



**Museu de Zoologia**  
**Universidade de São Paulo**

**Murilo Nogueira de Lima Pastana**

**Phylogeny of Stromateiformes (Teleostei; Percomorphacea)  
based on phenotypic data**

**Relações filogenéticas de Stromateiformes (Teleostei;  
Percomorphacea) com base em dados fenotípicos**

**Murilo Nogueira de Lima Pastana**

**Phylogeny of Stromateiformes (Teleostei; Percomorphacea)  
based on phenotypic data**

**Relações filogenéticas de Stromateiformes (Teleostei;  
Percomorphacea) com base em dados fenotípicos**

**Versão Original**

Tese apresentada ao Programa de Pós-Graduação do Museu de Zoologia da Universidade de São Paulo para obtenção do título de Doutor em Ciências (Sistemática, Taxonomia Animal e Biodiversidade).

Orientador: Prof. Dr. Aléssio Datovo

Não autorizo a reprodução e divulgação total ou parcial deste trabalho, por qualquer meio convencional ou eletrônico, para fins de estudo e pesquisa, desde que citada a fonte.

**Serviço de Biblioteca e Documentação**  
**Museu de Zoologia da Universidade de São Paulo**

**Catálogo na Publicação**

Pastana, Murilo Nogueira de Lima

Phylogeny of Stromateiformes (Teleostei; Percomorphacea) based on phenotypic data = Relações filogenéticas de Stromateiformes (Teleostei; Percomorphacea) com base em dados fenotípicos/ Murilo Nogueira de Lima Pastana; orientador Aléssio Datovo. São Paulo 2019.

309p.

Tese apresentada ao Programa de Pós-Graduação em Sistemática, Taxonomia e Biodiversidade, Museu de Zoologia, Universidade de São Paulo, 2019.

Versão original

1. Teleostei- filogenia. 2. Morfologia - Stromateiformes. I. Datovo, Alessio, orient. II. Título.

CDU 597.5

PASTANA, Murilo Nogueira de Lima

Phylogeny of Stromateiformes (Teleostei; Percomorphacea) based on phenotypic data

Relações filogenéticas de Stromateiformes (Teleostei; Percomorphacea) com base em dados fenotípicos

Tese apresentada ao Programa de Pós-Graduação do Museu de Zoologia da Universidade de São Paulo para obtenção do título de Doutor em Ciências (Sistemática, Taxonomia Animal e Biodiversidade).

Aprovado: \_\_\_\_/\_\_\_\_/\_\_\_\_

**Comissão Julgadora**

Prof. Dr. \_\_\_\_\_ Instituição: \_\_\_\_\_

Julgamento: \_\_\_\_\_ Assinatura: \_\_\_\_\_

Prof. Dr. \_\_\_\_\_ Instituição: \_\_\_\_\_

Julgamento: \_\_\_\_\_ Assinatura: \_\_\_\_\_

Prof. Dr. \_\_\_\_\_ Instituição: \_\_\_\_\_

Julgamento: \_\_\_\_\_ Assinatura: \_\_\_\_\_

Prof. Dr. \_\_\_\_\_ Instituição: \_\_\_\_\_

Julgamento: \_\_\_\_\_ Assinatura: \_\_\_\_\_

Prof. Dr. \_\_\_\_\_ Instituição: \_\_\_\_\_

Julgamento: \_\_\_\_\_ Assinatura: \_\_\_\_\_

## AGRADECIMENTOS

Expresso aqui meus sinceros agradecimentos a todos aqueles que de alguma maneira colaboraram com a conclusão deste trabalho.

Primeiramente registro aqui minha gratidão e admiração pelo Dr. Aléssio Datovo, não apenas pela orientação, mas também pela liberdade e confiança que depositou em mim ao longo dos anos de desenvolvimento desse projeto. O Aléssio exerceu não somente o papel de orientador acadêmico, mas também foi um grande amigo e conselheiro dos mais variados assuntos. Os momentos além do contexto acadêmico também foram sempre muito prazerosos, com ótimas companhias para conversas, risadas, culinária e jogos. Devo ao Aléssio boa parte do meu amadurecimento como pesquisador e como pessoa ao longo desses quatro anos.

Agradeço também aos professores Mario C. C. de Pinna, Naércio A. Menezes, Heraldo A. Britski e José L. de Figueiredo por terem aberto as portas do seu laboratório, e conseqüentemente facilitado meu ingresso na sessão de ictiologia do MZUSP. Ao Mario agradeço ainda pela amizade cultivada ao longo desses anos e pelos convites às reuniões em sua casa, sempre regadas de boas comidas, bebidas, e papos com muito bom humor. Adicionalmente, agradeço imensamente aos meus companheiros de laboratório no Museu de Zoologia que sempre tornaram o ambiente de trabalho um local bastante prazeroso. Obrigado Fernando D'agosta, Gustavo Ballen, Guilherme Dutra, Henrique Varella, Igor Mourão, Arthur de Lima, João Genova, Luiz Peixoto, Manoela Marinho, Marina Loeb, Michel Gianeti, Vitor Abrahão, Fábio Pupo, Paulo Presti, Priscila Camelier, Thiago Loboda, Túlio Teixeira, Verônica Slobodian, Vinícius Espíndola, Vinícius Carvalho e William Ohara pelas inúmeras discussões, auxílios, e parcerias acadêmicas. Agradeço especialmente ao Vitor pela paciência e pelas palavras de conselho que estiveram ali sempre que as procurei. Além disso, sua ajuda foi essencial para a conclusão desta tese dentro de seu prazo. Agradeço ainda ao Gustavo e Veronica, que por anos compuseram por anos minha sala e por lá mantiveram um bom astral; ao Luiz por sempre ter paciência em discutir e me ensinar sobre homologia de certos músculos, e por ser um dos poucos em compartilhar do meu interesse em miologia na sessão. Sou grato ao Vinícius Espíndola, que não hesitou ao me ajudar com literatura obscura. A Manu também teve uma sensibilidade e empatia ao conversar comigo na reta final da tese, e por isso sou muito grato. Também agradeço sinceramente ao apoio técnico desempenhado pelo Michel Gianeti e Osvaldo Oyakawa da sessão de peixes do Museu de Zoologia, e ao Alberto Carvalho do laboratório de Micro Tomografia. A ajuda dessas pessoas certamente facilitou o meu trabalho. Minha gratidão se estende aos funcionários e coordenadores da pós graduação em Sistemática, Taxonomia Animal, e Biodiversidade, que sempre se mostraram dispostos a enfrentar questões burocráticas ligadas à pós-graduação.

Naturalmente, meu vínculo com o LIRP (Laboratório de Ictiologia de Ribeirão Preto) se provou duradouro ao longo desses quatro anos, e nesse intervalo pude regressar às minhas origens ictiológicas em diferentes ocasiões. Agradeço imensamente aos mestres e colegas do Laboratório de Ictiologia de Ribeirão Preto (LIRP) Flávio Bockmann, Ricardo Castro, Pedro Rizzato, Dahyes Félix, João Pedro Trevisan, André Esguícero e Malu Araújo, e aos novos pós-graduandos que hoje compõem o LIRP. Estas pessoas me abriram as portas sempre que solicitei informações sobre a coleção, técnicas de preparação de espécimes, ou no uso da máquina de raio-X. Dentre estes, reservo um agradecimento particular ao André, que por tempos auxiliou no papel de curadoria da coleção do LIRP e, sempre que solicitado, me enviou prontamente espécimes e dados daquela coleção. Por sua vez, João Pedro me ajudou bastante atendendo aos meus pedidos de última hora e enviando prontamente literatura necessária para a conclusão dessa tese. O Pedro P. Rizzato teve um grande papel nessa jornada acadêmica. Agradeço em especial pelos convites para participar de eventos científicos, discursando desde sobre a linha lateral dos peixes até a (não) realidade da espécie biológica. Além disso, a habilidade expressa pelo Pedro em trabalhos envolvendo morfologia estabelece um novo padrão de qualidade de estudos anatômicos, me instigando a alcançar melhores resultados.

O tempo dedicado à execução deste projeto de doutorado contou também com um período sanduíche no exterior, realizado sob a supervisão do Dr. G. David Johnson na divisão de peixes do National Museum of Natural History (Smithsonian Institution). Esta oportunidade só se concretizou devido à enorme disposição e hospitalidade do Dave, que colaborou tanto nos processos burocráticos, quanto em importantes comentários acerca das relações filogenéticas de Percomorphacea. O Dave também incentivou minha participação e angariou boa parte dos recursos que me permitiram atender à Joint Meeting of Ichthyology and Herpetology em Austin – TX, em 2017. A ajuda e a hospitalidade do Dave também se expandiu para fora do ambiente do museu, e durante minha permanência em Washington – DC pude desfrutar de sincera amizade com o Dave e com sua esposa, Ai Nonaka. Esses dias certamente tornaram minha estadia no exterior mais especial. O ambiente de trabalho em Washington - DC foi bastante acolhedor também por conta da companhia de laboratório de David Santana, João Capretz, e Adela Roa-Varon. Durante a estadia no National Museum of Natural History, nos momentos de POETS ou de pausa para cafezinhos, pude me beneficiar de conversas produtivas com Bruce Colette, Thomas Munroe, Victor Springer, Carole Baldwin, Lynne Parenti, Roy McDiarmid, Rayna Bell, Aleta Quinn, e Kevin De Queiroz. Expresso ainda meus sinceros agradecimentos ao trabalho de curadoria de Jeff Clayton, Sandra Raredom, Kris Murphy, Diane Pitassy. Sou muito grato ainda pela ajuda da Ai Nonaka durante meu período de aclimação no NMNH. Agradeço ao Chad Walter pela hospedagem em DC. Agradeço a companhia de toda máfia brasileira do NMNH, fiéis colegas de almoço, café, POETS, museus, e ciclismo pela cidade de Washington. Estes colegas, mesmo em

períodos de contraturno do laboratório, apreciaram uma reunião acompanhada pelo bom papo de biólogo. Expresso ainda minha gratidão ao apoio de Rodolpho Menezes, Alexandre Cordeiro, João Capretz, Ismael Franz, Rodrigo CG, Ana Francisca Tamburus, Lucy Mila, Rafael Dell’Erba, Jonathan Lawley, Marcelo Pace, Manuela Dal Forno, e tantos outros colegas presentes no museu no primeiro semestre de 2017. A boa companha do Alex Eleotério também foi fundamental para me fazer esquecer das saudades do Brasil e aproveitar o período de intercâmbio no exterior. Destes, os que compartilharam a “república brasileira” na casa do Chad fizeram da minha rotina diária algo muito mais leve e prazerosa. Durante minha estadia no exterior pude desfrutar de uma semana de visitas ao laboratório de peixes do Virginia Institute of Marine Science em Gloucester Point – VA, e de participar de uma expedição de coletas ictiológicas nas drenagens da região. Pela hospitalidade durante a visita agradeço ao Pedro Rizzato, Diego Vaz, e Kate Bemis, e pela oportunidade de participar dessa expedição agradeço ao Dr. Eric Hilton.

Expresso meus sinceros agradecimentos aos curadores e/ou técnicos que enviaram espécimes fundamentais para a realização deste estudo. Estes foram Mark H. Sabaj (The Academy of Natural Sciences of Drexel University, ANSP), Brian Sidlauskas e Peter Konstantinidis (Oregon State University Ichthyological Collection, OS), Katherine Maslenikov (Burke Museum, UW), Karsten Hartel (Harvard Museum of Comparative Zoology, MCZ), Alastair Graham (Australian National Fish Collection, CSIRO), David Johnson (National Museum of Natural History – Smithsonian Institution, NMNH), e Marcelo Britto e Cristiano Moreira (Museu Nacional do Rio de Janeiro, UFRJ).

Por fim, quero expressar minha gratidão para pessoas que não são cientificamente ligadas a esse trabalho, mas que contribuíram muito com minha jornada acadêmica. Agradeço aos meus pais Firmo e Eliana Pastana, por sempre terem oferecido todo o apoio e incentivo, quaisquer que fossem minhas decisões. Meu irmão Marcelo, que desde nossa infância foi companheiro de aventuras em busca de peixes, em praias, várzeas, riachos e costões. Aos meus avós, maternos e paternos, que também sempre me incentivaram a seguir buscando por conhecimento. E por fim, ofereço minha especial gratidão à minha parceira de vida, Paula Thaísa Galdini Carvalho. Sua ajuda nessa minha conquista é algo imensurável. Adorei iniciar e dividir contigo essa nova jornada em São Paulo. Se não científico, meu aprendizado com você foi humano, e ao seu lado aprendi muito sobre o que é alegria, tristeza, paciência, perdão, companheirismo, e amor. Muito obrigado por ser esta pessoa incrível, sempre ao meu lado.

Este projeto foi financiado pela Bolsa de Doutorado concedidas pela Coordenação de Aperfeiçoamento de Pessoal de Nível Superior (CAPES), e pelo Programa de Doutorado Sanduíche no Exterior (PDSE – CAPES; vigência 01/04 a 01/11 de 2017).

## RESUMO

A divisão Percomorphacea engloba a maior diversidade de peixes vivos, somando mais da metade dos peixes de nadadeiras raiadas e o equivalente a praticamente um quarto de todos os vertebrados atuais. Entretanto, as interações entre a maioria das linhagens de Percomorphacea ainda est longe de uma resolu satisfatria. Dentre as 30 ordens de Percomorphacea reconhecidas atualmente, Stromateiformes agrupa 77 espcies organizadas em 16 gneros e seis famlias – Amarsipidae, Ariommatidae, Centrolophidae, Nomeidae, Stromateidae, e Tetragonuridae. Membros dessa ordem exibem distribu global em guas tropicais e temperadas, tanto em ambientes pelgicos ou costeiros, e so tradicionalmente agrupados por apresentar duas especializaes morfolgicas singulares: a presena de uma bolsa faringeana, e de uma rede de canais subdrmicos sobre a cabea e o tronco. O status filtico de Stromateiformes nunca foi testado de maneira apropriada com base em dados morfolgicos, e seu monofiletismo tem sido rejeitado por diferentes anlises filogenticas pautadas em dados moleculares. Alm disso, anlises morfolgicas e moleculares tm se mostrado indecisivas quanto s relaes de Stromateiformes com outros Percomorphacea. O presente estudo se prop a investigar estas questes e apresentou uma ampla reviso filogentica de Stromateiformes baseada em uma anlise exaustiva de 218 caracteres fenotpicos e 66 txons terminais, o que inclui todos os gneros vlidos de Stromateiformes bem como todas as famlias de Percomorphacea que de alguma maneira j foram alinhadas  ordem. A topologia resultante indica a ordem como monofiltica e suportada por quatro sinapomorfias. Amarsipidae, o nico representante de Stromateiformes a no apresentar uma bolsa faringeana,  posicionado como grupo irmo dos demais membros da ordem. Centrolophidae no  monofiltico, com cinco de seus gneros agrupados em um clado basal, enquanto outros dois aparecem como grupos irmos sucessivos de um clado composto pelas demais famlias de Stromateiformes. Todas estas famlias so recuperadas como monofilticas, arranjas da seguinte maneira: Nomeidae (Stromateidae (Tetragonuridae, Ariommatidae)). Um clado composto por Bramidae e Caristiidae  aqui hipotetizado como sendo o grupo irmo dos Stromateiformes, apesar desse arranjo ser suportado por apenas uma sinapomorfia no ambgua. O presente estudo ainda apresenta uma hiptese de que a relao simbitica singular entre juvenis de Stromateiformes e outros invertebrados gelatinosos (*e.g.* medusas e salpas) est provavelmente associado com a evoluo de algumas das mais notveis especializaes morfolgicas do grupo, tais como os cecos pilricos arranjas numa massa dendrtica, a presena de um plexo de canais subcutneos, e a presena de uma bolsa faringeana.

## ABSTRACT

The division Percomorphacea encompasses a major fraction of the extant fish diversity, including over half of all known ray-finned fishes and approximately one fourth of the living vertebrates. The interrelationships among the major percomorphacean lineages are still far from a satisfactory resolution. Among the 30 percomorphacean orders, Stromateiformes encloses 77 extant species distributed into 16 genera and six families – Amarsipidae, Ariommatidae, Centrolophidae, Nomeidae, Stromateidae, and Tetragonuridae. Members of this order are globally distributed in temperate and tropical oceans and exhibit two extraordinary morphological specializations: the presence of a pharyngeal sac and of a subdermal canal plexus over the head and trunk. The phyletic status of Stromateiformes has never been adequately tested on morphological grounds and the monophyly of the order has been recently rejected by multiple molecular analyses. Moreover, stromateiforms have been indecisively aligned with disparate percomorphacean taxa by both morphology- and molecular-based studies. The present work delved into these questions and presented a comprehensive phylogenetic revision of Stromateiformes based on an exhaustive analysis of 218 phenotypic characters and 66 terminal taxa encompassing all valid stromateiform genera, as well as all percomorphacean families somehow aligned with stromateiforms in prior studies. The resulting topology retrieves the order as monophyletic, supported by four unequivocal synapomorphies. Amarsipidae, the only stromateiform lacking a pharyngeal sac, is resolved as the sister group of the remaining members of the order. Centrolophidae is not monophyletic, with five of its genera grouped into a basal clade, whereas the other two appear as successive sister groups of a clade containing the remaining stromateiform families. All these families are recovered as monophyletic with the following cladistic arrangement: Nomeidae (Stromateidae (Tetragonuridae, Ariommatidae)). A clade composed by Bramidae and Caristiidae is herein hypothesized the sister group of stromateiforms, although this arrangement is supported by only a single unequivocal synapomorphy. The present study further hypothesizes that the remarkable symbiotic relationship between juvenile stromateiforms and gelatinous invertebrates (e.g. medusa and salps) is probably associated with the evolution of some of its most remarkable morphological specializations, such as the presence of dendritic pyloric caeca, subcutaneous canal plexuses, and the pharyngeal sac.

## LISTA DE TABELAS

<b>TABLE 1.</b> Specimen counts (left column) and normalized values (right column) used for Characters #0-15. Inapplicable characters are indicated by <i>in.</i> and data deficiency by a question mark .....	201
<b>TABLE 2.</b> Specimen standard length in millimeters (first column), and proportional specimen measurement and normalized values used for Characters #16-21. Proportions are relative to the specimen's standard length, offered in the first data column (mm SL). Question mark (?) indicates data deficiency .....	202
<b>TABLE 3.</b> <i>Fit</i> values for characters under 23 different values of K (K = 1-22, and K → ∞) and exhibiting 0 to 25 homoplasies. Column indicated by K → ∞ simulates <i>fit</i> values under equal weight methods.....	203
<b>TABLE 4.</b> <i>Fit</i> values for characters under 11 different K values and exhibiting 0 to 25 homoplasies. Values were calculated to generate a regular distribution of <i>fit</i> values in a character containing 12 homoplasies (indicated by the dashed bar) .....	204
<b>TABLE 5.</b> Published records for the association between percomorphacean fishes and different lineages of gelatinous invertebrates used to code Character #217 .....	205

## LISTA DE FIGURAS

- FIGURE 1:** The evolution of Stromateiformes according to Haedrich (1967). The diagram is constructed considering main changes on relative size and shape, fin pattern, presence or absence of palatal dentition, numbers of branchiostegals, vertebrae, and epurals + hypurals. Inset represents pharyngeal-sac rakers. Width of arrows are proportional to number of genera in the family. Image reproduced from Haedrich (1967: fig. 48) .....207
- FIGURE 2:** Hypotheses of the relationships of Stromateiformes inferred from morphological characters according to: A) Horn (1984) and B) Doiuchi *et al.* (2004). Highlighted taxa represent Amarsipidae (red), Centrolophidae (purple), Nomeidae (green), Tetragonuridae (pink), Stromateidae (orange), and Ariommatidae (light blue) .....208
- FIGURE 3:** Interrelationships of Stromateiformes according to Doiuchi & Nakabo (2006). Topology was obtained using molecular data and constructed using Maximum Likelihood methods. Image reproduced from Doiuchi & Nakabo (2006: fig. 4). Amarsipidae was not sampled .....209
- FIGURE 4:** Interrelationships of Pelagiaria according to Miya *et al.* (2013). Topology was obtained from mitogenome sequences and constructed using Maximum Likelihood methods. Image reproduced from Miya *et al.* (2013: fig. 5). Amarsipidae was not sampled .....210
- FIGURE 5:** Measurements used as continuous characters in the phylogenetic analysis shown in an alizarin red stained specimen of *Apogon maculatus* (Apogonidae: MZUSP 43155; 67.3 mm SL). Letters indicate: A) Predorsal length, B) dorsal-fin base length, C) pectoral-fin length, D) Prepevic length, E) Preanal length, F) Anal-fin base length .....211
- FIGURE 6:** *Fit* distribution for characters under 23 different values of K ( $K = 1-22$ , and  $K \rightarrow \infty$ ) and exhibiting 0 to 25 homoplasies. Note that higher values of K result in curves exhibiting similar concavities (darker curves). *Fit* values under an equal weight analysis ( $K \rightarrow \infty$ ) result in a straight line of *fit* distribution .....212
- FIGURE 7:** *Fit* distribution for characters under 11 different K values and exhibiting 0 to 25 homoplasies. Dashed line indicates a character exhibiting 12 homoplasies, chosen herein as the point where curves under different values of K exhibit a proportional *fit* variation .....213
- FIGURE 8:** Dorsal-fin musculoskeletal system of *Apogon maculatus* (Apogonidae: MZUSP 43155) in left lateral view. Note the epaxial musculature association with the dorsal-fin pterygiophores. Scale bar: 3 mm .....214

<b>FIGURE 9:</b> Left lateral view of an alizarin-red stained specimen of <i>Monocirrhus polyacanthus</i> (MZUSP 55122; 54.6 mm SL). Arrow indicates the membrane attaching the medial most pelvic-fin ray to the abdomen .....	215
<b>FIGURE 10:</b> Left pectoral girdle of <i>Morone mississippiensis</i> (Moronidae: MZUSP 123242) in (A) lateral and (B) medial view exhibiting associated muscles. Scale bar: 8 mm .....	216
<b>FIGURE 11:</b> Left pectoral girdle of <i>Nomeus gronovii</i> (Nomeidae: MZUSP 67590) in (A) lateral and (B) medial view exhibiting associated muscles. Scale bar: 5 mm .....	217
<b>FIGURE 12:</b> Left pectoral girdle of <i>Cubiceps pauciradiatus</i> (Nomeidae: MZUSP 80701) in (A) lateral and (B) medial view exhibiting associated muscles. Scale bar: 5 mm .....	218
<b>FIGURE 13:</b> Pelvic girdle of <i>Apogon maculatus</i> (Apogonidae: MZUSP 43155) in ventral view exhibiting associated muscles and ligaments. Scale bar: 1 mm .....	219
<b>FIGURE 14:</b> Caudal peduncle and caudal fin of (A) <i>Centropomus parallelus</i> (Centropomidae: MZUSP 108244) and (B) <i>Oplegnathus fasciatus</i> (Oplegnathidae: MZUSP 28867) showing the posterior limit of the trunk lateral line. Scale bar: 5 mm .....	220
<b>FIGURE 15:</b> Radiographs of the caudal skeleton of (A) <i>Amniataba caudavittata</i> (Terapontidae: USNM 173673), and (B) <i>Atherinella brasiliensis</i> (Atherinopsidae: MZUSP 67186) in left lateral view. Scale bar: 4 mm .....	221
<b>FIGURE 16:</b> Radiographs of the caudal skeleton of the centrolophids (A) <i>Hyperoglyphe perciformis</i> (MZUSP 119733), and (B) <i>Tubbia tasmanica</i> (CSIRO H 6979-03) in left lateral view. Scale bar: 5 mm .....	222
<b>FIGURE 17:</b> Caudal skeleton of a cleared and stained specimen of <i>Amarsipus carlsbergi</i> (Amarsipidae: SIO 75-122) in left lateral view. Scale bar: 2 mm .....	223
<b>FIGURE 18:</b> Radiographs of the occipital region and anterodorsal portion of the trunk of (A) <i>Lates niloticus</i> (Latidae: MZUSP 123243), and (B) <i>Centropomus parallelus</i> (Centropomidae: MZUSP 108244) in left lateral view. Scale bar: 4 mm .....	224
<b>FIGURE 19:</b> Head of <i>Holocentrus adscensionis</i> (Holocentridae: MZUSP 69190) in left lateral view. Scale bar: 7 mm .....	225
<b>FIGURE 20:</b> Head of <i>Centropomus parallelus</i> (Centropomidae: MZUSP 108244) in left lateral view. Scale bar: 10 mm .....	226

<b>FIGURE 21:</b> Head of <i>Arripis georgianus</i> (Arripidae: MZUSP 119735) in left lateral view. Scale bar: 10 mm .....	227
<b>FIGURE 22:</b> Superficial cranial musculoskeletal system of <i>Holocentrus adscencionis</i> (Holocentridae: MZUSP 69190) in left lateral view. Eye and infraorbital series removed. Scale bar: 7 mm .....	228
<b>FIGURE 23:</b> Superficial cranial musculoskeletal system of <i>Centropomus parallelus</i> (Centropomidae: MZUSP 108244) in left lateral view. Eye and infraorbital series removed. Scale bar: 10 mm .....	229
<b>FIGURE 24:</b> Superficial cranial musculoskeletal system of <i>Icichthys lockingtoni</i> (Centrolophidae: OS 16732) in left lateral view. Eye and infraorbital series removed. Scale bar: 7 mm .....	230
<b>FIGURE 25:</b> Superficial cranial musculoskeletal system of <i>Lateolabrax japonicus</i> (Lateolabracidae: MZUSP 123245) in left lateral view. Eye and infraorbital series removed. Scale bar: 10 mm .....	231
<b>FIGURE 26:</b> Superficial cranial musculoskeletal system of <i>Pomatomus saltatrix</i> (Pomatomidae: MZUSP 69784) in left lateral view. Eye and infraorbital series removed. Scale bar: 7 mm .....	232
<b>FIGURE 27:</b> Superficial cranial musculoskeletal system of <i>Raneya brasiliensis</i> (Ophidiidae: MZUSP 61358) in left lateral view. Eye and infraorbital series removed. Scale bar: 5 mm .....	233
<b>FIGURE 28:</b> Superficial cranial musculoskeletal system of <i>Sphyraena tome</i> (Sphyraenidae: MZUSP 47562) in left lateral view. Eye and infraorbital series removed. Scale bar: 10 mm .....	234
<b>FIGURE 29:</b> Superficial cranial musculoskeletal system of <i>Hyperoglyphe perciformis</i> (Centrolophidae: MZUSP 119733) in left lateral view. Eye and infraorbital series removed. Scale bar: 10 mm .....	235
<b>FIGURE 30:</b> Left <i>adductor mandibulae</i> and associated structures of <i>Pomatomus saltatrix</i> (Pomatomidae: MZUSP 69784) in (A) lateral and (B) medial views. Scale bar: 5 mm .....	236
<b>FIGURE 31:</b> Inset of palatal region of <i>Lates niloticus</i> (Latidae: MZUSP 123243) in left lateral view exhibiting associated muscles and bones. Eye, infraorbital series, and <i>adductor mandibulae</i> complex removed. Note the subocular shelf kept in place by ligamentous contact to the endopterygoid (anteriorly) and to the <i>levator arcus palatini</i> (posteriorly). Scale bar: 5 mm .....	237
<b>FIGURE 32:</b> Superficial cranial musculoskeletal system of <i>Apogon maculatus</i> (Apogonidae: MZUSP 43155) in left lateral view. Eye and infraorbital series removed. Scale bar: 3 mm .....	238
<b>FIGURE 33:</b> Superficial cranial musculoskeletal system of <i>Oplegnathus fasciatus</i> (Oplegnathidae: MZUSP 28867) in left lateral view. Eye and infraorbital series removed. Scale bar: 4 mm .....	239

- FIGURE 34:** Superficial cranial musculoskeletal system of *Cynoscion striatus* (Sciaenidae: MZUSP 68913) in left lateral view. Eye and infraorbital series removed. Scale bar: 8 mm .....240
- FIGURE 35:** Superficial cranial musculoskeletal system of *Polydactylus virginicus* (Polynemidae: MZUSP 67549) in left lateral view. Eye and infraorbital series removed. Scale bar: 6 mm .....241
- FIGURE 36:** Superficial cranial musculoskeletal system of *Cubiceps pauciradiatus* (Nomeidae: MZUSP 80701) in left lateral view. Eye and infraorbital series removed. Scale bar: 5 mm .....242
- FIGURE 37.** Superficial cranial musculoskeletal system of *Stromateus brasiliensis* (Stromateidae: MZUSP 51279) in left lateral view. Eye, infraorbital series, and RLA nerve removed. Scale bar: 5 mm .....243
- FIGURE 38:** Superficial cranial musculoskeletal system of *Paralichthys isosceles* (Paralichthyidae: MZUSP 72323) in left lateral view. Eye and infraorbital series removed. Scale bar: 8 mm .....244
- FIGURE 39.** Hyopalatine arch, opercular series, and associated musculature of *Ariomma melanum* (Ariommatidae: MZUSP 123246) in (A) lateral and (B) medial views. Scale bar: 10 mm .....245
- FIGURE 40.** Hyopalatine arch, opercular series, and associated musculature of *Paralichthys isosceles* (Paralichthyidae: MZUSP 72323) in (A) lateral and (B) medial views. Scale bar: 10 mm .....246
- FIGURE 41.** Hyopalatine arch, opercular series, and associated musculature of *Trichiurus lepturus* (Trichiuridae: MZUSP 8855) in lateral view. Scale bar: 8 mm .....247
- FIGURE 42.** Micro CT scanning of the branchial and pharyngeal-sac skeleton of *Ariomma bondi* (Ariommatidae: MZUSP 86717) in dorsal (A) and lateral views (B). Scale bar: 4 mm .....248
- FIGURE 43.** Micro CT scanning of the branchial and pharyngeal-sac skeleton of *Tubbia tasmanica* (Centrolophidae: CSIRO H 6979-03) in dorsal (A) and lateral views (B). Scale bar: 7 mm. A magnification of an enlarged raker associated to epibranchial 4 and ceratobranchial 5 is shown in C. Arrow indicates small pharyngeal-sac rakers associated to the large epibranchial raker. Scale bar: 2 mm .....249
- FIGURE 44.** Micro CT scanning of the branchial and pharyngeal-sac skeleton of *Tubbia tasmanica* (Centrolophidae: CSIRO H 6979-03). A) dorsal view, dorsal gill-arch elements removed; B) frontal view.; C) Parasagittal view, gill arch elements of the right side removed. A raker associated to epibranchial 4 and ceratobranchial 4 is highlighted in orange. Scale bar: 7 mm .....250

**FIGURE 45.** Micro CT scanning of the branchial and pharyngeal-sac skeleton of *Psenes cyanophrys* (Nomeidae: MZUSP 106392) in dorsal (A) and lateral views (B). Scale bar: 4 mm. A magnification of the upper pharyngeal tooth plates in ventral view is shown in C. Scale bar: 1 mm .....251

**FIGURE 46.** Branchial and pharyngeal sac musculoskeletal system of *Tetragonurus cuvieri* (Tetragonuridae: MZUSP 123241) in (A) dorsal and (B) lateral view. In C, the pharyngeal sac is cut laterally to expose its internal papillary lining and to show posteriorly elongate upper pharyngeal tooth plates. Scale bar: 5 mm .....252

**FIGURE 47.** Cranial and abdominal anatomy of *Icichthys lockingtoni* (Centrolophidae: OS 16732) depicting gill arches, pharyngeal sac, and anterior portion of the abdominal cavity. Orbital, *adductor mandibulae*, opercular, hyopalatal and pectoral-girdle complexes are removed. Scale bar: 6 mm ....253

**FIGURE 48.** Cranial and abdominal anatomy of *Tetragonurus cuvieri* (Tetragonuridae: MZUSP 123241). Gill arches, pharyngeal sac, and anterior portion of the abdominal cavity is depicted in A, after removal of the orbital, *adductor mandibulae*, opercular, hyopalatal and pectoral girdle complexes. In B, there is an inset of the gill-arch muscles and bones, and C depicts the pharyngeal sac and anteriormost abdominal organs. Scale bar: 10 mm .....254

**FIGURE 49:** Dorsal view of branchial and pharyngeal-sac musculoskeletal system of (A) *Ariomma melanum* (Ariommatidae: MZUSP 123246; scale bar: 5 mm) and (B) *Hyperoglyphe perciformis* (Centrolophidae: MZUSP 119733; scale bar: 5 mm) in dorsal view .....255

**FIGURE 50.** Branchial and pharyngeal-sac musculoskeletal system of *Icichthys lockingtoni* (Centrolophidae: OS 16732) in (A) dorsal, (B) lateral, and (C) ventral views. Scale bar: 5 mm .....256

**FIGURE 51.** Branchial and pharyngeal-sac musculoskeletal system of *Cubiceps whiteleggii* (Nomeidae: MZUSP 67590) in (A) dorsal, (B) lateral, and (C) ventral views. Scale bar: 6 mm .....257

**FIGURE 52.** Branchial and pharyngeal-sac musculoskeletal system of *Stromateus brasiliensis* (Stromateidae: MZUSP 51279) in (A) dorsal, (B) lateral, and (C) ventral view. Arrow indicates posterolateral set of *sphincter oesophagi* fibers. Scale bar: 5 mm .....258

**FIGURE 53.** Micro CT scanning of the pharyngeal-sac skeleton of *Ariomma bondi* (A-B; Ariommatidae: MZUSP 86717), and *Peprilus triacanthus* (C-D; Stromateidae: MZUSP 123240) in right lateral (A-C), and sagittal (B-D) views. Scale bar: 2 mm .....259

**FIGURE 54.** Stromateiform rakers from the gill arch and pharyngeal sac taken from *Psenopsis anomala* (A-D; Centrolophidae: MZUSP 119730) and *Ariomma bondi* (E-H; Ariommatidae: MZUSP 86717). First

column shows a raker associated to the anterior facet of ceratobranchial 1 (A, E); second column shows rakers from the posterior facet of ceratobranchial 2 (B, F); third column show rakers associated to the anterior facet of ceratobranchial 5 (C, G); and fourth column exhibits pharyngeal-sac rakers (D, H). Scale bar: 0.5 mm .....260

**FIGURE 55.** Stromateiform pharyngeal-sac raker. Dorsal (A) and lateral (B) views of the pharyngeal-sac raker of *Ariomma bondi* (Ariommatidae MZUSP 86717), exhibiting its elongate dorsoventral axis and round base. In *Peprilus triacanthus* (Stromateidae: MZUSP 123240) the pharyngeal-sac raker base is stellate (C), but the raker still elongate dorsoventrally (D). Stellate bases (E) also characterize *Psenes cyanophrys* (Nomeidae: MZUSP 106392), but the raker is less elongate (F) than in ariommatids or stromateids. Scale bar: 0.5 mm .....261

**FIGURE 56.** Inset of the muscular attachment of the pharyngeal-sac raker in Stromateiformes. Raker bases are visible after removal of the external most layer of the *sphincter oesophagi*. In A, Ariommatidae (*Ariomma melanum*: MZUSP 123246) the raker bases are large, round, and partially overlap each other. In B, Tetragonuridae (*Tetragonurus cuvieri*: MZUSP 123241) the round raker bases are small, do not overlap each other, and are poorly ossified. Both in C, Nomeidae (*Nomeus gronovii*: MZUSP 67590) and D, Stromateidae (*Stromateus brasiliensis*: MZUSP 51279) the raker bases exhibit large, well ossified, and exhibiting a stellate morphology. Scale bar: 0.5 mm .....262

**FIGURE 57.** Left lateral view of an alcohol preserved juvenile specimen of *Stromateus fiatola* (Stromateidae: USNM UNCAT; 68.7 mm SL). Arrow indicates the pelvic fin .....263

**FIGURE 58:** Caudal skeleton of a cleared and stained specimen of *Ariomma bondi* (Ariommatidae: MZUSP 86717) in left lateral view. Scale bar: 2 mm .....264

**FIGURE 59.** Pectoral and pelvic girdles and fins of *Cubiceps pauciradiatus* (Nomeidae: MZUSP 80701) in left lateral view. Note the lateral myoseptal ligament connecting the basipterygium to the postcleithrum. Scale bar: 5 mm .....265

**FIGURE 60:** Dorsal (A) and left lateral (B) views of the basipterygium of *Peprilus triacanthus* (Stromateidae: USNM 302441). In A, arrow indicates point of fusion between basipterygia; in B, arrow points to posteriorly oriented pelvic spine. Scale bar: 3 mm .....266

**FIGURE 61:** Left *adductor mandibulae* and associated structures of *Ariomma melanum* (Ariommatidae: MZUSP 123246) in (A) medial and (B) lateral views. Scale bar: 7 mm .....267

**FIGURE 62:** Left *adductor mandibulae* and associated structures of *Tetragonurus cuvieri* (Tetragonuridae: MZUSP 123241) in (A) lateral and (B) medial views. Scale bar: 5 mm .....268

**FIGURE 63:** Left *adductor mandibulae* and associated structures of *Trichiurus lepturus* (Trichiuridae: MZUSP 8855) in (A) medial and (B) lateral views. Scale bar: 10 mm .....269

**FIGURE 64.** Inset of the temporal region of *Peprilus paru* (Stromateidae: MZUSP 67608) in left lateral view exhibiting associated muscles and bones. Eye and infraorbital series removed. Note the *ramus lateralis accessorius* pattern 10, emerging from the sphenotic and following caudally superficial to the *levator arcus palatini*, *dilatator operculi*, and *levator operculi*. Scale bar: 4 mm .....270

**FIGURE 65.** Inset of the temporal region of *Icichthys lockingtoni* (Centrolophidae: OS 16732) in left lateral view exhibiting associated muscles and bones. Note the *ramus lateralis accessorius* in a pattern 10 emerging from the sphenotic. Scale bar: 2 mm .....271

**FIGURE 66.** Subdermal canal plexus of *Tubbia tasmanica* (Centrolophidae: CSIRO H 6979-03). In A, the subdermal canals are visible in a radiographed specimen (325.2 mm SL). A transverse section of the superficial layers of skin and axial musculature is shown in B. A magnification of the external appearance of the skin surface is offered in C, and a photograph of opposite surface of the same piece is shown in D. Note pores connecting the external surface to the interdermal space in pictures C and D. Scale bar: 1 mm .....272

**FIGURE 67.** Photographs of alizarin-red stained percomorphacean scales. The posterior margin of a cycloid scale of *Cubiceps whiteleggii* (Nomeidae: MZUSP 67590) is shown in A. The same region of a spinoid scale of *Beryx splendens* (Berycidae: MZUSP 121649) is shown in B; and of a transforming ctenoid scale of *Apogon maculatus* (MZUSP 43155) is shown in C. Scale sampling was standardized to the region behind the left pectoral fin. Scale bar: 0.5 mm .....273

**FIGURE 68.** Most parsimonious tree resultant from an analysis employing Implicit Weighting against homoplasies under  $K = 6.808$ . Highlighted clades represent: Stromateiformes (dark green), Ophidiiformes (blue), Scombriformes (red), Pleuronectiformes (yellow) Centropomidae (orange), Sciaenidae + Polynemidae (purple), and Mugiliformes + Atherinomorpha (light blue). The monophyly of Beryciformes (highlighted in grey) was not tested herein, as the analysis was rooted in *Beryx splendens* (Berycidae) .....274

**FIGURE 69.** Most parsimonious tree resultant from an analysis employing Implicit Weighting against homoplasies under  $K = 6.808$  exported with TNT native node numbers .....275

**FIGURE 70:** Interrelationships of the Stromateiformes resultant from an analysis employing Implicit Weighting against homoplasies, under  $K = 6.808$ . Highlighted taxa represent: Amarsipidae (red),

Centrolophidae (blue), Nomeidae (green), Stromateidae (orange), Tetragonuridae (pink), and Ariommatidae (light blue). Letters A to W represent clades within Stromateiformes .....276

**FIGURE 71:** Left lateral view of an alcohol preserved specimen of (A) *Amarsipus carlsbergi* (Amarsipidae: SIO 75-122; 50.4 mm SL), and (B) *Tetragonurus cuvieri* (Tetragonuridae: MZUSP 123241; 94.7 mm SL) .....277

# SUMÁRIO

Introduction .....	16
The taxonomy of Stromateiformes: an overview .....	16
Phylogeny of Stromateiformes: morphological approaches .....	20
Phylogeny of Stromateiformes: molecular approaches .....	23
Materials and methods .....	26
Anatomical terminology and specimen preparation .....	26
Taxonomic classification and taxon sampling .....	27
Data analysis.....	29
Results .....	33
Quantitative characters .....	33
Counts .....	33
Measurements .....	40
Qualitative characters .....	42
Osteology .....	42
Myology .....	78
Miscellanea .....	113
Phylogenetic analysis .....	138
Discussion .....	140
The phylogeny of Stromateiformes .....	140
The intrarelationships of Stromateiformes .....	140
The interrelationships of Stromateiformes .....	160
Further comments on the stromateiform morphology .....	162
Comments on the interrelationships of Percomorphacea .....	173
Bibliography .....	181
Tables .....	200
Figures .....	206
Appendix .....	278

# INTRODUCTION

## The taxonomy of stromateiformes: an overview

The division Percomorphacea (*sensu* Wiley & Johnson, 2010) encompasses a major fraction of the extant fish diversity, including over half of all known ray-finned fishes and approximately one fourth of the living vertebrates (Nelson, 2006; Van der Laan & Fricke, 2019). Recent classifications based on morphological data organize the 17,000+ known percomorphacean species into 30 distinct order (Wiley & Johnson, 2010). The monophyly of Percomorphacea is supported by studies based on both anatomical (Johnson & Patterson, 1993; Wiley & Johnson, 2010), molecular (Li *et al.*, 2007; Near *et al.*, 2012, 2013; Betancur-R *et al.*, 2013; Betancur-R *et al.* 2017), and combined morphological and molecular data (Mirande, 2016). The internal relationships among the dozens of percomorphacean orders, on the other hand, are still far from a satisfactory resolution. Conflicts between morphology- and DNA-based hypotheses are particularly striking, and the resolution of these discordances represents one of the biggest challenges of the systematics of bony fishes (Johnson & Patterson, 1993; Nelson, 2006, 2016; Wiley & Johnson, 2010).

Among the 30 percomorphacean orders recognized by Wiley & Johnson (2010), Stromateiformes encloses 77 extant species distributed into 16 genera and six families – Amarsipidae, Ariommatidae, Centrolophidae, Nomeidae, Stromateidae, and Tetragonuridae (Van der Laan & Fricke, 2019). Additionally, there is at least one fossil family, Propercarinidae, assigned to Stromateiformes (Bannikov, 1995; Prikryl *et al.* 2014). Members of this order generally exhibit broad geographical distributions in temperate and tropical ocean waters, both in pelagic and coastal environments, and in variable depths (Haedrich, 1967). At least part of the Stromateiformes inhabit deep pelagic waters (*e.g.* some Centrolophidae, Tetragonuridae, and Amarsipidae), a condition that has hampered the sampling and availability of these taxa in scientific collections. Other taxa, instead, inhabit coastal environments and are found in certain abundance in beaches and rocky shores. These species are often used as food resource and some may reach high prices on fish markets (*i.e.* *Peprilus* and *Pampus* spp.). Stromateiformes also exhibit a fair morphological variability, with pelagic taxa usually having shallow, cylindrical body (*i.e.* Tetragonuridae, Amarsipidae, some *Ariomma* species) and those inhabiting the shoreline with deeper and more compressed bodies (*i.e.* Stromateidae).

For over a century, anatomists have unequivocally recognized Stromateiformes as a natural assemblage. Fishes of the order have been traditionally grouped based on the sharing of an extraordinary specialization: the presence of a large and globular pharyngeal sac located on the proximal portion of the esophagus, immediately posterior to the last branchial arch (Günther, 1880;

Regan, 1902; Haedrich, 1967). This sac is covered externally by the *sphincter oesophagi* muscle (Datovo *et al.*, 2014) and internally lined by a series of small teeth-like structures that are covered by a thin epithelial tissue (Günther, 1880; Regan, 1902; Haedrich, 1967). This series of tissue-covered “teeth” are often referred as pharyngeal-sac papillae. Both the pharyngeal-sac dentition and its associated musculature present a notable degree of complexity among the Stromateiformes (Gilchrist, 1922; Buhler, 1930; Isokawa, 1965; Haedrich, 1967; Springer & Johnson, 2004; Datovo *et al.*, 2014) and the anatomical variations in these structures have been used as taxonomic characters (Isokawa, 1965; Haedrich, 1967).

The most important study on the systematics and taxonomy of Stromateiformes was published by Haedrich (1967). This work provided, for the first time, a detailed taxonomic revision of the entire order, identification keys for its families, and diagnosis, descriptions, and lists of synonyms for all its genera. Although presenting his ideas under a pre-cladistic perspective, Haedrich (1967) provided insightful thoughts regarding the interrelationships of the Stromateiformes. According to the author, these fishes could be diagnosed by presenting a “toothed sacular outgrowth in the gullet” (= pharyngeal sac), and small teeth approximately uniserial in the jaws. Within stromateiforms, Centrolophidae and Nomeidae would be “basal” lineages, while Tetragonuridae, Ariommatidae, and Stromateidae represented “specialized” forms (Fig. 1). In addition to the pharyngeal sac and the uniserial teeth, Haedrich (1967) also described an unusual characteristic present in almost all Stromateiformes: a subdermal canal system in the head and trunk, which connects an interdermal space in the skin to the outer surface through minute pores. According to the author, this was an unusual feature of stromateiforms. Indeed, this plexus of subcutaneous canals are only found in some unrelated taxa such as Trachipteridae (Walters, 1963) and some Gempylidae (Bone, 1972). As to the affinities of stromateiforms with other percomorphaceans, the author refrained himself of offering assertive opinions, but briefly stated that Stromateiformes, Kyphosidae, and Carangidae would share an overall similarity.

The taxonomic classification of Stromateiformes have undergone few, but important modifications after the publication of Haedrich’s (1967) seminal study. The main changes were the description two new families and one new genus, and the resurrection of another genus. The first of these was the discovery of *Amarsipus carlsbergi*. This species was described by Haedrich (1969) and placed in a monotypic family – Amarsipidae – just two years after the publication of his systematic revision of Stromateiformes. Curiously, Haedrich (1969) diagnosed *Amarsipus* from all other Stromateiformes by the absence of a pharyngeal sac, *i.e.* one of the two unique character used by himself to diagnose the order (Haedrich, 1967). To justify the placement of *Amarsipus* within

Stromateiformes, the author used a combination of characters shared by the new species and the other members of the order: a “perciform caudal skeleton”, an uniserial jaw teeth, an expanded lacrimal bone, an inflated and protruding top of the head, a bony bridge over the anterior vertical canal of the ear (*i.e.* pons moultoni *sensu* Haedrich, 1971), an overall similarity on external appearance, and the presence of a well-developed subdermal canal system on the head and body. As consequence, Haedrich (1969) implicitly provided a new definition for the order, which was no longer based on the presence of the pharyngeal sac and uniserial teeth, but rather on the combination of several characters.

Since its original description in the late 1920's, the genus *Propercarina* has been indecisively assigned to distinct percomorphacean taxa within Percomorphacea, with an initial suggestion of closer affinity with *Percarina* (Pauca, 1929, 1934), a percid genus from the Black Sea basin. However, subsequent studies rejected that proposition and demonstrated that *Propercarina* should be allocated in Stromateiformes (Bannikov, 1995; Prikryl, 2014). Yet, *Propercarina* species would not fit in any known stromateiform family, and a new family, Propercarinidae, was described to allocate this taxon within the order. As a diagnostic character of Propercarinidae, Bannikov (1995) listed the possession of widely separated dorsal fins and relatively large jaw teeth. Although the interrelationship of the family with the remaining Stromateiformes have not been explicitly tested, the author indicated shared similarities of Propercarinidae with Nomeidae and Amarsipidae in the postcranial skeleton, namely the increased number of vertebrae (about 35), the very slender vertebral spines, and the well-developed parapophyses on the posterior abdominal vertebrae. Moreover, *Propercarina* would share with *Amarsipus* a non-oligomerized caudal skeleton (hypurals free from each other), short-paired fins, most anal-fin rays below the posterior dorsal-fin, absence of pharyngeal sac, and presence of enlarged pharyngeal teeth. Bannikov (1995) listed the latter feature as a possible evidence that propecarinids and amarsipids would form a pre-centrolophid lineage. Propercarinidae was recently focus of a revisionary study, in which an additional species was described from the Oligocene of Romania (*Propercarina problematica*; Prikryl *et al.* 2004). Similar to Bannikov (1995), Prikryl *et al.* (2004) corroborated the affinities of Propercarinidae and Amarsipidae and reaffirmed their allocation within Stromateiformes.

In addition to the aforementioned new stromateiform families, the other two taxonomic novelties within Stromateiformes comprise erection of two new genera to allocate two previously known species of Centrolophidae. Haedrich (1967) considered *Tubbia* a junior synonym of *Schedophilus*. However, in Haedrich & Horn (1972), *T. tasmanica* appears in the key to the species of *Ichthyos*. This arrangement comes with a remark stating that it was provisional since *Tubbia*

*tasmanica* displayed characters intermediate between the genera *Schedophilus* and *Icichthys* and its position within Stromateiformes would represent an enigma. A few years later, Ahlstrom *et al.* (1976) drew attention to the high supraneural (= predorsal) count in *Icichthys* (up to 12 supraneurals) in contrast with that of *Tubbia* (three). The resurrection of *Tubbia*, however, was only formally made by McDowall (1979) based on a reanalysis of the type of *Tubbia tasmanica* and analysis of three additional specimens captured off the New Zealand coast. McDowall (1979) listed as main diagnostic character of *Tubbia* the distinct number of vertebrae, ranging from 43–44, which was substantially higher than that of *Schedophilus* (25–30), but still significantly lower than *Icichthys* (50–60). More recently, Last *et al.* (2013) described a second species of *Tubbia* and redefined the genus. According to the authors, *Tubbia* was characterized not only by the number of vertebrae, but also the number of fin rays, spines, and several details of the shape of the body, scales, and fins.

The second centrolophid genus described after Haedrich's (1967) study was *Pseudoicichthys*, erected by Parin & Permitin (1969) to allocate *Icichthys australis*. This species was originally described by Haedrich (1966) based on a 77.2 mm SL immature specimen that was placed in *Icichthys* due to its possession of high number of vertebrae (up to 51 bones) and three autogenous haemal spines, both uniquely shared by the other known species of *Icichthys* (*I. lockingtoni*). Other characteristics such as small pelvic fins, soft musculature, poorly calcified skeleton, and an insignificant ventral slit (or groove) were also used to allocate *I. australis* in *Icichthys* (Haedrich, 1966, 1967). However, shortly after its original description, Parin & Permitin (1969) redescribed by and reallocated *Icichthys australis* into a new genus. Based on the analysis of five additional individuals of that species, including adults, Parin & Permitin (1969) concluded that the "differences... are quite sufficient for separate distinction at the generic level" and erected the genus *Pseudoicichthys* to allocate *I. australis*. The authors distinguished the two genera based on the number of epurals (two in *Icichthys* and three in *Pseudoicichthys*), number and shape of pyloric caeca ("few" in *Icichthys*, "numerous" in *Pseudoicichthys*), details on the laterosensory ("seismosensory") canals of the head, squamation, number of pectoral-fin rays, and body depth. The authors, however, recognized the blatant similarities between *Icichthys* and *Pseudoicichthys* and stated that "the genus *Pseudoicichthys* established by us is undoubtedly extremely close to *Icichthys*".

The validity of *Pseudoicichthys* has been questioned since its original description. In the same year of the description of the genus, Krefft (1969) pointed out that the diagnostic features of *Pseudoicichthys* also occurred in other closely related genera. He further advocated in favor of a reduction in the number of genera in Centrolophidae and highlighted that most features used to diagnose these taxa were found in varying combinations across the family. Haedrich & Horn (1972)

also rejected the validity of *Pseudoicichthys* as both the taxonomic account of the Centrolophidae (Haedrich & Horn, 1972: p. 2) and the key to the species in *Icichthys* (Haedrich & Horn, 1972: p. 28) considered *I. australis* as belonging to *Icichthys*. McDowall (1982) made the same decision and commented that “*the broad relationships of these strange centrolophid fishes are poorly understood and that the situation is not helped by the proliferation of monotypic genera*”. The genus was also ignored in the phylogenetic studies of Horn (1984), Doiuchi *et al.* (2004), and Doiuchi & Nakabo (2006). Currently the validity of the genus is controversial. Most fish catalogues list it as a junior synonym of *Icichthys*: OBIS (Ocean Biogeographic Information System), WoRMS (World Register of Marine Species; Horton *et al.*, 2019), FishBase (Froese & Pauly, 2019), and FAO Fisheries and Aquaculture Department (Food and Agriculture Organization of the United Nations; Fisher & Bianchi, 1984). Yet, *Pseudoicichthys* is considered a valid genus in the Eschmeyer’s Catalog of Fishes (Fricke *et al.*, 2018), probably because it has never been explicitly synonymized. Taxonomic studies of Stromateiformes point to a split decision favoring its non-validity, with some studies accepting the genus (Rembiszewski, 1981; Haedrich, 1986; Parin & Piotrovstky, 2004; Stewart *et al.*, 2015), and several rejecting or simply ignoring its existence (Krefft, 1969; Haedrich & Horn, 1972; McDowall, 1982; Horn, 1984; Doiuchi *et al.*, 2004; Doiuchi & Nakabo, 2006; Nelson, 2006, 2016).

## **Phylogeny of Stromateiformes: morphological approaches**

The first phylogenetic analysis of Stromateiformes was published by Horn (1984), in a study aiming the ontogeny and phylogeny of the members of the order. The author used 27 characters, examined all 16 stromateiform genera, and corroborated the monophyly of the order including *Amarsipus* as a stromateiform member (Fig. 2A). The monophyly, however, was sustained by characteristics of the head and body squamation (presence and shape of scales on the preopercle and body) and by details of the caudal skeleton (number of hypurals). In the tree obtained by Horn (1984), *Amarsipus* was recovered as the sister-group of all remaining Stromateiformes; Centrolophidae was not monophyletic; and Nomeidae, along with Tetragonuridae, Ariommatidae, and Stromateidae, formed an apical clade. According to this topology, the pharyngeal sac was optimized as a synapomorphy for the non-Amarsipidae Stromateiformes, and no longer considered a synapomorphy for the order as traditionally treated by previous studies (*e.g.* Regan, 1902; Haedrich, 1967). Horn (1984) followed former predictions that Stromateiformes could be related to the Girellidae, Scorpididae, and Kyphosidae, and sampled these taxa as outgroups to his phylogenetic analysis. Kyphosidae was resolved as sister-group to the Stromateiformes, a relationship sustained by aspects of the dentition and color pattern of juveniles.

More recently, a second phylogenetic analysis based on morphological data sampling all stromateiform genera was published by Doiuchi *et al.* (2004). This study investigated 43 characters related to skeleton, muscle, and scales, taken from 17 representatives of the order (all 16 genera, plus a second species of *Psenes*) and two outgroups (Arripidae and Kyphosidae). Similar to Horn (1984), Doiuchi *et al.* (2004) recovered the monophyly of Stromateiformes (Fig. 2B), an arrangement supported by eight synapomorphies (Doiuchi *et al.*, 2004: Char. #7, 11, 20, 21, 22, 31, 40, and 43). Another convergence between these studies was the non-monophyly of Centrolophidae: representatives of this family appeared at a basal polytomy, separated from the other families that were grouped into an apical clade. However, a fundamental difference between the results of Doiuchi *et al.* (2004) and Horn (1984) was the placement of *Amarsipus*. While in Horn (1984) *Amarsipus* was allocated basally in Stromateiformes, figuring as the sister group of all other stromateiforms (Fig. 2A), in Doiuchi *et al.* (2004) the taxon appeared more apically within the order, as the sister-group of a lineage composed by Ariommatidae, Nomeidae, Tetragonuridae, and Stromateidae (Fig. 2B). Such differences implied directly on the interpretation of the pharyngeal-sac evolution in the order. In Horn (1984), the pharyngeal sac was not recovered as a synapomorphy for stromateiforms, but rather as a characteristic acquired after the divergence of *Amarsipus* from the remaining of the lineage. On the other hand, in Doiuchi *et al.* (2004), the pharyngeal sac constituted a synapomorphy for the order, with a secondary loss in *Amarsipus*.

Mentions about the affinity of Stromateiformes to other Percomorphacea are scarce in the anatomical literature. A possible relationship of Stromateiformes with the pelagic *Icosteus aenigmaticus* has been informally suggested by early studies (Jordan & Gilber, 1880; Steindachner, 1881), but basically due to a general external similarity between *Icosteus* and some Centrolophidae, particularly during larval and juvenile stages (Matarese *et al.*, 1984: fig. 306; Horn, 1984: fig. 333). In fact, young *Icosteus* and centrolophids are so similar that a juvenile specimen of *Icosteus* has once been described under the name *Schedophilopsis spinosus* (Steindachner, 1881), and thought to be related to the centrolophid genus *Schedophilus*. Similarly, the original description of *Icichthys lockingtoni* (Jordan & Gilbert, 1880) reveal that the authors believed in a relationship of this taxon with *Icosteus*, and the entire description is dedicated to list similarities and differences between them. However, all subsequent studies failed on finding “special similarities” (= synapomorphies) between Icosteiformes and Stromateiformes, and currently these orders are no longer believed to be closely related (Springer & Johnson, 2004). The alignment of Stromateiformes with pelagic taxa due an overall similarity is not restricted to *Icosteus*. Some other oceanic fishes that were once considered related to Stromateiformes are *Luvarus imperialis* (Luvaridae), *Coryphaena* spp. (Coryphaenidae), and *Gasterochisma melampus* (Scombridae). This grouping was proposed by Le Danois and Le Danois

(1963) as part of their classification of “Scombres”, which was based solely on the presence of two characteristics: hypurostergy (= fusion of hypurals) and erisme (= a bony crest on the skull). However, this hypothesis has received little attention by subsequent studies, possibly due to the common belief that these characteristics are likely convergences associated to the pelagic habit, rather than evidences of a natural assemblage. A more elaborated critic to this hypothesis, and a detailed comparison of *Luvarus* with the Stromateiformes, is provided by Tyler *et al.* (1989).

The latest morphological studies favor a hypothesis of closer relationship of Stromateiformes with the Kyphosidae and Girellidae (Freihofer, 1963; Haedrich, 1967; Johnson & Fritzsche, 1989). Freihofer (1963) offered one of the first mentions of a possible relationship among these taxa in a study dealing about the ramification pattern of a subdivision of the facial nerve, namely the *ramus lateralis accessorius* (RLA), in Teleostei. In a study encompassing 310 species of 130 families and 21 orders, Freihofer identified and described 17 different nerve-branching patterns and suggested several groupings in Teleostei based on the distribution of these patterns. One of those – the RLA pattern 10 – was shared by the Kyphosidae *lato sensu* (*i.e.* Kyphosidae plus Scorpididae, Girellidae, and Microcanthidae), Kuhliidae, Arripidae, Terapontidae, Pomatomidae, Nematistiidae, and all Stromateiformes. Based upon the restrict distribution of this pattern among Teleostei, Freihofer (1963) suggested that some (if not all) these taxa possibly constituted a natural assemblage. The distribution of RLA 10 branching pattern was later reassessed by Johnson & Fritzsche (1989), which tested Freihofer’s (1963) hypothesis on a broader taxon sampling within percomorphaceans. The authors also found an RLA-10 pattern in Oplegnathidae, but disagreed on the presence of this branching pattern in Pomatomidae and Nematistiidae. According to Johnson & Fritzsche (1989), pomatomids and nematistiids would be closely related to Scombriformes (following Johnson, 1986) and Carangiformes (according to Rosenblatt & Bell, 1976), respectively. Apart from these two taxa, Johnson & Fritzsche (1989) agreed with Freihofer (1963) and proposed that the remaining percomorphs with an RLA 10 pattern would form a monophyletic group. The RLA-10 group was later expanded to allocate the family Dichistiidae (Leis & Lingen, 1997), a percomorphacean family endemic to southern African oceans, which was historically related to microcanthids, scorpidids, girellids and kyphosids.

The last study to discuss the Stromateiformes interrelationship was Springer & Johnson (2004). In this study the authors mostly agreed with the monophyletic status of the RLA 10-group. However, the authors revealed that the stromateiform *Amarsipus* – which was not examined in Freihofer (1963) or Johnson & Fritzsche (1989) – lacks an RLA 10 pattern. They described the RLA opercular branch of this taxon as passing parallel to the pterotic and medial to the opercular

musculature, in a fashion that certainly diverges from Freihofer's RLA pattern 10. Based on that evidence, and a reevaluation of several other characters, Springer & Johnson (2004) questioned the inclusion of *Amarsipus* in Stromateiformes, stating that more studies would be needed to determine the allocation of *Amarsipus* within Percomorphacea. In fact, the allocation of *Amarsipus* within Stromateiformes has never been properly tested in a cladistic analysis using morphological data. Both phylogenies involving the Stromateiformes (*i. e.* Horn, 1984, and Doiuchi *et al.* 2004) had as primary objective the study of the intrarelationships among the stromateiform families, and not the monophyly of the order. In such analyses, the inclusion of *Amarsipus* to Stromateiformes could have been a spurious result due to the small outgroup sampling (3 taxa in Horn, 1984; 2 in Doiuchi *et al.* 2004). Until now, only the subdermal canal system can be listed as a strong evidence uniting Amarsipidae to Stromateiformes, even though this characteristic independently appears in unrelated taxa such as the lampridiform Trachipteridae (Walters, 1963) and the gempylid *Ruvettus prestiosus* (Bone, 1972). The other characteristics used to place *Amarsipus* within Stromateiformes (*i.e.* a perciform caudal skeleton, uniserial jaw teeth, expanded lacrimal bone, inflated and protruding top of the head, bony bridge over the anterior vertical canal of the ear) have been demonstrated to be present in a series of percomorphacean families including the Kyphosidae *lato sensu* (Springer & Johnson, 2004), and still await a formal analysis to test their synapomorphic status.

## Phylogeny of Stromateiformes: molecular approaches

The first phylogeny of Stromateiformes based on molecular data was conducted by Doiuchi & Nakabo (2006). This analysis did not include *Amarsipus* or tested the monophyly of the order since it used only a single outgroup (*i.e.* the RLA-10 family Arripidae). Nevertheless, the topology obtained by the authors was already strikingly conflicting with the trees resultant from anatomical studies (Fig. 3). For example, their hypothesis presented *Tetragonurus* as the sister group of the remaining Stromateiformes in a parsimony analysis (*vs.* *Amarsipus* in Horn, 1984; Centrolophidae in Doiuchi *et al.* 2004). Moreover, a monophyletic Centrolophidae was obtained by both the parsimony and the maximum likelihood analyses (*vs.* paraphyletic in Horn, 1984 and Doiuchi *et al.*, 2004). Subsequent molecular analyses sampling broader outgroups returned arrangements even more incongruent with preceding morphological hypotheses (Li *et al.*, 2007; Yagishita *et al.*, 2009; Near, 2013; Betancur-R *et al.*, 2013; Miya *et al.*, 2013; Betancur-R *et al.* 2017). Among these, that of Betancur-R *et al.* (2013) deserves special attention. Based on 21 sequences taken from 1410 taxa, which encompasses all orders traditionally recognized in Teleostei, Betancur-R *et al.* (2013) provided an unprecedented phylogenetic classification for bony fishes, redefining many taxa and naming several new others. As a

result, Scombriformes was modified to encompass not only some of the families traditionally assigned to the order (Johnson, 1986; Wiley & Johnson, 2010), but also representatives of Chiasmodontidae, Pomatomidae, Scombrilabracidae, Icosteidae, Caristiidae, Bramidae, and all families composing the Stromateiformes (Betancur-R *et al.*, 2013: fig. 5). The final topology, however, did not recover the monophyly of Stromateiformes, which were divided in three distinct lineages: Centrolophidae, as the sister group of part of the Scombridae; Stromateidae, as the sister group of an assemblage including bramids, caristiids, icosteids and scombrilabracids; and Nomeidae + Ariommatidae as the sister group of a subset of Scombridae. Amarsipidae and Tetragonuridae were not sampled in that study. Although exhibiting strong support for the Scombriformes clade, the authors recognized that the intrarelationships among the taxa composing the clade exhibit low support, and the monophyly of traditional taxa such as the Scombriformes *stricto sensu* would still require further studies (Betancur-R *et al.*, 2013: appendix 2).

Not long after the publication of Betancur-R's *et al.* (2013) phylogenetic classification of bony fishes, Miya *et al.* (2013) published a study on the evolutionary origin of Scombridae (tunas and mackerels). Based on analyses taken from an extensive database (*i.e.* DNA sequence of mitochondrial and nuclear genes of 5367 species allocated in 1558 genera and 215 families of Percomorphacea), the authors supported the existence of a larger clade corresponding to the Scombriformes *sensu* Betancur-R *et al.* (2013). Both the separated analyses for each of the six mitochondrial or three nuclear gene sequences and the combined-data analysis supported the existence of the Scombriformes *lato sensu*. That clade was therein renamed to Pelagia (= Pelagiaria *sensu* Betancur-R *et al.*, 2013). Again, the Stromateiformes (with all families sampled but Amarsipidae) did not result as a monophyletic entity and the members of the order were spread in three different assemblages (Fig. 4). Again, nodes within the Pelagia presented low support.

The first combined analyses of morphological and molecular data sampling Stromateiformes were that of Mirande (2017). The dataset used by the author contained 44 nuclear and mitochondrial markers and 274 morphological characters encompassing representatives of all orders of Actinopterygii. Once again, Stromateiformes was resolved as paraphyletic, with *Tetragonurus* appearing far removed from the remaining stromateiform families and forming a clade with Chiasmodontidae. The remaining stromateiforms formed a clade with Ariommatidae plus Nomeidae, and Centrolophidae plus Stromateidae. The taxon *Amarsipus* was not sampled by Mirande (2017). In fact, the relationships of the genus *Amarsipus* was only recently studied under a phylogenetic perspective using molecular data. That was possible after the discovery of a single fresh specimen at the Nagasaki Fish Market (Japan). According to the analysis of Campbell *et al.* (2018), which used the

datasets of Betancur *et al.* (2013), *Amarsipus* falls deeply nested within the Pelagiaria as the sister group of *Tetragonurus*. Similar to previous studies, the monophyly of Stromateiformes was not recovered and the nodal supports for the subgroups of Pelagiaria were low.

An important outcome from the analyses of Betancur-R *et al.* (2013), Miya *et al.* (2013), Mirande (2017), and Campbell *et al.* (2018), both of which recovering a polyphyletic Stromateiformes, is that complex morphological characters such as the pharyngeal sac or the subdermal canal system, necessarily had to evolve at least two (in Mirande, 2017) or three independent times (in the remaining studies) during the Pelagiaria radiation. In addition, these analyses place Stromateiformes distant from most RLA 10 taxa (*i.e.* Kyphosidae, Scorpididae, Microcanthidae, and Oplegnathidae, among others), which would be the stromateiform sister-group candidate according to some morphological studies (*e.g.* Freihofner, 1963; Johnson & Fritzsche, 1978). Until now, important systematics questions of Stromateiformes, such as its phyletic status, intrarelationships, affinities with enigmatic taxa such as *Amarsipus*, or its relationship with other Percomorphacea remain unsatisfactorily answered. Similarly, the evolution of complex anatomical structures, such as the pharyngeal sac, the subdermal canal system, and the RLA 10 innervation pattern are still unsolved.

## MATERIALS AND METHODS

### Anatomical terminology and specimen preparation

Osteological nomenclature follows Weitzman (1962), Rosenblatt & Bell (1986), Johnson (1986), and Johnson & Patterson (1993). The following modifications are made in order to match the terminology most commonly employed in other teleostean groups: mesethmoid instead of ethmoid, vomer instead of prevomer, epioccipital instead of epiotic, endopterygoid instead of mesopterygoid, intercalar instead of opisthotic, anterior ceratohyal instead of ceratohyal, posterior ceratohyal instead of epihyal, supraneural instead of predorsal or interneural, and basipterygium instead of pelvic bone. Counts of rays, spines, pterygiophores, vertebrae, supraneurals, hypurals, epurals, branchiostegals are given in Arabic numbers. On counts, fin spines are considered serially homologous to fin rays, but exhibiting azygous, unsegmented, and bilaterally fused hemitrichia. In some cases, the distinction between spines and rays are not possible and counts include the number of spines + rays. These are referred to as *total fin elements*. Finlets are considered serially homologous to soft fin rays and thus included in the counts of dorsal- and anal-fin rays. Myological terminology primarily follows Winterbottom (1974), except for the recent changes proposed by Springer & Johnson (2004) for dorsal branchial musculature, Datovo & Vari (2013) for the *adductor mandibulae* complex, and Datovo & Rizzato (2018) for the hyopalatal muscles. Muscle names mentioned throughout the text, when graphed in Latin, are italicized. Muscles or muscle sections not considered or not described on the abovementioned studies are named and described along the text. Laterosensory system terminology primary follows Webb (1989).

Taxa used to build the phylogenetic matrix were double stained for cartilage and bones following the protocol of Datovo & Bockmann (2010) and dissected to expose the skeleton and muscles. Besides the skeleton-stained specimens, additional cleared and double stained specimens were examined according to the necessity and availability. Those were prepared following the protocol of Taylor & van Dyke (1985). Specimens and dissected anatomical pieces were photographed using a digital camera Leica DFC420 attached to a Leica MZ16 stereomicroscope (for small-sized structures) or a Nikon D7000 with a 105 mm Micro-Nikkor lens (for larger specimens or structures). Images were edited in Adobe Photoshop CS6 and plates were built in Adobe Illustrator CS6.

## Taxonomic classification and taxon sampling

Taxonomic classification for higher ranks of Teleostei follows Wiley & Johnson (2010). Families not considered in that study follow Van der Laan & Fricke (2019). Stromateiformes classification follows Haedrich & Horn (1972), with some modifications: *Tubbia* is considered as a valid centrolophid genus (*sensu* McDowall, 1979) and *Pseudoicichthys* is considered synonym of *Icichthys* (*sensu* McDowall, 1982).

Taxon sampling includes only extant species. The analysis includes 66 terminals: 22 Stromateiformes and 44 outgroups. At least one representative of the 15 genera currently assigned to the Stromateiformes was sampled. Larger taxon sampling within Stromateiformes was carried on based on material availability, and prioritizing speciose genera or lineages known to exhibit greater morphological variability. Two species of the genera *Psenopsis*, *Psenes*, *Cubiceps*, and *Peprilus* and three of the genus *Ariomma* were sampled. Outgroup taxa includes two teleostean divisions, Beryceae (two terminal taxa), and Percomorphacea (42 terminal taxa). Within Beryceae, taxon sampling encompasses two Beryciformes (*Beryx splendens* and *Holocentrus adscencionis*) and, among Percomorphacea, 11 orders and 38 families. In order to test the morphological hypotheses of interrelationship of Stromateiformes, taxon sampling includes all percomorphacean families once aligned to stromateiforms according to the studies of Freihofer (1963), Johnson & Fritzsche (1989), and Springer & Johnson (2004). These encompass the RLA-10 families Pomatomidae, Arripidae, Kuhliidae, Oplegnathidae, Nematistiidae, Terapontidae, and the Kyphosidae *lato sensu* (girellins, microcanthins, scorpidins, and kyphosins). Additionally, in order to test the recent classifications of Stromateiformes based on molecular data, taxon sampling included all families of the Pelagiaria clade *sensu* Betancur-R *et al.* (2017) (*i.e.* Scombriformes *sensu* Betancur-R *et al.*, 2013; Pelagia *sensu* Miya *et al.*, 2013). These encompass the percomorphacean families Pomatomidae, Bramidae, Caristiidae, Arripidae, Chiasmodontidae, Icosteidae, Scombrilabracidae, Scombridae, Trichiuridae, and Gempylidae. Moreover, in order to provide outgroups for both hypotheses, 23 additional percomorphacean and two beryceean families are included in the analysis.

The specimens used on the present study comes from the following institutions: Museu de Zoologia da Universidade de São Paulo, Brazil (MZUSP); Museu Nacional da Universidade Federal do Rio de Janeiro, Brazil (MNRJ); National Museum of Natural History, Smithsonian Institution, USA (USNM); University of Washington Fish Collection, USA (UWFC); Scripps Institution of Oceanography, USA (SIO); Oregon State University Ichthyology Collection, USA (OS); and Australian National Fish Collection, Australia (CSIRO).

## LIST OF TAXA USED ON THE CLADISTIC ANALYSIS

**Beryciformes:** Berycidae: *Beryx splendens* (MZUSP 121649; 100.9 mm SL). Holocentridae: *Holocentrus ascensionis* (MZUSP 69190; 88.6 mm SL). **Ophidiiformes:** *Dinematichthys ilucoeteoides* (MZUSP 123258; 88.2 mm SL); *Raneya brasiliensis* (MZUSP 61358; 165.5 mm SL). **Gasterosteiformes:** Aulostomidae: *Aulostomus maculatus* (MZUSP 119736; 292.5 mm SL). **lcosteiformes:** *Icosteus aenigmaticus* (OS 6086; 220.8 mm SL). **Perciformes:** Apogonidae: *Apogon maculatus* (MZUSP 43155; 67.3 mm SL). Bramidae: *Brama caribbea* (MZUSP 78258; 98.1 mm SL). Caristiidae: *Caristius macropus* (UW 25832; 179.4 mm SL). Chiasmodontidae: *Pseudoscopelus altipinnis* (MZUSP 123250; 66.1 mm SL). Pomatomidae: *Pomatomus saltatrix* (MZUSP 69784; 114.6 mm SL). Arripidae: *Arripis georgianus* (MZUSP 119735; 172.78 mm SL). Scombrolabracidae: *Scombrolabrax heterolepis* (USNM 187565; 135.1 mm SL). Haemulidae: *Orthopristis ruber* (MZUSP 68061; 104.33 mm SL). Kuhliidae: *Kuhlia marginata* (USNM 342058; 105.23 mm SL). Girellidae: *Girella simplicidens* (USNM 321278; 88.1 mm SL). Kyphosidae: *Kyphosus sectatrix* (MZUSP 69433; 75.1 mm SL). Microcanthidae: *Microcanthus strigatus* (USNM 267047; 86.2 mm SL). Scorpionidae: *Scorpius chilensis* (USNM 218922; 114.2 mm SL). Lutjanidae: *Lutjanus analis* (MZUSP 65928; 102.9 mm SL). Sciaenidae: *Cynoscion striatus* (MZUSP 68913; 123.1 mm SL). Terapontidae: *Amniataba caudavittata* (USNM 173673; 80.4 mm SL). Serranidae: *Diplectrum radiale* (MZUSP 70776; 120.1 mm SL). Polycentridae: *Monocirrhus polyacanthus* (MZUSP 55122; 54.6 mm SL). Moronidae: *Morone mississippiensis* (MZUSP 123242; 121.9 mm SL). Lateolabracidae: *Lateolabrax japonicus* (MZUSP 123245; 149.5 mm SL). Latidae: *Lates niloticus* (MZUSP 123243; 146.4 mm SL). Centropomidae: *Centropomus parallelus* (MZUSP 108244; 166.5 mm SL). Oplegnathidae: *Oplegnathus fasciatus* (MZUSP 28867; 58.2 mm SL). Polynemidae: *Polydactylus virginicus* (MZUSP 67549; 114.5 mm SL). **Scombriformes:** Sphyraenidae: *Sphyraena tome* (MZUSP 47562; 235 mm SL). Gempylidae: *Thyrsopterus lepidopoides* (MZUSP 68416; 154.78 mm SL). Scombridae: *Auxis thazard* (MZUSP 51282; 210 mm SL); *Scomber* sp. (MZUSP 108155; 100.6 mm SL). Trichiuridae: *Trichiurus lepturus* (MZUSP 8855; 405 mm SL). **Stromateiformes:** Amarsipidae: *Amarsipus carlsbergi* (SIO 75-122; 50.4 mm SL). Ariommatidae: *Ariomma indicum* (MZUSP 123249; 129.9 mm SL); *Ariomma bondi* (MZUSP 86717; 125.3 mm SL). Centrolophidae: *Psenopsis anomala* (MZUSP 119730; 74.2 mm SL); *Psenopsis cyanea* (MZUSP 123244; 138.6 mm SL); *Centrolophus niger* (CSIRO H 2421-01; 245.1 mm SL); *Schedophilus medusophagus* (MCZ 161887; 89.2 mm SL); *Seriolaella porosa* (USNM 176593; 198.8 mm SL); *Tubbia tasmanica* (CSIRO H 6979-03; 325.2 mm SL); *Icichthys lockingtoni* (OS 16732; 102.3 mm SL); *Hyperoglyphe perciformis* (MZUSP 119733; 150.4 mm SL). Nomeidae: *Psenes cyanophrys* (MZUSP 106392; 152.6 mm SL); *Psenes sio* (MZUSP 123248; 184.3 mm SL).

SL); *Cubiceps baxteri* (= *Ariomma melanum*; MZUSP 123246; 134.9 mm SL); *Cubiceps whiteleggii* (MZUSP 123247; 107.5 mm SL); *Cubiceps pauciradiatus* (MZUSP 80701; 88.6 mm SL); *Nomeus gronovii* (MZUSP 67590; 81.3 mm SL). Stromateidae: *Peprilus triacanthus* (MZUSP 123240; 128.9 mm SL); *Peprilus paru* (MZUSP 67608; 80.9 mm SL); *Pampus cinereus* (MZUSP 119734; 72.4 mm SL); *Stromateus brasiliensis* (MZUSP 51279; 136.1 mm SL). Tetragonuridae: *Tetragonurus cuvieri* (MZUSP 123241; 94.7 mm SL). **Atheriniformes:** Atherinopsidae: *Atherinella brasiliensis* (MZUSP 67186; 105.2 mm SL). **Mugiliformes:** *Mugil curema* (MZUSP 67314; 87.1 mm SL). **Carangiformes:** Carangidae: *Trachinotus carolinus* (MZUSP 8798; 89.7 mm SL). Coryphaenidae: *Coryphaena hyppurus* (MNRJ 40643; 358.2 mm SL). Rachycentridae: *Rachycentron canadum* (MZUSP 69740; 149.6 mm SL). Nematistiidae: *Nematistius pectoralis* (MZUSP 119731; 46.3 mm SL). **Pleuronectiformes:** Paralichthyidae: *Paralichthys isosceles* (MZUSP 72323; 142.7 mm SL). Psettodidae: *Psettodes erumei* (MZUSP 63360; 130.9 mm SL). **Anabantiformes:** Channidae: *Parachanna obscura* (MZUSP 84470; 113.8 mm SL).

## COMPARATIVE MATERIAL

**Stephanoberyciformes:** Melamphaidae: *Poromitra crassiceps* (UNSM 296984; 111.4 mm SL). **Stromateiformes:** Amarsipidae: *Amarsipus carlsbergi* (SIO 75-221; 2C&S; 27.7-43.0 mm SL). Centrolophidae: *Psenopsis* sp.: (1 C&S; USNM 304398; 83.7 mm SL). *Icichthys lockingtoni* (OS 7703; 88.3 mm SL). Nomeidae: *Cubiceps pauciradiatus* (1 C&S; MZUSP 80702; 76.1 mm SL). Ariommatidae: *Ariomma bondi* (1 C&S; MZUSP 80659; 77.8 mm SL). Stromateidae: *Stromateus fiatola*: (USNM UNCAT; 68.7 mm SL). *Peprilus triacanthus* (1 C&S; USNM 302441; 80.3 mm SL). *Peprilus burti* (1 C&S; USNM 156148; 72.7 mm SL). *Pampus argenteus*: (1 C&S; USNM 85863; 77.8 mm SL). **Carangiformes:** Nematistiidae: *Nematistius pectoralis*: (1 musc; USNM 82203; 140 mm SL).

## Data analysis

A morphological character matrix was assembled using Microsoft Excel 2016. Discrete and continuous (measurements and counts) characters were coded in separated sheets and later concatenated into a combined matrix with a text editor (Notepad++). Quantitative characters were treated as continuous, and employed 6 measurements (Fig. 5) and 16 counts. These data were normalized to fit in a distribution ranging from 0 (lowest) to 1 (highest measurement or count), and then transferred to the TNT data matrix. Tables 1 and 2 provide raw and normalized numbers for Characters #0-15, and Characters #16-21, respectively. The remaining 196 discrete (= qualitative)

characters coded mostly variations on the osteology, myology, and external morphology. Discrete multistate characters were treated as ordered (= additive or minimally connected states; Slowinski, 1993) only when ontogenetic or morphoclinical evidence could be inferred between the most extreme states of the transformational series (Nixon & Carpenter, 2011: p. 8). Character numbering follows TNT default and were herein numbered from zero to 217. Continuous characters are analyzed according to Goloboff *et al.* (2006). Multistate characters 53, 68, 104, 110, 114, 115, 116, 124, and 130 were coded as ordered. The phylogenetic interrelationships between the taxa included in the analysis were inferred through a maximum parsimony analysis (Farris, 1983) run on TNT (Goloboff *et al.*, 2008a). Searches for the most parsimonious trees (MPTs) employed the four main algorithms of the “new technology search” (Goloboff *et al.*, 2008a), with the following parameters: 10 Ratchet total iterations (Nixon, 1999), with perturbation phases adjusted to eight, Tree-drift cycles (Goloboff, 1999) adjusted to 20, and Tree-fusing rounds adjusted to 10 (Goloboff, 1999). These parameters were used in a driven search adjusted to reach 50 hits of the best score, and with the Random Seed set to zero. All remaining search parameters were kept on their defaults. Searches using character weighting against homoplasies were also performed (Implied Weighting: Goloboff, 1993, 1997; Goloboff *et al.*, 2008b). Congruency indexes between characters and trees, as well as optimization of the transformations on the final cladograms, were analyzed on Mesquite v. 3.01 (Maddison & Maddison, 2014). Support index searches employed Bremer support (Bremer, 1994), sampling suboptimal trees with 15 extra steps. Consistency (CI; Farris, 1969) and retention (RI; Farris, 1989) indexes were calculated using the script *statsall* (designed by Peterson L. Lopes) and calculated on the final cladograms. Indexes are provided for each character, following the description of the character. Clades were named in the reference tree only for Stromateiformes and its subgroups (letters A to W). Remaining clades and terminals, when mentioned throughout the text, refer to the native node numbering of TNT and referred to as “TNT Clade”. Rooting was set on a representative of the Beryciformes (*Beryx splendens*, MZUSP 121649), an order recurrently treated as possessing plesiomorphic characteristics in relation to the Percomorphacea (Johnson & Patterson, 1993; Springer & Johnson, 2004; Wiley & Johnson, 2010) and invariably resolved as basal to percomorphaceans in both molecular and morphology-based hypotheses (Johnson & Patterson, 1993; Betancur-R. *et al.* 2014).

For searches using Implied Weighting (IW), the ideal value of the constant  $k$  (Goloboff *et al.*, 2008b) was determined through a new method proposed herein based on clade stability, which had the basic objective of avoiding a random choice of the constant  $K$  values in IW searches. In IW searches, high values of the constant  $K$  usually produce similar resultant topologies, while low values of  $k$  affect the results more drastically (Mirande, 2009). This happens due to the concave shape of the curve of

the character *fit* (Fig. 6; Tab. 3; Goloboff *et al.* 2008b). As consequence, trees obtained in weak weighting schemes (for example,  $k=13, 14,$  and  $15$ ) are more similar to each other than trees obtained by stronger weighting schemes ( $K=1, 2$  or  $3$ ). Based on this fact, the strategy adopted herein was to generate trees using  $K$  values that representing a regular distribution of the *fit* curves, rather than simply adopting regular intervals of  $K$  (Fig. 7; Tab. 4). A similar procedure was carried out by Mirande (2009), which justified these actions stating that a regular distribution of *fit* values would mean a better sample of the possible  $K$  values (and as consequence of the universe of trees) for a given analysis. Moreover, these trees may also represent a better input for tree comparison methods since they avoid biased results toward higher values of  $K$ , which produce topologies that are more similar.

The first step of this method was to identify the range of  $K$  values affecting the final topology. For that purpose, an initial search using equal weights (EW; adopting the parameters described above) was performed to find the most parsimonious trees, which was then used to serve as basis for subsequent comparisons. Then, several analyses using IW were performed using increasing  $K$  values and searching a topology that would be identical (or the most similar topology) to that resultant from analyses performed under EW. As an example, the first  $K$  value from an IW analysis to result in a topology equal from that obtained by searches employing Equal Weights was herein defined as the weakest  $K$  value ( $K_w$ ), and interpreted as the threshold at which weighting against homoplasies no longer affect the final topology. Thus, the universe of possible topologies was comprised between the strongest ( $K_s$ ; herein defined as  $K=1$ , which weight the character inversely proportional to its number of homoplasies) and weakest ( $K_w$ ) values of  $K$ . Once established the  $K_s - K_w$  range, the second step was to decide which values of  $K$  should be sampled in a way that they that would result in a regular distribution of *fit*. For that purpose, we used the number of homoplasies present on our *average* homoplastic character. This was obtained by calculating the characters with the lowest and highest number of homoplasies in the EW analysis and setting a midpoint between those values as the *average* homoplastic character. Once the *average* homoplasia number was discovered, this value was used to find  $K$  values with equidistant *fit* distribution between the  $K_s$  and  $K_w$ . The  $K$  values were obtained by using the *fit* formula for the IW searches:  $F = K / (S + K)$ ; where  $F$  is the *fit* value,  $S$  is the number of homoplastic steps, and  $K$  is the value of  $K$ . After establishing the number of homoplasies to be used, and the highest and lowest  $K$  values ( $K_s - K_w$  range), it was possible to define the lowest and highest *fit* values of our distribution. Taking this analysis as example, the average homoplastic character contain 12 homoplasies. In this example  $K_s$  ( $K=1$ ) would result in a *fit* of 0.0769, and  $K_w$  ( $K=22$ ) in a *fit* of 0.6471 (Tab. 4). If we decide to sample 10 intersects between  $K_s$  and  $K_w$ , the *fit* intervals would be of 0.0570. On total, 11 trees would be sampled, and the  $K$  values would be 1, 1.855,

2.849, 3.957, 5.267, 6.808, 8.654, 10.902, 13.702, 17.273, and 22 (Fig. 7). These values would then be used to perform searches for trees on TNT.

The trees generated on each search on TNT were imported to ViPhy (Bremm *et al.* 2011) and the topologies were compared under the *Element-Based* similarity score. This method differs from the regular leaf-based approaches (usually based on Robinson-Foulds distance) by considering not only congruence among the taxa included in each clade but also the nodes within each clade. Consequently, the element-based score has a higher discriminative power than other indices of topological comparison. As an outcome, ViPhy can sort the trees according to their global congruence relative to the universe of sampled trees. We adopted the ViPhy most congruent tree as the reference tree to our taxonomic and phylogenetic classifications. Trees generated by other values of K are offered as supplementary files (Appendix).

## RESULTS

### Quantitative characters:

#### COUNTS

##### **Char. #0 (RY01). Dorsal fin; total number of rays: 12 – 134**

*Description:* The percomorphacean dorsal fin is usually supported by spines (unsegmented and bilaterally fused fin rays) on its anterior portion and soft rays on its posterior region (Figs. 8, 9). The number of dorsal-fin rays varies considerably among percomorphaceans, ranging from a dozen (12 in *Atherinella brasiliensis*, Atherinidae; 13 in *Mugil curema*, Mugilidae) to more than 100 elements (134 in *Trichiurus lepturus*, Trichiuridae). This character refers to the total number of rays present in the dorsal fin, including spines, soft rays, and finlets.

*Remarks:* Finlets are short and widely spaced rays supported by pterygiophores with elongate, autogenous middle radials. These elements are present at the posterior portion of the dorsal and anal fin of most Scombridae and some Carangidae. Finlets are considered serially homologous to soft fin-rays and are thus included in the counts of total rays of the dorsal fin when applicable.

*Indexes:* CI = 0.250; RI = 0.478

##### **Char. #1 (RY02). Dorsal fin; number of spines: 1 – 19**

*Description:* Fin spines are azygous, unsegmented, and bilaterally fused rays present at the anterior portions of the dorsal and anal fins of most acanthomorphs. Within the Percomorphacea, fin spines are present either as a stiff and pungent element (Figs. 8, 9) or as a more delicate structure, commonly described in the literature as a smooth spine. The number of dorsal-fin spines greatly varies among the Percomorphacea, from one (*Caristius macropus*, Caristiidae) or three (*Trichiurus lepturus*, Trichiuridae) up to 19 elements (*Tetragonurus cuvieri*, Tetragonuridae).

*Inapplicability:* Taxa lacking dorsal-fin spines (Char. #65).

*Indexes:* CI = 0.126; RI = 0.367

##### **Char. #2 (RY03). Dorsal fin; number of soft rays: 7 – 131**

*Description:* Soft rays are simple, unfused, and segmented rays that typically follow posteriorly the dorsal-fin spines of acanthomorphs (Fig. 9). The number of soft rays in the percomorphacean dorsal fin is highly variable, ranging from less than ten (seven in *Atherinella brasiliensis*: Atherinopsidae) to more than a hundred (131 in *Trichiurus lepturus*: Trichiuridae).

*Remarks:* The posteriormost double ray, which is usually associated with a single dorsal-fin pterygiophore, is herein counted as a single element. Counts taken on the Scombridae include the series of seven to ten dorsal finlets located along the caudal peduncle, posterior to the main body of the dorsal fin. Occurrence of finlets, in turn, is coded as an independent character (Char. #86).

*Indexes:* CI = 0.248; RI = 0.521

**Char. #3 (RY04). Pectoral fin; total number of rays: 10 – 26**

*Description:* The pectoral fin of percomorphaceans is usually supported by one or a few unbranched soft rays (usually one or two), which are disposed on the dorsal border of the fin, and followed by a series of 10 to 20 branched soft rays (Figs. 10-12).

*Indexes:* CI = 0.147; RI = 0.383

**Char. #4 (RY05). Pectoral fin; number of unbranched rays: 1 – 3**

*Description:* Unbranched pectoral-fin rays are the dorsalmost rays of pectoral fin and vary in number from one to three among the analyzed percomorphaceans (Fig. 10-12).

*Inapplicability:* This character is inapplicable to taxa exhibiting all pectoral fin-rays unbranched (Fig. 9), which hampers the establishment the correct homology between the first to third anteriormost unbranched pectoral-fin rays. Taxa exhibiting unbranched pectoral-fin rays are: *Trichiurus lepturus* (Trichiuridae), *Polydactilus virginicus* (Polydactilidae), *Monocirrhus polyacanthus* (Polycentridae), and *Aulostomus maculatus* (Aulostomidae).

*Indexes:* CI = 0.222; RI = 0.300

**Char. #5 (RY06). Pectoral fin; number of branched rays: 8 – 24**

*Description:* Unbranched pectoral-fin rays are followed by a variable number of branched ones (Figs. 10-12). In the analyzed taxa, the number of branched pectoral-fin rays ranged from eight (*e.g.* *Paralichthys isosceles*: Paralichthyidae) to 24 (*Pampus cinereus*: Stromateidae). This count encompasses all rays following the unbranched pectoral-fin rays, including the last (*i.e.* ventralmost) pectoral-fin ray. Although this last ray may inter- or intraspecifically vary from a branched to an unbranched condition, it was indistinguishably added to this count.

*Inapplicability:* Taxa exhibiting all pectoral fin-rays in an unbranched condition, namely *Polydactylus virginicus* (Polydactilidae), *Monocirrhus polyacanthus* (Polycentridae), and *Aulostomus maculatus* (Aulostomidae), were coded as inapplicable for this character. The precise homology between the unbranched rays of these taxa and branched rays of remaining percomorphaceans could not be determined.

*Indexes:* CI = 0.137; RI = 0.394

**Char. #6 (RY07). Pelvic fin; total number of rays: 1 – 11.** (Johnson & Patterson, 1993: Char. #29, modified)

*Description:* The pelvic fin of the Percomorphacea is supported by a spine, or an unbranched soft ray, which is followed by a series of branched and segmented soft rays (Fig. 13). The total number of pelvic-fin rays in the group varies from one (*i.e.* Ophidiiformes) to six – one unbranched and five branched rays (*i.e.* most percomorphaceans). Although the total number of rays show little variation within the Percomorphacea, the most immediate outgroup taxa of percomorphaceans (*i.e.* Stephanoberyciformes, Lampridiformes, Beryciformes and Zeiformes) primitively have seven, eight, or 11 pelvic-fin rays (represented by one unbranched and, six, seven, eight, or 10 branched pelvic-fin rays, respectively).

*Remarks:* The reduction to six or less pelvic-fin rays is considered herein a synapomorphy for the Percomorphacea corroborating Johnson & Patterson (1993: Char. #29). According to and Wiley & Johnson (2010) there are few events of reversals to more than 6 pelvic-fin rays, *e.g.* the syngnathoid *Solenostomus* and a few Cyprinodontiformes and Pleuronectiformes (Johnson & Patterson, 1993).

*Inapplicability:* This character is inapplicable for taxa lacking the pelvic fin (*i.e.* representatives of the family Stromateidae and Trichiuridae). Pelvic-fin loss is treated on Character #72, and pelvic-girdle loss on Character #92.

*Indexes:* CI = 0.500; RI = 0.714

**Char. #7 (RY08). Anal fin; total number of rays: 8 – 153**

*Description:* Two or three spines followed by a series of branched rays support the anal fin of most acanthomorphs. In the analyzed taxa the total number of anal-fin rays vary from eight (*e.g. Centropomus paralellus*: Centropomidae) to 153 elements (*e.g. Trichiurus lepturus*: Trichiuridae). The present character refers to the total number of rays present in the anal fin, including spines, soft rays and finlets.

*Remarks:* Finlets, whenever present following the anal-fin, are considered serially homologues to soft fin-rays and therefore included in the anal-fin ray count.

*Indexes:* CI = 0.303; RI = 0.476

**Char. #8 (RY09). Anal fin; number of spines: 1 – 13**

*Description:* Anal-fin spines are azygous, unsegmented, and bilaterally fused anal-fin rays present either as a stiff and pungent element, or as a smooth spine. The number of anal-fin spines in percomorphaceans is usually three but may vary from one (*Sphyræna tome*: Sphyrænidae) to 13 elements (Fig. 9; *Monocirrhus polyacanthus*: Polycentridae).

*Remarks:* Although the number of anal-fin spines varies considerably across the percomorphacean families, the possession of three spines is the most common and possibly the primitive condition for the Percomorphacea. A reduction from four (present in the out-group taxa *Beryx splendens* and *Holocentrus adscensionis*) to three or less spines is herein recovered to be a synapomorphy for the division.

*Inapplicability:* Taxa lacking dorsal-fin spines (Char. #65, state 1).

*Indexes:* CI = 0.319; RI = 0.393

**Char. #9 (RY10). Anal fin; number of soft rays: 5 – 153**

*Description:* Soft fin rays are simple, unfused, and segmented rays that follow posteriorly the anal-fin spines (Fig. 9). The number of soft anal-fin rays is highly variable among the Percomorphacea,

ranging from a few (*e.g.* five in *Centropomus paralellus*: Centropomidae) to over a hundred rays (*i.e.* 153 in *Trichiurus lepturus*: Trichiuridae).

*Remarks:* The posteriormost anal-fin double ray, which articulates with a single anal-fin pterygiophore, is herein account as a single element. Counts presented for the Scombridae include the series of seven to ten finlets located along the caudal peduncle, posterior to the anal fin. Presence or absence of finlets is coded as an independent character (Char. #86).

*Indexes:* CI = 0.314; RI = 0.498

**Char. #10 (RY11). Caudal fin; number of branched rays:** 9 – 18 (Johnson & Patterson, 1993: Char. #33, modified).

*Description:* The percomorphacean caudal fin is supported by a dorsal and a ventral leading unbranched caudal-fin ray and a variable number of branched rays located in between these leading rays (Figs. 9, 14-17). The number of branched caudal-fin rays in the Percomorphacea ranges from nine (*i.e.* *Aulostomus maculatus*: Aulostomidae) to 18 (*i.e.* *Icosteus aenigmaticus*: Icosteidae), but with 15 being by far the most common count for representatives of the division.

*Remarks:* Johnson & Patterson (1993) proposed this character in a slightly modified manner as one of the eight synapomorphies supporting Percomorphacea. According to the authors the primitive ray count of acanthomorphs, which is also widespread among lower teleosts, is to exhibit 19 principal caudal-fin rays in a 1,9,8,1 pattern. This condition is exhibited by the immediate percomorphacean outgroups, such as Zeiformes, Lampridiformes, Stephanoberyciformes, and Beryciformes. A reduction in one branched caudal-fin ray (in a 1,8,8,1 pattern) is observed in *Polymixia* and Percopsiformes, and a reduction to 17 principal branched caudal-fin rays (*i.e.* 1,8,7,1) is unique to Percomorphacea. According to our analysis, the primitive euteleostean pattern of 17 branched rays is observed in the outgroup taxa (*i.e.* Beryciformes), and is reduced to 15 at the base of the Percomorphacea, corroborating the synapomorphic status of this character.

Within percomorphaceans, subsequent reductions of caudal-fin rays are often observed in some taxa (*e.g.* Ophidiiformes, Gasterosteiformes) but increase in this number are very rare. Among the analyzed taxa, numbers exceeding 17 branched anal-fin rays were exclusively observed in *Icosteus aenigmaticus* (Icosteiformes; 18 branched caudal-fin rays in a 1,8,8,1 pattern). In the literature, caudal-fin ray counts exceeding 15 branched rays are known to occur on some Mastacembelidae. According to Roberts (1986) the number of caudal-fin rays is highly variable among the representatives of this

family, and counts may reach up to 27 rays in some specimens (*i.e. Mastacembelus dayi*; Roberts, 1986: tab. 1).

*Inapplicability:* This character was coded as inapplicable to *Trichiurus lepturus* (Trichiuridae), in which the caudal skeleton is lost, and the fin is modified into a caudal filament.

*Indexes:* CI = 0.289; RI = 0.266

**Char. #11 (SN01). Supraneurals; total number:** 1 – 9 (Springer, 1983; Parenti, 1993; Imamura & Yabe, 2002; modified)

*Description:* Supraneurals are a series of small vertically elongated bones located between the posterior end of the skull and the anterior portion of the dorsal fin (Fig. 18). Within Percomorphacea the number of supraneurals is usually comprised between one (*e.g. Thysitops lepidopoides*: Gempylidae) and three (*i.e.* most analyzed taxa). Presence of more than three supraneurals are rare among the Percomorphacea and in the present analysis found only in *Icithys lockingtoni* (9 elements).

*Remarks.* Although not sampled herein, the Centrolophidae *Icithys australis* (= *Pseudoicithys australis sensu* Parin & Permitin, 1969), represents the only other event of increase of supraneural count that is comparable to *Icithys lockingtoni*. According to Parin & Permitin (1969) the species exhibits 9 to 10 interneurals (=supraneural bones).

*Inapplicability:* This character is coded as inapplicable for taxa lacking supraneurals (Char. #101, state 1).

*Indexes:* CI = 0.424; RI = 0.720

**Char. #12 (VE01). Vertebrae; total number:** 23 – 168

*Description:* Among percomorphaceans, the plesiomorphic count of vertebrae ranges from 24 to 26, numbers present in the out-group taxa (Beryciformes) and several Percomorphacea. While reduction in the number of vertebrae seem to be uncommon (23 in *Monocirrhus polyacanthus*; Polycentridae), counts exceeding 26 are known to have evolved in several lineages of percomorphaceans.

*Indexes:* CI = 0.341; RI = 0.429

**Char. #13 (PR01). Dorsal procurrent rays; total number: 1 – 15**

*Description:* The percomorphacean caudal fin usually exhibits a series of small-sized procurrent fin rays preceding the principal dorsal and ventral caudal-fin rays (Figs. 14-17). The number of procurrent rays greatly varies among the Percomorphacea, ranging from one (*e.g. Dinematchthys iluocoeteoides*: Bythitidae) to 15 (*Icichthys lockingtoni*: Centrolophidae) among the examined taxa. The number of dorsal procurrent caudal-fin rays usually exceeds the ventral ones in one or two elements, but this difference may be greater in some taxa (*i.e.* families Atherinidae, Mugilidae, Paralichthyidae).

*Remarks:* Among beryciforms, dorsal procurrent rays varies in number from four to six elements, while in percomorphaceans this number may reach up to 15 elements. The gain in number of dorsal procurrent rays (from 6 to 10 or more) is herein listed as an additional synapomorphy for percomorphaceans.

*Inapplicability:* This character is inapplicable for taxa lacking procurrent rays (*Raneya brasiliensis*: Ophidiidae) and taxa lacking a caudal fin (*Trichiurus lepturus*: Trichiuridae).

*Indexes:* CI = 0.132; RI = 0.377

**Char. #14 (PR02). Ventral procurrent rays; total number: 1– 15.**

*Description:* Ventral procurrent caudal-fin rays are a series of unbranched, small-sized rays that precede the principal rays of the ventral lobe of the caudal fin (Figs. 14-17).

*Remarks:* Similar to the dorsal procurrent rays, in Beryciformes the number of ventral procurrent elements vary from 4 to 6 elements. In percomorphaceans the number of elements is usually above 9 rays and may reach up to 15 elements. Accordingly, the transformation from 5 to 9 or more ventral procurrent rays is herein listed as an additional synapomorphy for percomorphaceans.

*Inapplicability:* This character is inapplicable for taxa lacking procurrent rays (*Raneya brasiliensis*: Ophidiidae), and taxa lacking a caudal fin (*Trichiurus lepturus*: Trichiuridae).

*Indexes:* CI = 0.134; RI = 0.345

**Char. #15 (BR01). Branchiostegal rays; total number: 4 – 8**

*Description:* This character accounts to the number of branchiostegal rays.

*Remarks:* All analyzed non-percomorphaceans exhibit eight branchiostegal rays, a number that is also present in pre-percomorphaceans (e.g. Zeiformes: McAllister, 1968; Johnson & Patterson, 1993). A reduction to seven branchiostegal rays is herein listed as a synapomorphy for the Percomorphacea, with further reductions to six or less rays independently evolving in several percomorphacean subgroups.

*Indexes:* CI = 0.364; RI = 0.759

## MEASUREMENTS

**Char. #16 (PP01). Dorsal fin; predorsal length; proportion in relation to the standard length: 7.9% – 61.5% (Chapleau, 1993: Char #2, modified):**

*Description:* The relative position of the dorsal-fin origin is variable among the Percomorphacea and possibly informative in a phylogenetic context. A proportion of the relative position of the dorsal fin is herein incorporated in order to evaluate events of displacement of the dorsal fin across percomorphaceans. Measurements were taken from the tip of the upper jaw to the base of the anteriormost dorsal-fin ray or spine and divided by the standard length in order to obtain a proportion of the predorsal length (Fig. 5A).

*Remarks:* This character is modified from Chapleau, 1993 (Char. #2). According to Chapleau (1993) one of the synapomorphies of flatfishes is their long dorsal fin that overlaps the neurocranium and sometimes extends in front of the jaws, a condition that differs from most other percomorphaceans. However, according to our results this character does not stand as a synapomorphy for Pleuronectiformes. A reduction in the predorsal length (compatible to an anterior displacement of the dorsal-fin origin) is synapomorphic for a broader clade composed by Pleuronectiformes + Scombriformes.

*Indexes:* CI = 0.179; RI = 0.346

**Char. #17 (PP02). Dorsal fin; base length; proportion in relation to the standard length: 19% – 88.9%**

*Description:* The dorsal-fin base length is taken from the base of the anteriormost dorsal-fin ray or spine to the base of the last dorsal-fin ray (Fig. 5B). This measurement includes the space in between the anterior and posterior dorsal fins in taxa exhibiting two separated dorsal fins (*i.e.* taxa exhibiting the condition 1 of Char. #67). Finlets are serially homologous to the remaining fin rays and were accordingly considered part of the dorsal fin; in such instances, the dorsal-fin base length was then taken from the bases of the anteriormost dorsal-fin ray to the last dorsal finlet.

*Indexes:* CI = 0.161; RI = 0.374

**Char. #18 (PP03). Pectoral fin; fin length; proportion in relation to the standard length: 4.8% – 40.8%**

*Description:* The pectoral-fin length accounts for the length between the pectoral-fin base to the tip of the longest pectoral-fin ray (Fig. 5C). This measurement varies across percomorphacean lineages from 5% (*e.g.* *Trichiurus lepturus*: Trichiuridae; *Aulostomus maculatus*: Aulostomidae) to 40% of the standard length (*e.g.* *Peprilus paru* and *Pampus cinereus*: Stromateidae). The pectoral-fin length is relatively stable among certain percomorphacean subgroups herein sampled (*i.e.* suborders and less inclusive taxa).

*Indexes:* CI = 0.158; RI = 0.474

**Char. #19 (PP04). Pelvic fin; prepelvic length; proportion in relation to the standard length: 8.3% – 60.6%**

*Description:* Prepelvic length is taken from the tip of the upper jaw to the base of the lateralmost pelvic-fin ray (Fig. 5D). The relative position of the pelvic fin on the body is highly variable among the Percomorphacea, but it is most commonly located in the anterior half of the body, ventral to the pectoral girdle. In some taxa, however, there is a shift on the insertion site of the pelvic fin. Representatives of the Mugiliformes, Atheriniformes, and Aulostomidae have a posteriorly placed pelvic girdle, with its insertion near the half of the body length. The Ophidiiformes, on the other hand, exhibit an anterior shift in the pelvic fin, with cases of pelvic-fin insertion located on the vertical passing through the orbit (*Raneya brasiliensis*: Ophidiidae).

*Remarks:* The pectoral fin of the examined specimen of *Centrolophus niger* was damaged and the prepelvic length of this taxon was obtained from Ueno (1954).

*Inapplicability:* This character was coded as inapplicable for fishes lacking a pelvic fin (Char. #72).

*Indexes:* CI = 0.234; RI = 0.338

**Char. #20 (PP05). Anal fin; preanal length; proportion in relation to the standard length: 32.6% – 79.5%**

*Description:* Measurements of the pre-anal length is herein incorporated in order to evaluate the variation of the anal-fin insertion among the percomorphacean fishes. This measurement is taken from the tip of the upper jaw to the base of the anteriormost anal-fin ray or spine (Fig. 5E).

*Indexes:* CI = 0.135; RI = 0.394

**Char. #21 (PP06). Anal fin; base length; proportion in relation to the standard length: 6.8% – 69.6%**

*Description:* Anal-fin base length was taken from the base of the anteriormost anal-fin ray or spine to the base of the last anal-fin ray (Fig. 5F). Finlets are serially homologous to the remaining fin rays and are thus considered part of the anal fin; in such instances, the anal-fin base length was taken from bases of the anteriormost anal-fin ray to the last anal finlet.

*Indexes:* CI = 0.130; RI = 0.469

## **Qualitative characters:**

### **OSTEOLOGY**

#### **Skull**

**Char. #22 (BH01). Supramaxilla; occurrence: (0) absent; (1) present.**

*Description:* The supramaxilla is a small dermal bone lying immediately above or partially overlapping the posterodorsal region of the maxilla (Figs. 19-30).

*Remarks:* The absence of a supramaxilla resulted herein as a synapomorphy for Percomorphacea. Nevertheless, our analysis reveals that variation in the presence of a supramaxilla is

higher than previously documented for subgroups within Percomorphacea, and the supramaxilla appears at least 13 times independently within this clade under six different reconstructions.

Haedrich (1967) reported the presence of supramaxilla as a diagnostic feature of Centrolophidae, which would be absent in the remaining Stromateiformes. However, our analysis does not support this character distribution within stromateiforms. The examined specimens *Psenes cyanophrys* (Nomeidae), and *Ariomma bondi* and *A. melanum* (Ariommatidae) unequivocally exhibit a well-developed supramaxilla. As for the Centrolophidae, which were characterized by Haedrich (1967) by the possession of this bone, the ossification is absent in *Centrolophus*, *Tubbia*, *Schedophilus*, and both *Psenopsis* species. Similarly, the presence of a supramaxilla has been listed as a synapomorphy for the Carangidae (Smith-Vaniz, 1984), but our analysis failed on finding this bone in *Trachinotus carolinus* (Carangidae).

*Indexes:* CI = 0.071; RI = 0.480

**Char. #23 (BH02). Free prenasals; occurrence:** (0) absent; (1) present (Smith-Vaniz, 1984: Char. #2).

*Description:* The nasal bone is typically located anterior to the frontal and associates with the anteriormost portion of the supraorbital canal of the laterosensory system. Among percomorphaceans, additional tubular ossifications located anterior to the nasal are known to occur in toxotids, lutjanids, and the carangiforms (Freihofer, 1978; Smith-Vaniz, 1984). These ossifications retain an association with the supraorbital canal and are referred to as prenasals (Smith-Vaniz, 1984).

*Remarks:* Freihofer (1978) reported the occurrence of up to two separate sets of prenasals in the Carangidae, Coryphaenidae, Rachycentridae, and Echeneidae. Among non-Carangiformes percomorphaceans, the author recorded autogenous prenasals in Toxotidae and Lutjanidae. The presence of these ossifications was later optimized as a synapomorphy for the Carangiformes by Smith-Vaniz (1984: Char. #2), who credited Freihofer (1978) for this observation. Curiously, the carangiform circumscription of Freihofer (1978) did not include the Nematistiidae, but the confirmation of the presence of prenasals in that family was provided by Johnson (1984) in the same volume, a few pages before Smith-Vaniz's (1984) phylogeny.

Our observation indicates that in small specimens of *Nematistius pectoralis* (46.3 mm SL) the prenasal segment of the supraorbital canal is unossified. The canal leaves the anterior portion of the nasal bone and extends anteriorly over the nape, where it curves laterally and proceeds along the premaxilla. A similar path of the supraorbital canal is observed in other analyzed Carangiformes

(carangids, rachycentrids, coryphaenids). However, in Carangiformes in general, and in large specimens of *N. pectoralis* (140 mm SL), the anterior segment of the supraorbital canal is fully ossified into a recognizable prenasal (Freihofer, 1978; Johnson, 1984; Smith-Vaniz, 1984). This observation is compatible to Johnson's (1984) descriptions, which report a single *partly ossified* prenasal unit in *Nematistius pectoralis*. It is possible that this supraorbital canal segment develops early during ontogeny in *Nematistius* but exhibits a late and not complete ossification. Freihofer (1978) also stated that all scombriforms have a prenasal fused with the nasal and forming a long compound bone. Among the scombriforms herein examined, free prenasals are observed only in *Trichiurus lepturus* (Trichiuridae). In *Thyrsitops lepidopoides* (Gempylidae), the prenasal bones, if present, are fused to the nasal bone and thus coded as character state 0 herein.

Although documented for Lutjanidae, the analyzed taxon *Lutjanus analis* lacks free prenasal ossifications. On the other hand, an additional event of prenasal occurrence is documented herein, occurring in Ophidiiformes.

*Indexes:* CI = 0.250; RI = 0.500

**Char. #24 (BH03). Infraorbital 1 (= lachrymal or lacrimal); serrations on the ventral margin; occurrence: (0) absent; (1) present.**

*Description:* Several percomorphaceans exhibit serrations on the distal margin of some dermal bones. These serrations are commonly observed along the infraorbital and opercular bones, and often present on elements of the pectoral girdle (*e.g.* extrascapular, posttemporal and supracleithrum). Marginal serrations along the ventral margin of infraorbital 1 (= lacrimal or lachrymal) occur in some analyzed taxa (Figs. 19-21).

*Indexes:* CI = 0.143; RI = 0.500

**Char. #25 (BH04). Subocular shelf; occurrence: (0) present; (1) absent**

*Description:* The subocular shelf is a bony lamina that extends inward from the infraorbitals and forms a bony wall along the ventral region of the orbit (Fig. 31). In percomorphaceans, the subocular shelf occurs most frequently in infraorbitals 3 and 4, but sometimes extending from infraorbitals 3 to IO5 (*i.e.* *Holocentrus adscensionis*: Holocentridae) or restricted to infraorbitals four

and five (e.g. *Tubbia tasmanica*: Centrolophidae; analyzed specimens of the Channidae, Trichiuridae, and Apogonidae).

*Remarks:* In the present analysis, the subocular shelf of *Nematistius pectoralis* (Nematistiidae) is coded as present based on the description of Rosenblatt & Bell (1976). The specimen used on the analysis is a juvenile, presenting poorly ossified circumorbital bones. Although previously reported as present in sphyraenids (Johnson, 1986), the *Sphyraena* species herein examined lacks any vestiges of subocular projection, and the structure is coded as absent.

*Indexes:* CI = 0.067; RI = 0.533

**Char. #26 (BH05). Sclerotic bone; occurrence: (0) present; (1) absent**

*Description:* Sclerotic bones are ossifications of the eyeball's sclera (Fig. 19, 21).

*Remarks:* The degree of ossification of the sclerotic bones are highly variable and not accounted herein. It may range from little ossification restricted to the lateral edges of the eyes (i.e. Nomeidae, Paralichthyidae) to almost full ossification of the sclera around the eyeball (i.e. *Sphyraena tome*: Sphyraenidae; *Auxis thazard*: Scombridae).

*Indexes:* CI = 0.071; RI = 0.316

**Char. #27 (BH06). Opercle; spines; occurrence: (0) present, (1) absent**

*Description:* Opercular spines are posteriorly oriented pointy projections at the dorsal portion of the opercular margin. Beryciformes (Figs. 19, 22) and many percomorphacean families (Figs. 21, 24-27, 29, 32-34) exhibit spines on the posterior margin of the opercle.

*Remarks:* Most percomorphs have a single opercular spine. Some taxa exhibit an increase in number to two, and rarely three opercular spines. Imamura & Yabe (2002) hypothesized a backwardly-directed opercular spine (i.e. a third spine) crossing the subopercle as synapomorphy of his Scorpaeniformes (= Scorpaenoidei + Serranidae). Although not coded herein in a separated character, the backwardly oriented spine of Imamura & Yabe (2002) is the ventralmost opercular spine, which is present in the herein analyzed representative of Serranidae (*Diplectrum radiale*). According to Johnson (1983) the only other taxa to present a homoplastic condition of three opercular spines, with the ventralmost crossing the subopercle, are *Sphyraenops* (Epigonidae) and Trachinidae.

*Indexes:* CI = 0.083; RI = 0.577

**Char. #28 (BH07). Opercle, spines; degree of rigidity:** (0) stiff and pungent; (1) soft, not pungent.

*Description:* Opercular spines are located at the posterodorsal margin of the opercle and may vary from as a stiff and pungent element (Figs. 19, 21, 22, 25-27, 32, 33) to a weak, flat structure (Figs. 24, 29, 34).

*Inapplicability:* This character is coded as inapplicable for taxa lacking an opercular spine (Char. #27, state 1).

*Indexes:* CI = 0.200; RI = 0.636

**Char. #29 (BH08). Opercle; serrations on distal margin; occurrence:** (0) absent; (1) present.

*Description:* Several percomorphaceans exhibit serrations on the distal margin of dermal bones. These serrations are commonly observed along the infraorbital preopercle, opercle, and occasionally present on elements of the pectoral girdle (*e.g.* extrascapular, posttemporal, supracleithrum, and cleithrum). When present in the opercle, serrations are usually limited to the ventral half of the bone (Fig. 22). In taxa lacking opercular serrations, the posterior edge of this bone is represented by a straight margin (Figs. 23, 25, 32-38)

*Indexes:* CI = 0.200; RI = 0.200

**Char. #30 (BH09). Preopercle; spines; occurrence:** (0) absent; (1) present. (Otero, 2004: Char. #13).

*Description:* Spines on the preopercle are usually present on its posteroventral margin of this bone, projecting over the subopercle. Preopercular spines are commonly observed as a single element at the point of flexion of this bone, although some taxa may exhibit an increased number of three to five spines (Otero, 2004: Char. #13). Such a numerical variation was not observed among the terminal taxa included in the present study and, accordingly, this character accounts only for the presence of preopercular spines (Figs. 19, 20, 22, 23, 25, 31, 35).

*Indexes:* CI = 0.333; RI = 0.500

**Char. #31 (BH10). Preopercle; serrations; occurrence: (0) absent; (1) present.**

*Description:* Serrations on the preopercle are usually present on its posterior margin as a crenation at the distal margin of this bone (Figs. 19, 20, 22, 23, 25, 31, 32, 35). These crenations are widespread among the analyzed specimens; including the analyzed outgroup taxa (*i.e.* Beryciformes). In taxa lacking opercular serrations, the posterior edge of this bone is represented by a straight margin (Figs. 36-38)

*Indexes:* CI = 0.100; RI = 0.710

**Char. #32 (BH11). Quadrate and metapterygoid; articulation; type: (0) not sutured; (1) sutured** (Sasaki, 1989; Johnson, 1993; Kang *et al.* 2017).

*Description:* In most taxa, the metapterygoid and quadrate are separated by a narrow strip of cartilage (Figs. 31, 39-41). In sciaenids and polynemids the articulation between these bones lack cartilage and is made through an interdigitated bony suture.

*Remarks:* A suture between quadrate and metapterygoid returns as a synapomorphy for Sciaenidae + Polynemidae (TNT clade 123). Sasaki (1989), in a morphological cladistic analysis of the Sciaenidae, proposed the interdigitating quadrate and metapterygoid bones as one of the 21 synapomorphies for the family. These characters were later reevaluated by Johnson (1993) who reported that at least five of the 21 sciaenid synapomorphies were also present in polynemids, including the interdigitation between quadrate and metapterygoid. The author thus advanced that Sciaenidae and Polynemidae would be sister groups. More recently, Kang *et al.* (2017: p. 11) confirmed that feature as a synapomorphy for the clade Polynemidae + Sciaenidae.

*Indexes:* CI = 0.500; RI = 0.500

**Char. #33 (BH12). Posttemporal; serrations on the posterior margin: (0) absent; (1) present.**

*Description:* Serrations on the distal margin of the posttemporal are present as a marginal crenation of this bone (Figs. 18-20, 22, 23, 25, 33).

*Indexes:* CI = 0.143; RI = 0.600

**Char. #34 (BH13). Parasphenoid; posterior myodome; bony window: (0) absent; (1) present.**

*Description:* The parasphenoid of percomorphaceans is usually a long and cross-shaped bone placed at the ventral surface of the skull. Anteriorly, this bone articulates to the vomer, laterally with the prootic, and posteriorly it connects to the basioccipital. The parasphenoid-prootic contact is the landmark of the anterior portion of the posterior myodome, *i.e.* a bony furrow that serves as origin site for the *recti* muscles of the eye. The myodome is constituted by the spaces left between the contacts of the lateral arms of the parasphenoid to the ventral ridges of the prootic. From this point, the myodome continues through a tunnel along the parasphenoid, which will end at the parasphenoid-basioccipital contact.

The ossification of the posterior walls of the posterior myodome is variable among percomorphaceans. When fully ossified, fibers of the *recti* eye muscles are completely enclosed in bones and are not visible at the posteroventral portion of the skull. However, several taxa exhibit a parasphenoid bony window delimited by posterolateral walls of the parasphenoid and the anteroventral margin of the basioccipital (Collette & Chao, 1975: figs. 15-19; Rosenblatt & Bell, 1976: fig. 2). In such cases, the posterior portion of the posterior myodome is not enclosed by the parasphenoid, and fibers of the *recti* muscles, mostly the *rectus internus* (the longest of the eye muscles with origin at the posterior myodome), are visible originating from the parasphenoid and basioccipital.

*Indexes:* CI = 0.067; RI = 0.548

## Teeth

**Char. #35 (TH01). Premaxillary teeth; series; number: (0) one; (1) multiple.**

*Description:* This character accounts to the number of premaxillary-teeth series.

*Remarks:* The presence of a single row of premaxillary teeth returns herein as a synapomorphy for Stromateiformes, with a single event of homoplasy in mugilids.

*Indexes:* CI = 0.333; RI = 0.917

**Char. #36 (TH02). Vomer; teeth; occurrence: (0) present; (1) absent.**

*Description:* This character accounts to the presence of teeth on the vomer.

*Indexes:* CI = 0.077; RI = 0.613

**Char. #37 (TH03). Palatine; teeth; occurrence: (0) present; (1) absent.**

*Description:* This character accounts to the presence of teeth on the palatine (Fig. 41).

*Indexes:* CI = 0.083; RI = 0.645

**Char. #38 (TH04). Ectopterygoid; teeth; occurrence: (0) present; (1) absent.**

*Description:* This character accounts to the presence of teeth on the ectopterygoid.

*Indexes:* CI = 0.200; RI = 0.200

**Char. #39 (TH05). Endopterygoid; teeth; occurrence: (0) present; (1) absent.**

*Description:* This character accounts to the presence of teeth on the endopterygoid.

*Indexes:* CI = 0.333; RI = 0.500

**Char. #40 (TH06). Basihyal/ hypobranchial/ basibranchial; teeth; occurrence: (0) present; (1) absent.**

*Description:* This character accounts to the presence of teeth on the ventral surface of the mouth, *i.e.* on the basihyal, hypobranchial, and basibranchials 1–3 (see Nelson, 1969: figs 8-12).

*Remarks:* The present character codes indiscriminately the occurrence of basihyal, basibranchial and hypobranchial tooth plates. This decision was made due to the poor limits between tooth patches, which in several occasions, did not respect the limits within branchial bones (Nelson, 1969: figs 8-12). Therefore, this character could be also described as presence of teeth on the surface of ventral branchial bones. Basibranchial teeth is uncommon among stromateiforms (Figs. 42-44). However, tooth plates are present in the basibranchial of most nomeids (Fig. 45).

*Indexes:* CI = 0.125; RI = 0.462

**Char. #41 (TH07). Basibranchials; teeth; alignment:** (0) not aligned; (1) aligned.

*Description:* This character describes the arrangement of basibranchial teeth. Usually, stromateiforms lack tooth plates associated to the basibranchials (Char. #40, state 0). However, several nomeids exhibit uniserial, aligned teeth along basibranchials bones (Fig. 45; Barnard, 1948: fig. 12).

*Indexes:* CI = 0.333; RI = 0.667

*Inapplicability:* This character is inapplicable for taxa lacking basibranchial teeth (Char. #40, state 0).

**Char. #42 (TH08). Epibranchial 2; teeth; occurrence:** (0) present; (1) absent.

*Description:* This character accounts to the presence of a toothplate associated to the second epibranchial (Fig. 44).

*Indexes:* CI = 0.143; RI = 0.571

**Char. #43 (TH09). Epibranchial 3; teeth; occurrence:** (0) present; (1) absent.

*Description:* This character accounts to the presence of a toothplate associated to the third epibranchial.

*Indexes:* CI = 0.067; RI = 0.500

**Char. #44 (TH10). Fourth pharyngeal tooth plate; length:** (0) roughly as long as wide; (1) considerably longer than wide (Johnson, 1986: Char. #8, modified).

*Description:* Most percomorphaceans have a fourth pharyngeal toothplate associated to the pharyngobranchial 4 with comparable length and width, and with overall roundish limits (*e.g.* Johnson, 1986: fig. 6, A-B; Sasaki, 1989: fig. 39). Stromateiformes instead have a notably elongated and often digitiform fourth pharyngeal toothplate (Figs. 44-46; Barnard, 1948: fig. 10, e-g; Doiuchi *et al.* 2004:

fig. 6, A). This expansion, particularly pronounced in centrolophids and tetragonurids, where it enters the pharyngeal sac and provides a toothed dorsal roof to the sac (Figs. 43, 44, 46).

*Remarks:* This character is herein proposed as a synapomorphy for non-Amarsipidae Stromateiformes. A similarly elongated fourth pharyngobranchial toothplate has been proposed as synapomorphy for the Scombriformes *sensu* Johnson (1986: Char. #8), condition which is corroborated herein.

*Indexes:* CI = 0.333; RI = 0.923

**Char. #45 (TH11). Pharyngeal sac; dorsal portion; tooth patches; occurrence: (0) absent; (1) present.**

*Description:* The presence of pharyngeal-sac dorsal patches of teeth is exclusive of ariommatid and stromateid Stromateiformes. These taxa have a series of three pairs of teeth patches attached to the dorsal wall of the pharyngeal sac that follow the fourth pharyngeal toothplates posteriorly (Fig. 42).

*Indexes:* CI = 0.500; RI = 0.833

**Char. #46 (TH12). Pharyngeal sac; proximal region; ventral portion; teeth patches; occurrence: (0) absent; (1) present**

*Description:* Like the dorsal pharyngeal-sac patches of teeth, the presence of teeth on the ventral midline of the pharyngeal sac occur in Stromateidae.

*Indexes:* CI = 1.000; RI = 1.000

## **Hyoid skeleton**

**Char. #47 (HY01). Anterior ceratohyal and posterior ceratohyal; lateral view; contact: (0) cartilaginous; (1) bony sutured.**

*Description:* In lateral view, the anterior and posterior ceratohyals are usually separated from each other by a thin strip of cartilage (Fig. 42, 47). This is the most common condition among percomorphaceans, which is also present in Stephanoberyciformes and Beryciformes. However, some

of the analyzed specimens exhibit a bony contact between anterior and posterior ceratohyals in which both elements are connected to each other through an interdigitated bony suture.

*Remarks:* Bony sutures between anterior and posterior ceratohyals are present in several Teleostei. This condition is recorded in percopsiforms, ophidiiforms, gadiforms, lophiiforms, batrachoidiforms, atheriniforms, zeiforms, syngnathiforms, gasterosteiforms, and several other percomorphacean subgroups (McAllister; 1968). Given the absence of ceratohyal sutures in lampridiforms, polymixiiforms, stephanoberyciforms, and beryciforms, Johnson & Patterson (1993) hypothesized the presences of this suture as a possible percomorphacean synapomorphy. Optimization conflict due to the presence of sutures in some of the so-called Paracanthopterygii (*e.g.* Lophiiformes, Batrachoidiformes, Ophidiiformes) was resolved after their inclusion in the Percomorphacea (Wiley & Johnson, 2010).

*Indexes:* CI = 0.077; RI = 0.538

**Char. #48 (HY02). Anterior and posterior ceratohyals; medial view; contact: (0) cartilaginous; (1) bony sutured** (Doiuchi *et al.* 2004: Char. #13).

*Description:* Sutured bony contact between anterior and posterior ceratohyals occur independently on the lateral and medial faces of the hyoid bar. While some specimens presented ceratohyals not sutured in a lateral view, sutures on medial side is common to nearly all sampled percomorphaceans.

*Remarks:* The medial suture between anterior and posterior ceratohyals is herein proposed for the first time as a synapomorphy for the Percomorphacea. This characteristic was listed as “*Other Possible Percomorph Characters*” but not included in the list of percomorphacean synapomorphies by Johnson & Patterson (1993) or Wiley & Johnson (2010).

*Indexes:* CI = 0.100; RI = 0.182

**Char. #49 (HY03). Ceratohyals; hyoid artery; path: (0) in a canal or groove lateral to anterior and posterior ceratohyals; (1) lying dorsal to the anterior and posterior ceratohyals.**

*Description:* Percomorphaceans usually exhibit a canal or groove along the lateral side of anterior and posterior ceratohyals that serves as passage of the hyoid artery (Fig. 42). Representatives of a few families, however, exhibited the artery shifted dorsally in relation to the hyoid bones,

intermingled with the tissue covering the hyoid bar. In such taxa, no canal or groove is present on the lateral side of the anterior and posterior ceratohyals.

*Remarks:* This character figures independently as synapomorphy for Sciaenidae + Polynemidae (TNT clade 123) and for Mugiliformes + Atherinomorpha (TNT clade 124).

*Inapplicability:* This character is inapplicable for *Aulostomus maculatus* (Aulostomidae) due to its highly modified ceratohyal bones.

*Indexes:* CI = 0.333; RI = 0.600

**Char. #50 (HY04). Anterior ceratohyal; foramen (*i.e.* beryciform foramen); occurrence: (0) absent; (1) present.**

*Description:* The anterior ceratohyal of percomorphaceans is usually displayed as a longitudinal bony bar that contains one dorsal groove or canal housing the hyoid artery (Fig. 42). Other grooves or foramina in the anterior ceratohyal are of a more restricted occurrence. In the Beryciformes, the anterior ceratohyal is represented by a dorsal and ventral thin rim of bone encircling a large aperture (*i.e.* beryciform foramen of McAllister, 1968; ceratohyal window of Collette & Chao, 1975: fig. 42). No nerves or blood vessels are noted piercing this foramen, which is covered by skin on both sides (Doiuchi *et al.* 2004: fig. 5, A-B).

*Indexes:* CI = 0.077; RI = 0.586

**Char. #51 (HY05). Anterior ceratohyal; foramen; dorsal bar: (0) present; (1) absent.**

*Description:* In some taxa, the dorsal rim of the anterior ceratohyal foramen is lost, and only the ventral bone bridge is present. However, a dorsal bony prong correspondent to reminiscent of the dorsal bony bridge is still present on the anterior and/ or posterior edges of the anterior ceratohyal.

*Inapplicability:* This character is inapplicable for taxa lacking the anterior ceratohyal foramen (Char. #50: state 1).

*Indexes:* CI = 0.200; RI = 0.636

**Char. #52 (HY06). Penultimate branchiostegal ray; articulation: (0) with the posterior ceratohyal; (1) with the joint between anterior and posterior ceratohyals; (2) with the anterior ceratohyal.**

*Description:* The presence of two branchiostegal rays articulating with the posterior ceratohyal is the most common condition among the analyzed percomorphaceans (Fig. 42), and possibly the plesiomorphic condition for the division (McAllister 1968: plates 12-21). Modifications in this pattern are observed towards a gradual anterior displacement of the ray attachment site in relation to the hyoid bar. In an intermediate configuration, the penultimate branchiostegal ray articulates with joint between the anterior and posterior ceratohyals; in a more extreme condition, that ray articulates with the anterior ceratohyal.

*Remarks:* The articulation of the penultimate branchiostegal ray with the anterior ceratohyal (= a single branchiostegal articulating with the posterior ceratohyal) is returned herein as a synapomorphy for Sciaenidae + Polynemidae. This characteristic is one of the 21 synapomorphies currently supporting the monophyly of Sciaenidae (Sasaki, 1989: Char. #18). However, as noted by Johnson (1993) this and other four supposed synapomorphies are also present in the Polynemidae, indicating a possible sister-group relationship between the two families. Among percomorphaceans, that condition is also known to occur in some Pseudochromidae and Gobiiformes (Johnson, 1993).

*Indexes:* CI = 0.154; RI = 0.154

**Char. #53 (HY07). Third last branchiostegal ray; articulation: (0) with the anterior ceratohyal; (1) with the joint between anterior and posterior ceratohyals; (2) with the posterior ceratohyal [multistate additive].**

*Description:* The possession of three branchiostegal rays articulating with the posterior ceratohyal is uncommon among percomorphaceans and possibly a modification from the widespread condition of two branchiostegal connected to this bone (McAllister 1968: plates 12-21). An intermediate state between these two conditions is the third last branchiostegal ray laying in between the anterior and posterior ceratohyals.

*Remarks:* Among the analyzed specimens, an increase on the number of associated elements to the posterior ceratohyal was observed in some Scombriformes, where the third last branchiostegal ray is either completely associated to the posterior ceratohyal or is lying in the point of connection between anterior and posterior ceratohyals (Collete & Chao, 1975: fig. 42; Johnson, 1986).

*Inapplicability:* This character is coded as inapplicable to taxa with the penultimate branchiostegal ray articulating with the anterior ceratohyal or the joint between this bone and the posterior ceratohyal (Char. #52, states 1 or 2).

*Indexes:* CI = 0.200; RI = 0.467

**Char. #54 (HY08). Dorsal and ventral hypohyals; medial view; contact:** (0) bony sutured; (1) cartilaginous. (Doiuchi, 2004: Char. #11, modified).

*Description:* In the outgroups and most percomorphaceans, the dorsal and ventral hypohyals are usually connected to each other by a bony suture in medial view. Some analyzed taxa, however, have these bones separated from each other by a thin layer of cartilage (Doiuchi, 2004: Char. # 11).

*Inapplicability:* This character is inapplicable for *Schedophilus medusophagus* (Centrolophidae). The juvenile specimen analyzed herein still exhibits a completely unossified hyoid skeleton.

*Indexes:* CI = 0.111; RI = 0.652

**Char. #55 (HY09). Dorsal hypohyal; hyoid artery; path:** (0) piercing the dorsal hypohyal; (1) lying on a dorsal sulcus over the dorsal hypohyal.

*Description:* When exiting the ceratohyals, the hyoid artery usually pierces the dorsal hypohyal through the cartilaginous contact between this and the anterior ceratohyal. The artery trespasses this bone from its lateral to medial side, where it follows to the branchial chamber. Representatives of the Polynemidae, Sciaenidae, Mugilidae, and Atherinopsidae, however, exhibit a shift on the hyoid artery path over the dorsal hypohyal. In these taxa, the artery lies on a dorsal sulcus on dorsal hypohyal, and not in a canal that bypasses this bone.

*Remarks:* This character figures independently as synapomorphy for Sciaenidae + Polynemidae (TNT clade 123) and for Mugiliformes + Atherinomorpha (TNT clade 124).

*Inapplicability:* Inapplicable for *Aulostomus maculatus* (Aulostomidae), which exhibits the foramen along the anterior ceratohyal, and not piercing the dorsal hypohyal.

*Indexes:* CI = 0.500; RI = 0.667

## Branchial skeleton

**Char. #56 (BQ01). Interarcual cartilage; occurrence: (0) absent; (1) present** (Travers, 1981; Johnson & Patterson, 1993; Wiley & Johnson, 2010).

*Description:* The interarcual cartilage is a cartilaginous rod-like element located between the uncinated process of the epibranchial 1 and pharyngobranchial 2 (Rosen & Greenwood, 1976; Travers, 1981). This structure is present, and widespread among percomorphaceans, and currently considered a synapomorphy for the group (Johnson & Patterson, 1993; Wiley & Johnson, 2010). Similar, but non-homologous, oval cartilages are often present in some Stephanoberyciformes (*e.g.* anomalopids, melamphoids) and Beryciformes (Johnson & Patterson, 1993; Wiley & Johnson, 2010).

*Remarks:* The synapomorphic status of the interarcual cartilage for the Percomorphacea is recovered herein, corroborating the predictions of Johnson & Patterson, 1993 and Wiley & Johnson, 2010.

Although present in some Channoidei (Travers, 1981: fig. 3), the interarcual cartilage is absent in the analyzed specimen of *Parachanna obscura* (Channidae).

*Indexes:* CI = 0.167; RI = 0.286

**Char. #57 (BQ02). Basibranchial 4; number: (0) one; (1) two**. (Doiuchi *et al.* 2004: Char. #19, modified).

*Description:* Teleostean fishes usually exhibit four basibranchials, which develop independently from two cartilage precursors: basibranchials 1-3 from the anterior, and basibranchial 4 from the posterior cartilage (Nelson, 1969). In adults, the general morphology is to exhibit basibranchials 1-3 ossified, while the basibranchial 4 is retained as a cartilaginous element. The pattern of three ossified basibranchials (1-3) followed by a cartilaginous basibranchial 4 is widespread among the observed Percomorphacea, and also present in both analyzed Beryciformes. However, a modified morphology was observed in the stromateiforms *Icichthys lockingtoni* (Centrolophidae) and in Stromateidae. These fishes exhibited two cartilaginous pieces posterior to basibranchials 1-3: one corresponding to basibranchial 4 (surrounded by the anterior facets of the ceratobranchials 3 and 4, and never reaching the proximal portion of ceratobranchial 5), and an extra basibranchial cartilage (comprised between the proximal portions of ceratobranchials 4 and 5; Doiuchi *et al.* 2004: Fig. 7, C).

*Remarks:* An additional cartilaginous basibranchial is uniquely found among stromateiforms, occurring independently in *Icichthys lockingtoni* (Centrolophidae) and in Stromateidae.

*Indexes:* CI = 0.500; RI = 0.750

### Pharyngeal-sac osteology

**Char. #58 (PH01). Pharyngeal sac; occurrence:** (0) absent; (1) present.

*Description:* For over a century stromateiform fishes have been treated as a natural assemblage. One of the main characteristics of fishes of this order is the possession of the pharyngeal sac, which can be described as a saccular outgrowth located posterior to the gill arches, and internally covered by numerous tooth-like structures (Figs. 42-52; Regan, 1902; Gilchrist, 1922; Bühler, 1930; Barnard 1948; Haedrich, 1967; Doiuchi *et al.* 2004; Datovo *et al.* 2014). With exception of *Amarsipus carlsbergi* (Amarsipidae), whose inclusion stromateiforms has been recurrently questioned (Springer & Johnson, 2004; Datovo *et al.* 2014), all Stromateiformes exhibit a pharyngeal sac.

*Remarks:* Although lacking a pharyngeal sac, Haedrich (1969) placed *Amarsipus carlsbergi* (Amarsipidae) within the Stromateiformes based on other putatively derived characteristics shared by with stromateiforms, such as subdermal canals on the head and body. According to the author, *Amarsipus* represented an aberrant stromateiform that “*can neither be derived from any living stromateoid group, nor have they given rise to any. They may represent the last vestiges of some early stromateoid experiment which never succeeded*”. Horn (1984) interpreted the presence of a pharyngeal sac as a homoplasy-free unambiguous synapomorphy for the non-Amarsipidae Stromateiformes (Fig. 2). Doiuchi *et al.* (2004), on the other hand, obtained a contrasting hypothesis, in which *Amarsipus* figured as sister-group of a clade encompassing the Nomeidae, Ariommatidae, Tetragonuridae, and Stromateidae (Fig. 3). In that configuration, the presence of a pharyngeal sac would be synapomorphic for the Stromateiformes, with a reversal in *Amarsipus*.

*Indexes:* CI = 1.000; RI = 1.000

**Char. #59 (PH02). Pharyngeal sac; lining:** (0) wrinkled; (1) papillary.

*Description:* The internal surface of the stromateiform pharyngeal sac varies from wrinkled (or folded) to papillary (or polypoid). A wrinkled lining corresponds to the folded aspect of the internal

surface of the pharyngeal sac (Fig. 44; Isokawa *et al.*, 1965: fig. 3). On the other hand, a papillary lining (Fig. 46C) is consequence of the presence of several papillae (= polypoid processes *sensu* Isokawa *et al.*, 1965: fig. 4) projecting from the dorsal and lateral walls of the pharyngeal sac and pointing to the sac lumen.

*Inapplicability:* This character is inapplicable for fishes lacking a pharyngeal sac (Char. #58, state 0).

*Indexes:* CI = 1.000; RI = 1.000

**Char. #60 (PH03). Pharyngeal sac; enlarged gill rakers associated to the last gill arch: (0) present; (1) absent.**

*Description:* In some stromateiforms (*e.g.* Centrolophidae, Nomeidae, Ariommatidae), the pharyngeal sac exhibits a set of greatly enlarged gill rakers that originate from the posteriormost gill-arch elements (*i.e.* ceratobranchials 4 and 5, and epibranchial 4) and attach internally to the lateral walls of the sac (Fig. 44).

*Remarks:* Gill rakers associated to the last gill arches (*i.e.* ceratobranchial 4 and 5, epibranchial 4) are rare among percomorphaceans, and among the analyzed taxa are present only in Stromateiformes and in the mugilid *Mugil curema*. While in mugiliforms these rakers are restricted to the anterior face of the bones, and are morphologically similar to that present in the remaining gill arches, in Stromateiformes the rakers are greatly enlarged and folded backwards to the proximal portion of the pharyngeal sac (Fig. 44). Therefore, the mugiliform and stromateiform rakers are herein considered non-homologous, and only the stromateiform raker (Fig. 44C) is coded on this character. Further descriptions and a discussion on the homology of the pharyngeal sac elements of Stromateiformes are offered in the discussion (Section *Gill arch and pharyngeal-sac evolution*).

*Inapplicability:* This character is inapplicable for fishes lacking a pharyngeal sac (Char. #58, state 0).

*Indexes:* CI = 0.500; RI = 0.750

**Char. #61 (PH04). Pharyngeal sac; ventral surface; associated rakers; occurrence: (0) present; (1) absent.**

*Description:* In stromateiforms, the pharyngeal-sac lining (*i.e.* the sac papillae) is constituted of modified gill rakers, which grows from the internal walls of the sac. Among stromateiform families, the distribution of pharyngeal-sac associated rakers varies from covering the entire internal surface of the sac (Fig. 53, C-D) to a condition in which they are lacking on the ventral surface of this organ (Fig. 53, A-B).

*Remarks:* Further comments on the stromateiform pharyngeal-sac homology is provided in the discussion, Section *Gill arch and pharyngeal-sac evolution*.

*Inapplicability:* This character is inapplicable for fishes lacking a pharyngeal sac (Char. #58, state 0).

*Indexes:* CI = 1.000; RI = 1.000

**Char. #62 (PH05). Pharyngeal sac; associated rakers; vertical axis: (0) absent; (1) present.**

*Description:* Among Stromateiformes, the pharyngeal-sac raker morphology (= pharyngeal-sac papilla) varies from a small conic structures without a distinct dorsoventral axis (Fig. 54D; Haedrich, 1967: fig. 50, A-A1), to columnar structure (Figs. 53B-D; Fig. 54H; Fig. 55; Haedrich, 1967: fig. 50, B-D).

*Remarks:* Short and convex rakers lacking a well-defined dorsoventral axis are restricted to Centrolophidae, while rakers exhibiting a dorsoventral orientation are present in the remaining non-amarsipid Stromateiformes. The longest columnar rakers occur in Ariommatidae and Stromateidae (Figs. 53B-D, 55B-D).

*Inapplicability:* This character is inapplicable for fishes lacking a pharyngeal sac (Char. #58, state 0).

*Indexes:* CI = 1.000; RI = 1.000

**Char. #63 (PH06). Pharyngeal sac; associated rakers; base: (0) asymmetrical; (1) symmetrical.**

*Description:* The pharyngeal-sac raker base varies regarding its symmetry. In a symmetrical condition, the rakers exhibit either a round or a stellate base (Figs. 42, 45, 53, 54H, 55, 56). Asymmetrical rakers are small convex structures with irregular margins (Figs. 43, 44, 54D).

*Remarks:* Symmetrical teeth bases occur in Ariommatidae, Nomeidae, Tetragonuridae, and Stromateidae.

*Inapplicability:* This character is inapplicable for fishes lacking a pharyngeal sac (Char. #58, state 0).

*Indexes:* CI = 1.000; RI = 1.000

**Char. #64 (PH07). Pharyngeal sac; associated rakers; base; shape: (0) round; (1) stellate.**

*Description:* Symmetrical pharyngeal-sac raker bases vary from stellate (Figs. 45, 53C-D, 55C-F, 56C-D) to round (Figs. 42, 53A-B, 54H, 55A-B, 56A-B).

*Remarks:* Raker bases are round in Tetragonuridae and Ariommatidae, and stellate in Nomeidae and Stromateidae.

*Inapplicability:* This character is inapplicable for fishes lacking a pharyngeal sac (Char. ##58, state 0), and for stromateiforms with pharyngeal-sac rakers with irregular base (Char. #63, state 0).

*Indexes:* CI = 1.000; RI = 1.000

## Fins

**Char. #65 (FN01). Dorsal fin; spines; occurrence: (0) present, (1) absent**

*Description:* See Character #1.

*Indexes:* CI = 0.333; RI = 0.333

**Char. #66 (FN02). Dorsal fin; spinous, pungent spine; occurrence (0) present, (1) absent**

*Description:* See Character #1 (Figs. 8, 9, 18).

*Inapplicability:* Inapplicable for taxa lacking dorsal-fin spines (Char. #65, state 1).

*Indexes:* CI = 0.125; RI = 0.741

**Char. #67 (FN03). Dorsal fin; anterior and posterior portions:** (0) continuous to each other; (1) separated from each other.

*Description:* The dorsal fin of percomorphacean fishes are often divided in an anterior spinous portion and a posterior non-spinous portion (Fig. 8). Most percomorphaceans have the anterior and posterior portions continuous to each other. A few taxa (*e.g.* Mugilidae, Atherinopsidae), however, have a complete separation between into an anterior and a posterior dorsal fin. The landmark herein used to separate the continuous from a non-continuous dorsal fin is the presence of a continuous interradiial membrane uniting the last fin ray of the anterior portion to the first ray of the posterior portion.

*Indexes:* CI = 0.091; RI = 0.545

**Char. #68 (FN04). Dorsal fin; insertion; location:** (0) on first interneural space; (1) on second interneural space; (2) on third interneural space [multistate additive].

*Description:* Among percomorphaceans, the dorsal-fin insertion (*i.e.* the position of the first dorsal-fin pterygiophore) is usually between the second and third neural spines (= second interneural space *sensu* Johnson, 1984; Fig. 18). Nevertheless, shifts on the dorsal-fin insertion are not uncommon, and these result in the dorsal fin inserting in the first or third interneural spaces.

*Remarks:* More conspicuous shifts of the dorsal-fin insertion (anterior or posterior) do happen in some taxa. These variations usually affect the taxon's pre-dorsal length and are coded in Character #16

*Inapplicability:* This character is inapplicable for taxa exhibiting a dorsal-fin insertion in interneural spaces other than the first three.

*Indexes:* CI = 0.286; RI = 0.286

**Char. #69 (FN05). Dorsal fin; supernumerary anteriormost dorsal-fin rays or spines; articulation with the first dorsal-fin pterygiophore; occurrence:** (0) present; (1) absent (Johnson, 1986: Char. #2, modified).

*Description:* Percomorphaceans have either one or two supernumerary rays or spines articulating with the first dorsal-fin pterygiophore (Fig. 18). A modified condition describes a situation in which all dorsal-fin rays (or spines) are in serial association to the dorsal-fin pterygiophores (*i.e.* there is no supernumerary ray articulating to the first pterygiophore).

*Remarks:* This character results a synapomorphy for Ophidiiformes. Both *Dinematichthys ilucoeteoides* and *Raneya brasiliensis* have no supernumerary rays articulating to the first dorsal-fin pterygiophore.

*Inapplicability:* This character is inapplicable for *Brama caribbea* (Bramidae), which exhibits supernumerary dorsal-fin pterygiophores rather than supernumerary spines.

*Indexes:* CI = 1.000; RI = 1.000

**Char. #70 (FN06). Dorsal fin; supernumerary anteriormost dorsal-fin rays or spines; articulation with the first dorsal-fin pterygiophore; number: (0) two; (1) one (Johnson, 1986: Char. #2, modified).**

*Description:* Most generalized percomorphaceans have two supernumerary rays or spines articulating with the first dorsal-fin pterygiophore, both with non-serial association with the remaining pterygiophores (Fig. 18; Rosenblatt & Bell, 1976: Fig. 12). A modified, less frequent condition describes a single supernumerary spine without serial association to the first dorsal-fin pterygiophore.

*Inapplicability:* This character is inapplicable for taxa lacking supernumerary anteriormost rays or spines (Char. #69, state 1), and for *Brama caribbea* (Bramidae) that exhibits supernumerary dorsal-fin pterygiophores.

*Indexes:* CI = 0.077; RI = 0.571

**Char. #71 (FN07). Dorsal fin; anteriormost dorsal-fin rays: (0) not blade-like; (1) blade-like.**

*Description:* In Stromateidae, the anteriormost three (in *Peprilus*) or eight dorsal-fin rays (in *Pampus*) are modified into flat, keeled, bladelike spines with pointy ends oriented both anterior and posteriorly.

*Remarks:* The presence of blade-like anteriormost dorsal-fin rays constitute a synapomorphy for *Pampus* + *Peprilus* (see Clade V).

*Indexes:* CI = 1.000; RI = 1.000

**Char. #72 (FN08). Pelvic fin; occurrence: (0) present; (1) absent**

*Description:* Pelvic fins are primitively present in gnathostomes, with several independent events of loss occurring in specific subgroups. Among the examined percomorphaceans, pelvic fins are absent in the Stromateidae and Trichiuridae.

*Remarks:* Pelvic fins are absent in all life stages of stromateids, except in juveniles of *Stromateus fiatola*. Young specimens of *S. fiatola* (*i.e.* < 100 mm SL) exhibit a small pelvic fin that progressively reduces during specimen growth. A 68.7 mm SL juvenile (USNM, uncatalogued) has a pelvic fin with four (I+3) rays (Fig. 57). Adult *Stromateus fiatola* completely lack pelvic fins, as do other stromateids.

Absence of pelvic fins constitutes a synapomorphy for the Stromateidae and an autapomorphy for *Trichiurus lepturus* (Trichiuridae).

*Indexes:* CI = 0.500; RI = 0.750

**Char. #73 (FN09). Pelvic fin; lateralmost pelvic ray: (0) spinous, pungent spine, (1) soft spine**

*Description:* The pelvic fin of acanthopterygians is usually supported by a lateralmost spine, and followed by a series of branched and segmented soft rays. The lateralmost, leading pelvic-fin ray varies from a stiff, robust, and pungent spine to a slender, rather fragile, soft spine.

*Inapplicability:* Inapplicable for specimens lacking pelvic fins (Char. #72).

*Indexes:* CI = 0.167; RI = 0.762

**Char. #74 (FN10). Pelvic fin; medialmost branched pelvic-fin ray; membranous attachment with the abdominal wall; occurrence: (0) absent; (1) present.**

*Description:* In the generalized teleostean condition, the pelvic fins attach to the abdomen only at its basal portion. In several percomorphaceans, however, an additional attachment occurs by means of a thin expansion of the interradiial membrane, which connects the last pelvic-fin ray to the ventral surface of the abdomen (Fig. 9).

*Inapplicability:* Inapplicable for specimens lacking pelvic fins (Char. #72).

*Indexes:* CI = 0.083; RI = 0.476

**Char. #75 (FN11). Pelvic fin; free pelvic radials; occurrence:** (0) absent; (1) present. (Johnson, 1992; Johnson & Patterson, 1993: Char. #31).

*Description:* Free pelvic radials are either cartilaginous or ossified round structures that lie between the proximal portions of the pelvic-fin rays, articulating the fin to the pelvic bone.

*Remarks:* Johnson & Patterson (1993) proposed the absence of pelvic radials as a synapomorphy for the Percomorphacea. According to the authors, all percomorphacean immediate outgroups have at least one free pelvic radial at the posterior margin of the pelvic bone, associated either to the pelvic spine or to some of the pelvic-fin rays. Loss of free pelvic radials occur in nearly all percomorphacean lineages, and in this context, such absence could be optimized as an additional synapomorphy for the clade (Johnson & Patterson, 1993: Char. #31). Stiassny and Moore (1992) also listed the absence of free pelvic radials as a synapomorphy of their *higher percomorphs*. However, by placing the atherinomorphs outside Percomorphacea, the loss of free radials would require independent losses in both lineages. Johnson & Patterson (1993) solved this character conflict by placing Smegmamorpharia (atherinomorphs included) into Percomorphacea.

The synapomorphic status of the absence of pelvic radials for Percomorphacea is confirmed by our study. Reversals within this character are uncommon within the group, and among the sampled taxa, occur Caristiidae and Ophidiiformes. In *Caristius macropus*, there are two cartilaginous radials: one very large fused to the medial most pelvic-fin ray, and a small one immediately lateral to it. In Ophidiiformes, there is a single cartilaginous radial articulating to its only pelvic-fin ray. In the literature, reversals of this condition are reported for callionymids and gobiesocids (Gosline, 1970; Johnson & Patterson, 1993).

*Inapplicability:* Inapplicable for specimens lacking pelvic fins (Char. #72).

*Indexes:* CI = 0.333; RI = 0.600

**Char. #76 (FN12). Anal fin; spines; occurrence:** (0) present, (1) absent

*Description:* See Character #8.

*Remarks:* Anal-fin spines are primitively present in the examined taxa and lost in the Ophidiiformes, *Icosteus*, and *Paralichthys*.

*Indexes:* CI = 0.500; RI = 0.667

**Char. #77 (FN13). Anal fin; spinous, pungent spines; occurrence: (0) present, (1) absent**

*Description:* See Character #8.

*Indexes:* CI = 0.167; RI = 0.815

**Char. #78 (FN14). Caudal fin; posterior margin, shape: (0) concave; (1) straight; (2) convex [multistate non-additive].**

*Description:* In the examined taxa, the posterior margin of the caudal fin is either concave, straight, or convex (Fig. 14). Concave caudal fins exhibit the median fin rays progressively shorter than the remaining dorsal and ventral principal rays, and this category encompasses the so-called forked, lunate, and emarginate caudal fins. Codification of these subtypes is often ambiguous as there is a series of intermediate conditions between them. Truncate caudal fins are characterized by a vertical straight line delimitating the posterior margin of the fin. Convex caudal fins exhibit the median fin rays longer than the remaining ones, which are gradually shorter both dorsally and ventrally.

*Inapplicability:* Inapplicable for *Trichiurus lepturus* (Trichiuridae), which lacks a caudal fin.

*Indexes:* CI = 0.286; RI = 0.444

**Char. #79 (FN15). Caudal fin; paired fleshy caudal keels; occurrence: (0) absent; (1) present (Johnson, 1986, Char. #14).**

*Description:* Caudal keels are a pair of horizontal, longitudinal fleshy keels lying at the base of the caudal fin.

*Optimization:* On the present analysis, paired fleshy caudal keels are present in the scombroids *Auxis thazard* and *Scomber* sp. and constitute a unique synapomorphy for the Scombridae. Among Scombriformes, these structures are present in all scombrids, istiophorids and the gempylid *Lepidocybium* (Johnson, 1986).

*Inapplicability:* Inapplicable for *Trichiurus lepturus* (Trichiuridae), which lacks a caudal fin.

*Indexes:* CI = 1.000; RI = 1.000

**Char. #80 (FN16). Caudal fin; first and second hypurals; fusion: (0) not fused; (1) fused.**

*Description:* This character accounts to the number of free (*i.e.* unfused) hypural elements on the lower caudal-fin lobe (Figs 15-17, 58).

*Remarks:* Although not coded herein as an independent character, the reduction from six to five hypural bones has been proposed to be a synapomorphy for the Percomorphacea (Johnson & Patterson, 1993; Wiley & Johnson, 2010). The choice of not using this character on the analysis can be explained by the outgroup choice. Previous studies point that Beryciforms primitively have six hypurals, but this number was independently reduced berycids and holocentrids, both taxa used as percomorphacean outgroups on the present analysis.

*Inapplicability:* Inapplicable for *Trichiurus lepturus* (Trichiuridae), which lacks a caudal fin.

*Indexes:* CI = 0.111; RI = 0.704

**Char. #81 (FN17). Caudal fin; third and fourth hypurals; fusion: (0) not fused; (1) fused.**

*Description:* This character accounts to the number of free (*i.e.* unfused) hypural elements on the upper caudal-fin lobe (Figs 15-17, 58).

*Remarks:* Fusion of hypurals can occur independently on the upper and lower caudal-fin lobe, which justifies coding both variables in different characters. On the present analysis, the fusion of lower hypural elements not followed by the upper elements was observed in *Atherinella brasiliensis* (Atherinopsidae; Fig. 15B).

*Inapplicability:* This character is inapplicable for *Trichiurus lepturus* (Trichiuridae), which lacks a caudal fin.

*Indexes:* CI = 0.111; RI = 0.692

**Char. #82 (FN18). Caudal fin; first and second hypurals; relationships with the parhypural: (0) not fused; (1) fused**

*Description:* The caudal fin of percomorphacean fishes is highly variable in several attributes, including ray count (Char. #10, #13, #14), ray morphology (Char. #84, #85), and bone fusion (Char. #80, #81). One of the most remarkable examples is observed in representatives of Ariommatidae. In these fishes the ventral hypural plate (formed by hypurals 1 and 2 in adults) is completely fused to the parhypural (Fig. 58). A broad contact between the parhypurals and hypurals 1-2 do occur in other percomorphaceans (e.g. *Psenopsis cyanea*; *Tubbia tasmanica*: Centrolophidae; Fig. 16B). Such morphology, however, contrast from Ariommatidae by never occurring at the preural and ural centra and by leaving a suture line along the parhypural-hypural contact.

*Remarks:* Aside ariommatids, a complete parhypural-hypural fusion is also reported for some scombrids (i.e. *Gymnosarda*, *Acanthocybium*, and variably present in species of *Scomberomorus*: Collette & Chao, 1975: fig. 56e).

*Inapplicability:* This character is inapplicable for *Trichiurus lepturus* (Trichiuridae), which lacks a caudal fin.

*Indexes:* CI = 1.000; RI = 1.000

**Char. #83 (FN19). Caudal fin; epurals; number: (0) three; (1) two**

*Description:* Epurals are a series of small bones of the caudal skeleton located between the last neural spine and the dorsalmost hypural plate. Number of epurals varies little among percomorphaceans, being three epurals the most common condition among these fishes (Figs 15A, 16, 17, 58). Reduction to two epurals (Fig. 15B) is uncommon among percomorphaceans, and often mentioned as phylogenetically informative (Hilton & Johnson, 2007).

*Inapplicability:* This character is inapplicable for taxa lacking epural bones (*Raneya brasiliensis*: Ophidiidae), taxa lacking a caudal fin (*Trichiurus lepturus*: Trichiuridae), and taxa known to exhibiting fusion (and not loss) of epurals (e.g. carangids, *sensu* Hilton & Johnson, 2007).

*Indexes:* CI = 0.125; RI = 0.417

**Char. #84 (FN20). Caudal fin; posteriormost ventral procurrent ray; procurrent spur; occurrence:**  
(0) absent; (1) present

*Description:* The procurrent spur is a bony process that projects from the posteriormost (= last) ventral procurrent ray and partially overlaps the preceding ray (Fig. 15A, arrow; Johnson, 1975: fig. 2). When present, this spur is used as attachment site for a tendon of the ventral bundle of the of the *flexor ventralis inferior*. Taxa lacking the procurrent spur (Fig. 15B) have that tendon attaching directly to the main body of the procurrent ray. The occurrence of the procurrent spur is variable in higher levels of the Percomorphacea, but apparently stable within its families.

*Inapplicability:* This character is inapplicable for *Trichiurus lepturus* (Trichiuridae) that lacks a caudal fin.

*Indexes:* CI = 0.091; RI = 0.655

**Char. #85 (FN21). Caudal fin; penultimate ventral procurrent ray; ray base: (0) not shortened; (1) shortened** (Johnson & Patterson, 1993: Char. #24).

*Description:* Fishes with a procurrent spur often exhibit a shortening on the base of the procurrent ray preceding the procurrent spur (Fig. 15A, 16). In such a condition, the base of penultimate procurrent ray may, or may not extend forward proximally to meet the bases of the remaining procurrent rays, but often originates slightly posterior to the overlapping procurrent spur. The preceding ray base is coded as not shortened only when its anteriormost tip is completely aligned to tip of other procurrent fin rays (Fig. 15B). A shortened state, in its turn, is coded when the procurrent ray exhibit a shortening of its base. Although the presence of a procurrent spur is often associated with a shortening of the base of the penultimate ventral procurrent ray, these attributes are not always dependent, and are herein tested in two independent characters.

*Remarks:* The present character is adapted from the studies of Johnson (1975). The author treated the degree of reduction of the second last ventral procurrent ray as a multistate character: the procurrent ray base could be shortened, slightly shortened, or not shortened. In order to avoid ambiguity over the slightly shortened/ shortened states, the present character is expressed herein in only two variables.

*Inapplicability:* This character is inapplicable for *Trichiurus lepturus* (Trichiuridae) due to the absence of a caudal fin.

*Indexes:* CI = 0.091; RI = 0.600

**Char. #86 (FN22). Finlets; occurrence: (0) absent; (1) present.** (Johnson, 1986: Char. #12).

*Description:* Finlets are short, widely spaced fin rays not interconnected by interradial membrane present at the dorsal and ventral profiles of the caudal peduncle of most Scombriformes. Finlets are supported by pterygiophores with elongate, autogenous middle radials, and are considered serially homologous to the regular fin rays of the dorsal anal fins.

*Remarks:* Outside the Scombriformes, finlets are also known to occur only in some Carangidae (e.g. *Megalaspis* spp.).

*Indexes:* CI = 0.500; RI = 0.500

## **Pectoral girdle**

**Char. #87 (PE01). Cleithrum; serrations on the posterior margin: (0) absent; (1) present** (Otero, 2004: Char. #27).

*Description:* Marginal serrations along the distal margin of the cleithrum is uncommon and observed in a few percomorphaceans. When present, these serrations are located on the distal margin of the cleithrum (Figs. 10, 19, 22, 33) and often covered by skin.

*Indexes:* CI = 0.333; RI = 0.600

**Char. #88 (PE02). Third postcleithrum; attachment to the anal fin: (0) absent; (1) present.**

*Description:* Percomorphaceans usually have two or three postcleithra, which contact the cleithrum dorsally, and each other ventrally (*i.e.* postcleithra 1 with 2, and postcleithra 2 with 3). The third postcleithrum is usually a very long and narrow ossification that runs along a myoseptum from the pectoral-fin base to the ventral edge of the body. The location of the third postcleithrum posterior edge varies among the analyzed taxa. In the most common condition, the postcleithrum reaches the ventral profile of the body, falling short in a region situated posterodorsally to the pelvic girdle (Fig. 59). In *Pepriulus* (Stromateidae) and in *Amniataba caudavittata* (Terapontidae), however, the postcleithrum extends posteriorly reaching the first anal-fin pterygiophore.

*Remarks:* This characteristic results as a synapomorphy for the genus *Peprilus*, with a parallel acquisition in *Amniataba caudavittata* (Terapontidae).

*Indexes:* CI = 0.500; RI = 0.500

**Char. #89 (PE03). Coracoids; anteroventral portion; contact with the cleithrum: (0) straight; (1) curved.**

*Description:* The coracoid of percomorphacean fishes occupy the ventromedial portion of the pectoral girdle. Although the coracoid morphology varies considerably throughout percomorphaceans, this bone exhibits stable limits concerning its contact with other bones. Dorsally the coracoid contacts the scapula and the medial surface of the cleithrum, and anteriorly it contacts the ventral portion of the cleithrum through a long and nearly straight ventral limb or bony process (Collette & Chao, 1975: fig. 72; Rosenblatt & Bell, 1976: fig. 8; Tyler *et al.* 1989: fig. 11). The lateral surface of the coracoid serves almost entirely as site of origin of the *abductor profundus* muscle, which also originates from the ventral and posterior sides of the cleithrum.

In most of the analyzed specimens, the ventral limb of the coracoid meets the cleithrum in a straight line (Fig. 10). This contrasts to the morphology observed in Nomeidae, which always exhibit an anterior coracoidal flexion before contacting the cleithrum (Figs. 11, 12, 59) This flexion can either be discrete and restricted to its anterior portion (Fig. 11), or a large posteroventral expansion before contacting the cleithrum (Figs. 12, 59). In either case, these modifications are consequence of a hypertrophied *abductor* and *adductor profundus* muscles. While most percomorphaceans exhibit the *abductor* and the *adductor profundus* roughly comparable in size to the *superficialis* section, in Nomeidae these muscles are enlarged and occupy a vast ventro lateral portion below the pectoral fin.

*Remarks:* The flexed anterior portion of the coracoid results as a synapomorphy for the Nomeidae, with homoplastic events in *Beryx splendens* (Berycidae) and *Brama caribbea* (Bramidae). Further modifications on the coracoid morphology (*i.e.* Chars. #90, #91 below) are informative within the internal arrangement of Nomeidae, and are treated below.

*Indexes:* CI = 0.333; RI = 0.667

**Char. #90 (PE04). Coracoids; anteroventral portion; margin: (0) not exposed on ventral midline of the body; (1) exposed on ventral midline of the body.**

*Description:* The *abductor* and *adductor profundus* enlargement is variable within Nomeidae and, as consequence, the posteroventral expansion of the coracoids are expressed in different degrees. In *Nomeus gronovii* (Fig. 11), it takes form as a rather discrete flexion on its anterior portion, with the coracoids never being exposed on the ventral midline of the body. In other Nomeidae (Figs. 12, 59) and in a few outgroup taxa, the expanded coracoids reach the ventral profile of the body and meet the cleithrum in a perpendicular angle. In the latter taxa, the coracoids are visible after a simple removal of the skin covering the ventral portion of the body.

*Inapplicability:* This character is inapplicable for taxa exhibiting a straight coracoid ventral margin (Char. #89, state 0).

*Indexes:* CI = 1.000; RI = 1.000

**Char. #91 (PE05). Coracoids; ventral margin: (0) not angled; (1) angled.**

*Description:* Among the taxa exhibiting an enlarged coracoid, the ventral margin of this bone can exhibit a smooth curve (Fig. 11), or a nearly perpendicular angle (Figs. 12, 59).

*Remarks:* Angled coracoids are exclusively present in the genus *Cubiceps* (Nomeidae).

*Inapplicability:* This character is inapplicable for taxa exhibiting a straight coracoid ventral margin (Char. #89, state 0).

*Indexes:* CI = 0.500; RI = 0.500

## **Pelvic girdle**

**Char. #92 (PV01). Pelvic girdle; occurrence: (0) present; (1) absent**

*Description:* Pelvic girdle and fins are primitively present in fishes. Losses of pelvic fins, however, do not imply on loss of the pelvic girdle, in such a way that some taxa lacking a pelvic fin may still exhibit a rudimentary pelvic girdle.

*Remarks:* Pelvic girdle loss occur exclusively in Trichiuridae. This is an autapomorphy for the family according to the present analysis.

*Indexes:* CI = 1.000; RI = 1.000

**Char. #93 (PV02). Pelvic girdle; relationship between contralateral basipterygia: (0) tightly attached to each other; (1) loosely attached to each other** (Stiassny & Moore, 1992: Char. #01, modified).

*Description:* Percomorphaceans usually exhibit the contralateral basipterygia strongly bound or sutured to each other at their medial borders (Fig. 13). The median suture is more-or-less straight on the ventral surface of the girdle, although deep interdigitating sutures are often visible in this region. Some percomorphaceans, however, have the basipterygia loosely attached to each other. In such cases, they are observed overlapping each other, or simply lying on the abdominal tissue.

*Remarks:* The Beryciformes (Stiassny & Moore, 1992: fig. 5, A) and Stephanoberyciformes exhibit pelvic halves overlapping each other, but not sutured medially. This is also present in Atheriniformes (Stiassny & Moore, 1992: Fig. 9B) and in *Icosteus*. In the mugilid *Mugil curema* the pelvic girdles are tightly bound medially (character state 0) but lacking a bony suture. In the stromateid *Stromateus brasiliensis* and *Pampus cinereus*, the pelvic fins are lost, and the pelvic girdles are reduced to two long rods of bones, that do not exhibit a medial fusion (character-state 1).

*Inapplicability:* This character is inapplicable for *Trichiurus lepturus* (Trichiuridae), which lacks a pelvic girdle (Char. #92, state 1).

*Indexes:* CI = 0.167; RI = 0.375

**Char. #94 (PV03). Pelvic girdle; fusion between the contralateral basipterygia: (0) absent; (1) present**

*Description:* Percomorphaceans usually exhibit the contralateral basipterygia strongly bound or sutured to each other. In the stromateid *Peprilus* both bones are fused to each other at their posterior portions, leaving no trace of bony suture between the basipterygia (Fig. 60A).

*Remarks:* Fused basipterygia were not observed in any other taxon and constitutes a unique synapomorphy for *Peprilus* (Stromateidae).

*Inapplicability:* This character is inapplicable for *Trichiurus lepturus* (Trichiuridae), which lacks a pelvic girdle (Char. #92, state 1).

*Indexes:* CI = 1.000; RI = 1.000

**Char. #95 (PV04). Pelvic girdle; posteriorly oriented spine: (0) absent; (1) present.**

*Description:* Spines modified from pelvic-fin rays are of common occurrence among percomorphacean fishes (Char. #73, state 0). However, spiny projections emerging directly from the basipterygia are rare in Percomorphacea. A round, posteriorly projected spine is uniquely observed in fishes of the genus *Peprilus* (Stromateidae; Fig. 60B).

*Optimization:* The presence of a pelvic-girdle spine, which is visible externally preceding the anal fin, is a unique synapomorphy for the genus *Peprilus* (Stromateidae). This feature has often been used to diagnose the genus from the other stromateiforms (Haedrich, 1967; Horn, 1970).

*Inapplicability:* This character is inapplicable for *Trichiurus lepturus* (Trichiuridae), which lacks a pelvic girdle (Char. #92, state 1).

*Indexes:* CI = 1.000; RI = 1.000

**Char. #96 (PV05). Pelvic girdle; basipterygia, length: (0) anterior edge of the basipterygia touching the cleithrum; (1) anterior edge of basipterygia not touching the cleithrum.**

*Description:* Primitively in percomorphaceans, the basipterygium is positioned anteroventrally in the body. Often, its anterior edge reaches the cleithrum and/ or the coracoid, attaching to these bones through a strong conjunctive tissue. However, in several taxa the basipterygium is shortened and does not reach the pectoral-girdle bones anteriorly. In these cases, the connection between the pectoral and pelvic girdles is either wanting, or made through an anteromedial ligament (Char. #194).

*Inapplicability:* This character is inapplicable for *Trichiurus lepturus* (Trichiuridae), which lacks a pelvic girdle (Char. #92, state 1).

*Indexes:* CI = 0.167; RI = 0.545

## **Axial skeleton**

**Char. #97 (AX01). Epineural 1; proximal attachment; location: (0) on the neural arch; (1) on a laterally expanded parapophysis (Johnson & Patterson, 1993: Char. #34).**

*Description:* Stephanoberyciformes, Beryciformes, and most Percomorphacea exhibit the proximal portion of the first two epineurals attached to the neural arch of the first vertebrae, or to

the vertebral body. This morphology contrasts that observed in *Mugil curema* (Mugilidae) and *Atherinella brasiliensis* (Atherinopsidae), which exhibit the epineural 1 connected to a large lateral parapophysis on the first vertebra.

*Remarks:* This character has been proposed as the single synapomorphy for the smegmamorphs according to Johnson & Patterson (1993) (= Smegmamorpharia *sensu* Wiley & Johnson, 2010). This group unites the Synbranchidae, Mastacembelidae, Elasmobranchiidae, Gasterosteiformes, Mugiliformes, and Atheriniformes (and is named after an anagram of their initials, which spells the word smegma). According to Johnson & Patterson (1993), besides the epineural 1 originating from a lateral expanded parapophysis, fishes of this group also shares 33 putative derived characteristics (Johnson & Patterson, 1993: table 2). These would further strengthen the monophyly of this clade, or arrangements within them. Currently, the Smegmamorpharia is placed inside the Percomorphacea *sensu* Wiley & Johnson, 2010, and compose one of the few resolved clades within the division.

According to our results, the attachment of the epineural 1 on a laterally expanded parapophysis can be optimized as a synapomorphy for the smegmamorphs Mugiliformes + Atherinomorphs under certain character reconstructions.

*Inapplicability:* This character is coded as inapplicable for *Aulostomus maculatus* (Aulostomidae) due to the impossibility to homologize which epineural is associated to its highly elongated first vertebral centrum. *Icosteus aenigmaticus* (Icosteidae) and *Monocirrhus polyacanthus* (Polycentridae) lack epineurals.

*Indexes:* CI = 1.000; RI = 1.000

**Char. #98 (AX02). Epineural 1; morphology:** (0) not expanded anteroposteriorly; (1) expanded anteroposteriorly.

*Description:* In most analyzed taxa, the epineurals are observed as a series of long rod-like bones. However, in the kyphosids *Kyphosus sectatrix* and *Microcanthus strigatus*, the kuhliid *Kuhlia marginata*, and the oplegnathid *Oplegnathus fasciatus*, the first epineural exhibits a flat anteroposterior expansion.

*Inapplicability:* See Char. #97.

*Indexes:* CI = 0.333; RI = 0.333

**Char. #99 (AX03). Epineural 3; proximal attachment; location: (0) on vertebra 3; (1) on rib 1** (Johnson & Patterson, 1993: Char. #32, modified).

*Description:* Most percomorphaceans exhibit the epineural 3 and subsequent bones attaching proximally to the first ribs. This morphology contrasts to that observed in some taxa, which exhibit the epineural 3 and the remaining bones of the series contacting the vertebral centrum or parapophysis.

*Remarks:* Johnson & Patterson (1993) proposed this and the following character in a slightly modified fashion as one of the eight synapomorphies supporting their Percomorpha (currently Percomorphacea *sensu* Wiley & Johnson, 2010). The character was originally proposed as “*point of origin of all but first two epineurals displaced ventrally, and distal parts of all epineurals displaced ventrally into horizontal septum*”. Although initially proposed as a single character, there are at least two independent modifications occurring in the percomorphacean epineurals: 1) a ventral shift on its point of origin; and 2) its distal-tip position in relation to the horizontal septum. These are coded herein in two independent characters (current Char. #99, and following Char. #100).

Our results indicate that the proximal attachment of epineural 3 to the first rib is plesiomorphically present in percomorphaceans, as well as in the Beryciformes analyzed herein. We therefore do not corroborate the synapomorphic status of this character to the Percomorphacea node.

*Inapplicability:* See Char. #97.

*Indexes:* CI = 0.143; RI = 0.400

**Char. #100 (AX04). Epineurals 4 – last; distal portion; location: (0) above the horizontal septum; (1) along the horizontal septum.** (Johnson & Patterson, 1993: Char. #32, modified).

*Description:* The general Percomorphacea arrangement of the epineural series to exhibit their proximal portions attached to the vertebra or ribs, and their distal portion lying along the horizontal septum with their tips visible just beneath the skin (Johnson & Patterson, 1993; Patterson & Johnson, 1995: fig. 15, b-d; Tyler *et al.*, 1989: figs. 23-33). This morphology is contrasting to that observed in Beryciformes, which exhibits the epineural 4 and the following epineural series bending in an ascending and progressively drifting dorsally from the horizontal septum (Patterson & Johnson, 1995: Fig. 15b).

*Remarks:* We corroborate the presence of epineural 4 to the last along the horizontal septum as a synapomorphy for the Percomorphacea.

*Inapplicability:* In *Raneya brasiliensis* (Ophidiidae), the epineurals 2 to 5 are along the horizontal septum, but from epineural 6 and on are below the horizontal septum. In *Trichiurus lepturus* (Trichiuridae), there is no evident separation of a horizontal septum. In *Tetragonurus cuvieri* (Tetragonuridae), the location of epineurals along the septum could not be attested since epineurals 4 and following are unossified. These taxa were coded as inapplicable for this character. For the remaining taxa coded as inapplicable, see *remarks* from Character #97.

*Indexes:* CI = 1.000; RI = 1.000

**Char. #101 (AX05). Supraneurals; occurrence: (0) present, (1) absent.**

*Description:* Supraneurals (=predorsals *sensu* Smith & Bailey, 1961) are elongate splinter bones that precede the pterygiophores supporting the dorsal and anal fins (Fig. 18; Mabee, 1988). Occurrence of supraneurals is variable among percomorphaceans, as this bone is absent in a few groups (*i.e.* most Scombriformes, some Carangiformes, and in Pleuronectiformes). Number of supraneurals is also variable across the analyzed taxa, and these are accounted in Character #11.

*Remarks:* Absence of supraneurals have been independently proposed as synapomorphy for the superorder Atherinomorphae (Parenti, 1993), Gobiiformes (Springer, 1983), Acanthuriformes (Wiley & Johnson, 2010), Cottiformes (Imamura & Yabe, 2002), Elasmobranchii (Johnson & Patterson, 1993), and Echeoichthyoidei (Smith-Vaniz, 1984). According to our results, absence of supraneurals is synapomorphic to subgroups within Carangiformes, Scombriformes, and independently absent in Atherinopsidae.

*Indexes:* CI = 0.143; RI = 0.600

**Char. #102 (AX06). First supraneural bone; location: (0) between supraoccipital and first neural spine; (1) between first and second neural spines.**

*Description:* The arrangement of supraneural bones in relation to the anteriormost vertebral neural spines is fairly variable among percomorphaceans, and together with the number of these structures, it is an important taxonomic character for percomorphaceans (*e.g.* Centrolophidae:

Ahlstrom *et al.* 1976; Carangidae: Springer & Smith-Vaniz, 2008). The supraneural number and arrangement in relation to the neural spines or dorsal-fin pterygiophores have been traditionally treated under the complex character named *predorsal formula* (Ahlstrom, 1976; Johnson, 1984: tab. 120). The putative primitive percomorphacean predorsal formula would exhibit three supraneurals, which would display the following arrangement: the first supraneural would precede the first neural spine, the second supraneural would lie between the first and second neural spines (first interneural space), and the third supraneural would be placed between the second and third neural spines (second interneural space). In addition, the primitive predorsal formula would also contain the first dorsal-fin pterygiophore inserted in second interneural space, sharing this location with the third supraneural bone (Ahlstrom *et al.*, 1976; Johnson, 1984).

The innumerable possible changes on the primitive predorsal formula clearly indicates that this character express several independent evolutionary events (*e.g.* gain or loss of supraneurals; shift on supraneural position in relation to neural spines; shift of the dorsal-fin insertion in relation to neural spines; number of dorsal-fin pterygiophores comprised in a given interneural space). In order to analyze these events independently, the present study offers each one of these variables as a distinct phylogenetic characters. The present character evaluated the location of the first supraneural bone, which among the analyzed taxa varies from the space between the posterior portion of the skull and the first vertebral neural spine (Fig. 18), or between neural spines 1 and 2. The location of second and third supraneurals are coded in the following characters (#103 and #104, respectively). Additionally, character #11 accounts for the total number of supraneurals, and Characters #16 and #68 evaluates differences on the dorsal-fin insertion.

*Inapplicability:* This character is inapplicable for taxa lacking supraneural bones. This character is inapplicable for *Ariomma bondi*, in which the first supraneural bone is absent. Although *Mugil curema* (Mugilidae) exhibits three supraneurals, they insert posterior to neural spines 2, 3 and 4, respectively. This condition is autapomorphous to this taxon and thus not coded herein.

*Indexes:* CI = 0.500; RI = 0.000

**Char. #103 (AX07). Second supraneural bone; location: (0) between supraoccipital and first neural spine; (1) between first and second neural spines; (2) between second and third neural spines.**

*Description:* This character accounts the location of the second supraneural bone (Fig. 18).

*Inapplicability:* This character is inapplicable for taxa lacking supraneural bones.

*Indexes:* CI = 0.667; RI = 0.000

**Char. #104 (AX08). Third supraneural bone; location:** (0) between supraoccipital and first neural spine; (1) between first and second neural spines; (2) between second and third neural spines; (3) between third and fourth neural spines [multistate additive].

*Description:* This character accounts the location of the third supraneural bone (Fig. 18).

*Inapplicability:* This character is inapplicable for taxa lacking supraneural bones.

*Indexes:* CI = 0.600; RI = 0.600

## MYOLOGY

### ***Adductor mandibulae* muscle complex**

**Char. #105 (AD01). *Adductor mandibulae; segmentum facialis; pars rictalis*; insertion:** (0) solely on the lower jaw; (1) on both lower and upper jaws; (2) solely on the upper jaw [multistate additive].

*Description:* Among percomorphaceans, the *rictalis* section of the *adductor mandibulae* usually originates from the ventrolateral region of the suspensorium, attaching onto the ventrolateral portions of the quadrate and the horizontal arm of the preopercle (Figs. 22-29, 32-38). It inserts onto the lower jaw via intersegmental aponeurosis, which is contiguous with the mandibular segment of the adductor mandibulae (*i.e.* the *segmentum mandibularis*; Figs. 30, 61-63). In some of the analyzed percomorphaceans (in mugilids, atherinids, and polycentrids), part, or all fibers associated to the *rictalis*, extend over and insert onto the upper jaw *via* retrojugal lamina and/or its embedded ligaments.

*Indexes:* CI = 1.000; RI = 1.000

**Char. #106 (AD02). *Adductor mandibulae; segmentum facialis; pars rictalis*; subdivision into *ectorictalis* and *endorictalis* subsections:** (0) absent; (1) present.

*Description:* In a primitive configuration among percomorphaceans, the *adductor mandibulae pars rictalis* does not exhibit segmentations or subdivisions. However, in some of the examined taxa

the *riotalis* is differentiated into an external subsection, referred to as the *ectoriotalis*, and an internal subsection, named *endoriotalis*.

*Indexes:* CI = 0.500; RI = 0.000

**Char. #107 (AD03). *Adductor mandibulae; segmentum facialis; pars malaris; origin: (0) restricted to the suspensorium; (1) on the suspensorium and neurocranium.***

*Description:* Among acanthopterygians the *malaris* section usually originates from the posterodorsal region of the suspensorium, mainly from the lateral surfaces of the hyomandibula and the posterodorsal portion (= vertical arm) of the preopercle (Figs. 22-26, 29, 32-34; 36-37). In some taxa, the *malaris* subsection exhibits a dorsal expansion, with fibers also originating from the frontal, sphenotic, and pterotic (Figs. 27-28, 35, 38).

*Remarks:* Other sites of origin of the *malaris* may involve the subocular shelf (*Lutjanus analis*: Lutjanidae) and the palatine (*Cynoscion striatus*: Sciaenidae). These conditions, however, were not included on the analysis due to their restricted occurrence on the abovementioned taxa.

A *malaris* originating from the skull bones is herein optimized as independent synapomorphies for the clade comprised by Pleuronectiformes + Scombriformes (reversed in Scombridae), Ophidiiformes, for the terminal taxa *Polydactylus virginicus* (Polynemidae), and *Pseudoscopelus altipinnis* (Chiasmodontidae).

*Indexes:* CI = 0.200; RI = 0.500

**Char. #108 (AD04). *Adductor mandibulae; segmentum facialis; pars malaris; origin on the preopercle: (0) origin not reaching the preopercular canal laterally; (1) origin reaching the preopercular canal laterally.***

*Description:* Among the examined acanthopterygians, the origin of the *malaris* section is usually restricted to the dorsolateral surface of the suspensorium, involving the hyomandibula and the posterior portion of the preopercle. In the preopercle, fibers of the *malaris* originate mostly from its vertical arm but vary in relation to its posterior extent. In most percomorphaceans and the analyzed beryciforms, the fibers of the *malaris* are restricted to the anterolateral region of the preopercle, which is often delimited by a vertical keel present on this bone (Figs. 22, 23, 25, 27, 32, 34, 38). This keel separates the anterior surface of the preopercle from the lateral one, which contains the vertical

limb of the preopercular canal (state 0). In a modified state (state 1), fibers of the *malaris* expands posteriorly and invades the lateral surface of the preopercle (Figs. 24, 26, 28, 29, 35-37). This posterior expansion is better comprehended using the preopercular canal as a landmark to map the lateral extension of the *malaris*: in such cases the fibers trespass to the lateral surface of the preopercle and covers the vertical limb of the preopercular canal.

*Inapplicability*: This character is inapplicable for *Kuhlia marginata* (Kuhliidae), which exhibits a narrow preopercle in comparison to other taxa. As consequence, the *malaris* does attach to the posterior limit of the preopercle of *Kuhlia* even though there is no apparent posterolateral expansion of the *malaris* fibers.

*Indexes*: CI = 0.083; RI = 0.607

**Char. #109 (AD05). Adductor mandibulae; segmentum facialis; pars malaris; origin on the preopercle:** (0) origin not reaching the dorsolateral edge of the preopercle; (1) origin reaching the dorsolateral edge of the preopercle.

*Description*: Among taxa exhibiting a posterior extension on the *malaris* origin, this expansion may vary in two unambiguous states: one in which fibers trespass to the lateral surface of the preopercle, cover the vertical limb of the preopercular canal, but does not reach the posterior edge of this bone (Figs. 24, 29, 36); and a more extreme condition in which the fibers extend until the posterior margin of the preopercle (Figs. 28, 30).

*Inapplicability*: This character is inapplicable for taxa not exhibiting a posterior expansion on the *malaris* origin (Char. #108, state 0).

*Indexes*: CI = 0.167; RI = 0.615

**Char. #110 (AD06). Adductor mandibulae; segmentum facialis; pars malaris; insertion:** (0) only to the lower jaw; (1) on both the lower jaw and the retrojugal lamina; (2) only to the retrojugal lamina and/or its embedded ligaments [multistate additive].

*Description*: In a typical acanthopterygian condition (state 1), the *malaris* section inserts to the lower jaw via intersegmental aponeurosis and to the retrojugal lamina via and embedded ligaments (e.g. the endomaxillar ligament; Figs. 22-30, 32-35). Modification in this pattern are expressed as two diverging morphologies. In the first (state 0), the *malaris* loses its connection with the retrojugal

lamina and embedded ligaments, so that the insertion is restricted to the lower jaw by means of the intersegmental aponeurosis (Fig. 36-37, 61-63). A second and less frequent condition (state 2) describes a *malaris* is exclusively associated with the retrojugal lamina and/or ligaments attached to the maxilla and the connection of the section with the intersegmental aponeurosis and lower jaw is completely lost. Such condition is exclusively found in the analyzed Haemulidae (*Orthopristis ruber*), Kyphosidae (*Microcanthus strigatus*), and Polycentridae (*Monocirrhus polyacanthus*).

*Indexes:* CI = 0.222; RI = 0.682

**Char. #111 (AD07). *Adductor mandibulae; segmentum facialis; pars malaris; subdivision into retromalaris and promalaris subsections:* (0) absent; (1) present.**

*Description:* Events of subdivision of the *pars malaris* of the *adductor mandibulae* is variably present among percomorphaceans. These subdivisions often occur towards the insertion of the section, near the maxilla and the posterolateral portion of the retrojugal lamina (Figs. 23-24, 27-29, 33-35). The two resultant subsections are referred to as *retromalaris* for the posterolateral subsection and *promalaris* for the anterodorsal subsection.

*Indexes:* CI = 0.125; RI = 0.741

**Char. #112 (AD08). *Adductor mandibulae; segmentum facialis; pars malaris; retromalaris and promalaris subsections; degree of subdivision:* (0) sections not completely subdivided; (1) sections completely subdivided.**

*Description:* Among the taxa exhibiting differentiated *retromalaris* and *promalaris*, the degree of subdivision between these subsections varies from a differentiation towards the muscle insertion (Figs. 23-24, 29, 33) to a complete separation between subsections (Figs. 27-28, 34-35).

*Inapplicability:* This character is inapplicable for taxa lacking subdivisions of the *pars malaris* of the *adductor mandibulae* (Char. #111, state 0).

*Indexes:* CI = 0.250; RI = 0.500

**Char. #113 (AD09). *Adductor mandibulae; segmentum facialis; pars stegalis; subdivision into epistegalis and substegalis subsections:* (0) absent; (1) present.**

*Description:* The *adductor mandibulae, pars stegalis* is the innermost component of the *segmentum facialis*, usually not visible laterally. The section originates from the lateral surfaces of the metapterygoid and the anterior portion of the hyomandibula, and ventrally converges to the meckelian tendon and/or the ventral portion of the intersegmental aponeurosis (Figs. 30, 61-63). Most frequently, the *stegalis* appears as a single unit, lacking any type of segmentation. However, in some of the examined taxa, the *stegalis* is differentiated into an anterodorsal subsection, *epistegalis*, and a posteroventral subsection, *substegalis*.

*Indexes:* CI = 0.200; RI = 0.200

**Char. #114 (AD10). *Adductor mandibulae; segmentum facialis; rictalis* and *malaris*; degree of separation:** (0) completely separated; (1) partially separated; (2) completely continuous [multistate additive].

*Description:* The *segmentum facialis* of the *adductor mandibulae* is often differentiated in three main sections, namely the *rictalis*, *malaris*, and *stegalis*. In several instances, two or more facial sections of the *adductor mandibulae* may be continuous to each other. The coalescence between these sections is observed as either some shared fibers between clearly recognizable sections (usually towards the point of insertion), or as a total continuum between the muscle fibers. Among the examined acanthopterygians, the degree of separation between the *rictalis* and *malaris* exhibits three types of recognizable variation. These sections may be separated from each other along their entire extent (state 0; Fig. 61), separated at origin but gradually continuous to each other towards insertion (state 1), or completely non-separated and forming a compound section (state 2; Figs. 22-25, 30, 32, 33, 37, 62, 63). This resulting compound section may correspond to either the *ricto-malaris*, in the taxa with undivided *malaris*, or the *ricto-retromalaris* (e.g., Centrolophidae and *Pseudoscopelus*), in species with *malaris* differentiated into *promalaris* and *retromalaris* (Char. #111, state 1).

*Remarks:* Completely fused muscle bundles are considered only in cases where there is no trace of separation between bundles. If bundles are somewhat detectable (e.g. muscle bundles are superficially, or proximally separated), these are coded as character state 1. Accordingly, character state 2 describes only cases where muscle bundles are completely separated (i.e. there are no muscle fibers shared between bundles).

*Indexes:* CI = 0.069; RI = 0.386

**Char. #115 (AD11). *Adductor mandibulae; segmentum facialis; rictalis and stegalis; degree of separation:* (0) completely separated; (1) partially separated; (2) completely continuous [multistate additive].**

*Description:* In percomorphaceans, the separation between fibers of the *rictalis* and *stegalis* vary from complete (state 0), partial (state 1), or absent (state 2). The resulting compound section formed by the non-differentiation between these sections is termed *ricto-stegalis* (Figs. 34-36, 61).

*Remarks:* Same as Character #114.

*Indexes:* CI = 0.095; RI = 0.345

**Char. #116 (AD12). *Adductor mandibulae; segmentum facialis; malaris and stegalis; degree of separation:* (0) completely separated; (1) partially separated; (2) completely continuous [multistate additive].**

*Description:* As in the case of the two preceding characters, the degree of separation between the *malaris* and *stegalis* exhibit a clinal series of three states (total, partial, or no separation), with the undifferentiated compound section been termed *stego-malaris*.

*Remarks:* Same as Character #114.

*Indexes:* CI = 0.091; RI = 0.355

**Char. #117 (AD13). *Adductor mandibulae; segmentum mandibularis; anterior portion:* (0) not notched anteriorly; (1) notched anteriorly.**

*Description:* The *segmentum mandibularis* is the portion of the *adductor mandibulae* primarily connected to the medial surface of the lower jaw. The *segmentum mandibularis* usually exhibits a non-notched and often pointy anterior end (Figs. 30B, 61A; Datovo & Vari, 2013: fig. 2B, 9B). However, in taxa exhibit the anterior portion of the *segmentum mandibularis* exhibits notch that divides the anterior tip of this muscle in dorsal and ventral anterior portion (Figs. 62B, 63A).

*Indexes:* CI = 0.063; RI = 0.167

*Inapplicability:* This character is inapplicable for *Aulostomus maculatus* (Aulostomidae), which lacks a *segmentum mandibularis*.

**Char. #118 (AD14). Adductor mandibulae; segmentum mandibularis; separation in a pars coronalis and a pars mentalis:** (0) separation in a pars coronalis and a pars mentalis superficially distinguishable, visible only in medial view; compounds not completely differentiated; (1) separation in a pars coronalis and a pars mentalis complete.

*Description:* The *segmentum mandibularis* of the *adductor mandibulae* is usually nearly bipinnate along its medial surface, exhibiting a visible separation between a dorsal portion, namely the *pars coronalis*, and a ventral portion, a *pars mentalis*. In most of the examined taxa, these sections are only superficially (medially) distinguishable; they are often distinguishable posteriorly, while non-differentiable on its anterior portion (Datovo & Vari, 2013: fig. 2B). In just a few of the examined taxa, the separation of *segmentum mandibularis* subsection is complete and clearly differentiated along the anteroposterior axis (Datovo & Vari, 2013: fig. 9A).

*Inapplicability:* This character is inapplicable for *Aulostomus maculatus* (Aulostomidae), which lacks a *segmentum mandibularis*.

*Indexes:* CI = 0.200; RI = 0.600

**Char. #119 (AD15). Adductor mandibulae; segmentum mandibularis; pars coronalis; posterodorsal extent:** (0) not trespassing the posterodorsal border of the lower jaw; (1) trespassing the posterodorsal border of the lower jaw.

*Description:* In the most common condition among percomorphaceans, the *segmentum mandibularis* of the *adductor mandibulae* is completely covered laterally by the lower jaw. However, in several Stromateiformes, Scombriformes, and some Perciformes, the *coronalis* section of the *segmentum mandibularis* is posterodorsally expanded, trespassing the posterior limits of the lower jaw and being partially exposed in a lateral view. A good landmark of the posterodorsal expansion of the coronalis is its confluence with the anterior portion of the *segmentum facialis* that forms a laterally visible mandibular raphe (Figs. 22, 28, 37, 61, 63; Datovo & Vari, 2013: fig. 3).

*Indexes:* CI = 0.091; RI = 0.643

*Inapplicability:* This character is inapplicable for *Aulostomus maculatus* (Aulostomidae), which lacks a *segmentum mandibularis*.

**Char. #120 (AD16). Adductor mandibulae; segmentum mandibularis; pars mentalis; differentiation into prementalis and postmentalis subunits: (0) absent; (1) present.**

*Description:* In some percomorphaceans, the *pars mentalis* of the *segmentum mandibularis* is differentiated into two subunits: an anterodorsal *prementalis* and a posteroventral *postmentalis*. In such configuration, the *coronalis* and the *prementalis* are usually associated to the intersegmental aponeurosis, while *postmentalis* arises from the faucal ligament and/or the buccopharyngeal membrane (Fig. 61A).

*Indexes:* CI = 0.083; RI = 0.476

*Inapplicability:* This character is inapplicable for *Aulostomus maculatus* (Aulostomidae), which lacks a *segmentum mandibularis*.

**Char. #121 (AD17). Adductor mandibulae; segmentum mandibularis; intersegmental aponeurosis; accessory tendon; occurrence: (0) present; (1) absent.**

*Description:* The intersegmental aponeurosis is a strong tendinous complex that primarily interconnects the *facialis* and *mandibularis* segments of the *adductor mandibulae*. In the simplest arrangement of this aponeurosis, it gives origin to two main tendons: an anterodorsal component – the mandibular tendon – and an anteroventral component – the meckelian tendon. In some taxa, a third tendinous branch emerges from the intersegmental aponeurosis, the accessory tendon (Datovo & Vari, 2013: fig. 2B). This tendon runs near to the meckelian tendon and anchors either to the coronomeckelian bone or to the dentary (see Char. #122).

*Indexes:* CI = 0.056; RI = 0.414

*Inapplicability:* This character is inapplicable for *Aulostomus maculatus* (Aulostomidae), which lacks a *segmentum mandibularis*.

**Char. #122 (AD18). Adductor mandibulae; segmentum mandibularis; intersegmental aponeurosis; accessory tendon; distal attachment: (0) coronomeckelian bone; (1) dentary.**

*Description:* In percomorphaceans exhibiting a well differentiated accessory tendon (Char. #121, state 0), the tendon is most almost always attached to the coronomeckelian bone (Datovo &

Vari, 2013: fig. 2B). However, in most Stromateiformes the accessory tendon anchoring site is shifted anteriorly and attaches to the posterior portion of the dentary.

*Inapplicability:* This character is inapplicable for *Aulostomus maculatus* (Aulostomidae), which lacks a *segmentum mandibularis*. This character is also inapplicable for taxa lacking a differentiated accessory tendon (Char. #121, state 0).

*Indexes:* CI = 1.000; RI = 1.000

## Opercular myology

**Char. #123 (OP01). *Levator operculi*; insertion:** (0) only on the medial surface of the opercle; (1) on both lateral and medial surfaces of the opercle.

*Description:* The *levator operculi* is visible on the lateral surface of the head, with origin involving the sphenotic, pterotic, and posttemporal bones, and insertion commonly on the dorsal or dorsomedial face of the opercle (Figs. 22-27, 29, 32-41). In some taxa, however, the insertion site of the *levator operculi* is laterally expanded and attaches also to the lateral surface of the opercle (Fig. 28).

*Indexes:* CI = 0.500; RI = 0.667

**Char. #124 (OP02). *Levator operculi*; origin; degree of subdivision:** (0) undivided; (1) partially divided in two sections; (2) completely divided in two sections [multistate additive].

*Description:* In the outgroup and most analyzed taxa, the *levator operculi* is a single, undivided muscle extending from the sphenotic and/or pterotic to the dorsal or dorsomedial portion of the opercle (state 0). In several taxa (e.g. *Microcanthus strigatus*: Kyphosidae; some stromateiforms) the *levator operculi* is partially (state 1) or completely (state 2) subdivided into two sections toward its origin. In these conditions, the origin of the *levator operculi* may expand posteriorly, involving both the pterotic (anterior section) and posttemporal (posterior section). In state 1, both the anterior and posterior muscle slips converge onto a common insertion at the medial side of the opercle (Fig. 40), while in state 2 the *levator operculi* exhibits a complete subdivision on both its origin and insertion (Fig. 32, 37, 65).

*Indexes:* CI = 0.118; RI = 0.063

**Char. #125 (OP03). *Levator operculi*; origin: (0) origin solely from the neurocranium; (1) origin from both neurocranium and pectoral girdle.**

*Description:* In the outgroup taxa *Beryx splendens* (Berycidae), *Holocentrus adscensionis* (Holocentridae), and most analyzed taxa the *levator operculi* originates from the sphenotic and pterotic. In some taxa, however, the *levator operculi* exhibits a posterior expansion of its origin, in which its posteriormost fibers (or the posterior section of the muscle) also attaches to the dorsalmost elements of the pectoral girdle, *i.e.* posttemporal, extrascapular, or supracleithrum (Figs. 32, 37, 40, 65).

*Remarks:* Origins of the *levator operculi* involving different bones does not necessarily imply in separated bundles of this muscle, as not all taxa exhibiting this character exhibit a divided *levator operculi* (Char. #124, state 1).

*Indexes:* CI = 0.091; RI = 0.333

**Char. #126 (OP04). *Dilatator operculi*; origin: (0) restricted to the sphenotic; (1) allocated on a fronto-sphenotic fossa** (Johnson, 1986: Char. #3, modified).

*Description:* In a typical percomorphacean condition, the *dilatator operculi* lies posterodorsal to the *levator arcus palatini* and connects the opercle with the postorbital region of the skull. This muscle has its origins on a notch or a *fossa* on the sphenotic, region often referred to as the *dilatator fossa*. In most taxa, this *fossa* is restricted to the sphenotic, with the *dilatator operculi* running parallel to the articulation between hyomandibula and skull. In a less frequent condition, the *dilatator fossa* is expanded anteriorly, forming a lateral groove that spans through both the frontal and sphenotic (Allis, 1903: Plt IV, *dgr*; Johnson, 1986: Fig. 4, B-C). This morphology is obviously associated to an associated anterior expansion of the *dilatator operculi* (Figs. 26, 28, 41).

*Remarks:* *Sphyraena tome* (Sphyraenidae) exhibits a remarkable anterior expansion of the *dilatator operculi*. In this taxon, the anterior limit of the *dilatator fossa* opens into a fenestra, which connects the fossa to the roof of the orbit. The *dilatator operculi* invades the orbit and expands anteriorly to reach the anterior half of the orbital cavity. In *Arripis georgianus* (Arripidae), the *dilatator operculi* is also anteriorly expanded and originates from a dilatator fossa that extends to the anteriormost portion of the frontal. The fossa is, however, mostly contained on sphenotic-pterotic boundary, and not as long as observed in pomatomids or Scombriformes.

Johnson (1986) discussed an equivalent character for the Scombriformes (Johnson, 1986: Char. #3 – *Pomatomus* + Scombroids). His character, however, dealt with two variables: the presence of an “enlarged and reoriented fronto-sphenotic shelf” and the “altered infraorbital-supraorbital sensory canal junction, medially and somewhat anteriorly displaced”. According to Johnson (1986), the enlarged *dilatator operculi* of *Pomatomus* and the Scombriformes not only fits a large and reoriented fronto-sphenotic shelf (*i.e.* the *dilatator fossa*), but also shifts the supraorbital-infraorbital connection medially when compared to taxa with a plesiomorphic condition. According to the author, both states characterize *Pomatomus* + scombriforms. However, due to the codependence of both characters (*i.e.* the anterior expansion of the *dilatator operculi* is related to both the enlarged fronto-sphenotic shelf and the altered infraorbital-supraorbital junction) they are combined herein in a single character dealing with the *dilatator operculi* origin.

Similar, but not homologous morphologies of the anterior expansion of the *dilatator operculi* occur in at least two additional sampled taxa: *Polydactylus virginicus* (Polynemidae) and *Mugil curema* (Mugilidae). In both taxa, the *dilatator operculi* originates from the frontal, but the resultant morphologies differ from that observed in the Scombriformes and Pomatomidae. In *Polydactylus* the expanded origin of the *dilatator operculi* involves the ventral surface of the frontal bone (*i.e.* the roof of the orbit), and the expanded *dilatator fossa* is not visible laterally as ridge or groove. In *Mugil*, the *dilatator operculi* originates from the dorsolateral surface of the frontal, but it is not contained in a distinct fossa. Both taxa are herein coded as zero (*i.e.* not containing an anteriorly expanded fronto-sphenotic fossa).

*Indexes:* CI = 0.500; RI = 0.800

**Char. #127 (OP05). *Ramus lateralis accessorius*; orbitopectoral branch (RLA-OP); position relative to the levator operculi:** (0) medial to the levator operculi; (1) lateral to the levator operculi.

*Description:* The *ramus lateralis accessorius* (RLA) is a head nerve that originates from the geniculate ganglion and extends onto the posterodorsal region of the head, trunk, and fins (Freihofer, 1963). Along its path through the head, the RLA subdivides in at least two main trunks: the orbitopectoral branch (RLA-OP) and the parietodorsal branch (RLA-PD). In the trunk, this nerve may exhibit several additional subdivisions (*e.g.* RLA-AF, RLA-M, RLA-V, RLA-T1, RLA-T2, etc...).

Sixteen different RLA branching patterns are recognized in teleostean fishes based on different combinations of head and trunk elements, and at least nine of these patterns occur on percomorphaceans (Freihofer, 1963: tab. 1, figs. 16-28). Among these, the so-called pattern 10 is one

of the simplest to recognize in Percomorphacea, since it does not need special specimen preparations and can be quickly assessed by a dissection of preserved specimens. Only in pattern 10 the RLA-OP reaches the pectoral fin overlying the *levator arcus palatini*, *dilatator*, and *levator operculi* muscles (Figs. 33, 64, 65). In taxa presenting pattern 9 for example (the most common among the examined percomorphaceans and the most similar to pattern 10), the RLA-OP is never visible immediately beneath the skin or lateral to the abovementioned muscles.

*Remarks:* Based solely on the shared pattern 10 of the *ramus lateralis accessorius* (RLA), Freihofner (1963) delimited for the first time a percomorphacean group that would include: Kuhliidae, Arripidae, Terapontidae, (except *Scorpiis*, which has pattern 8), Kyphosidae *latu sensu* (including girellins, scorpidins, microcanthins), Pomatomidae, Nematistiidae, and Stromateiformes. This hypothesis was later reassessed by Johnson & Fritzsche (1989), which corroborated the possible monophyly of the group with a few changes: the inclusion of *Graus* and oplegnathids and exclusion of Pomatomidae and Nematistiidae. *Pomatomus*, according to Johnson (1986) would be sister-group of the Scombriformes, and *Nematistius* of the Carangiformes. Leis & Lingen (1997) later expanded this group to allocate Dichistiidae, a taxon also containing an RLA-10 pattern.

Our analysis does not corroborate an RLA-10 natural assemblage of fishes. It suggests that such branching pattern appeared at least four times along the percomorphacean evolution: 1) in Oplegnathidae; 2) in a clade comprising Kyphosidae + Haemulidae + Terapontidae + Kuhliidae (deltran); 3) in Pomatomidae + Arripidae; and 4) in non-Amarsipidae Stromateiformes.

*Indexes:* CI = 0.100; RI = 0.625

**Char. #128 (OP06). *Dilatator operculi* and *levator arcus palatini*, degree of separation: (0) partially separated from each other; (1) completely separated from each other.**

*Description:* The *dilatator operculi* and *levator arcus palatini* are subdivisions of a single muscle named *constrictor mandibularis dorsalis* (Datovo & Rizzato, 2018), which is found in cartilaginous fishes and in earlier ontogenetic stages of bony fishes. In a common configuration, adult percomorphaceans have the *dilatator operculi* and the *levator arcus palatini* completely separated from each. However, in some of the analyzed taxa, that separation is incomplete, and these muscles exhibit a common insertion at the suspensorium, yet retaining a separation at their points of origin.

*Indexes:* CI = 0.100; RI = 0.100

## Hyopalatal myology

**Char. #129 (AP01).** *Levator arcus palatini*; insertion; subdivisions: (0) single; (1) partially divided in lateral and medial sections, sandwiching the *segmentum facialis* of the *adductor mandibulae*.

*Description:* In the most common configuration among percomorphaceans, the *levator arcus palatini* is formed by a single bundle of fibers that inserts medial to the *segmentum facialis* of the *adductor mandibulae*, on the vertical arm of the metapterygoid, preopercle and/or hyomandibula. Modifications in this common pattern involves the *levator arcus palatini* subdivided into a lateral and medial section near its point of insertion at the suspensorium. These sections are separated ventrally by an interposing *malaris* section of the *adductor mandibulae* (Figs. 23, 34).

*Indexes:* CI = 0.200; RI = 0.333

**Char. #130 (AP02).** *Levator arcus palatini*; insertion; position relative to the *segmentum facialis* of the *adductor mandibulae*: (0) medial in relation to the *segmentum facialis*; (1) dividing bundles of the *segmentum facialis* (2) lateral in relation to the *segmentum facialis* [multistate additive].

*Description:* In the most common configuration among percomorphaceans, the *levator arcus palatini* is placed medial to the *segmentum facialis* of the *adductor mandibulae*. Nevertheless, in some events the *levator arcus palatini* is sandwiched (state 1) or completely lateral (state 2) to the the *segmentum facialis*.

*Inapplicability:* This character is inapplicable for taxa exhibiting a subdivided *levator arcus palatini* (Char. #129, state 1).

*Indexes:* CI = 0.400; RI = 0.250

**Char. #131 (AP03).** *Levator arcus palatini*; insertion: (0) restricted to lateral/dorsolateral surface of suspensorium; (1) invading the medial face of the hyomandibula.

*Description:* The *levator arcus palatini* has its origin on the braincase (mainly the sphenotic), and insertion only on the lateral faces of the metapterygoid, preopercle and/or hyomandibula. In a few taxa, however, some fibers of the *levator arcus palatini* pass through a gap of variable size between the hyomandibula and metapterygoid and reach the medial surface of the hyomandibula.

*Remarks:* Datovo & Rizzato (2018) reported a condition similar to the described in character-state 1 in *Elops*. In the elopid, however, the division of the *levator arcus palatini* invading the medial face of the suspensorium (termed *pars pharyngealis* by Datovo & Rizzato, 2018) emerges from a gap located between the hyomandibula and preopercle, rather than between hyomandibula and metapterygoid as in the examined percomorphaceans.

*Indexes:* CI = 0.100; RI = 0.250

**Char. #132 (AP04). *Levator arcus palatini*; insertion on the suspensorium; type: (0) muscular; (1) aponeurotic.**

*Description:* In coryphaenids and rachycentrids, the lateralmost portion of the *levator arcus palatini* is modified into a very thin sheet of fibers that dissipates ventrally into a wide and delicate aponeurosis. This sheet of conjunctive tissue covers the *adductor mandibulae* and attaches to the lateral borders of the hyomandibula and the preopercle.

*Remarks:* This character is recovered as a unique synapomorphy for Coryphaenidae + Rachycentridae.

*Indexes:* CI = 1.000; RI = 1.000

**Char. #133 (AP05). *Levator arcus palatini*; origin: (0) sphenotic; (1) expanded anteriorly, involving both the sphenotic and frontal bones.**

*Description:* In the most common configuration among percomorphaceans, the *levator arcus palatini* is conical in shape, placed at the rear of the orbit, and originates primarily from the sphenotic spine (Figs. 39, 40, 65). Some taxa, however, exhibits an anterior expansion of the *levator arcus palatini* origin, which extends on the ventral surface of the frontal bone (Fig. 26, 27, 35).

*Indexes:* CI = 0.167; RI = 0.000

**Char. #134 (AP06). *Levator arcus palatini*; *pars temporalis*; occurrence: (0) absent; (1) present.**

*Description:* Among the specializations observed in the *levator arcus palatini*, one of the most remarkable is the subdivision of part of this muscle into a *pars temporalis*. This is represented by a

dorsolateral segmentation of the *levator arcus palatini* that laterally overlays the *dilatator operculi* and attaches to the borders of the dilatator fossa (Fig. 41).

*Remarks:* Presence of a *levator arcus palatini pars temporalis* is of restrict occurrence among percomorphaceans, and among analyzed taxa, it is uniquely found in the scombriforms *Trichiurus lepturus* (Trichiuridae) and *Thyrsitops lepidopoides* (Gempylidae). Nevertheless, a similar condition has also been described for lower teleosts (Datovo & Rizzato, 2018: fig 8), and listed as a synapomorphy for Elopiformes.

*Indexes:* CI = 0.500; RI = 0.000

**Char. #135 (AP07). *Adductor hyomandibulae pars primordialis*; insertion: (0) not involving the endopterygoid; (1) involving the endopterygoid:**

*Description:* The *adductor hyomandibulae* of percomorphaceans typically stretches between the skull and the suspensorium at the rear of the orbit, with insertion on the hyomandibula and metapterygoid (Figs. 22, 26, 28, 32, 36, 38-41). Nevertheless, in a certain number of taxa this muscle expands anteroventrally and also attaches to the endopterygoid (Figs. 24, 27, 29, 33-35, 37, 60).

*Indexes:* CI = 0.071; RI = 0.567

**Char. #136 (AP08). *Adductor hyomandibulae*; origin: (0) not expanded anteriorly; (1) expanded anteriorly, origin involving the orbital roof:**

*Description:* The *adductor hyomandibulae* of percomorphaceans usually originates from the prootic and parasphenoid. Some of the analyzed taxa exhibit an anterodorsal expansion in the origin of this muscle that involves the basisphenoid, pterosphenoid and/or orbitosphenoid.

*Indexes:* CI = 0.250; RI = 0.000

## Eye myology

**Char. #137 (EY01). *Rectus internus*; origin: (0) restricted to the posterior portion of the posterior myodome; (1) originating from the first vertebra.**

*Description:* In fishes exhibiting a non-ossified posterior myodome (Char. #34, state 1), the origin of the *rectus internus* eye muscle can be directly observed through the parasphenoid-basioccipital window. In some of these taxa, however, the paired *recti interni* exhibit a posterior expansion of its origin sites, which also involve the lateral and ventral facets of the first vertebra.

*Inapplicability:* This character is inapplicable for taxa lacking a parasphenoid-basioccipital window (Char. #34, state 0).

*Indexes:* CI = 0.250; RI = 0.250

### **Pharyngea-sac myology**

**Char. #138 (PS01). Pharyngeal sac; sagittal sulcus: (0) present; (1) absent.**

*Description:* The pharyngeal-sac morphology has long been used an important source of taxonomic information for the Stromateiformes. Variations of the overall external and internal anatomy of the pharyngeal sac (*i.e.* pharyngeal-sac raker morphology, pharyngeal-sac folds) have been successfully explored in a phylogenetic perspective and used to define families within the order (*e.g.* Horn, 1984: Char. #4-8).

Among Stromateiformes exhibiting a pharyngeal sac, the overall external shape of the organ varies from roughly elliptical (Figs. 46, 48, 49A, 52; Barnard, 1943: fig. 10, b; Datovo *et al.* 2014: fig. 15), to a grooved or kidney-shaped sac (Figs. 47, 49B, 50, 51; Isokawa *et al.*, 1965; Springer & Johnson, 2004: pl. 177). Spherical pharyngeal sacs exhibit such morphology due to an extra set of the *sphincter oesophagi* muscle fibers uniting both sides of the organ and covering the dorsal and ventral sagittal sulci. Contrastingly, kidney-shaped sacs retain the sagittal sulci dividing the sac in two lateral compartments (Barnard, 1943: fig 10, a, c-d; Springer & Johnson, 2004: pl. 177).

*Remarks:* Elliptical sacs lacking the sagittal sulcus are present in stromateids, tetragonurids, and ariommatids. Kidney-shaped organs are present in centrolophids and nomeids.

*Inapplicability:* This character is inapplicable to fishes lacking a pharyngeal sac (Char. #58, state 0).

*Indexes:* CI = 1.000; RI = 1.000

**Char. #139 (PS02). Pharyngeal sac; posterolateral set of the *sphincter oesophagi* fibers; occurrence: (0) absent; (1) present.**

*Description:* As mentioned on the previous character, taxa exhibiting spherical pharyngeal sacs deserve its morphology to an extra dorsal set of *sphincter oesophagi* fibers linking the left and right sac hemispheres (Figs. 46A, 49A, 52). Stromateidae exhibits a further modification of the *sphincter oesophagi* fibers associated to the posterior portion of the pharyngeal sac. In this taxon, differentiated fibers of the *sphincter oesophagi* also attach to the posterolateral portion of the organ, linking the sac hemispheres dorsally and ventrally (Fig. 52B, arrow; Datovo *et al.* 2014: fig. 15).

*Remarks:* A posterolateral set of *sphincter oesophagi* fibers is uniquely present in Stromateidae.

*Inapplicability:* This character is inapplicable to fishes lacking a pharyngeal sac (Char. #58, state 0), or exhibiting a grooved pharyngeal-sac (Char. #138, state 1).

*Indexes:* CI = 1.000; RI = 1.000

**Char. #140 (PS03). Pharyngeal sac; transversal sulci: (0) present; (1) absent.**

*Description:* The pharyngeal-sac morphology of centrolophids and nomeids further differs from the remaining families by exhibiting a set of transversals, regularly-spaced sulci or striae on its external surface (Figs. 49B, 50, 51; Barnard, 1948: fig. 10c; transversal bands *sensu* Haedrich, 1967). The sulci hold nerves and vessels that supply the pharyngeal-sac muscular layers. Although similar nerves and vessels attach to the pharyngeal-sac of ariommatids, nomeids, and stromateids, these are distinct on not forming regularly-spaced sulci or striae over the sac's surface.

*Remarks:* Transversal pharyngeal-sac sulci are uniquely present in Centrolophidae and Nomeidae.

*Inapplicability:* This character is inapplicable to fishes lacking a pharyngeal sac (Char. #58, state 0).

*Indexes:* CI = 1.000; RI = 1.000

**Char. #141 (PS04). Pharyngeal sac; dorsal portion: (0) not expanded anteriorly; (1) expanded anteriorly.**

*Description:* The pharyngeal sac of Stromateiformes is located posterior to the last gill arches, attached to epibranchials 4 and ceratobranchials 5. In dorsal view, the organ is visible immediately posterior to the *transversi* muscles that link the contralateral pharyngobranchials 3 and 4, and epibranchials 4 (TPb3-Pb4-Eb3 of Springer & Johnson, 2004), and to the *retractores dorsales* (Figs.46A, 49B, 50A, 51A, 52A); Springer & Johnson, 2004: pl. 177). In Ariommatidae, the pharyngeal sac contrasts from this morphology on exhibiting an anterodorsal outgrowth that laterally surrounds the *retractores dorsales* and partially covers the posteriormost *transversi* muscles (Fig. 49A).

*Remarks:* An anterior pharyngeal-sac outgrowth is restrict to Ariommatidae.

*Inapplicability:* This character is inapplicable to fishes lacking a pharyngeal sac (Char. #58, state 0).

*Indexes:* CI = 1.000; RI = 1.000

**Char. #142 (PS05). Pharyngeal sac; attachment to cleithrum; accessory muscle: (0) absent; (1) present.**

*Description:* The stromateiform pharyngeal sac is fixed to the gill-arch bones through a direct muscle attachment to epibranchials 4 and ceratobranchials 5. Accessory pharyngeal-sac muscular attachments are of restrict occurrence and found uniquely among ariommatids. These fishes exhibit a modification from the ventral fibers of the *sphincter oesophagi*, which converge to a tendon and attach to the anteromedial portion of the cleithrum.

*Remarks:* Accessory cleithral attachment of the pharyngeal sac are restrict to Ariommatidae.

*Inapplicability:* This character is inapplicable to fishes lacking a pharyngeal sac (Char. #58, state 0).

*Indexes:* CI = 1.000; RI = 1.000

## **Branchial myology**

**Char. #143 (BR01). Levatores externi; levator externus 1; separation from levatores externi 2-4 by interposed levatores interni 1-2; occurrence: (0) absent; (1) present** (Stiassny, 1990; Stiassny, 1993).

*Description:* The common morphology among acanthomorphs is to have the *levatores externi* muscles originating from the postorbital region of the neurocranium and overlying superficially the *levatores interni* (Figs. 46B, 47, 48B, 50B, 51B, 52B; Stiassny, 1990: fig. 3; Stiassny, 1993: fig. 2A; Springer & Johnson, 2004). A modified condition is observed in Mugiliformes and the Atherinomorpha, in which the first external levator is separated from the remaining *levatores* by interposing *levatores interni* 1 and 2 (Stiassny, 1990: Fig. 4; Stiassny, 1993: Fig. 2B, C).

*Remarks:* This character is recovered as a synapomorphy for the clade composed by *Mugil curema* (Mugilidae) and *Atherinella brasiliensis* (Atherinopsidae).

*Indexes:* CI = 1.000; RI = 1.000

**Char. #144 (BR02). *Levatores externi*; levator externus 3; occurrence: (0) present; (1) absent** (Springer & Orrell, 2004: Char. #3).

*Description:* Acanthomorphs usually exhibit five external *levatores* muscles (namely *levatores externi* 1 to 4, and a *levator posterior*), with origin on the cranium and insertion on the epibranchials 1 to 4, respectively (both *levator externus* 4 and *levator posterior* insert on epibranchial 4). Losses of *levatores* muscles are uncommon among the percomorphaceans, and absence of *levator externus* 3 is of restricted distribution among the analyzed taxa.

*Remarks:* This character is optimized as a synapomorphy for Pleuronectiformes. Homoplastic losses occur in *Brama caribbea* (Bramidae) and *Monocirrhus polyacanthus* (Polycentridae).

*Indexes:* CI = 0.333; RI = 0.333

**Char. #145 (BR03). *Levator posterior*; occurrence: (0) present; (1) absent** (Springer & Johnson, 2004).

*Description:* The *levator posterior* presumably represents the fifth *levator externus* with a posteriorly displaced origin on the skull (Winterbottom, 1974). It is a thin muscle with origin on the prootic, pterotic, epiotic, intercalar, or exoccipital, and insertion on epibranchial 4, the cartilaginous epibranchial 5, and/or ceratobranchial 5 (Springer & Johnson, 2004). This muscle is usually present in percomorphaceans, but it is herein reported as absent in Scombridae (*Auxis thazard* and *Scomber* sp.) and in Chiasmodontidae (*Pseudoscopelus altipinnis*).

*Remarks:* The *levator posterior* exhibits a mosaic distribution among Teleostei. Among non-Acanthomorpha, the *levator posterior* is present in Clupeiformes (but absent in *Denticeps*), in *Chanos* (Gonorynchiformes), and in Characiformes (Springer & Johnson, 2004). This muscle appears again in acanthomorphs, with confirmed presence in all non-percomorphacean Acanthomorpha (*i.e.* Lampridiformes, Percopsiformes, Gadiformes, Stephanoberyciformes, Zeiformes, Polymixiiformes, and Beryciformes (Springer & Johnson, 2004). Within Percomorphaceans, this muscle occurs in most lineages except Batrachoidiformes, Lophiiformes, Caproiformes, Synbranchiformes, and Scombridae (Springer & Johnson, 2004; Springer & Orrell, 2004: char. #4).

Although reported as absent in Ophidiiformes (Springer & Johnson, 2004), both *Raneya brasiliensis* (Ophidiidae) and *Dinematichthys ilucoeteoides* (Dinematichthyidae) exhibit a *levator posterior*. Nevertheless, the *levator posterior* of ophidiiforms is reduced to few fibers attached to epibranchial 4, which may have been overlooked by previous studies. A similar atrophied *levator posterior* is present in Beryciformes and Pleuronectiformes.

*Indexes:* CI = 0.500; RI = 0.500

**Char. #146 (BR04). *Obliquus posterioris*; origin: (0) solely from ceratobranchial 5; (1) from ceratobranchial 5 and esophageal raphe** (Springer & Orrell, 2004: Char. #33, modified).

*Description:* The *obliquus posterioris* is a branchial muscle located at the posterior portion of the gill arches, with origin on ceratobranchial 5 and attachment at the posterior surface of epibranchial 4. In some percomorphaceans, the *obliquus posterioris* originates not only from ceratobranchial 5, but also from a raphe (esophageal raphe of Springer & Johnson, 2004) shared with other posterior branchial muscles, *i.e.* the *adductor 5* and/ or the *sphincter oesophagi*.

*Remarks:* This character is modified from Springer & Orrell's Character #33, which accounts to the presence of an esophageal raphe. The esophageal raphe is defined as a thin line of connective tissue, or a myoseptum, that transversely divides the *obliquus posterioris*. The presence of the esophageal raphe is used to demarcate the limits between the *obliquus posterioris*, *adductor 5* and/ or the *sphincter oesophagi*. According to Springer & Johnson (2004) the presence of an esophageal raphe is of restrict occurrence among percomorphaceans, although it is frequently observed in pre-acanthomorphs.

*Indexes:* CI = 0.500; RI = 0.750

**Char. #147 (BR05). *Sphincter oesophagi*; section *dorsalis*; occurrence: (0) present; (1) absent** (Springer & Orrell, 2004: Char. #18, modified).

*Description:* The *sphincter oesophagi* is an unpaired muscle that encircles the anterior portion of the esophagus. Anteriorly, this muscle attaches to epibranchial 4 and ceratobranchial 5, and posteriorly it encircles the proximal portion of the esophagus. In some taxa, the *sphincter oesophagi* exhibits an extra muscle band (*i.e.* *sphincter oesophagi dorsalis*: Springer & Johnson, 2004) that is separated from its main body and lies dorsally to the *retractores dorsalis* (Figs. 50A, 52A). This muscle band is usually located immediately posterior to *transversus epibranchialis* 3, and often shares some fiber with it.

*Indexes:* CI = 0.143; RI = 0.714

**Char. #148 (BR06). *Retractor dorsalis*: (0) not vestigial; (1) vestigial.**

*Description:* The *retractor dorsalis* is a dorsal branchial muscle with origin on the anteriormost vertebrae and insertion on the dorsal bone elements of the posterior gill arches (*i.e.* pharyngobranchials 3 and/ or 4; epibranchial 4; pharyngeal tooth plates 4 and/or 5). The percomorphacean *retractor dorsalis* is usually present as a conspicuous pair of muscle disposed transversally in relation to the remaining dorsal gill-arch muscles (Figs. 46AB, 48C, 49B, 50A, 51A, 52A). Nevertheless, in some of the analyzed specimens the *retractor dorsalis* is atrophied. In the analyzed Ariommatidae the *retractor dorsalis* is reduced to vestigial muscle, and the few, almost imperceptible fibers corresponding to the *retractores dorsales* are represented by a pair of discrete muscle stripes emerging in between the contralateral pharyngeal-sac hemispheres (Fig. 49A).

*Remarks:* Vestigial *retractores dorsales* are uniquely found in Ariommatidae.

*Indexes:* CI = 1.000; RI = 1.000

**Char. #149 (BR07). *Sternobranchialis tendon*; ventral attachment: (0) emerging from differentiated fibers of the sternohyoideus; (1) emerging from the dorsal edge of the urohyal.**

*Description:* In percomorphaceans (and in most teleosts), the *sternohyoideus* originates from the anteroventral portion of the cleithrum. It exhibits a muscular insertion at the dorsal and lateral surfaces of the urohyal, and an additional tendinous attachment at the ventral surface of the gill arch,

which is made via sternobranchialis tendon. This tendon is represented by a strengthened oblique band of collagen modified from the membranous tissue that laterally covers the *sternohyoideus*.

In the most common condition, the sternobranchialis tendon is observed at the lateral surface of the *sternohyoideus* converging anteriorly and dorsally to attach to the ventral limb of hypobranchial 3 (state 0). Some taxa, however, exhibit a modified sternobranchialis that no longer is represented by a strengthened collagenous band covering the *sternohyoideus*, but as a distinct ligament linking the urohyal directly to hypobranchial 3 (state 1).

*Inapplicability:* This character is inapplicable for *Icosteus aenigmaticus* (Icosteidae) and *Aulostomus maculatus* (Aulostomidae), taxa that lack a differentiated sternobranchialis tendon.

*Indexes:* CI = 0.250; RI = 0.000

**Char. #150 (BR08). Sternobranchialis tendon; position in relation to the *rectus communis*:** (0) lateral;  
(1) medial.

*Description:* Most percomorphaceans exhibit the sternobranchialis tendon's distal attachment at the ventral limbs of hypobranchials 3 (Stiassny, 1996: fig. 9A). The tendon is typically visible passing laterally in relation to the *rectus communis*, a muscle that originates from hypobranchial 3 and/ or the urohyal. A modification of this pattern is observed in Ophidiiformes. In these taxa, the sternobranchialis tendon passes medially in relation to the *rectus communis* to attach to the hypobranchial 3.

*Remarks:* A sternobranchialis tendon that is medial to the *rectus communis* is herein retrieved as a novel and unambiguous synapomorphy for Ophidiiformes.

*Inapplicability:* This character is inapplicable for taxa exhibiting the sternobranchialis attachment site displaced anteriorly and involving hypobranchial 2 and basibranchial 2. In such conditions, the sternobranchialis tendon is anterior to the *rectus communis*, and could not be classified as lateral or medial to it. The sternobranchialis tendon is untraceable in *Icosteus aenigmaticus* (Icosteidae) and *Aulostomus maculatus* (Aulostomidae), for which the character is coded as inapplicable.

*Indexes:* CI = 1.000; RI = 1.000

**Char. #151 (BR09). *Rectus communis*; origin at the urohyal: (0) present (1) absent** (Datovo *et al.* 2014: Char. #25, modified)

*Description:* In percomorphaceans, the *rectus communis* originates from the urohyal or from fibers of the *sternohyoideus*, and inserts via tendon to lateral projections of ceratobranchial 5. Yet, a *rectus communis* with partial or total origin on hypobranchial 3 is present in some percomorphaceans herein examined (*i.e.* Pleuronectiformes, Trichiuridae, Aulostomidae). When partial, origin sites of the *rectus communis* are the hypohyals 3, the urohyal, and occasionally the *sternohyoideus*, when this last muscle is involved (Stiassny, 1996: fig. 9B, 9E). When the shift on the origin of the *rectus communis* is complete, the muscle attaches to the ventral limb of hypobranchial 3 (Stiassny, 1996: fig. 9A, 9C-D). The present character investigates the origin of the *rectus communis* at the urohyal, while the following character (#152) evaluates its origins at hypobranchial 3.

*Remarks:* According to Lauder (1983), the partial association of the *rectus communis* with the urohyal is a synapomorphy for Ctenosquamata. Stiassny (1996) reported that a hypobranchial 3 no longer representing a site of origin for the *rectus communis* is a characteristic of holacanthopterygians. Contrastingly, Datovo *et al.* (2014) states that hypobranchial 3 still serves as a site of origin of the *rectus communis* on some percomorphaceans, and that it was not clear whether the attachment of this muscle to hypobranchial 3 would be plesiomorphic or apomorphic.

Our reconstructions for Chars. #151 and #152 (below) indicate that both the urohyal and hypobranchial 3 primitively serve as origin sites for the *rectus communis*. In this scenario, ventral and dorsal shifts of the *rectus communis* origin are specializations acquired by different lineages within Percomorphacea.

*Inapplicability:* This character is inapplicable for *Mugil curema* (Mugilidae), in which the *rectus communis* is comprised between hypobranchial 3 and the urohyal. In this taxon, the *rectus communis* has completely lost its connection to ceratobranchial 5.

*Indexes:* CI = 0.333; RI = 0.500

**Char. #152 (BR10). *Rectus communis*; origin at hypobranchial 3: (0) present (1) absent** (Datovo *et al.* 2014: Char. # 25, modified)

*Description:* This character accounts to the presence of fibers of the *rectus communis* originating from hypobranchial 3. For further descriptions, see Character #151.

*Remarks:* See Char. #151.

*Inapplicability:* See Char. #151.

*Indexes:* CI = 0.125; RI = 0.774

**Char. #153 (BR11). *Rectus communis*; insertion at hypobranchial 3: (0) present (1) absent.**

*Description:* Variation of the *rectus communis* origin (treated on Characters #151 and #152, above) are occasionally observed among the analyzed taxa, but expansions on its sites of insertion are restricted to few groups of fishes. In percomorphaceans, the *rectus communis* inserts at the lateral projections of ceratobranchial 5 via a consolidated tendon (Winterbottom, 1974: fig. 30, 31), and in most analyzed taxa, this represents the only insertion site for this muscle. However, in *Pseudoscopelus altipinnis* (Chiasmodontidae), *Mugil curema* (Mugilidae), and in almost all Stromateiformes, fibers of the *rectus comunis* that origin from the urohyal also insert at the anteroventral facet of hypobranchial 3. In *Mugil curema* this condition is further modified, and the taxon exhibits the entire *rectus communis* confined between the urohyal and hypobranchial 3.

*Inapplicability:* This character is inapplicable for taxa exhibiting the *rectus communis* origin confined between hypobranchial 3 – ceratobranchial 5 (Char. 151, state 1; #152, state 0).

*Indexes:* CI = 0.167; RI = 0.737

**Char. #154 (BR12). *Rectus ventralis I*; occurrence: (0) absent; (1) present (Datovo *et al.* 2014: Char. #6).**

*Description:* *Rectus ventralis I* is a muscle possibly derived from a subdivision and/or expansion of *obliquus ventralis I*. This muscle extends from the anterior margin of hypobranchial 1 to the dorsal hypohyal (Datovo *et al.* 2014: fig. 8).

*Remarks:* The occurrence of a *rectus ventralis I* is restrict among percomorphaceans, registered to some Acanthuriformes, Anabantiformes, Gobiiformes, Batrachoidiformes, among other percomorphaceans (Datovo *et al.*, 2014: Char. #16). We expand its distribution to some Stromateiformes (Nomeidae and Tetragonuridae), and to *Monocirrhus polyacanthus* (Polycentridae).

*Indexes:* CI = 0.200; RI = 0.000

**Char. #155 (BR13). *Pharyngoclavicularis externus*; intermediate aponeurosis; occurrence: (0) absent; (1) present** (Datovo *et al.* 2014, Char. # 13).

*Description:* The *pharyngoclavicularis externus* generally originates from the anteroventral margin of the cleithrum and inserts at the lateroventral face of ceratobranchial 5 (Datovo *et al.* 2014: fig. 3). This muscle usually lacks any intermediate aponeurosis and its fibers are continuous from the cleithrum to ceratobranchial 5 (Figs. 46B-C, 47, 48B, 50B-C, 51B-C, 52B-C). Scombriformes, in contrast, exhibit a well-developed aponeurosis running across the *pharyngoclavicularis externus*, observed as a laminar, flattened tendon along the anteroposterior expanse of this muscle (Datovo *et al.* 2014: Char. #13).

*Remarks:* According to Datovo *et al.* (2014), the presence of an intermediate aponeurosis is present in all lineages of Scombriformes, including the billfishes, and has been interpreted as an additional synapomorphy for the Scombriformes (*sensu* Johnson, 1986). Within scombriforms, a reversal event occurs in the Trichiuridae, and among the percomorphaceans, a homoplastic presence of the aponeurosis occurs in *Kyphosus sectatrix* (Kyphosidae).

This study confirms the presence of an intermediate aponeurosis on the *pharyngoclavicularis externus* of Scombriformes, and this character is recovered as a synapomorphy for a clade composed by all non-trichiurid Scombriformes (TNT Clade 88). I also report a homoplastic presence of this character-state in *Centropomus parallelus* (Centropomidae).

*Indexes:* CI = 0.500; RI = 0.750

**Char. #156 (BR14). *Pharyngoclavicularis externus*; origin: (0) lateral to the *sternohyoideus*; (1) dividing bundles of the *sternohyoideus*.**

*Description:* The *pharyngoclavicularis externus* usually originates from the cleithrum and inserts at the anterior portion of ceratobranchial 5. On its site of origin, the *pharyngoclavicularis externus* may be lateral to the *sternohyoideus* (Howes, 1992: fig. 29, A), or be sandwiched by this muscle (Fig. 48B; Stiassny, 1990: fig. 4; Stiassny, 1993: fig. 2 A-C).

*Indexes:* CI = 0.071; RI = 0.278

**Char. #157 (BR15). *Pharyngoclavicularis externus*; insertion; subdivisions; occurrence: (0) absent; (1) present.** (Datovo *et al.* 2014: Char. 11).

*Description:* Most percomorphaceans, and all examined outgroup taxa exhibit a non-subdivided *pharyngoclavicularis externus*, which originates from the cleithrum and inserts at the anterior portion of ceratobranchial 5. In Mugiliformes and Atherinomorpha (except exocoetid beloniforms) instead, the *pharyngoclavicularis externus* (= *pharyngocleithralis* of Stiasny, 1993) splits in an anterior and posterior portion towards its insertion, attaching to both the antero- and posteroventral portions of ceratobranchial 5.

*Remarks:* The dorsally subdivided *pharyngoclavicularis externus* has been proposed as a synapomorphy for the Atherinomorpha + Mugiliformes clade (Stiasny, 1990; Stiasny, 1993; Datovo *et al.*, 2014). This analysis corroborates the synapomorphic status of this character, which results as an additional synapomorphy for *Mugil curema* (Mugilidae) + *Atherinella brasiliensis* (Atherinopsidae).

*Indexes:* CI = 1.000; RI = 1.000

**Char. #158 (BR16). *Pharyngoclavicularis internus*; insertion; subdivisions; occurrence: (0) absent; (1) present.**

*Description:* In percomorphaceans, the *pharyngoclavicularis internus* arises from the anterodorsal face of the cleithrum and inserts on the anteroventral region of ceratobranchial 5 (Datovo *et al.* 2014: fig. 3). Variation on the morphology of the *pharyngoclavicularis internus* involves the presence of subdivisions of this muscle towards its point of insertion. In such cases, the *pharyngoclavicularis internus* exhibits a single origin on the cleithrum but splits in two well-separated insertion sites: one at the anterior edge of ceratobranchial 5, and other on the mid length of this bone (Fig. 48B).

*Indexes:* CI = 0.125; RI = 0.125

**Char. #159 (BR17). *Pharyngoclavicularis internus*; medial contact with its antimere: (0) absent; (1) present.** (Datovo *et al.* 2014: Char. #15).

*Description:* In a typical percomorphacean condition, each *pharyngoclavicularis internus* insert solely to the anteroventral edge of ceratobranchial 5, and the contralateral muscles do not contact each other. In most stromateiforms, in *Icosteus aenigmaticus* (Icosteidae), and in *Brama caribbea*

(Bramidae) each *pharyngoclavicularis internus* insert onto a sagittal raphe or tendon that is shared with its antimere (Figs. 50C, 51C, 52C).

*Remarks:* The contact between contralateral *pharyngoclaviculares interni* result herein as a synapomorphy for non-Amarsipidae stromateiforms. Homoplastic events occur in Bramidae and Icosteidae.

*Indexes:* CI = 0.333; RI = 0.909

**Char. #160 (BR18).** *Pharyngoclavicularis internus*; medial contact with its antimere; extension: (0) along the entire length of the muscle; (1) restricted to its anterior portion.

*Description:* Among taxa exhibiting contact between the contralateral *pharyngoclaviculares interni*, the extension in which the muscles contact each other vary from a long sagittal raphe encompassing the entire length of this muscle, to a small raphe or ligament restricted to its anterior portion.

*Remarks:* A reduced area of contact between both *pharyngoclaviculares interni* is a synapomorphy for Tetragonuridae + Ariommatidae.

*Indexes:* CI = 1.000; RI = 1.000

**Char. #161 (BR19).** *Pharyngoclavicularis internus*; medial contact; type: (0) in a sagittal raphe; (1) tendinous.

*Description:* In taxa exhibiting contact between the contralateral *pharyngoclaviculares interni*, the connection between antimere muscles can be either tendinous, or made through a sagittal raphe.

*Remarks:* Tendinous contact between *pharyngoclaviculares interni* are present in *Tetragonurus cuvieri* (Tetragonuridae) and *Ariomma indicum* (Ariommatidae).

*Indexes:* CI = 0.500; RI = 0.000

**Char. #162 (BR20).** *Pharyngoclavicularis internus*; insertion in relation to *pharyngoclavicularis externus*: (0) anterior to *pharyngoclavicularis externus* (1) disposed side by side; (2) posterior to *pharyngoclavicularis externus*. [multistate non-additive] (Datovo *et al.* 2014: Char. #27, modified).

*Description:* The typical percomorphacean condition exhibits both *pharyngoclaviculares* with insertion to ceratobranchial 5, where the *pharyngoclavicularis internus* inserts anteriorly in relation to the *pharyngoclavicularis externus* (e.g. Datovo *et al.* 2014: fig. 14). However, some taxa exhibit a posterior shift of the *pharyngoclavicularis internus*, which may be disposed side-by-side or even posterior to the *pharyngoclavicularis externus*.

*Inapplicability:* This character is coded as inapplicable for *Cynoscion striatus* (Sciaenidae), *Microcanthus strigatus* (Kyphosidae), and *Mugil curema* (Mugilidae). In *Cynoscion* and *Microcanthus* the *pharyngoclavicularis internus* is divided in two segments, one inserting anterior and another posterior to the *pharyngoclavicularis externus*. In *Mugil curema* (Mugilidae) it is the *pharyngoclavicularis externus* that is divided in anterior and posterior segments.

*Indexes:* CI = 0.167; RI = 0.286

**Char. #163 (BR21). *Transversus ventralis 5*; sagittal raphe; occurrence: (0) absent; (1) present** (Datovo *et al.* 2014: Char. #22, modified).

*Description:* *Transversus ventralis 5* is an unpaired ventral branchial muscle that connects the contralateral ceratobranchials 5. In the primitive percomorphacean condition, this muscle exhibits a sagittal raphe of variable length (Figs. 50C, 51C). However, several analyzed taxa lack any trace of raphe along *transversus ventralis 5*.

*Indexes:* CI = 0.091; RI = 0.286

**Char. #164 (BR22). *Transversus ventralis 5*; sagittal raphe; extension: (0) partial, restricted to the posterior portion of the muscle; (1) complete.** (Datovo *et al.* 2014: Char. #22, modified).

*Description:* In taxa exhibiting a sagittal raphe on *transversus ventralis 5*, this structure can either be restricted to the posterior portion of the muscle or extend along its entire length (Figs. 50C, 51C).

*Inapplicability:* Inapplicable for taxa lacking a raphe on *transversus ventralis 5* (Char. #163, state 1). This character is inapplicable for *Parachanna obscura* (Channidae), *Rachycentron canadum* (Rachycentridae), and *Orthopristis ruber* (Haemulidae). These taxa exhibit a raphe restricted to the median portion of *transversus ventralis 5*. This character is also inapplicable for both *Peprilus* spp., for which the raphe restricted to the anterior portion the *transversus* muscle.

*Indexes:* CI = 1.000; RI = 1.000

**Char. #165 (BR23). *Transversus ventralis 5*; subdivisions:** (0) absent; (1) present (Datovo *et al.* 2014: Char. #24).

*Description:* In most percomorphaceans, *transversus ventralis 5* is undifferentiated into subsections. However, in a few examined taxa this muscle exhibits well differentiated anterior and posterior subsections.

*Indexes:* CI = 0.200; RI = 0.000

**Char. #166 (BR24). *Sphincter oesophagi*; continuity to *transversus ventralis 5*:** (0) absent; (1) present (Datovo *et al.* 2014: Char. #23).

*Description:* Ventrally, the *sphincter oesophagi* is usually separated from *transversus ventralis 5* (*i.e.* these muscles do not share fibers). However, in some examined taxa, the *sphincter oesophagi* is partially continuous with *transversus ventralis 5*.

*Indexes:* CI = 0.100; RI = 0.400

## **Axial myology**

**Char. #167 (AM01). *Epaxialis*; lateral segment; association with the neurocranium:** (0) insertion on the posttemporal and epiotic only; (1) insertion involving the pterotic and frontal bones.

*Description:* The association of epaxial musculature with the neurocranium is variable among percomorphacean fishes (Stiassny, 1986), and its large diversity represents a rich source of phylogenetic information. Aside the usual attachment sites of the *epaxialis* to the posterior portion of the skull (*i.e.* between the supraoccipital and epiotic, at the posterodorsal margin of the posttemporal, and between the posttemporal and exoccipital), this muscle may exhibit differentiation and expansion on the attachment site of three of its segments, namely the lateral, medial, and posteroventral *epaxialis* segments. The present character deals with anterior expansions of the lateral segment of the *epaxialis*, while insertions of the medial and posteroventral segments are treated in the following Characters #170-174.

In state 0 the lateral segment of the epaxialis is poorly differentiated and inserts only to the posterior facets of the epiotic and posterodorsal margin of the posttemporal. This contrasts from character state 1, which describes the most common condition among the Acanthomorpha (Stiassny, 1986): the lateral bundle of the epaxialis inserts in several elements of the neurocranium, including crests on the frontal, parietal, pterotic, and supraoccipital (*i.e.* advances onto the posttemporal fossa). In such cases, the epaxial muscle is encircled dorsally by the extrascapulars, laterally by the pterotic, and medially by the epiotic (Figs. 20-29; 31-38, 47, 64).

*Remarks:* An *epaxialis* that advances onto the neurocranium and attaches to the crests of the frontal, parietal, pterotic, and supraoccipital is widespread among the analyzed taxa. It is present in the sampled beryciforms (although covered laterally by expansions of the parietal and extrascapular bones), and primitively present in Percomorphacea. This agrees with the predictions of Stiassny (1986), which listed this condition as common to Acanthomorpha. Among the analyzed taxa, the only event of regression of the epaxial musculature from the skull surface is found in the clade formed by *Parachanna obscura* (Channidae) and *Aulostomus maculatus* (Aulostomidae).

*Indexes:* CI = 1.000; RI = 1.000

**Char. #168 (AM02). *Epaxialis*; lateral segment; anterior expansion:** (0) not reaching the vertical through the middle of the orbit; (1) reaching the vertical through the middle of the orbit.

*Description:* Among fishes exhibiting an expansion of the *epaxialis* onto the neurocranium, the degree in which this musculature advances anteriorly is variable. In most taxa, the lateral *epaxialis* segment is restricted to the posterolateral portions of the pterotic, parietal, and posteriormost portions of the frontal (Figs. Figs. 22, 23, 25-28, 31-35, 47). A modified condition (state 1) describes the lateral epaxialis bundle advancing anteriorly and reaching the vertical through the middle of the orbit. In such taxa, namely the stromateiforms, carangiforms, bramids, caristiids, and *Beryx*, the lateral *epaxialis* segment inserts also to the lateral wings of the frontal (Figs. 24, 29, 36, 37, 64).

*Indexes:* CI = 0.200; RI = 0.840

**Char. #169 (AM03). *Epaxialis*; lateral segment; anterior expansion:** (0) not reaching the vertical through the lateral ethmoid; (1) reaching the vertical through the lateral ethmoid.

*Description:* Within the taxa exhibiting an anterior expansion of the lateral *epaxialis* bundle, this muscle usually falls short along the lateral wings of the frontal. Yet, in some analyzed specimens, the *epaxialis* is further expanded and reaches the anterior portions of the frontal bone, frequently extending through the vertical through the anterior limit of the orbit (*i.e.* the lateral ethmoid) and reaching the vertical through the lateral ethmoid. This morphology is uniquely observed in the stromateid genera *Stromateus* and *Peprilus* (Figs. 37, 64).

*Indexes:* CI = 0.500; RI = 0.500

**Char. #170 (AM04). *Epaxialis*; medial segment; association with the neurocranium:** (0) insertion on the posterior portion of epioccipital and supraoccipital; (1) medial segment advancing onto neurocranium.

*Description:* The medial *epaxialis* segment is also variable regarding its association to dorsal skull bones. In state 0, the medial segment of the epaxial musculature is poorly differentiated from the lateral one and is restricted to a fossa delimited by the posterodorsal facets of the epi- and supraoccipital bones (Figs. 22, 23, 25, 27, 32-34). In a modified condition, the medial *epaxialis* advances anteriorly, and attaches to the dorsal surface of the supraoccipital, parietal, and posterior portions of the frontal, and in extreme cases it reaches the mesethmoid (Figs. 24, 29, 30, 35-37, 64).

*Remarks:* In Pleuronectiformes (Fig. 38), the medial segment of the *epaxialis* advances onto the neurocranium in a degree compatible with state 1 (*i.e.* invading the neurocranium). However, the attachment sites of this muscle are not the same from other percomorphaceans due to the modified arrangement of the skull bones. As results, the fibers of the medial segment of the *epaxialis* attach not only to the parietal and frontal, but also to the rear portions of the sphenotic and pterotic of the ocular side.

*Indexes:* CI = 0.091; RI = 0.524

**Char. #171 (AM05). *Epaxialis*; medial segment; anterior expansion:** (0) medial segment of the *epaxialis* not reaching anteriorly the vertical through the middle of the orbit; (1) medial segment of the *epaxialis* trespassing the vertical through the middle of the orbit.

*Description:* The extension to which the medial epaxial muscle expands onto the skull bones is also variable among percomorphaceans. In most taxa exhibiting expansions, the anterior limit of

this segment never trespasses the vertical through the middle of the orbit. In some taxa, however, the medial epaxial segment trespasses this point and attaches to the anterior portions of the frontal and/or mesethmoid (Figs. 36, 37, 64).

*Indexes:* CI = 0.200; RI = 0.800

**Char. #172 (AM06). *Epaxialis*; posteroventral segment; occurrence: (0) absent; (1) present.**

*Description:* Aside the lateral and medial segments of the *epaxialis*, which attach to different sites of the dorsal surface of the skull, some percomorphacean fishes exhibit a third and ventral differentiation of the *epaxialis* that attaches to different sites at the ventrolateral portions of the neurocranium.

Usually the ventralmost attachment site of the *epaxialis* onto the skull is the posttemporal fossa, and delimited by the pterotic, intercalar, and dorsal facet of the exoccipital (*i.e.* the ventral portions of the posttemporal fossa; Otero, 2004: figs. 12-13). Yet, in some analyzed specimens, fibers of the *epaxialis* trespass the ventral limits of the posttemporal fossa and reach the lateral surface of the exoccipital, basioccipital, and occasionally the posterior portion of the parasphenoid. Further modifications of the epaxial insertion on this region are represented by a muscle segment completely differentiated from its main body, constituting a third segment of the *epaxialis*, namely the posteroventral segment.

A consistent landmark to recognize the posteroventral *epaxialis* segment is its relative position to other muscles and ligaments. Fishes lacking a posteroventral segment retain the *epaxialis* confined to a horizontal plane that is always dorsal to the *adductor operculi*'s origin. Contrastingly, the occurrence of a posteroventral *epaxialis* segment is noted by fibers positioned lateral, and sometimes ventral to the *adductor operculi*. In addition, fishes with a well developed posteroventral *epaxialis* has its ventralmost fibers attaching to the lateral facets of the epioccipital and basioccipital, and occasionally sandwiching the Baudelot's ligament at the base of the skull.

*Indexes:* CI = 0.071; RI = 0.381

**Char. #173 (AM07). *Epaxialis*; posteroventral segment; insertion: (0) well developed; (1) reduced.**

*Description:* When present, the posteroventral *epaxialis* segment varies in relation to its size, and two unambiguous states can be delimited from its degree of development. In a well-developed

state, this muscle segment is observed as a conspicuous bundle of *epaxialis* musculature with an independent attachment from the remaining segments of *epaxialis*. In this condition, most of the *epaxialis* fibers are located ventral to the horizontal plane through the *adductor operculi*'s origin, attaching to the basioccipital. Contrastingly, fishes with a reduced posteroventral *epaxialis* segment exhibit a discrete bundle of fibers not completely differentiated from the *epaxialis* main body. These fibers are observed immediately posterior to the *adductor operculi*'s origin, but never expanding ventrally to reach the basioccipital or to sandwich the Baudelot's ligament.

*Inapplicability*: This character is inapplicable for taxa lacking a posteroventral segment of the *epaxialis* (Char. #172, state 0).

*Indexes*: CI = 0.333; RI = 0.714

**Char. #174 (AM09). *Epaxialis*; posteroventral segment; origin:** (0) anteriormost vertebrae and ribs;  
(1) origin also involving the swim bladder.

*Description*: Subsequent modifications of the posteroventral segments of the *epaxialis* occur in some of the analyzed percomorphacean fishes. A particular modification involving this muscle segment was perceived in the analyzed Ophidiiformes. These fishes exhibited a well developed posteroventral *epaxialis* segment, which originates from the first vertebra, first ribs, and at the anterior wall of the swim bladder, and attaches to the exoccipital and basioccipital. This contrasts from other percomorphaceans exhibiting a posteroventral segment, in which its origin is always restricted to the anteriormost vertebrae and ribs, but never the swim bladder.

*Remarks*: The direct link between the posteroventral segment of the *epaxialis* and the swim bladder constitutes a novel synapomorphy for Ophidiiformes. The association between the *epaxialis* musculature, the swim bladder, and the first three ribs and vertebrae in Ophidiiformes has been richly described and illustrated by Howes (1992: figs. 17-18, 20-26). The author identified two different types of swim bladder-vertebral connections, both of which involved the posteroventral *epaxialis* segment. Notably, in the taxa assigned to the group 1, the *epaxialis* – swim bladder connection is part of a general modification related to the ophidiiform sexual dimorphism involving a sound-production mechanism. Additional sexual dimorphic traits of these taxa include a direct attachment of the swim bladder to the first ribs, and ossification of the lateral walls of the bladder. Despite never used as a phylogenetic character, the general morphology and biomechanics of this system has already been extensively explored by previous studies (Courtenay & McKittrick, 1970; Tyler, 1970; Markle & Olney, 1990; Parmentier & Diogo, 2006)

*Inapplicability:* This character is inapplicable for taxa lacking a posteroventral segment of the *epaxialis* (Char. #172, state 0).

*Indexes:* CI = 1.000; RI = 1.000

**Char. #175 (AM10). *Epaxialis*; association with the dorsal-fin pterygiophores: (0) absent; (1) present.**

*Description:* The main body of the *epaxialis* muscle runs laterally along the flanks of percomorphacean fishes, disposed laterally in relation to the neural spines and dorsal-fin pterygiophores. Attachment of the *epaxialis* to the dorsal portion of the pterygiophores is of restrict distribution among percomorphaceans. Yet, an *epaxialis* association with dorsal-fin pterygiophores do occur in some of the analyzed taxa (Fig. 8).

*Remarks:* Among the specimens analyzed herein, an association between the dorsal-fin pterygiophores and the epaxial musculature is present in the percomorphacean families Apogonidae, Haemulidae, Serranidae, Sciaenidae, and *Lates* (= Centropomidae). From these, Apogonidae, Haemulidae, Serranidae and *Lates* were once included in a putative monophyletic group shared with centrogeniids, champsodontids, cheimarrhichthyids, grammatids, percids, blennioids and some cirrhitoids (Mooi & Gill, 1995). This grouping was based on the shared *type 1* morphology of the association between the *epaxialis* and the dorsal-fin pterygiophores (Fig. 8). Our results do not support such grouping. Character reconstruction of the *type 1 epaxialis* association reveals that, at least among the analyzed percomorphacean, it evolved four time independently: in Apogonidae, Haemulidae, Serranidae, and *Lates*.

*Indexes:* CI = 0.250; RI = 0.000

## **Pectoral-fin myology**

**Char. #176 (PC01). *Adductor medialis*; occurrence: (0) absent; (1) present.**

*Description:* Teleost fishes usually exhibit three main muscles associated to the medial surface of the pectoral girdle, namely the *adductor superficialis*, *adductor profundus*, and the *arrector dorsalis* (Winterbottom, 1974). Some Percomorphacea exhibit a fourth pectoral-fin muscle attached to the medial face of the girdle, namely the *adductor medialis* (Figs. 10, 11). It originates from the cleithrum

(sometimes also from the coracoid) and inserts tendinously on the middle fin rays (vs. on the first pectoral-fin ray).

*Remarks:* Winterbottom (1974) considered the *adductor medialis* of erratic occurrence among teleosts and restricted mainly to percomorphaceans. Instead, our survey reveals a wider distribution of this muscle than previously suspected, and report its occurrence in 49 of the 66 examined taxa. A character-reconstruction of the *adductor medialis* reveals that this muscle is primitively present in percomorphaceans and that losses occurred independently among different lineages.

*Indexes:* CI = 0.111; RI = 0.500

### **Caudal-fin myology**

**Char. #177 (CF01). Caudal fin; *interradialis*; origin:** (0) restricted to the fin rays; (1) on fin rays and distal portion of hypural 3.

*Description:* The *interradialis* consists of several bundles of muscle fibers interconnecting the principal caudal fin rays. These fibers link adjacent rays from the upper and lower caudal-fin lobes. *Interradialis* attachments involve the dorsal and ventral portion of the middlemost caudal-fin rays and the lateral region of surrounding rays. In some of the analyzed taxa, the anteriormost portion of the *interradialis* is expanded anteriorly and also attach to hypural 3.

*Remarks:* The *interradialis* apparently develops from fibers of the last few myomeres, as in some basal teleosts (*i.e. Elops*) it still retains indications of the horizontal septum that would separate the *epaxialis* and *hypaxialis* muscles (Winterbottom, 1974).

*Inapplicability:* This character is inapplicable for *Trichiurus lepturus* (Trichiuridae), which lacks a caudal fin.

*Indexes:* CI = 0.111; RI = 0.619

**Char. #178 (CF02). Caudal fin; *adductor dorsalis*; occurrence:** (0) absent; (1) present (Imamura & Yabe, 2002: Char. #SS4).

*Description:* The *adductor dorsalis* is a caudal muscle located on the deeper layers of the fin. The muscle originates from the lateral faces of the upper hypurals and inserts at the proximal portion

of the dorsalmost ventral caudal-fin rays (*i.e.* first rays of the lower lobe of the caudal fin). The homology of the *adductor dorsalis* is still unresolved, but it most likely develops from a dorsal migration and expansion of the dorsalmost *interradiales* from the ventral caudal-fin lobe (Winterbottom, 1974).

*Remarks:* Until the present date, this muscle has been reported as having a relatively restricted distribution among percomorphaceans: present in some Tetraodontiformes, Serranidae, Callanthiidae, Centrarchidae, Kuhliidae, Lutjanidae, Terapontidae, Sparidae, Pinguipedidae, and Nototheniidae (Nag, 1963; Nursall, 1967; Winterbottom, 1974; Imamura & Yabe, 2002). Presence of an *adductor dorsalis* has also been considered a synapomorphy for the Scorpaeniformes (including Serranidae; *sensu* Imamura & Yabe, 2002).

The *adductor dorsalis* distribution is herein broadened to also encompass the percomorphacean families Haemulidae and Kyphosidae (*sensu lato*). The presence of an *adductor dorsalis* results as an unambiguous synapomorphy for the clade composed by Kuhliidae, Lutjanidae, Terapontidae, Serranidae, Haemulidae and Kyphosidae.

*Inapplicability:* This character is inapplicable for *Trichiurus lepturus* (Trichiuridae), which lacks a caudal fin.

*Indexes:* CI = 1.000; RI = 1.000

## MISCELLANEA

### External morphology

**Char. #179 (MS01). Upper jaw complex; mobility:** (0) protrusible; (1) non-protrusible

*Description:* Most percomorphaceans exhibit the maxilla and premaxilla free to move independently from each other and from the snout, allowing the anterior protrusion of the upper jaw. This mobility plays an important role in the suction feeding, in which the fish captures food by creating a low-pressure region inside the mouth cavity. During upper jaw protrusion, both the premaxilla and maxilla are projected anteriorly, the rostral cartilage slides along the mesethmoid, and the buccal membrane (*sensu* Datovo & Vari, 2013) is quickly expanded. Together with upper jaw protrusion, the low pressured area is also created by a lateral expansion of the *suspensoria*, the abduction and lateral expansion of the lower jaw, and the posteroventral shift and lateral expansion of the hyoid bar. These

processes greatly and rapidly expand the buccopharyngeal cavity, causing the suction feeding of items (Lauder, 1982).

The present character used as landmark a premaxilla free from the snout that slides through the rostral cartilage to attest the upper jaw mobility. In some of the analyzed percomorphaceans, the ability of upper jaw protrusion has been secondarily lost. These taxa have in common a premaxilla bound to the snout by a ligamentous frenum, the maxilla partially or sometimes completely covered by the lachrymal, and the rostral cartilage bound to the ethmoid region of the neurocranium.

*Indexes:* CI = 0.500; RI = 0.962

**Char. #180 (MS02). Branchial opening; anteroventral limit: (0) at region of the isthmus; anterior limit of branchial opening delimited by fused contralateral branchial membranes; (1) located anterior to the region of the isthmus; anterior limit of branchial opening delimited by crossed, unfused, contralateral branchial membranes.**

*Description:* The evolution of the branchiostegal membranes and its association to the gill slits have been recently demonstrated to bear phylogenetic signal (Farina *et al.*, 2015). Accordingly, two distinct types of branchial openings could be categorized within the sampled taxa. Character-state 0 describes a branchial opening that starts at the posterodorsal edge of the opercle and extends ventrally to the (often) fused contralateral branchiostegal membranes that partially cover the isthmus. This condition contrasts to that described by character-state 1, which describes an anteriorly expanded branchial opening. In the second condition, the anteroventral margin of the gill slit is limited by the contralateral branchial membranes crossing over each other near the posteroventral portion of the urohyal.

*Remarks:* This character is partially related to the fusion of the branchiostegal membranes to the isthmus, another character commonly mentioned on morphological descriptions. Among the abovementioned character-states, a fusion of the branchiostegal membrane to the isthmus is restricted to specimens coded under state 1. Yet, within the analyzed taxa, branchiostegal fusion to the isthmus is uniquely observed in *Icosteus aenigmaticus* (Icosteidae), thus not coded as an independent character.

*Inapplicability:* This character is inapplicable for *Pampus cinereus* (Stromateidae), which exhibits a branchial opening restricted to a small lateral slit located at the posterior margin of the opercle. This condition is considered an autapomorphy for the genus *Pampus*.

*Indexes:* CI = 0.083; RI = 0.450

**Char. #181 (MS03). Nostrils, number of openings on each side of the head: (0) two; (1) one:**

*Description:* Paired anterior and posterior nostrils on each side of the head are present in almost all examined taxa (Figs. 19-21). A single, unpaired, nostril opening characterizes *Brama caribbea* (Bramidae) and *Trichiurus lepturus* (Trichiuridae).

*Remarks:* Although recovered as independent acquisitions for each one of the analyzed taxa, these conditions are informative in other taxonomic levels. According to Johnson (1986), a single nostril opening is a synapomorphy of the subfamily Trichiurinae. Other percomorphaceans not included in the present analysis are also reported as having a single nostril opening, such as the Zoarcoidei, Nototheniiformes, and some Callionymidae (Gosline, 1970).

*Indexes:* CI = 0.500; RI = 0.000

**Char. #182 (MS04). Nostrils; distance between anterior and posterior openings: (0) close to each other, separated only by a skinfold; (1) distant from each other, with a long olfactory duct:**

*Description:* Anterior and posterior nostril openings can be either closely set one to the other, separated by just a flap of skin (Figs. 19-21), or distant from each other, separated by an elongate olfactory duct.

*Inapplicability:* This character was coded as inapplicable for taxa exhibiting a single nostril opening (Char. #181, state 1): *Brama caribbea* (Bramidae) and *Trichiurus lepturus* (Trichiuridae).

*Indexes:* CI = 0.100; RI = 0.526

**Char. #183 (MS05). Eyes; adipose eyelid; occurrence: (0) absent; (1) present.**

*Description:* The adipose membrane of the eye is a thick, crystalline membrane disposed along the anterior and posterior margins of the orbit (Fig. 21).

*Remarks:* Although its conceived name alludes to an adipose tissue, the eyelid is composed of epithelial and connective tissue. The structure possible develops a function of blocking harmful

ultraviolet light into eyes and protecting against impacts of sediment of the aquatic environment (Chang *et al.*, 2009).

*Indexes:* CI = 0.200; RI = 0.429

**Char. #184 (MS06). Eyes; bilateral symmetry in adults: (0) symmetric; (1) asymmetric.** (Chapleau, 1993: Char. #1, modified).

*Description:* Ontogenetic migration of one eye from one side to the top or the opposite side of the head has long been recognized as the most remarkable synapomorphy for adult flatfishes (Pleuronectiformes). Many morphological studies support the homology of this character, which involves several associated cranial musculoskeletal modifications (Fig. 38). The most remarkable ones are the relocation of the frontal of the blind side to the ocular side and the enlargement of the lateral ethmoid of the blind side (Brewster, 1987; Chapleau, 1993). Among the examined taxa, eye and associated cranial musculoskeletal asymmetry was observed in *Paralichthys isosceles* (Paralichthyidae) and *Psettodes erumei* (Psettodidae).

*Remarks:* Eye asymmetry in adults result herein as an unambiguous synapomorphy for Pleuronectiformes.

*Indexes:* CI = 1.000; RI = 1.000

**Char. #185 (MS07). Pseudobranch; occurrence: (0) present; (1) absent.**

*Description:* The pseudobranch is a vestigial hemibranch primitively associated with the spiracle that is attached to the inner surface of the suspensorium or opercle of teleosts.

*Remarks:* Pseudobranch loss is uncommon, and exhibit a mosaic distribution within the analyzed percomorphaceans. Among the examined taxa, absence of pseudobranch occur independently in *Coryphaena hippurus* (Coryphaenidae), *Parachanna obscura* (Channidae), *Trachinotus carolinus* (Carangidae), and *Monocirrhus polyacanthus* (Polycentridae).

*Indexes:* CI = 0.250; RI = 0.000

**Char. #186 (MS08). Head; subcutaneous canal plexus; occurrence: (0) absent; (1) present** (Haedrich, 1967; Doiuchi, 2004: Char. #43, modified).

*Description:* Some teleosts, most notably the stromateiform fishes, exhibit a well-developed system of interconnected canals located under the skin covering the head and trunk. This network of canals is herein termed subcutaneous canal plexus. The plexus is mostly located between the external and internal layers of skin and communicate with the external surface through minute pores. The pores are densely scattered along the whole head and trunk. Taxa with canal plexus have the outer and inner skin layers separated from each other (but also kept together) by a cushion-like connective tissue traversed by blood vessels and nerves. The degree of development of the subcutaneous canal plexus is highly variable, ranging from thin and barely visible isolated tubules running through extensive blocks of connective tissue (*e.g.* Stromateidae) to a labyrinthine net of coalescent canals separated by nearly cylindrical columns of cushion-like connective tissue (*e.g.* the centrolophids *Tubbia* and *Centrolophus*).

The presence of subcutaneous canals in any part of the body has been traditionally treated as a single character in previous analyses involving the Stromateiformes. However, canal plexus on the head occurs independently from that on the trunk (*e.g.* *Arripis georgianus* – Arripidae, and *Brama caribbea* – Bramidae, have canal plexus on the head only). Moreover, the plexus of each region exhibits marked differences. The pores of the cephalic canal plexus are minute and densely scattered on the surface of skin (Fig. 21, 29; Horn, 1972: figs. 5, 6). The connective tissue enclosing these canals is predominantly amorphous and, most importantly, the entire network of cephalic canals is ultimately connected with the cephalic laterosensory system. Each pore leads to a short canal that intercommunicate laterally with the adjacent ones and coalesce internally into larger canals that, finally, connect with the main cephalic laterosensory canals (Fig. 29). The canal plexus of the trunk, in turn, has a small number of relatively larger pores and the entire system has no connection with the lateral line. In addition, most part of the connective tissues surrounding the trunk plexus has a cushion-like arrangement (Fig. 66). Therefore, subdermal canal plexuses on the head and trunk are coded in separate characters, with the present one concerning only that on the head and the following character (Char. #MS08) that on the trunk.

Taxa with a cephalic canal plexus were coded herein by exhibiting a large amount of closely set pores scattered on the surface of the cephalic skin (Horn, 1972: figs. 5, 6). Each pore leads to a short canal that intercommunicate laterally with the adjacent ones and coalesce internally into larger canals. These larger canals, on their turn, connect to the main cephalic laterosensory canals (Fig. 29).

*Remarks:* Contrasting with previous studies (*i.e.* Bone, 1972; Bone & Brook, 1973) the present analysis concludes that the subdermal canal plexus of the head is linked with the cephalic laterosensory system. Connections between these two systems were observed in the head of all stromateiform genera. Such connections are of difficult visualization in smaller and poorly preserved specimens, but clearly observed in large sized centrolophids (*i.e.* *Tubbia tasmanica*, 325 mm SL). The wide subcutaneous canal segments eventually lead to the main cephalic canals of the head (*i.e.* supraorbital, postotic). In such scenario, the cephalic canal plexus is most likely the result of a highly dendritic pattern of subdivision in the superficial tubules of the cephalic laterosensory system. A relationship of homology between the subdermal canal plexus and the lateral-line system has been previously hypothesized (Bone & Brook, 1973), but subsequently refused because of the failure in finding cells with sensory structures of any kind in the lumen of these canals. However, the lack of sensory cells on the canals forming the plexus do not refute its connection with the laterosensory system. Neuromasts, which are the lateral-line sensory cells, are typically located inside the main, deeper laterosensory canals (*i.e.* supraorbital, infraorbital, otic, postotic, etc.) and not on its branches and sub-branches. Sensory cells, therefore, would not be expected to be found on the lumen of the subdermal canal plexus, but only on the main canals of the cephalic lateral line.

*Optimization:* In the present study, a cephalic canal plexus was observed in all Stromateiformes and in the following percomorphaceans: *Pomatomus saltatrix* (Pomatomidae), *Arripis georgianus* (Arripidae), *Brama caribbea* (Bramidae), *Sphyræna tome* (Sphyrænidae), *Trichiurus lepturus* (Trichiuridae), *Orthopristis ruber* (Haemulidae), *Lutjanus analis* (Lutjanidae), *Centropomus parallelus* (Centropomidae), *Oplegnathus fasciatus* (Oplegnathidae), *Polydactilus virginicus* (Polynemidae), and all representatives of the Kyphosidae.

*Indexes:* CI = 0.100; RI = 0.667

**Char. #187 (MS09). Trunk; subcutaneous canal plexus:** (0) absent; (1) present (Haedrich, 1967; Doiuchi, 2004: Char. #43, modified).

*Description:* The subcutaneous canal plexus is described in Character MS08. Like the cephalic canal plexus, a trunk plexus is externally identifiable by the closely set pores scattered on the surface of skin, often piercing the body scales (Fig. 66C-D). These pores lead to interconnected canals embedded into the intradermal space, which is kept together by cushion-like pillars of connective tissue. The deeper canals may exhibit a sophisticated internal arrangement that is unequivocally identifiable only in larger specimens with a good state of preservation. Among the examined taxa, the

stromateiform *Hyperoglyphe perciformis* (Centrolophidae) presented the trunk canal plexus in better conditions. In this species (and similarly in most stromateiforms), the surface pores are spread all over the scaled areas of the trunk and along the dorsal and anal-fin bases. These pores lead to a series of small canals, which anastomoses under the skin forming a dendritic plexus. The anastomosed canals eventually converge into deeper canals running along the lateral surface of each myoseptum (Fig. 59). These myoseptal canals, in turn, connect to three larger, bilaterally-paired canals running longitudinally along the lateral surfaces of the horizontal septum, dorsal-fin base, and anal-fin base. A similar layout is illustrated by Bone & Brook for *Schedophilus medusophagus* (1973: fig. 1). The canal of the horizontal septum extends from the head to caudal-fin base. The dorsal and anal-fin canals span from the anterior portion of the fin to the posteriormost ray. Each of these canals connects to its antimere via a series of transverse tubules running in between the base of each fin ray. In some taxa, the canals at the dorsal-fin base also opens to the surface by means of a series of external pores (*Peprilus triacanthus*: Horn, 1970; *Schedophilus maculatus*: McDowall, 1981). The canal at the anal-fin base never opens externally into pores. A fourth main, deeper canal of the subcutaneous plexus of the trunk of *Hyperoglyphe perciformis* is associated with the caudal fin. This canal is unpaired bilaterally, lying at the sagittal plane. It begins at the fourth or fifth procurrent ray and runs in between the hemitrichia of the procurrent and principal rays of the caudal fin. The dorsal and ventral *rami* of the caudal canal meet each other and the posterior end of the canal at the horizontal septum at the joint between the dorsal and ventral hypurals (Fig. 16).

*Remarks:* The trunk canal plexus is universal but not unique to stromateiforms – similar structures are also reported for the Trachipteridae (Walters, 1963) and at least two scombriforms, *Ruvettus* (Bone, 1972) and *Makaira* (LaMonte, 1958).

Despite its taxonomic and phylogenetic importance, little has been published about the trunk canal plexus, and its ontogeny and function remain virtually unknown. Previous studies suggested this system would be related to the lateral line, oil storage, or water storage for swimming assistance. One of the first mentions to the stromateiform subcutaneous plexus was made by Gilchrist (1922). In a study focused on the pharyngeal-sac teeth of the Stromateiformes, the author briefly commented that the surface pores of a *Centrolophus* led to a network of larger canals spread over the body and filled with a very viscid oily substance. Gilchrist (1922) further warned that eating *Centrolophus* (and some other stromateiforms) could lead to “sickness or gastric disturbances”, which would possibly be due to the accumulation of lipids on the subcutaneous region. LaMonte (1965), in a very detailed description of the skin of *Makaira* (Istiophoridae; Scombriformes), also concluded the subcutaneous

plexus in this taxon is at least partially filled by fat, which was soluble in alcohol and xylol (LaMonte, 1965).

Alternative hypotheses for the function of the trunk canal plexus propose that this system would be filled with water, not lipids. Walters (1963) provided functional calculations that suggested that the subcutaneous canal plexuses of trachipterids (Lampridiformes) would function as a hydrodynamic organ. The increase on the water pressure against the skin caused by drag would make the water sink through the pores and enter the subcutaneous plexus. The water would flow from high to low pressured areas inside the canals, and then it would exit the body. This hydrodynamic flow would maintain a laminar boundary layer that could inject momentum during swimming, and at the same time damp the fluid disturbance (Walters, 1963: p. 260). Walter's (1963) hydrodynamic hypothesis for trachipterids was later reassessed and slightly modified by Bone (1972) in a study with *Ruvettus prestiosus* (Gempylidae), a fish also known to exhibit an extensive trunk canal plexuses. In Bone's (1972) hypothesis, the water stored in the trunk canal plexus would be forced out from the subdermal canals during muscle contraction. By reaching the boundary layer, the outflowing fluid would add momentum and reduce drag during swimming.

Inspired by prior descriptions (Walters, 1963; Bone, 1972), Bone & Brook (1973) revisited the swimming hypothesis in a study of the subdermal canals of centrolophid *Schedophilus ovalis* (Centrolophidae). The authors contrasted their observations to the stromateoid subdermal descriptions of Gilchrist (1922), author which suggested that the subcutaneous canals would store lipids. Bone & Brook (1973) observed "*only occasional mucus cells in the outer layer of the integument, but none have been observed in the walls of the canals*". Based on this finding, Bone & Brook (1973) suggested that the plexus would be filled with water (*sensu* Walters, 1963; Bone, 1972), and postulated that the oily substance reported by Gilchrist (1922) in *Centrolophus* was likely "*derived from the underlying tissues*" of a poorly preserved specimen. Nevertheless, the hydrodynamic importance of the trunk canal plexus would possibly be reduced in *Schedophilus* and most remaining stromateiforms (except Stromateidae) because these fishes display a sedentary lifestyle, following medusas rather than being active swimmers (Bone & Brook, 1973). No conclusive study has been performed to date, and the function of the subcutaneous canal plexus of Stromateiformes remains open to debate.

*Optimization:* The subcutaneous canal plexus on the trunk is herein recovered as an unambiguous synapomorphy for the Stromateiformes. Trachipterids and the scombriforms *Ruvettus* (Gempylidae) and *Makaira* (Istiophoridae) were not included in the present analysis, but given the fact

that these taxa are nested into relatively distant clades, the presence of their trunk canal plexuses are most parsimoniously interpreted as homoplastic events.

*Indexes:* CI = 0.500; RI = 0.950

**Char. #188 (MS10). Ventral groove; occurrence:** (0) absent; (1) present.

*Description:* Some examined taxa exhibit a groove of variable length and depth at the ventral profile of the body. This groove is usually comprised between the pelvic and anal fins and contains the urogenital papillae. The ventral groove is present in *Caristius macropus* (Caristiidae) and stromateiforms in general, with exception of *Amarsipus carlsbergi* (Amarsipidae), *Hyperoglyphe perciformis* and *Ichthys lockingtoni* (Centrolophidae), and *Tetragonurus cuvieri* (Tetragonuridae).

*Remarks:* The presence of a ventral groove results herein as a synapomorphy for non-Amarsipidae Stromateiformes. A parallel acquisition is reported for Caristiidae, and reversals in some Centrolophidae, and in Tetragonuridae.

*Indexes:* CI = 0.167; RI = 0.737

**Char. #189 (MS11). Ventral groove; length:** (0) broad, from pelvic-fin insertion to anal-fin origin; (1) reduced to area around the urogenital papillae.

*Description:* The ventral groove usually spans from the pelvic-fin base to the anal-fin origin. In *Centrolophus niger*, *Tubbia tasmanica*, *Serirolella porosa*, and in Stromateidae, the groove is much reduced in length, being restricted to a ventral skin fold that envelops the urogenital papillae.

*Inapplicability:* This character is inapplicable for taxa lacking a ventral slit (Char. #188, state 0).

*Indexes:* CI = 0.500; RI = 0.833

## Ligaments

**Char. #190 (LG01). Subocular shelf and metapterygoid; ligamentous contact:** (0) absent; (1) present.

*Description:* The subocular shelf is usually located below the eyeball and wrapped in the connective tissue surrounding the orbit. In some taxa, the subocular shelf exhibits a rather steady

position, kept in place and fixed by two ligaments (aferred herein in Character #190 and #191): 1) one links the subocular shelf posterior portion to the metapterygoid, and another attaches to the shelf's ventral surface, linking it to the ectopterygoid, endopterygoid, or the palatoquadrate cartilage separating these bones (Fig. 31, 39). The present character deals with the occurrence of a ligament extending from the posterior process of the subocular shelf to the anterior edges of the metapterygoid, usually located between the facial muscles *levator arcus palatini* and the the *adductor mandibulae pars malaris*.

*Remarks:* A peculiar, hook-like subocular shelf has been described for the snook *Centropomus undecimalis* (Smith & Bailey, 1962: p. 4). The authors commented that the hook-like process would attach to a ligament that would serve “as a guy to steady the suborbital ring”. According to the authors, a similar process would present in the moronid *Morone chrysops*. Other taxa exhibiting a posterior ligament attached to the subocular shelf are the lutjanid *Lutjanus* (Lutjanidae), the carangid *Caranx* (Carangidae), and the mullid *Pseudupeneus maculatus* (Smith & Bailey, 1962). In *Lates niloticus* (Latidae) a comparable ligament is present, but it attaches to a strengthened sheet that covers the anterior portion of the *levator arcus palatini*. This condition is coded as primarily homologous to the ligament present in other taxa that typically has a direct attachment to the metapterygoid (Fig. 31).

*Inapplicability:* Inapplicable for fishes lacking a subocular shelf (Char. #25, state 1).

*Indexes:* CI = 0.250; RI = 0.786

**Char. #191 (LG02). Subocular shelf and ectopterygoid/palatine; ligamentous contact: (0) absent; (1) present.**

*Description:* As described above in Character #190, two ligaments may attach to the subocular shelf and provide a steady position for this bone. The present character evaluates the occurrence of a ligament stretching between the ventral portion of the subocular shelf and the ectopterygoid, endopterygoid, or the palatoquadrate cartilage separating these bones. When present, this ligament is located medial to the *pars malaris* of the *adductor mandibulae* (Fig. 31, 39).

*Inapplicability:* Inapplicable for fishes lacking a subocular shelf (Char. #25, state 1).

*Indexes:* CI = 0.200; RI = 0.714

**Char. #192 (LG03). Baudelot's ligament; proximal site of attachment:** (0) at the basioccipital; (1) on the first vertebral centrum.

*Description:* The Baudelot's ligament is a stiff, round, ligament that connects the inner part of the supracleithrum to the basioccipital or anteriormost vertebral centra.

*Remarks:* A Baudelot's ligament attaching to the basioccipital is the primitive and most common condition among percomorphaceans. A posterior shift on the Baudelot's site of attachment is uncommon, and among the examined taxa occurs only in *Aulostomus maculatus* (Aulostomidae), *Icosteus aenigmaticus* (Icosteidae), and *Trichiurus lepturus* (Trichiuridae).

*Indexes:* CI = 0.333; RI = 0.333

**Char. #193 (LG04). Pelvic girdle; contralateral ligamentous association; occurrence:** (0) present; (1) absent (Stiassny & Moore, 1992; char. #6).

*Description:* Primitively in Acanthomorphata, a pair of intra-pelvic ligaments extend from either side of the pelvic fins and pass to the median process of the same basipterygium (Stiassny & Moore, 1992: fig. 9B; Stiassny, 1993). In most Percomorphaceans this general layout is modified, and the ligaments attach to the contralateral basipterygia (inter-pelvic ligament) bonding the two pelvic halves (Fig. 13; Stiassny & Moore, 1992: fig. 9C).

*Remarks:* Stiassny & Moore (1992) listed the presence of inter-pelvic ligaments in Holocentridae and "higher percomorphs" as evidence for the monophyly of a higher assemblage, in which Holocentridae is more closely related to the remaining Percomorphacea than to Beryciformes (Stiassny & Moore, 1992: fig. 14). We confirm the presence of such ligament in *Holocentrus adscensionis*, but we are unable to question the monophyly of Beryciformes due to the rooting choice in a beryciform taxon (*Beryx splendens*: Berycidae), and to a restrict sampling of taxa belonging to this order.

*Inapplicability:* This character is inapplicable for taxa lacking the pelvic girdle (Char. #92, state 1) or presenting both basipterygia fused to each other (Char. #94, state 1). This character is inapplicable for *Beryx splendens* (Berycidae), a taxon that lacks modified ligaments associated to the pelvic fins.

*Indexes:* CI = 0.250; RI = 0.571

**Char. #194 (LG05). Pelvic girdle; anteromedial ligament connecting to the cleithrum or coracoid; occurrence: (0) present; (1) absent.** (Stiassny & Moore, 1992: Char. #5, modified).

*Description:* Primitively in percomorphaceans, the pelvic girdle is positioned anteroventrally in the body, just posteroventral to the pectoral girdle (Fig. 59). In these taxa, the pelvic girdle is tightly bound to the pectoral girdle via ligaments in two distinct sites: (1) an anteromedial ligament connecting the basiptyrgium with the cleithrum or coracoid; and (2) a lateral myoseptal ligament connecting the lateral side of the basiptyrgium to the postcleithrum (Stiassny & Moore, 1992: fig. 7C-D). The present character refers to the former ligament (the later is treated in the following character, Char. #195).

*Remarks:* According to Stiassny & Moore (1992: Char. #5) the attachment of the pelvic girdle to the cleithrum or coracoid would be widespread among percomorphaceans. We corroborate these predictions and list such connection as primitively present in Beryciformes and Percomorphacea. Apomorphic loss of pectoral-pelvic girdle connection occur at least three times within percomorphaceans: in a clade comprised by Mugilidae and Atherinopsidae; in *Sphyraena tome* (Sphyraenidae); and in a clade comprised by *Pseudoscopus altipinnis* (Chiasmodontidae), *Parachanna obscura* (Channidae), *Aulostomus maculatus* (Aulostomidae), *Icosteus aenigmaticus* (Icosteidae), and Ophidiiformes (with a reversal in ophidiiforms).

*Inapplicability:* This character is inapplicable for *Trichiurus lepturus* (Trichiuridae), which lacks a pelvic girdle (Char. #92, state 1).

*Indexes:* CI = 0.250; RI = 0.571

**Char. #195 (LG06). Pelvic girdle; lateral myoseptal ligament; occurrence: (0) present; (1) absent.** (Stiassny & Moore, 1992: char. #2, modified; Stiassny, 1993; Johnson & Patterson, 1993: Char. #25, modified).

*Description:* Two distinct ligaments bound the pelvic girdle to the pectoral girdle: (1) an anteromedial ligament between basiptyrgium and cleithrum or coracoid; and (2) a lateral ligament between basiptyrgium and postcleithrum. The anteromedial ligamentous connection between the pectoral and pelvic girdles was coded in Character #194. The present character refers to the occurrence of the lateral myoseptal ligament between the anterolateral portion of the basiptyrgium and the anterior surface of the third postcleithrum (Fig. 59; Stiassny & Moore, 1992: Fig. 7C-D).

*Remarks:* In a few taxa, the distal attachment of the lateral myoseptal ligament is secondarily shifted to the body rib or peritoneum (see Char. #196). When present, this myoseptal ligament is developed in varying degrees, from a strengthening band of the myoseptal fascia to a round and robust ligament. Nevertheless, this basipterygium – peritoneum/body rib ligament is still considered homologous to that attaching to the postcleithrum. Some other taxa (*e.g. Parachanna obscura* – Channidae; *Coryphaena hyppurus* – Coryphaenidae) exhibit a strong connective tissue attaching to the anterolateral portion of the pelvic girdle, resultant from a strengthening of the skin covering the basipterygium. However, this tissue never forms a true ligament or attaches distally to the postcleithrum or body ribs. In such cases, the taxa were coded as lacking a myoseptal ligament.

The myoseptal ligament has once been hypothesized as a synapomorphy for the Acanthomorphata by Stiassny & Moore (1992). Johnson & Patterson (1993) mentioned that the sparse occurrence and variable configuration of such ligament among lower Acanthomorphata would bring doubt on the synapomorphic status of this character, and that it would better fit as a synapomorphy for a higher clade within acanthopterygian fishes (Johnson & Patterson, 1993). This analysis indicates that a myoseptal ligament between the postcleithrum and the basipterygium is primitively present among percomorphaceans, also occurring in both beryciforms sampled as outgroup.

*Inapplicability:* This character is inapplicable for taxa lacking a pelvic girdle (Char. #92).

*Indexes:* CI = 0.063; RI = 0.464

**Char. #196 (LG07). Pelvic girdle; myoseptal ligament; anterior attachment:** (0) postcleithrum; (1) ribs; (2) peritoneum [multistate non-additive]. (Stiassny & Moore, 1992: Char. #2, modified; Stiassny, 1993; Johnson & Patterson, 1993: Char. #25, modified).

*Description:* The lateral myoseptal ligament (Char. #195) typically links the pelvic girdle to the postcleithrum (Fig. 59). However, some taxa exhibit the anterior attachment of this ligament shifted to the ribs or the peritoneum.

*Remarks:* A basipterygium-rib ligamentous connection is uniquely found in the atherinopsid *Atherinella brasiliensis*. A ligamentous attachment between the basipterygium and the peritoneum occur in *Caristius macropus* (Caristiidae), and *Psenes cyanophrys* (Nomeidae).

*Inapplicability:* This character is inapplicable for taxa lacking a pelvic girdle (Char. #92, state 1) or lacking a lateral myoseptal ligament (Char. #195, state 1, respectively).

*Indexes:* CI = 0.667; RI = 0.000

## **Squamation**

### **Char. #197 (ES01). Scales; occurrence: (0) present; (1) absent**

*Description:* Scales are primitively present on the body of percomorphacean fishes with several reductions or losses occurring in specific taxa.

*Remarks:* In the present analysis, complete absence of scales was observed in *Trichiurus lepturus* (Trichiuridae) and in *Icosteus aenigmaticus* (Icosteidae). Absence of scales are optimized as independent autapomorphies for each taxon.

*Indexes:* CI = 0.500; RI = 0.000

### **Char. #198 (ES02). Head; dorsal region; scales; occurrence: (0) present; (1) absent**

*Description:* In scaled fishes, scales are either restricted to the body or also present on the head. Cephalic scales may be independently distributed along the dorsal, lateral, and/or ventral portions of the head. Among the percomorphaceans, a dorsal region of the head lacking scales is the most common condition. In this morphology scales are usually restricted to the posterior or posterolateral portion of the head and cover the lateral and medial bundles of the associated lateral *epaxialis* segment (Figs. 20, 21). However, such condition is modified in several taxa, in which scales trespass the anterior limits of the epaxial musculature and advance anteriorly over the neurocranium (Horn, 1972: Fig. 4).

*Remarks:* In taxa exhibiting scales on the dorsal portion of the head, the degree of scale coverage varies from few, restricted to the posterior portion of the frontal and parietal (*i.e. Atherinella brasiliensis*: Atherinopsidae) to a condition in which scales advance anteriorly and reach the tip of the upper lip (*i.e. Cynoscion striatus*: Sciaenidae; *Parachanna obscura*: Channidae). However, there is a gradation of intermediate states between these two extreme conditions that hampers the delimitation of clearly defined discrete states.

*Inapplicability:* Inapplicable for specimens completely lacking scales (Char. #197, state 1).

*Indexes:* CI = 0.067; RI = 0.517

**Char. #199 (ES03). Head; lateral surface; scales; occurrence: (0) present; (1) absent**

*Description:* Scales on the lateral portion of the head are commonly present in most analyzed taxa. When present, these scales spread over the opercular surface, cheek, and occasionally the lachrymal and upper jaw bones (Figs. 19-21).

*Remarks:* Absence of scales on the lateral portion of the head is uniquely present and independently acquired by *Pseudoscopelus altipinis* (Chiasmodontidae) and *Aulostomus maculatus* (Aulostomidae).

*Inapplicability:* Inapplicable for specimens completely lacking scales (Char. #197, state 1).

*Indexes:* CI = 0.500; RI = 0.000

**Char. #200 (ES04). Head; ventral region; scales; occurrence: (0) present; (1) absent**

*Description:* Scales on the ventral portion of the head are present in a few analyzed taxa, spreading over the ventral portion of the preopercle, dentary and occasionally the branchiostegal membrane.

*Remarks:* Presence of scales associated to the lower suspensorium and lower jaw bones occurred at least 7 times independently within percomorphaceans. Among these events, the presence of scales on the ventral and ventrolateral portions of the head result as independent synapomorphy for Sciaenidae + Polynemidae, and Bramidae + Caristiidae.

*Inapplicability:* Inapplicable for specimens completely lacking scales (Char. #197, state 1).

*Indexes:* CI = 0.125; RI = 0.222

**Char. #201 (ES05). Dorsal fin; interradial membrane; scales; occurrence: (0) absent; (1) present**

*Description:* Scales along the interradial membrane are independently found on the pectoral, pelvic, dorsal, anal, and caudal fins. When present in the dorsal fin, these scales are typically observed on the ventroposterior region of the fin covering the base of the finrays (Fig. 9). In several taxa, the occurrence of scales is more evident on, or even restricted to, the base of the posteriormost branched dorsal-fin rays.

*Remarks:* Stromateiform fishes present minute and deciduous scales on the body and fins, which may fall during specimen capture, preservation, and/or preparation methods. Direct observation of this character on some centrolophids and nomeids was not possible due to complete lack of scales on the body, which is probably a preservation artifact. These taxa were coded according to the descriptions of Haedrich (1967) and/ or Haedrich (1986).

*Inapplicability:* Inapplicable for specimens completely lacking scales (Char. #197, state 1).

*Indexes:* CI = 0.091; RI = 0.667

**Char. #202 (ES06). Pectoral fin; interradial membrane; scales; occurrence: (0) absent; (1) present**

*Description:* When present, scales on the interradial membrane of the pectoral fin cover the proximal half of the fin.

*Remarks:* Same as Char. #201.

*Inapplicability:* Inapplicable for specimens completely lacking scales (Char. #197, state 1).

*Indexes:* CI = 0.067; RI = 0.391

**Char. #203 (ES07). Pelvic fin; interradial membrane; scales; occurrence: (0) absent; (1) present**

*Description:* When present, scales on the interradial membrane of the pelvic fin are observed on the proximal half of the fin.

*Remarks:* Same as Char. #201.

*Inapplicability:* Inapplicable for specimens completely lacking scales (Char. #197, state 1) or lacking pelvic fins (Char. #72, state 1).

*Indexes:* CI = 0.077; RI = 0.455

**Char. #204 (ES08). Anal fin; interradial membrane; scales; occurrence: (0) absent; (1) present**

*Description:* When present, scales on the anal-fin are present along the proximal half of the fin covering the proximal portion of the fin rays (Fig. 9). In several taxa, the occurrence of scales on

the proximal portion of the fin is more evident at, or restricted to, the posteriormost branched anal-fin rays.

*Remarks:* Same as Char. #201.

*Inapplicability:* Inapplicable for specimens completely lacking scales (Char. #197, state 1).

*Indexes:* CI = 0.091; RI = 0.643

**Char. #205 (ES09). Caudal fin; interradiial membrane; scales; occurrence: (0) absent; (1) present**

*Description:* Most percomorphaceans exhibit scales advancing onto the caudal fin. These scales are typically attached to the interradiial membrane and cover at least the anterior half of the caudal fin (Fig. 9, 14). In some taxa, the scale coverage advances posteriorly and reach the posterior tip of the caudal-fin.

*Remarks:* Same as Char. #201.

*Inapplicability:* Inapplicable for specimens completely lacking scales (Char. #197, state 1).

*Indexes:* CI = 0.200; RI = 0.200

**Char. #206 (ES10). Scale; type: (0) ctenoid; (1) cycloid, (2) spinoid [multistate non-additive] (Johnson 1983, Roberts 1993, Johnson & Patterson 1993).**

*Description:* Four main scale-types are traditionally recognized in the Percomorphacea: cycloid, crenate, spinoid, and ctenoid. Among these, the cycloid scale is the simplest and hypothesized to be primitive for teleosts (Roberts, 1993). Cycloid scales are found in all major teleost lineages and are characterized by a smooth posterior margin devoid of spiny projections (Fig. 67A). Crenate, spinoid, and ctenoid scales, on the other hand, exhibit projections arising from their posterior margins.

The crenate is rather simple and comprise scales with irregular modifications on their posterior margins, such as projections and indentations. This type of scale was not found in any of the examined in the present study. As for the spinoid and ctenoid scales, for a long time these scales with a spiny posterior margin were classified under the term “ctenoid” (*e.g.*, Rosen, 1973, 1985). Johnson (1984, 1992) suggested the existence of two different and possibly non-homologous types of “ctenoid” scales (termed Ct and Ct’). Roberts (1993) latter confirmed Johnson’s (1984, 1992)

hypothesis and restricted the term spinoid for those scales presenting spines projecting posteriorly and sometimes laterally as continuations of the main body of the scale (Fig. 67B). The term ctenoid was then restricted for scales presenting true *ctenii* arising as separate ossifications that later fuse to the posterior edge of the scale (Fig. 67C).

Ctenoid scales are further distinguished in two types: transforming ctenoid scales, in which the two or three rows of *ctenii* transform into truncated spines near the scale margin (Fig. 67C); and peripheral ctenoid scales, with non-truncated *ctenii* arranged into a simple row. The transforming ctenoid type is the most common condition among the Percomorphacea, being uniquely found in this clade. This type of scale is currently hypothesized to be a synapomorphy for the Percomorphacea (Johnson & Patterson, 1993; Wiley & Johnson, 2010).

*Remarks:* Our analysis confirms the presence of transforming ctenoid scales as a synapomorphy for Percomorphacea. The presence of cycloid scales have been independently proposed as reversals, and synapomorphy for several subgroups of Percomorphacea (*e.g.* Stromateiformes: Horn, 1984; Carangiformes: Smith-Vaniz, 1984; Scombriformes: Johnson, 1986). Our analysis suggests otherwise: the shift from ctenoid to cycloid scales occurred only twice. It represents an autapomorphy for *Atherinella brasiliensis* (Atherinopsidae), and a synapomorphy for a large percomorphacean clade including several pelagic lineages (TNT Clade 76).

*Inapplicability:* Inapplicable for specimens completely lacking scales (Char. #197, state 1).

*Indexes:* CI = 0.250; RI = 0.769

## Lateral-line system

**Char. #207 (LL01). Trunk lateral line; truncation:** (0) truncated, not reaching the caudal-fin base; (1) not truncated, reaching the caudal-fin base.

*Description:* Teleosts usually present a single trunk lateral line canal (Coombs *et al.*, 1988; Webb, 1989) that follows either a straight or an arched course. The trunk lateral line generally starts at the posterior edge of the supracleithrum, and follows through the midline of the body flanks until the caudal-fin base. Although plesiomorphically present in teleosts, the trunk lateral line is completely lost in several percomorphaceans, especially in miniaturized or fossorial taxa. When present, the trunk lateral line can either be truncated, *i.e.* falling short anterior to the caudal-fin base, or complete (= not truncated), representing cases in which the lateral line reaches the caudal-fin base (Fig. 14).

*Remarks:* Same as Char. #201. In *Mugil curema* (Mugilidae) all trunk scales have an associated lateral-line segment (Freihofer, 1972; Ishida *et al.* 2015). The homology of the scale row containing a trunk canal homologous to the remaining percomorphacea was based on the descriptions of Ishida *et al.* (2015).

*Inapplicability:* This character is inapplicable for taxa completely lacking a trunk lateral line (*i.e.* *Trichiurus lepturus*: Trichiuridae). This character is inapplicable for *Dinematichthys ilucoeteoides* (Dinematichthyidae). In this taxon, the trunk lateral line is present as a series of superficial neuromasts and its completeness could not be ascertained.

*Indexes:* CI = 0.333; RI = 0.000

**Char. #208 (LL02). Trunk lateral line; extension on caudal-fin:** (0) not reaching the caudal-fin posterior margin; (1) reaching the caudal-fin posterior margin.

*Description:* Fishes exhibiting a complete lateral line may exhibit variation on the posterior extension of the lateral line (Fig. 14). These cases can be sorted in two unambiguously recognized states: 1) in which the lateral-line canal falls short between the caudal-fin base and the posterior margin of the fin (Fig. 14B), and other 2) where the canal reaches the posterior border of the caudal fin (Fig. 14A).

*Remarks:* Same as Char. #201 and #207. A trunk lateral line extending onto the posterior margin of the caudal fin resulted as independent synapomorphies for the Pleuronectiformes, for the clade comprised by Sciaenidae + Polynemidae, and for Centropomidae *sensu* Greenwood (1976).

*Inapplicability:* Same as Char. #207. This character is inapplicable for *Raneya brasiliensis* (Ophidiidae) and *Mugil curema* (Mugilidae). In both taxa, the posterior limit of the trunk lateral line could not be identified.

*Indexes:* CI = 0.250; RI = 0.500

**Char. #209 (LL03). Infraorbital canal; suborbital portion:** (0) present; (1) absent.

*Description:* In the plesiomorphic teleostean condition, a complete infraorbital canal is present and associated with the lachrymal, infraorbitals 2 to 5, and dermosphenotic (Fig. 20). Segmentation of the infraorbital canal is usually associated with truncations in the development of the cephalic

laterosensory system. When present, this process often results in losses of the canal segments associated with the infraorbital bones 2 and 3 and consequent segmentation into an anterior (associated with the lachrymal and infraorbital 2) and a posterior infraorbital segment (associated with infraorbital 5 and the dermosphenotic).

*Remarks:* More severe ontogenetic truncations lead to losses of anterior and/ or posterior portions of the infraorbital canal, independently. These were coded separately in the two following Characters #210 and #211.

*Indexes:* CI = 0.333; RI = 0.500

**Char. #210 (LL04). Infraorbital canal; anterior portion: (0) present; (1) absent.**

*Description:* Truncations in the development of the infraorbital canal often result in a segmented pattern formed by an anterior and a posterior infraorbital canal fragment (see Character #209, remarks). In taxa with more severe ontogenetic truncations, the anterior portion of the infraorbital canal is also lost.

*Inapplicability:* This character is coded as inapplicable for taxa with a contiguous, non-segmented infraorbital canal (Char. #209, state 0).

*Indexes:* CI = 1.000; RI = 1.000

**Char. #211 (LL05). Infraorbital canal; posterior portion: (0) present; (1) absent.**

*Description:* As described in Character #209, truncations in the development result in a fragmented pattern of the infraorbital canal. In some instances, severe truncations lead to the loss of the posterior portion of the infraorbital canal.

*Inapplicability:* This character is coded as inapplicable for taxa with a contiguous, non-segmented infraorbital canal (Char. #209, state 0).

*Indexes:* CI = 1.000; RI = 1.000

**Char. #212 (LL06). Postotic canal; association with the supracleithrum: (0) present; (1) absent.**  
(Stiassny, 1993, *pectoral girdle*, 1<sup>st</sup> character, pg. 207, modified)

*Description:* Primitively in Percomorphacea, the supracleithrum is a vertically elongated blade-like bone that laterally overlies the dorsal limb of the cleithrum. Dorsally, the supracleithrum receives the posteriormost portion of the postotic canal, which appears as a distinct sensory canal or groove at the lateral surface of the bone (Figs. 10, 12). Posterior to that point, the postotic canal is contiguous to the trunk lateral line and continues along the first body scales. A modification of this condition is observed in a few taxa, which exhibit a small triangular supracleithrum confined within the dorsal limits of the cleithrum (Stiassny, 1993: fig. 6). Accompanying this modification, these taxa lack an association of the postotic canal with the supracleithrum. The canal, however, is not interrupted in this region and follows from the posttemporal directly to the first dorsolateral body scales.

*Remarks:* This character was first proposed by Stiassny (1993) to support a monophyly between the Mugiliformes and Atherinomorpha. Stiassny's character regarded a "*supracleithrum reduced to a small plate confined to the dorsal limits of the cleithrum and lacking a sensory canal or groove*". The author offered an explanation to this phenomenon hypothesizing that a reduction in size of the supracleithrum would lead to the absence of the postotic canal in that bone. A similar interpretation is followed herein. Since the postotic canal is not interrupted, but rather continues directly from the posttemporal to the first lateral-line scales, it is plausible to assume that the non-association of that canal with the supracleithrum is due to a shrinking of the bone. Accordingly, we modify Stiassny's character to include only a single variable, *i.e.* the association of the postotic canal to the supracleithrum. The present character is also partially compatible to Parenti's (1993) Char. #9: supracleithrum reduced or absent. However, Parenti (1993) limits her discussion to the size of the supracleithrum, without mentioning the association with the lateral-line canals.

The optimization of this character reveals that it is no longer synapomorphic for Mugiliformes + Atherinomorpha. According to our analysis, this character-state defines a broader clade (TNT Clade 80) that includes Apogonidae, Polycentridae, Mugilidae, and Atherinopsidae. Homoplastic acquisition of this character also supports the monophyly a clade encompassing Aulostomidae, Channidae, Icosteidae, and the Ophidiiformes. A third parallel acquisition of this characteristic occurs in Bramidae.

*Indexes:* CI = 0.333; RI = 0.778

**Char. #213 (LL07). Cephalic canals; type of opening:** (0) a single tubule and pore; (1) dendritic tubules with multiple pores.

*Description:* Lateral-line pores are openings that connect the lateral-line canal lumen to the external surface. These pores are usually present along the lateral-line canal and disposed between

two adjacent neuromasts (*i.e.* a group of sensitive cells, which are the functional unity of the lateral-line system; Webb, 1989). Among percomorphaceans, pore openings are observed in two distinct categories: simple openings, with each canal tubule leading to a single pore, or a dendritic pattern, in which a main tubule subdivides into multiple *rami* with many pores covering a broad surface of the epithelium (Fig. 20, 21).

*Remarks:* A multiple, dendritic tubule branching is plesiomorphically present among Percomorphacea. Simple pores occur in two distinct percomorphacean clades: 1) in Polycentridae + Mugilidae + Atherinopsidae; and 2) in a larger clade including Rachycentridae, Coryphaenidae, Aulostomidae, Channidae, Icosteidae, and the Ophidiiformes (reversed to multiple pores in coryphaenids plus rachycentrids).

*Indexes:* CI = 0.333; RI = 0.800

## Viscera

**Char. #214 (IO1). Swim bladder; occurrence in adults: (0) present; (1) absent.**

*Description:* Teleost fishes primitively have a functional swim bladder responsible, among other functions, for buoyancy control. Nevertheless, approximately half of the extant teleostean species lack a swim bladder in the adult stage (Fänge, 1966), although it is possible that this organ is present during larval forms of many of these taxa.

*Remarks:* According to our analysis, the swim bladder is primitively present in Percomorphacea. Losses of swim bladder occur at least five times within percomorphaceans, which include the Bramidae + Caristiidae + Stromateiformes clade.

*Indexes:* CI = 0.143; RI = 0.800

**Char. #215 (IO2). Pyloric caeca; occurrence: (0) present; (1) absent.**

*Description:* Pyloric caeca are blind diverticula located at the proximal portion of the intestine of fishes (Fig. 48C). This structure is widespread among percomorphacean fishes and serves as an expansion of the gut area that enhances the fish's nutrient uptake capacity (Rahimullah & Osmania, 1945; Buddington & Diamond, 1986).

*Remarks:* Pyloric caecae are primitively present in percomorphaceans. Absence of caeca are reported herein for *Cynoscion striatus* (Sciaenidae) and *Brama caribbea* (Bramidae).

*Indexes:* CI = 0.500; RI = 0.000

**Char. #216 (IO3). Pyloric caeca; number: (0) few; (1) numerous** (Haedrich, 1967, modified).

*Description:* Although variable in their occurrence and shape among different lineages, the pyloric caeca of stromateiforms are notorious due to its complexity. These fishes exhibit numerous pyloric caeca aggregated in a dendritic mass branching from the proximal portion of the intestine (Fig. 48C). However, at least two centrolophid genera, *i.e.* *Icichthys* and *Centrolophus*, exhibit a contrasting and simplified morphology. These fishes have about 10 long arborescent pyloric caeca not forming a dendritic mass.

*Remarks:* Haedrich (1967) stated that both *Centrolophus* and *Icichthys* exhibited few (about 10) digitiform pyloric caeca. This would contrast from the other Stromateiformes that would exhibit numerous pyloric caeca enrolled in a large dendritic mass (or, in Haedrich's words, resembling a raspberry, as in *Hyperoglyphe*: Haedrich, 1967: pg. 56). According to our analysis, few pyloric caecae are plesiomorphically present in percomorphacean fishes, and do not result as a synapomorphy grouping *Centrolophus* and *Icichthys*. In fact, numerous caeca are the apomorphic state, which define higher clades within stromateiforms.

*Inapplicability:* This character is inapplicable for taxa lacking pyloric caeca (Char. #1215, state 1).

*Indexes:* CI = 0.143; RI = 0.600

## **Behavior**

**Char. #217 (BE01). Fishes; juveniles; association to gelatinous organisms: (0) present; (1) absent** (Horn, 1984: Char. #17, modified).

*Description:* Several lineages of fishes associate to floating matter in the ocean. This matter can include a variety of animals (cnidarian, ctenophore, salps, pyrosomes, other fishes), macroalgae (sargassum, kelps, other kinds of seaweed), and inanimate objects such as floating logs, wreckage, and even boats (Matthews & Shoemaker, 1952; Mansueti, 1963; Merriner *et al.* 1970; Janssen & Harbison,

1981; Quigley, 1986; Arai, 1988; Safran & Omori, 1990; Harbison, 1993; Kingsford, 1993; Purcell & Arai, 2001; Wells & Rooker, 2004). Although the association of fishes to general floating matter is a common behavior of some percomorphaceans (*i.e.* pilot fish, remoras, fish fauna associated to drift algae and flotsam), a reduced number of fishes associate to *gelata*, *i.e.* medusas, ctenophores, siphonophores, salps, pyrosomes, among others (Mansueti, 1963; Arai, 1988; Harbison, 1993; Kingsford, 1993; Purcell & Arai, 2001). The association between fish-gelata is frequently observed among young jacks (*i.e.* carangids), and occasionally mentioned for some bramids (Johnson, *pers. com.*), myctophids, girellids, sparids, zaprorids, gadiforms, and bythitids (Mansueti, 1963; Auster *et al.* 1992; Kingsford, 1993; Lynam & Brierley, 2006; Drazen & Robison, 2004). Such interactions include fish-coelenterates competition for prey (Purcell & Arai, 2001), predation by fishes on medusa and ctenophores (Arai, 1988; Harbison, 1993), coelenterate as parasite vector to fish (Arai, 1988), commensalism between fish and medusa (Mansueti, 1963; Harbison, 1993; Purcell & Arai, 2001), and fish mimicry (Jenkins, 1983; Arai, 1988; Tan, 2008; Greer *et al.* 2016).

Contrastingly, fish-*gelata* association is widespread and well documented across all lineages of Stromateiformes, especially during early life stages (Tab. 5). The young fishes initially develop the interactions as a simple commensalism, in which the fish presumably uses its host for shelter and protection from other animals (Mansueti, 1963; Duffy, 1998). Most of the time, fish-*gelata* interaction is kept as a commensalism, but cases in which the fish bites off chunks of its host has been described for several taxa (*i.e.* grazing behavior, predation). The commensalism can be observed in vast array of behaviors, with the fish actively swimming around and between the jellyfish tentacles; sitting on the jellyfish umbrella; or even entering the body cavity of jellyfish or other gelata. The most common and widespread behavior among stromateiforms is also the least specialized one: swimming around the tentacles of the medusa. This behavior was first described in detail and illustrated by Mansueti (1963: fig. 5) on a study of the association of *Peprilus aepidotus* to the scyphomedusa *Chrysaora quinquecirrha*. The fish specimens swim “freely in and out of the tentacles. They alternated between swimming three to six inches from the floating, pulsating medusa when undisturbed... They sometimes dove toward the depths away from the medusa, occasionally returning to it, however, after a short period”. When feeling threatened, these fishes may occasionally enter its host body cavity (subumbrellar area, or in between the oral arms) as an attempt to evade from possible predators (Mansueti, 1963; Haedrich, 1967: pl. 1; Lawley & Junior, 2018: fig. 1). Identical behavior has been depicted for the nomeid man-of-war fish (= *Nomeus gronovii*; Jenkins, 1983), and medusaefish (= *Schedophilus maculatus* and *S. ovalis*; Maul, 1964), *Peprilus cf. crenulatus* (Lawley & Junior, 2018), and mentioned for stromateiforms in general (Mansueti, 1963, Haedrich, 1967; Janssen & Harbison, 1981; Harbison, 1993; Purcell & Arai, 2001). Another stereotyped commensal behavior restricted to small

juvenile fishes is sitting on the top of the medusa umbrella. In these cases, the fish is described as drifting (or surfing) on the top of a medusa (Karplus, 2014: fig. 5.2). Similar behavior is known to occur in Bramidae (Johnson, *pers. com*). Although still not published, young bramids even have a modified anteriormost pelvic-fin ray that may serve as a gripping tool to attach to the medusa's umbrella.

The stromateiform commensal association develops with at least three invertebrate phyla: ctenophore, cnidarian, and tunicates, and involves different orders within each of these taxa (see the reviews of Mansueti, 1963; Janssen & Harbison, 1981; Harbison, 1993). Events of proto-cooperation (*i.e.* a non-obligatory, relaxed mutualism), parasitism (fish stealing food from jellyfish), or mimicry, although rarer among stromateiforms, do occur between fish and gelata. Such cases indicate a gain in complexity between the initial interactions between the two involved taxa. Notwithstanding, only the commensal behavior during juveniles is accounted in the present character. This choice is made in order to standardize both the behavior (commensalism) and semaphoront (juvenile fishes) considered on the present character. Different, and possibly more specialized, types of association between Stromateiformes and gelata are mentioned in the Discussion section, topic: *Stromateiform morphological adaptations related to symbiosis with gelatinous invertebrates*.

*Remarks:* Character coding applied herein was taken from available literature for the taxa used in the present analysis. These data are compiled in Table 5, which offers a full list of taxa known to develop some kind of commensal behavior with gelata.

When compared to the fish-gelata association, the general behavior of following drifting objects is much broader among percomorphaceans and possibly a primitive behavior among teleostean fishes. The behavior of hovering on floating objects is present in families of several different lineages (Kingsford, 1993: table 1), and provide not only shelter and protection but also aids on spatial orientation and enhances underwater visibility (Helfman, 1981; Kingsford, 1993). Aside gelatinous organisms, adult Stromateiformes also follow and associate to general floating objects in the ocean. Adult specimens of Centrolophidae, Nomeidae, and Stromateidae are often observed hovering around wreckage, sargassum, or flotsam (Mansueti, 1963; Merriner *et al.*, 1970; Dawson, 1971; Quigley, 1986; Kingsford, 1993; Duffy *et al.* 2000). This earns them scientific names referring floating objects, such as: *Palinurichthys* (*syn. of Hyperoglyphe*), in allusion to the Roman mythology of Palinurus, earned due to the common habit of this fish to follow boats; and *Schedophilus*, which is Greek for raft friend. Common stromateiform names also allude to their hovering-in-shade behavior. For example barrelfish (= *Hyperoglyphe*), rudderfish (= *Centrolophus*); driftfish (= nomeids in general); flotsamfish (= *Psenes pellucidus*). Accordingly, capture records of these fishes are often correlated to sargassum accumulation near the shoreline (Merriner *et al.*, 1970) or associated to floating objects in the ocean

(e.g. floating boxes: Schwartz, 1963; floating wreckage, weed, barnacle-covered log, or boats: Quigley, 1986).

*Indexes:* CI = 0.250; RI = 0.880

## Phylogenetic analysis

The present analysis sampled 218 morphological characters in 66 terminal taxa, including 22 Stromateiformes and 44 outgroup species that represent 14 orders and 40 families. The characters were categorized in continuous (22, encompassing counts and measurements), osteological (83), myological (74), and miscellaneous (39).

A phylogenetic analysis based on Equal Weights (EW), employing “new technology search” adjusted to reach 50 hits of the best score, resulted into two most parsimonious trees (MPTs) with a score of 1254.440 (offered in the appendix). These trees were employed to calculate the average homoplastic character of the EW analysis, which was then used to search for the optimal K values for different searched under Implicit Weighting (IW). In trees resultant from EW searches, the lowest number of homoplasies present in a character was zero (= a single transformation) and the most homoplastic character was Char. #114, with 24 homoplasies. Thus, the average homoplasy number used in this analysis was set at the midpoint between both values, i.e., 12 (Fig. 7). The resultant EW MPT's were also used for comparisons with the IW searches. This analysis revealed that the first K value to not inflict in changes on the topology under IW searches was K=22, and this value was set as  $K_w$ . Trees generated from K=23 to K=1000 (highest K value supported by TNT 1.6) were equal to each other and resulted in topologies nearly identical to that obtained by  $K_w=22$  and to EW searches. As for the first (i.e. strongest) K value sampled herein, this was set as  $K_s=1$ , which is equivalent to weighting based on the character's consistency index (= ci).

By adopting 12 as an *average* of homoplasies and 22 as a maximum K number, it was possible to calculate the *fit* intersection between  $K_s - K_w$  values. For K=1, *fit* is of 0.0769, and K=22 is 0.6471, and thus the range between both values is a *fit* intersect of 0.5701. Eleven regular *fit* intervals were sampled within this range starting on K=1 and stopping on K=22. The resultant K values were 1, 1.855, 2.849, 3.957, 5.267, 6.808, 8.654, 10.902, 13.702, 17.273, and 22 (Tab. 4; Fig. 7). These values were used to perform searches on TNT and resulted in 11 different topologies (available in the appendix). The trees were then imported to ViPhy (Bremm *et al.* 2011) and compared under the *Element-Based* similarity measure. As outcome, ViPhy indicated the topology obtained under 6.808 as being the tree

that is most congruent to the universe of imported trees, and thus we follow this topology as reference to our taxonomic and phylogenetic classifications.

## DISCUSSION

### The phylogeny of the Stromateiformes:

The present study is by far the largest cladistic analysis to test the monophyly, inter- and interrelationships of the Stromateiformes based on phenotypic data. Our final matrix includes 218 phenotypic characters examined in 66 terminal taxa, including 22 stromateiforms and 44 outgroup species that represent 14 orders and 40 families of Acanthopterygii. Previous morphology-based phylogenies of the order analyzed only a small fraction of these characters and taxa (Horn, 1984; Doiuchi *et al.*, 2004). Moreover, none of these studies properly tested the monophyly of the order, as only a few outgroup taxa were included in the analyses. Monophyly of Stromateiformes has been challenged by recent molecular or combined data phylogenies that repeatedly recovered the order as a para- or polyphyletic assemblage (Miya *et al.*, 2013; Betancur-R *et al.*, 2013; Near *et al.*, 2013; Mirande, 2017; Betancur-R *et al.*, 2017; Campbell *et al.*, 2018), as well as by a few morphological studies that questioned the inclusion of Amarsipidae in the order (Springer & Johnson, 2004; Datovo *et al.*, 2014). Our analysis result in one most parsimonious tree (Fig. 68), which supports Stromateiformes as monophyletic, including Amarsipidae and other five families: Ariommatidae, Centrolophidae, Nomeidae, Stromateidae, and Tetragonuridae (Fig. 70). Our study also indicates that a clade formed by the percomorphacean families Bramidae and Caristiidae represents the immediate sister-group of the Stromateiformes (Fig. 68). In the subsequent sections, all 23 resolved clades within Stromateiformes are listed and discussed and a list of unambiguous synapomorphies is offered for each one of them. In addition, further comments on the bramid-caristiids-stromateiform relationship are also provided.

### The intrarelations of Stromateiformes:

**Clade A (TNT clade 92) = Order Stromateiformes:** *Amarsipus carlsbergi*, *Serirolella violacea*, *Hyperoglyphe perciformis*, *Centrolophus niger*, *Tubbia tasmanica*, *Icichthys lockingtoni*, *Psenopsis anomala*, *Psenopsis cyanea*, *Schedophilus* sp., *Psenes sio*, *Psenes cyanophrys*, *Nomeus gronovii*, *Cubiceps whiteleggii*, *Cubiceps pauciradiatus*, *Tetragonurus cuvieri*, *Ariomma indicum*, *Ariomma bondi*, *Ariomma melanum*, *Stromateus brasiliensis*, *Pampus cinereus*, *Peprilus triacanthus*, *Peprilus paru*.

*Synapomorphies:* Char. #35 (1>0), Char. #37 (0>1), Char. #85 (0>1), Char. #187 (0>1).

*Support:* relative Bremer = 59%

*Remarks:* The monophyly of Stromateiformes (Clade A) is herein supported by four unambiguous synapomorphies and a moderate relative Bremer value. The order encompasses six families, namely Amarsipidae, Centrolophidae, Nomeidae, Tetragonuridae, Ariommatidae, and Stromateidae. The two most distinctive synapomorphies for the order are the presence of uniserial teeth in the jaws (Char. #35) and a subcutaneous canal plexus in the trunk (= subdermal canal system of Haedrich, 1967; Fig. 66; Char. #187, secondarily reversed in *Tetragonurus*;). Within the analyzed taxa, homoplastic occurrences of uniserial teeth appears only in the scombrid *Scomber* sp. (Scombridae) and in the mugilid *Mugil curema*, and the presence of the subcutaneous-canal plexus is uniquely present in Stromateiformes, with a reversal in Tetragonuridae. The other two unambiguously synapomorphies for the order involve characters that are highly homoplastic within Percomorphacea, namely the absence of palatine teeth (Char. #37) and presence of a shortened base on the penultimate ventral procurent ray (Char #85; Fig. 16).

Haedrich (1969) placed Amarsipidae within Stromateiformes based on five characteristics: a greatly expanded lachrymal bone, a protruding top of the head, a bony bridge over the anterior vertical canal of the inner ear (= *pons moultoni sensu* Haedrich, 1971), the jaws with uniserial teeth, and an extensive subdermal canal system over the body (head and trunk). Although not explicitly discussed by the author, these characters would represent a novel and expanded diagnosis for Stromateiformes. The former definition of the order (offered by Haedrich, 1967) included only the pharyngeal sac and uniserial jaw teeth as stromateiform characteristics. We have reanalyzed two of the five characters of Haedrich (1969): the uniserial jaw teeth and the subdermal canal system over the body. While the first feature is confirmed as a synapomorphy for Stromateiformes, the latter proved to be a compound character that was herein split into with two independent characters: the subcutaneous canals of the head (Char. #186; Fig. 29) and of the trunk (Char. #187; Fig. 66). The cephalic subcutaneous canals are highly homoplastic across percomorphs and only the trunk canals were recovered as a stromateiform synapomorphy. The remaining Haedrich's (1969) synapomorphies for the order are either vaguely delimited (*i.e.* lachrymal bone expansion, protruding top of the head) or demanded destructive dissections (*pons moultoni*), and thus were not coded herein.

The allocation of *Amarsipus* within Stromateiformes, and consequently the discussion over which synapomorphies sustain the order, have been subjects of recurrent debate. For example, the placement of Amarsipidae as sister group of the remaining Stromateiformes as obtained herein is compatible with Horn's (1984) topology (Fig. 2A). In Horn's (1984) study *Amarsipus* supposedly shared with the remaining stromateiforms the apomorphic possession of cycloid scales, a scaled preopercular

bone, and the possession of six hypurals. Nevertheless, our analysis demonstrates that none of these supposed synapomorphies are valid. The high hypural count for *Amarsipus* is obviously a misidentification of the parhypural as a first hypural (Fig. 17; Haedrich, 1967: figs. 10, 12, 17, 24, 33, 36, 42, 47; Haedrich, 1969: fig. 5; Horn, 1984). Regarding the amarsipid scale type, its optimization as synapomorphy for the Stromateiformes is due to the restrict outgroup comparison employed in Horn's analysis, which included only one species of Scorpidae, Girellidae, and Kyphosidae. Our analysis recovers a cycloid-scale type (Char. #206) as synapomorphy for a larger percomorphacean clade (Fig. 69: TNT Clade 76). As for the presence of scale on the lateral surface of the head (Char. #199, a necessary modification of Horn's character 16 about the preopercular squamation), this feature is plesiomorphically present in percomorphaceans. Notwithstanding these divergences, the basal position of *Amarsipus* within Stromateiformes in Horn's (1984) analysis was primarily by the absence of a pharyngeal sac, a finding corroborated by our analysis.

Doiuchi et al. (2004) offered a change in the amarsipid placement, and consequently a modification on the characters supporting the stromateiform monophyly. In that study, the Centrolophidae formed a basal stromateiform polytomy, while Amarsipidae was deeply nested within Stromateiformes as the sister group of the clade containing Ariommatidae, Nomeidae, Tetragonuridae, and Stromateidae (Fig. 2B). Eight characters supported the monophyly of Stromateiformes on that arrangement (Doiuchi *et al.*, 2004: p. 209), which also included the presence of a pharyngeal sac, and would be secondarily reverted in *Amarsipus*.

The contentious positioning of the Amarsipidae is partially due to the fact *Amarsipus* does exhibit a mosaic of primitive and derived stromateiform features. Characters supporting its basal placement within the order involve the absence of the pharyngeal sac, unfused hypurals, three epurals (Fig. 17), and an epaxial musculature not covering the skull roof. Yet, *Amarsipus* displays some derived characteristics such as an elevated vertebral count (47), which is paralleled only in a few stromateiforms (*e.g.* *Stromateus*, 47; *Tetragonurus*, 53; *Icichthys*, 60); a reduced number of branchiostegal rays (6); and the symbiosis with gelatinous invertebrates (= gelata). Contrary to previous assumptions (*e.g.* Horn, 1984: Char. #27), young amarsipids do associate with gelata, more specifically with salps and pyrosomes (Tab. 5). In contrast with the generalized stromateiform association with medusae, symbiosis with salps and pyrosomes are rare among stromateiforms and reported elsewhere only for some *Cubiceps* and tetragonurids (Janssen & Harbison, 1981). Amarsipidae and Tetragonuridae seem to be particularly more specialized in living inside and feeding on salps (Harbison, 1993), a behavior possibly secondary to the preexisting association with medusae.

The relatively long and compressed bodies of *Amarsipus* and *Tetragonurus* might be adaptations for the life in such confined spaces (Fig. 71).

A sister-group relationship between Amarsipidae and Tetragonuridae was recently proposed by the molecular analysis of Campbell *et al.* (2018). However, this clade was resolved as more related to Scombridae, while the remaining Stromateiformes were grouped with Bramidae, Icosteidae, and Caristiidae. A clade Tetragonuridae + Amarsipidae was not supported by our analysis in any scenario, and the placement of *Tetragonurus* within Ariommatidae and Stromateidae is strongly supported by a series of morphological characters (see discussion below: clades P and Q).

**Clade B (TNT clade 19) = Suborder Amarsipoidei (new name, containing Amarsipidae):** *Amarsipus carlsbergi*.

*Autapomorphies:* Char. #1: (8-9>11); Char. #2: (28-30>23); Char. #12: (31-38>47); Char. #13: (10-11>13); Char. #14: (9>13); Char. #15: (7>6); Char. #17: (56.5%>32%); Char. #19: (34%-36%>21.8%); Char. #20: (54.2%-54.7%>45.9%); Char. #48: (1>0); Char. #67: (0>1); Char. #102: (0>1); Char. #103: (1>2); Char. #104: (2>3); Char. #111: (0>1); Char. #114: (1>0); Char. #115: (1>2); Char. #168: (1>0); Char. #171: (1>0); Char. #172: (0>1); Char. #182: (0>1); Char. #205: (1>0).

*Support:* ---

*Remarks:* Amarsipidae is a monotypic family containing the sole species *Amarsipus carlsbergi*. This taxon was obtained herein as sister group of the remaining Stromateiformes. Twenty-two characters are optimized as autapomorphies for *Amarsipus*. Haedrich (1969) taxonomically diagnosed *Amarsipus carlsbergi* from the remaining Stromateiformes by the combination of anteriorly displaced pelvic fins, toothed vomer, six hypurals, two epurals, and absence of the pharyngeal sac. These characteristics are compatible with our Characters #19, #36, #58, #80, #81. Among these, only Char. #19 is optimized as an apomorphy for Amarsipidae, while the remaining characters are considered retained plesiomorphies.

A subordinal treatment for Amarsipidae was suggested for the first time by Haedrich (1969). However, the author refrained himself of raising that suborder because it could mask the relationship of this taxon with the remaining Stromateiformes. This was a valid argument in a context where stromateiforms were still being treated as Stromateoidei, a suborder within the non-monophyletic Perciformes. However, as current classifications raised Stromateiformes to an ordinal level (Wiley &

Johnson, 2010), the formal ranking of Amarsipoidei (Clade B) as the sister group of the Stromateoidei (Clade C, treated below) is an appropriate taxonomic adjustment.

**Clade C (TNT clade 100) = Stromateoidei (new usage for non-Amarsipidae Stromateiformes):** *Seriolella violacea*, *Hyperoglyphe perciformis*, *Centrolophus niger*, *Tubbia tasmanica*, *Icichthys lockingtoni*, *Psenopsis anomala*, *Psenopsis cyanea*, *Schedophilus* sp., *Psenes sio*, *Psenes cyanophrys*, *Nomeus gronovii*, *Cubiceps whiteleggii*, *Cubiceps pauciradiatus*, *Tetragonurus cuvieri*, *Ariomma indicum*, *Ariomma bondi*, *Ariomma melanum*, *Stromateus brasiliensis*, *Pampus cinereus*, *Peprilus triacanthus*, *Peprilus paru*.

*Synapomorphies:* Char. #3: (18>19-20); Char. #5: (16>17-18); Char. #12: (31-38>25); Char. #16: (32%-33.2%>34%-35.8%); Char. #18: (20.8%-22.8%>23.6%); Char. #26: (1>0); Char. #31: (0>1); Char. #36: (0>1); Char. #44: (0>1); Char. #58: (0>1); Char. #70: (1>0); Char. #127: (0>1); Char. #135: (0>1); Char. #147: (0>1); Char. #152: 1>0; Char. #153: (0>1); Char. #159: (0>1); Char. #188: (0>1); Char. #201: (0>1); Char. #204: (0>1).

*Support:* relative Bremer = 55%

*Remarks:* The suborder Stromateoidei is herein proposed to encompass all non-amarsipid Stromateiformes, namely the families Centrolophidae, Nomeidae, Tetragonuridae, Ariommatidae, and Stromateidae. The monophyly of this clade is supported by several morphological characters and obtained under all searching parameters employed in this study. Among the characters supporting Clade C, the presence of the pharyngeal sac (Char. #58) is obviously the most remarkable as this organ is, to our knowledge, unparalleled in vertebrates (Figs. 42-53). Accordingly, a natural assemblage comprising the pharyngeal-sac bearing stromateiform fishes has long been recognized by morphological studies (*e.g.* Regan, 1902; Gilchrist, 1922; Bühler, 1930; Barnard 1948; Haedrich, 1967; Horn, 1984; Datovo *et al.* 2014). In addition, these fishes also share a long and streamlined upper pharyngeal tooth plate (Char. #44; Figs. 43A, 44C, 45C, and 46C), the absence of the section dorsalis of the *sphincter oesophagi* (Char. #147, with a reversal in *Icichthys* and Stromateidae; Figs. 46A, 49A, and 51A), the presence of a medial contact between the *pharyngoclaviculares interni* (Char. #159; Figs. 49C, 50C, 51C, and 52C), and presence of a ventral abdominal groove (Char. #188).

Under an explicit phylogenetic context, a Stromateoidei clade was surprisingly obtained by only one previous study (Horn, 1984) based on two synapomorphies: the presence of the pharyngeal sac (Char. #58) and the juvenile association with floating objects (Char. #217). However, as mentioned above (Clade A, *Remarks*), an association between small fishes and gelatinous organisms has already

been reported for juvenile amarsipids (Janssen & Harbison, 1981; Harbison, 1993) as well as some other non-stromateiform percomorphaceans (Tab. 5). Our analysis reveals that feature (Char. #217) as synapomorphic for a larger clade including Bramidae, Caristiidae, and Stromateiformes (Figs. 68, 69).

**Clade D (TNT clade 104; new, unnamed):** *Seriolella violacea*, *Hyperoglyphe perciformis*, *Centrolophus niger*, *Tubbia tasmanica*, *Icichthys lockingtoni*

*Synapomorphies:* Char. #21: (32%-37.5%>27.7%); Char. #34: (0>1); Char. #43: (1>0); Char. #189: (0>1).

*Support:* relative Bremer = 39%

*Remarks:* The family Centrolophidae, as defined by Haedrich's (1967) taxonomic revision, encompass stromateiforms with pelvic fins present in adults (Char. #72), continuous dorsal fin (Char. #67), toothless palate (Char. #37), seven branchiostegal rays (our Char. #15), six "hypurals" (actually five hypurals + parhypural; see Chars. #80 and #81; Fig. 16), pharyngeal-sac papillae with irregular bases (Char. #63) and arranged in a number of transversal bands (Char. #140). According to this diagnosis the family would encompass the following genera: *Hyperoglyphe*, *Seriolella*, *Centrolophus*, *Tubbia*, *Icichthys*, *Schedophilus*, and *Psenopsis*. However, such arrangement never resulted in a monophyletic group in our study (Fig. 70), as five of its representatives (namely *Seriolella*, *Hyperoglyphe*, *Centrolophus*, *Tubbia*, and *Icichthys*) comprise the Clade D, and three other form successive sister groups of the clade that includes all remaining stromateiform families (Clades H, I, and J). According to our analysis, all characteristics used by Haedrich (1967) to define Centrolophidae result in plesiomorphies within Stromateiformes. Thus, it is not surprising that the family is not resolved as a monophyletic assemblage.

The previous morphological analyses of Horn (1984) and Doiuchi et al. (2004) also recovered a non-monophyletic Centrolophidae, although with distinct arrangements. In Horn's (1984) cladogram, the centrolophid *Tubbia* and *Icichthys* formed an unresolved tritomy with the remaining non-centrolophid stromateoids (Fig. 2A; Clade K below). Doiuchi *et al.* (2004), on the other hand, posited *Psenopsis* as sister group to a clade comprising the other five stromateiform families (Amarsipidae, Ariommatidae, Nomeidae, Tetragonuridae, and Stromateidae; Fig. 2B). Interestingly, a monophyletic Centrolophidae has been obtained only by the few molecular analyses that sampled more than one member of the family (Doiuchi & Nakabo, 2006; Miya *et al.*, 2013; Figs. 3, 4).

A clade grouping *Seriolella*, *Hyperoglyphe*, *Centrolophus*, *Tubbia*, and *Icichthys* is herein proposed for the first time. The clade is supported by four synapomorphies, which include the presence of a bony window at the posterior myodome (Char. #34); and of tooth plates associated to epibranchial 3 (Char. #43).

**Clade E (TNT clade 103; new, unnamed):** *Hyperoglyphe perciformis*, *Centrolophus niger*, *Tubbia tasmanica*, *Icichthys lockingtoni*.

*Synapomorphies:* Char. #3: (19-20>21); Char. #5: (17-18>19); Char. #14: (9>10); Char. #111: (0>1); Char. #171: (1>0); Char. #172: (0>1); Char. #202: (0>1); Char. #203: (0>1).

*Support:* relative Bremer = 39%

*Remarks:* For the first time *Hyperoglyphe*, *Centrolophus*, *Tubbia*, and *Icichthys* are grouped in a monophyletic lineage (Fig. 70). The clade is supported by eight synapomorphies. These include an increase in number of pectoral-fin rays (Chars. #3 and #5) and of ventral procurrent rays (Char. #14), and the presence of a posteroventral section of the *epaxialis* musculature.

**Clade F (TNT clade 102; new, unnamed):** *Centrolophus niger*, *Tubbia tasmanica*, *Icichthys lockingtoni*.

*Synapomorphies:* Char. #1: (8>5); Char. #13: (10-11>12-13); Char. #14: (10>11-12); Char. #18: (23.5%>11.8%-13.5%); Char. #19: (34%-36.2%>27.5%); Char. #20: (54.2%-60.2%>53.8%); Char. #50: (1>0); Char. #68: (1>2); Char. #74: (1>0); Char. #114: (1>2).

*Support:* relative Bremer = 44%

*Remarks:* Within Centrolophidae, a clade composed of *Centrolophus*, *Tubbia*, and *Icichthys* is proposed herein for the first time. Members of this clade share several morphological novelties, including the lack of a membrane connecting the medial most pelvic-fin ray to the body wall (Char. #74); a posteriorly displaced dorsal-fin insertion (Char. #68); and the highest counts of dorsal and ventral procurrent fin-rays among Stromateoidei (Chars. #13 and #14).

Although never recovered as a clade, a possible relationship between these centrolophid genera has been suggested by previous studies. Concerning *Centrolophus*, Haedrich (1967) stated that it “shows much affinity of form towards *Icichthys*, from which it differs mainly in having far fewer vertebrae”. Bolch et al. (1994) have indicated a relationship between *Centrolophus* and *Tubbia* in a

phylogenetic study of the Australian Centrolophidae based on allozyme electrophoresis. According to the authors, both taxa would be grouped when analyzed on a UPGMA tree method (unweighted pair-group method with arithmetic means) based on genetic distance (Bolch *et al.*, 1994: fig. 1). Nevertheless, when analyzed by distance-Wagner tree or cladistic maximum-parsimony, a different topology is obtained, with *Centrolophus* and *Tubbia* as successive sister groups of *Hyperoglyphe*, *Seriolella*, *Psenopsis*, and some *Schedophilus* (Bolch *et al.*, 1994: fig. 2 and 3). The genus *Icichthys* was not sampled in Bolch's study.

**Clade G (TNT clade 105; new, unnamed):** *Tubbia tasmanica*, *Icichthys lockingtoni*.

*Synapomorphies:* Char. #7: (27>32); Char. #9: (24>29); Char. #12: (25>42); Char. #21: (27.7%>32.3%); Char. #29: (0>1); Char. #34: (1>0); Char. #70: (0>1); Char. #173: (1>0).

*Support:* relative Bremer = 53%

*Remarks:* The sister-group relationship between *Tubbia* and *Icichthys* is herein proposed for the first time (Fig. 70). Derived features such as high numbers of vertebrae (Char. #12) and anal-fin rays (Chars. #7 and #9), a single supernumerary spine without serial association with the dorsal-fin pterygiophores (Char. #70), and a well-developed posteroventral bundle of the *epaxialis* muscle attaching to the back of the skull (Char. #173) support the clade. Evidences toward a *Tubbia-Icichthys* relationship has been indirectly considered by Haedrich & Horn (1972) as the authors listed *Tubbia* (then considered a synonym of *Schedophilus*) among the species of *Icichthys* based on a high vertebral count.

The genus *Icichthys* originally included a single species, *I. lockingtoni* (Jordan & Gilbert, 1880). *Icichthys australis* was described almost a century later by Haedrich (1966) for the New Zealand coast. The species was then raised to the genus level (Parin & Permitin, 1969) under the name *Pseudoicichthys*. However, this taxonomic decision was harshly criticized (Krefft, 1969; McDowall, 1982) and the species has been variably treated as *Icichthys* (*e.g.* Haedrich & Horn, 1972; McDowall, 1982) or *Pseudoicichthys* (*e.g.* Haedrich, 1986; Stewart *et al.*, 2015; Fricke *et al.*, 2018). Although not sampled herein, information from the literature allow me to infer that *Icichthys australis* would fall in the centrolophid Clade G, most likely as sister group to *Icichthys lockingtoni*. According to the descriptions of Haedrich (1966) and Parin & Permitin (1969), *Icichthys australis* shares with Clade G high vertebral (50-52; Char. #12) and anal-fin ray counts (27-28; Char. #9), and with *Icichthys lockingtoni* an absence of the ventral groove (Char. #188), an unparallel elevated number of supraneural bones (9-10; Char. #11), and the highest predorsal length among centrolophids (42-43 %

of SL; Char. #16). Once corroborated the sister-group relationship between *I. lockingtoni* and *I. australis*, the erection of a separate genus for the latter taxon is completely unjustifiable. Parin & Permitin (1969) claimed that the differences between the two species were sufficient to separate them at the generic level, an argument that is obviously flawed. The diagnosis offered to *Pseudoicichthys* was based on characters that are either homoplastic to other centrolophids (*i.e.* scales on the top of the head, pyloric caeca numerous, three epurals), or synapomorphic to *Icichthys* (great predorsal length, high vertebral count, 9-11 supraneurals). In this sense, I see no reason to raise a monotypic genus to allocate *Icichthys australis* and advocate against the usage of the name *Pseudoicichthys*.

**Clade H (TNT clade 99; new; unnamed):** *Psenopsis anomala*, *Psenopsis cyanea*, *Schedophilus* sp., *Psenes sio*, *Psenes cyanophrys*, *Nomeus gronovii*, *Cubiceps whiteleggii*, *Cubiceps pauciradiatus*, *Tetragonurus cuvieri*, *Ariomma indicum*, *Ariomma bondi*, *Ariomma melanum*, *Stromateus brasiliensis*, *Pampus cinereus*, *Peprilus triacanthus*, *Peprilus paru*.

*Synapomorphies:* Char. #1: (8>7); Char. #216: (0>1).

*Support:* relative Bremer = 99%

*Remarks:* Clade H is a newly proposed clade for the Stromateiformes. It contains the Centrolophidae genera *Psenopsis* and *Schedophilus*, and the stromateoid families Nomeidae, Tetragonuridae, Ariommatidae, and Stromateidae. The clade exhibits a high relative Bremer value and is supported by two unambiguous synapomorphies: a reduction in number of dorsal-fin spines (Char. #1), and the presence of numerous and dendritic pyloric caeca (Char. #216; Fig. 48C).

Similar to the topology offered herein, Doiuchi's *et al.* (2004) Clade B also retrieves the genus *Psenopsis* closer to the remaining Stromateiformes than to the Centrolophidae (Fig. 2B). His clade is supported by two synapomorphies (Doiuchi *et al.*, 2004: Char. #3>1, 9>1). However, his Clade B differs from our topology in not including *Schedophilus*, which is rather grouped with *Seriolella* (for further comments on the intrarelationships of *Schedophilus* see our remarks on Clade J).

**Clade I (TNT clade 98; new, unnamed):** *Psenopsis cyanea*, *Schedophilus* sp., *Psenes sio*, *Psenes cyanophrys*, *Nomeus gronovii*, *Cubiceps whiteleggii*, *Cubiceps pauciradiatus*, *Tetragonurus cuvieri*, *Ariomma indicum*, *Ariomma bondi*, *Ariomma melanum*, *Stromateus brasiliensis*, *Pampus cinereus*, *Peprilus triacanthus*, *Peprilus paru*.

*Synapomorphies*: Char. #50: (1>0); Char. #85: (1>0); Char. #115: (1>2).

*Support*: relative Bremer = 43%

*Remarks*: For the first time, the centrolophid genus *Psenopsis* is sampled by more than one species in a cladistic analysis. Interestingly, our results do not recover the monophyly of the genus, with *Psenopsis cyanea* appearing as more closely related to other stromateiform families than to *P. anomala* (Fig. 70). The genus is currently composed by six valid species (Fricke *et al.*, 2018) and diagnosed from other centrolophids by a combination of characteristics that involves a similar number of dorsal and anal-fin rays, absence of supramaxilla, position of the pelvic fins, among others (Haedrich, 1967).

*Psenopsis* is one of the most obscure genus within Stromateiformes. Little information has been published on this taxon and the available data on the genus is mostly summarized to geographical records for some of its valid species (*e.g.* Thomas & Rohit, 2007). Some studies have suggested that *Psenopsis* species might be organized in two groups based on their body shape: a “narrow-bodied” and a “deep-bodied” species group (Thomas & Rohit, 2007). Among the species sampled herein, *Psenopsis cyanea* is classified as “narrow-bodied” and *P. anomala* as a “deep-bodied” taxon and our analysis indicates that these species groups are not sister to each other (Fig. 70).

**Clade J (TNT clade 97; new, unnamed)**: *Schedophilus* sp., *Psenes sio*, *Psenes cyanophrys*, *Nomeus gronovii*, *Cubiceps whiteleggii*, *Cubiceps pauciradiatus*, *Tetragonurus cuvieri*, *Ariomma indicum*, *Ariomma bondi*, *Ariomma melanum*, *Stromateus brasiliensis*, *Pampus cinereus*, *Peprilus triacanthus*, *Peprilus paru*.

*Synapomorphies*: Char. #12: (25>33); Char. #15: (7>6); Char. #17: (57%>60.6%); Char. #25: (0>1); Char. #31: (1>0); Char. #80: (0>1); Char. #81: (0>1); Char. #118: (0>1); Char. #119: (0>1); Char. #120: (0>1).

*Support*: relative Bremer = 99%

*Remarks*: The phylogenetic position of the centrolophid *Schedophilus* herein obtained contrasts with prior hypotheses (Horn, 1984; Bolch *et al.*, 1994; Doiuchi *et al.*, 2004; Doiuchi & Nakabo, 2006). Our *Schedophilus* sp. appears as sister group of the non-centrolophid stromateoids (Fig. 70). These taxa are grouped in our analysis on the basis of the apomorphic sharing of 33 vertebrae (Char. #12), six branchiostegal rays (Char. #15), fused hypurals (Chars. #80 and #81), *coronalis* and *prementalis* sections of the *adductor mandibulae* completely separated from each other (Char. #118),

a *coronalis* posteriorly expanded and trespassing the dorsal limit of the dentary (Char. #119; Figs. 37, 61), and a *postmentalis* completely separated from the *prementalis* (Char. #120; Fig. 61).

The taxonomy of *Schedophilus* is highly problematic. The genus currently includes eight valid species (Fricke *et al.*, 2018), which have been suggested to form two species groups: one including the fishes with compressed, elongated, and soft bodies and the other formed by species with short, stout, thick, and hard bodies (McDowall, 1982). Variations between the two *Schedophilus* species groups include a wide range of dorsal-fin rays (30 to 60), dorsal-fin spines (zero to nine), and vertebrae (25 to 31) (Haedrich, 1967; Haedrich & Horn, 1972; McDowall, 1979, 1982). Additionally, four different arrangements of predorsal bones are observed across the genus (Ahlstrom *et al.* 1976). Taxonomically, at least some species of *Schedophilus* (*S. griseolineatus* or *S. labyrinthicus*) have been proposed as closely related, or even belonging, to the genus *Seriolella* (McDowall, 1982) based on the sharing of a deep and thick body. In contrast, *Schedophilus* species with compressed, elongate, and soft bodies, such as *S. huttoni*, greatly resemble the elongate centrolophids *Tubbia*, and *Icichthys*, additionally sharing with these genera increased numbers of dorsal-fin rays and vertebrae (see remarks on Clade G).

The morphological variability among the species of *Schedophilus* and its apparent lacking of unequivocal synapomorphies suggest the genus is not monophyletic. Indeed, an exploratory study based on allozymes indicates the possible polyphyly of the genus (Bolch *et al.*, 1994). This might also explain the recalcitrant allocation of the genus across different cladistic analyses that sampled only one species of *Schedophilus* (Horn, 1984; Doiuchi *et al.*, 2004; Doiuchi & Nakabo, 2006; present study; Figs. 2, 3, 70).

**Clade K (TNT clade 96) = Nomeidae + Tetragonuridae + Ariommatidae + Stromateidae (Doiuchi *et al.*, 2004: Clade D):** *Psenes sio*, *Psenes cyanophrys*, *Nomeus gronovii*, *Cubiceps whiteleggii*, *Cubiceps pauciradiatus*, *Tetragonurus cuvieri*, *Ariomma indicum*, *Ariomma bondi*, *Ariomma melanum*, *Stromateus brasiliensis*, *Pampus cinereus*, *Peprilus triacanthus*, *Peprilus paru*.

*Synapomorphies:* Char. #1: (7>11); Char. #62: (0>1); Char. #63: (0>1); Char. #110: (1>0).

*Support:* relative Bremer = 83%

*Remarks:* The families Nomeidae, Ariommatidae, Tetragonuridae, and Stromateidae form a clade mostly supported by characters related to the morphology of the pharyngeal-sac rakers. At this

node of the stromateiform tree, sac raker acquire a distinct vertical axis (Char. #62; Fig. 55) and distinct symmetrical basis (Char. #63; Figs. 55, 56), hence losing its primitive conical morphology.

The monophyly of a clade including Nomeidae, Tetragonuridae, Ariommatidae, and Stromateidae is in accordance with all morphology-based phylogenies of Stromateiformes (Horn, 1984; Doiuchi *et al.* 2004). In Horn (1984), this clade was also supported by aspects of the pharyngeal-sac rakers, as well as by a reduced number of branchiostegal rays and hypurals (which are synapomorphies listed herein for Clade J). Doiuchi's *et al.* (2004) analysis retrieved no pharyngeal-sac character supporting this clade, as the authors deliberately unsampled characters from this organ arguing that they would not be applicable to the outgroup taxa. Curiously, most molecular analyses do not recover a monophyletic Clade K (Doiuchi & Nakabo, 2006; Li *et al.*, 2007; Betancur-R *et al.*, 2013; Miya *et al.*, 2013; Betancur-R *et al.*, 2017; Campbell *et al.*, 2018), mainly because of the indecisive grouping of Tetragonuridae with disparate taxa (often non-stromateiforms). Only under Bayesian inference, the molecular analysis of Doiuchi & Nakabo (2006) grouped Tetragonuridae with Stromateidae and resolved a monophyletic Clade K (Fig. 3), but it should be noticed that this study included only one non-stromateiform as the outgroup taxon.

Our analysis indicates that Nomeidae is sister-group of the remaining families of Clade K. This is corroborated by the overall morphology of the nomeid pharyngeal sac that, in many details, retain plesiomorphic conditions present in the centrolophid organ, such as the pharyngeal-sac externally grooved and roughly kidney-shaped (Figs. 49B, 50, 51; Char. #138; Isokawa *et al.*, 1965; Springer & Johnson, 2004: pl. 177), with lateral sulci for the passage of main nerves and vessels (Char. #140). Internally, the nomeid pharyngeal sac also exhibits the same wrinkled lining found in centrolophids, versus the apomorphic papillary pattern observed in tetragonurids, ariommatids, and stromateids (Fig. 46; Char. #59).

Clade K arrangement is almost identical to that obtained by Horn (1984), but contrasting with the predictions of Haedrich (1967) and the phylogenetic analysis of Doiuchi *et al.* (2004). Haedrich (1967) posited that nomeids would constitute one of the "basal stocks" of Stromateiformes (the other constituted by the Centrolophidae), from which ariommatids and tetragonurids would have derived (Fig. 1). On the other hand, Doiuchi *et al.* (2004) retrieved Ariommatidae as sister group of the remaining stromateoid families, and Nomeidae aligned with Tetragonuridae and Stromateidae (Fig. 2B).

**Clade L (TNT clade 107) = Nomeidae:** *Psenes sio*, *Psenes cyanophrys*, *Nomeus gronovii*, *Cubiceps whiteleggii*, *Cubiceps pauciradiatus*

*Synapomorphies:* Char. #89: (0>1); Char. #198: (1>0); Char. #202: (0>1).

*Support:* relative Bremer = 77%

*Remarks:* The monophyly of Nomeidae has never been questioned on the grounds of morphology (Haedrich, 1967; Horn, 1984; Doiuchi *et al.* 2004; Doiuchi & Nakabo, 2006) and accordingly these families are recovered herein as natural assemblage. One of the most distinctive characteristics of nomeid fishes is their modified pectoral fin, which has a ventral expansion on the coracoid that anchors a hypertrophied *abductor profundus* muscle (Figs. 11, 12; Char. #89). As consequence, the coracoid of these fishes exhibits an anteroventral curvature before contacting the cleithrum. This morphology contrasts with that from all other stromateiforms, in which the ventral limb of the coracoid meets the cleithrum in a straight line and the *abductor profundus* is never hypertrophied (*e.g.* Figs. 13, 29).

According to Haedrich (1967) nomeid fishes could be grouped based on a combination of characteristics that would include the anterior and posterior dorsal fins separated from each other, six branchiostegal rays, vomer and palatine toothed, hypurals 1-2 and 3-5 fused, and three epurals (Chars. #67, #15, #36, #37, #80, #81, and #82, respectively). Horn (1984), in turn, listed the stellate base of the pharyngeal-sac associated raker (Char. #64; Figs. 55E-F, 56C) and the separated dorsal fins (Char. #67) as synapomorphy for Nomeidae. While we confirm the presence of these features in nomeids, our analysis indicated that none of them results in actual synapomorphies for the family. These are actually synapomorphic for different levels of the stromateiform tree. As to Doiuchi's *et al.* (2004) supposed synapomorphies for Nomeidae (their char. #4>2, and #33>1), these characters were excluded from the present analysis because of the verified ambiguity in the distinction between the proposed states.

Taxonomically, nomeid fishes have often been characterized by the presence of tooth plates associated with the palatine, basihyal, and basibranchial (Fig. 45A-B; *e.g.* Haedrich, 1967). However, basihyal and basibranchial teeth have been reported as absent in some species of *Psenes*, including the *P. sio* sampled herein (Haedrich, 1970). Accordingly, our analysis indicates that the presence of palatine, basihyal and basibranchial tooth plates define a lesser inclusive clade of nomeids (see Clade M, remarks).

**Clade M (TNT clade 106; new, unnamed):** *Psenes cyanophrys*, *Nomeus gronovii*, *Cubiceps whiteleggii*, *Cubiceps pauciradiatus*

*Synapomorphies:* Char. #18: (23.7%-24.9%>29.4%-29.7%); Char. #36: (1>0); Char. #37: (1>0); Char. #40: (1>0); Char. #118: (1>0).

*Support:* relative Bremer = 28%

*Remarks:* Clade M is herein proposed for the first time for Stromateiformes and supported by five synapomorphies. Fishes of this clade exhibit teeth on the vomer (Char. #36), palatine (Char. #37), and basihyal plus basibranchials (Char. #40). Curiously, Clade M indicates the non-monophyly of the genus *Psenes* since *P. cyanophrys* is more closely related to the remaining nomeid genera than to *Psenes sio*. This arrangement is similar to that obtained by Doiuchi *et al.* (2004) that also resolved *P. cyanophrys* as more closely related to other nomeids than to *P. pellucidus* (Fig. 2B).

Haedrich (1967, 1970) already pointed out that *Psenes cyanophrys* displayed a morphology discrepant from the remaining species of the genus, namely *P. sio*, *P. arafurensis*, *P. maculatus*, and *P. pellucidus*. While *P. cyanophrys* has small and conical teeth on the lower jaw, the other congeners bear large and blade-like dentary teeth. Such differences have been used to justify the description of new genera (*i.e.* *Icticus* and *Caristioides*; Fricke *et al.*, 2018) that were subsequently synonymized within *Psenes* by Haedrich (1967). The author agreed that forms like *Psenes pellucidus* were indeed very odd, but argued that the remaining *Psenes* species would represent intermediates between *Psenes cyanophrys* and *P. pellucidus*. This hypothesis has not been corroborated by any phylogenetic analysis, which either recovered alternative arrangements within a monophyletic *Psenes* (Doiuchi & Nakabo, 2006) or even a paraphyletic genus (Doiuchi *et al.*, 2004; present study).

**Clade N (TNT clade 109; new, unnamed):** *Nomeus gronovii*, *Cubiceps whiteleggii*, *Cubiceps pauciradiatus*

*Synapomorphies:* Char. #17: (60.6%>53.5%-57.4%); Char. #20: (51%-54.9%>56.9%-58.3%); Char. #21: (37.6%-39.5%>31.3%-31.6%); Char. #96: (0>1); Char. #135: (1>0); Char. #216: (1>0).

*Support:* relative Bremer = 83%

*Remarks:* Our analysis grouped *Nomeus* and *Cubiceps* into a clade that is sister to *Psenes cyanophrys*. The monophyly of the clade *Nomeus* + *Cubiceps* is supported by six synapomorphies, which includes a shortened pelvic bone that fails to reach the cleithrum anteriorly (Char. #96), the lack

of an anteroventral expansion of the *adductor hyomandibulae* (Char. #135; Fig. 36), and few fingerlike pyloric caeca (Char. #216).

The grouping of *Nomeus* and *Cubiceps* obtained herein has also been recovered by the morphological analyses Horn (1984) and Doiuchi *et al.* (2004). However, this hypothesis contrasts with the molecular analysis of Doiuchi & Nakabo (2006), which allocated *Cubiceps paradoxus* as sister group of a clade including *Psenes* and *Cubiceps squamiceps*, with latter genus being paraphyletic (Fig. 3). Our morphological data do not corroborate the paraphyly of *Cubiceps* (see Clade O, remarks).

**Clade O (TNT clade 108) = *Cubiceps*: *Cubiceps whiteleggii*, *Cubiceps pauciradiatus***

*Synapomorphies*: Char. #0: (34-35>30); Char. #2: (23>17); Char. #7: (27-29>20); Char. #9: (24-26>17); Char. #16: (35%>35.5%); Char. #91: (0>1); Char. #163: (0>1).

*Support*: relative Bremer = 33%

*Remarks*: This is the first cladistic analysis based on morphology to sample more than one species of *Cubiceps*. In our topology, *Cubiceps* occupies an apical position in the nomeid phylogeny. Members of this genus share some unique features, such as a highly modified pectoral-fin skeleton with a ventrally expanded coracoid with angled margins (Char. #91; Figs. 12, 59), as well as reductions in the number of dorsal- (Chars. #0 and #2) and anal-fin rays (Chars. #7 and #9).

The genus *Cubiceps* has been traditionally characterized by a combination of features that includes an elongate body, wing-like pectoral fins, scales on the top of the head, cheek, and opercle, and toothed basihyal (Haedrich, 1967). Yet, none of these characteristics proved to be valid synapomorphies for the genus in our analysis. Haedrich (1967) also believed that *Cubiceps* would occupy a “central” position in the nomeid evolution, whereas *Nomeus* and *Psenes* would be “derived” from an ancestral *Cubiceps* stock. This hypothesis sharply contrasts with our analysis that presents *Cubiceps* as a highly modified nomeid taxon.

**Clade P (TNT clade 95) = Tetragonuridae + Ariommatidae + Stromateidae: *Tetragonurus cuvieri*, *Ariomma indicum*, *Ariomma bondi*, *Ariomma melanum*, *Stromateus brasiliensis*, *Pampus cinereus*, *Peprilus triacanthus*, *Peprilus paru*.**

*Synapomorphies*: Char. #59: (0>1); Char. #115: (2>1); Char. #138: (0>1); Char. #140: (0>1); Char. #166: (0>1).

*Support:* relative Bremer = 55%

*Remarks:* Our analysis grouped Stromateidae, Ariommatidae, and Tetragonuridae into a monophyletic lineage mostly supported by several evolutionary novelties associated with the pharyngeal-sac morphology, including the spherical shape of the sacs (*i.e.* lacking sagittal sulcus; Char. #138; Figs. 48, 49A, 52), the absence of transversal sulci on the pharyngeal-sac (Char. #140), and a papillary pharyngeal-sac lining (Char. #59; Fig. 48C). In addition, the occurrence of a series of teeth attached to the dorsal portion of the pharyngeal sac, posterior to the upper pharyngeal tooth plates (Fig. 42A) can also be optimized as synapomorphy for Clade P, with a secondary reversal in Tetragonuridae (Char. #45).

An arrangement compatible with our Clade P was obtained only by Horn (1984). In the analysis of Doiuchi *et al.* (2004), Ariommatidae is the sister group of Nomeidae + Tetragonuridae + Stromateidae (Fig. 2B). We think this relationship was possibly biased due to the absence of pharyngeal-sac characters, which were deliberately left out by the authors. A third hypothesis was proposed by the molecular analysis of Doiuchi & Nakabo (2006) that resolved Ariommatidae as sister to Nomeidae, and Tetragonuridae as sister to Stromateidae (Fig. 3). In the remaining analyses sampling Tetragonuridae (based on molecular or combined data), the genus appears far removed from Ariommatidae and Stromateidae (Miya *et al.*, 2013; Mirande, 2017; Campbell *et al.*, 2018).

**Clade Q (TNT clade 94) = Tetragonuridae + Ariommatidae:** *Tetragonurus cuvieri*, *Ariomma indicum*, *Ariomma bondi*, *Ariomma melanum*.

*Synapomorphies:* Char. #0: (34-35>30); Char. #2: (23-28>15); Char. #7: (27-29>18); Char. #9: (24-26>15); Char. #20: (51%-54.7%>59.5%-61.2%); Char. #64; (1>0); Char. #160; (0>1).

*Support:* relative Bremer = 22%

*Remarks:* A clade composed by Tetragonuridae and Ariommatidae was recovered herein based on seven synapomorphies (Fig. 70). Clade Q is mostly supported by evolutionary novelties associated with the ventral branchial musculature and pharyngeal-sac morphology. Among these are the presence of pharyngeal-sac teeth with round bases (Char. #64; Fig. 56A-B) and a reduced area of contact between the contralateral *pharyngo-claviculares interni* (Char. #160).

The phylogenetic affinities of Tetragonuridae is, along with that of Amarsipidae, the most contentious among the Stromateiformes. The hypothesis proposed herein with a Tetragonuridae + Amarsipidae has been previously recovered only by Horn's (1984) phylogenetic study (Fig. 2A). Doiuchi

*et al.* (2004) and Doiuchi & Nakabo (2006), instead, grouped Tetragonuridae with Stromateidae (Figs. 2B, 3, respectively). In the precladistic scheme presented by Haedrich (1967; Fig. 1), tetragonurids branch off directly from a “nomeid stem” (Fig. 1). Molecular analyses with more reasonable sampling of outgroup taxa presented even more surprising hypotheses: in Miya *et al.* (2013) Tetragonuridae is sister to the non-stromateiform Chiasmodontidae (Fig. 4) and in Campbell *et al.* (2018) it is grouped with Amarsipidae in a clade that is closer to scombrids (Scombriformes) than to remaining stromateiforms.

**Clade R (TNT clade 40) = Tetragonuridae: *Tetragonurus cuvieri*.**

*Autapomorphies:* Char. #1: (11-12>19); Char. #2: (15>11); Char. #3: (19-21>16); Char. #5: (17-19>14); Char. #7: (18>12); Char. #8: (3>1); Char. #9: (15>11); Char. #11: (3>0); Char. #12: (33-36>53); Char. #13: (9>11); Char. #16: (36.3%-36.6%>41.2%); Char. #17: (61%>34.8%); Char. #18: (23.7%-24.9%>13.6%); Char. #19: (34%-37.3%>30.7%); Char. #21: (31.6%-39.5%>10.7%); Char. #26: (0>1); Char. #29: (0>1); Char. #31: (0>1); Char. #36: (1>0); Char. #37: (1>0); Char. #40: (1>0); Char. #48: (1>0); Char. #56: (1>0); Char. #101: (0>1); Char. #109: (0>1); Char. #115: (1>0); Char. #117: (0>1); Char. #118: (1>0); Char. #119: (1>0); Char. #120: (1>0); Char. #127: (1>0); Char. #128: (1>0); Char. #154: (0>1); Char. #156: (1>0); Char. #158: (0>1); Char. #162: (1>0); Char. #168: (1>0); Char. #171: (1>0); Char. #182: (0>1); Char. #187: (1>0); Char. #188: (1>0); Char. #206: (1>2).

*Support:* ---

*Remarks:* The family Tetragonuridae encompasses one genus and three valid species, namely *Tetragonurus atlanticus*, *T. pacificus*, and *T. cuvieri* (Fricke *et al.*, 2018). The genus represents the most modified lineage of Stromateiformes as evidenced by its long branch with 42 autapomorphies. These include a set of unique features among Stromateiformes, such as the highest count of dorsal-fin spines (Char. #1), the lowest count of anal-fin spines (Char. #8), small dorsal- (Char. #17) and anal-fin base lengths (Char. 21), absence of supraneural bones (Char. #101), absence of a subcutaneous canal system over the body (Char. #187), and presence of spinoid scales (Char. 206).

Tetragonurids also exhibit differences on its primary association with gelatinous invertebrates. Juveniles and young adults of *Tetragonurus* are always observed associated to salps and pyrosomes, while other stromateiforms are usually symbiotic with jellyfish and ctenophores. According to the behavioral study of Janssen & Harbison (1981), juvenile tetragonurids spend most of their life confined inside salps and pyrosomes, feeding from their guts and gonads. This highly specific association might correlate with some of the aberrant tetragonurid morphological modifications, such as the specialized

jaw and teeth (Fig. 62) and the elongate and shallow body (Fig. 71A). The symbiosis of *Tetragonurus* with tunicates, rather than jellyfishes, might also explain the absence of a subcutaneous canal plexus on their bodies, as one of the possible functions of this system is to protect the fishes against the cnidarian stings. Nevertheless, according to some studies, *Tetragonurus* still possesses a water-filled channel system composed by their modified scale rows that communicate the inter-scale space to the boundary layer in a morphology that is analogous to the remaining stromateiforms (Bone & Brook, 1972).

**Clade S (TNT clade 93) = Ariommatidae:** *Ariomma indicum*, *Ariomma bondi*, *Ariomma melanum*.

*Synapomorphies:* Char. #0: (30>27); Char. #3: (19-21>22); Char. #5: (17-19>20); Char. #12: (33-36>31); Char. #25: (1>0); Char. #61: (0>1); Char. #82: (0>1); Char. #135: (1>0); Char. #141: (0>1); Char. #142: (0>1); Char. #148: (0>1); Char. #198: (1>0); Char. #201: (1>0); Char. #204: (1>0).

*Support:* relative Bremer = 75%

*Remarks:* The family Ariommatidae currently comprises the genus *Ariomma* with seven valid species (Fricke *et al.*, 2018). Monophyly of ariommatids is herein strongly supported by 14 synapomorphies, including unique characteristics such as a parhypural-hypural fusion (Char. #82; Fig. 58), pharyngeal-sac teeth restricted to the dorsal lining of the sac (Char. #61), an anterodorsal expansion of the pharyngeal-sac over the posteriormost gill arch muscles and bones (Char. #141; Fig. 49A), an accessory muscular attachment of the *sphincter oesophagi* that connects the pharyngeal sac to the cleithrum (Char. #142), and a reduced/vestigial *retractor dorsalis* muscle (Char. #148; Fig. 49A).

The monophyly of Ariommatidae has been recovered by all previous analyses, both those based on morphological (Doiuchi *et al.*, 2004) and molecular data (Doiuchi & Nakabo, 2006; Miya *et al.*, 2013; Campbell *et al.*, 2018). Haedrich (1967) grouped these fishes based on the presence of pelvic fins, separation of the dorsal fins, absence of teeth on basihyal and basibranchials, six branchiostegal rays, fusion of hypural bones, and ossified sclerotic bones. In addition, the author listed the shape and distribution of the pharyngeal-sac papillae as diagnostic to the family. Similarly, Horn (1984) used the distribution of these papillae as diagnostic to members of the family, as well as the head squamation and number of hypurals. According to the present analysis, only the number of hypurals (coded herein as parhypural-hypural fusion; Char. #82), results as a valid ariommatid synapomorphy. The remaining characters are either symplesiomorphies within all Stromateiformes (*e.g.* presence of pelvic fin, ossification of the sclerotic bones), or within Ariommatidae (*e.g.* pharyngeal-sac papillae with round bases). Although examining two *Ariomma* species, Doiuchi *et al.* (2004) listed the genus as a single

terminal on his phylogenetic analysis. As a result, Ariommatidae resulted as a long branch exhibiting 10 autapomorphies (Doiuchi *et al.* 2004, chars. #2>1, 3>0, 4>1, 5>0, 10>1; 11>0, 18>1, 27>1, 34>1, 41>1). From these, Doiuchi's characters #5 and #10 are compatible to our characters #25 and #135 (presence of a subocular shelf, and *adductor hyomandibulae* not expanded onto the endopterygoid, respectively; Fig. 39). These are corroborated herein as valid synapomorphies for Ariommatidae.

**Clade T (TNT clade 101) = Elongate ariommatids (*sensu* Horn, 1970):** *Ariomma bondi*, *Ariomma melanum*.

*Synapomorphies:* Char. #20: (59.5%-61.2%>63%); Char. #22: (0>1); Char. #54: (1>0); Char. #115: (1>2).

*Support:* relative Bremer = 8%

*Remarks:* Clade T is composed by two ariommatid species and supported by four synapomorphies. These include the presence of a supramaxilla (Char. #22), and the *adductor mandibulae* exhibiting undifferentiated *rictalis* and *stegalis* sections (Char. #115; Fig. 61).

According to Horn (1972), ariommatids can be reasonably divided into two groups of species based on their body depth: a deep-bodied group (body depth greater than 33% of the SL), and an elongated group (body depth less than 28% of the SL). Although sampling only three from the seven valid *Ariomma* species, our analysis includes two elongate (*Ariomma bondi*, and *A. melanum*), and one deep-bodied taxon (*A. indicum*) and recovers a monophyletic elongate-ariommatid clade.

**Clade U (TNT clade 112) = Stromateidae:** *Stromateus brasiliensis*, *Pampus cinereus*, *Peprilus triacanthus*, *Peprilus paru*.

*Synapomorphies:* Char. #0: (34-35>45); Char. #2: (23-28>34); Char. #7: (27-29>40-43); Char. #9: (24-26>34-39); Char. #17: (60.9%>62.1%-63.3%); Char. #21: (37.6%-39.5%>52.2%); Char. #46: (0>1); Char. #57: (0>1); Char. #70: (0>1); Char. #72: (0>1); Char. #125 (0>1); Char. #189: (0>1); Char. #193: (0>1).

*Support:* relative Bremer = 70%

*Remarks:* The family Stromateidae (Clade U) is resolved herein as monophyletic based on the sharing of 13 synapomorphies. Clade U is diagnosed, among other characteristics, by an extra

basibranchial bone (Char. #57), a series of tooth plates disposed ventrally on the proximal portion of the esophagus (Char. #46), a posterolateral set of *sphincter oesophagi* fibers linking the dorsal and ventral hemispheres of the pharyngeal-sac (Char. #139; Fig. 52A), a reduced ventral groove (Char. #189), absence of pelvic fins in adults (Char. #72), and a high number of dorsal- (Char. #0) and anal-fin rays (Char. #7).

Similar to our analysis, previous cladistic studies (Horn, 1984; Doiuchi *et al.*, 2004; Doiuchi & Nakabo, 2006; Miya *et al.*, 2013; Campbell *et al.*, 2018) have always recovered the monophyly of Stromateidae with robust support. Those prior phylogenies based on morphological data have also listed a number of unique synapomorphies for the family. These agree with Haedrich's (1967) predictions that Stromateidae was the current "zenith" of stromateiform evolution.

**Clade V (TNT clade 112; new, unnamed):** *Pampus cinereus*, *Peprilus triacanthus*, *Peprilus paru*.

*Synapomorphies:* Char. #0: (45>47-49); Char. #1: (11>9); Char. #2: (34>40); Char. #13: (9>6-7); Char. #14: (8-9>5-7); Char. #18: (25%>34.3%-38.2%); Char. #21: (52.2%>57.5%-60.7%); Char. #66: (1>0); Char. #71: (0>1); Char. #77: (1>0).

*Support:* relative Bremer = 16%

*Remarks:* According to our data, *Peprilus* and *Pampus* form an apical clade that is the sister group of *Stromateus*. Monophyly of Clade V is based on ten synapomorphies, among which only Char. #71 (dorsal-fin spines blade-like) is recovered as unique.

Despite the highly and universally supported monophyly of Stromateidae (see Clade U), the internal relationships of the family are largely irresolute. Although only three genera compose Stromateidae, all three possible alternative hypotheses among them have been proposed. An arrangement of *Stromateus* as sister group of *Peprilus* + *Pampus* was first suggested by Haedrich (1967), which commented that *Stromateus* would contain the most primitive species of the family. His view was supported by the occurrence of three epurals and the presence of pelvic fins in juveniles of *Stromateus fiatola* (Fig. 57). Accordingly, Haedrich (1967) considered both *Peprilus* and *Pampus* to be "more derived" than *Stromateus*, although he did not provide characters supporting this opinion. The two other possible interrelationship hypotheses for the interrelationship for stromateids were offered by Horn (1984: *Stromateus* + *Pampus*; Fig. 2A) and Doiuchi *et al.* (2004: *Stromateus* + *Peprilus*; Fig. 2B). A *Stromateus*-*Peprilus* relationship was also recovered and strongly supported by the molecular phylogeny of Doiuchi & Nakabo (2006; Fig. 3).

**Clade W (TNT clade 110) = *Peprilus*: *Peprilus triacanthus*, *Peprilus paru*.**

*Synapomorphies*: Char. #1: (9>7); Char. #3: (19-21>18); Char. #5: (17-19>16); Char. #12: (33-36>32); Char. #88: (0>1); Char. #94: (0>1); Char. #95: (0>1).

*Support*: relative Bremer = 92%

*Remarks*: *Peprilus* (Clade W) represents one of the most modified stromateiform taxa. The monophyly of the genus is supported herein by seven synapomorphies, two of which are unique. The most remarkable synapomorphies for *Peprilus* are the long postcleithrum reaching the anteriormost anal-fin rays (Char. #88), the rod-like basipterygia which are fused posteriorly (Char. #94; Fig. 60), and a posteriorly projected pelvic spine that emerges from the basipterygium (Char. #95; Fig. 60). Moreover, upon certain character-optimizations, the genus is additionally diagnosed phylogenetically by the *rectus internus* eye-muscle traversing the braincase through the parasphenoid-basioccipital window and attaching to the lateral facets of the first vertebrae (Char. #137, state 1).

Although often untested in comprehensive phylogenies, the monophyly of *Peprilus* has never been questioned by previous studies (*e.g.* Haedrich, 1967; Horn, 1970a; Miya *et al.* 2013; Campbell *et al.*, 2018). The genus was the focus of a systematic revision by Horn (1970a), who diagnosed *Peprilus* from the remaining stromateids by the combination of the following characteristics: long pectoral fins, two to four small spines ahead of the dorsal and anal fins, a ventral spine on the pelvic bone, and no pelvic fins. However, when included in our comprehensive phylogenetic analysis, only the pelvic-bone spine (our Char. #95) is flagged as a synapomorphy for the genus, whereas the other character-states are also present in *Pampus* and/or *Stromateus*. Horn (1970a) also offered a tree representing the supposed evolution of *Peprilus* species, but this analysis employed Camin & Sokal's (1965) methodology based on 14 characters taken from seven species. The data summarized in Horn's (1970a) figure 44 indicate the existence of two species-groups within *Peprilus*, being *P. snyderi* the sister taxon of the remaining congeners.

## **The interrelationships of Stromateiformes:**

### **Bramidae + Caristiidae + Stromateiformes (TNT clade 84)**

*Synapomorphies*: Char. #186: (0>1)

*Support: relative Bremer = 59%*

In the cladogram resultant from the present analysis (Figs. 68, 69), Stromateiformes is resolved as sister-group of a clade composed by Bramidae and Caristiidae. This is a novel hypothesis of relationships for the order. The bramid + caristiid + stromateiform clade (Fig. 68) is supported by one unequivocal synapomorphy, the presence of a subcutaneous canal plexus on the head (Char. #186, state 1), and exhibits a relative Bremer support of 59%. As discussed on Character #186, the presence of head subcutaneous canals represents a specialization of the cephalic laterosensory system, as the minute pores perforating the epidermal surface on the head is ultimately connected with the cephalic lateral-line canals (Figs. 20, 21, 29). This cephalic canal plexus has long been recognized as a peculiar stromateiform specialization (Haedrich, 1967; Bone & Brook, 1973), but the present analysis reveals that this feature is much more widely distributed. Besides Clade 84 (Fig. 69), this character state independently evolved six more times within Percomorphacea.

Other character states with ambiguous optimizations may also support the monophyly of Clade 84. Likewise, adults of Stromateiformes, Bramidae, and Caristiidae lack a swim bladder (Char. #214, state 1) and the juveniles exhibit the peculiar behavior of associating with gelatinous invertebrates (= gelata; Char. #217, state 1). The absence of the swim bladder has been seldom incorporated into phylogenetic studies (*e.g.* Wiley & Johnson, 2010) although this feature is often reported for pelagic fishes (Fänge, 1966; Horn, 1970b; Bone, 1972; Magnuson, 1973; Horn, 1975). In our analysis, the absence of a swim bladder in adult specimens could be interpreted as an additional synapomorphy for the bramid-caristiid-stromateiform clade, with a reversal in *Hyperoglyphe perciformis* (Centrolophidae). In alternative optimizations, this character state is synapomorphic for more inclusive clades (Fig. 69: Clades 74, 75, or 85) with multiple reversals, thus not resulting in a synapomorphy for Clade 84.

Juvenile bramids also hang on jellyfishes by resting their chin or pectoral fin on the jellyfish's umbrella in a behavior very similar to that described for Stromateiformes (Johnson, *pers. com.*; Char. #217, state 1). According to Johnson (*unpublished data*), juvenile bramids even exhibit a modification on its first pelvic-fin ray, which is probably related to their habit of anchoring to and resting on gelata. Although information for caristiid-gelata association is still scarce in the literature, two brief descriptions of a caristiid hanging around a siphonophore has been published (Janssen *et al.* 1989; Benfield *et al.*, 2009; Tab. 5), indicating that they possibly display a juvenile association homologous with that of stromateiforms and bramids (this character is provisory coded as unknown for caristiids). In the present hypothesis of relationship, one of the two alternative optimizations of Character 217 indicate that the juvenile association with gelata is a synapomorphy for the clade Bramidae +

Caristiidae + Stromateiformes, with a homoplastic event in the carangid *Trachinotus carolinus* (vs. a synapomorphy for a more inclusive clade, with a reversal in *Nematistius pectoralis* – Nematistiidae: Fig. 69: Clade 85).

The new hypothesis of stromateiform interrelationships proposed herein is highly contrasting with previous studies based on morphology. These have suggested a closer relationship between stromateiforms and the Kyphosidae *sensu lato* (including Scorpidae, Girellidae, and Microcanthidae), Oplegnathidae, Kuhliidae, Arripidae, Terapontidae (Freihofer, 1963; Johnson & Fritzsche, 1989), and Dichistiidae (Leis & Lingen, 1997). These hypotheses were based solely on the shared pattern 10 of the *ramus lateralis accessorius* (RLA), in which a branch of the facial nerve overlies the *levator arcus palatini*, *dilatator*, and *levator operculi* muscles (Figs. 33, 64, 65; see Char. #127). Contrasting with these hypotheses, our analysis does not support the monophyly of an RLA-10-pattern assemblage. Our topology indicates that this branching pattern has arisen five times independently in: 1) Oplegnathidae (Fig. 69: Clade 62); 2) a clade comprising Kyphosidae *lato sensu*, Kuhliidae, and Terapontidae (Fig. 69: Clade 115); 3) the clade *Pomatomus* + *Arripis* (Fig. 69: Clade 86); 4) Stromateoidei (Fig. 70: Clade C; Fig. 69: Clade 100; with reversal events in *Tubbia*, both *Psenes* species, and in *Tetragonurus*); and 5), in the clade *Nomeus* + *Cubiceps* (Fig. 70: Clade N; Fig. 69: Clade 109).

The interrelationships of Stromateiformes presented herein is also highly conflicting with the current classifications based on molecular data. These have placed a polyphyletic Stromateiformes into a large clade named Pelagiaria that also included representatives of Scombriformes, Chiasmodontidae, Pomatomidae, Arripidae, Scombrobracidae, Icosteidae, Caristiidae, and Bramidae (Fig. 4). Such grouping has never been proposed under morphological grounds, and our analysis do not support the monophyly of Pelagiaria. Although that clade encompasses bramids, caristiids, and stromateiforms, these taxa were always hypothesized to be more closely aligned to other pelagiarians than to each other. As an example, the latest molecular classification of bony fishes grouped Bramidae with Gempylidae, Caristiidae with Scombrobracidae, and the different stromateiform families with Scombridae, Gempylidae, and Trichiuridae (Betancur-R *et al.*, 2017).

## **Further comments on the stromateiform morphology**

### **Gill arch and pharyngeal-sac evolution:**

Our study provides for the first time an exhaustive comparative analysis combined with explicit hypotheses of homology for the skeletal and muscular components of the pharyngeal sac. The

organ has been recurrently listed as one of the most extraordinary morphological characteristics of stromateiforms (Gill, 1884; Regan, 1902; Haedrich, 1967), being often considered a synapomorphy for the order (Doiuchi *et al.*, 2004; Doiuchi & Nakabo, 2006). Yet, the homology of its components and their relationship with the gill arches and the esophagus have never been properly addressed. Extensive studies of the stromateiform pharyngeal sacs do exist (Bühler, 1930; Isokawa, 1966), but they focus solely on an anatomical characterization of this organ in few specific taxa, thus lacking an evolutionary perspective. Until now, specific hypotheses of homology for the pharyngeal-sac elements were limited to a few dispersed statements in the studies of Gill (1884), Regan (1902), Gilchrist (1922), and Barnard (1948).

The pharyngeal sac has been initially described as an *oesophageal* outgrowth of stromateiforms (*e.g.* Regan, 1902). Subsequent studies claimed that the organ had a pharyngeal origin (Gilchrist, 1922; Bühler, 1930) as all its skeletal constituents were serially homologous to gill-arch ossifications. The present analysis confirms the gill-arch origin of the bony elements of the pharyngeal sac but also corroborate that its muscles derive from the *sphincter oesophagi* (Datovo *et al.*, 2014). The organ, therefore, is more accurately described as having a compound origin from both the gill arches and the esophagus. In any event, the widely used name ‘pharyngeal sac’ is herein retained for the sake of nomenclatural stability.

Externally, the pharyngeal-sac muscular layer is represented by two thick sheets of the *sphincter oesophagi* attached to the fourth and fifth gill-arch bones (Figs. 46-52). The external muscular layer has transversally oriented fibers, and in Nomeidae and Centrolophidae these fibers are supplied by sets of regularly spaced nerves and vessels that gives the organ a banded aspect (Figs. 49B, 50, 51). A second and internal layer of fibers encircles the sac longitudinally and attach to the so-called pharyngeal-sac “teeth” (Fig. 56), structures that are actually serially homologous to gill rakers (see below). Stromateids, ariommatids and tetragonurids additionally exhibit a third and outer set of transversal fibers of the *sphincter oesophagi* connecting the contralateral sac hemispheres (Figs. 46, 49A, 52). In conjunction, the set of *sphincteres oesophage* layers that constitute the pharyngeal sac form a very strong muscular pharyngeal organ.

Internally, the pharyngeal sac contains a pair of very long upper pharyngeal tooth plates that form a spiny roof for the organ (Figs. 43, 44, 45C, 46C; Barnard, 1948: fig. 10, e-g; Doiuchi *et al.* 2004: fig. 6, A). The ventral lining of the sac is also spiniferous and composed by two long and toothed medial projection of ceratobranchials 5 (Fig. 44). Laterally, the internal surface of the organ contains sets of greatly enlarged and toothed gill rakers (Fig. 43C), that originate from the posteriormost arch elements (*i.e.* ceratobranchials 4 and 5 and epibranchial 4) and directed posteriorly, paralleling the

internal walls of the pharyngeal sac (Fig. 44). Differing from the regular rakers of the anteriormost gill arches, the enlarged posterior rakers are firmly attached to the internal walls of the sac. Modified gill rakers associated with the posteriormost gill arch bones are uniquely found in stromateiforms (Char. #60, state 1). The conjunction of dorsal and ventral bony projections (*i.e.* upper pharyngeal tooth plates and ceratobranchial 5) with the elongate gill rakers of ceratobranchials 4 and 5 and epibranchial 4 function as a complex shredding toothed mechanism to process food. These elements are probably coordinated by fine contractions of the different layers of *sphincter oesophagi* and branchial muscles.

The internal walls of the pharyngeal-sac also exhibit an intricate morphology. Historically, the inner lining of this organ has been classified as wrinkled (= folded, plicate) or papillary (= polypoid). A wrinkled aspect (*e.g.* Bühler, 1930: fig. 1; Isokawa *et al.* 1965: fig. 3) is due to the presence of the elongate rakers that fold backwards over the proximal portion of the organ of centrolophids and nomeids (Fig. 44; Doiuchi & Nakabo, 2006: fig. 5a). Each raker supports a skin fold that connects to the walls of the esophagus and partially compartmentalize the sac lumen. Attached to the skin-fold tegument are several minute conical ossifications with bristle-like teeth at its apex (Fig. 43C, arrow; Fig. 54D; Barnard, 1948: fig. 11d; Haedrich, 1969: fig. 50a-b) that projects from the folds and provide a spiny surface for the pharyngeal-sac compartments. Ariommatidae, Tetragnuridae, and Stromateidae, instead, have a papillary pharyngeal-sac lining (Fig. 46C). In this morphology, the rakers associated with the last gill arches are proportionally smaller (Figs. 54G; Ariommatidae) or absent (Tetragnuridae and Stromateidae). The rakers no longer form the raker-fold pattern of compartments and most of the pharyngeal-sac surface is covered by the so-called papillae (= polyps). These papillae are internally supported by a bony axis with numerous projecting conical teeth and a round or stellate bases (Figs. 53, 55, 56). These structures resemble spiked clubs and are much larger than the conical ossifications found in the wrinkled pharyngeal sacs (Fig. 54D, H).

All morphological evidences indicate the conical and club-like ossifications covering the inner walls of the pharyngeal sac are serially homologous to gill rakers. For instance, the ossifications of the pharyngeal sac have a morphology strikingly similar to the gill rakers associated with the posterior facet of gill arch 1 and to both anterior and posterior facets of gill arches 2, 3 and 4 (Fig. 54). These gill rakers are lens-like (*i.e.* exhibit a convex surface) and bear elongate teeth at its convex apex, which is the same morphology of the conical pharyngeal-sac ossifications exhibited by the Centrolophidae (compare Fig. 54D with 54B, F). Other stromateiform families have further modified pharyngeal-sac rakers. The structures become gradually larger, start to exhibit a dorsoventral orientation, and a symmetrical basis that attaches to the inner walls of the sac (Figs. 54E-H, 55). In Ariommatidae and Stromateidae they reach their most specialized morphology, exhibiting either round or stellate bases,

and a very long dorsoventral axis (Figs. 53, 54H, 55A-D). Yet, they still exhibit a general resemblance to the non-modified rakers of arches 2-4.

Evidences indicating that the pharyngeal-sac ossifications were homologous to modified gill rakers are mentioned ever since the 19<sup>th</sup> century. Gill (1884) defined the Stromateiformes by the possession of “*peculiar appendages representing and homologous with the gill-rakers of ordinary fishes, developed from the last branchial arch, and extending into the oesophagus*”. Gilchrist (1922) reached to similar conclusions for the ariommatid and stromateid pharyngeal-sac ossifications. The author further hypothesized that those structures could have arisen from a backward extension of the last gill-arch epithelium. Yet, subsequent studies, have treated the pharyngeal-sac rakers generally as papillae (*e.g.* Haedrich, 1967), without providing a more conclusive homology hypothesis for its parts (Doiuchi *et al.*, 2004; Doiuchi & Nakabo, 2006). Most of the times, the pharyngeal-sac components were characterized in “types” and optimized within an evolutionary framework (*e.g.* Haedrich, 1967: figs. 48-49; Doiuchi & Nakabo, 2006: fig. 5). The first and only attempt to use pharyngeal-sac morphology as phylogenetic information is still Horn’s (1984) study, which sampled five pharyngeal-sac related characters in his cladistic study.

Our analysis represents the most complete study of the morphology and evolution of the pharyngeal sac of stromateiforms. We were able to identify several major evolutionary changes that have marked the pharyngeal-sac evolution in the group, and which revealed to be highly informative in a phylogenetic context. For that, we constructed fourteen discrete characters (Chars. #45-46; #58–64, #138–142) related to the pharyngeal-sac anatomy, and the evolution of this organ within Stromateiformes is synthesized below:

1. The pharyngeal sac appears in Clade C, Stromateoidei (Char. #58). In a primitive condition the organ has two bilaterally paired, kidney-shaped hemispheres, a sagittal sulcus (Char. #138, state 0), and a series of bands that receive larger nerves and vessels (Char. #140, state 0) (Figs. 49B, 50, 51). Internally, the upper pharyngeal tooth plates provide the roof of the organ (Char. #44, state 1) (Fig. 43A, 44C) and posteriorly directed elongate gill rakers from the posteriormost gill arches are disposed along the ventrolateral walls of the sac (Char. #60, state 0) (Fig. 44). The internal surface of the organ is wrinkled (Char. #59, state 0) and covered by conical rakers with irregular basis (Char. #63, state 0) and no obvious dorsoventral axis (Char. #62, state 0) (Fig. 54D).

2. Nomeids, tetragonurids, ariommatids, and stromateids (Clade K) exhibit modifications mainly in the pharyngeal-sac raker morphology. These ossifications exhibit a symmetrical basis (Char. #63, state 1) and a dorsoventral axis (Char. #62, state 1) (Fig. 55).

3. Major changes affect the organ morphology in Clade P (Tetragonuridae, Ariommatidae, and Stromateidae). An outer band of muscle connects the two lateral hemispheres, so the pharyngeal-sac acquires an external spherical appearance (Char. #138, state 1), and the sac lacks transversal bands (Char. #140, state 1) (Figs. 46, 48, 49A, 52). The elongate and posteriorly directed rakers from the last gill arches are reduced to one pair (Ariommatidae) or absent (Tetragonuridae and Stromateidae) and, consequently, the internal surface of the organ loses the wrinkled aspect, being rather papillary (Char. #59, state 1) (Fig. 46C). They also exhibit a set of tooth plates on the dorsal surface of the pharyngeal sac (Char. #45, state 1) that follows posteriorly the upper pharyngeal tooth plates (Fig. 42A). This series of teeth is possibly optimized as a synapomorphy for this clade, but secondarily lost in Tetragonuridae (AccTran).

4. Tetragonuridae and Ariommatidae (Clade Q) share pharyngeal-sac rakers with a round base (Char. #64, state 0) (Figs. 42, 53A-B, 56A-B).

5. Tetragonurids (Clade R) have small, poorly ossified sac rakers (Figs. 46C, 56B). In addition, these fishes exhibit the proportionally longest pharyngeal sacs among stromateoids (Figs. 46, 48). These represent autapomorphies for the family not coded in the matrix.

6. Ariommatidae (Clade S) has an anterodorsal outgrowth of the pharyngeal sac (Char. #141, state 1) (Fig. 49A) and lacks rakers associated with the ventral surface of the organ (Char. #61, state 1) (Fig. 53A-B). An accessory muscular attachment of the pharyngeal-sac on the cleithrum is additionally present (Char. #142, state 1).

7. Stromateids (Clade U) exhibit an additional outer posterolateral set of fibers of the *sphincter oesophagi* linking the dorsal and ventral hemispheres of the pharyngeal sac (Char. #139, state 1) (Fig. 52B, arrow), and also a set of dorsal and ventral patches of teeth on the pharyngeal sac, just anterior to the esophagus (Chars. #45 and 46, state 1).

### **Stromateiform morphological adaptations related to symbiosis with gelatinous invertebrates**

Some gelatinous marine organisms, such as jellyfishes, comb jellies, men-o'-war, and salps (so-called "gelata"; Haddock, 2004; Thiebot *et al.*, 2017) play an important role in the life history of stromateiforms. These drifting invertebrates provide shelter and protection to the juveniles and constitute most of the diet of adult stromateiforms (Mansueti, 1963; Jenkins, 1983; Arai, 1988; Harbison, 1993). However, this interesting symbiotic relationship is possibly related with the evolution of some of the most extraordinary morphological features of stromateiforms, such as the presences

of subcutaneous canal plexus of the trunk, pharyngeal sac, dendritic pyloric caeca, and the absence of a swim bladder. In light of the new hypothesis of phylogenetic relationships recovered herein (Figs. 68-70), these adaptations revealed either be plesiomorphic or synapomorphic to stromateiforms, an indication that they may have played a key role in the evolution of the group.

The association with floating objects is a widespread and probably primitive behavior for many pelagic fishes. Hovering in the shade of floating matter enhances the fish visibility, spatial orientation, and helps on evading from possible predators (Helfman, 1981). To varying degrees, this type of behavior has been documented for several actinopterygian lineages (Kingsford, 1993). Large cnidarians may provide visual benefits similar to floating objects, but the fact that they are harmful to most of other animals may provide further protection for those fishes that can somehow associate with these organisms. Scyphomedusae and siphonophores produce toxins that are lethal to most fishes even in low doses (Lane, 1960; Mansueti, 1963) and only a small number of specialized fishes are able to use these cnidarians as hosts (Arai, 1988). Stromateiforms are one of these exceptions, as most species of the group spend their early life stages in association with cnidarians (Tab. 5; Lane, 1960; Mansueti, 1963; Horn, 1975; Ahlstrom *et al.*, 1976; Janssen & Harbison, 1981; Arai, 1988; Harbison, 1993; Purcell & Arai, 2001).

Most associations between juvenile stromateiforms and their host gelata are taxonomically variable, with a certain fish using different gelata as host, and a same host sheltering different species of fishes (Tab. 5; Mansueti, 1963; Janssen & Harbison, 1981; Harbison, 1993). Moreover, in most of these interactions the stromateiform is a commensal that, therefore, is neither benefit or harm its host. However, this generalized symbiosis evolved into different and more complex interactions in some lineages. These include, for instance, a fish-coelenterate competition for prey (Purcell & Arai, 2001), fish predation on medusa and ctenophores (Arai, 1988; Harbison, 1993), coelenterate as intermediate host for fish parasites (Arai, 1988), fish as gelata parasites (Janssen & Harbison, 1981), fish-gelata protocoooperation (Riascos *et al.* 2012), or even a possible mimicry (Arai, 1988; Jenkins, 1983; Tan, 2008; Greer *et al.* 2016). One interesting example of a more elaborate fish-gelata interaction is the facultative mutualism (or protocoooperation) between the centrolophid *Seriolella violacea* and the scyphozoan *Chrysaora plocamia* off the northern Chilean coast. According to Riascos *et al.* (2012), young *Seriolella* feeds heavily on hyperiid amphipods that parasite the jellyfish. During the months of November to March, period in which hyperiids are in a pelagic and parasitic life stage, these organisms constitute near 97% of the diet *Seriolella*, which enters through the oral disks of the medusa to feed on the amphipods living inside the jellyfish gastric pouches.

Another unique symbiotic interaction occurs between the man-of-war-fish *Nomeus gronovii* and the poisonous siphonophore *Physalia physalis*. This nomeid is well known to develop a lifelong interaction with siphonophores, but not only it uses its host as shelter and protection, but it also feeds actively from the *Physalia* gonozooids and dactylozooids. The *Nomeus-Physalia* interaction is the one of the most well documented cases of lifelong association between a stromateiform and its host, and the numerous observations of the fish following siphonophores indicate that the commensalism-parasitism might be obligatory for the fish (Lane, 1960; Mansueti, 1963; Jenkins, 1983). Accordingly, *Nomeus* displays some unique adaptations that may be related to its interaction with *Physalia*. They have the longest pelvic fins among all stromateiforms, which can be open like a fan and may contribute to its maneuverability avoiding direct contact with the man-of-war tentacles (Jenkins, 1983). In addition, *N. gronovii* is the only stromateiform species to keep the juvenile mottled blue and silver color pattern even in adult stages (Karpplus, 2014). This coloration, which resembles the bluish hues of the tentacles of the man-of-war (Ahlstron *et al.*, 1976: fig. 27; Horn, 1984: fig. 333D), is possibly a type of fish-jellyfish mimicry.

Another remarkable fish-gelata association is documented for Tetragonuridae. Contrasting to other stromateiforms that usually interact with cnidarians, *Tetragonurus* seems to have specialized as a tunicate parasite, using salps and pyrosomes as shelter and food resource (Janssen & Harbison, 1981). *Tetragonurus* has the longest body among stromateiforms (Fig. 71A), their dorsal and anal-fin spines are short and soft and can be depressed to fit into dorsal and anal-fin grooves, and the mandibular teeth are long, sharp, and arranged into a row resembling a saw's edge (Fig. 62). According to laboratory experiments, *Tetragonurus* preferentially associate with tunicates, ignoring medusa or other gelatinous organisms as hosts (Janssen & Harbison, 1981). The authors relate that when exposed to salps and pyrosomes, these fishes readily enter their body cavity where it feeds on the salps gonads, gill bars, and stomachs. The tunicate parasitism, however, seems not unique to *Tetragonurus*, as some behavioral reports for *Amarsipus*, another elongated stromateiform (Fig. 71B), indicate its preference for hosting inside the salp *Cyclosalpa affinis* (Harbison, 1993).

Different hypotheses have been proposed on how stromateiforms return unharmed from their associations with cnidarians. Some of these hypotheses report an exceptional swimming ability to avoid direct contact with the tentacles (Mansueti, 1963; Jenkins, 1983), while others point to the existence of some physiological resistance or protection against the cnidocysts (Lane, 1960; Mansueti, 1963; Maul, 1964; Jenkins, 1983; Arai, 1988; Duffy *et al.* 2000). In fact, these fishes have been observed surviving to eventual contacts with the jellyfish tentacles. Both *Seriola* (Centrolophidae) and *Peprilus* (Stromateidae) have been observed entering the gastric pouches of medusas (Riascos *et al.*, 2012;

Lawley & Junior, 2018), which would be improbable to achieve without being stung by jellyfish cnidocysts. In addition, reports of stung *Schedophilus* (Centrolophidae) kept in aquarium describe that the wound marks left by the tentacles would eventually peel off and reveal a healthy skin underneath it (Maul, 1964). Laboratory studies carried out with *Nomeus gronovii*, show that the fish actively feeds on *Physalia* dactylozooids and is often stung by its cnidocysts (Jenkins, 1983). When contact is forced against the tentacles, the fish swims erratically for a moment, but recovers itself after a relatively short time (Lane, 1960; Jenkins, 1983). However, recurrent forced contacts between *Nomeus* and *Physalia* results in the fish death and indicate that the species is not immune to the man-of-war toxin (Lane, 1960). According to the unpublished thesis of Mayo (1968), *N. gronovii* is about ten times more resistant to *Physalia* toxins than regular fishes and may produce at least one antibody against these toxins. Yet, the nature of the stromateiform physiological resistance to the cnidarian toxins still pends further studies across the order.

An additional mechanism of resistance to jellyfish interaction may be the contact insulation provided by the specialized stromateiform skin and its reported external layer of mucus (Lane, 1960; Maul, 1964; Dawson, 1971; Jenkins, 1983; Arai, 1988). A correlation between these features and the existence of a subcutaneous canal plexus in trunk of these fishes is a natural unfolding. As described in detail under Character #187, stromateiform fishes exhibit a trunk canal plexus running under the skin (Figs. 16B, 59) and externally identifiable by innumerable pores open to the surface of skin, which internally lead to interconnected net of canals embedded into an intradermal space (Fig. 66). Information on the morphology and function of the subcutaneous canal plexus (= subdermal canal system of previous studies) are scarce and mostly conflicting. Similar canals have been described to Trachipteridae (Walters, 1963) and Gempylidae (Bone, 1972). For trachipterids, Walters (1963) provided evidence that the canal system would enhance swimming performance. For *Ruvettus*, Bone (1972) hypothesized that the canals would inject momentum on the boundary skin layer by expelling water and this mechanism would be used to increase burst speed during hunting. However, none of these hypotheses seems to be suitable for explaining the subcutaneous canals of Stromateiformes. These fishes are notable by not being active swimmers and rather exhibit a preference to hang around sargassum, wreckage, gelatinous zooplankton, or other floating objects during most of its life.

Considering the stromateiform lifestyle and its interaction with jellyfishes, a hypothesis where the subcutaneous canal plexus functions as mucous system or a “keratin shield” (*sensu* Bone & Brook, 1972) would seem suitable to explain the function of this organ. To begin with, a double layer of skin would give these fishes an extra resistance against the cnidarian cnidocysts. The stromateiform external skin layer is relatively thick, composed of several layers of connective tissue and, according

to some authors, this morphology would even resemble a terrestrial keratinized skin (Bone & Brook, 1972: p. 758). In fact, the skin of some centrolophids are extra thick (Fig. 66A-B), and there should be little doubt that it does represent a stronger physical barrier against the cnidocysts. Moreover, the external skin layer is pierced by regularly spaced pores that provide a direct contact between the lumen of subcutaneous canal plexus with the outer surface, a morphology that is compatible to a secretory system (Fig. 66C-D). Laboratory experiment performed with the gadid *Gadus merlangus*, a fish that also associate with cnidarians, have shown that the tentacles of jellyfish are not very liable to produce cnidocyst discharge when in contact to their skin (Dahl, 1961). In this experiment, the number of cnidocysts attached to skin of *Gadus* were 5 to 20 times lower than in the gobiid *Gobius flavescens* (control group), and a possible explanation offered by the author is that a mucus coat would be secreted by gadids to prevent the cnidocyst attachment. Similar mucous protection has been reported to protect damselfishes from the cnidocysts of sea anemone (Davenport & Norris, 1958). Interestingly, pomacentrids secrete mucus only during a fish-host acclimation period, and not permanently, and it is not expected to find mucus in these fishes while they are not sheltering among anemone tentacles. Similarly, it is possible that stromateiforms will only secrete mucus when swimming around the cnidarian tentacles evading from possible predators, or while nibbling on cnidarians tentacles during feeding. This may explain why reports on mucus secretion in Stromateiformes are scarce.

Salps, pyrosomes, and jellyfish (Harbison, 1993) compose most of the adult stromateiform diet (Harbisson, 1993; Arai, 2005). This is a common diet of slow-moving oceanic fishes (*e.g.* Icosteidae, Alepocephalidae, Molidae and Balistidae; Ates, 1988; Harbisson, 1993; Allen, 2001) and the capture of these drifting preys does not demand active swimming. In general, adult centrolophids and nomeids inhabit open seas and often follow large medusae, drifting sargassum, or ships (Mansueti, 1963; Merriner *et al.*, 1970; Dawson, 1971; Quigley, 1986; Kingsford, 1993; Duffy *et al.* 2000). This contrasts with the stromateiform juvenile swimming style, which is notable by its constant hovering and maneuvering around jellyfishes (Horn, 1975). In these fishes, the transition to adulthood is concomitant with a shrinking of their gas bladders. The organ, which is functional in juveniles, is reduced in adults to a gas gland that is below the critical point that provide neutral buoyancy (Horn, 1970b) and thus inefficient for buoyancy control (Horn, 1975). The absence of a swim bladder in large stromateiforms is probably compensated by oil storage, as these fishes are considerably oily when compared to other taxa. Among the analyzed stromateiforms, the largest quantities of oil were noticed in *Tubbia tasmanica* (Centrolophidae). This taxon exhibited oil in its skin, flesh, and inside the trabeculae present on most of its bones (*e.g.* Fig. 16B, 43, 44). According to Nichols *et al.* (2001) about 80% of the oil present on *Tubbia tasmanica* is squalene, an oil common in deep-sea sharks (Nichols *et al.*, 2001; Last *et al.*, 2013) but extremely unusual among teleosts. Mentions to a flesh with high oil

concentration are also present for other stromateiforms, such as nomeids, ariommatids, and stromateids (Gilchrist, 1922; Abe, 1955; Haedrich, 1967). The centrolophid *Centrolophus niger*, for example, has been reported to contain a viscid oily substance on its skin that, if ingested, could lead to “sickness or gastric disturbances” (Gilchrist, 1922). Oily flesh has also been described in *Cubiceps* and *Tetragonurus*, and these were compared to the flesh of the gempylid oil fish, *Ruvettus prestiosus* (Abe, 1955), which is known to have purgative properties when consumed in large quantities (Cox & Reid, 1932). Nevertheless, the oil present in the flesh of stromateids does not seem to harm humans when eaten. These fishes, commonly known as butterfishes, are much appreciated and largely consumed in Asian countries due to its fine flavor (Gilchrist, 1922; Haedrich, 1967; Ghosh *et al.*, 2009).

Other distinctive morphological features of stromateiforms may also be related to their feeding habits. These fishes all have a relatively large stomach, long intestines, and dendritic pyloric caecae. In some taxa (*e.g.* *Stromateus* spp.), the intestines may reach four times the fish’s standard length (Harbison, 1993). The large mass of pyloric caeca and the long intestines (Fig. 48) are possibly adaptations to a low-energetic diet based on gelatinous zooplankton, as these characteristics seems to enhance the efficiency of nutrient uptake (Rahimullah & Osmania, 1945; Buddington & Diamond, 1986).

Yet, the most interesting Stromateiform adaptation toward medusivory is the presence of the pharyngeal-sac. The organ is a result of specializations of the gill-arch bones and esophageal musculature and is probably used to process food (mostly gelata). The pharyngeal sac of stromateiform seems to work together with the upper pharyngeal bones and the spiny surface of the fish’s pharynx and esophagus to shatter its gelatinous prey until it is reduced to a shredded material (Figs. 43, 44). Surprisingly, both the morphology and the function of this organ remain little explored, and up to date one of the few studies to address the issue was that of Bühler (1930). The author provided extensive descriptions of the digestive epithelium of these fishes, including the pharyngeal sac, and similarly concluded that these morphological particularities were adaptations towards a medusivorous diet. It is interesting to note that Bühler’s speculations were offered in a context where little was known about the stromateiform diet, and that the medusivory inferred by his morphological observations were corroborated only decades later (Harbison, 1993; Ates, 1998). Some different ideas have also been suggested for the pharyngeal sac function. Harbison (1993) compared the stromateiform pharyngeal sac to the gastric mills (= pharyngeal mills) present on herbivorous fishes (*i.e.* the triturating surfaces of upper and lower pharyngeal tooth plates). According to the author, both the large stomach, long intestine, and the pharyngeal sac of stromateiforms had a parallel in herbivorous taxa, which would indicate that medusivory evolved from herbivory, or vice versa.

Although Harbison's hypothesis points to an interesting morphological resemblance, our study does not support a stromateiform relationship with herbivorous fishes. Our final cladogram resolved Stromateiformes as sister group of Bramidae and Caristiidae (Fig. 68). Bramids are mostly carnivorous, feeding on other fishes and invertebrates (Júnior *et al.*, 2008), while caristiids are generalist invertebrate eaters (Janssen *et al.*, 1989; Benfield *et al.*, 2009), and none of those exhibit the abovementioned digestive adaptations.

Morphological parallels of the stromateiform spiny esophagus do exist in other vertebrates, and similarly, these structures are used to develop a function of grabbing and shredding gelatinous food. Aside stromateiform fishes, a spiny or papillary lining over the tongue, cheeks, palate, or esophagus are present on several species of penguins, some turtles, and even some mammals (Den Hartog & Van Nierop, 1984; Kobayashi *et al.* 1998; Vogt *et al.*, 1998; Pérez *et al.*, 2012). These spines or papillae are related to grabbing, processing, adhering, or spreading food over the mouth, and its definitive function will depend on its size and shape, and its distribution over the oropharyngeal cavity (Noel & Hu, 2018). According to biomechanical studies, a large, sharp and rigid papillae-type is mostly related to enhance grip on soft-bodied prey (Noel & Hu, 2018). These are frequently found in marine animals (*e.g.* penguins – Kobayashi *et al.*, 1998: fig. 1; leatherback turtles - Den Hartog & Van Nierop, 1984), and its backward-oriented angle functions as a one-way valve to avoid food to slide out of the mouth (Noel & Hu, 2018).

Perhaps the most striking morphological resemblance of a pharyngeal sac organ occurs in the leatherback sea turtle *Dermochelys coriacea*. This turtle is a notorious medusivorous animal, and a single adult turtle may eat up to 50% its body mass of jellyfish per day, which represents over 200 kilos of gelata (Heaslip *et al.*, 2011). Accordingly, several morphological adaptations toward medusivory are present on the digestive tract of *Dermochelys*. Its oral and esophageal cavity are equipped with a set of large, conical, and cornified, which presumably avoid food to slide out of its mouth. In addition, *Dermochelys* exhibit a unique stomach morphology: the organ is compartmentalized in an anterior sac-like, and a posterior tubular portion (Den Hartog & Van Nierop, 1984: pl. 4, fig. a-b; pl. 5 a-d). The anterior sac-like stomach is characterized by being thick and muscular, and containing a complex surface marked by longitudinal furrows and ridges. Contrastingly, the posterior stomach has thinner walls and is subdivided in several small compartments, each provided with its own sphincter muscle.

Den Hartog & Van Nierop (1984) offered an elaborate hypothesis for the function of the *Dermochelys* stomach that would be deeply related to the turtle's diet. They first considered that if an adult turtle can eat 200 kilos of gelata, it would have to excrete a comparable volume of liquid since only 0.5-2.5% of a jellyfish is organic matter. Moreover, the turtle would still have to deal with extreme

amounts of salt on its system, as the bodies of gelata are isotonic in relation to seawater, but hypertonic in relation to the turtle's organism. However, a daily elimination of 200 liters of water would sound an implausible hypothesis, and Den Hartog & Van Nierop (1984) offered an alternative water-eliminating mechanism that takes place in the anterior, muscular stomach. The organ would provide a partial mechanical and chemical digestion that would liberate the water contained in the body of the gelata, and once shredded, the contraction of the stomach's muscle would eliminate the excess of salt water by oral expulsion. During contraction, the posteriorly-oriented esophageal papillae could function as a sift, avoiding the shredded food particles to slip off the turtle's mouth.

Although water-elimination stands as a suitable explanation for the function of the *Dermochelys*' muscular stomach, marine teleosts may not suffer from salt-water intake from its prey as much as sea turtles. Most marine fishes actively ingest seawater to balance water-loss through the skin due osmosis (*e.g.* Smith, 1930) and excrete the extra ions through their gills and concentrate urine (Evans *et al.*, 2005). Thus, a mechanism to eliminate salt water from food seems implausible on stromateiforms, and the use of the pharyngeal sacs to shred food still stands as its most suitable function.

## **Comments on the interrelationships of Percomorphacea**

The main objective of this study was to perform a phylogeny of Stromateiformes that would test both the inter- and intrarelationships of the group. Accordingly, taxon sampling encompassed lineages that were suspected to be related to the Stromateiformes based on hypotheses presented by both morphological and molecular studies. Reconstructed relationships among the outgroup taxa in this study are not discussed for every clade, since taxon sampling outside Stromateiformes was much sparser and not with the proper effort to resolve outgroup interrelationships. Nevertheless, some of the results were congruent to previous hypotheses (either morphological or molecular), and exhibited strong morphological support. We offer a brief discussion on some of these groups and list the characters that were corroborated, or that possibly represent novel synapomorphies for these clades.

### **Ophidiiformes (TNT clade 69):**

*Synapomorphies*: Char. #0: (54>73); Char. #2: (54>73); Char. #3: (19>20); Char. #5: (18>20); Char. #6: (5>1); Char. #7: (37>57); Char. #9: (37>57); Char. #13: (4-7>1); Char. #14: (4-5>1); Char. #17:

(68.5%>69%); Char. #18: (16.4%>13.2%); Char. #19: (29.6%>22.9%); Char. #21: (38.5%>54.7%); Char. #22: (0>1); Char. #23: (0>1); Char. #42: (1>0); Char. #43: (1>0); Char. #49: (0>1); Char. #50: (0>1); Char. #69: (0>1); Char. #75: (0>1); Char. #80: (0>1); Char. #81: (0>1); Char. #96: (1>0); Char. #107: (0>1); Char. #111: (0>1); Char. #121: (1>0); Char. #130: (0>1); Char. #146: (0>1); Char. #156: (1>0); Char. #174: (0>1); Char. #194: (1>0).

*Support:* relative Bremer = 74%

Although for long recognized as a natural assemblage, no synapomorphy for the Ophidiiformes has been listed so far. The order is provisionally considered monophyletic, but still awaits confirmation from cladistic analyses (Nielsen *et al.*, 1999; Wiley & Johnson, 2010). Previous morphological studies (*e.g.* Rosen, 1985; Howes, 1992; Nielsen *et al.* 1999) have failed on finding synapomorphies for ophidiiforms. Features used to unite these fishes rely on a combination of characters that include: pelvic fins absent or with 1 or 2 soft rays; pelvics inserted at the level of the preopercle or anteriorly; pelvic-fin bases close together; dorsal and anal fins with long bases; soft (spineless) fin rays; dorsal- and anal-fin pterygiophores more numerous than adjacent vertebrae; nostrils paired on each side of the head (Nielsen *et al.*, 1999).

Our analysis is the first to test Ophidiiformes in a cladistic framework based on morphological data. The monophyly of the order is sustained by 32 synapomorphies, representing one of the longest branches of our reference tree (Figs. 68, 69). Although taxon sampling included only two ophidiiforms, a literature survey reveals that several of the synapomorphies listed herein are indeed unique to ophidiiforms, or of restricted occurrence among Percomorphacea. As an example, Characters #111 and #130, when analyzed together, describe a unique arrangement between the *adductor mandibulae* and the *levator arcus palatini* muscles of these fishes (Fig. 27). Both taxa analyzed herein have the *adductor mandibulae pars malaris* divided in *pro-* and *retromalaris* (Char. 111, state 1). The *promalaris* is further subdivided into an outer and inner section and separated by an interposing *levator arcus palatini* (Char. #130, state 1). A literature survey reveals that this arrangement is widespread among Ophidiiforms (Howes, 1992; Parmentier *et al.* 2000; Parmentier & Vandewalle, 2003). Given the wide distribution of this character across the order and its absence in other percomorphaceans, the disposition of the *adductor mandibulae* and the *levator arcus palatini* is likely a derived myological condition of the order.

Another remarkable evolutionary novelty present in these taxa is the association between the posteroventral segment of the *epaxialis* musculature and the swim bladder (Char. #174, state 1). An *epaxialis*-swim bladder connection is widespread among ophidiiforms (Courtenay & McKittrick, 1970;

Tyler, 1970; Carter & Musick, 1985; Markle & Olney, 1990; Howes, 1992; Parmentier & Diogo, 2006) and a well-known characteristic of the order. However, morphological descriptions of this character have always focused on the sound-production system involving this connection, and/ or the sexually dimorphic nature of the modifications. In this context, the attachment of the posteroventral segment of the *epaxialis* musculature to the swim bladder (Char. #174, state 1) is for the first time interpreted in an evolutionary context and reported to be a unique synapomorphy for the order.

Several other characters resulted as synapomorphic for the Ophidiiformes. These include many of Nielsen's *et al.* (1999) diagnostic features for the group (*e.g.* Chars. #6, #17, #19, #21). Similar to our results, molecular and combined analyses have also indicated the monophyly of Ophidiiformes based on strong support indexes (*e.g.* Betancur-r *et al.* 2013, 2017; Mirande, 2017; Møller *et al.*, 2016).

#### **Mugiliformes + Atherinomorphae (TNT clade 124):**

*Synapomorphies:* Char. #0: (16-24>13); Char. #1: (7-10>5); Char. #16: (50.1%>53.4%); Char. #27: (0>1); Char. #49: (0>1); Char. #55: (0>1); Char. #80: (0>1); Char. #96: (0>1); Char. #110: (1>0); Char. #115: (1>0); Char. #120: (0>1); Char. #121: (0>1); Char. #143: (0>1); Char. #147: (0>1); Char. #156: (0>1); Char. #157: (0>1); Char. #194: (0>1).

*Support:* relative Bremer = 46%

The sister-group relationship between Mugiliformes and Atherinomorphae was first proposed by Stiassny (1990) based on a series of morphological novelties. This hypothesis has been recurrently corroborated by anatomical studies (*e.g.* Stiassny, 1993; Datovo *et al.*, 2014), and is likewise recovered herein, supported by 17 synapomorphies (Figs. 68, 69).

Some of the most distinct characters supporting the Mugiliformes + Atherinomorphae clade represent modification on the pectoral and pelvic girdle, and branchial myology. These characteristics have been for long listed as putative synapomorphies for mugiliforms and atherinomorphs (*e.g.* Stiassny, 1990, 1993; Datovo *et al.*, 2014), but are herein for the first time analyzed in a cladistic analysis *sensu stricto* (*e.g.* Chars. #96, #143, #157 and #194). Accordingly, these modifications result in valid synapomorphies for this clade. Contrastingly, molecular approaches have never recovered a sister-group relationship between Mugiliformes and Atherinomorphae. Although both taxa are placed within Ovalentariae (fishes with sticky eggs), Atherinomorphae results sister-group of polycentrids, cichlids and pholidichthyids, while Mugiliformes is related to Embiotocidae and Ambassidae (Betancur-R *et al.* 2013, 2017). Similarly, combined analysis of morphological and molecular data also

rejects a Mugiliformes and Atherinomorphae relationship. According to Mirande (2017), Mugilidae forms a clade with Ambassidae and Congrogadidae, while Atherinomorphae is more related to Embiotocidae, Pomacentridae, Pseudochromidae, and the blenniiforms.

***Lates + Centropomus (TNT clade 130) = (Centropomidae sensu Greenwood, 1976):***

*Synapomorphies:* Char. #0: (21-24>19); Char. #1: (10>9); Char. #24: (0>1); Char. #38: (1>0); Char. #51: (1>0); Char. #198: (0>1); Char. #203: (0>1); Char. #208: (0>1).

*Support:* relative Bremer = 30%

Nile perches and snooks have long been allied to each other (Regan, 1913; Greenwood, 1976; Otero, 2004). These fishes are grouped in the family Centropomidae, which was first proposed by Greenwood (1976) based on an extensive osteological study. The monophyly of the family is supported by two putative synapomorphies: 1) a pored lateral-line scale series extending to the posterior margin of the caudal fin (Fig. 14A); and 2) an expansion of the second neural spines in an anteroposterior direction (Fig. 18).

According to Greenwood (1976), Centropomidae would be constituted of two subfamilies: Latinae (*Lates + Psammoperca*) and Centropominae (*Centropomus* spp.). However, Mooi & Gill (1995) contested this circumscription stating that: 1) the lateral line extending to reach the caudal-fin margin also occurred on several unrelated taxa (such as pempherids, rhyacichthyids, polynemids and sciaenids), and 2) that the homology of the second neural-arch expansion between *Centropomus* and *Lates* was not convincing. In addition, they noted that their *type 1* epaxial morphology (Fig. 8; Char #175) was absent *Centropomus*, but present in *Lates* and *Psammoperca*. Based on these evidences, Mooi & Gill (1995) removed Latinae from Centropomidae and raised it to a family level, the Latidae. According to the authors, Latidae would probably be related to other *type 1* taxa, (*i.e.* Apogonidae, Centrogeniidae, Champsodontidae, Cheimarrichthyidae, Grammatidae, Haemulidae, Percidae, and Serranidae), and not to Centropomidae. More recently, Otero (2004) also rejected the monophyly of Centropomidae (*sensu* Greenwood, 1976) in a systematic study of recent and fossil latine fishes. Otero's cladistic analysis sampled 29 morphological characters and 11 taxa, and recovered Latinae as sister-group to *Niphon*, while Centropominae would form a clade with *Ambassis*. A third and contrasting centropomid arrangement was published by Whitlock (2010). The author recovered *Centropomus* as sister-group of a large clade including *Lates*, Percichthyidae, Lateolabracidae, Moronidae, and Centrarchidae (an arrangement similar to our Clade 128: Fig. 69).

Our results strongly support a *Lates* and *Centropomus* sister-group relationship that is compatible to Greenwood's (1976) Centropomidae. The clade is supported, among other characteristics, by a pored lateral line which extends to the posterior margin of the caudal fin (Fig. 14; Char. #208, state 1), Greenwood's first character for Centropomidae. Nevertheless, the expansion of the second neural spine (Greenwood's second character) was not sampled herein due to the impossibility to create unambiguous character-states for its morphological variation when analyzing a large number of perciforms.

The proper elucidation of the limits of Centropomidae is beyond the scope of our study. Such investigation would demand the sampling of several taxa perciform taxa not sampled herein, such as *Niphon*, *Ambassis*, *Glaucosoma*, and *Siniperca*. In this sense, our analysis cannot be used to reject Otero's (2004) or Whitlock's (2010) hypotheses. However, we do refute Mooi & Gill's (1995) intrarelationships of Latidae. Our character reconstruction for the *type 1 epaxialis* association to the dorsal-fin pterygiophores (Char. #175) reveals that that it evolved five times within the analyzed perciforms and is homoplastically present in Sciaenidae, Serranidae, Apogonidae, Haemulidae, and Latinae.

Recent analyses based on molecular data mostly support Greenwood's (1976) composition of Centropomidae. A sister-group relationship between Latinae and Centropominae is recovered by the analyses of Li *et al.* (2011), Betancur-R *et al.* (2013), and Betancur-R *et al.* (2017). However, Mirande's (2017) phylogeny of ray-finned fishes based on combined morphological and molecular data recovers *Lates* (their Latidae) as sister-group of Lactariidae, and this clade as sister-group of Psettodidae. Centropomidae, instead, is grouped with Sphyraenidae.

#### **Sciaenidae + Polynemidae (TNT clade 123):**

*Synapomorphies*: Char. #16: (39.3%>37.6%); Char. #32: (0>1); Char. #49: (0>1); Char. #52: (0>2); Char. #55: (0>1); Char. #74: (1>0); Char. #112: (0>1); Char. #114: (1>0); Char. #115: (1>2); Char. #158: (0>1), Char. #200: (1>0); Char. #203: (0>1); Char. #208: (0>1).

*Support*: relative Bremer = 59%

Johnson (1993) proposed for the first time a relationship between Sciaenidae and Polynemidae. The author noted that five of the 21-sciaenid synapomorphies listed by Sasaki (1989) would also be present on polynemids. These include the insertion of a single branchiostegal ray on the posterior ceratohyal, an interdigitation between the metapterygoid and quadrate, the absence of

trisegmental pterygiophores (*i.e.* fusion between proximal and medial pterygiophores), absence of a supramaxilla, and an extension of the epaxial musculature onto the frontals. Of these, the last three would be homoplastically present in several other percomorphs, but the first two were of restrict distribution, or unique to sciaenids and polynemids. Kang et al. (2017) also discussed a possible sciaenid + polynemid relationship in a morphological investigation of the Polynemidae inter- and intrarelationships. The authors suggested Sciaenidae as immediate sister-group of Polynemidae based on six putatively derived characters. These included most characters listed by Johnson (1993) with a few modifications: the exclusion of the anterior epaxial expansion (considered by the authors of dubious polarity), and inclusion of a specialization of the anterior portion of the nasal, plus a posterior interdigitation between pelvic bones.

Our analysis strongly supports a Sciaenidae + Polynemidae relationship (Figs. 68, 69). This clade is sustained by 13 synapomorphies, which include the following Sasaki's (1989) characters: insertion of a single branchiostegal ray on the posterior ceratohyal (Char. #52), and interdigitation between the metapterygoid and quadrate (Char. #32). In addition, we also list Characters #49 and #55 as newly recognized synapomorphies for Sciaenidae + Polynemidae: these describe a series of specialization of the hyoid-artery path in these taxa. The hyoid-artery foramen is absent, and the hyoid artery follows dorsally to the ceratohyals (Char. #49). When it reaches the dorsal-hypohyal, the hyoid artery lays on a sulcus on the dorsal surface of this bone, instead of piercing it (Char. #55).

Yet, molecular analyses never recover a Polynemidae + Sciaenidae sister-group relationship. Based on molecular data, Polynemidae is considered a member of the Carangaria (=Carangimorphariae), and placed among Carangiformes, Pleuronectiformes, Sphyraenidae, Menidae, Leptobramidae, Toxotidae, Xiphiidae, and Istiophoridae. Sciaenidae, on the other hand, falls within a large Percomorpharia clade and sister-group of the Emmelichthyidae (Near *et al.*, 2013; Betancur-R *et al.* 2013, 2017). None of these relationships is supported by our data.

#### **Scobriformes *sensu* Johnson (1986) (TNT clade 89):**

*Synapomorphies:* Char. #44: (0>1); Char. #119: (0>1); Char. #126: (0>1); Char. #186: (0>1).

*Support:* relative Bremer = 11%

The limits and interrelationships of Scobriformes (*sensu* Wiley & Johnson, 2010) is among the most extensively studied topics of percomorphaceans (*e.g.* Collette & Chao, 1975; Nakamura & Fujii, 1983; Collette *et al.* 1984; Johnson, 1986). Yet, the exact composition or the internal resolution

of the order has suffered variation over time, mostly regarding the position of Sphyraenidae, Xiphiidae, Istiophoridae, and Luvaridae in Scombriformes. Recent morphological hypotheses (e.g. Collette *et al.* 1984; Johnson, 1986; Tyler *et al.*, 1989; Datovo *et al.* 2014) have agreed with the inclusion of billfishes, and the removal of *Luvarus* from the order. However, a monophyletic Scombriformes has never been corroborated by molecular analyses. Although most scombriform families are included in a common clade named Pelagiaria (*sensu* Betancur-R *et al.*, 2017), the internal arrangement of pelagiarian fishes never recovers the monophyly of this order. In addition, molecular data has never supported the inclusion of Xiphiidae and Istiophoridae among scombriforms. The most recent classifications place billfishes within a large clade named Carangaria (*sensu* Betancur-R *et al.*, 2017), which also includes the families Menidae, Lactariidae, Polynemidae, Sphyraenidae, Leptobramidae, Toxotidae, Centropomidae, Pleuronectiformes, and Carangiformes (Miya *et al.*, 2013; Near *et al.*, 2013; Betancur-R *et al.* 2013, 2017).

Our analysis agrees with the monophyly of Scombriformes and retrieves a clade that is compatible to Johnson's 1986 composition of Scombroidei (Figs. 68, 69). It includes sphyraenids, gempylids, thrichiurids and scombrids (billfishes were not sampled). This arrangement is supported by four synapomorphies, which includes two of Johnson's former synapomorphies for the group (our Chars. #44 and #126). Yet, our final hypothesis differs from Johnson (1986) regarding the scombriforms sister-group. While in Johnson's (1986) hypothesis, Scombroidei and Pomatomidae are successive sister-groups of his Scombroidei, our analysis offers Scombriformes as sister-group of Pleuronectiformes, *Pomatomus* in a clade with Arripidae, and *Scombrolabrax* as sister-group of a large clade containing several pelagic lineages.

#### **Pleuronectiformes (TNT clade 131):**

*Synapomorphies:* Char. #19: (34%-36.2%>32.8%); Char. #25: (0>1); Char. #52: (0>1); Char. #108: (1>0); Char. #124: (0>1); Char. #144: (0>1); Char. #184: (0>1); Char. #198: (1>0); Char. #206: (1>0); Char. #208: (0>1).

*Support:* relative Bremer = 29%

Flatfishes are unique among vertebrates to exhibit a bilateral asymmetry where the eye of one side of the head migrates to the opposing side during larval metamorphosis (Fig. 38). Accordingly, most anatomical studies have accepted the monophyly of the group (e.g. Regan, 1910; Hubbs, 1945; Lauder & Liem, 1983; Hensley & Ahlstrom, 1984; Chapleau, 1993). Current morphological classifications consider Pleuronectiformes monophyletic, and the clade is supported by three

synapomorphies: 1) ontogeny characterized by eye migration; 2) dorsal-fin origin shifted anteriorly; and 3) presence of a *recessus orbitalis* – a muscular sac-like evagination that is filled with water and helps on eye-protrusion when these fishes are buried in the substrate (Chapleau, 1993).

Our results strongly corroborate the monophyly of Pleuronectiformes and the clade is herein supported by 10 synapomorphies. These include newly recognized character-states such as a partially divided *levator operculi* (Fig. 38; Char. #124, state 1) and the absence of the branchial muscle *levator externus 3* (Char. #144, state 1). In addition, we have sampled two of the three Chapleau's (1993) synapomorphies for Pleuronectiformes, but only the ontogeny characterized by eye migration resulted as a valid synapomorphy (Char. #184). A dorsal fin insertion that is shifted anteriorly resulted as a synapomorphy for the Pleuronectiformes + Scombriformes clade (Figs. 68, 69: Clade 90). Moreover, we have detected no modification on the eye musculature compatible to the *recessus orbitalis*, and thus this character was not tested in our phylogeny.

Molecular analyses are inconsistent when regarding the monophyly of Pleuronectiformes, mostly because *Psettodes* (Psettodidae) often figures as more related to non-flatfishes than to the remaining pleuronectiforms (Li *et al.*, 2011; Near *et al.*, 2013; Betancur *et al.* 2013; Campbell *et al.*, 2013). It has been only recently that analyses including larger datasets and sampling ultraconserved DNA elements (UCE's) recovered the monophyly of flatfishes (Harrington *et al.* 2016; Betancur-R *et al.*, 2017), but a final decision on this matter still awaits further investigations.

## BIBLIOGRAPHY

- ABE T. 1954-1955. New, rare or uncommon fishes from Japanese waters. V. Notes on the rare fishes of the suborders Stromateoidei and Tetragonuroidei (Berg). *Japan Journal of Ichthyology*, 3: 113-118.
- AHLSTROM EH, BUTLER JL, SUMIDA BY. 1976. Pelagic stromateoid fishes (Pisces, Perciformes) of the eastern Pacific: kinds, distributions, and early life histories and observations on five of these from the northwest Atlantic. *Bulletin of marine science*, 26(3): 285-402
- ALLEN GH. 2001. The ragfish, *Icosteus aenigmaticus* Lockington, 1880: a synthesis of historical and recent records from the North Pacific Ocean and the Bering Sea. *Marine Fisheries Review*, 63(4): 1-31.
- ALLIS EP. 1903. The skull, and the cranial and first spinal muscles and nerves in *Scomber scomber*. *Journal of Morphology*, 18(1-2): 45-328.
- ARAI MN. 1988. Interactions of fish and pelagic coelenterates. *Canadian Journal of Zoology*, 66(9): 1913-1927.
- ARAI MN. 2005. Arai, M. N. (2005). Predation on pelagic coelenterates: a review. *Journal of the Marine Biological Association of the United Kingdom*, 85(3): 523-536.
- AUSTER PJ, GRISWOLD CA, YOUNGBLUTH MJ, BAILEY TG. 1992. Aggregations of myctophid fishes with other pelagic fauna. *Environmental Biology of Fishes*, 35(2): 133-139.
- BANNIKOV AF. 1995. Morphology and phylogeny of fossil stromateoid fishes (Perciformes). *Geobios*, 19: 177-181.
- BARNARD KH. 1948. Further notes on South African marine fishes. *Annals of the South African Museum*, 36: 341-406.
- BENFIELD MC, CARUSO JH, SULAK KJ. 2009. In situ video observations of two manefishes (Perciformes: Caristiidae) in the mesopelagic zone of the northern Gulf of Mexico. *Copeia*, 2009(4): 637-641.
- BETANCUR-R R, WILEY EO, ARRATIA G, ACERO A, BAILLY N, MIYA M, LECOINTRE G, ORTI G. 2017. Phylogenetic classification of bony fishes. *BMC Evolutionary Biology*, 17(1): 162.
- BETANCUR-RR, BROUGHTON RE, WILEY EO, CARPENTER K, LÓPEZ JA, LI C, HOLCROFT NI, ARCILA D, SANCIANGCO M, CURETON JC, ZHANG F, BUSER T, CAMPBELL MA, BALLESTEROS JA, ROA-VARON A, WILLIS S, BORDEN WC, ROWLEY T, RENEAU PC, HOUGH DJ, LU G, GRANDE T, ARRATIA G, ORTÍ G. 2013.

The tree of life and a new classification of bony fishes. *PLOS Currents Tree Of Life* 2013: Apr 18 [Last Modified: 2013 Jun 3]. Edition 1.

BOLCH CJ, WARD RD, LAST PR. 1994. Biochemical systematics of the marine fish family Centrolophidae (Teleostei: Stromateoidei) from Australian waters. *Marine and Freshwater Research*, 45(7): 1157-1172.

BONE Q, BROOK CER. 1973. On *Schedophilus medusophagus* (Pisces: Stromateoidei). *Journal of the Marine Biological Association of the United Kingdom*, 53(4): 753-761.

BONE Q. 1972. Buoyancy and hydrodynamic functions of integument in the castor oil fish, *Ruvettus pretiosus* (Pisces: Gempylidae). *Copeia*, 1972: 78-87.

BREMMER K. 1994. Branch support and tree stability. *Cladistics*, 10: 295-304.

BREMM S, VON LANDESBERGER T, HEß M, SCHRECK T, WEIL P, HAMACHER K. 2011. *Interactive visual comparison of multiple trees*. In: IEEE Conference on Visual Analytics Science and Technology (VAST). Providence, Rhode Island. p. 31-40.

BREWSTER B. 1987. Eye migration and cranial development during flatfish metamorphosis: a reappraisal (Teleostei: Pleuronectiformes). *Journal of Fish Biology*, 31(6): 805-833.

BUDDINGTON RK, DIAMOND JM. 1986. Aristotle revisited: the function of pyloric caeca in fish. *Proceedings of the National Academy of Sciences*, 83(20): 8012-8014.

BÜHLER, H. 1930. Die Verdauungsorgane der Stromateidae (Teleost.). *Zoomorphology*, 19: 59-115.

CAMIN JH, SOKAL RR. 1965. A method for deducing branching sequences in phylogeny. *Evolution*, 19(3): 311-326.

CAMPBELL MA, CHEN WJ, LÓPEZ A. 2013. Are flatfishes (Pleuronectiformes) monophyletic? *Molecular Phylogenetics and evolution*, 69: 664-673.

CAMPBELL MA, SADO T, SHINZATO C, KOYANAGI R, OKAMOTO M, MIYA M. 2018. Multilocus phylogenetic analysis of the first molecular data from the rare and monotypic Amarsipidae places the family within the Pelagia and highlights limitations of existing data sets in resolving pelagian interrelationships. *Molecular Phylogenetics and Evolution*, 124: 172-180.

CARTER HJ, MUSICK JA. 1985. Sexual dimorphism in the deep-sea fish *Barathrodemus manatinus* (Ophidiidae). *Copeia*, 1985(1): 69-73.

- CHANG C-H, CHIAO C-C, YAN HY. 2009. The structure and possible functions of the milkfish *Chanos chanos* adipose eyelid. *Journal of fish biology*, 75: 87-99.
- CHAPLEAU F. 1993. Pleuronectiform relationships: a cladistic reassessment. *Bulletin of Marine Science*, 52(1): 516-540.
- COLLETTE BB, CHAO LN 1975. Systematics and morphology of the bonitos (*Sarda*) and their relatives (Scombridae, Sardini). *Fishery Bulletin*, 73(3): 516-625.
- COLLETTE BB, POTTHOFF T, RICHARDS WJ, UEYANAGI S, RUSSO JO, NISHIKAWA Y. 1984. Scombroidei: development and relationships. In: MOSER HG, RICHARDS WJ, COHEN DM, FAHAY MP, KENDALL JR AW, RICHARDSON SL. Eds. *Ontogeny and systematics of fishes*. American Society of Ichthyologists and Herpetologists: 591-620. Special Publication Number 1.
- COOMBS S, JANSSEN J, WEBB JF. 1988. Diversity of lateral line systems: evolutionary and functional considerations. In: ATEMA J, FAY RR, POPPER AN AND W. N. TAVOLGA WN. Eds. *Sensory biology of aquatic animals*. Springer, New York. p. 553-593.
- COURTENAY WR, MCKITTRICK FA. 1970. Sound-producing mechanisms in carapid fishes, with notes on phylogenetic implications. *Marine Biology*, 7(2): 131-137.
- COX JR WM, REID EE. 1932. The chemical composition of oil of *Ruvettus pretiosus*, the "Castor oil fish". *Journal of the American Chemical Society*, 54(1): 220-229.
- DAHL E. 1961. The association between young whiting, *Gadus merlangus*, and the jelly-fish *Cyanea capillata*. *Sarsia*, 3(1): 47-55.
- DATOVO A, BOCKMANN FA. 2010. Dorsolateral head muscles of the catfish families Nematogenyidae and Trichomycteridae (Siluriformes: Loricarioidei): comparative anatomy and phylogenetic analysis. *Neotropical Ichthyology*, 8(2): 193-246.
- DATOVO A, de PINNA MCC, JOHNSON GD. 2014. The infrabranchial musculature and its bearing on the phylogeny of percomorph fishes (Osteichthyes: Teleostei). *PLOS ONE* 9(10): E110129.
- DATOVO A, RIZZATO PP. 2018. Evolution of the facial musculature in basal ray-finned fishes. *Frontiers in zoology*, 15(1): 40.
- DATOVO A, VARI RP. 2013. The Jaw adductor muscle complex in teleostean fishes: Evolution, homologies and revised nomenclature (Osteichthyes: Actinopterygii). *PLOS ONE*, 8: E60846.

- DAVENPORT D, NORRIS KS. 1958. Observations on the symbiosis of the sea anemone *Stoichactis* and the pomacentrid fish, *Amphiprion percula*. *The Biological Bulletin*, 115(3): 397-410.
- DAWSON CE. 1971. Notes on juvenile black driftfish, *Hyperoglyphe bythites*, from the northern Gulf of Mexico. *Copeia*, 1971(4): 732-735.
- DEN HARTOG JC, VAN NIEROP MM. 1984. A study on the gut contents of six leathery turtles *Dermochelys coriacea* (Linnaeus) (Reptilia: Testudines: Dermochelyidae) from British waters and from the Netherlands. *Zoologische Verhandelingen*, 209: 1–36.
- DOIUCHI R, SATO T, NAKABO T. 2004. Phylogenetic relationships of the Stromateoid fishes (Perciformes). *Ichthyological Research*, 51: 202–212.
- DOIUCHI, R. & NAKABO, T. 2006. Molecular phylogeny of the stromateoid fishes (Teleostei: Perciformes) inferred from mitochondrial DNA sequences and compared with morphology-based hypotheses. *Molecular Phylogenetics and Evolution*, 39: 111-123.
- DRAZEN JC, ROBISON BH. 2004. Direct observations of the association between a deep-sea fish and a giant scyphomedusa. *Marine and Freshwater Behaviour and Physiology*, 37(3): 209-214.
- DUFFY CAJ, STEWART AL, YARRALL R. 2000. First record of pre-settlement juvenile bluenose, *Hyperoglyphe antarctica*, from New Zealand. *New Zealand Journal of Marine and Freshwater Research*, 34(2): 353-358.
- DUFFY DC. 1988. Predator-prey interactions between common terns and butterfish. *Ornis Scandinavica*, 19(2): 160-163.
- EVANS DH, PIERMARINI PM, CHOE KP. 2005. The multifunctional fish gill: dominant site of gas exchange, osmoregulation, acid-base regulation, and excretion of nitrogenous waste. *Physiological reviews*, 85(1): 97-177.
- FÄNGE R. 1966. Physiology of the swimbladder. *Physiological reviews*, 46(2): 299-322.
- FARINA SC, NEAR TJ, BEMIS WE. 2015. Evolution of the Branchistegal Membrane and Restricted gill openings in Actinopterygian fishes. *Journal of morphology*, 276: 681-694.
- FARRIS JS. 1969. A successive approximations approach to character weighting. *Systematic Biology*, 18(4): 374-385.

FARRIS JS. 1983. The logical basis of phylogenetic analysis. In: PLATNICK N, FUNK VA. Eds. *Advances in Cladistics*, 2. Proceedings of the second meeting of the Willi Hennig Society. New York, Columbia University Press. p. 7-36.

FARRIS JS. 1989. The retention index and the rescaled consistency index. *Cladistics*, 5(4): 417-419.

FISCHER W, BIANCHI G. 1984. *FAO species identification sheets for fishery purposes. Western Indian Ocean (Fishing Area 51)*. Prepared and printed with the support of the Danish International Development Agency (DANIDA). Rome, Food and Agricultural Organization of the United Nations. v. 1-6, 62p.

FREIHOFER WC. 1963. Patterns of ramus lateralis accessorius and their systematic significance in teleostean fishes. *Stanford Ichthyological Bulletin*, 8(2): 80-189.

FREIHOFER WC. 1972. Trunk lateral line nerves, hyoid arch gill rakers, and olfactory bulb location in atheriniform, mugilid, and percoid fishes. *Occasional Papers of the California Academy of Sciences*, 95: 1-31.

FREIHOFER WC. 1978. Cranial nerves of a percoid fish, *Polycentrus schomburgkii* (family Nandidae), a contribution to the morphology and classification of the order Perciformes. *Occasional Papers of the California Academy of Sciences*, 128: 1-78.

FRICKE R, ESCHMEYER WN, VAN DER LAAN R. 2018. *Eschmeyer's catalog of fishes: genera, species, references*. Retrieved from <http://researcharchive.calacademy.org/research/ichthyology/catalog/fishcatmain.asp>. Access in 8 Mar 2018.

FROESE R, PAULY D. 2019. *FishBase. World Wide Web electronic publication*. Retrieved from [www.fishbase.org](http://www.fishbase.org). Access in 8 Mar 2019.

GHOSH S, MOHANRAJ G, ASOKAN PK, DHOKIA HK, ZALA MS, BHINT HM. 2009. Fishery and stock estimates of the silver pomfret, *Pampus argenteus* (Euphrasen), landed by gill netters at Veraval. *Indian Journal of Fisheries*, 56(3): 177-182.

GILCHRIST JDF. 1922. On the oesophageal teeth of the Stromateidae. *The Annals and Magazine of Natural History, Ser. 9*, 9: 249-255.

GILL T. 1884. Notes on the Stromateidæ. *Proceedings of the American Philosophical Society*, 21(116): 664-672.

- GOLOBOFF PA. 1993. Estimating character weights during tree search. *Cladistics*, 9: 83-91.
- GOLOBOFF PA. 1997. Self-weighted optimization: Tree searches and character state reconstructions under implied transformation costs. *Cladistics*, 13: 225–245.
- GOLOBOFF PA. 1999. Analyzing large data sets in reasonable time: Solution for composite optima. *Cladistics*, 15: 415–428.
- GOLOBOFF PA, FARRIS JS, NIXON KC. 2008a. TNT, a free program for phylogenetic analysis. *Cladistics*, 24: 774-786.
- GOLOBOFF PA, CARPENTER JM, SALVADOR ARIAS J, MIRANDA ESQUIVEL DR. 2008b. Weighting against homoplasy improves phylogenetic analysis of morphological data sets. *Cladistics*, 24: 758-773.
- GOLOBOFF PA, MATTONI CI, QUINTEROS AS. 2006. Continuous characters analyzed as such. *Cladistics*, 22: 589-601.
- GOSLINE WA. 1970. A reinterpretation of the teleostean fish order Gobiesociformes. *Proceedings of the California Academy of Sciences*, 38(19): 363-382.
- GREENWOOD PH. 1976. A review of the family Centropomidae (Pisces, Perciformes). *Bulletin of the British Museum of Natural History. Zoology series*, 29: 1-81.
- GREER AT, WOODSON CB, GUIGAND CM, COWEN RK. 2016. Larval fishes utilize Batesian mimicry as a survival strategy in the plankton. *Marine Ecology Progress Series*, 551: 1-12.
- GÜNTHER A. 1880. *An introduction to the study of fishes*. London, Taylor & Francis, 524p.
- HADDOCK SH. 2004. A golden age of gelata: past and future research on planktonic ctenophores and cnidarians. *Hydrobiologia*, 530(1-3): 549-556.
- HAEDRICH RL. 1966. The stromateoid fish genus *Icichthys*: notes and a new species. *Videnskabelige Meddelelser fra Dansk Naturhistorisk Forening, Kjøbenhavn*, 129: 199-213.
- HAEDRICH RL. 1967. The stromateoid fishes: systematics and a classification. *Bulletin of the Museum of Comparative Zoology*, 135(2): 310-139.
- HAEDRICH RL. 1969. A new family of aberrant stromateoid fishes from the equatorial indo-pacific. *Dana-Reports*, 76: 1-14.
- HAEDRICH RL. 1971. The pons moultoni, a significant character. *Copeia*, 1971(1): 167-169.

HAEDRICH RL. 1986. Suborder Stromateoidei. In: SMITH, MM, HEEMSTRA PC. Eds. *Smiths' Sea Fishes*. Johannesburg, Macmillan. p. 841-851.

HAEDRICH RL, HORN MH. 1972. *A key to the stromateoid fishes*. Woods Hole Oceanographic Institution. Technical Report WHOI-72-15. 46p.  
<https://darchive.mblwhoilibrary.org/bitstream/handle/1912/99/WHOI-72-15.pdf?sequence=1&isAllowed=y>

HARBISON GR. 1993. The potential of fishes for the control of gelatinous zooplankton. In: *ICES C.M. Documents*, 74: 1–10.

HEASLIP SG, IVERSON SJ, BOWEN WD, JAMES MC. 2012. Jellyfish support high energy intake of leatherback sea turtles (*Dermochelys coriacea*): video evidence from animal-borne cameras. *PLoS one*, 7(3): e33259.

HELFMAN GS. 1981. The advantage to fishes of hovering in shade. *Copeia*, 1981(2): 392-400.

HENSLEY DA, AHLSTROM EH. 1984. Pleuronectiformes: Relationships. In: MOSER HG, RICHARDS WJ, COHEN DM, FAHAY MP, KENDALL JR AW, RICHARDSON SL. Eds. *Ontogeny and systematics of fishes. Based on an International Symposium dedicated to the memory of Elbert Halvor Ahlstrom*. New York, American Society of Ichthyologists and Herpetologists. p. 670–687. (Special Publication Number 1).

HILTON EJ, JOHNSON GD. 2007. When two equals three: developmental osteology and homology of the caudal skeleton in carangid fishes (Perciformes: Carangidae). *Evolution & Development*, 9(2): 178–189.

HORN MH. 1970a. Systematic and biology of the stromateid fish genus *Peprilus*. *Bulletin of the Museum of Comparative Zoology*, 140(5): 165-262.

HORN MH. 1970b. The swimbladder as a juvenile organ in stromateoid fishes. *Breviora, Museum of Comparative Zoology*, 359: 1-9.

HORN MH. 1972. Systematic status and aspects of the ecology of the elongate ariommid fishes (Suborder Stromateoidei) in the Atlantic. *Bulletin of Marine Science*, 22(3): 537-558.

HORN MH. 1973. Systematic comparison of the stromateid Fishes *Stromateus brasiliensis* fowler and *Stromateus stellatus* Cuvier from coastal South America with a review of the genus. *Bulletin of the British Museum (Natural History) Zoology*, 24(7): 317-339.

HORN MH. 1975. Swim-bladder state and structure in relation to behavior and mode of life in stromateoid fishes. *Fishery bulletin*, 73(1): 95-109.

HORN MH. 1984. *Stromateoidei: development and relationships*. In: MOSER HG, RICHARDS WJ, COHEN DM, FAHAY MP, KENDALL JR AW, RICHARDSON SL. Eds. *Ontogeny and systematics of fishes. Based on an International Symposium dedicated to the memory of Elbert Halvor Ahlstrom*. New York, American Society of Ichthyologists and Herpetologists. p. 620–636. (Special Publication Number 1).

HORTON T, KROH A, AHYONG S, *et al.* 2019. *World Register of Marine Species*. Retrieved from <http://www.marinespecies.org/aphia.php?p=taxdetails&id=234546>. Access in 08 Mar 2019.

HOWES GJ. 1992. Notes on the anatomy and classification of ophidiiform fishes with particular reference to the abyssal genus *Acanthonus* Gunther, 1878. *Bulletin of the British Museum (Natural History) Zoology*, 52: 95-131.

HUBBS CL. 1945. Phylogenetic position of the Citharidae, a family of flatfishes. *Miscellaneous Publications. Museum of Zoology. University of Michigan*, 63: 1-38.

IMAMURA H, YABE M. 2002. Demise of the Scorpaeniformes (Actinopterygii: Percomorpha): an alternative phylogenetic hypothesis. *Bulletin of Fisheries Sciences, Hokkaido University*, 53(3): 107-128.

ISHIDA Y, ASAOKA R, NAKAE M, SASAKI K. 2015. The trunk lateral line system and its innervation in *Mugil cephalus* (Mugilidae: Mugiliformes). *Ichthyological Research*, 62(3): 253-257.

ISOKAWA S, KUBOTA K, KOSAIKAI T, SATOMURA I, TSUBOUCHI M, SERA A. 1956. Some contributions to study of esophageal sacs and teeth of fishes. *The Journal of Nihon University School of Dentistry*, 7(3): 103-111.

JANSSEN J. 1989. Association of *Caristius* sp. (Pisces: Caristiidae) with a siphonophore, *Bathypusa conifera*. *Copeia*, 1989(1): 198-201.

JANSSEN J, HARBISON GR. 1981. Fish in salps: the association of squaretails (*Tetragonurus* spp.) with pelagic tunicates. *Journal of the Marine Biological Association of the United Kingdom*, 61(4): 917-927.

JENKINS RL. 1983. Observations on the commensal relationship of *Nomeus gronovii* with *Physalia physalis*. *Copeia*, 1983(1): 250-252.

JOHNSON GD. 1975. The procurrent spur: an undescribed perciform caudal character and its phylogenetic implications. *Occasional Papers of the California Academy of Sciences*, 121: 1-23.

JOHNSON GD. 1984. *Percoidei: development and relationships*. In: MOSER HG, RICHARDS WJ, COHEN DM, FAHAY MP, KENDALL JR AW, RICHARDSON SL. Eds. *Ontogeny and systematics of fishes Based on an International Symposium dedicated to the memory of Elbert Halvor Ahlstrom*. New York, American Society of Ichthyologists and Herpetologists. p. 464–499. (Special Publication Number 1).

JOHNSON GD. 1986. Scombroid phylogeny: an alternative hypothesis. *Bulletin of Marine Science*, 39(1): 1-41.

JOHNSON GD. 1992. Monophyly of the euteleostean clades: Neoteleostei, Eurypterygii, and Ctenosquamata. *Copeia*, 1992(1)2: 8-25.

JOHNSON GD. 1993. Percomorph phylogeny-Progress and problems. *Bulletin of Marine Science*, 52(1): 3-28.

JOHNSON GD, FRITZSCHE RA. 1989. *Graus nigra*, an omnivorous girellid, with a comparative osteology and comments on relationships of the Girellidae (Pisces: Perciformes). *Proceedings of the Academy of Natural Sciences of Philadelphia*, 141: 1-27.

JOHNSON GD, PATTERSON C. 1993. Percomorph phylogeny: a survey of acanthomorphs and a new proposal. *Bulletin of Marine Science*, 52(1): 554-626.

JORDAN DS, GILBERT CH. 1880. Description of a new species of deep-water fish (*Ichthyos lockingtoni*), from the coast of California. *Proceedings of the United States National Museum*, 154(3): 305-308.

JÚNIOR TV, LESSA RP, BARBOSA TM, TOLOTTI MT, RIBEIRO ACB. 2008. Stomach contents of the Caribbean pomfret *Brama caribbea* (Mead, 1972) from stomach contents of great pelagic predators from Southwestern equatorial Atlantic. *Boletín del Instituto de Pesca*, 34: 241-249.

KANG S, IMAMURA H, KAWAI T. 2018. Morphological evidence supporting the monophyly of the family Polynemidae (Teleostei: Perciformes) and its sister relationship with Sciaenidae. *Ichthyological Research*, 65(1): 29-41.

KARPLUS I. 2014. *Symbiosis in Fishes. The Biology of interspecific partnerships*. Hoboken, N J, John Wiley & Sons. 449p.

KINGSFORD MJ. 1993. Biotic and abiotic structure in the pelagic environment: importance to small fishes. *Bulletin of Marine Science*, 53(2): 393-415.

KOBAYASHI K, KUMAKURA M, YOSHIMURA K, INATOMI M, ASAMI T. 1998. Fine structure of the tongue and lingual papillae of the penguin. *Archives of Histology and Cytology*, 61(1): 37-46.

- KONOVALENKO II, PIOTROVSKIY AS. 1989. First description of a sexually mature *Amarsipa*, *Amarsipus carlsbergi*. *Journal of Ichthyology*, 28: 86-89.
- KREFFT F. 1969. Ergebnisse der Forschungsreisen des FFS "Walther Herwig" nach Süd Amerika. VI. Fische der Familie Centrolophidae (Perciformes, Stromateoidei). *Archiv für Fishereiwissenschaft*, 20: 1-9.
- LA MONTE FR. 1958. Scales of the Atlantic species of *Makaira*. *Atlantic Marlins*, 61: 381-411.
- LANE CE. 1960. The Portuguese man-of-war. *Scientific American*, 202: 158-168.
- LAST PR, DALEY RK, DUHAMEL G. 2013. A review of the rudderfish genus *Tubbia* (Stromateoidei: Centrolophidae) with the description of a new species from the Southern Hemisphere. *Zootaxa*, 3616(5): 461-477.
- LAUDER GV. 1982. Patterns of evolution in the feeding mechanism of actinopterygian fishes. *American Zoologist*, 22(2): 275-285.
- LAUDER GV. 1983. Functional design and evolution of the pharyngeal jaw apparatus in euteleostean fishes. *Zoological Journal of the Linnean Society*, 77(1): 1-38.
- LAUDER CV, LIEM KF. 1983. The evolution and interrelationships of the actinopterygian fishes. *Bulletin of the Museum of Comparative Zoology*, 150: 95-197.
- LAWLEY JW, JÚNIOR EF. 2018. First record of association between *Tamoya haplonema* (Cnidaria: Cubozoa) and stromateid fish, with a review on interactions between fish and cubozoan jellyfishes. *Plankton and Benthos Research*, 13(1): 32-38.
- LE DANOIS E, LE DANOIS Y. 1963. L'Ordre des Scombres. *Memoires de l' Institut Francois d' Afrique Noire*, 68: 153-192.
- LEIS JM, VAN DER LINGEN CD. 1997. Larval development and relationships of the perciform family Dichistiidae (= Coracinidae), the galjoen fishes. *Bulletin of Marine Science*, 60(1): 100-116.
- LI B, DETTAI A, CRUAUD C, COULOUX C, DESOUTTER-MENIGER M, LECOINTRE G. 2007. RNF213, a new nuclear marker for acanthomorph phylogeny. *Molecular Phylogenetics and Evolution*, 50: 345–363.
- LI C, BETANCUR-R R, SMITH WL, ORTÍ G. 2011. Monophyly and interrelationships of Snook and Barramundi (Centropomidae sensu Greenwood) and five new markers for fish phylogenetics. *Molecular Phylogenetics and Evolution*, 60(3): 463-471.

- LINDSAY DJ, HUNT JC, HAYASHI KI. 2001. Associations in the midwater zone: the penaeid shrimp *Funchalia sagamiensis* Fujino 1975 and pelagic tunicates (Order: Pyrosomatida). *Marine Freshwater Behaviour & Physiology*, 34(3): 157-170.
- LYNAM CP, BRIERLEY AS. 2007. Enhanced survival of 0-group gadoid fish under jellyfish umbrellas. *Marine Biology*, 150(6): 1397-1401.
- MABEE PM. 1988. Supraneural and predorsal bones in fishes: development and homologies. *Copeia*, 1988(4): 827-838.
- MADDISON WP, MADDISON DR. 2014. *Mesquite: A modular system for evolutionary analysis*. Version 3.6. Retrieved from <http://mesquiteproject.org>. Access in 11 Mar 2018.
- MAGNUSON JJ. 1973. Comparative study of adaptations for continuous swimming and hydrostatic equilibrium of scombroid and xiphoid fishes. *Fishery Bulletin*, 71(2): 337-356.
- MANSUETI R. 1963. Symbiotic behavior between small fishes and jellyfishes, with new data on that between the stromateid, *Peprilus alepidotus*, and the scyphomedusa, *Chrysaora quinquecirrha*. *Copeia*, 1963: 40-80.
- MARKLE DF, OLNEY JE. 1990. Systematics of the pearlfishes (Pisces: Carapidae). *Bulletin of Marine Science*, 47(2): 269-410.
- MATARESE AC, STEVENS G, WATSON DW. 1984. *Icosteioidei: Development and Relationships*. In: MOSER HG, RICHARDS WJ, COHEN DM, FAHAY MP, KENDALL JR AW, RICHARDSON SL. Eds. *Ontogeny and systematics of fishes Based on an International Symposium dedicated to the memory of Elbert Halvor Ahlstrom*. New York, American Society of Ichthyologists and Herpetologists. p. 576-577. (Special Publication Number 1).
- MATTHEWS JE, SHOEMAKER HH. 1952. Fishes using ctenophores for shelter. *Copeia*, 1952(4): 270-270.
- MAUL GE. 1964. Observations on young live *Mupus maculatus* (Günther) and *Mupus ovalis* (Valenciennes). *Copeia*, 1964(1): 93-97.
- MAYO CA. 1968. *Physiology and behavior of the man-of-war fish, Nomeus gronovii, in the Florida current*. Unpublished Master's Thesis. University of Miami.

- MCALLISTER DE. 1968. The evolution of branchiostegals and associated opercular, gular and hyoid bones and the classification of teleostome fishes, living and fossil. *National Museum of Canada Bulletin*, 221: 1-239.
- MCDOWALL RM. 1979. The centrolophid genus *Tubbia* (Pisces: Stromateoidei). *Copeia*, 1979(4): 733-738.
- MCDOWALL RM. 1981. A sub-dorsal fin pore/canal system in the centrolophid fish *Schedophilus maculatus* (Pisces: Stromateoidei). *Copeia*, 1981(2): 492-494.
- MCDOWALL RM. 1982. The centrolophid fishes of New Zealand (Pisces: Stromateoidei). *Journal of the Royal Society of New Zealand*, 12(2): 103-142.
- MECKLENBURG CW. 2003. Family Icosteidae Jordan & Gilbert 1880 - Ragfishes. *California Academy of Sciences Annotated checklist of fishes*, 14: 1-4.
- MERRINER JV, FOSTER WA, SCHWARTZ FJ. 1970. The Barrelfish, *Hyperoglyphe perciformis* (Pisces: Stromateidae), in Pamlico Sound, NC, and Adjacent Atlantic Ocean. *Journal of the Elisha Mitchell Scientific Society*: 28-30.
- MIRANDE JM. 2009. Weighted parsimony phylogeny of the family Characidae (Teleostei: Characiformes). *Cladistics*, 25(6): 574-613.
- MIRANDE JM. 2017. Combined phylogeny of ray-finned fishes (Actinopterygii) and the use of morphological characters in large-scale analyses. *Cladistics*, 33(4): 333-350.
- MIYA M, FRIEDMAN M, SATOH TP, TAKESHIMA H, SADO T, IWASAKI W, YAMANOUE Y, NAKATANI M, MABUCHI K, INOUE JG, POULSEN J, FUKUNAGA T, SATO Y, NISHIDA M. 2013. Evolutionary origin of the Scombridae (tunas and mackerels): Members of a Paleogene adaptive radiation with 14 other pelagic fish families. *Plos ONE* 8(9): E73535.
- MØLLER PR, KNUDSEN SW, SCHWARZHANS W, NIELSEN JG. 2016. A new classification of viviparous brotulas (Bythitidae)—with family status for Dinematichthyidae—based on molecular, morphological and fossil data. *Molecular Phylogenetics and Evolution*, 100: 391-408.
- MØLLER PR, SCHWARZHANS W, NIELSEN JG. 2004. Review of the American Dinematichthyini (Teleostei, Bythitidae). Part I. *Dinematichthys*, *Gunterichthys*, *Typhliasina* and two new genera. *Aqua*, 8(4): 141-192.

- MOOI R, GILL A. 1995. Association of epaxial musculature with dorsal-fin pterygiophores in acanthomorph fishes, and its phylogenetic significance. *Bulletin of the Natural History Museum of London (Zoology)*, 61: 121-137.
- NAG AC. 1967. Functional morphology of the caudal region of certain clupeiform and perciform fishes with reference to the taxonomy. *Journal of Morphology*, 123(4): 529-558.
- NAKAMURA I, FUJII E. 1983. A new genus and species of Gempylidae (Pisces: Perciformes) from Tonga Ridge. *Publications of the Seto Marine Biological Laboratory*, 28: 173-191.
- NEAR TJ, DORNBURG A, EYTAN RI, KECK BP, SMITH WL, KUHN KL, MOORE JA, PRICE SA, BURBRINK FT, FRIEDMAN M, WAINWRIGHT PC. 2013. Phylogeny and tempo of diversification in the superradiation of spiny-rayed fishes. *Proceedings of the National Academy of Sciences*, 110(31): 12738-12743.
- NEAR TJ, EYTAN RI, DORNBURG A, KUHN KL, MOORE JA, DAVIS MP, WAINWRIGHT PC, FRIEDMAN M, SMITH WL. 2012. Resolution of ray-finned fish phylogeny and timing of diversification. *Proceedings of the National Academy of Sciences*, 109(34): 13698–13703.
- NELSON G. 1969. Gill arches and the phylogeny of fishes, with notes on the classification of vertebrates. *Bulletin of the American Museum of Natural History*, 141(4): 475-552.
- NELSON JS. 2006. *Fishes of the World*. 4. Ed. New York, John Wiley & Sons. 601p.
- NELSON JS, GRANDE TC, WILSON MV. 2016. *Fishes of the World*. 5. ed. Hoboken, N.J., John Wiley & Sons. 707p.
- NICHOLS PD, MOONEY BD, ELLIOTT NG. 2001. Unusually high levels of non-saponifiable lipids in the fishes escolar and rudderfish: identification by gas and thin-layer chromatography. *Journal of Chromatography*, A936(1-2): 183-191.
- NIELSEN JG, COHEN DM, MARKLE DF, ROBINS CR. 1999. An annotated and illustrated catalogue of pearlfishes, cusk-eels, brotulas and other ophidiiform fishes known to date. In: *Ophidiiform fishes of the world (Order Ophidiiformes)*. Rome, FAO. 178p. (FAO Fisheries Synopsis, 125 n.18, 178).
- NIXON K. 1999. The parsimony Ratchet, a new method for rapid parsimony analysis. *Cladistics*, 15: 407-414.
- NIXON K, CARPENTER JM. 2011. On Homology. *Cladistics*, 28: 160-169.
- NOEL AC, HU DL. 2018. The tongue as a gripper. *Journal of Experimental Biology*, 221: jeb176289.

- NURSALL JR. 1963. The caudal musculature of *Hoplopagrus guntheri* Gill (Perciformes: Lutjanidae). *Canadian Journal of Zoology*, 41(5): 865-880.
- OBIS (Ocean Biogeographic Information System). Available from <https://obis.org/taxon/234723>. Access in 11 Mar 2019.
- OHTSUKA S, KOIKE K, LINDSAY D, NISHIKAWA J, MIYAKE H, KAWAHARA M, MULYADI M, MUJIONO N, HIROMI J, KOMATSU H. 2009. Symbionts of marine medusae and ctenophores. *Plankton and Benthos Research*, 4(1): 1-13.
- OTERO O. 2004. Anatomy, systematics and phylogeny of both recent and fossil latid fishes (Teleostei, Perciformes, Latidae). *Zoological Journal of the Linnean Society*, 141(1): 81-133.
- PARENTI LR. 1993. Relationships of atherinomorph fishes (Teleostei). *Bulletin of Marine Science*, 52(1): 170-196.
- PARIN NV, PERMITIN YY. 1969. Materials on the pelagic fish fauna of the Antarctic. A new genus of stromateoid fishes—*Pseudoicichthys* (Pisces, Centrolophidae). *Voprosy Ikhtiologii*, 9(6): 981-987.
- PARIN NV, PIOTROVSKY AS. 2004. Stromateoid fishes (suborder Stromateoidei) of the Indian Ocean (species composition, distribution, biology, and fisheries). *Journal of Ichthyology*, 44(1): S33-SS62.
- PARMENTIER E, CASTILLO G, CHARDON M, VANDEWALLE P. 2000. Phylogenetic analysis of the pearlfish tribe Carapini (Pisces: Carapidae). *Acta Zoologica*, 81(4): 293-306.
- PARMENTIER E, DIOGO R. 2006. Evolutionary trends of swimbladder sound mechanisms in some teleost fishes. In: LADICH F, COLLIN SP, MOLLER P, KAPOOR BG. Eds. *Communication in fishes*. Enfield, NH, Science Publishers. v.1, p. 45–70.
- PARMENTIER E, VANDEWALLE P. 2003. Morphological adaptations of pearlfish (Carapidae) to their various habitats. In: VAL AL, KAPOOR BG. Eds. *Fish adaptations*. New Delhi, Oxford & IBH. p. 261–276.
- PATTERSON C, JOHNSON GD. 1995. The intermuscular bones and ligaments of teleostean fishes. *Smithsonian Contributions to Zoology*, 559: 1–85.
- PAUCĂ, M. 1929. Fossile Fische aus dem rumänischen Alttertiär. *Bulletin de la Section Scientifique de l'Académie Roumaine*, 12: 206-212.

- PAUCĂ, M. 1934. Die fossile Fauna und Flora aus dem Oligozän von Suslănesti-Muscel in Rumänien. Eine systematische und paläobiologische Studie. *Annales de l'institut Géologique Roumanie*, 16: 575–668.
- PÉREZ W, MICHEL V, JERB H, VAZQUEZ N. 2012. Anatomía de la Boca de la Jirafa (*Giraffa camelopardalis rothschildi*). *International Journal of Morphology*, 30(1): 322-329.
- PRIKRYL T, BANNIKOV AF, GRADIANU I, KANIA I, KRZEMINSKI W. 2014. Revision of the family Propercarinidae (Perciformes, Stromateoidei) with description of a new species from the Oligocene of the Carpathians. *Comptes Rendus Palevo*, 13(8): 691-700.
- PURCELL JE, ARAI MN. 2001. Interactions of pelagic cnidarians and ctenophores with fish: a review. *Hydrobiologia*, 451: 27-44.
- QUIGLEY DTG. 1986. A specimen of the barrel-fish *Hyperoglyphe perciforma* Mitchill 1818 (*Lirus perciformis* Regan 1902) from Achill Island, Co Mayo. *Irish Naturalists' Journal*, 22: 77-78.
- RAHIMULLAH M, OSMANIA FSZ. 1945. A comparative study of the morphology, histology and probable functions of the pyloric caeca in Indian fishes, together with a discussion on their homology. *Proceedings: Plant Sciences*, 21(1): 1-37.
- REGAN CT. 1902. A Revision of the fishes of the family Stromateidae. *The Annals and Magazine of Natural History, Ser. 7*, 10: 115-131.
- REGAN CT. 1910. The origin and evolution of the Teleostean fishes of the order Heterosomata. *Annals and Magazine of Natural History, Ser. 6*, (35): 484-496.
- REGAN CT. 1913. The classification of the Percoid fish. *Annals and Magazine of Natural History. Serie 8*, 12: 11–145.
- REMBISZEWSKI JM. 1981. *Pseudoicichthys australis* (Haedrich, 1966) and *Anotopterus pharao* Zugmayer, 1911, rare fishes from Antarctic waters. *Annales zoologici - Polska Akademia Nauk Instytut Zoologii*, 36(12): 241-245.
- RIASCOS JM, VERGARA M, FAJARDO J, VILLEGAS V, PACHECO AS. (2012). The role of hyperiid parasites as a trophic link between jellyfish and fishes. *Journal of Fish Biology*, 81(5): 1686-1695.
- ROBERTS CD. 1993. Comparative morphology of spined scales and their phylogenetic significance in the Teleostei. *Bulletin of Marine Science*, 52(1): 60-113.

- ROBERTS TR. 1986. Systematic Review of the Mastacembelidae or Spiny Eels of Burma Thailand, with Description of Two New Species of *Macrognathus*. *Japanese Journal of Ichthyology*, 33(2): 95-109.
- ROSEN DE. 1973. Interrelationships of higher euteleostean fishes. In: GREENWOOD PH, MILES RS, PATTERSON C. Eds. *Interrelationships of fishes*. New York, Academic Press. p. 397-513.
- ROSEN DE. 1985. An essay on euteleostean classification. *American Museum Novitates*, 2827: 1-57.
- ROSEN DE, GREENWOOD PH. 1976. A fourth neotropical species of synbranchid eel and the phylogeny and systematics of synbranchiform fishes. *Bulletin of the American Museum of Natural History*, 157(1): 1-69.
- ROSENBLATT RH, BELL MA. 1976. Osteology and relationships of the roosterfish, *Nematistius pectoralis* Gill. *Contributions in Science, Los Angeles County Museum of Natural History*, 279: 1-23.
- SAFRAN P, OMORI M. 1990. Some ecological observations on fishes associated with drifting seaweed off Tohoku coast, Japan. *Marine Biology*, 105(3): 395-402.
- SASAKY K. 1989. Phylogeny of the family Sciaenidae, with notes on its zoogeography (Teleostei, Perciformes). *Memoirs of the Faculty of Fisheries Hokkaido University*, 36(1-2): 1-137.
- SCHWARTZ FJ. 1963. The barrelfish from Chesapeake Bay and the Middle Atlantic bight, with comments on its zoogeography. *Chesapeake Science*, 4(3): 147-149.
- SLOWINSKI JB. 1993. "Unordered" versus "Ordered" characters. *Systematic Biology*, 42(2): 155-165.
- SMITH CL, BAILEY RM. 1961. Evolution of the dorsal-fin supports of percoid fishes. *Michigan Academy of Science, Arts, and Letters*, 46: 345-363.
- SMITH CL, BAILEY RM. 1962. The subocular shelf of fishes. *Journal of Morphology*, 110(1): 1-17.
- SMITH HW. 1930. The absorption and excretion of water and salts by marine teleosts. *American Journal of Physiology-Legacy Content* 93(2): 480-505.
- SMITH-VANIZ WF. 1984. Carangidae: relationships. In: MOSER HG, RICHARDS WJ, COHEN DM, FAHAY MP, KENDALL JR AW, RICHARDSON SL. Eds. *Ontogeny and systematics of fishes. Based on an International Symposium dedicated to the memory of Elbert Halvor Ahlstrom*. New York, American Society of Ichthyologists and Herpetologists. p. 522-530. (Special Publication Number 1).

- SPRINGER VG. 1983. *Tyson belos*, new genus and species of Western Pacific fish (Gobiidae, Xenisthminae): with discussions of gobioid osteology and classification. *Smithsonian Contributions to Zoology*, 390: 1-39.
- SPRINGER VG, JOHNSON GD. 2004. Study of the dorsal gill-arch musculature of Teleostome fishes, with special reference to the Actinopterygii. *Bulletin of the Biological Society of Washington*, 11: vi+1–260+pl. 001–205.
- SPRINGER VG, ORRELL TM. 2004. Phylogenetic analysis of 147 families of acanthomorph fishes, based primarily on dorsal gill-arch muscles and skeleton. *Bulletin of the Biological Society of Washington*, 11: 237-260.
- SPRINGER VG, SMITH-VANIZ WF. 2008. Supraneural and pterygiophore insertion patterns in carangid fishes, with description of a new Eocene carangid tribe, †Paratrachinotini, and a survey of anterior anal-fin pterygiophore insertion patterns in Acanthomorpha. *Bulletin of the Biological Society of Washington*, 16(1): 1-74.
- STEINDACHNER F. 1881. Ichthyologische Beiträge (XI). *Sitzungsberichte der Kaiserlichen Akademie der Wissenschaften. Mathematisch-Naturwissenschaftliche Classe V.* 83(1): 393-408.
- STEWART AL, LAST PR, STRUTHERS CD. 2015. Family Centrolophidae (235). In: ROBERTS CD, STEWART AL, STRUTHERS CD. Eds. *The Fishes of New Zealand. Systematics accounts*. Wellington, Te Papa Press. v. 4, p. 1648-1661.
- STIASSNY ML. 1986. The limits and relationships of the acanthomorph teleosts. *Journal of Zoology*, 1(2): 411-460.
- STIASSNY ML. 1990. Notes on the anatomy and relationships of the bedotiid fishes of Madagascar: with a taxonomic revision of the genus *Rheocles* (Atherinomorpha, Bedotiidae). *American Museum Novitates*, 2979: 1-33.
- STIASSNY ML. 1993. What are grey mullets? *Bulletin of Marine Science*, 52(1): 197-219.
- STIASSNY ML. 1996. Basal ctenosquamate relationships and the interrelationships of the myctophiform (scopelomorph) fishes. In: STIASSNY MLJ, PARENTI LR, JOHNSON GD. Eds. *Interrelationships of Fishes*. San Diego, CA, Academic Press. p.405–426.
- STIASSNY ML, MOORE JA. 1992. A review of the pelvic girdle of acanthomorph fishes, with comments on hypotheses of acanthomorph intrarelationshps. *Zoological Journal of the Linnean Society*, 104(3), 209-242.

- TAN HH. 2008. Apparent mimicry of jellyfish by juvenile pomfret, *Pampus chinensis* (Teleostei: Stromateidae). *Nature in Singapore*, 1: 139-142.
- TAYLOR WR, VAN DYKE GC. 1985. Revised procedures for staining and clearing small fishes and other vertebrates for bone and cartilage study. *Cybiurn*, 9 (2): 107-119.
- THIEBOT JB, ARNOULD JP, GÓMEZ-LAICH A, ITO K, KATO A, MATTERN T, MITAMURA H, NODA T, POUPART T, QUINTANA F, RACLOT T, ROPERT-COUDERT Y, SALA JE, SEDDON PJ, SUTTON GJ, YODA K, TAKAHASHI A. 2017. Jellyfish and other gelata as food for four penguin species—insights from predator-borne videos. *Frontiers in Ecology and the Environment*, 15(8): 437-441.
- THOMAS S, ROHIT P. 2007. New record of the stromateoid fish *Psenopsis intermedia* (Piontrovskiy, 1987) from Indian waters. *Indian Journal of Fisheries*, 54(1): 127-130.
- TOLLEY SG. 1987. Association of young *Chloroscombrus chrysurus* (Pisces: Carangidae) with the jellyfish *Aurelia aurita*. *Copeia*, 1987(1): 216-219.
- TRAVERS RA. 1981. The interarcual cartilage; a review of its development, distribution and value as an indicator of phyletic relationships in euteleostean fishes. *Journal of Natural History*, 15(5): 853-871.
- TYLER JC, JOHNSON GD, NAKAMURA I, COLLETTE BB. 1989. Morphology of *Luvarus imperialis* (Luvaridae) with a phylogenetic analysis of the Acanthuroidei (Pisces). *Smithsonian Contributions to Zoology*, 485: 1-78.
- TYLER JC. 1970. A redescription of the inquiline carapid fish *Onuxodon parvibrachium*, with a discussion of the skull structure and the host. *Bulletin of Marine Science*, 20(1): 148-164.
- UENO T. 1954. First record of a strange bathypelagic species, referable to the genus *Centrolophus* (Centrolophidae, Stromateiformes) from Japanese water, with remarks on the specific differentiation. *Bulletin of the Faculty of Fisheries, Hokkaido University*, 5(3): 240-247.
- VAN DER LAAN R, FRICKE R. 2019. *Eschmeyer's Catalog of fishes. Family-group names*. Retrieved from <http://Research.Calacademy.Org/Research/Ichthyology/Catalog/Speciesbyfamily.Asp>. Access in 01 Nov 2018.
- VOGT RC, SEVER DM, MOREIRA G. 1998. Esophageal papillae in pelomedusid turtles. *Journal of Herpetology*, 32(2): 279-282.
- WALTERS V. 1963. The trachipterid integument and an hypothesis on its hydrodynamic function. *Copeia*, 1963: 260-270.

WEBB JF. 1989. Gross morphology and evolution of the mechanosensory lateral line system in teleost fishes. *Brain Behavior and Evolution*, 33: 34–53.

WEITZMAN SH. 1962. The osteology of *Brycon meeki*, a generalized characid fish, with an osteological definition of the family. *Stanford Ichthyological Bulletin*, 8: 1-77.

WELLS RJ, ROOKER JR. 2004. Spatial and temporal patterns of habitat use by fishes associated with Sargassum mats in the northwestern Gulf of Mexico. *Bulletin of Marine Science*, 74(1): 81-99.

WHITLOCK JA. 2010. Phylogenetic relationships of the Eocene percomorph fishes †*Priscacara* and †*Mioplosus*. *Journal of Vertebrate Paleontology*, 30(4): 1037-1048.

WILEY EO, JOHNSON GD. 2010. A Teleost classification based on monophyletic groups. In: NELSON JS, SCHULTZE H-P, WILSON MVH. Eds. *Origin and phylogenetic interrelationships of teleosts*. München, Verlag Dr. Friedrich Pfeil. p. 123–182.

WILLIAMS A, HAMER P, HADDON M, ROBERTSON S, ALTHAUS F, GREEN M, KOOL J. 2017. *Determining Blue-eye Trevalla stock structure and improving methods for stock assessment*. Hobart, Tasmania, Fisheries Research and Development Corporation Report. 124p.

WINTERBOTTOM R. 1974. A descriptive synonymy of the striated muscles of the Teleostei. *Proceedings of the Academy of Natural Sciences of Philadelphia*, 125: 225–317.

YAGISHITA N, MIYA M, YAMANOUE Y, SHIRAI SM, NAKAYAMA K, SUZUKI N, SATOH TP, MABUCHI K, NISHIDA M, NAKABO T. 2009. Mitogenomic evaluation of the unique facial nerve pattern as a phylogenetic marker within the perciform fishes (Teleostei: Percomorpha). *Molecular Phylogenetics and Evolution*, 53: 258–266.

## **TABLES**

**TABLE 1.** Specimen counts (left column) and normalized values (right column) used for Characters #0-15. Inapplicable characters are indicated by *in.* and data deficiency by a question mark.

Character	#0	#0	#1	#1	#2	#2	#3	#3	#4	#4	#5	#5	#6	#6	#7	#7	#8	#8	#9	#9	#10	#10	#11	#11	#12	#12	#13	#13	#14	#14	#15	#15
Specimen	RY01	NOR	RY02	NOR	RY03	NOR	RY04	NOR	RY05	NOR	RY06	NOR	RY07	NOR	RY08	NOR	RY09	NOR	RY10	NOR	RY11	NOR	SN01	NOR	VE01	NOR	PR01	NOR	PR02	NOR	BR01	NOR
<i>Beryx splendens</i>	17	0,04	4	0,17	13	0,05	16	0,38	2	0,50	14	0,38	11	1,00	26	0,12	4	0,25	22	0,11	17	0,89	3	0,25	24	0,01	4	0,21	4	0,21	8	0,00
<i>Holocentrus adscensionis</i>	27	0,12	11	0,56	16	0,07	16	0,38	2	0,50	14	0,38	8	0,70	15	0,05	4	0,25	11	0,04	17	0,89	2	0,13	27	0,03	6	0,36	5	0,29	8	0,00
<i>Dinematchthys iluocetooides</i>	73	0,50	<i>in.</i>	-	73	0,53	22	0,75	1	0,00	21	0,81	1	0,00	57	0,34	<i>in.</i>	-	57	0,35	14	0,56	<i>in.</i>	-	43	0,14	1	0,00	1	0,00	7	0,25
<i>Raneya brasiliensis</i>	117	0,86	<i>in.</i>	-	117	0,89	20	0,63	1	0,00	20	0,75	1	0,00	95	0,60	<i>in.</i>	-	95	0,61	9	0,00	<i>in.</i>	-	64	0,28	<i>in.</i>	-	<i>in.</i>	-	7	0,25
<i>Apogon maculatus</i>	16	0,03	7	0,33	9	0,02	12	0,13	2	0,50	10	0,13	6	0,50	10	0,01	2	0,08	8	0,02	15	0,67	2	0,13	24	0,01	10	0,64	8	0,50	7	0,25
<i>Aulostomus maculatus</i>	39	0,22	13	0,67	26	0,15	16	0,38	<i>in.</i>	-	<i>in.</i>	-	6	0,50	28	0,14	2	0,08	26	0,14	9	0,00	?	-	58	0,24	4	0,21	4	0,21	4	1,00
<i>Icosteus aenigmaticus</i>	54	0,34	<i>in.</i>	-	54	0,38	19	0,56	1	0,00	18	0,63	5	0,40	37	0,20	<i>in.</i>	-	37	0,22	18	1,00	<i>in.</i>	-	67	0,30	7	0,43	5	0,29	6	0,50
<i>Brama caribbea</i>	36	0,20	5	0,22	31	0,19	18	0,50	2	0,50	16	0,50	6	0,50	28	0,14	2	0,08	26	0,14	14	0,56	3	0,25	38	0,10	7	0,43	6	0,36	7	0,25
<i>Caristius macropus</i>	36	0,20	1	0,00	35	0,23	18	0,50	2	0,50	16	0,50	6	0,50	22	0,10	1	0,00	21	0,11	15	0,67	<i>in.</i>	-	38	0,10	7	0,43	9	0,57	7	0,25
<i>Pseudoscopus altipinnis</i>	30	0,15	10	0,50	20	0,10	13	0,19	2	0,50	11	0,19	6	0,50	16	0,06	3	0,17	13	0,05	15	0,67	<i>in.</i>	-	37	0,10	10	0,64	10	0,64	7	0,25
<i>Pomatomus saltatrix</i>	29	0,14	8	0,39	21	0,11	18	0,50	2	0,50	16	0,50	6	0,50	30	0,15	2	0,08	28	0,16	15	0,67	3	0,25	26	0,02	9	0,57	9	0,57	7	0,25
<i>Arripis georgianus</i>	22	0,08	9	0,44	13	0,05	15	0,31	2	0,50	13	0,31	6	0,50	12	0,03	3	0,17	9	0,03	15	0,67	3	0,25	25	0,01	8	0,50	8	0,50	7	0,25
<i>Scombrorlabrax heterolepis</i>	29	0,14	13	0,67	16	0,07	16	0,38	2	0,50	14	0,38	6	0,50	20	0,08	2	0,08	18	0,09	15	0,67	<i>in.</i>	-	30	0,05	10	0,64	10	0,64	7	0,25
<i>Sphyræna tome</i>	15	0,02	6	0,28	9	0,02	13	0,19	2	0,50	11	0,19	6	0,50	11	0,02	1	0,00	10	0,03	15	0,67	<i>in.</i>	-	25	0,01	9	0,57	9	0,57	7	0,25
<i>Thyrsopterus lepidopoides</i>	37	0,20	18	0,94	19	0,10	15	0,31	2	0,50	13	0,31	6	0,50	21	0,09	3	0,17	18	0,09	15	0,67	1	0,00	33	0,07	8	0,50	8	0,50	7	0,25
<i>Auxis thazard</i>	18	0,05	9	0,44	9	0,02	23	0,81	2	0,50	21	0,81	6	0,50	13	0,03	<i>in.</i>	-	13	0,05	15	0,67	<i>in.</i>	-	39	0,11	13	0,86	15	1,00	7	0,25
<i>Scomber sp.</i>	26	0,11	9	0,44	17	0,08	22	0,75	2	0,50	20	0,75	6	0,50	18	0,07	2	0,08	16	0,07	15	0,67	<i>in.</i>	-	31	0,06	11	0,71	10	0,64	7	0,25
<i>Trichiurus lepturus</i>	134	1,00	3	0,11	131	1,00	10	0,00	<i>in.</i>	-	<i>in.</i>	-	<i>in.</i>	-	153	1,00	<i>in.</i>	-	153	1,00	<i>in.</i>	-	<i>in.</i>	-	168	1,00	<i>in.</i>	-	<i>in.</i>	-	7	0,25
<i>Amarsipus carlsbergi</i>	34	0,18	11	0,56	23	0,13	18	0,50	2	0,50	16	0,50	6	0,50	27	0,13	3	0,17	24	0,13	15	0,67	3	0,25	47	0,17	13	0,86	13	0,86	6	0,50
<i>Ariomma indicum</i>	24	0,10	10	0,50	20	0,10	13	0,19	2	0,50	11	0,19	6	0,50	18	0,06	3	0,17	13	0,07	15	0,67	<i>in.</i>	-	31	0,06	9	0,57	8	0,50	6	0,50
<i>Ariomma bondi</i>	27	0,12	13	0,67	14	0,06	22	0,75	2	0,50	20	0,75	6	0,50	22	0,10	3	0,17	19	0,09	15	0,67	2	0,13	31	0,06	10	0,64	9	0,57	6	0,50
<i>Psenopsis anomala</i>	34	0,18	6	0,28	28	0,17	20	0,63	2	0,50	18	0,63	6	0,50	30	0,15	3	0,17	27	0,15	15	0,67	3	0,25	25	0,01	9	0,57	8	0,50	7	0,25
<i>Psenopsis cyanea</i>	30	0,15	7	0,33	23	0,13	20	0,63	2	0,50	18	0,63	6	0,50	27	0,13	3	0,17	24	0,13	15	0,67	3	0,25	25	0,01	10	0,64	9	0,57	7	0,25
<i>Centrolophus niger</i>	44	0,26	5	0,22	39	0,26	21	0,69	2	0,50	19	0,69	6	0,50	27	0,13	3	0,17	24	0,13	15	0,67	3	0,25	25	0,01	13	0,86	12	0,79	7	0,25
<i>Schedophilus sp.</i>	46	0,28	7	0,33	39	0,26	19	0,56	2	0,50	17	0,56	6	0,50	33	0,17	3	0,17	30	0,17	15	0,67	3	0,25	33	0,07	9	0,57	9	0,57	6	0,50
<i>Seriola lalandi</i>	44	0,26	8	0,39	36	0,23	19	0,56	2	0,50	17	0,56	6	0,50	24	0,11	3	0,17	21	0,11	15	0,67	3	0,25	25	0,01	11	0,71	9	0,57	7	0,25
<i>Tubbia tasmanica</i>	48	0,30	5	0,22	43	0,29	21	0,69	2	0,50	19	0,69	6	0,50	34	0,18	3	0,17	31	0,18	15	0,67	3	0,25	42	0,13	12	0,79	11	0,71	7	0,25
<i>Ichthyos lockingtoni</i>	40	0,23	5	0,22	35	0,23	20	0,63	2	0,50	18	0,63	6	0,50	32	0,17	3	0,17	29	0,16	15	0,67	9	1,00	60	0,26	15	1,00	15	1,00	7	0,25
<i>Hyperglypheus perciformis</i>	29	0,14	8	0,39	21	0,11	23	0,81	2	0,50	21	0,81	6	0,50	20	0,08	3	0,17	17	0,08	15	0,67	3	0,25	25	0,01	10	0,64	10	0,64	7	0,25
<i>Psenes cyanophrys</i>	34	0,18	11	0,56	23	0,13	18	0,50	2	0,50	16	0,50	6	0,50	32	0,17	3	0,17	29	0,16	14	0,56	3	0,25	31	0,06	7	0,43	7	0,43	6	0,50
<i>Psenes sio</i>	35	0,19	12	0,61	23	0,13	18	0,50	2	0,50	16	0,50	6	0,50	25	0,12	2	0,08	23	0,12	14	0,56	3	0,25	36	0,09	9	0,57	8	0,50	6	0,50
<i>Cubiceps baxteri</i> (=Ariomma melanum)	27	0,12	12	0,61	15	0,06	22	0,75	2	0,50	20	0,75	6	0,50	17	0,06	3	0,17	14	0,06	15	0,67	3	0,25	31	0,06	9	0,57	8	0,50	6	0,50
<i>Cubiceps whiteleggi</i>	30	0,15	13	0,67	17	0,08	20	0,63	2	0,50	18	0,63	6	0,50	20	0,08	3	0,17	17	0,08	15	0,67	3	0,25	31	0,06	9	0,57	9	0,57	6	0,50
<i>Cubiceps pauciradiatus</i>	25	0,11	10	0,50	15	0,06	18	0,50	2	0,50	16	0,50	6	0,50	17	0,06	2	0,08	15	0,07	15	0,67	3	0,25	31	0,06	8	0,50	7	0,43	6	0,50
<i>Nomeus granovii</i>	37	0,20	11	0,56	26	0,15	22	0,75	2	0,50	20	0,75	6	0,50	29	0,14	3	0,17	26	0,14	15	0,67	3	0,25	40	0,12	10	0,64	9	0,57	6	0,50
<i>Pepilurus triacanthus</i>	47	0,29	4	0,17	43	0,29	18	0,50	2	0,50	16	0,50	<i>in.</i>	-	43	0,24	3	0,17	40	0,24	15	0,67	3	0,25	32	0,06	7	0,43	7	0,43	6	0,50
<i>Pepilurus paru</i>	48	0,30	7	0,33	41	0,27	18	0,50	2	0,50	16	0,50	<i>in.</i>	-	43	0,24	4	0,25	39	0,23	15	0,67	3	0,25	29	0,04	6	0,36	5	0,29	6	0,50
<i>Pampus cinereus</i>	49	0,30	9	0,44	40	0,27	26	1,00	2	0,50	24	1,00	<i>in.</i>	-	40	0,22	6	0,42	34	0,20	15	0,67	3	0,25	36	0,09	6	0,36	5	0,29	6	0,50
<i>Stromateus brasiliensis</i>	45	0,27	11	0,56	34	0,22	21	0,69	2	0,50	19	0,69	<i>in.</i>	-	44	0,25	3	0,17	41	0,24												

**TABLE 2.** Specimen standard length in millimeters (first column), and proportional specimen measurement and normalized values used for Characters #16-21. Proportions are relative to the specimen's standard length, offered in the first data column (mm SL). Question mark (?) indicates data deficiency.

Character	#16	#16	#16	#17	#17	#17	#18	#18	#18	#19	#19	#19	#20	#20	#20	#21	#21	#21	
Specimen	mm SL	PP01	PP01 rel	PP01 nor	PP02	PP02 rel	PP02 nor	PP03	PP04rel	PP03 nor	PP04	PP04 rel	PP04 nor	PP05	PP05 rel	PP05 nor	PP06	PP06 rel	PP06 nor
<i>Beryx splendens</i>	100,90	48,59	48,16	0,75	19,14	18,97	0,00	31,25	30,97	0,73	43,34	42,95	0,66	63,24	62,68	0,64	38,33	37,99	0,50
<i>Holocentrus adscensionis</i>	88,57	33,12	37,39	0,55	50,88	57,45	0,55	20,00	22,58	0,49	32,99	37,25	0,55	64,10	72,37	0,85	12,98	14,66	0,12
<i>Dinematichthys iluocoteoides</i>	88,22	28,41	32,20	0,45	60,87	69,00	0,72	11,64	13,19	0,23	20,15	22,84	0,28	43,64	49,47	0,36	48,28	54,73	0,76
<i>Raneya brasiliensis</i>	165,55	42,74	25,82	0,33	126,75	76,56	0,82	14,23	8,60	0,11	13,86	8,37	0,00	65,80	39,75	0,15	97,98	59,18	0,83
<i>Apogon maculatus</i>	67,31	28,88	42,91	0,65	20,91	31,07	0,17	15,83	23,52	0,52	24,93	37,04	0,55	40,84	60,67	0,60	7,60	11,29	0,07
<i>Aulostomus maculatus</i>	292,53	148,86	50,89	0,80	117,06	40,02	0,30	13,82	4,72	0,00	177,24	60,59	1,00	232,53	79,49	1,00	34,55	11,81	0,08
<i>Icosteus aenigmaticus</i>	220,85	55,41	25,09	0,32	151,20	68,46	0,71	35,88	16,25	0,32	65,31	29,57	0,41	101,86	46,12	0,29	84,99	38,48	0,50
<i>Brama caribbea</i>	98,06	42,45	43,29	0,66	55,40	56,50	0,54	32,08	32,71	0,78	43,06	43,91	0,68	56,59	57,71	0,53	45,66	46,56	0,63
<i>Caristius macropus</i>	179,44	36,94	20,59	0,24	140,22	78,14	0,85	41,08	22,89	0,50	58,76	32,75	0,47	90,31	50,33	0,38	73,84	41,15	0,55
<i>Pseudoscopelus altipinnis</i>	66,09	22,51	34,06	0,49	37,09	56,12	0,53	12,33	18,66	0,39	22,17	33,55	0,48	35,75	54,09	0,46	24,74	37,43	0,49
<i>Pomatomus saltatrix</i>	114,65	45,81	39,96	0,60	56,88	49,61	0,44	19,97	17,42	0,35	41,40	36,11	0,53	70,11	61,15	0,61	31,86	27,79	0,33
<i>Arripis georgianus</i>	172,78	62,69	36,28	0,53	85,07	49,24	0,43	30,99	17,94	0,37	64,25	37,19	0,55	126,07	72,97	0,86	23,71	13,72	0,11
<i>Scombrobrax heterolepis</i>	135,13	49,70	36,78	0,54	69,21	51,22	0,46	39,33	29,11	0,68	56,19	41,58	0,64	98,47	72,87	0,86	27,36	20,25	0,21
<i>Sphyræna tome</i>	235,00	105,60	44,94	0,69	74,48	31,69	0,18	24,36	10,37	0,16	104,09	44,29	0,69	164,64	70,06	0,80	16,10	6,85	0,00
<i>Thyrstitops lepidopoides</i>	154,78	44,99	29,07	0,39	98,86	63,87	0,64	21,84	14,11	0,26	56,01	36,19	0,53	110,27	71,24	0,82	35,13	22,70	0,25
<i>Auxis thazard</i>	210,00	69,73	33,20	0,47	137,52	65,49	0,66	28,60	13,62	0,25	64,64	30,78	0,43	151,53	72,16	0,84	56,80	27,05	0,32
<i>Scomber sp.</i>	100,61	38,01	37,78	0,56	58,04	57,69	0,55	13,08	13,00	0,23	35,23	35,02	0,51	66,91	66,50	0,72	26,96	26,80	0,32
<i>Trichiurus lepturus</i>	405,50	46,08	11,36	0,07	333,37	82,21	0,90	19,54	4,82	0,00	?	?	?	154,20	38,03	0,11	137,36	58,10	0,82
<i>Amarsipus carlsbergi</i>	50,40	16,14	32,02	0,45	24,03	47,68	0,41	10,50	20,83	0,45	11,00	21,83	0,26	23,13	45,89	0,28	16,21	32,16	0,40
<i>Ariomma indicum</i>	129,92	47,85	36,83	0,54	79,07	60,86	0,60	40,95	31,52	0,74	52,45	40,37	0,61	77,34	59,53	0,57	52,31	40,26	0,53
<i>Ariomma boni</i>	125,30	43,51	34,72	0,50	76,04	60,69	0,60	32,60	26,02	0,59	46,85	37,39	0,56	80,05	63,89	0,67	38,42	30,66	0,38
<i>Psenopsis anomala</i>	74,17	29,03	39,14	0,58	39,89	53,78	0,50	20,76	27,99	0,64	30,52	41,15	0,63	40,21	54,21	0,46	32,46	43,76	0,59
<i>Psenopsis cyanea</i>	138,61	49,59	35,78	0,52	78,91	56,93	0,54	31,62	22,81	0,50	44,71	32,26	0,46	75,79	54,68	0,47	48,35	34,88	0,45
<i>Centrolophus niger</i>	245,10	78,75	32,13	0,45	147,43	60,15	0,59	??	8,56	0,11	67,56	27,56	0,37	132,05	53,88	0,45	68,02	27,75	0,33
<i>Schedophilus sp.</i>	89,29	27,07	30,32	0,42	54,16	60,66	0,60	21,18	23,72	0,53	37,13	41,58	0,64	49,61	55,56	0,49	33,60	37,63	0,49
<i>Seriolaella porosa</i>	198,84	67,88	34,14	0,49	116,26	58,47	0,56	46,96	23,62	0,52	67,72	34,06	0,49	119,75	60,22	0,59	54,90	27,61	0,33
<i>Tubbia tasmanica</i>	325,20	119,15	36,64	0,54	184,10	56,61	0,54	38,59	11,87	0,20	89,74	27,60	0,37	153,60	47,23	0,31	137,36	42,24	0,56
<i>Ichthyos lockingtoni</i>	102,35	43,03	42,04	0,64	55,11	53,84	0,50	13,93	13,61	0,25	27,89	27,25	0,36	54,87	53,61	0,45	35,05	32,29	0,41
<i>Hyperaglyphe perciformis</i>	150,37	58,25	38,74	0,58	82,91	55,14	0,52	36,53	24,29	0,54	55,43	36,86	0,55	95,93	63,80	0,66	37,34	24,83	0,29
<i>Psenes cyanophrys</i>	152,58	53,39	34,99	0,51	99,15	64,98	0,66	51,67	33,86	0,81	60,54	39,68	0,60	77,13	50,55	0,38	71,58	46,91	0,64
<i>Psenes sio</i>	184,29	63,82	34,63	0,50	112,37	60,97	0,60	33,17	18,00	0,37	59,37	32,22	0,46	94,10	51,06	0,39	72,84	39,52	0,52
<i>Cubiceps baxteri (=Ariomma melanum)</i>	134,89	48,95	36,29	0,53	80,10	59,38	0,58	30,90	22,91	0,50	50,41	37,37	0,56	85,08	63,07	0,65	42,69	31,65	0,40
<i>Cubiceps whiteleggii</i>	107,55	40,71	37,85	0,56	61,70	57,37	0,55	31,92	29,68	0,69	45,02	41,86	0,64	61,22	56,92	0,52	34,05	31,66	0,40
<i>Cubiceps pauciradiatus</i>	88,63	31,63	35,69	0,52	45,00	50,77	0,45	28,05	31,65	0,75	39,57	39,57	0,60	55,59	62,72	0,64	19,19	21,65	0,24
<i>Nomeus gronovii</i>	81,32	27,42	33,72	0,48	43,47	53,46	0,49	23,92	29,41	0,68	29,19	35,90	0,53	47,41	58,30	0,55	25,46	31,31	0,39
<i>Peprius triacanthus</i>	128,93	45,97	35,66	0,52	81,62	63,31	0,63	44,34	34,39	0,82	?	?	?	57,93	44,93	0,26	74,24	57,58	0,81
<i>Peprius paru</i>	80,68	36,53	45,28	0,70	55,74	69,09	0,72	32,92	40,80	1,00	?	?	?	39,37	48,80	0,34	50,30	67,30	0,96
<i>Pampus cinereus</i>	72,40	30,42	42,02	0,64	44,98	62,13	0,62	27,68	38,23	0,93	?	?	?	40,65	56,15	0,50	43,95	60,70	0,86
<i>Stromateus brasiliensis</i>	136,10	47,51	34,91	0,50	86,49	63,55	0,64	33,91	24,92	0,56	?	?	?	61,17	44,94	0,26	71,08	52,23	0,72
<i>Tetragonurus cuvieri</i>	94,73	39,09	41,26	0,62	33,00	34,84	0,23	12,86	13,58	0,25	29,10	30,72	0,43	57,96	61,18	0,61	10,13	10,69	0,06
<i>Orthopristis ruber</i>	104,33	42,48	40,72	0,61	58,54	56,11	0,53	29,03	27,83	0,64	40,59	38,91	0,58	70,82	67,88	0,75	18,53	17,76	0,17
<i>Kuhlia marginata</i>	105,23	41,52	39,46	0,59	48,19	45,79	0,38	21,12	20,07	0,43	41,23	39,18	0,59	63,26	60,12	0,59	29,10	27,65	0,33
<i>Girella simplicidens</i>	88,00	34,66	39,39	0,59	51,28	58,27	0,56	22,60	25,68	0,58	32,81	37,28	0,55	57,09	64,88	0,69	18,18	20,66	0,22
<i>Kyphosus sectatrix</i>	74,99	35,90	47,87	0,75	33,77	45,03	0,37	14,54	19,39	0,41	29,82	39,77	0,60	46,32	61,77	0,62	17,54	23,39	0,26
<i>Microcanthus strigatus</i>	86,20	41,14	47,73	0,74	54,04	62,69	0,62	23,60	27,38	0,63	38,53	44,70	0,70	61,30	71,11	0,82	23,84	27,66	0,33
<i>Scorpius chilensis</i>	114,19	44,98	39,39	0,59	62,88	55,07	0,52	26,47	23,18	0,51	45,71	40,03	0,61	65,99	57,79	0,54	46,23	40,49	0,54
<i>Lutjanus analis</i>	102,98	46,33	44,99	0,69	51,08	49,60	0,44	27,92	27,11	0,62	42,47	41,24	0,63	69,22	67,22	0,74	17,12	16,62	0,16
<i>Cynoscion striatus</i>	123,11	43,10	35,01	0,51	60,34	49,01	0,43	25,34	20,58	0,44	46,47	37,75	0,56	91,95	74,69	0,90	9,75	7,92	0,02
<i>Amniataba caudavittata</i>	80,44	35,03	43,55	0,66	43,82	54,48	0,51	15,80	19,64	0,41	33,23	41,31	0,63	56,70	70,49	0,81	14,41	17,91	0,18
<i>Diplectrum radiale</i>	120,11	42,71	35,56	0,52	63,20	52,62	0,48	28,23	23,50	0,52	38,14	31,75	0,45	72,53	60,39	0,59	19,84	16,52	0,15
<i>Atherinella brasiliensis</i>	105,23	64,75	61,53	1,00	22,77	21,64	0,04	23,91	22,72	0,50	44,48	42,27	0,65	63,37	60,22	0,59	23,38	22,22	0,24
<i>Mugil curema</i>	87,14	46,58	53,45	0,85	30,44	34,93	0,23	19,09	21,91	0,48	38,58	44,27	0,69	63,84	73,26	0,87	10,73	12,31	0,09
<i>Monocirrhus polyacanthus</i>	54,57	27,34	50,10	0,79	31,20	57,17	0,55	6,14	11,25	0,18	23,70	43,43	0,67	32,27	59,14	0,57	24,47	44,84	0,61
<i>Trachinotus carolinus</i>	89,73	35,03	39,04	0,58	53,92	60,09	0,59	19,66	21,91	0,48	33,23	37,03	0,55	49,63	55,31	0,48	34,91	38,91	0,51
<i>Coryphaena hippurus</i>	358,02	55,36	15,46	0,14	285,03	79,61	0,87	54,70	15,28	0,29	98,11	27,40	0,36	197,57	55,18	0,48	135,60	37,87	0,49
<i>Rachycentron canadum</i>	149,65	42,07	28,11	0,38	87,07	58,18	0,56	33,02	22,06	0,48	44,24	29,56	0,41	81,24	54,29	0,46	51,59	34,47	0,44
<i>Nematistius pectoralis</i>	46,33	14,72	31,77	0,45	29,21	63,05	0,63	7,24	15,63	0,30	16,99	36,67	0,54	31,42	67,82	0,75	9,87	21,30	0,23
<i>Morone mississippiensis</i>	121,88	52,35	42,95	0,65	50,70	41,60	0,32	27,56	22,61	0,50	45,97	37,72	0,56	86,17	70,70	0,81	15,06	12,36	0,09
<i>Lateolabrax japonicus</i>	149,49	56,18	37,58	0,55	70,74	47,32	0,												

**TABLE 3.** *Fit* values for characters under 23 different values of K (K = 1-22, and K → ∞) and exhibiting 0 to 25 homoplasies. Column indicated by K → ∞ simulates *fit* values under equal weight methods.

Homoplasies/ K	1	2	3	4	5	6	7	8	9	10	11	12	13	14	15	16	17	18	19	20	21	22	∞
0	1	1	1	1	1	1	1	1	1	1	1	1	1	1	1	1	1	1	1	1	1	1	1
1	0,500	0,667	0,750	0,800	0,833	0,857	0,875	0,889	0,900	0,909	0,917	0,923	0,929	0,933	0,938	0,941	0,944	0,947	0,950	0,952	0,955	0,957	1
2	0,333	0,500	0,600	0,667	0,714	0,750	0,778	0,800	0,818	0,833	0,846	0,857	0,867	0,875	0,882	0,889	0,895	0,900	0,905	0,909	0,913	0,917	1
3	0,250	0,400	0,500	0,571	0,625	0,667	0,700	0,727	0,750	0,769	0,786	0,800	0,813	0,824	0,833	0,842	0,850	0,857	0,864	0,870	0,875	0,880	1
4	0,200	0,333	0,429	0,500	0,556	0,600	0,636	0,667	0,692	0,714	0,733	0,750	0,765	0,778	0,789	0,800	0,810	0,818	0,826	0,833	0,840	0,846	1
5	0,167	0,286	0,375	0,444	0,500	0,545	0,583	0,615	0,643	0,667	0,688	0,706	0,722	0,737	0,750	0,762	0,773	0,783	0,792	0,800	0,808	0,815	1
6	0,143	0,250	0,333	0,400	0,455	0,500	0,538	0,571	0,600	0,625	0,647	0,667	0,684	0,700	0,714	0,727	0,739	0,750	0,760	0,769	0,778	0,786	1
7	0,125	0,222	0,300	0,364	0,417	0,462	0,500	0,533	0,563	0,588	0,611	0,632	0,650	0,667	0,682	0,696	0,708	0,720	0,731	0,741	0,750	0,759	1
8	0,111	0,200	0,273	0,333	0,385	0,429	0,467	0,500	0,529	0,556	0,579	0,600	0,619	0,636	0,652	0,667	0,680	0,692	0,704	0,714	0,724	0,733	1
9	0,100	0,182	0,250	0,308	0,357	0,400	0,438	0,471	0,500	0,526	0,550	0,571	0,591	0,609	0,625	0,640	0,654	0,667	0,679	0,690	0,700	0,710	1
10	0,091	0,167	0,231	0,286	0,333	0,375	0,412	0,444	0,474	0,500	0,524	0,545	0,565	0,583	0,600	0,615	0,630	0,643	0,655	0,667	0,677	0,688	1
11	0,083	0,154	0,214	0,267	0,313	0,353	0,389	0,421	0,450	0,476	0,500	0,522	0,542	0,560	0,577	0,593	0,607	0,621	0,633	0,645	0,656	0,667	1
12	0,077	0,143	0,200	0,250	0,294	0,333	0,368	0,400	0,429	0,455	0,478	0,500	0,520	0,538	0,556	0,571	0,586	0,600	0,613	0,625	0,636	0,647	1
13	0,071	0,133	0,188	0,235	0,278	0,316	0,350	0,381	0,409	0,435	0,458	0,480	0,500	0,519	0,536	0,552	0,567	0,581	0,594	0,606	0,618	0,629	1
14	0,067	0,125	0,176	0,222	0,263	0,300	0,333	0,364	0,391	0,417	0,440	0,462	0,481	0,500	0,517	0,533	0,548	0,563	0,576	0,588	0,600	0,611	1
15	0,063	0,118	0,167	0,211	0,250	0,286	0,318	0,348	0,375	0,400	0,423	0,444	0,464	0,483	0,500	0,516	0,531	0,545	0,559	0,571	0,583	0,595	1
16	0,059	0,111	0,158	0,200	0,238	0,273	0,304	0,333	0,360	0,385	0,407	0,429	0,448	0,467	0,484	0,500	0,515	0,529	0,543	0,556	0,568	0,579	1
17	0,056	0,105	0,150	0,190	0,227	0,261	0,292	0,320	0,346	0,370	0,393	0,414	0,433	0,452	0,469	0,485	0,500	0,514	0,528	0,541	0,553	0,564	1
18	0,053	0,100	0,143	0,182	0,217	0,250	0,280	0,308	0,333	0,357	0,379	0,400	0,419	0,438	0,455	0,471	0,486	0,500	0,514	0,526	0,538	0,550	1
19	0,050	0,095	0,136	0,174	0,208	0,240	0,269	0,296	0,321	0,345	0,367	0,387	0,406	0,424	0,441	0,457	0,472	0,486	0,500	0,513	0,525	0,537	1
20	0,048	0,091	0,130	0,167	0,200	0,231	0,259	0,286	0,310	0,333	0,355	0,375	0,394	0,412	0,429	0,444	0,459	0,474	0,487	0,500	0,512	0,524	1
21	0,045	0,087	0,125	0,160	0,192	0,222	0,250	0,276	0,300	0,323	0,344	0,364	0,382	0,400	0,417	0,432	0,447	0,462	0,475	0,488	0,500	0,512	1
22	0,043	0,083	0,120	0,154	0,185	0,214	0,241	0,267	0,290	0,313	0,333	0,353	0,371	0,389	0,405	0,421	0,436	0,450	0,463	0,476	0,488	0,500	1
23	0,042	0,080	0,115	0,148	0,179	0,207	0,233	0,258	0,281	0,303	0,324	0,343	0,361	0,378	0,395	0,410	0,425	0,439	0,452	0,465	0,477	0,489	1
24	0,040	0,077	0,111	0,143	0,172	0,200	0,226	0,250	0,273	0,294	0,314	0,333	0,351	0,368	0,385	0,400	0,415	0,429	0,442	0,455	0,467	0,478	1
25	0,038	0,074	0,107	0,138	0,167	0,194	0,219	0,242	0,265	0,286	0,306	0,324	0,342	0,359	0,375	0,390	0,405	0,419	0,432	0,444	0,457	0,468	1

**TABLE 4.** *Fit* values for characters under 11 different K values and exhibiting 0 to 25 homoplasies. Values were calculated to generate a regular distribution of *fit* values in a character containing 12 homoplasies (indicated by the dashed bar).

Homoplasies/K	1	1,855	2,849	3,957	5,267	6,808	8,654	10,902	13,702	17,273	22
0	1	1	1	1	1	1	1	1	1	1	1
1	0,5000	0,6497	0,7402	0,7983	0,8404	0,8719	0,8964	0,9160	0,9320	0,9453	0,9565
2	0,3333	0,4812	0,5875	0,6643	0,7248	0,7729	0,8123	0,8450	0,8726	0,8962	0,9167
3	0,2500	0,3821	0,4871	0,5688	0,6371	0,6941	0,7426	0,7842	0,8204	0,8520	0,8800
4	0,2000	0,3168	0,4160	0,4973	0,5684	0,6299	0,6839	0,7316	0,7740	0,8120	0,8462
5	0,1667	0,2706	0,3630	0,4418	0,5130	0,5766	0,6338	0,6856	0,7326	0,7755	0,8148
6	0,1429	0,2362	0,3220	0,3974	0,4675	0,5315	0,5906	0,6450	0,6955	0,7422	0,7857
7	0,1250	0,2095	0,2893	0,3611	0,4294	0,4930	0,5528	0,6090	0,6619	0,7116	0,7586
8	0,1111	0,1882	0,2626	0,3309	0,3970	0,4598	0,5196	0,5768	0,6314	0,6835	0,7333
9	0,1000	0,1709	0,2404	0,3054	0,3692	0,4307	0,4902	0,5478	0,6036	0,6574	0,7097
10	0,0909	0,1565	0,2217	0,2835	0,3450	0,4050	0,4639	0,5216	0,5781	0,6333	0,6875
11	0,0833	0,1443	0,2057	0,2646	0,3238	0,3823	0,4403	0,4978	0,5547	0,6109	0,6667
12	0,0769	0,1339	0,1919	0,2480	0,3050	0,3620	0,4190	0,4760	0,5331	0,5901	0,6471
13	0,0714	0,1249	0,1798	0,2334	0,2883	0,3437	0,3996	0,4561	0,5131	0,5706	0,6286
14	0,0667	0,1170	0,1691	0,2204	0,2734	0,3272	0,3820	0,4378	0,4946	0,5523	0,6111
15	0,0625	0,1101	0,1596	0,2087	0,2599	0,3122	0,3659	0,4209	0,4774	0,5352	0,5946
16	0,0588	0,1039	0,1511	0,1983	0,2477	0,2985	0,3510	0,4052	0,4613	0,5191	0,5789
17	0,0556	0,0984	0,1435	0,1888	0,2365	0,2860	0,3373	0,3907	0,4463	0,5040	0,5641
18	0,0526	0,0934	0,1366	0,1802	0,2264	0,2744	0,3247	0,3772	0,4322	0,4897	0,5500
19	0,0500	0,0889	0,1304	0,1724	0,2170	0,2638	0,3129	0,3646	0,4190	0,4762	0,5366
20	0,0476	0,0849	0,1247	0,1652	0,2085	0,2540	0,3020	0,3528	0,4066	0,4634	0,5238
21	0,0455	0,0812	0,1195	0,1586	0,2005	0,2448	0,2918	0,3417	0,3948	0,4513	0,5116
22	0,0435	0,0778	0,1147	0,1524	0,1932	0,2363	0,2823	0,3313	0,3838	0,4398	0,5000
23	0,0417	0,0746	0,1102	0,1468	0,1863	0,2284	0,2734	0,3216	0,3733	0,4289	0,4889
24	0,0400	0,0717	0,1061	0,1415	0,1800	0,2210	0,2650	0,3124	0,3634	0,4185	0,4783
25	0,0385	0,0691	0,1023	0,1367	0,1740	0,2140	0,2571	0,3037	0,3540	0,4086	0,4681

**TABLE 5.** Published records for the association between percomorphacean fishes and different lineages of gelatinous invertebrates used to code Character #217.

Family	Genus	Species	Size (SL)	Object of association	Behavior	References
Amarsipidae	<i>Amarsipus</i>	<i>A. carlsbergi</i>	15 mm	Salp: <i>Cyclosalpa affinis</i>	commensalism; parasitism	Janssen & Harbisson (1981); Harbisson (1993)
Ariommatidae	<i>Ariomma</i>	<i>A. indica</i>	-	-	-	Haedrich (1967)
	<i>Psenopsis</i>	<i>P. anomala</i>	"young"	Scyphozoa: <i>Cyanea nozakii</i>	-	Haedrich (1967); Ohtsuka <i>et al.</i> (2009)
		<i>Psenopsis</i> spp.	"young"	"Medusae"	-	Haedrich (1967)
	<i>Centrolophus</i>	<i>C. niger</i>	30–40 mm	Scyphozoa: <i>Rhizostoma pulmo</i>	-	Mansueti (1963); Parin & Piotrovsky (2004)
		<i>S. ovalis</i>	31–37 mm	Hydrozoa: <i>Physalia</i> sp.	-	Mansueti (1963); Maul (1964)
	<i>Schedophilus</i>	<i>S. medusophagus</i>	85–180 mm	Scyphozoa: <i>Pelagia noctiluca</i> , <i>Phacellophora camtschatica</i>	-	Maul (1964); Bone & Brooke (1973)
	<i>Seriotelella</i>	<i>S. violacea</i>	66–98 mm	Scyphozoa: <i>Chrysaora plocamia</i>	non-obligatory mutualism	Riascos <i>et al.</i> (2012)
Centrolophidae	<i>Tubbia</i>	<i>Tubbia tasmanica</i>	-	-	-	Mansueti (1963)
	<i>Icichthys</i>	<i>I. australis</i>	-	Scyphozoa: <i>Periphylla periphylla</i>	-	Purcell & Arai (2001)
		<i>I. lockingtoni</i>	55–180.5 mm	Scyphozoa: <i>Pelagia noctiluca</i>	-	Haedrich (1966); Haedrich (1967)
		<i>H. bythites</i>	12 mm	Ctenophora: <i>Beroe</i> sp.	commensalism	Matthews & Shoemaker (1952); Dawson (1971)
	<i>Hyperglyphe</i>	<i>H. antarctica</i>	"young"	Kelp: <i>Phyllospora comosa</i> ; sargassum, drift algae, flotsam	commensalism	Duffy <i>et al.</i> (2000); Williams <i>et al.</i> (2017)
		<i>H. japonica</i>	3.6–27.6 mm	Drifting seaweed	commensalism	Safran & Omori (1990)
		<i>H. perciformis</i>	345 mm	Sargassum, wreckage, floating boxes	commensalism	Schwartz (1963); Merriner <i>et al.</i> (1970); Quigley (1986); Horn (1984)
	<i>Psenes</i>	<i>P. cyanophrys</i>	-	"Salp"	-	Janssen & Harbisson (1981)
		<i>P. arafurensis</i>	58 mm	Scyphozoa: <i>Cepha cepha</i>	-	Mansueti (1963); Karplus (2014)
Nomeidae	<i>Cubiceps</i>	<i>C. capensis</i>	9 mm	"Salp"	-	Janssen & Harbisson (1981); Harbisson (1993)
		<i>C. gracilis</i>	"young"	"Medusae"	-	Mansueti (1963); Haedrich (1967); Harbisson (1993)
	<i>Nomeus</i>	<i>N. granovii</i>	all sizes	Hydrozoa: <i>Stomolophus meleagris</i> ; <i>Physalia pelagica</i> ; <i>Physalia physalis</i> ; <i>Forksalia tholoides</i>	symbiosis; mimicry; parasitism	Lane (1960); Mansueti (1963); Jenkins (1983); Purcell & Arai (2001); Karplus (2014)
		<i>P. triacanthus</i>	-	Scyphozoa: <i>Cyanea capillata</i>	-	Duffy (1988)
		<i>P. cf. crenulatus</i>	"young"	Cubozoa: <i>Tamoya haplonema</i>	commensalism; sheltering	Lawley & Junior (2018)
	<i>Peprilus</i>	<i>P. alepidotus</i>	"young"	Scyphozoa: <i>Dactyometra</i> sp., <i>Chrysaora quinquecirrha</i>	commensalism; predation	Matthews & Shoemaker (1952); Mansueti (1963); Purcell & Arai (2001)
		<i>P. simillimus</i>	-	Scyphozoa: <i>Chrysaora achlyosa</i>	-	Purcell & Arai (2001)
		<i>P. paru</i>	-	Scyphozoa: <i>Aurelia aurita</i>	-	Tolley (1987); Purcell & Arai (2001)
	<i>Pampus</i>	<i>P. chinensis</i>	"young"	Scyphozoa: <i>Thyanostoma</i> sp.	mimicry; predation	Tan (2008)
	<i>Stromateus</i>	<i>S. fiatola</i>	10–40 mm	Scyphozoa: <i>Rhizostoma pulmo</i> , <i>Cotylorhiza tuberculata</i>	commensalism	Mansueti (1963)
		<i>T. atlanticus</i>	8–16 mm			
Tetragonuridae	<i>Tetragonurus</i>	<i>T. pacificus</i>	7–17 mm	Salp: ( <i>Salpa</i> spp., <i>Pegea</i> spp., <i>Cyclosalpa</i> spp., <i>Ihlea asymmetrica</i> ); Pyrosome: ( <i>Pyrosoma</i> sp.)	parasitism	Janssen & Harbisson (1981)
		<i>T. cuvieri</i>	7–53 mm			
Icosteidae	<i>Icosteus</i>	<i>I. aenigmaticus</i>	"young"	"Medusae"	commensalism	Mecklenburg (2003)
Bramidae	<i>Brama</i>	<i>Brama</i> spp.	"young"	"Medusae"	commensalism	Johnson ( <i>pers. com.</i> )
	<i>Caristius</i>	<i>Caristius</i> sp.	63 mm	Hydrozoa: <i>Bathyphysa confiera</i>	commensalism; parasitism	Janssen <i>et al.</i> (1989)
Caristiidae	<i>Paracaristius</i>	<i>Paracaristius</i> sp.	150–200 mm	Hydrozoa: Apolemiidae	commensalism	Benfield <i>et al.</i> (2009)
	<i>Caristiidae</i> sp.	<i>Caristiidae</i> sp.	-	Hydrozoa: <i>Praya</i> sp.	commensalism	Lindsay <i>et al.</i> (2001)
Kyphosidae	<i>Girella</i>	<i>G. nigricans</i>	"young"	"Medusae"	commensalism	Mansueti (1963)

## FIGURES

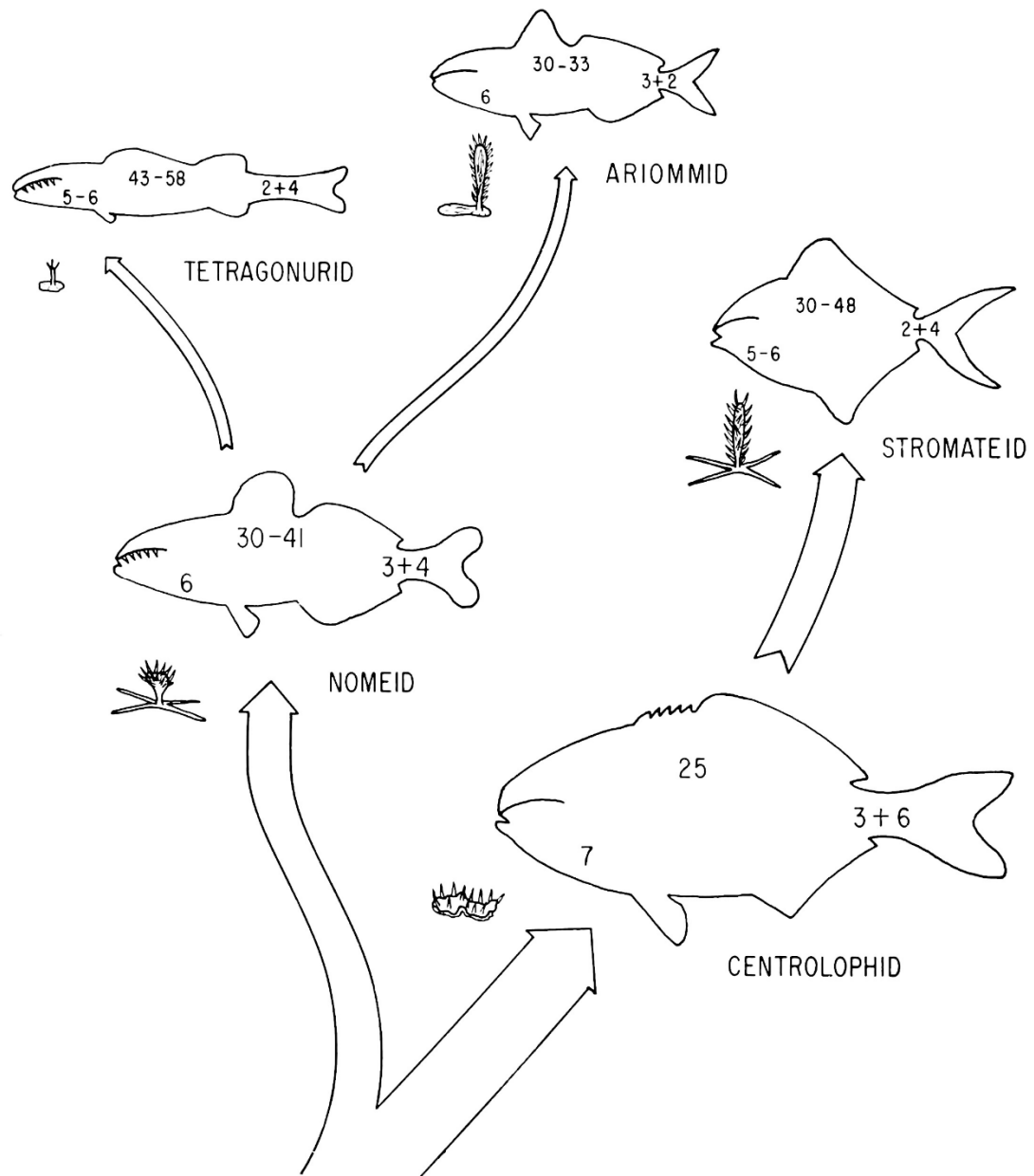


**FIGURE 1:** The evolution of Stromateiformes according to Haedrich (1967). The diagram is constructed considering main changes on relative size and shape, fin pattern, presence or absence of palatal dentition, numbers of branchiostegals, vertebrae, and epurals + hypurals. Inset represents pharyngeal-sac rakers. Width of arrows are proportional to number of genera in the family. Image reproduced from Haedrich (1967: fig. 48).

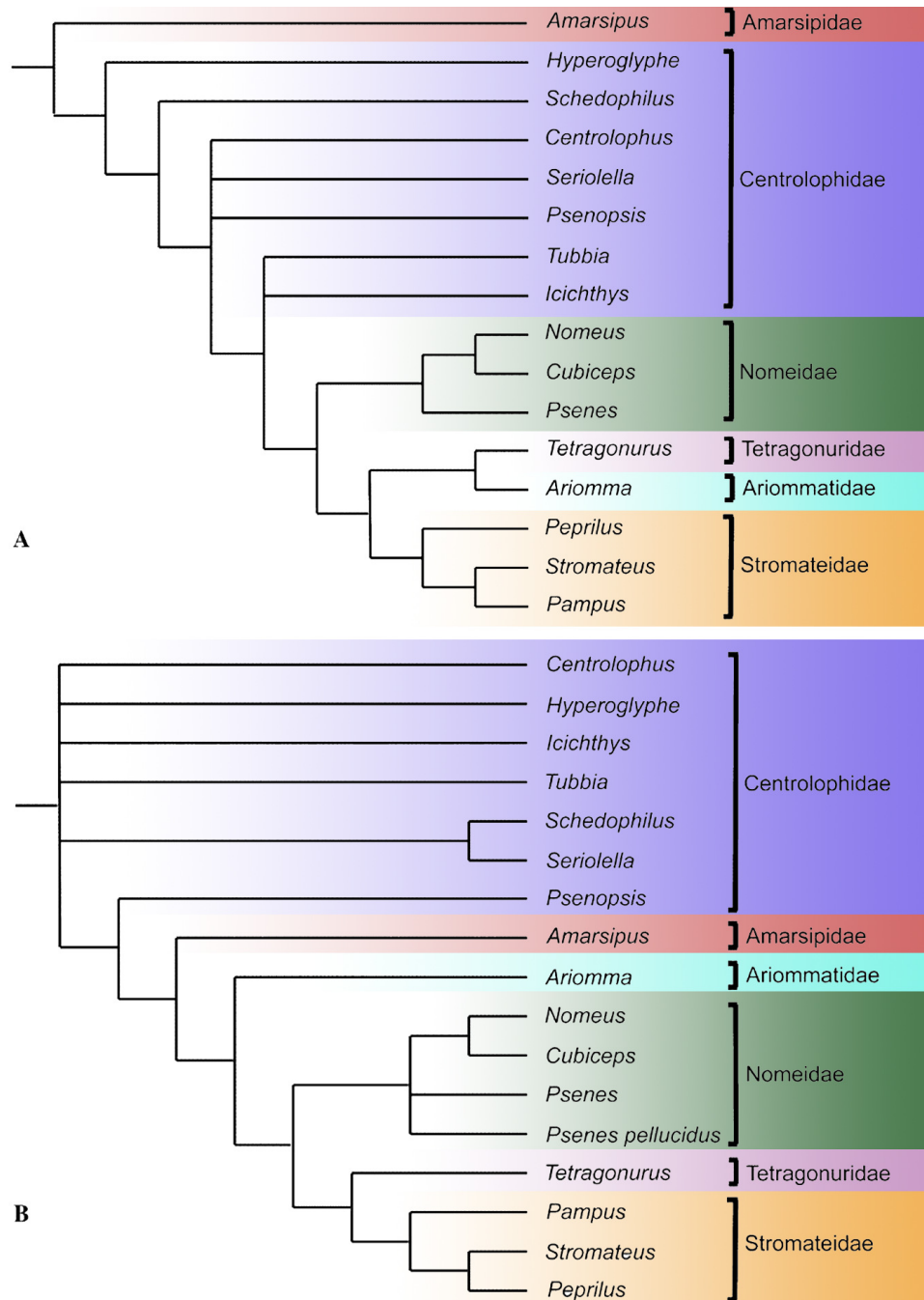


**FIGURE 2:** Hypotheses of the relationships of Stromateiformes inferred from morphological characters according to: A) Horn (1984) and B) Doiuchi *et al.* (2004). Highlighted taxa represent Amarsipidae (red), Centrolophidae (purple), Nomeidae (green), Tetragonuridae (pink), Stromateidae (orange), and Ariommatidae (light blue).

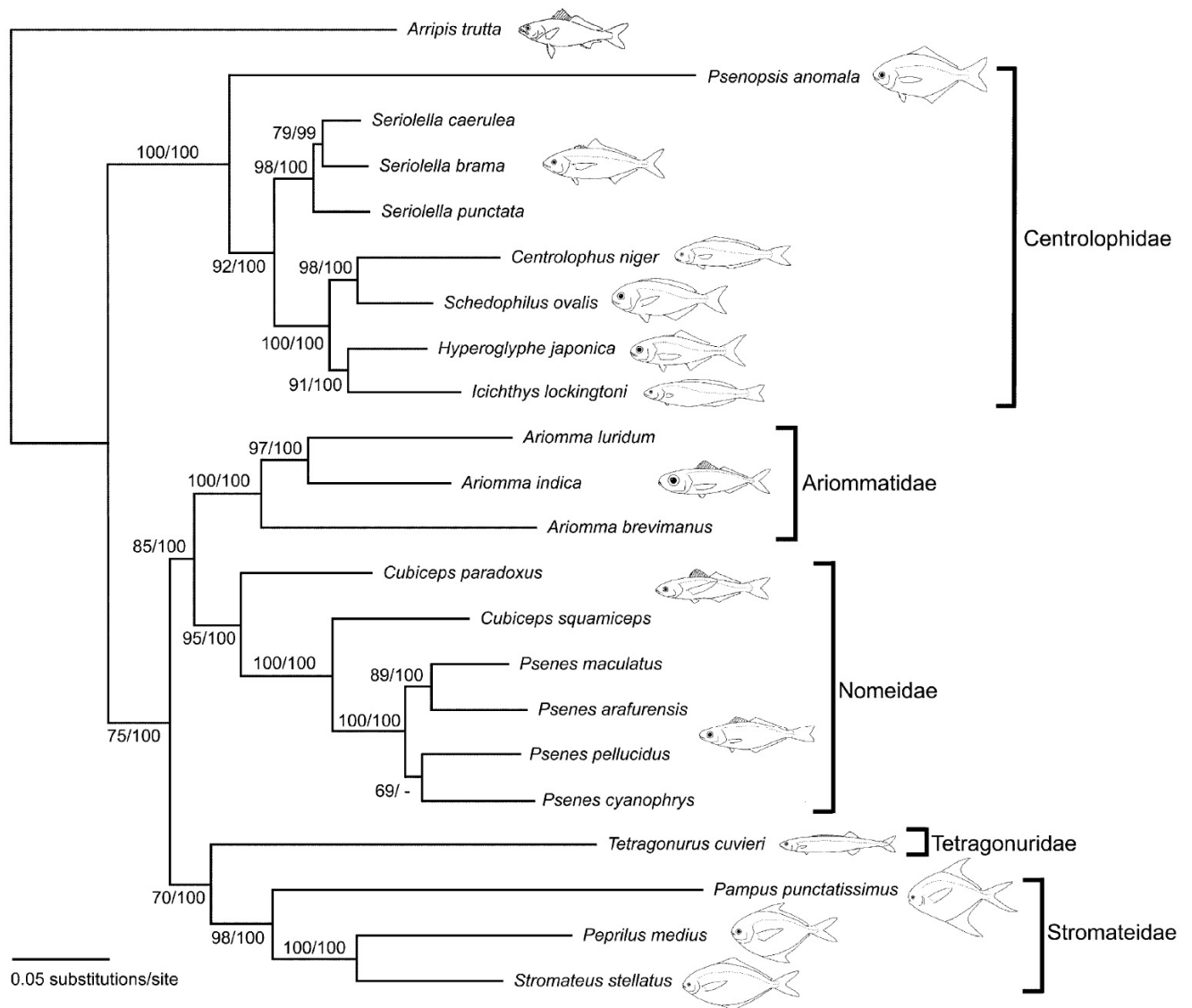


**FIGURE 3:** Interrelationships of Stromateiformes according to Doiuchi & Nakabo (2006). Topology was obtained using molecular data and constructed using Maximum Likelihood methods. Image reproduced from Doiuchi & Nakabo (2006: fig. 4). Amarsipidae was not sampled.

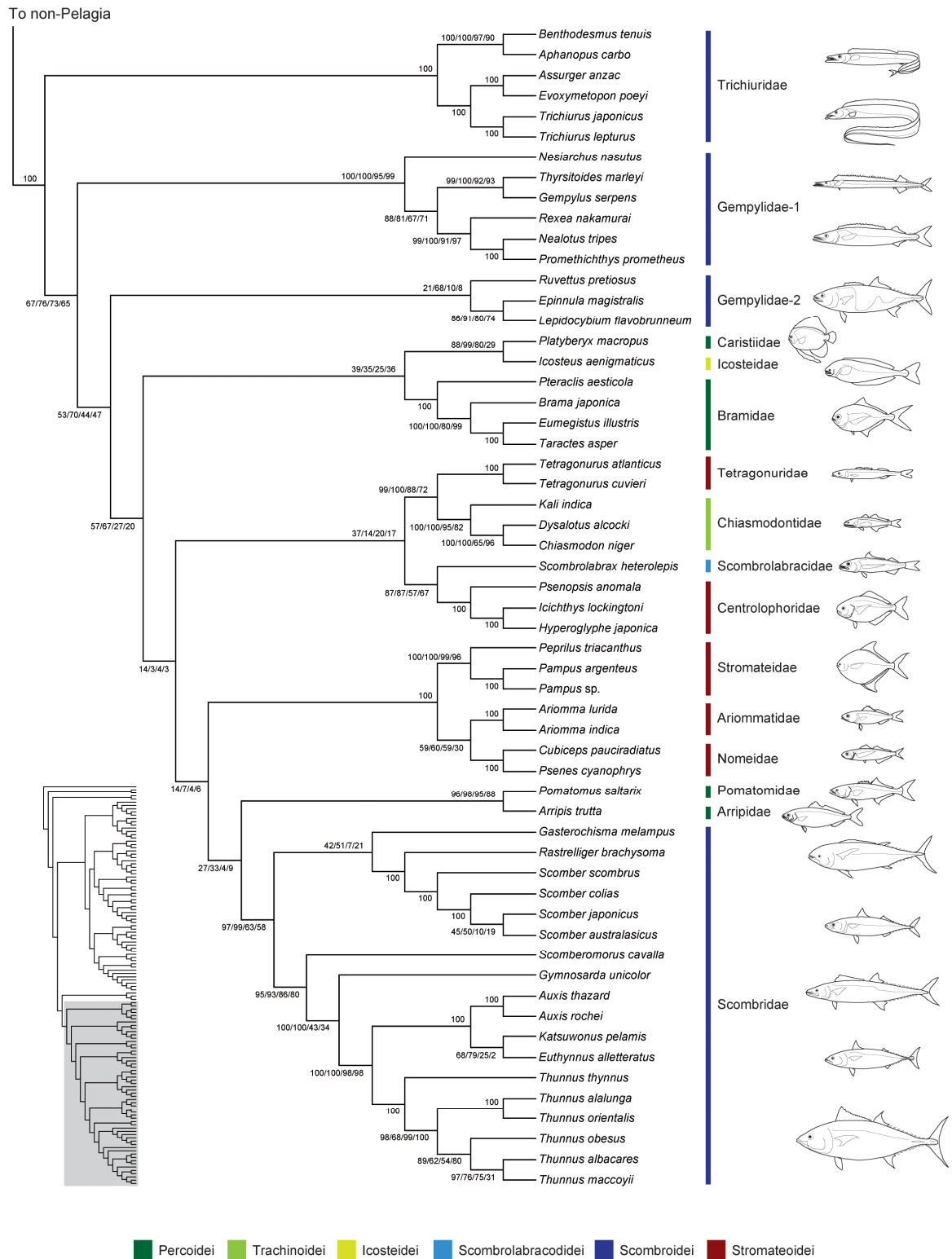


**FIGURE 4:** Interrelationships of Pelagiaria according to Miya et al. (2013). Topology was obtained from mitogenome sequences and constructed using Maximum Likelihood methods. Image reproduced from Miya et al. (2013: fig. 5). Amarsipidae was not sampled.

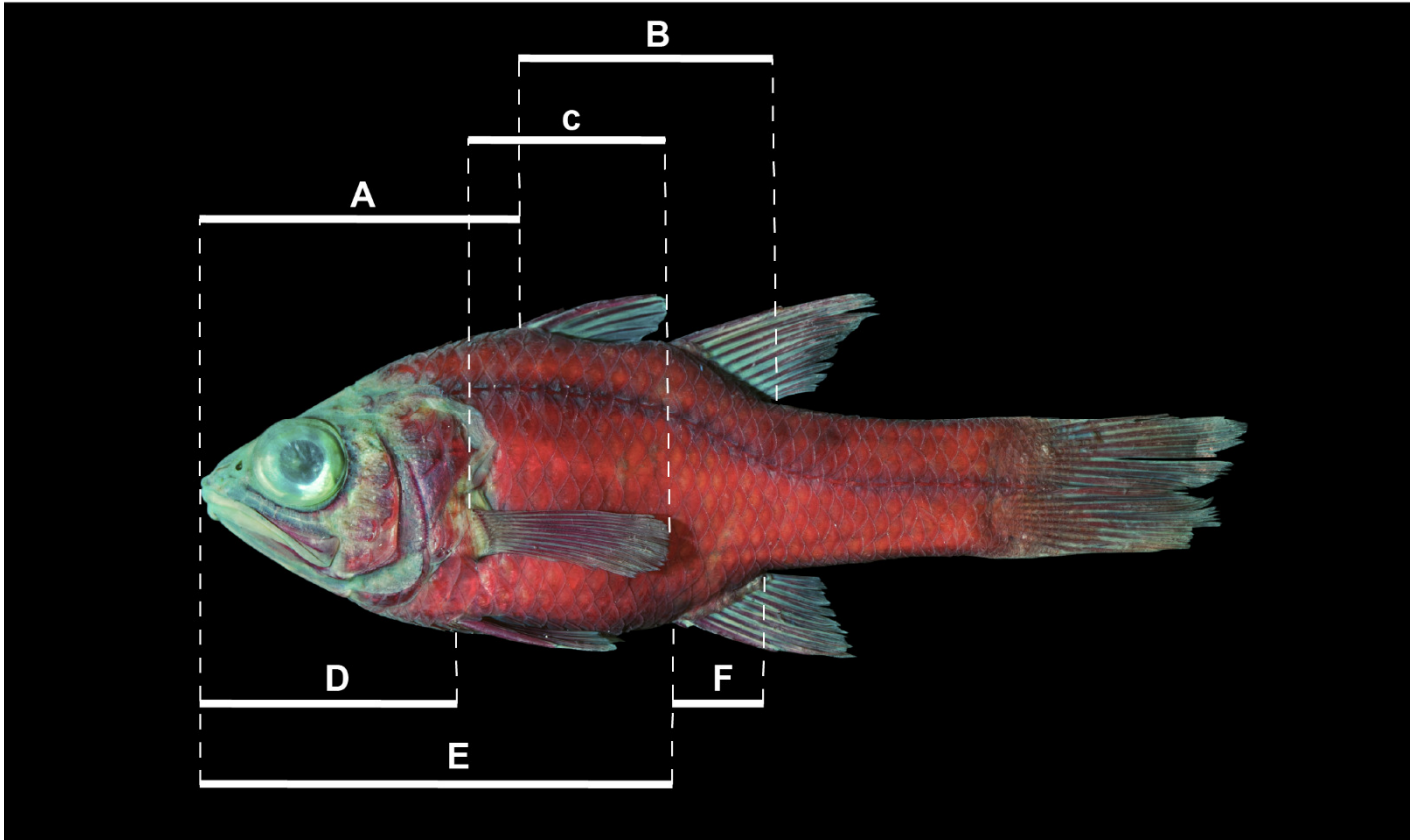


**FIGURE 5:** Measurements used as continuous characters in the phylogenetic analysis shown in an alizarin red stained specimen of *Apogon maculatus* (Apogonidae: MZUSP 43155; 67.3 mm SL). Letters indicate: A) Predorsal length, B) dorsal-fin base length, C) pectoral-fin length, D) Prepevic length, E) Preanal length, F) Anal-fin base length.

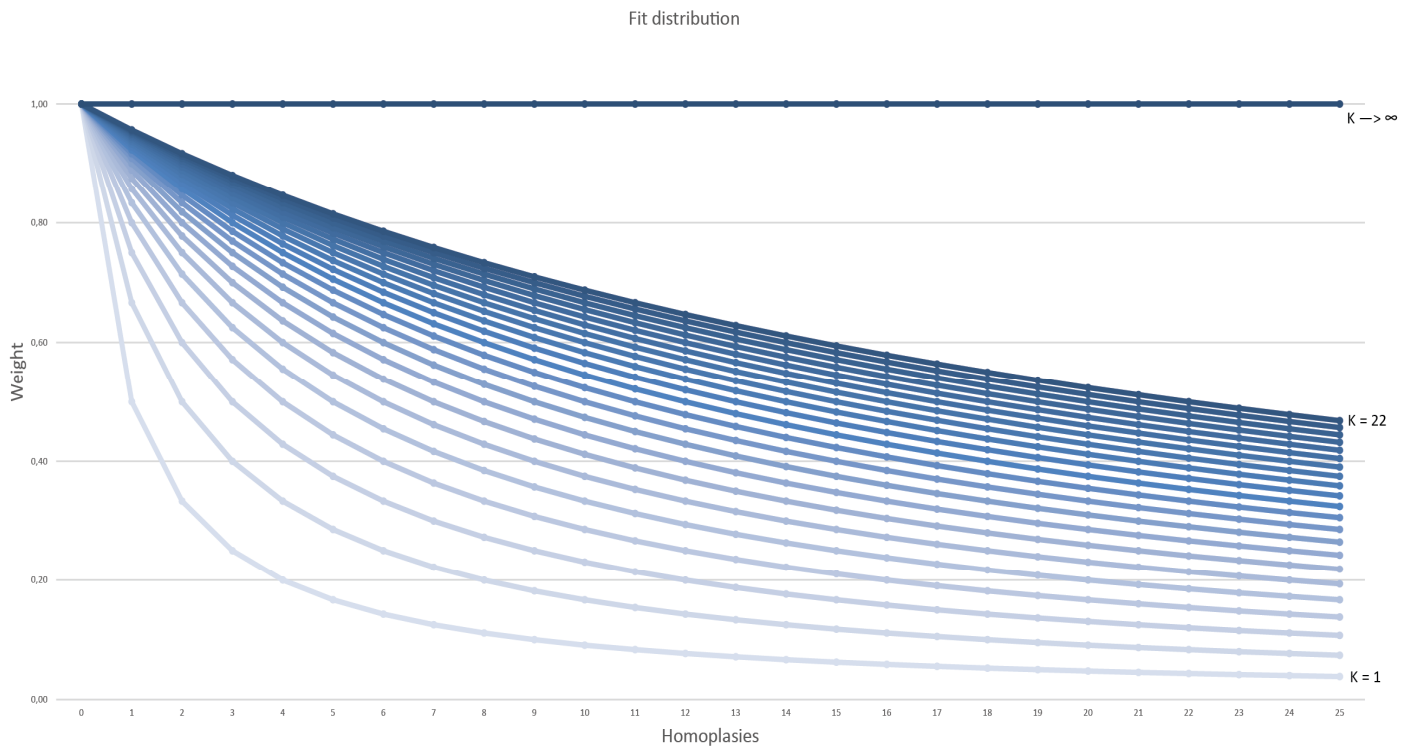


**FIGURE 6:** *Fit* distribution for characters under 23 different values of  $K$  ( $K = 1-22$ , and  $K \rightarrow \infty$ ) and exhibiting 0 to 25 homoplasies. Note that higher values of  $K$  result in curves exhibiting similar concavities (darker curves). *Fit* values under an equal weight analysis ( $K \rightarrow \infty$ ) result in a straight line of *fit* distribution.

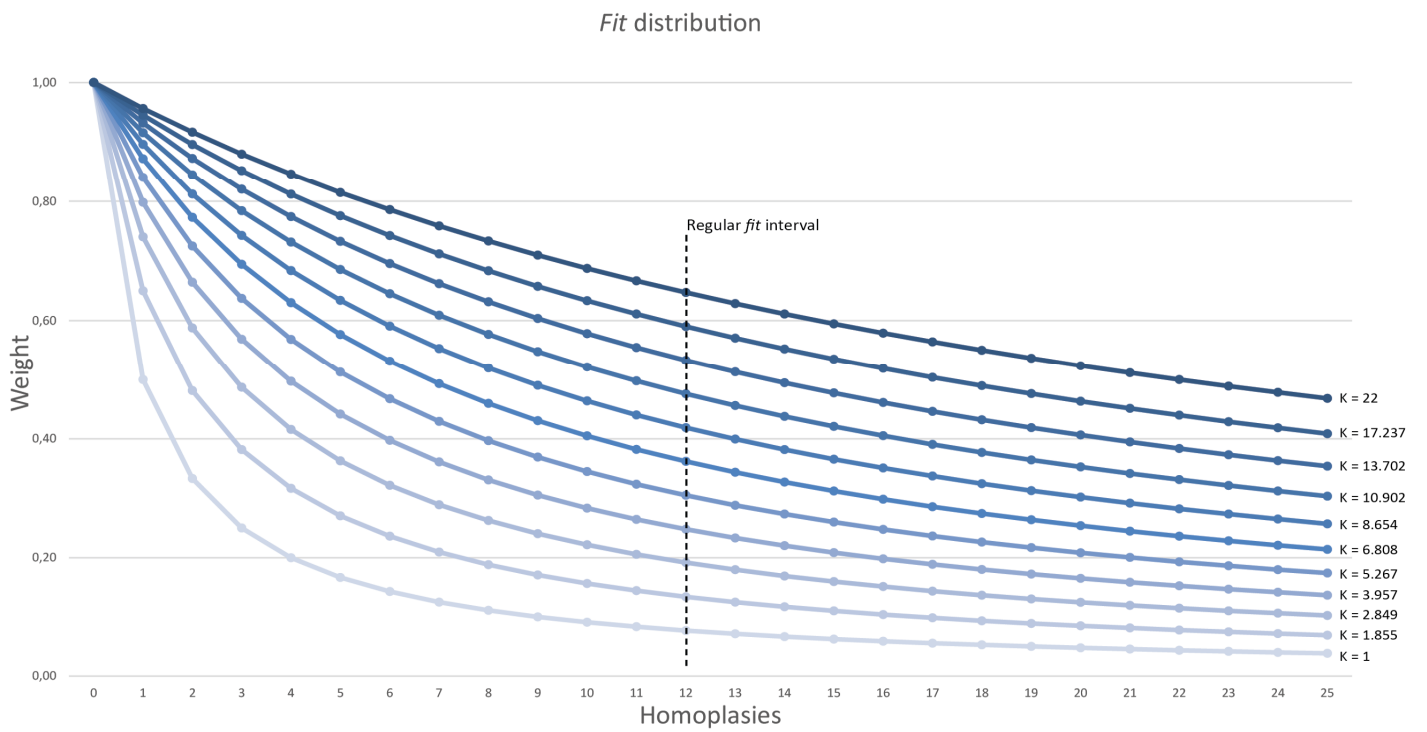


**FIGURE 7:** *Fit distribution* for characters under 11 different K values and exhibiting 0 to 25 homoplasies. Dashed line indicates a character exhibiting 12 homoplasies, chosen herein as the point where curves under different K values exhibit a proportional *fit* variation.

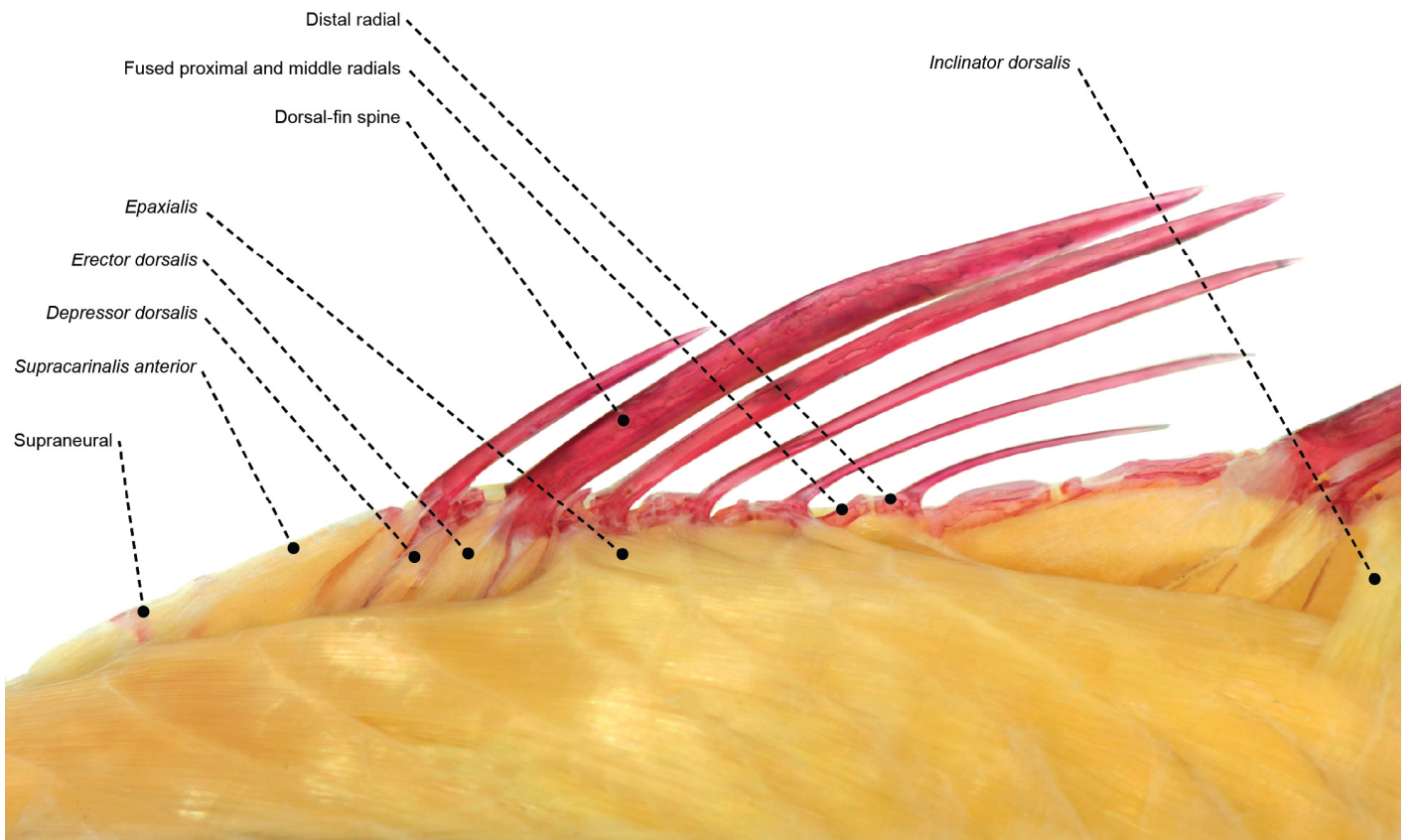


**FIGURE 8:** Dorsal-fin musculoskeletal system of *Apogon maculatus* (Apogonidae: MZUSP 43155) in left lateral view. Note the epaxial musculature association with the dorsal-fin pterygiophores. Scale bar: 3 mm.

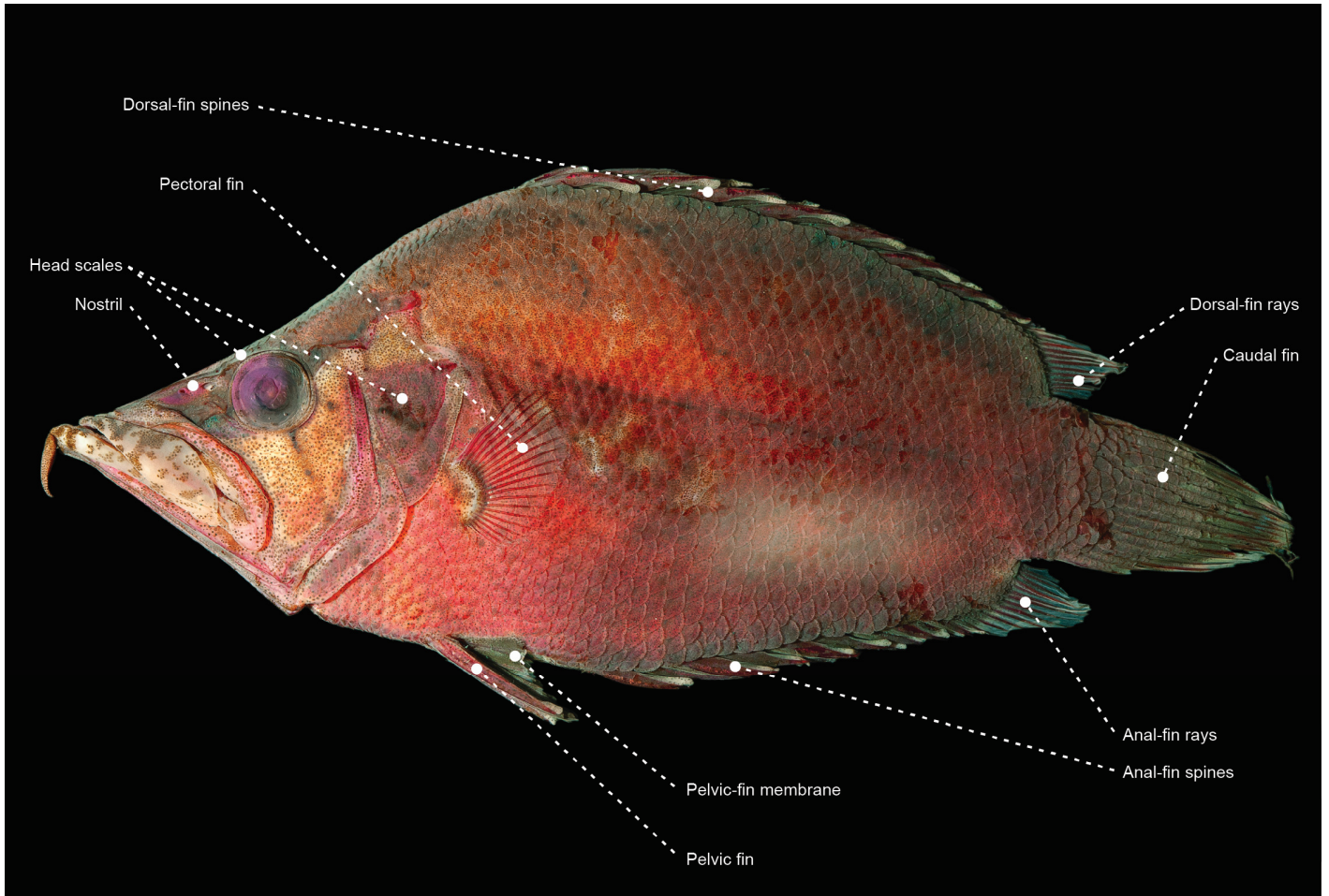


**FIGURE 9:** Left lateral view of an alizarin-red stained specimen of *Monocirrhus polyacanthus* (MZUSP 55122; 54.6 mm SL). Arrow indicates the membrane attaching the medial most pelvic-fin ray to the abdomen.

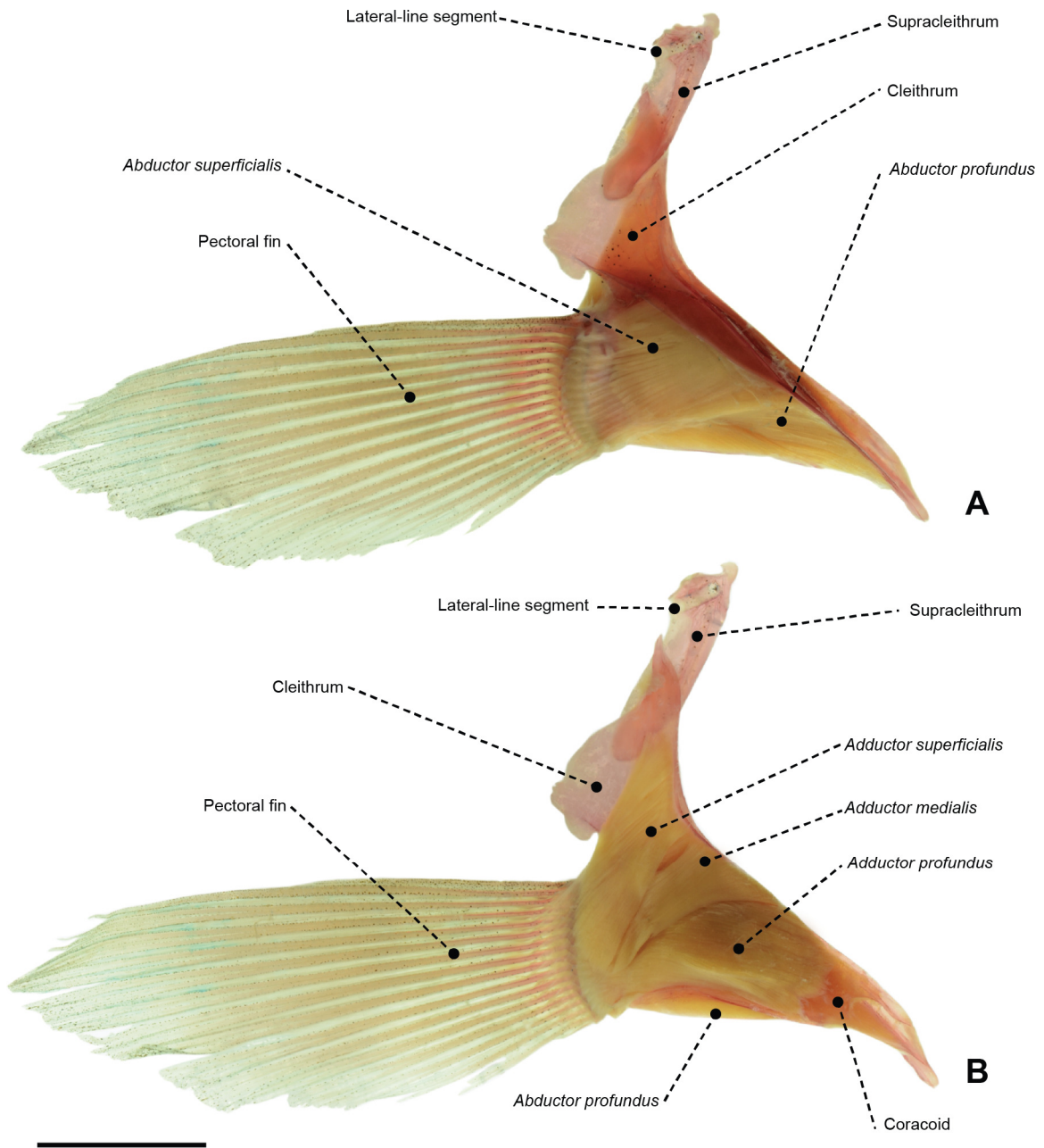


**FIGURE 10:** Left pectoral girdle of *Morone mississippiensis* (Moronidae: MZUSP 123242) in (A) lateral and (B) medial view exhibiting associated muscles. Scale bar: 8 mm.

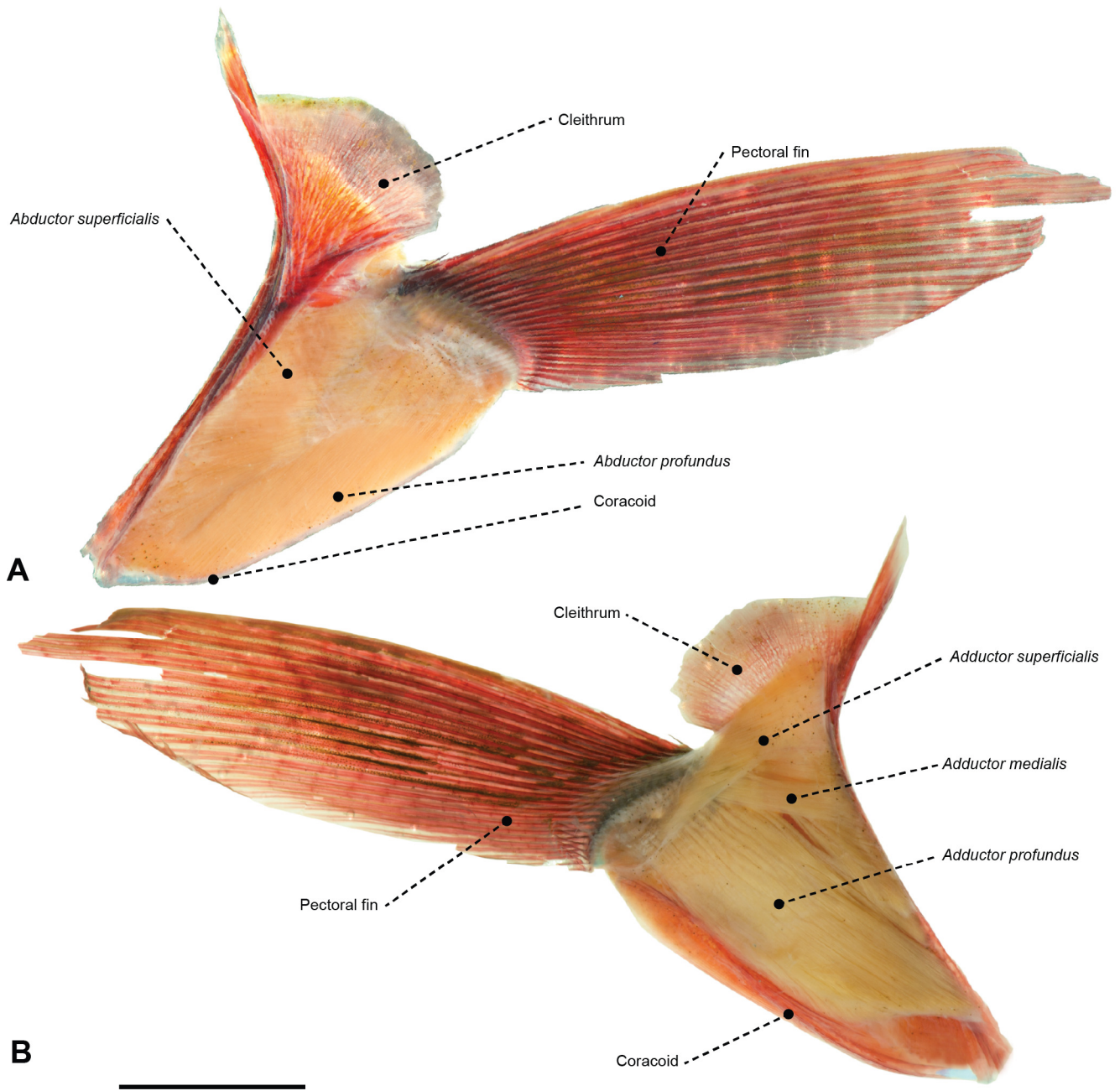


**FIGURE 11:** Left pectoral girdle of *Nomeus gronovii* (Nomeidae: MZUSP 67590) in (A) lateral and (B) medial view exhibiting associated muscles. Scale bar: 5 mm.

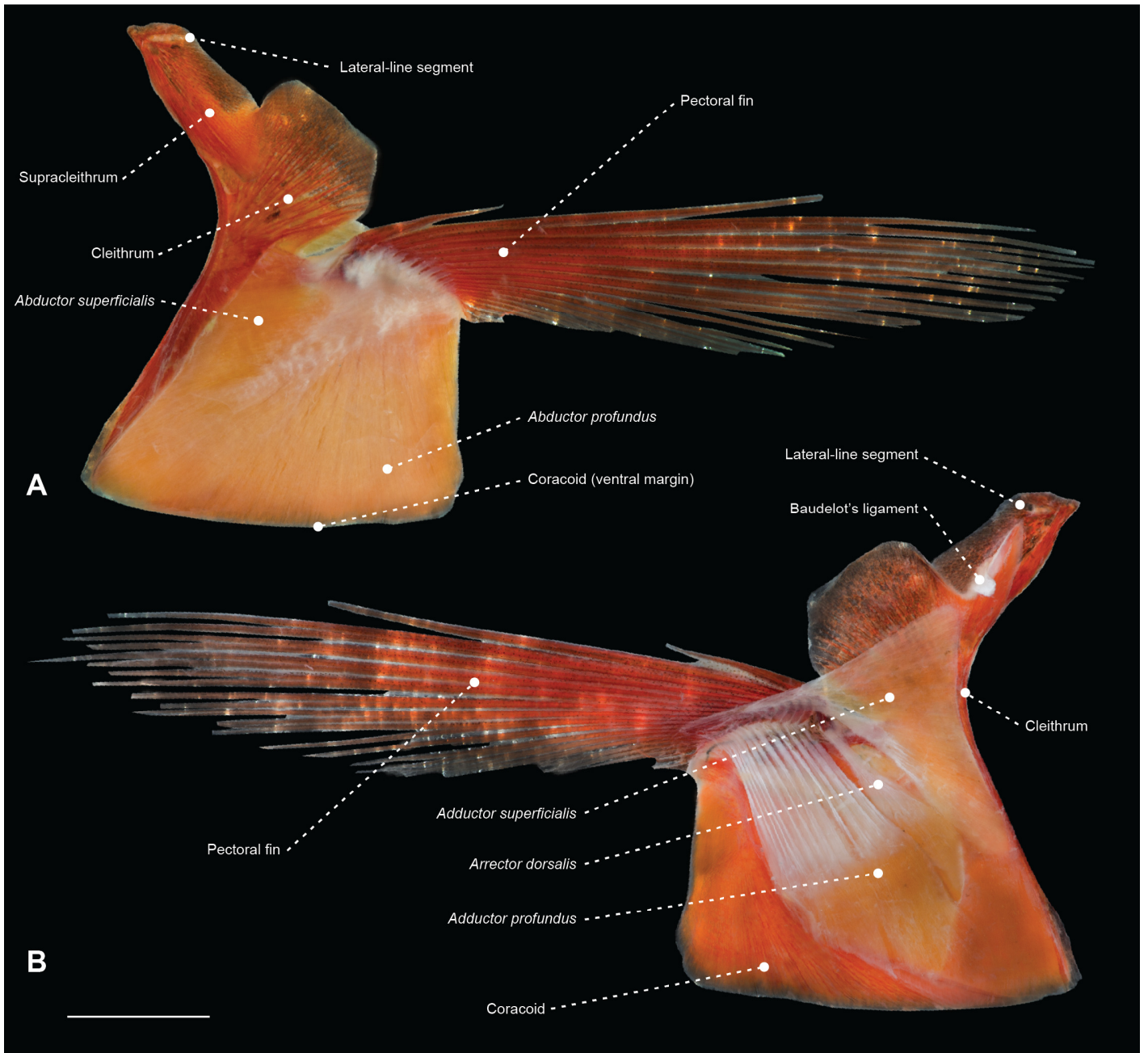


**FIGURE 12:** Left pectoral girdle of *Cubiceps pauciradiatus* (Nomeidae: MZUSP 80701) in (A) lateral and (B) medial view exhibiting associated muscles. Scale bar: 5 mm.

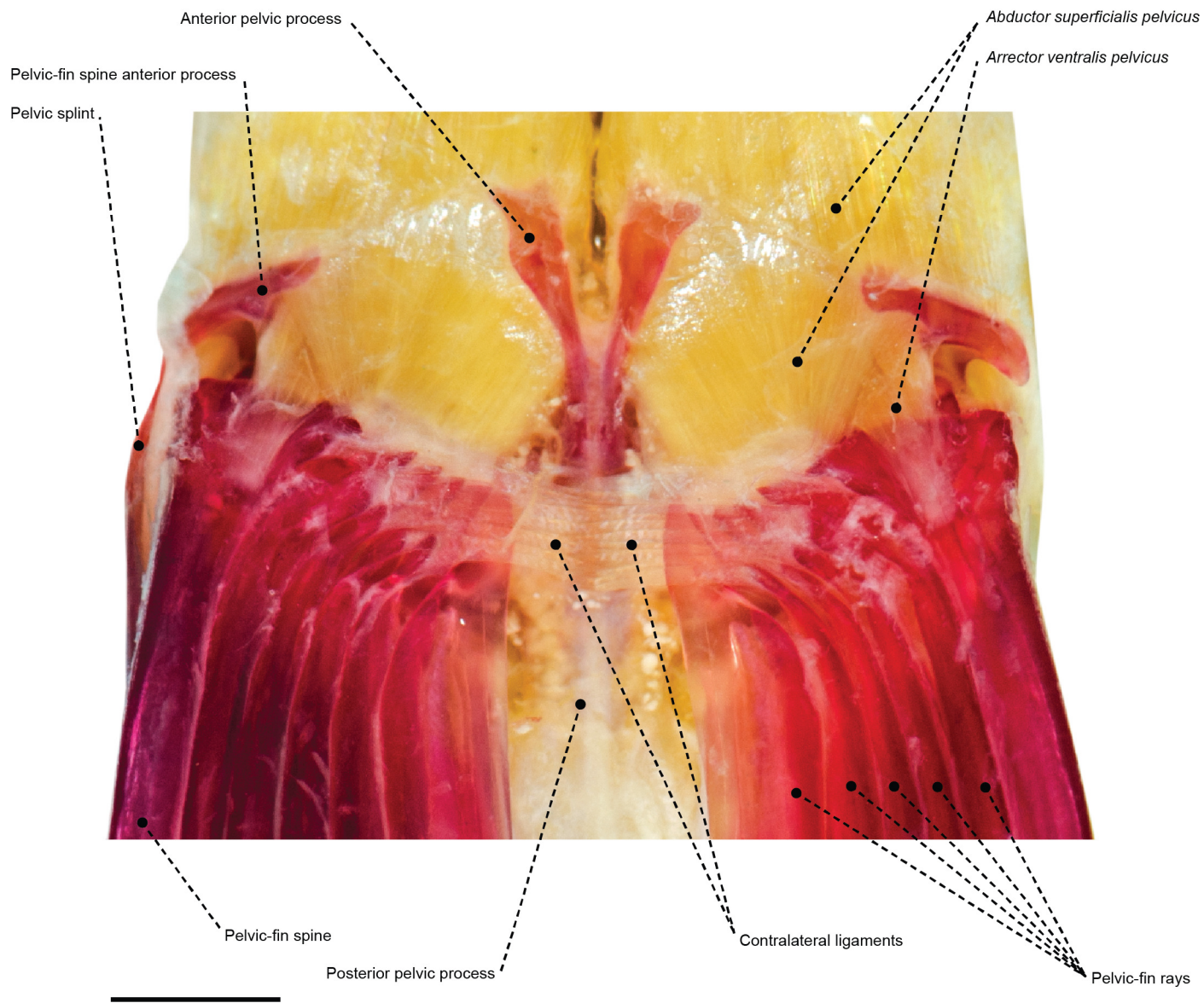


**FIGURE 13:** Pelvic girdle of *Apogon maculatus* (Apogonidae: MZUSP 43155) in ventral view exhibiting associated muscles and ligaments. Scale bar: 1 mm.

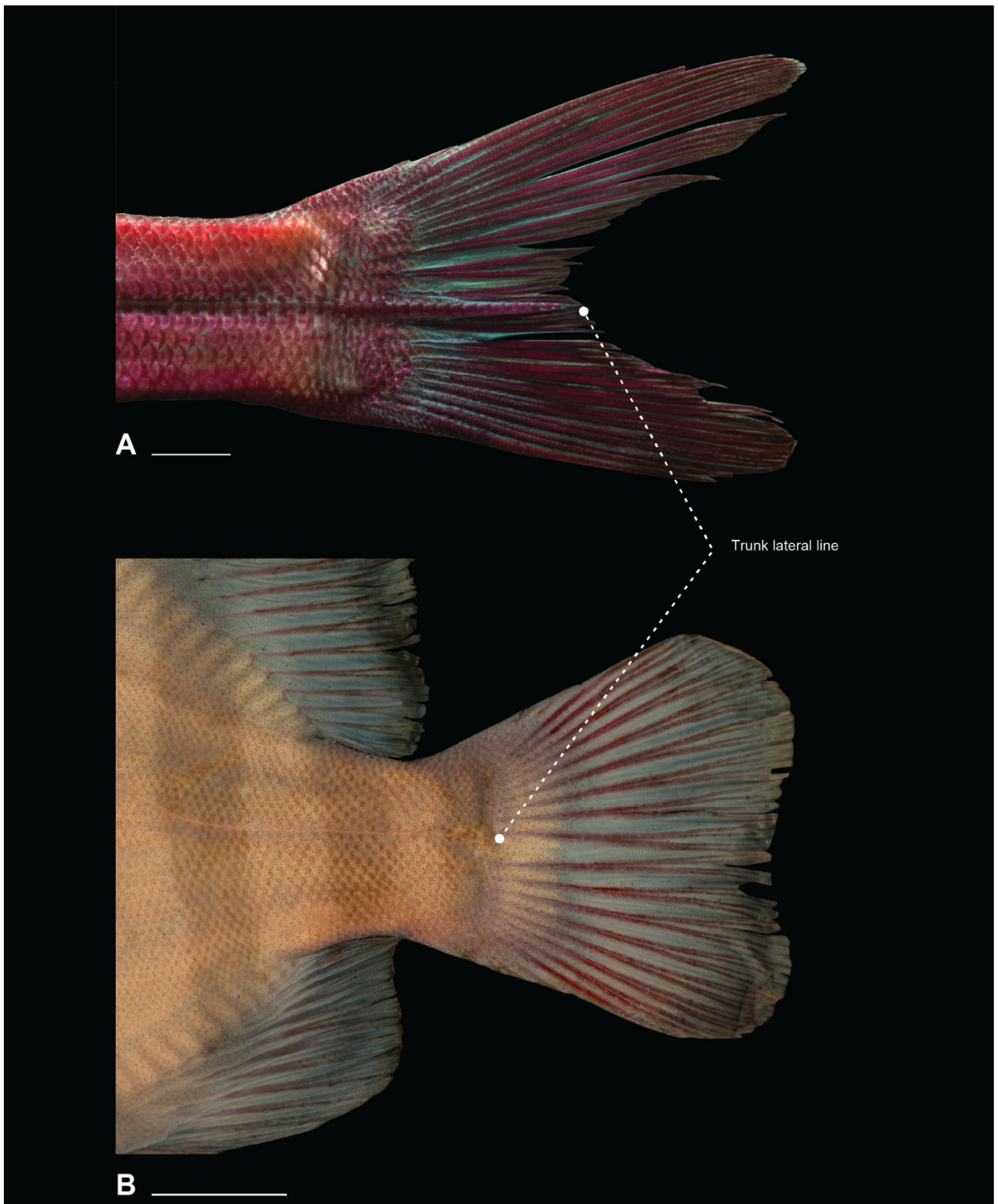


**FIGURE 14:** Caudal peduncle and caudal fin of (A) *Centropomus parallelus* (Centropomidae: MZUSP 108244) and (B) *Oplegnathus fasciatus* (Oplegnathidae: MZUSP 28867) showing the posterior limit of the trunk lateral line. Scale bar: 5 mm.

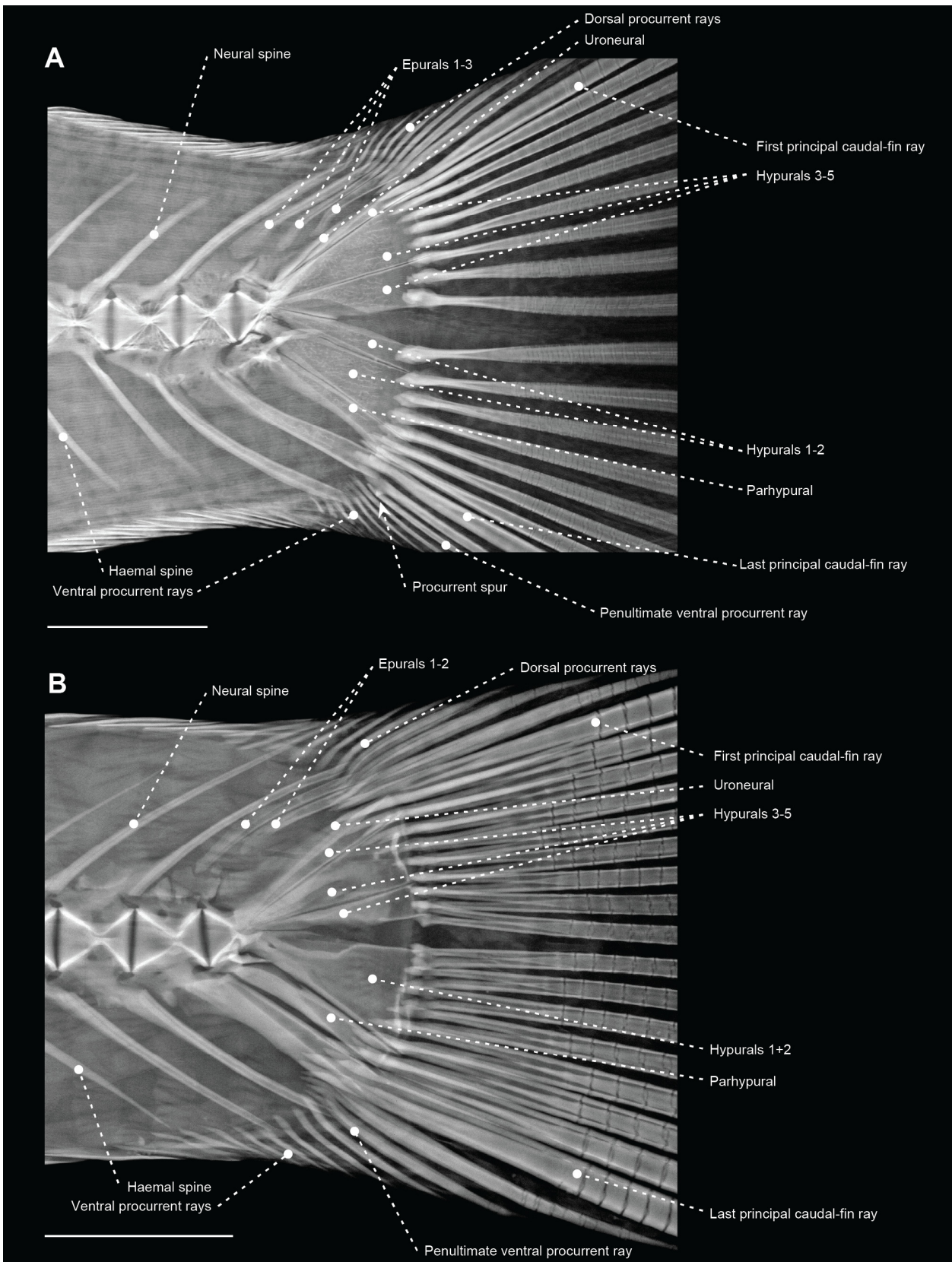


**FIGURE 15:** Radiographs of the caudal skeleton of (A) *Amniataba caudavittata* (Terapontidae: USNM 173673), and (B) *Atherinella brasiliensis* (Atherinopsidae: MZUSP 67186) in left lateral view. Scale bar: 4 mm.

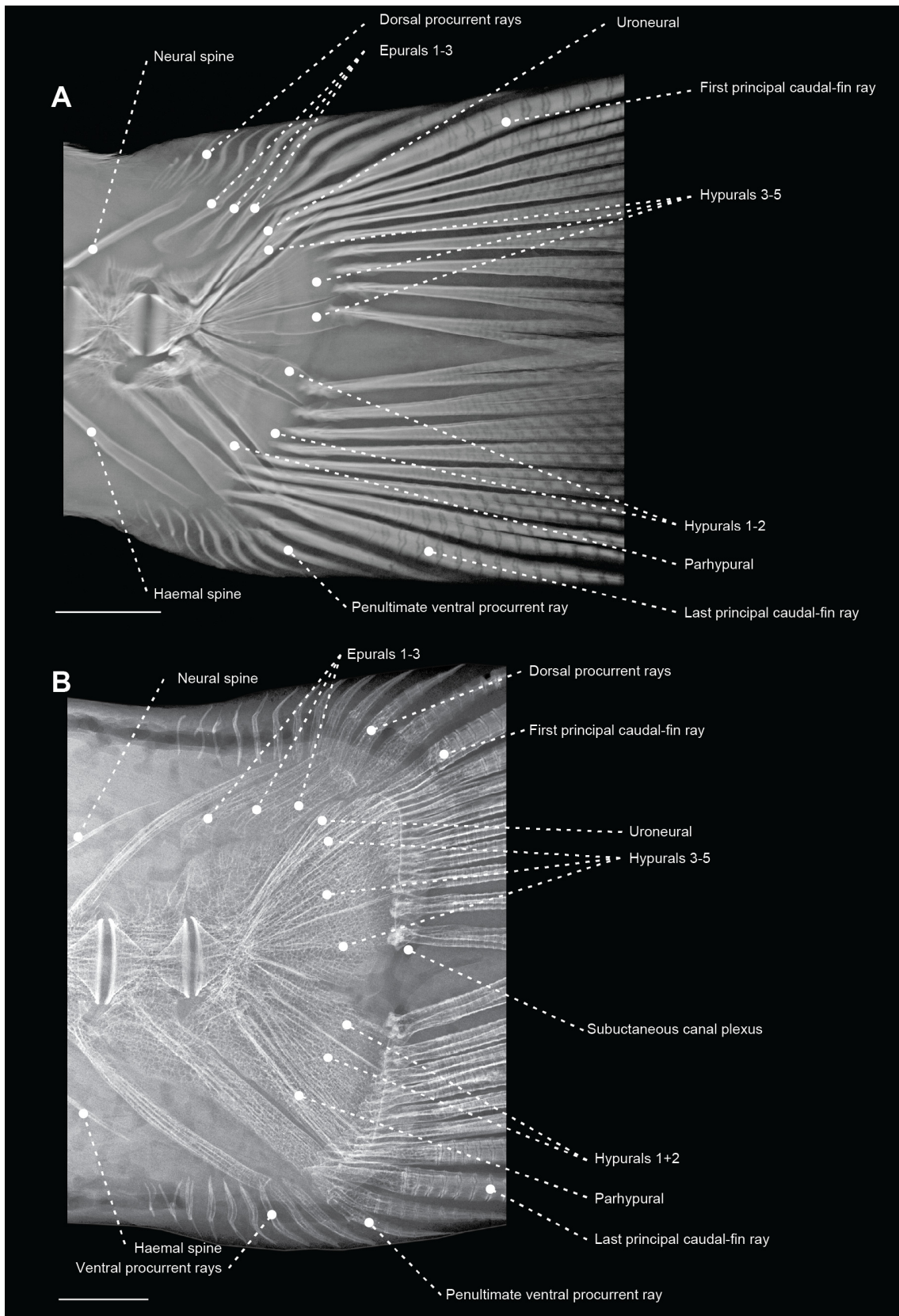


**FIGURE 16:** Radiographs of the caudal skeleton of the centrolophids (A) *Hyperoglyphe perciformis* (MZUSP 119733), and (B) *Tubbia tasmanica* (CSIRO H 6979-03) in left lateral view. Scale bar: 5 mm.

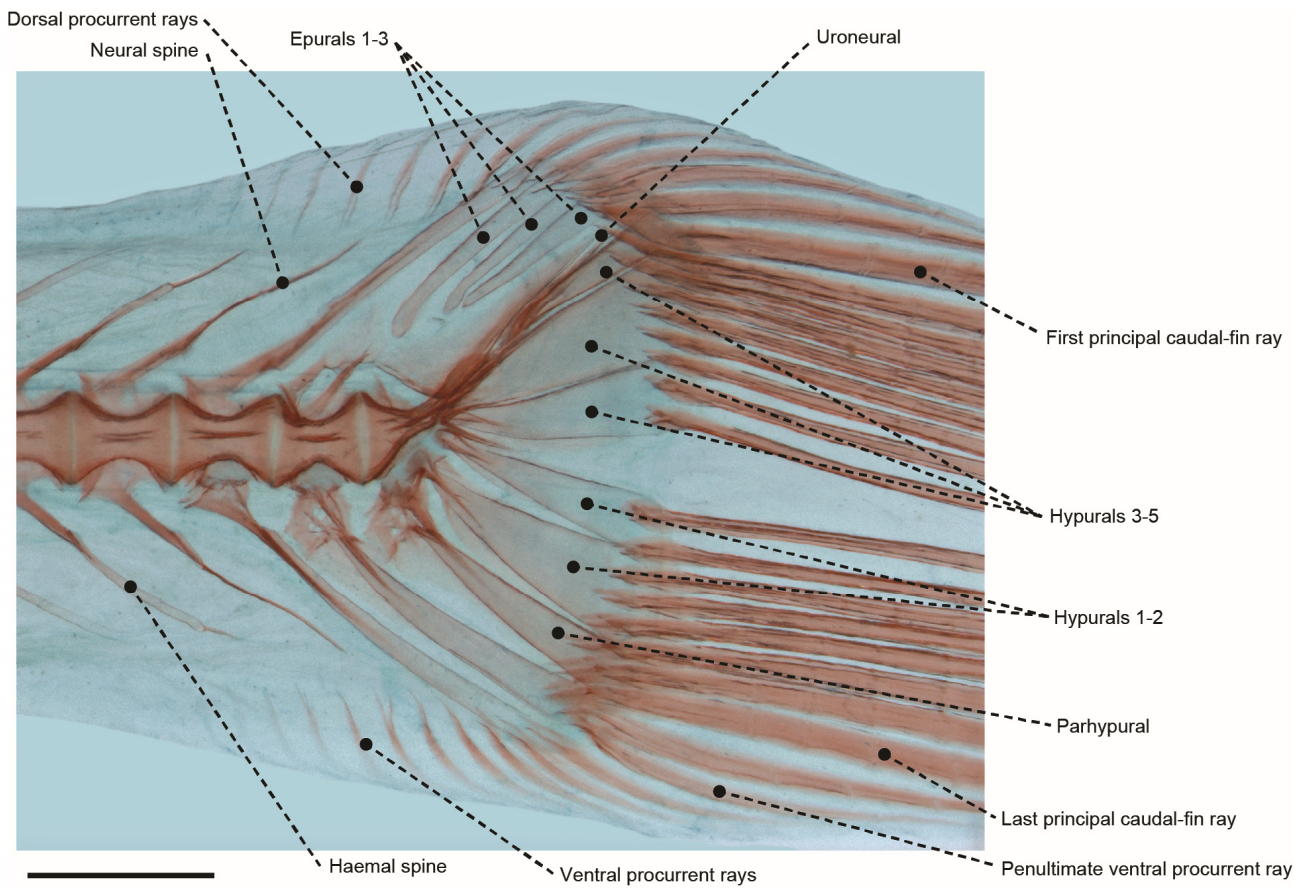


**FIGURE 17:** Caudal skeleton of a cleared and stained specimen of *Amarsipus carlsbergi* (Amarsipidae: SIO 75-122) in left lateral view. Scale bar: 2 mm.

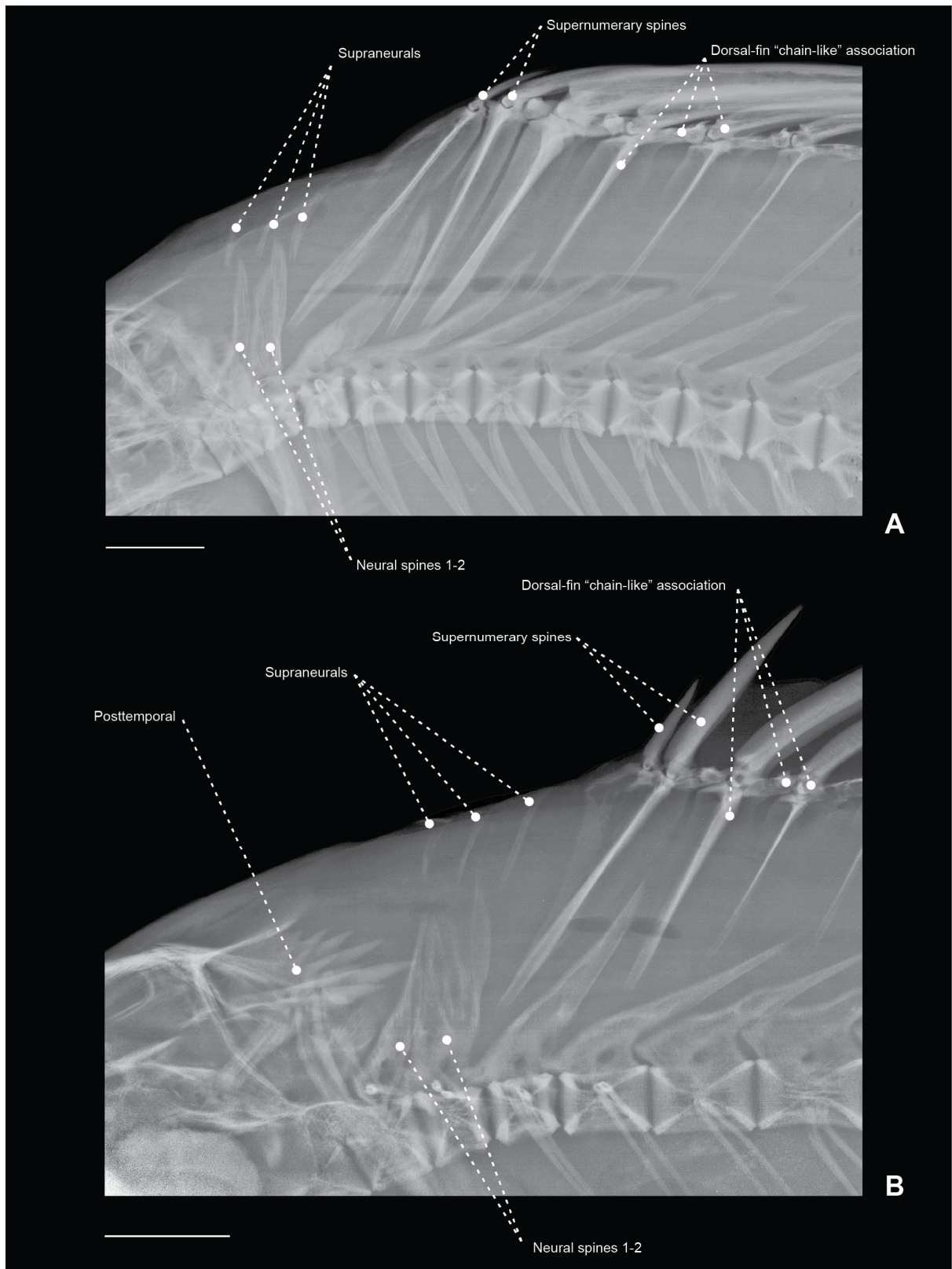


**FIGURE 18:** Radiographs of the occipital region and anterodorsal portion of the trunk of (A) *Lates niloticus* (Latidae: MZUSP 123243), and (B) *Centropomus parallelus* (Centropomidae: MZUSP 108244) in left lateral view. Scale bar: 4 mm.

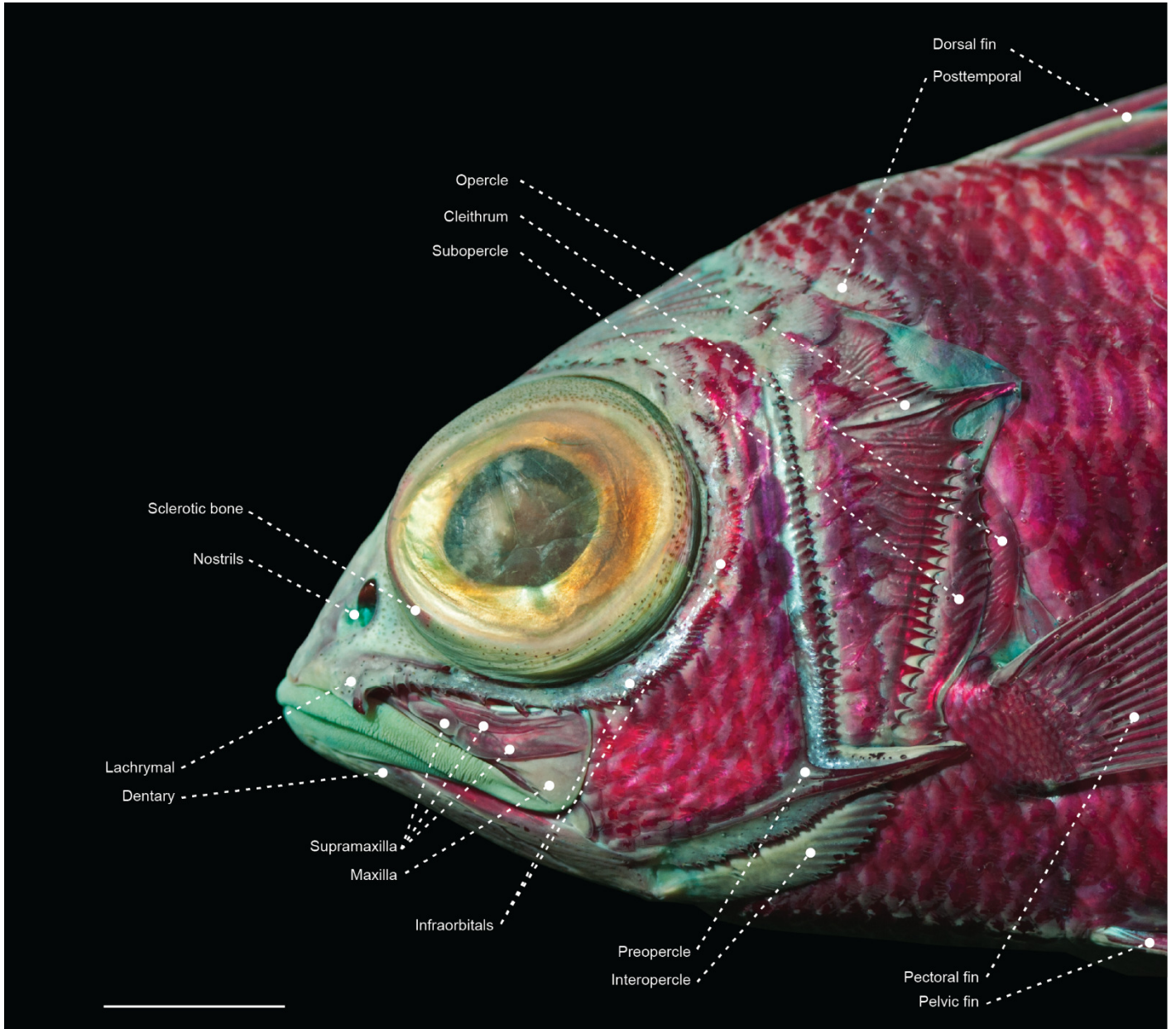


**FIGURE 19:** Head of *Holocentrus adscencionis* (Holocentridae: MZUSP 69190) in left lateral view. Scale bar: 7 mm.

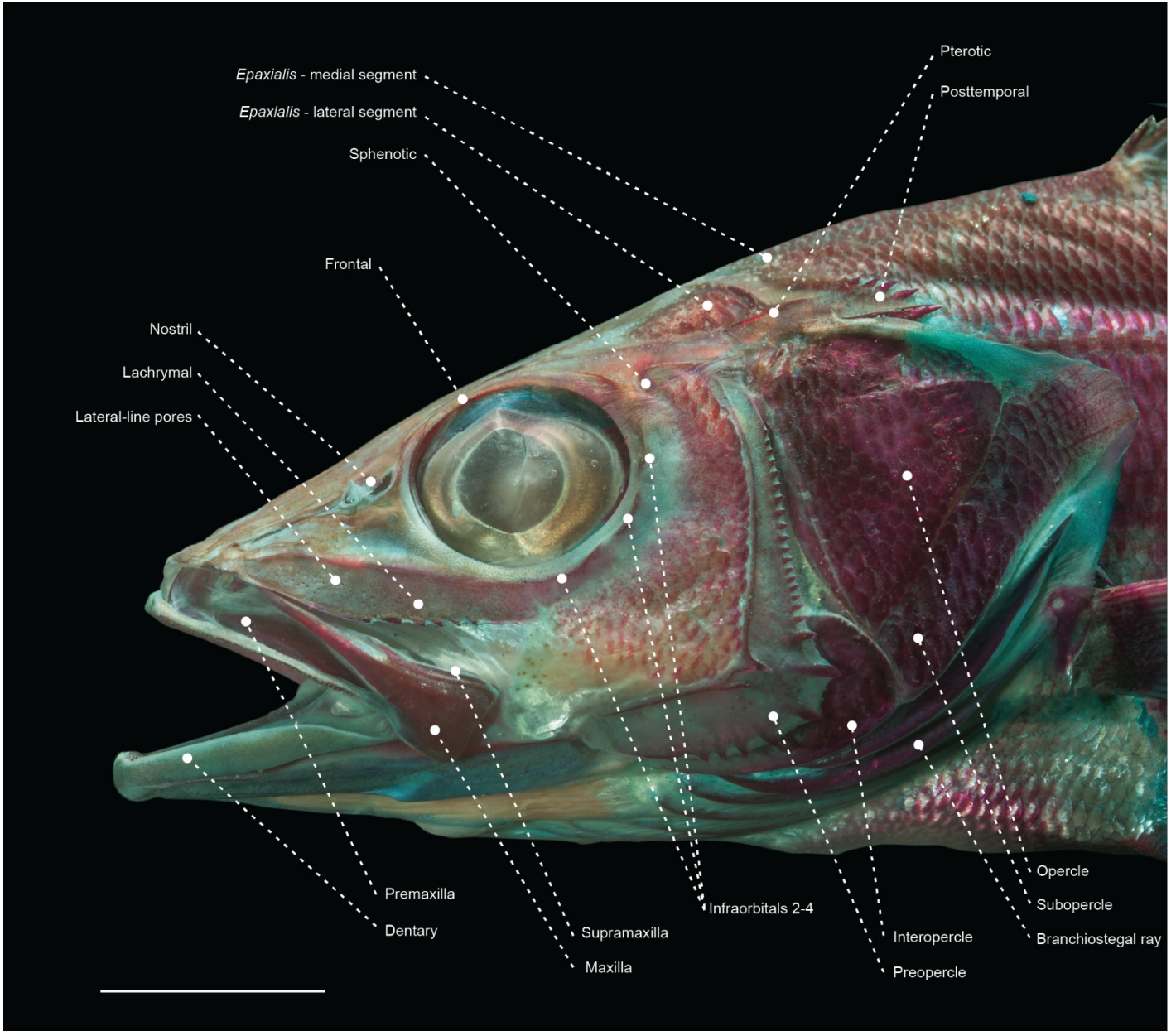


**FIGURE 20:** Head of *Centropomus parallelus* (Centropomidae; MZUSP 108244) in left lateral view. Scale bar: 10 mm.

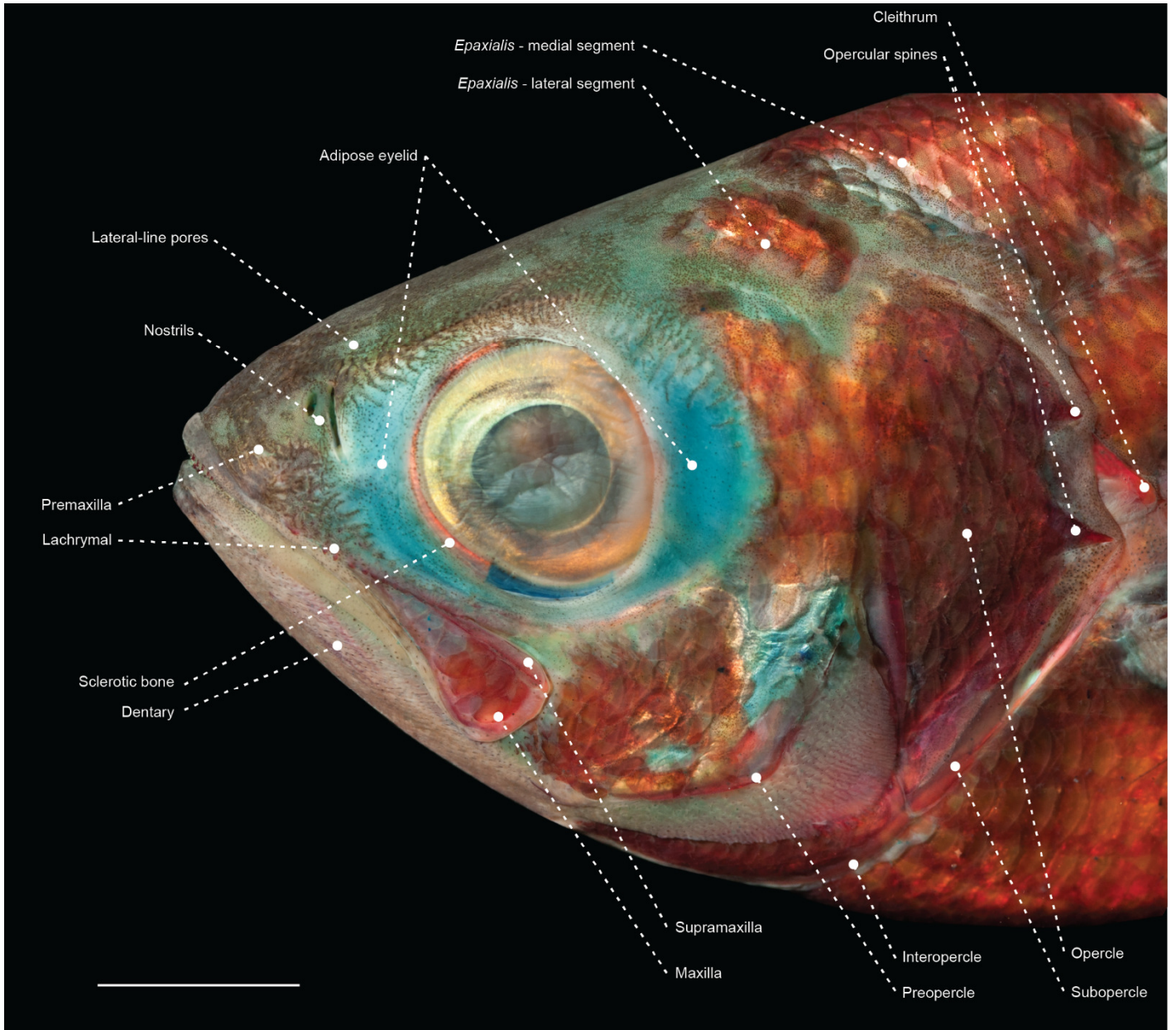


**FIGURE 21:** Head of *Arripis georgianus* (Arripidae; MZUSP 119735) in left lateral view. Scale bar: 10 mm.

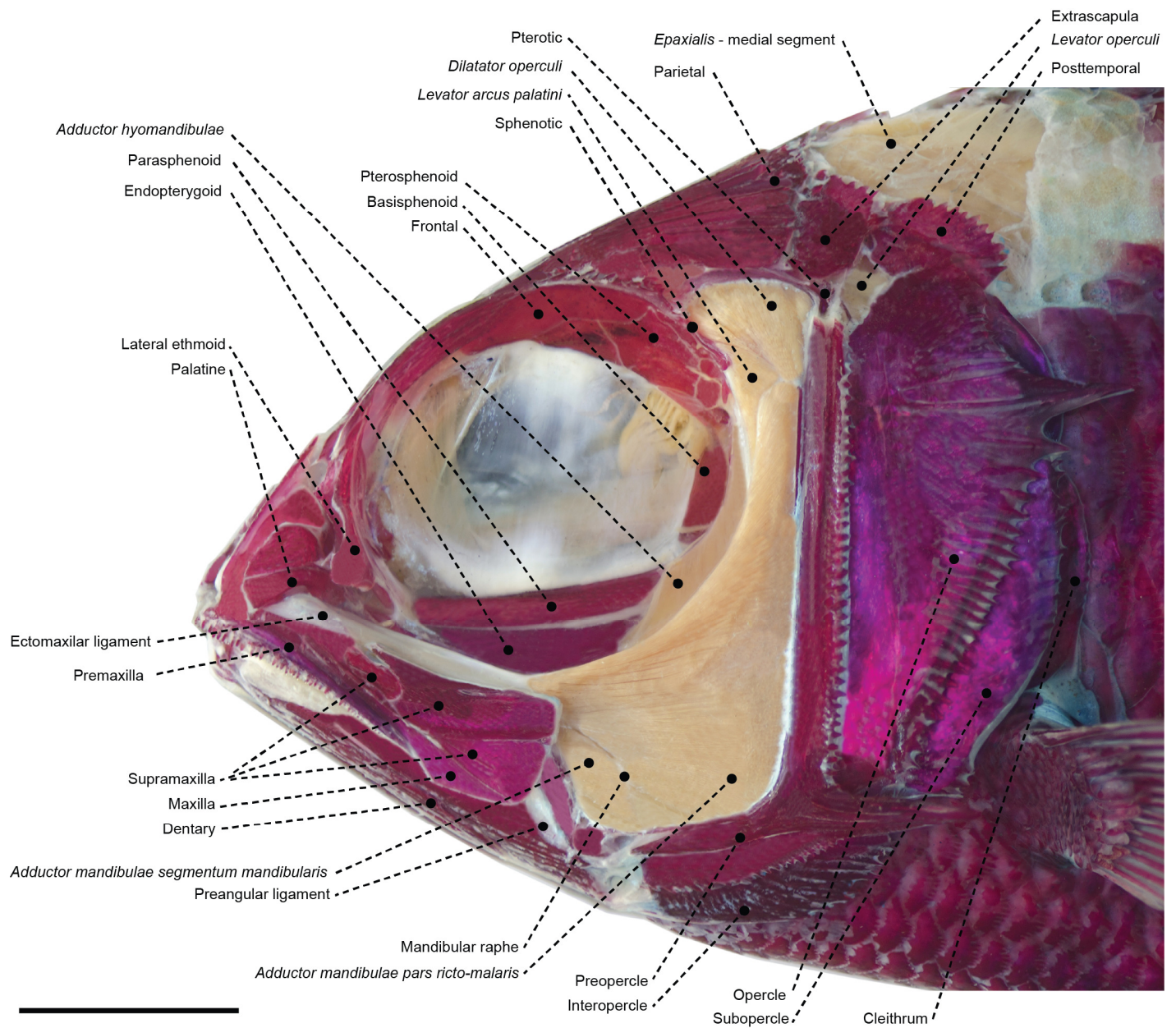


**FIGURE 22:** Superficial cranial musculoskeletal system of *Holocentrus adscencionis* (Holocentridae: MZUSP 69190) in left lateral view. Eye and infraorbital series removed. Scale bar: 7 mm.

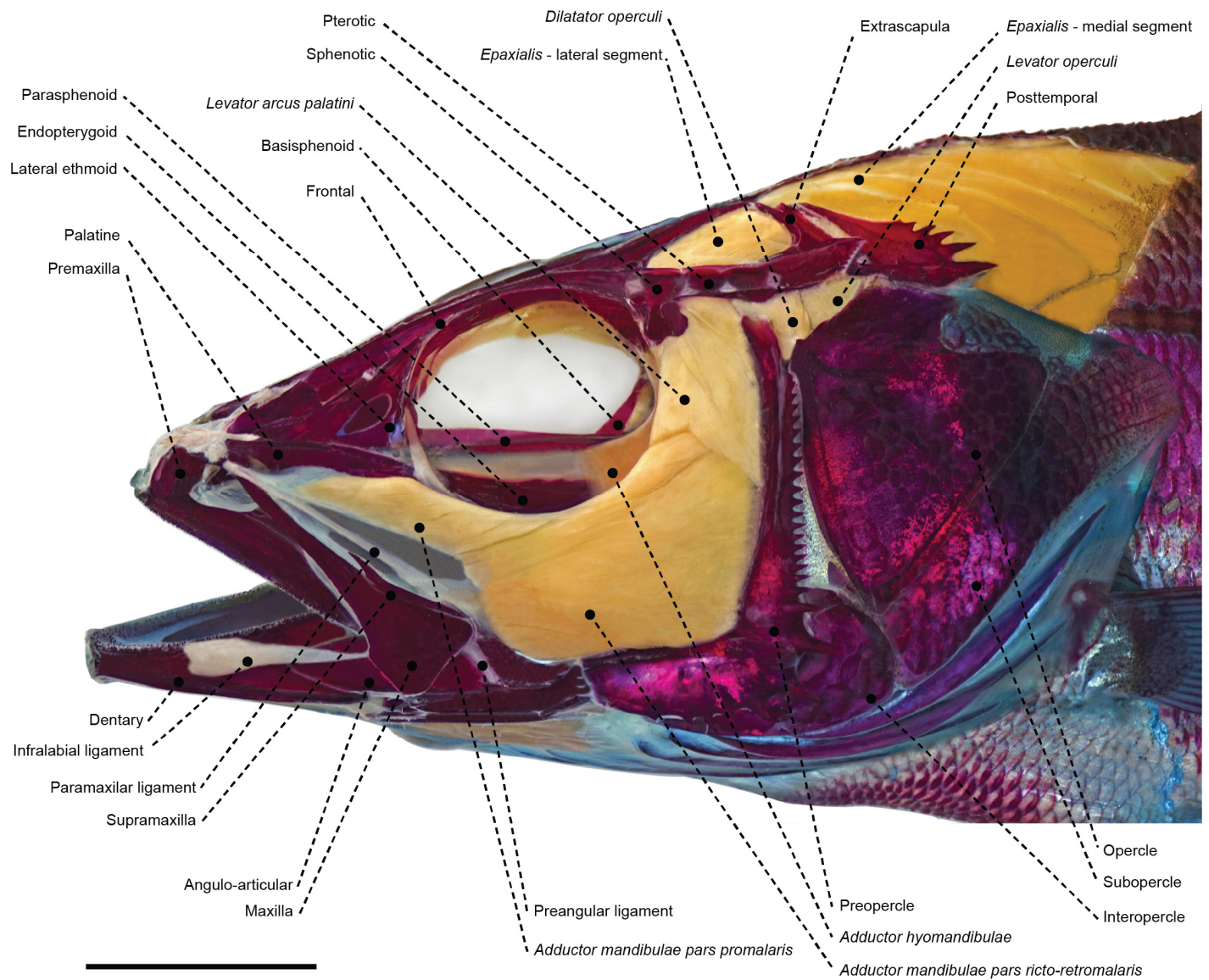


**FIGURE 23:** Superficial cranial musculoskeletal system of *Centropomus parallelus* (Centropomidae: MZUSP 108244) in left lateral view. Eye and infraorbital series removed. Scale bar: 10 mm.

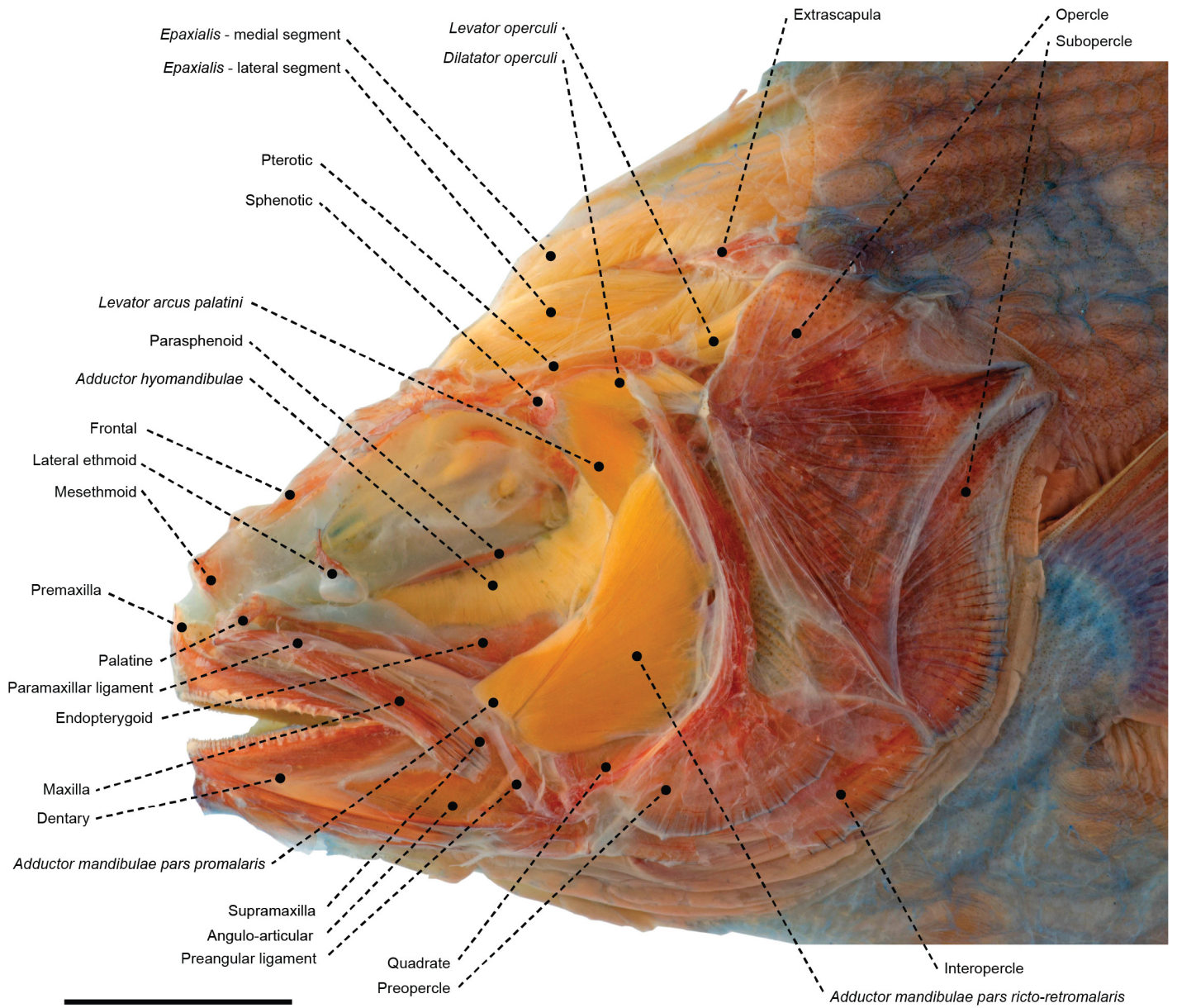


**FIGURE 24:** Superficial cranial musculoskeletal system of *Icichthys lockingtoni* (Centrolophidae: OS 16732) in left lateral view. Eye and infraorbital series removed. Scale bar: 7 mm

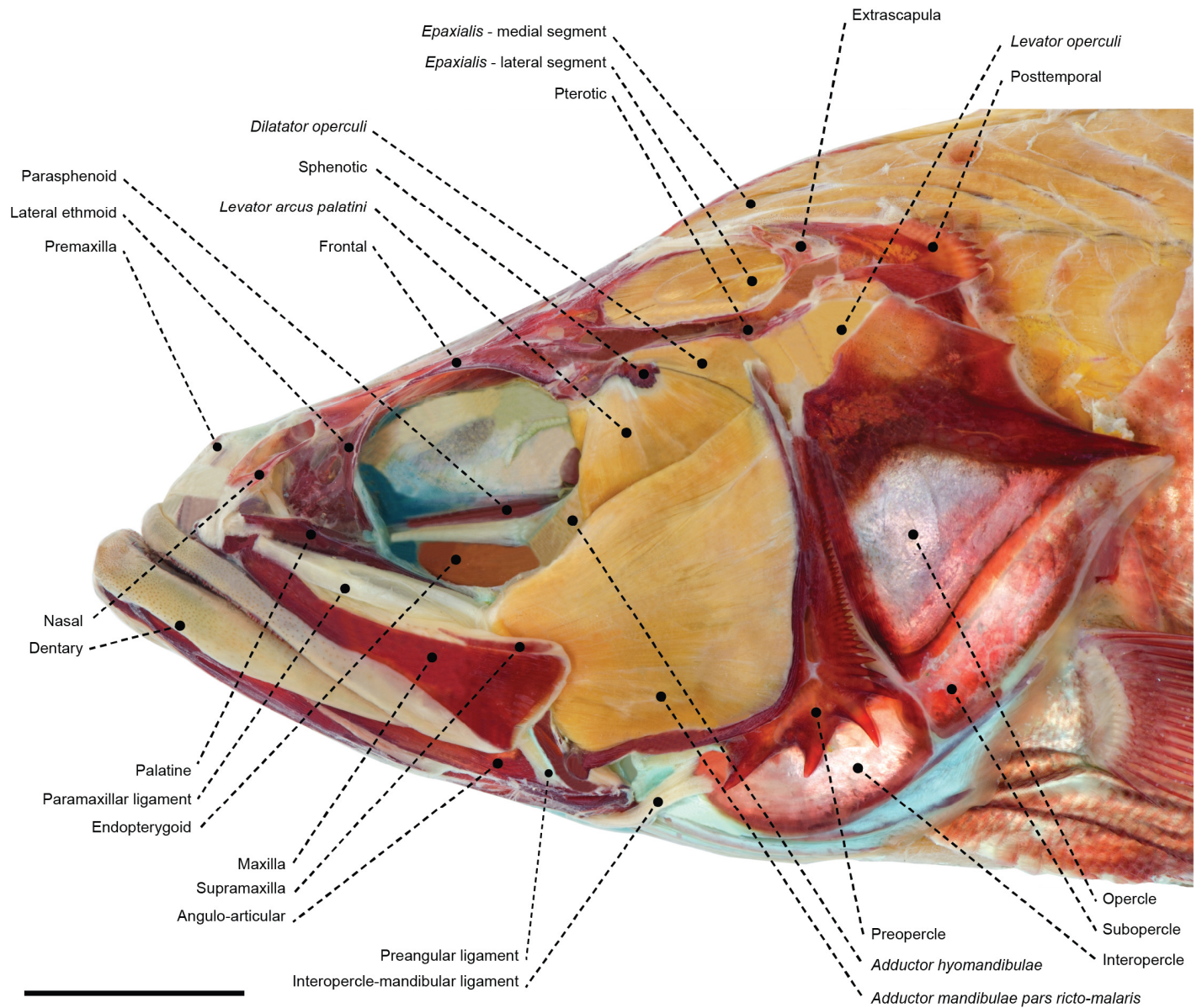


**FIGURE 25:** Superficial cranial musculoskeletal system of *Lateolabrax japonicus* (Lateolabracidae: MZUSP 123245) in left lateral view. Eye and infraorbital series removed. Scale bar: 10 mm.

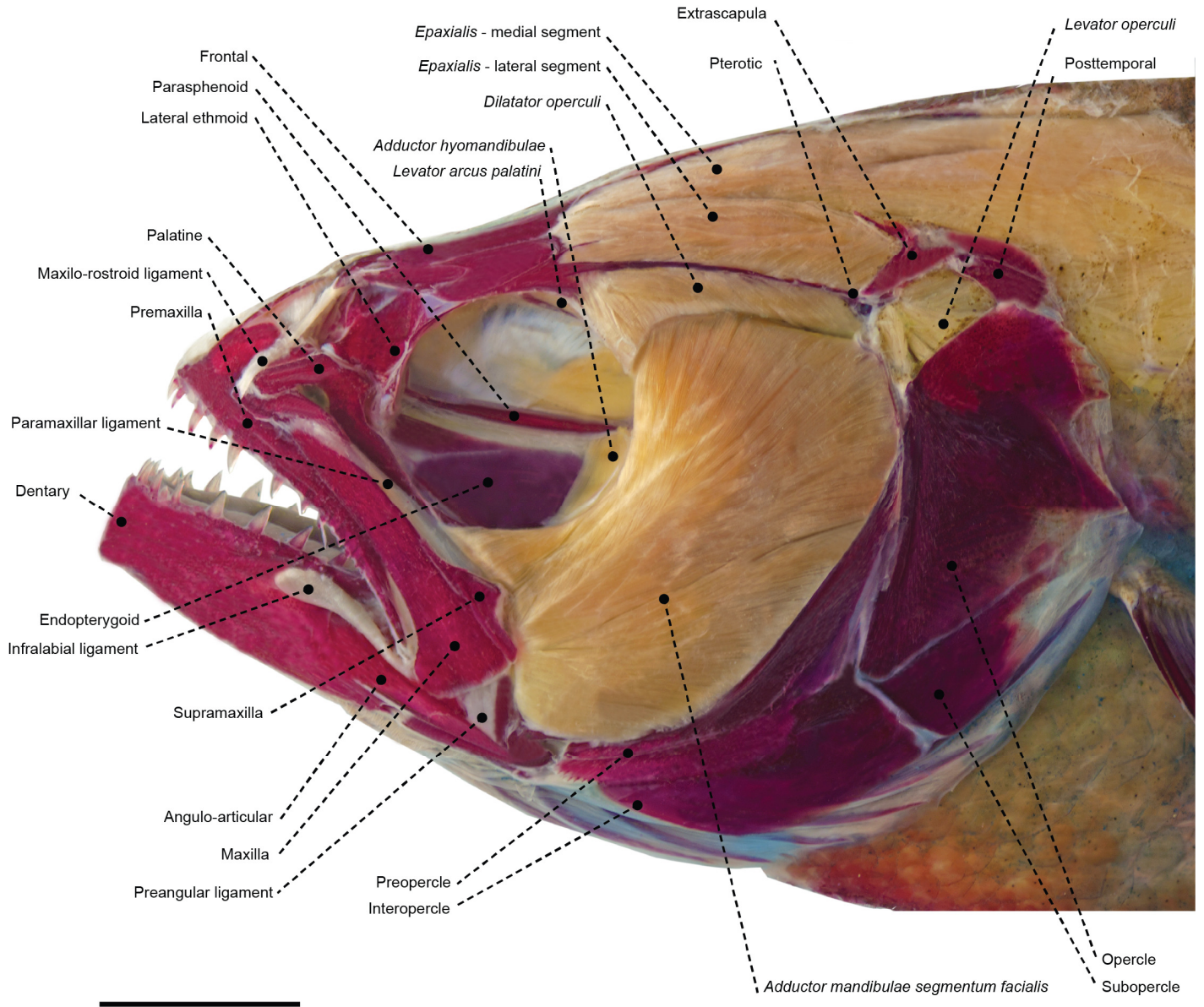


**FIGURE 26:** Superficial cranial musculoskeletal system of *Pomatomus saltatrix* (Pomatomidae: MZUSP 69784) in left lateral view. Eye and infraorbital series removed. Scale bar: 7 mm.

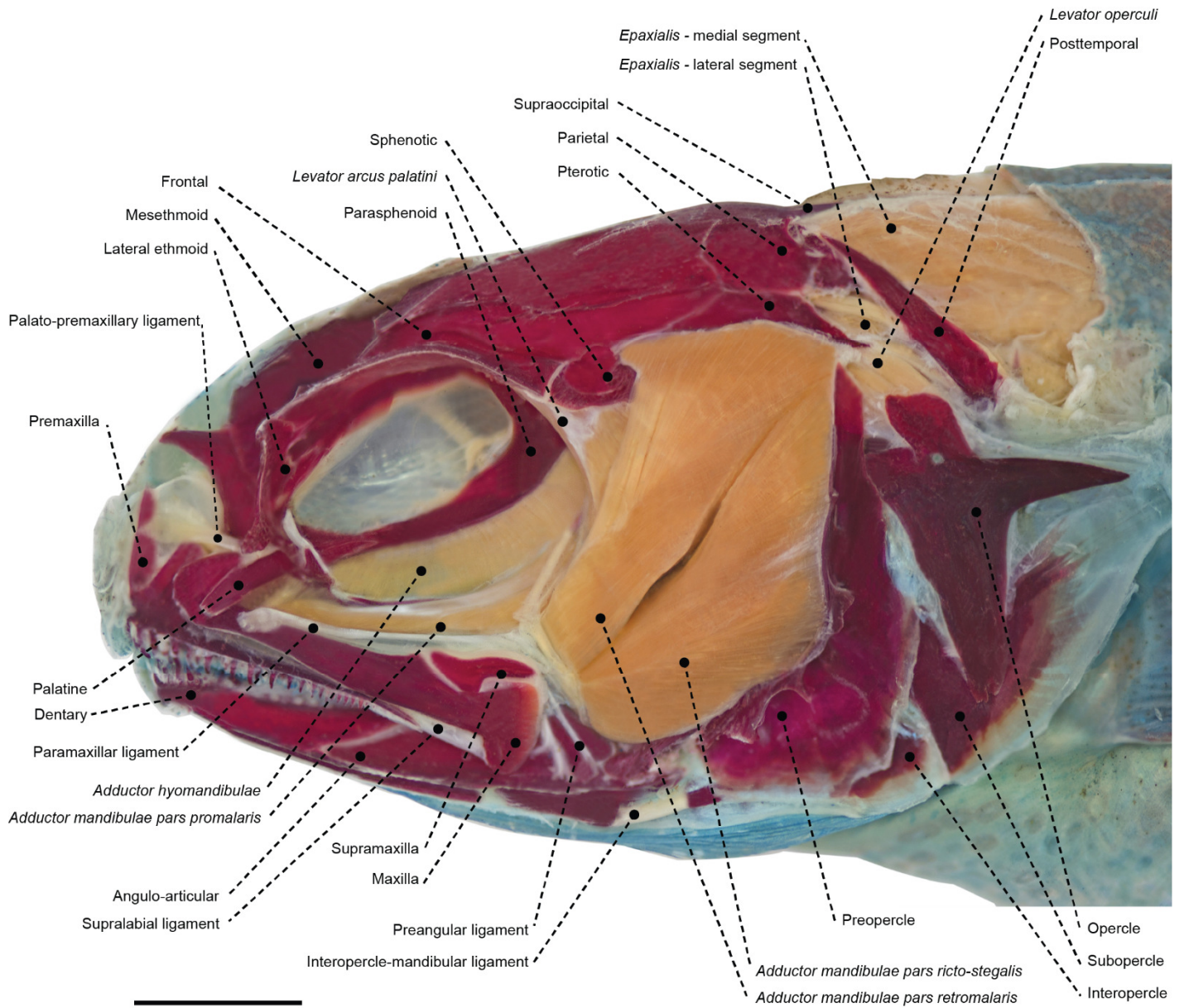


**FIGURE 27:** Superficial cranial musculoskeletal system of *Raneya brasiliensis* (Ophidiidae: MZUSP 61358) in left lateral view. Eye and infraorbital series removed. Scale bar: 5 mm.

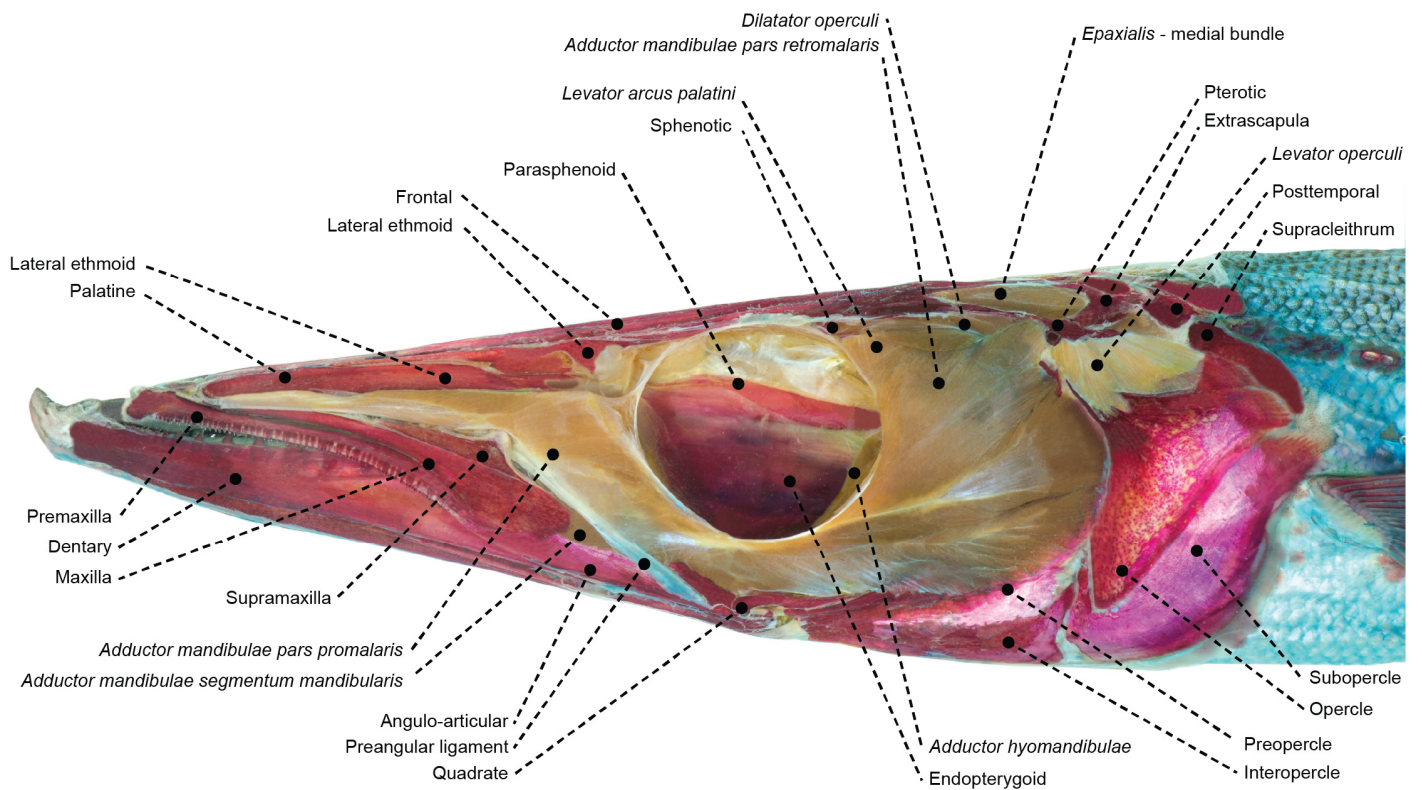


**FIGURE 28:** Superficial cranial musculoskeletal system of *Sphyraena tome* (Sphyraenidae: MZUSP 47562) in left lateral view. Eye and infraorbital series removed. Scale bar: 10 mm.

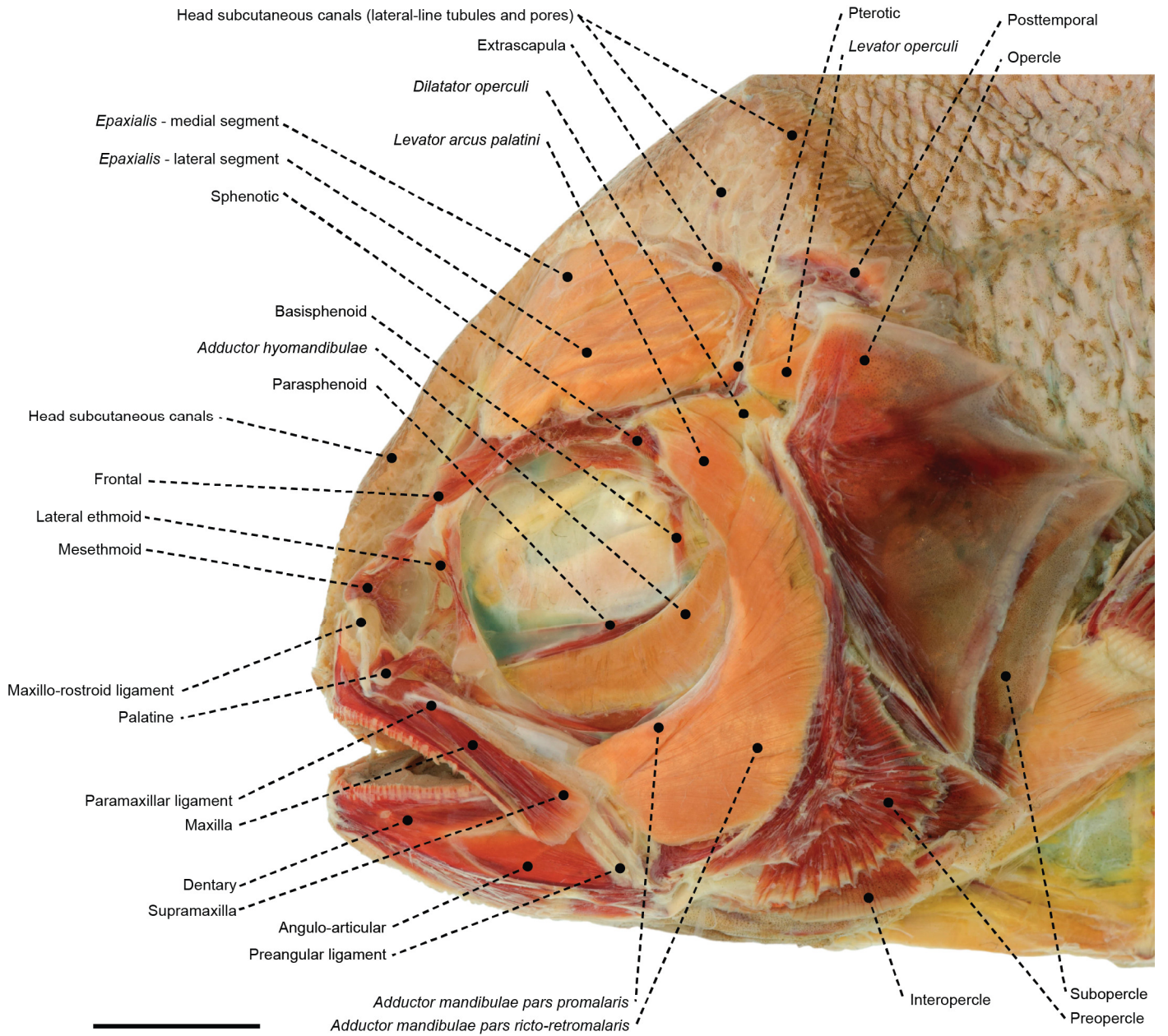


**FIGURE 29:** Superficial cranial musculoskeletal system of *Hyperoglyphe perciformis* (Centrolophidae: MZUSP 119733) in left lateral view. Eye and infraorbital series removed. Scale bar: 10 mm.

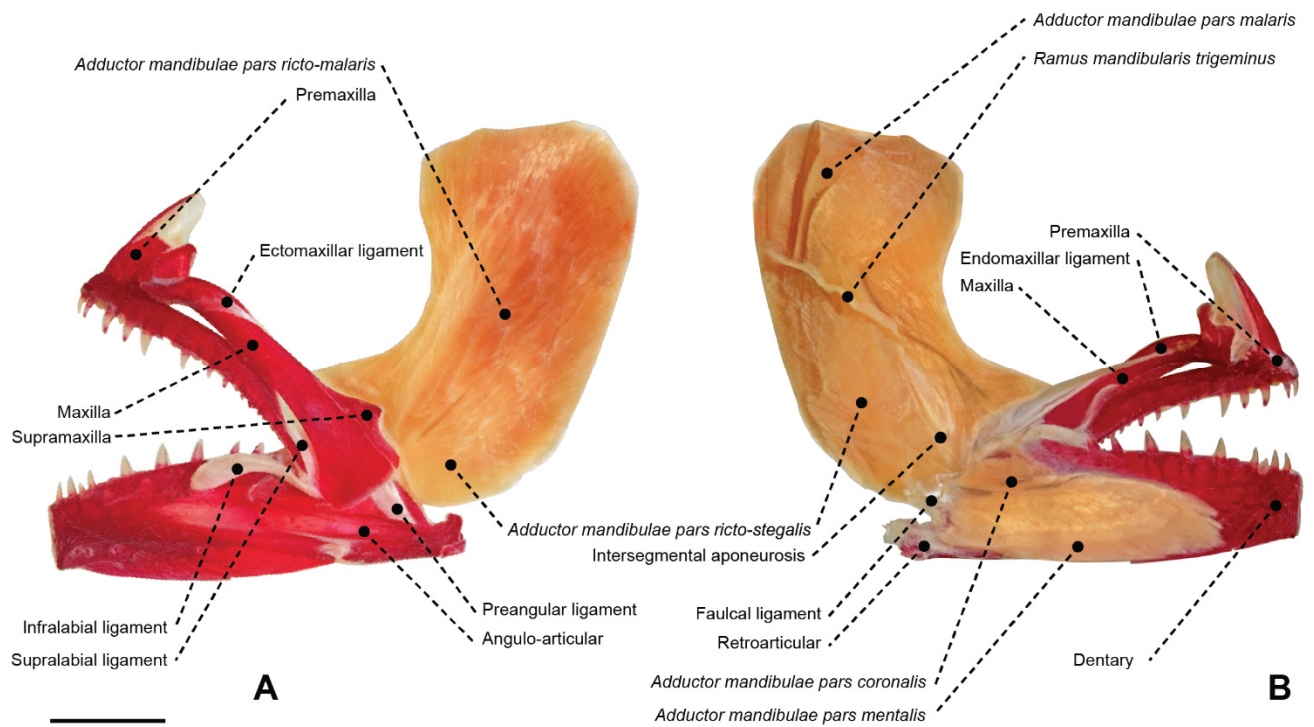


**FIGURE 30:** Left *adductor mandibulae* and associated structures of *Pomatomus saltatrix* (Pomatomidae: MZUSP 69784) in (A) lateral and (B) medial views. Scale bar: 5 mm.

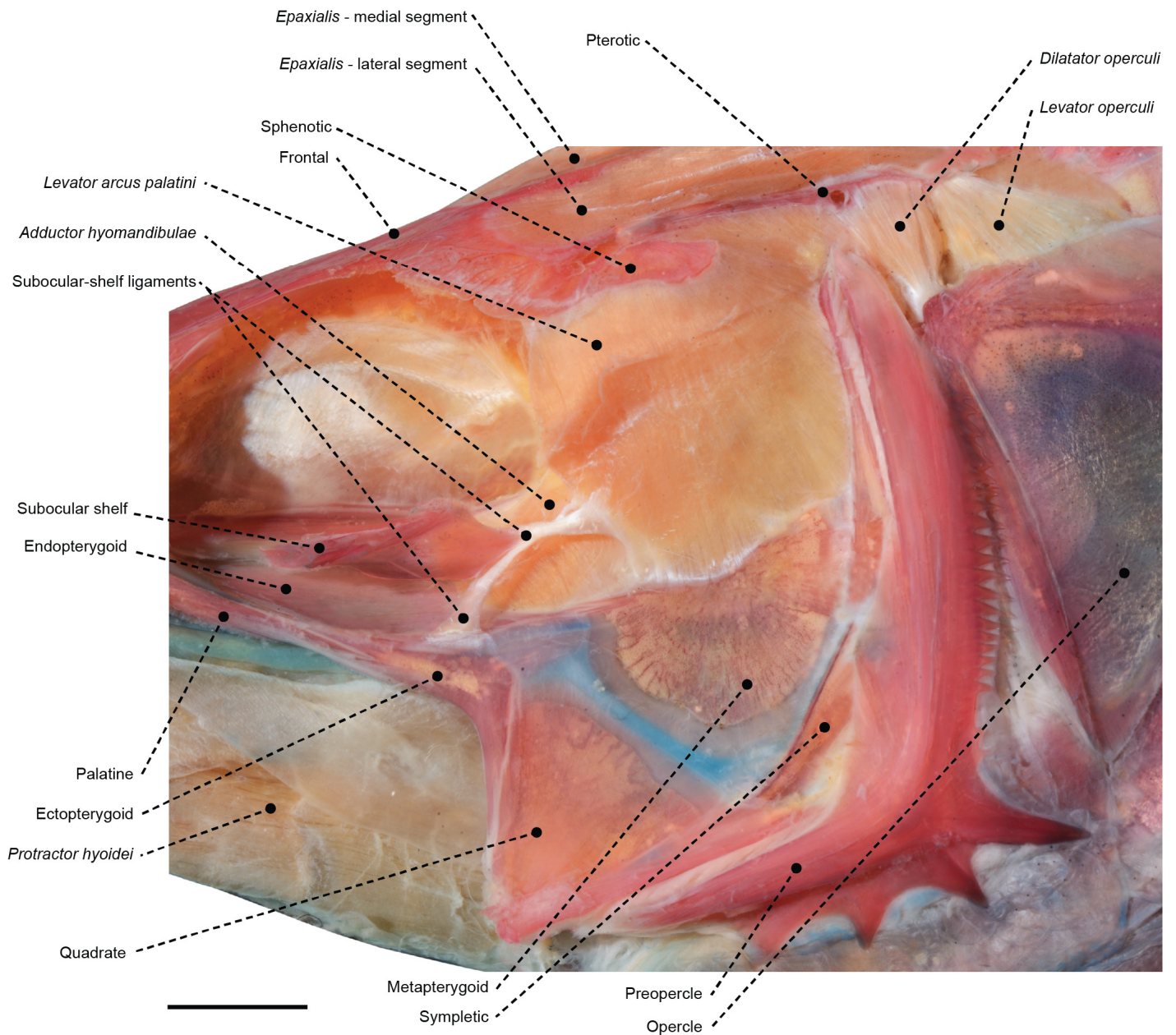


**FIGURE 31:** Inset of palatal region of *Lates niloticus* (Latidae: MZUSP 123243) in left lateral view exhibiting associated muscles and bones. Eye, infraorbital series, and *adductor mandibulae* complex removed. Note the subocular shelf kept in place by ligamentous contact to the endopterygoid (anteriorly) and to the *levator arcus palatini* (posteriorly). Scale bar: 5 mm.

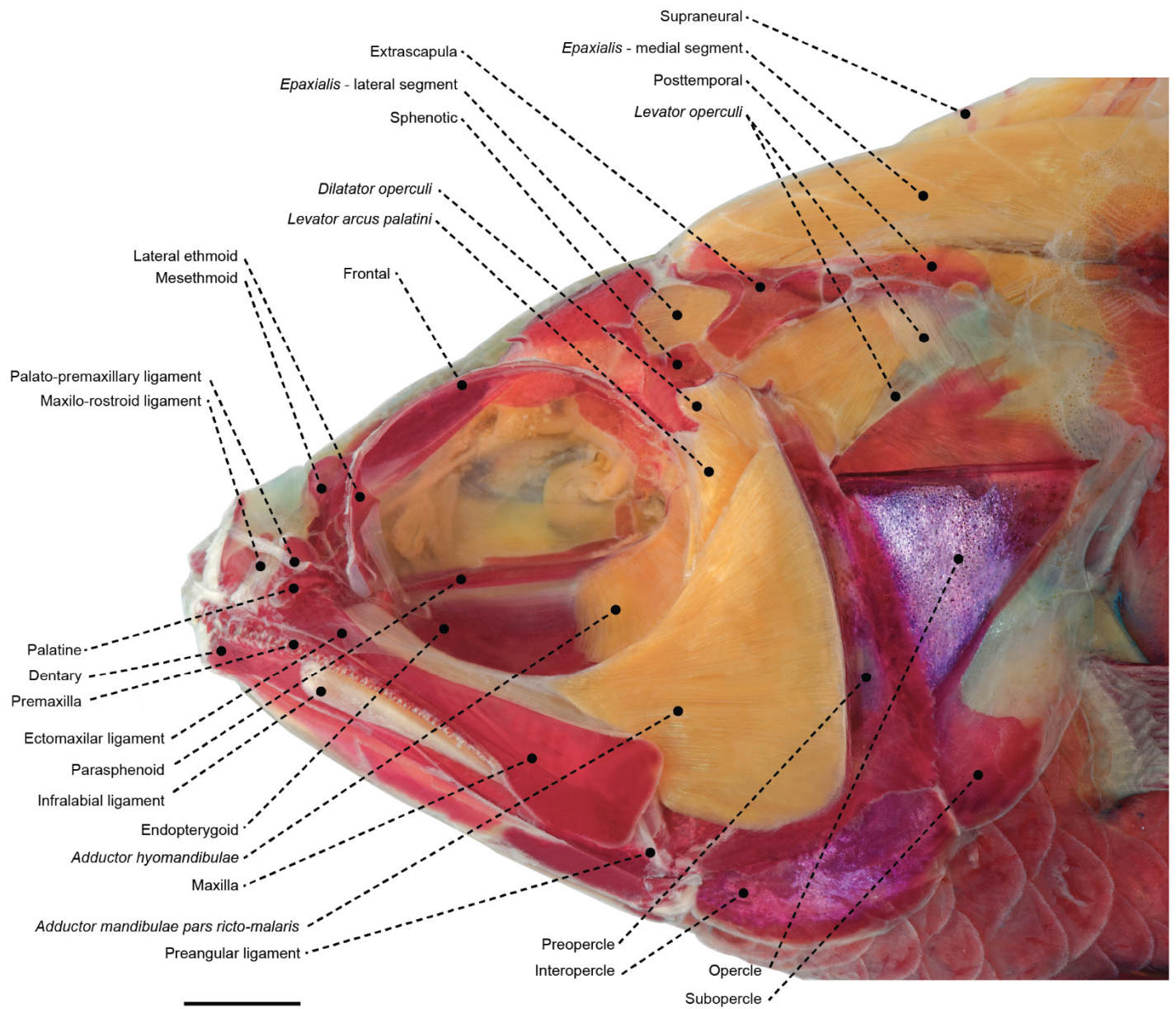


**FIGURE 32:** Superficial cranial musculoskeletal system of *Apogon maculatus* (Apogonidae: MZUSP 43155) in left lateral view. Eye and infraorbital series removed. Scale bar: 3 mm.

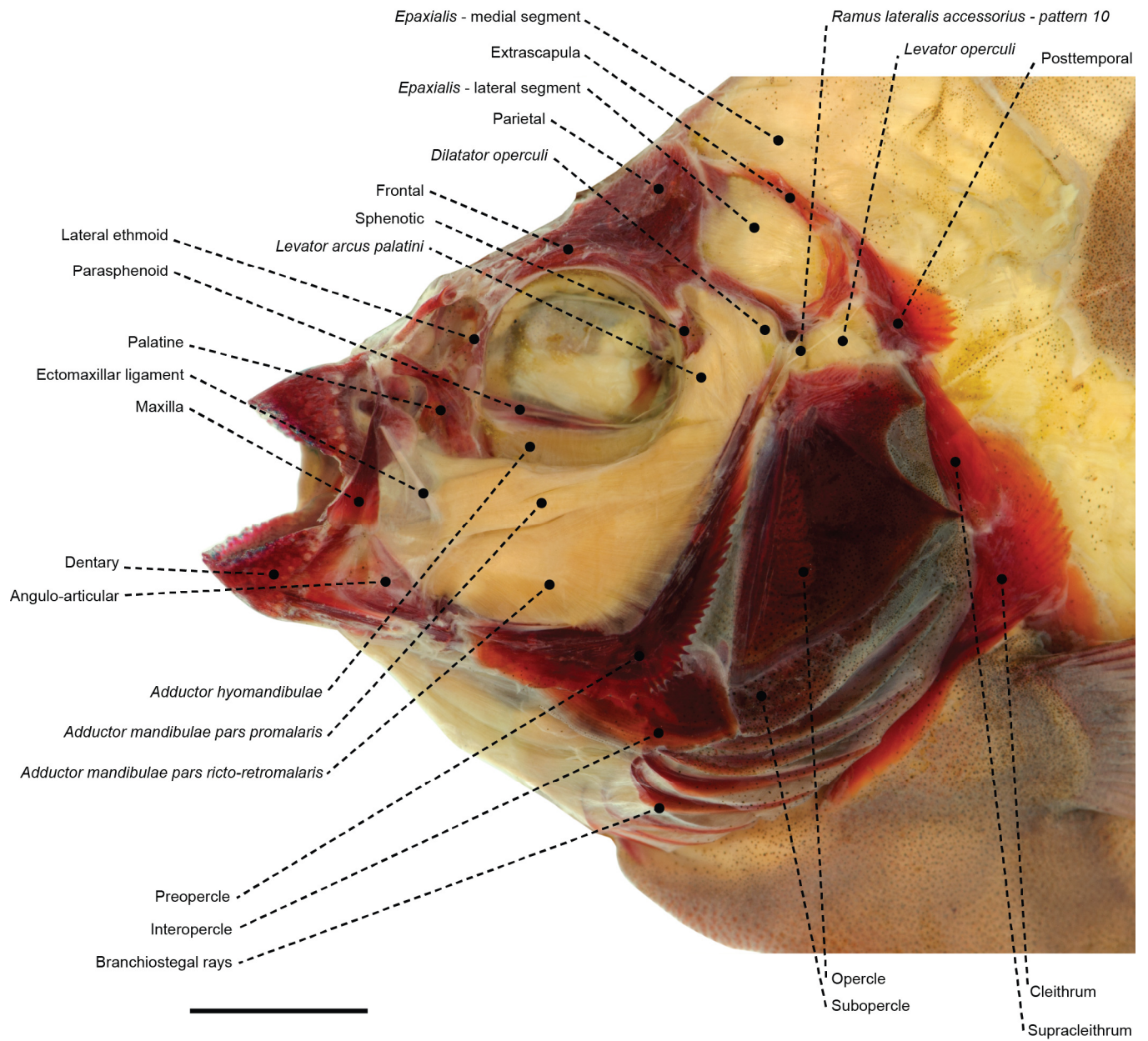


**FIGURE 33:** Superficial cranial musculoskeletal system of *Oplegnathus fasciatus* (Oplegnathidae: MZUSP 28867) in left lateral view. Eye and infraorbital series removed. Scale bar: 4 mm.

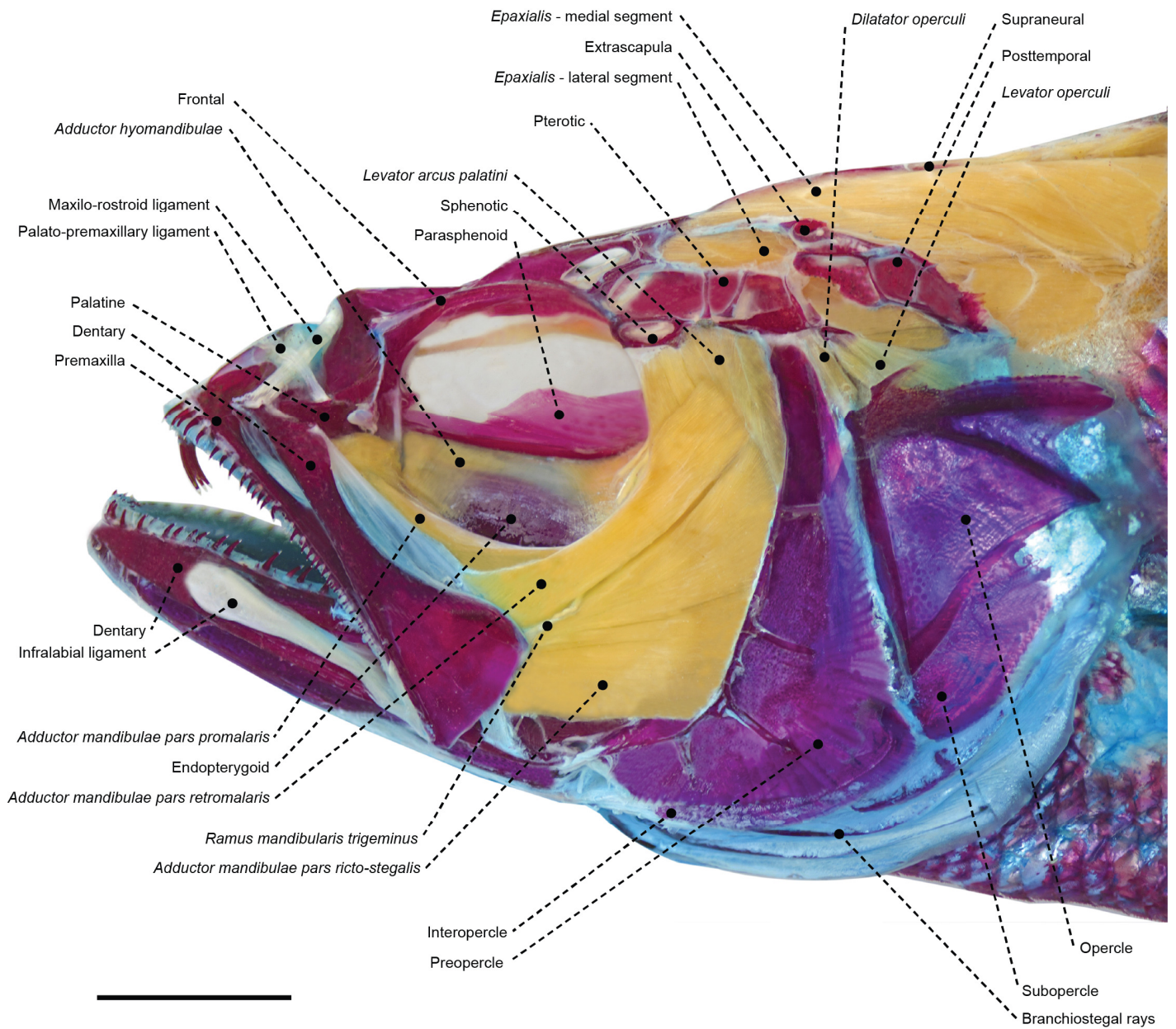


**FIGURE 34:** Superficial cranial musculoskeletal system of *Cynoscion striatus* (Sciaenidae: MZUSP 68913) in left lateral view. Eye and infraorbital series removed. Scale bar: 8 mm.

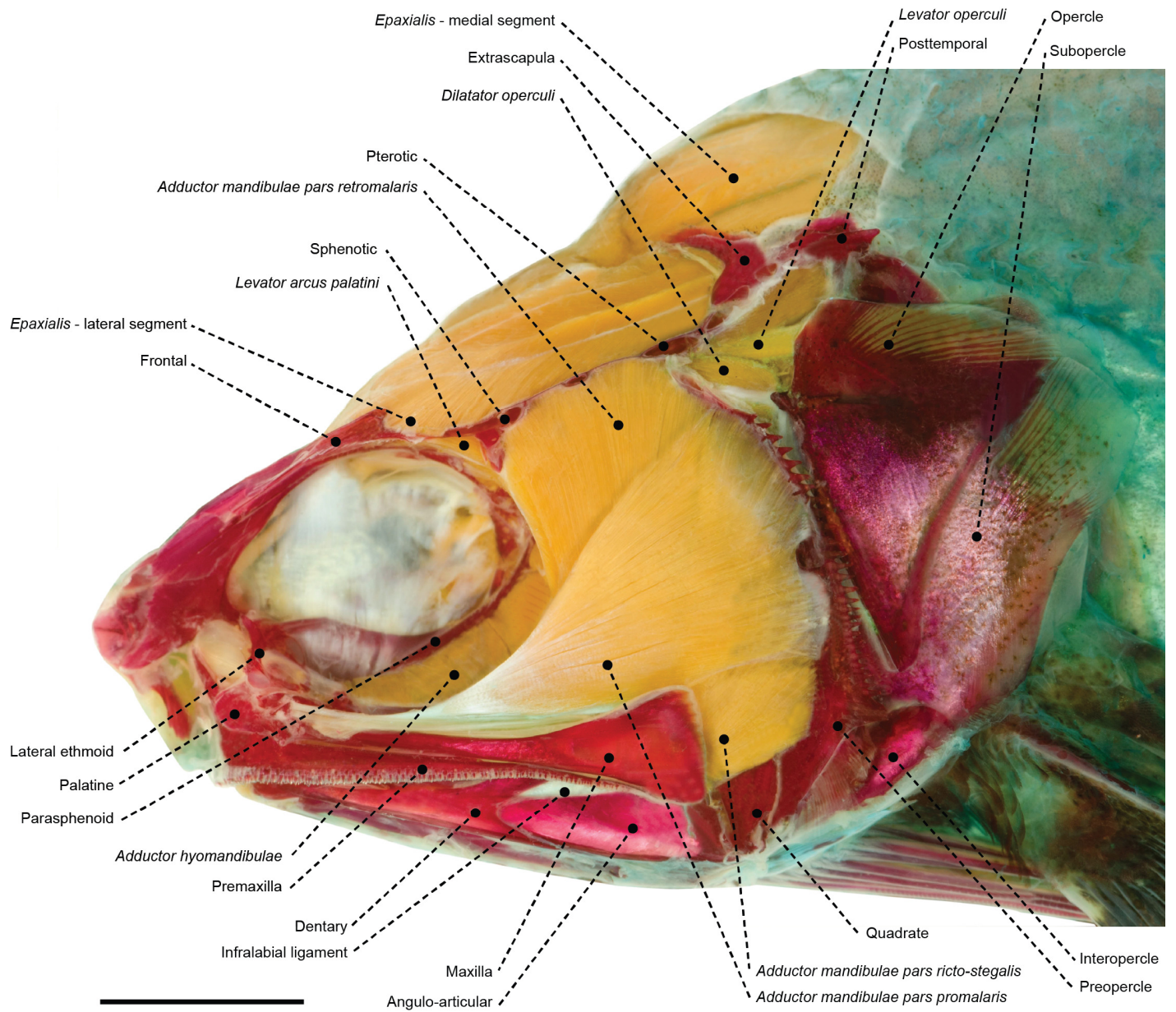


**FIGURE 35:** Superficial cranial musculoskeletal system of *Polydactylus virginicus* (Polynemidae: MZUSP 67549) in left lateral view. Eye and infraorbital series removed. Scale bar: 6 mm.

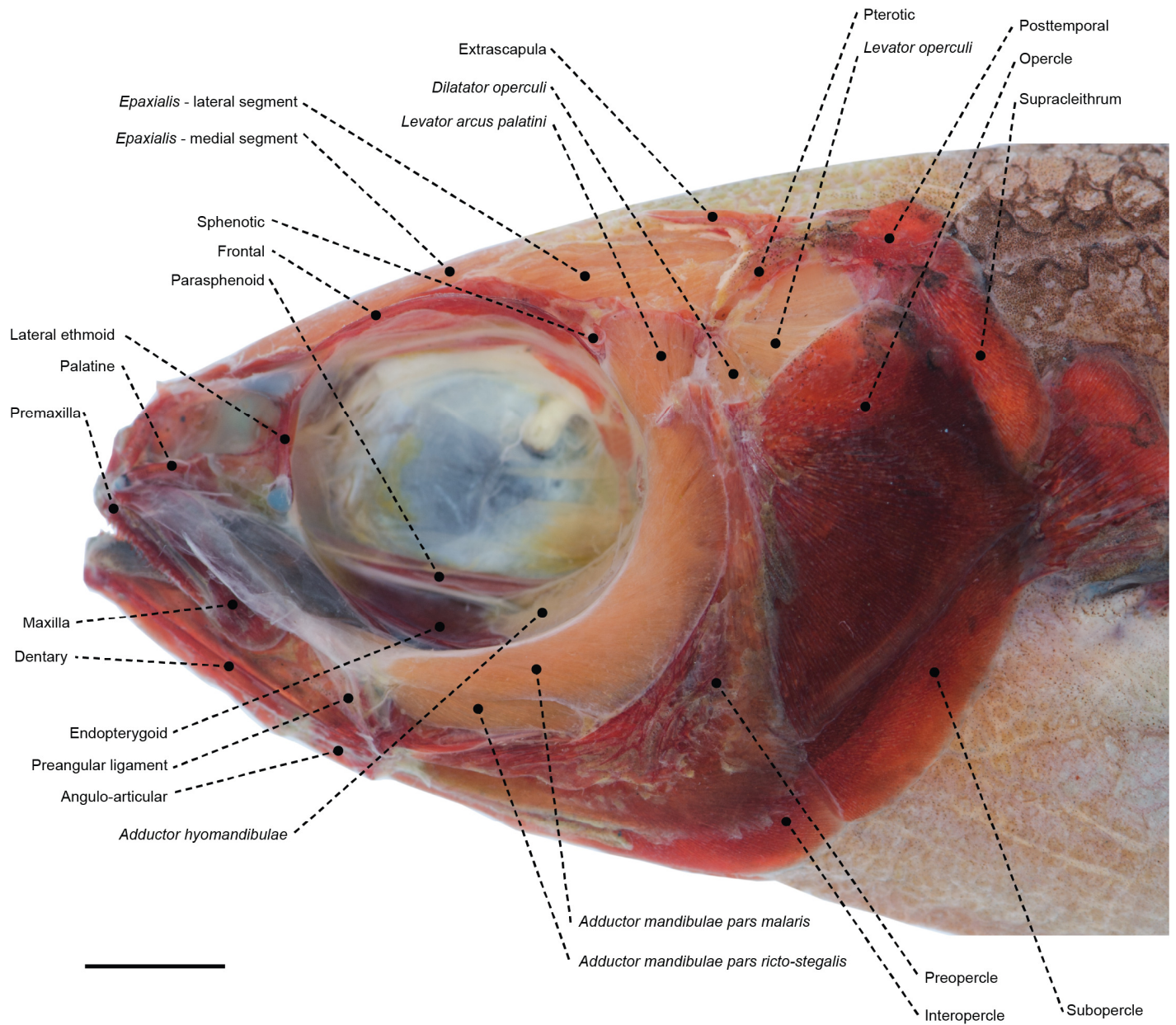


**FIGURE 36:** Superficial cranial musculoskeletal system of *Cubiceps pauciradiatus* (Nomeidae: MZUSP 80701) in left lateral view. Eye and infraorbital series removed. Scale bar: 5 mm.

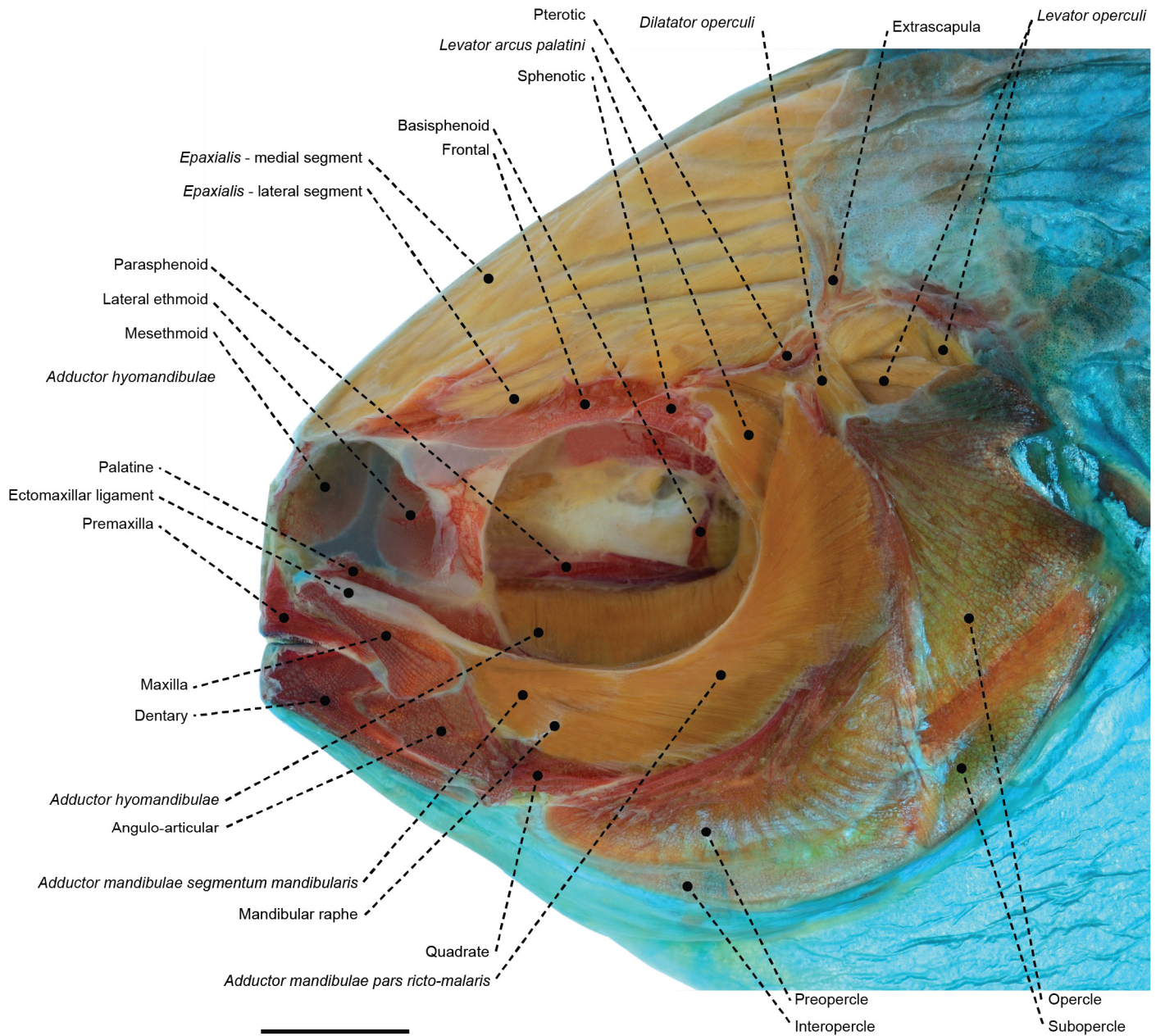


**FIGURE 37.** Superficial cranial musculoskeletal system of *Stromateus brasiliensis* (Stromateidae: MZUSP 51279) in left lateral view. Eye, infraorbital series, and RLA nerve removed. Scale bar: 5 mm.

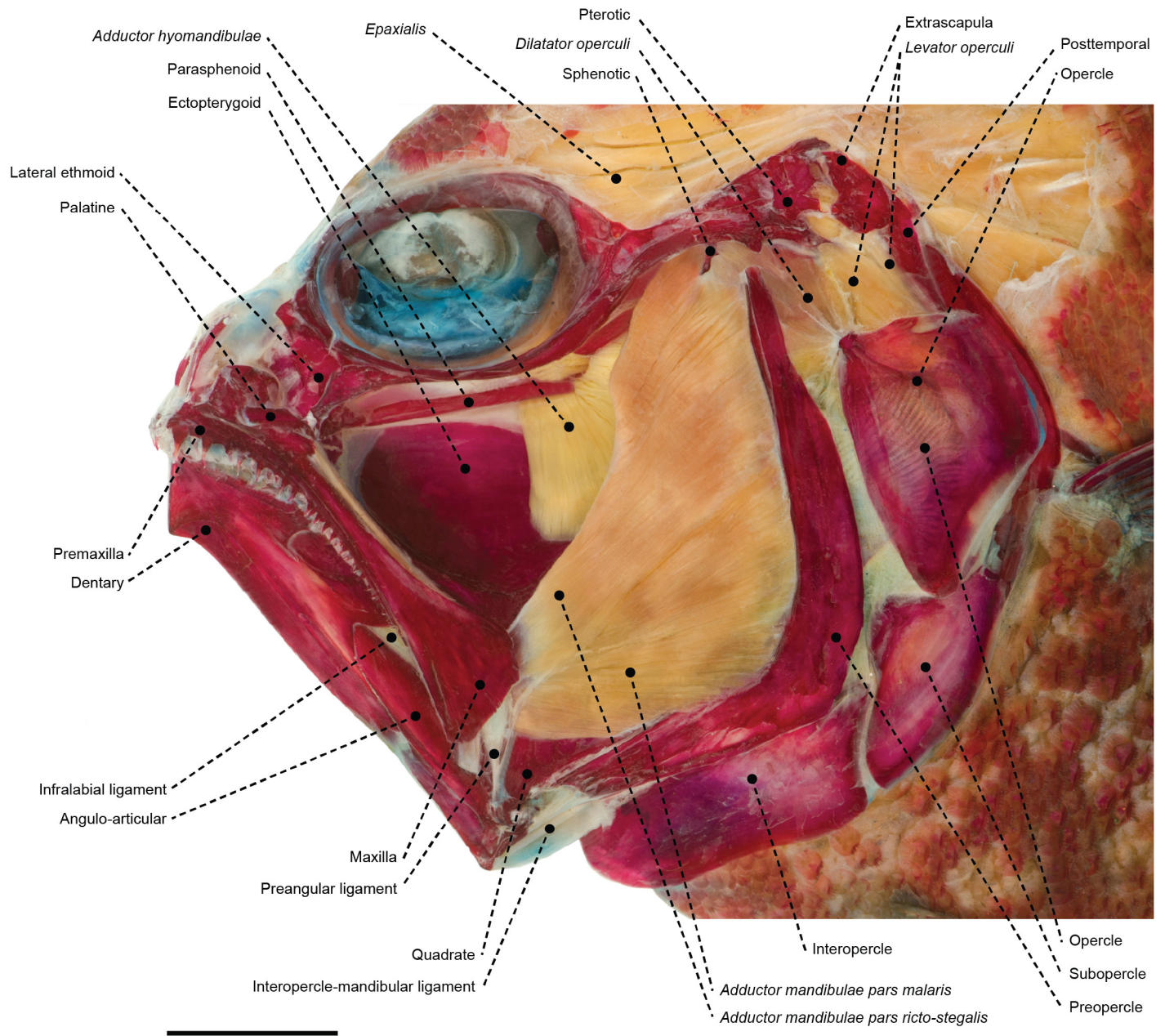


**FIGURE 38:** Superficial cranial musculoskeletal system of *Paralichthys isosceles* (Paralichthyidae: MZUSP 72323) in left lateral view. Eye and infraorbital series removed. Scale bar: 8 mm.

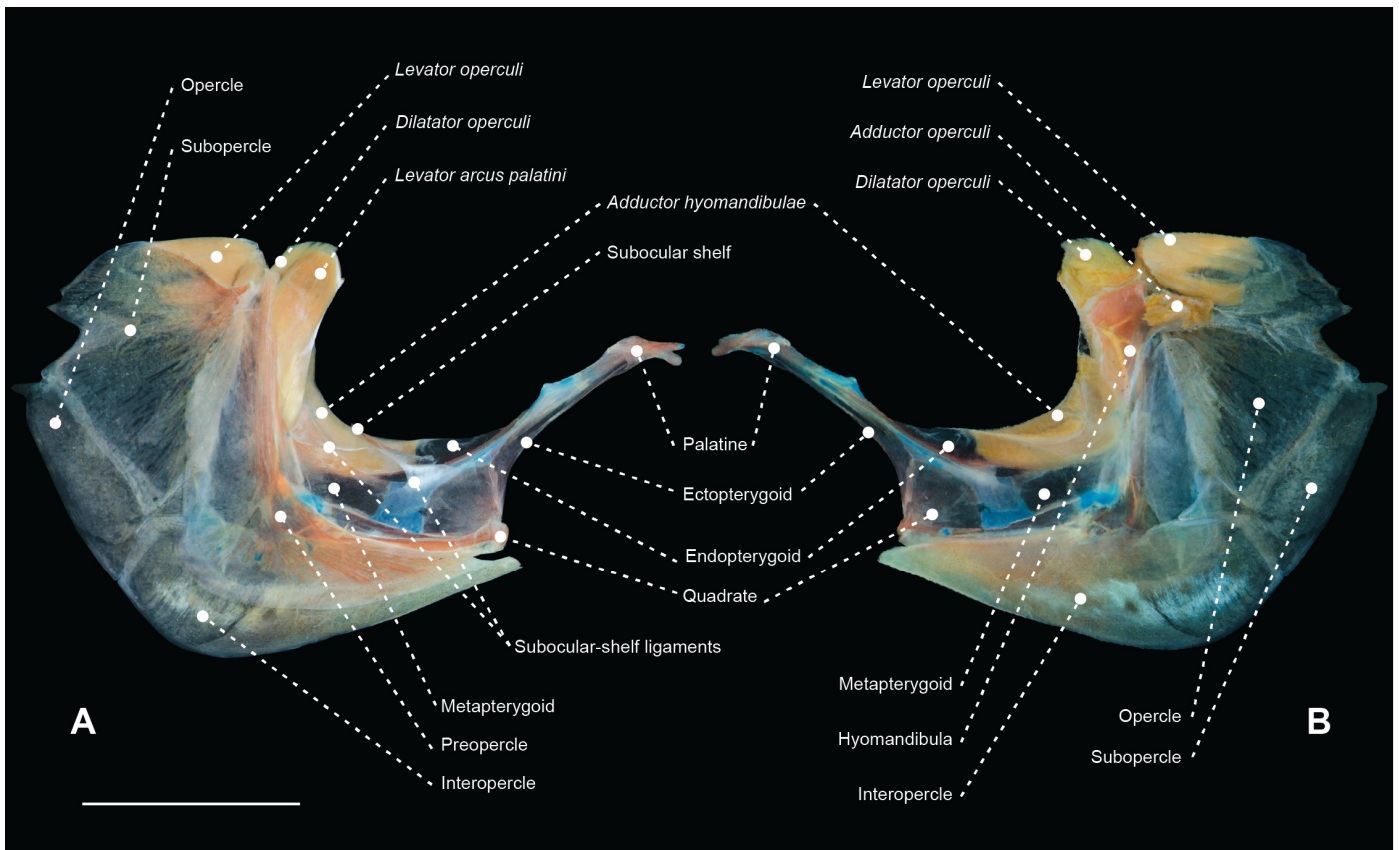


**FIGURE 39.** Hyopalatine arch, opercular series, and associated musculature of *Ariomma melanum* (Ariommatidae: MZUSP 123246) in (A) lateral and (B) medial views. Scale bar: 10 mm.

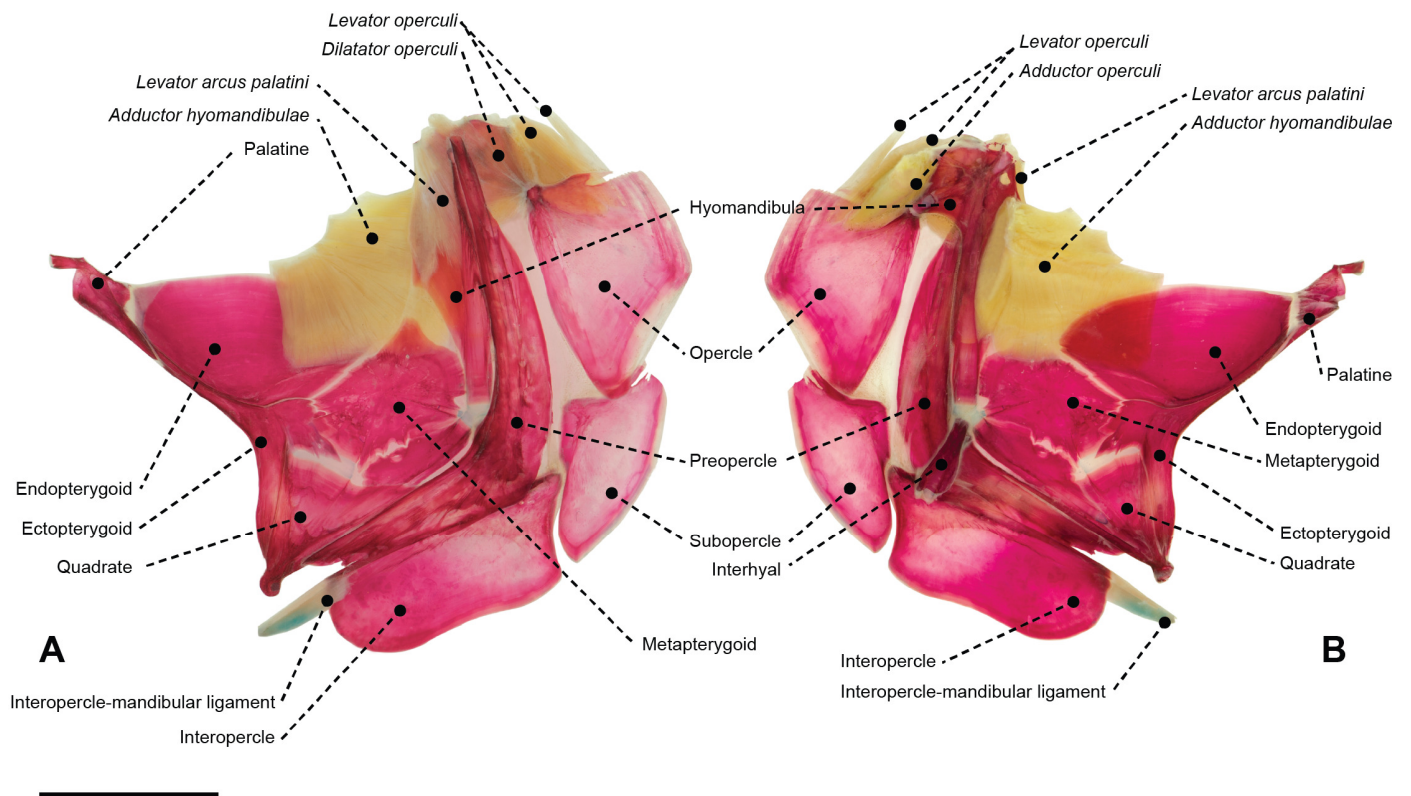


**FIGURE 40.** Hyopalatine arch, opercular series, and associated musculature of *Paralichthys isosceles* (Paralichthyidae: MZUSP 72323) in (A) lateral and (B) medial views. Scale bar: 10 mm.

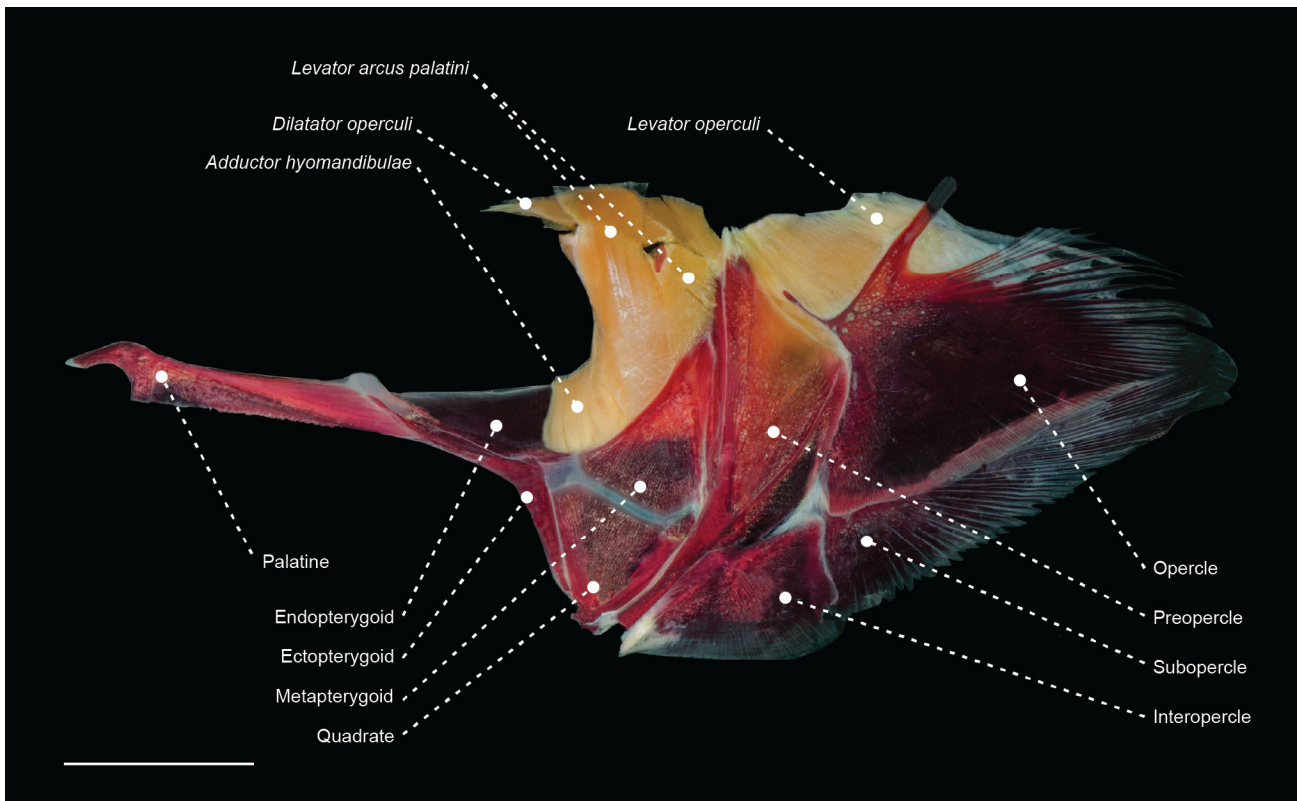


**FIGURE 41.** Hyopalatine arch, opercular series, and associated musculature of *Trichiurus lepturus* (Trichiuridae: MZUSP 8855) in lateral view. Scale bar: 8 mm.

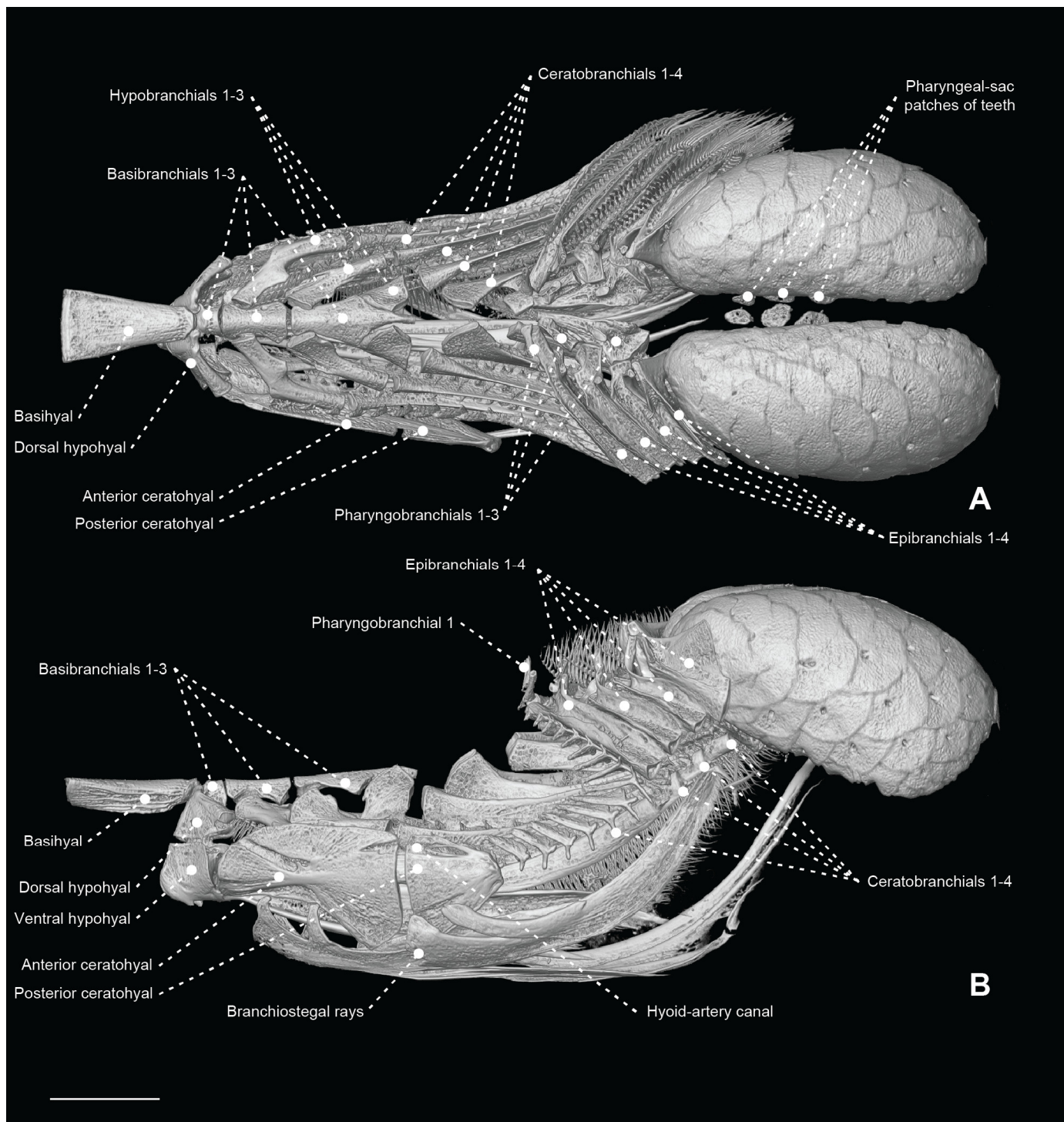


**FIGURE 42.** Micro CT scanning of the branchial and pharyngeal-sac skeleton of *Ariomma bondi* (Ariommatidae: MZUSP 86717) in dorsal (A) and lateral views (B). Scale bar: 4 mm.

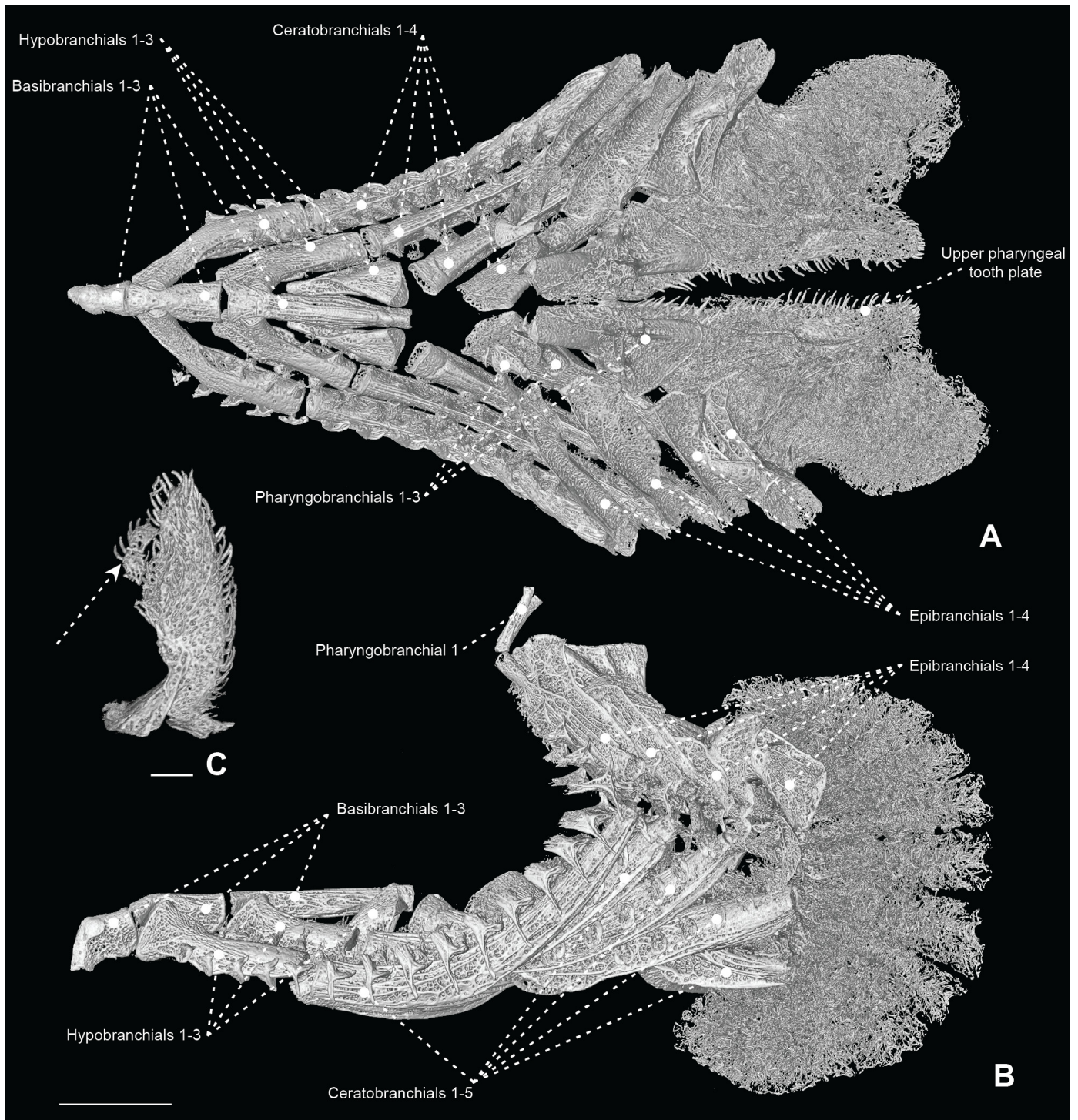


**FIGURE 43.** Micro CT scanning of the branchial and pharyngeal-sac skeleton of *Tubbia tasmanica* (Centrolophidae: CSIRO H 6979-03) in dorsal (A) and lateral views (B). Scale bar: 7 mm. A magnification of an enlarged raker associated to epibranchial 4 and ceratobranchial 5 is shown in C. Arrow indicates small pharyngeal-sac rakers associated to the large epibranchial raker. Scale bar: 2 mm.

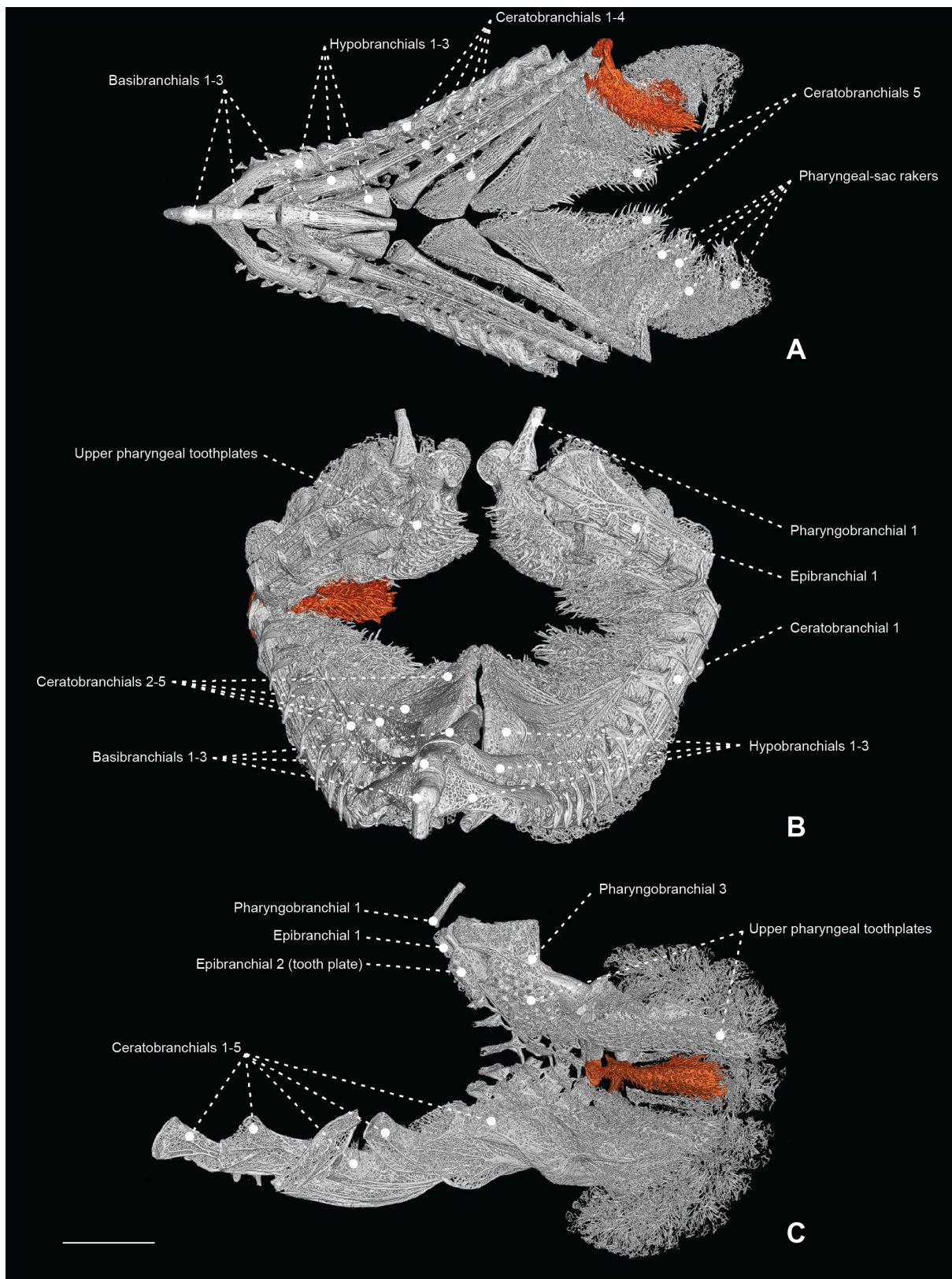


**FIGURE 44.** Micro CT scanning of the branchial and pharyngeal-sac skeleton of *Tubbia tasmanica* (Centrolophidae: CSIRO H 6979-03). A) dorsal view, dorsal gill-arch elements removed; B) frontal view.; C) Parasagittal view, gill arch elements of the right side removed. A raker associated to epibranchial 4 and ceratobranchial 4 is highlighted in orange. Scale bar: 7 mm.

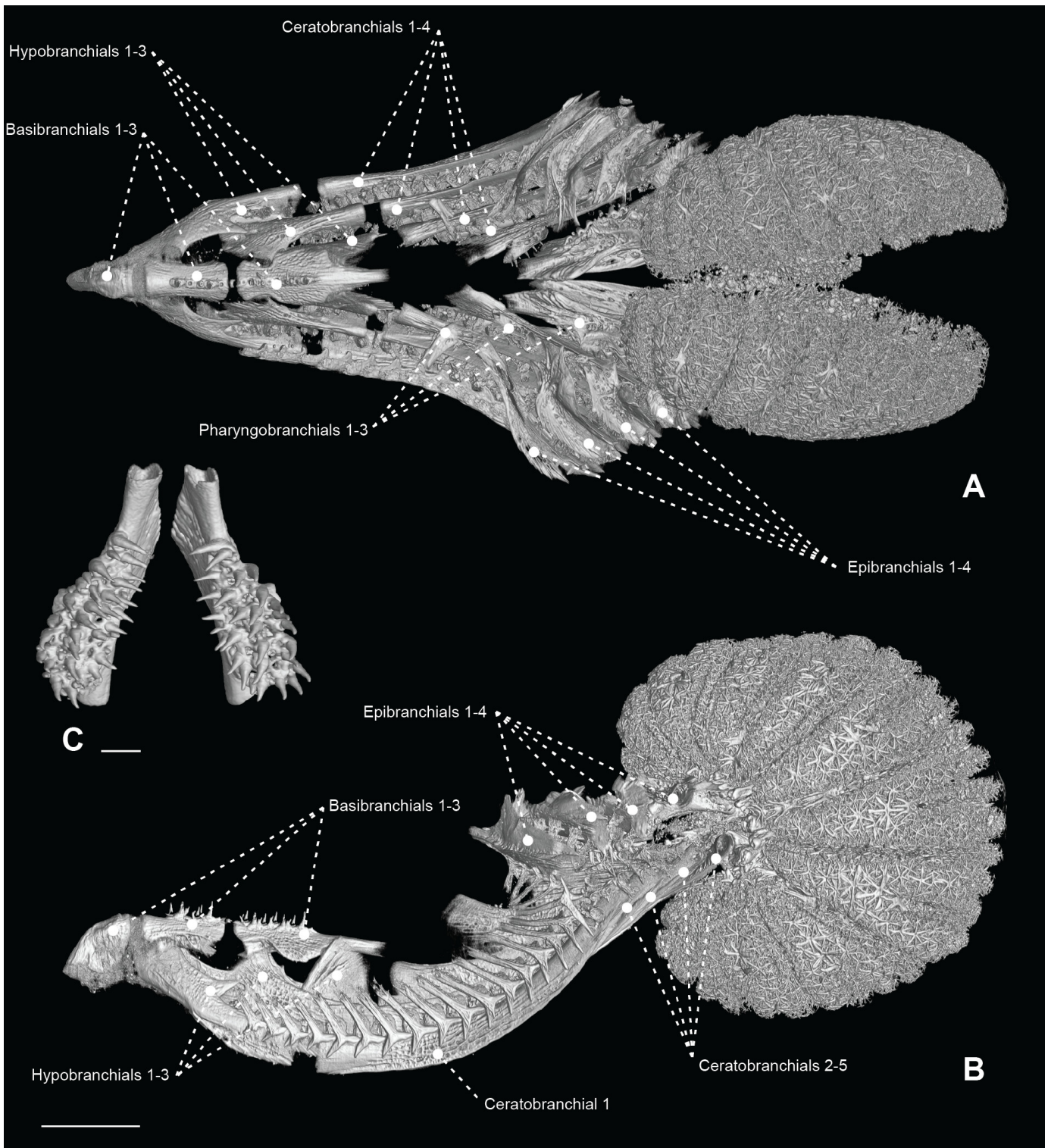


**FIGURE 45.** Micro CT scanning of the branchial and pharyngeal-sac skeleton of *Psenes cyanophrys* (Nomeidae: MZUSP 106392) in dorsal (A) and lateral views (B). Scale bar: 4 mm. A magnification of the upper pharyngeal tooth plates in ventral view is shown in C. Scale bar: 1 mm.

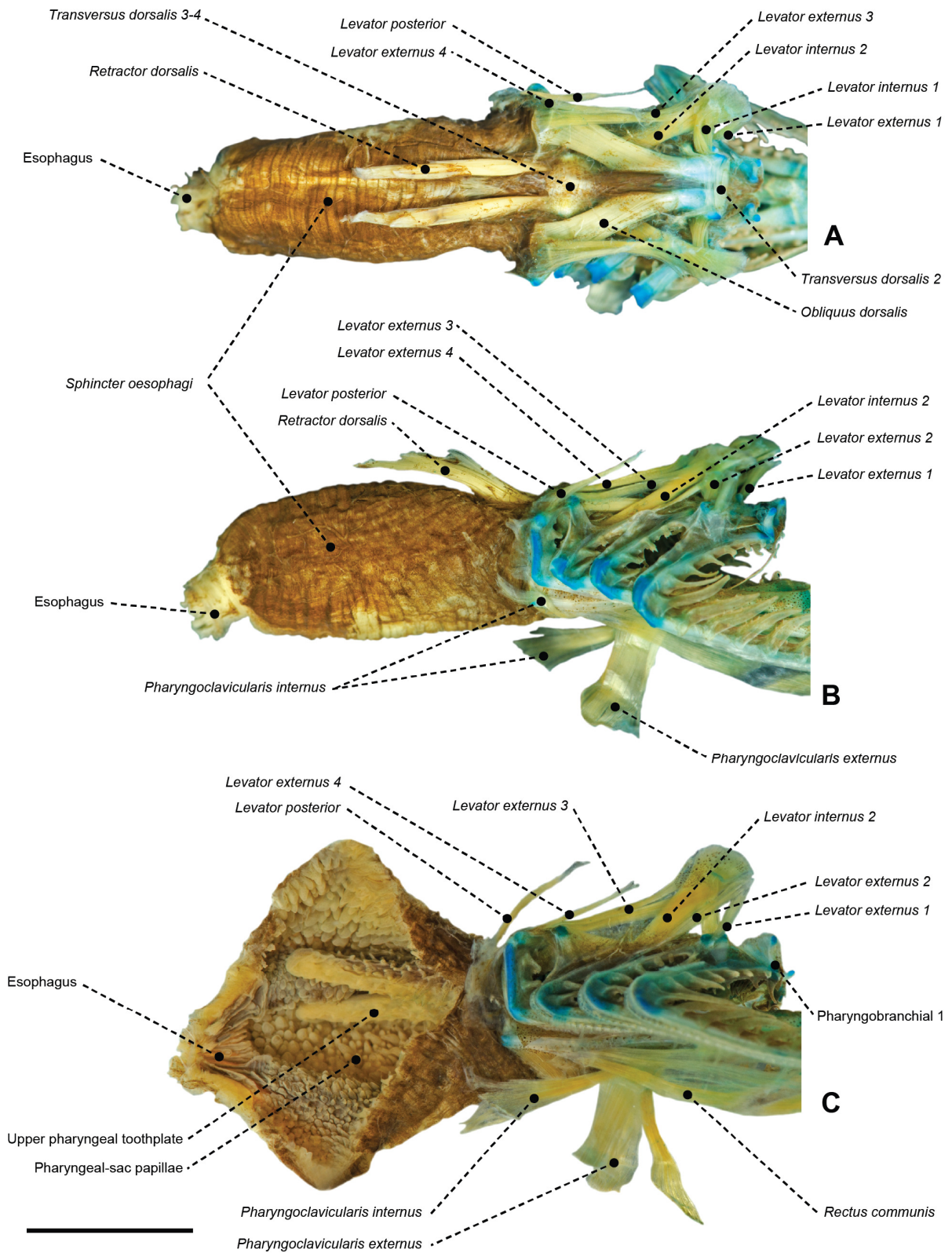


**FIGURE 46.** Branchial and pharyngeal sac musculoskeletal system of *Tetragnurus cuvieri* (Tetragnuridae: MZUSP 123241) in (A) dorsal and (B) lateral view. In C, the pharyngeal sac is cut laterally to expose its internal papillary lining and to show posteriorly elongate upper pharyngeal tooth plates. Scale bar: 5 mm.

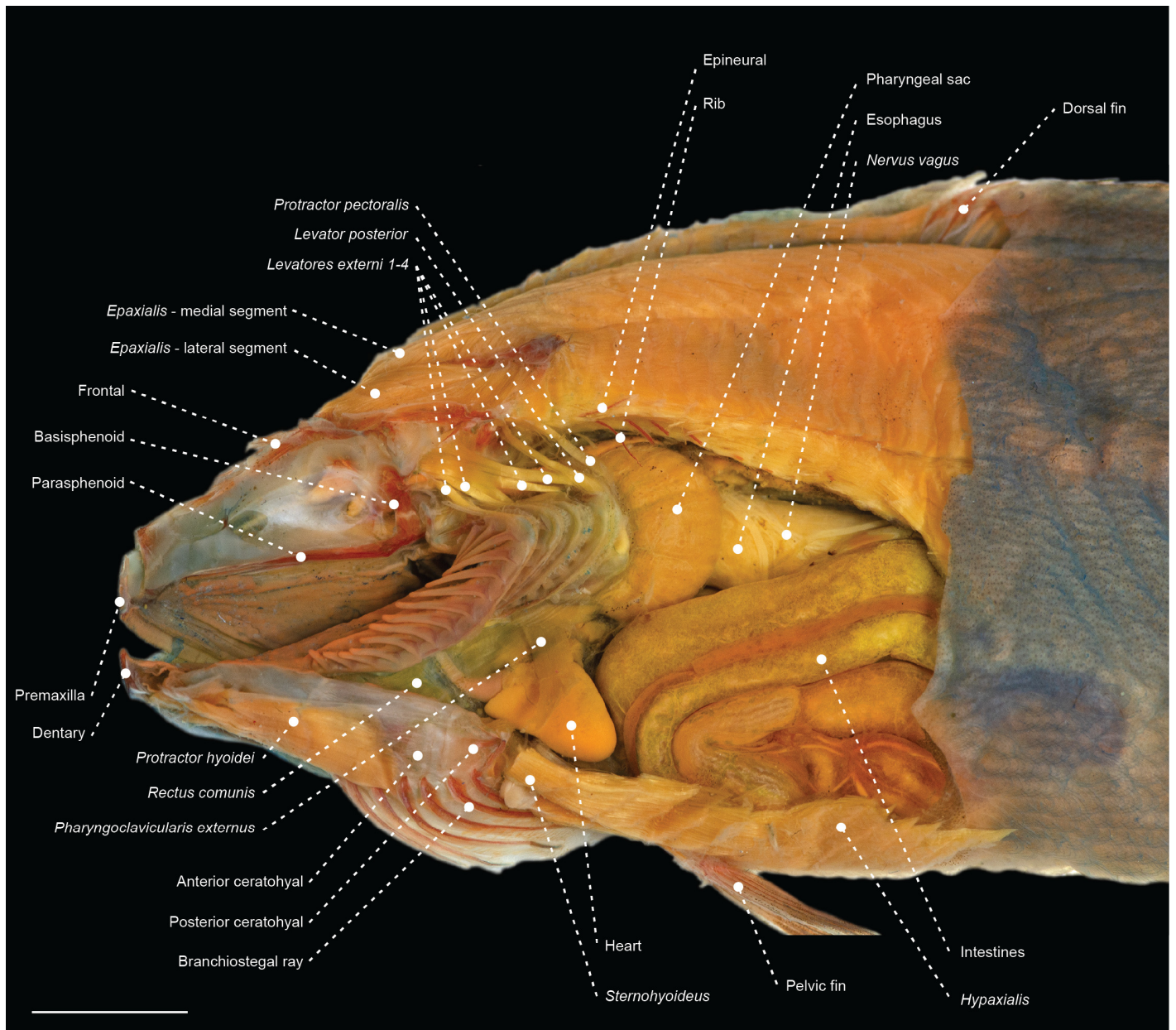


**FIGURE 47.** Cranial and abdominal anatomy of *Icichthys lockingtoni* (Centrolophidae: OS 16732) depicting gill arches, pharyngeal sac, and anterior portion of the abdominal cavity. Orbital, *adductor mandibulae*, opercular, hyopalatal and pectoral-girdle complexes are removed. Scale bar: 6 mm.

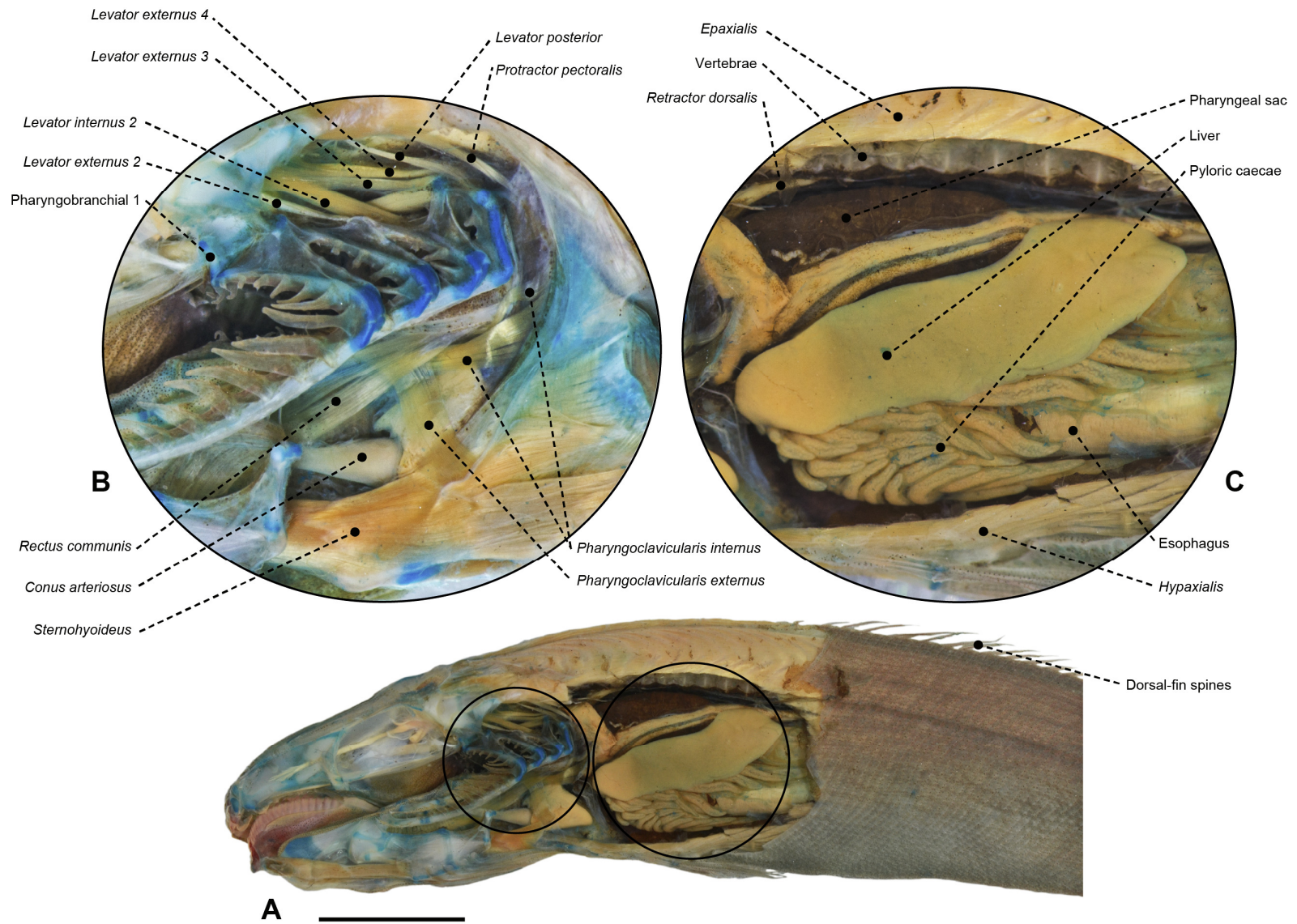


**FIGURE 48.** Cranial and abdominal anatomy of *Tetragonurus cuvieri* (Tetragonuridae: MZUSP 123241). Gill arches, pharyngeal sac, and anterior portion of the abdominal cavity is depicted in A, after removal of the orbital, *adductor mandibulae*, opercular, hyopalatal and pectoral girdle complexes. In B, there is an inset of the gill-arch muscles and bones, and C depicts the pharyngeal sac and anteriormost abdominal organs. Scale bar: 10 mm.

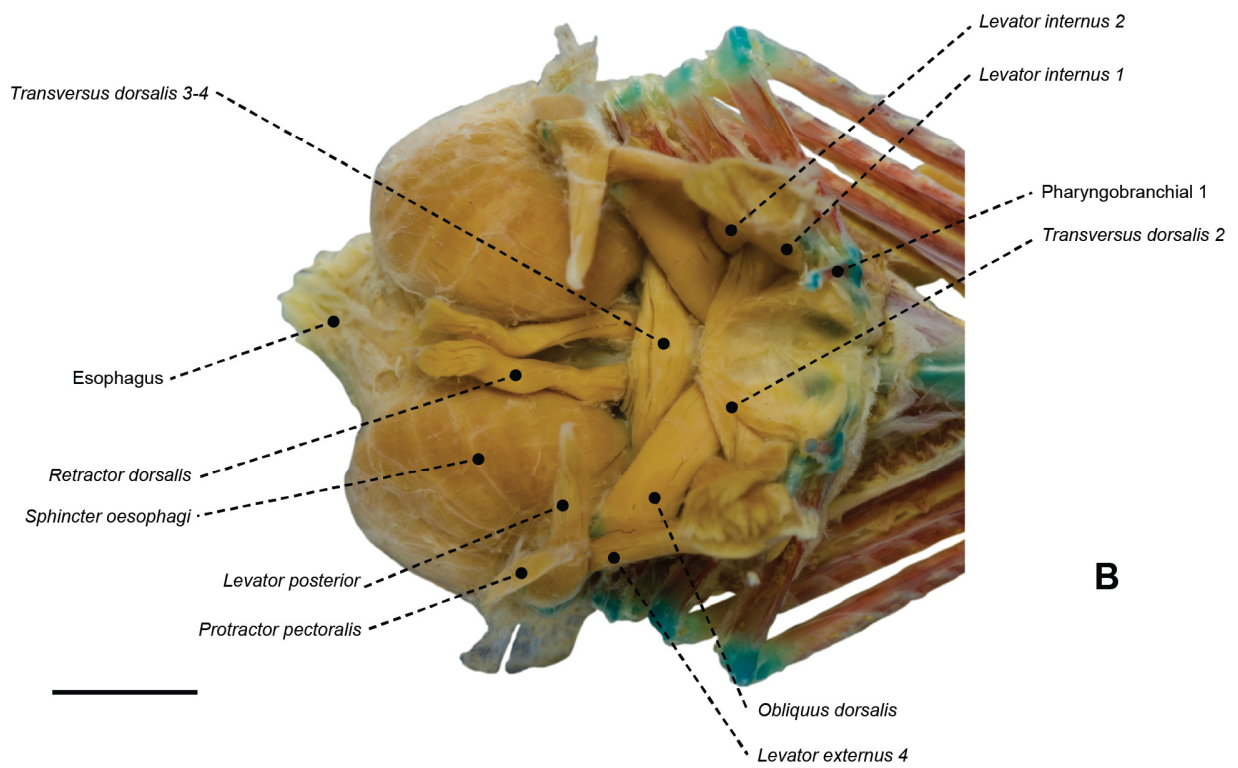
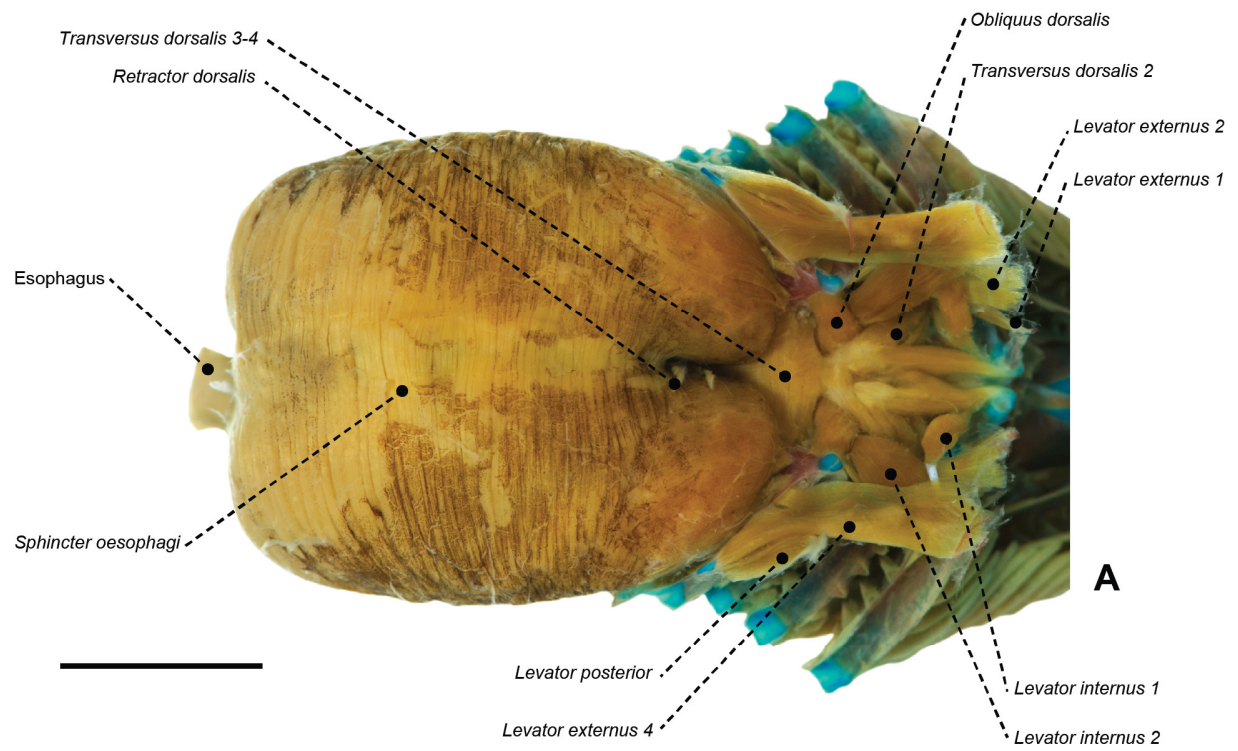


**FIGURE 49:** Dorsal view of branchial and pharyngeal-sac musculoskeletal system of (A) *Ariomma melanum* (Ariommatidae: MZUSP 123246; scale bar: 5 mm) and (B) *Hyperoglyphe perciformis* (Centrolophidae: MZUSP 119733; scale bar: 5 mm) in dorsal view.

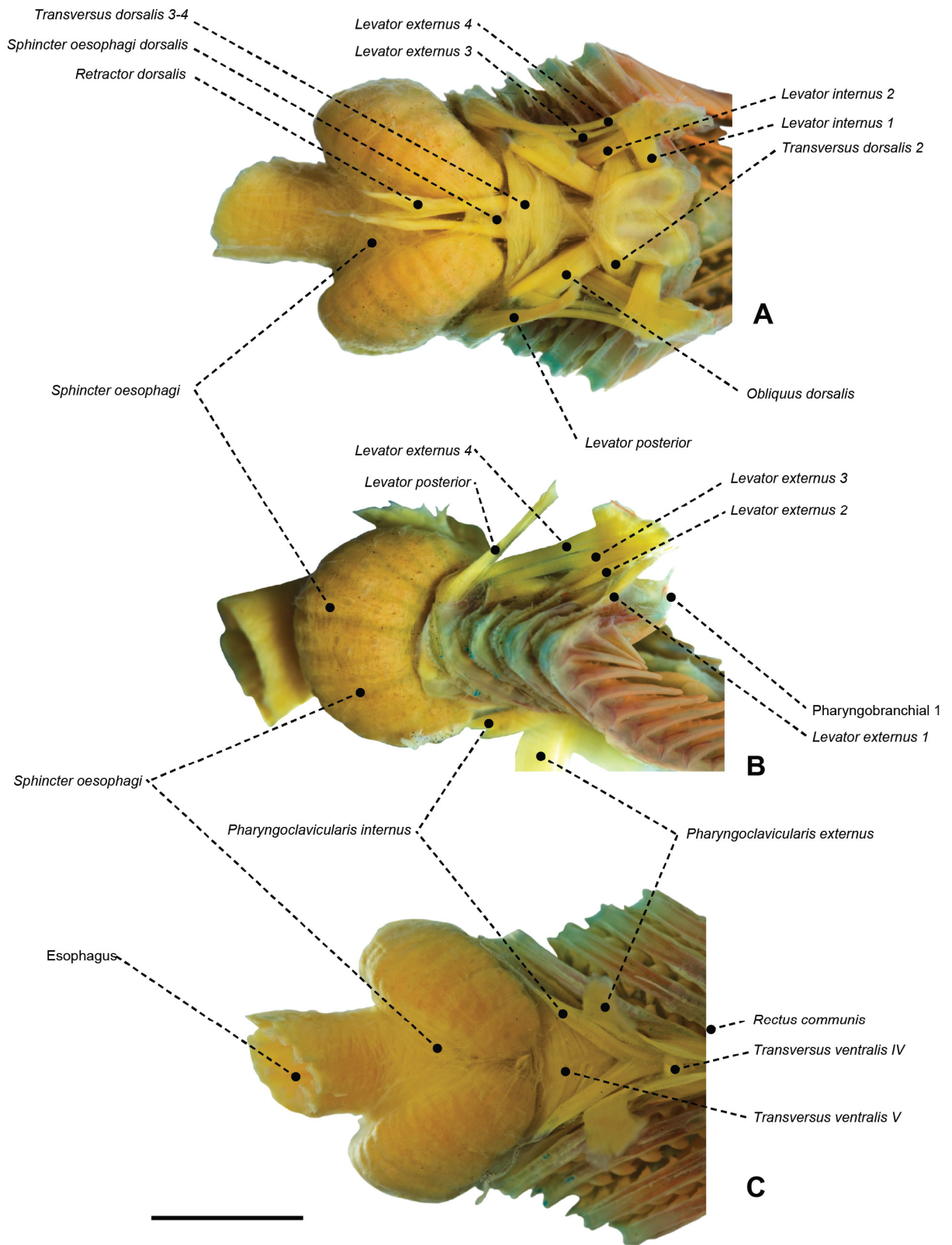


**FIGURE 50.** Branchial and pharyngeal-sac musculoskeletal system of *Ichthyoscypha lockingtoni* (Centrolophidae: OS 16732) in (A) dorsal, (B) lateral, and (C) ventral views. Scale bar: 5 mm.

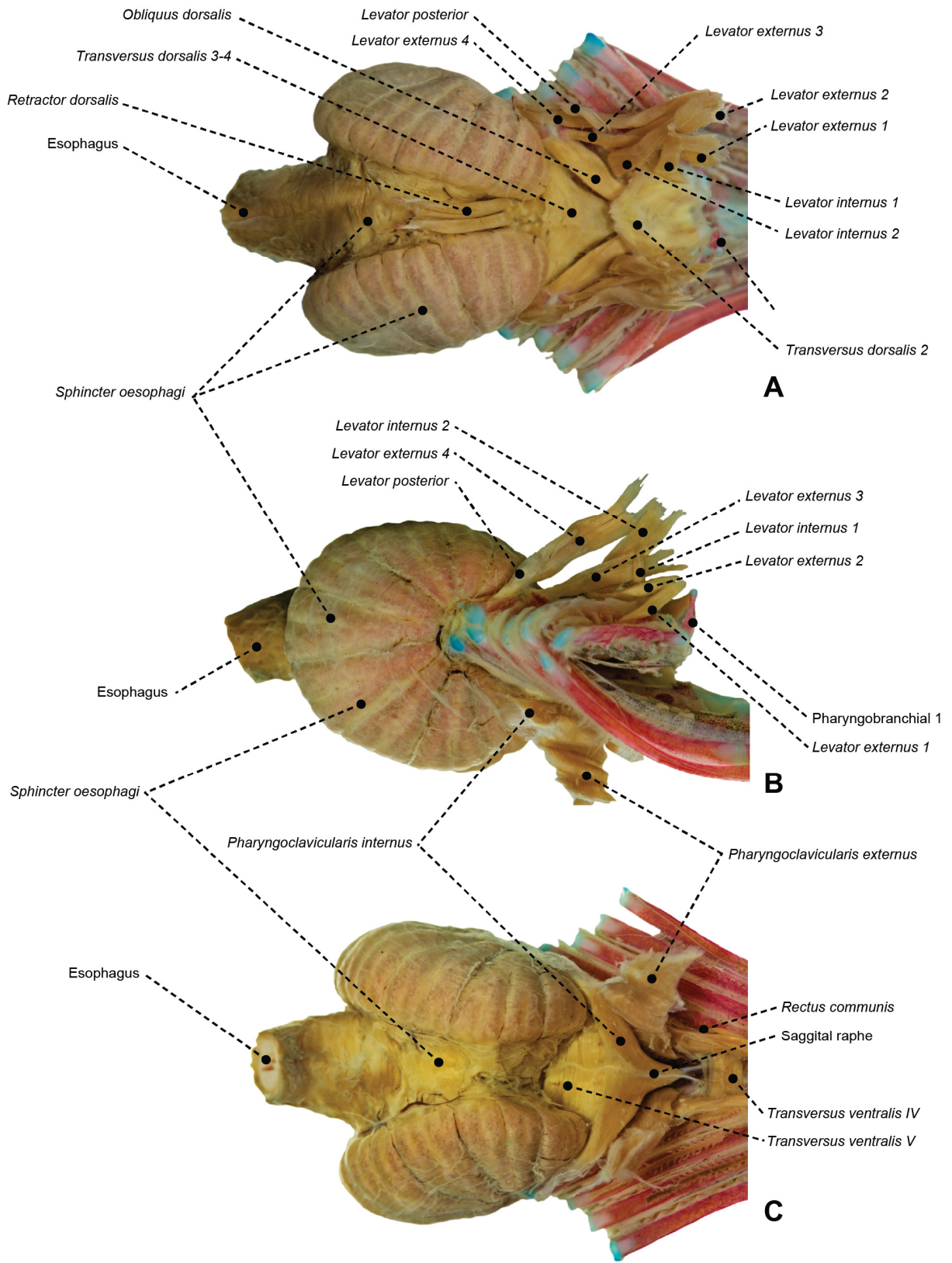


**FIGURE 51.** Branchial and pharyngeal-sac musculoskeletal system of *Cubiceps whiteleggii* (Nomeidae: MZUSP 67590) in (A) dorsal, (B) lateral, and (C) ventral views. Scale bar: 6 mm.

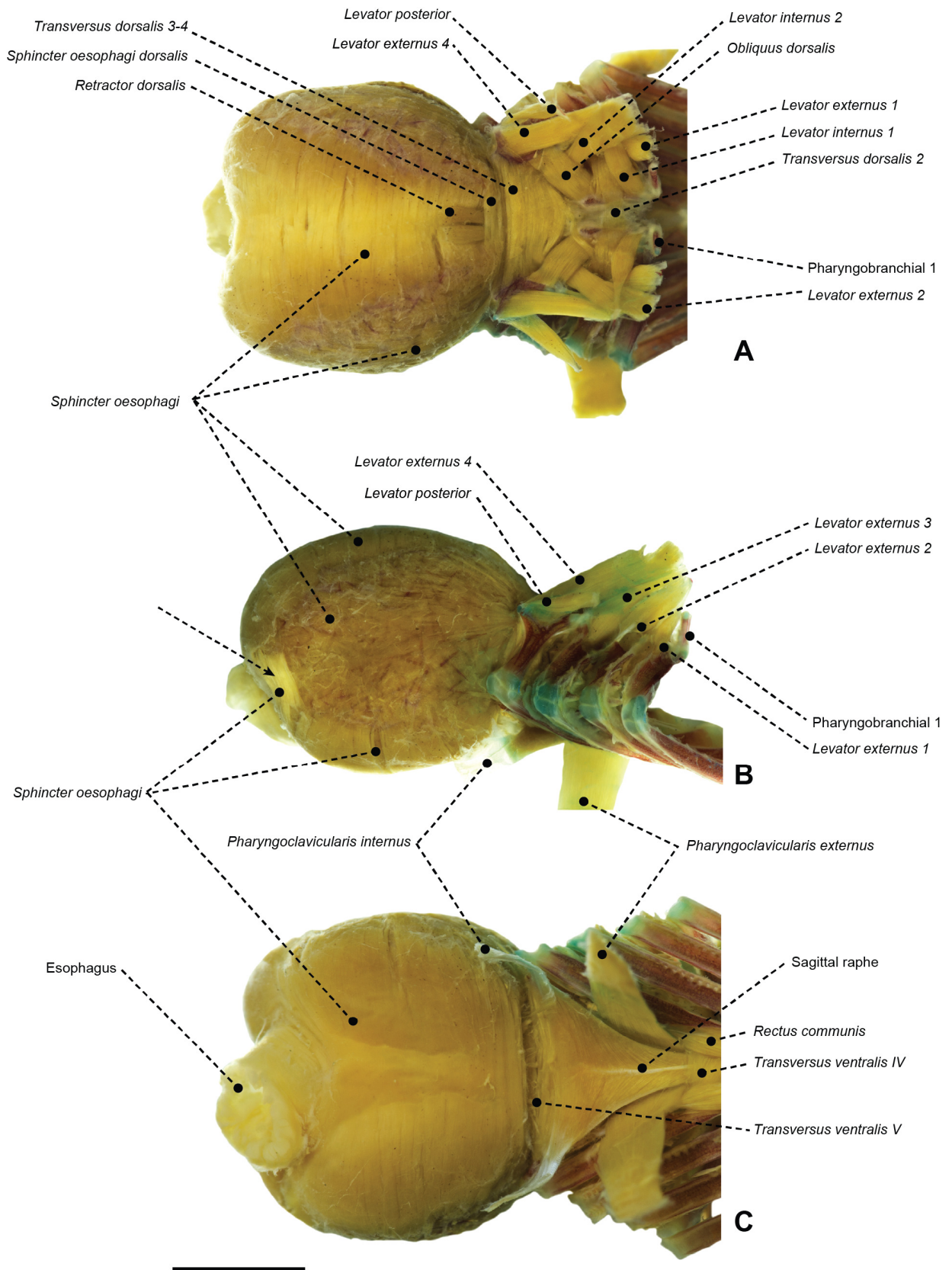


**FIGURE 52.** Branchial and pharyngeal-sac musculoskeletal system of *Stromateus brasiliensis* (Stromateidae: MZUSP 51279) in (A) dorsal, (B) lateral, and (C) ventral views. Arrow indicates posterolateral set of *sphincter oesophagi* fibers. Scale bar: 5 mm.

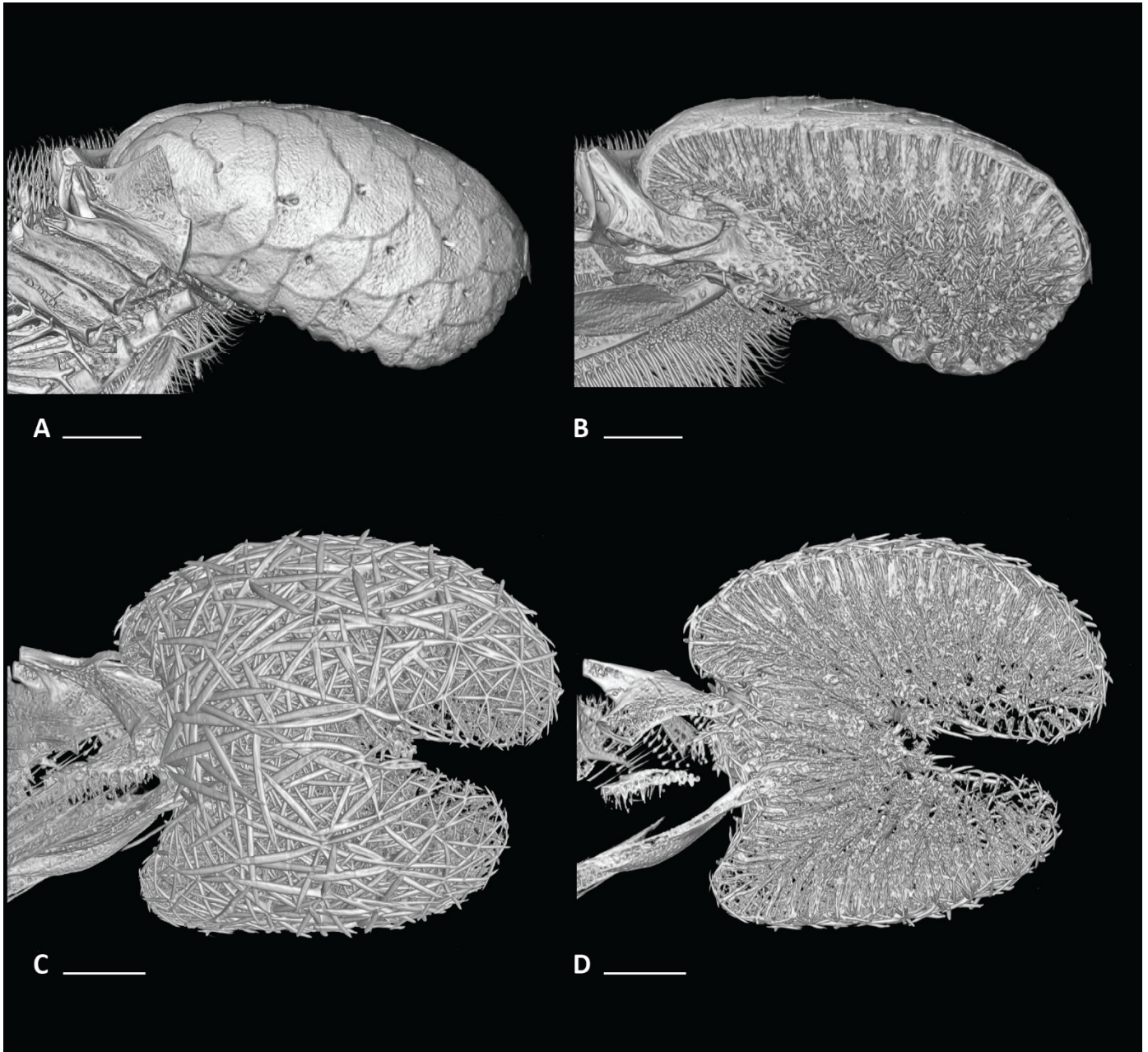


**FIGURE 53.** Micro CT scanning of the pharyngeal-sac skeleton of *Ariomma bondi* (A-B; Ariommatidae: MZUSP 86717), and *Peprilus triacanthus* (C-D; Stromateidae: MZUSP 123240) in right lateral (A-C), and sagittal (B-D) views. Scale bar: 2 mm.

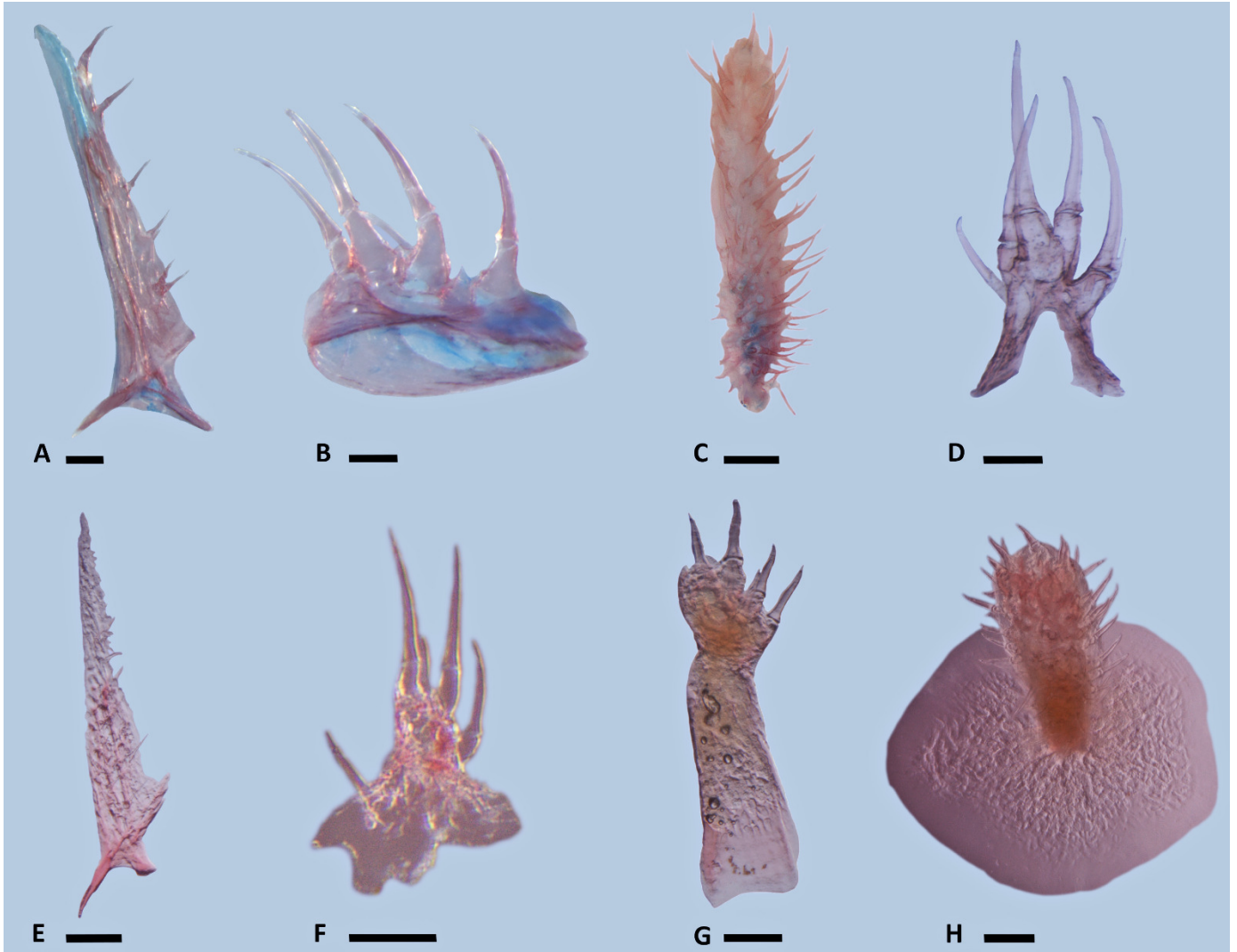


**FIGURE 54.** Stromateiform rakers from the gill arch and pharyngeal sac taken from *Psenopsis anomala* (A-D; Centrolophidae: MZUSP 119730) and *Ariomma bondi* (E-H; Ariommatidae: MZUSP 86717). First column shows a raker associated to the anterior facet of ceratobranchial 1 (A, E); second column shows rakers from the posterior facet of ceratobranchial 2 (B, F); third column show rakers associated to the anterior facet of ceratobranchial 5 (C, G); and fourth column exhibits pharyngeal-sac rakers (D, H). Scale bar: 0.5 mm.

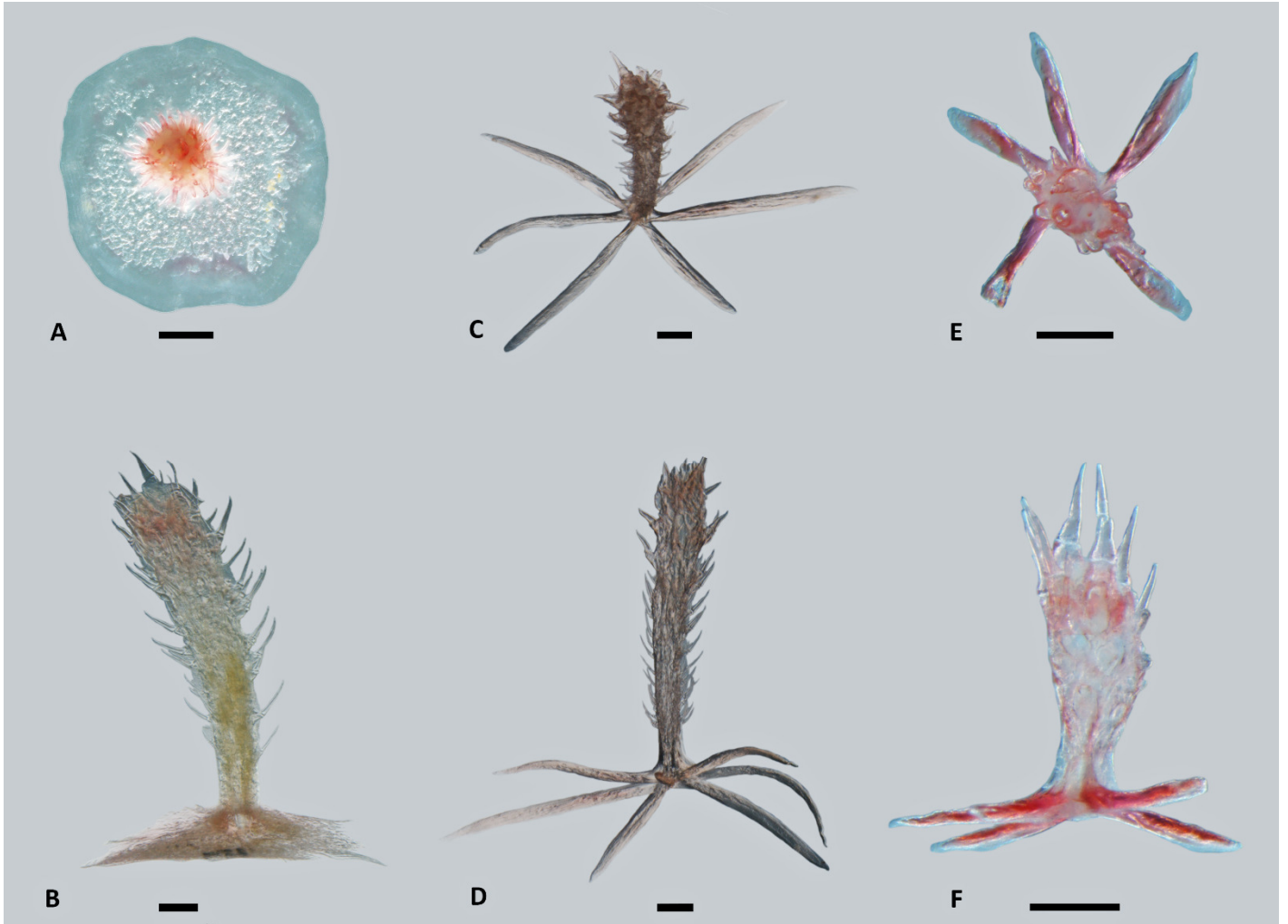


**FIGURE 55.** Stromateiform pharyngeal-sac raker. Dorsal (A) and lateral (B) views of the pharyngeal-sac raker of *Ariomma bondi* (Ariommatidae MZUSP 86717), exhibiting its elongate dorsoventral axis and round base. In *Peprilus triacanthus* (Stromateidae: MZUSP 123240) the pharyngeal-sac raker base is stellate (C), but the raker still elongate dorsoventrally (D). Stellate bases (E) also characterize *Psenes cyanophrys* (Nomeidae: MZUSP 106392), but the raker is less elongate (F) than in ariommatids or stromateids. Scale bar: 0.5 mm.

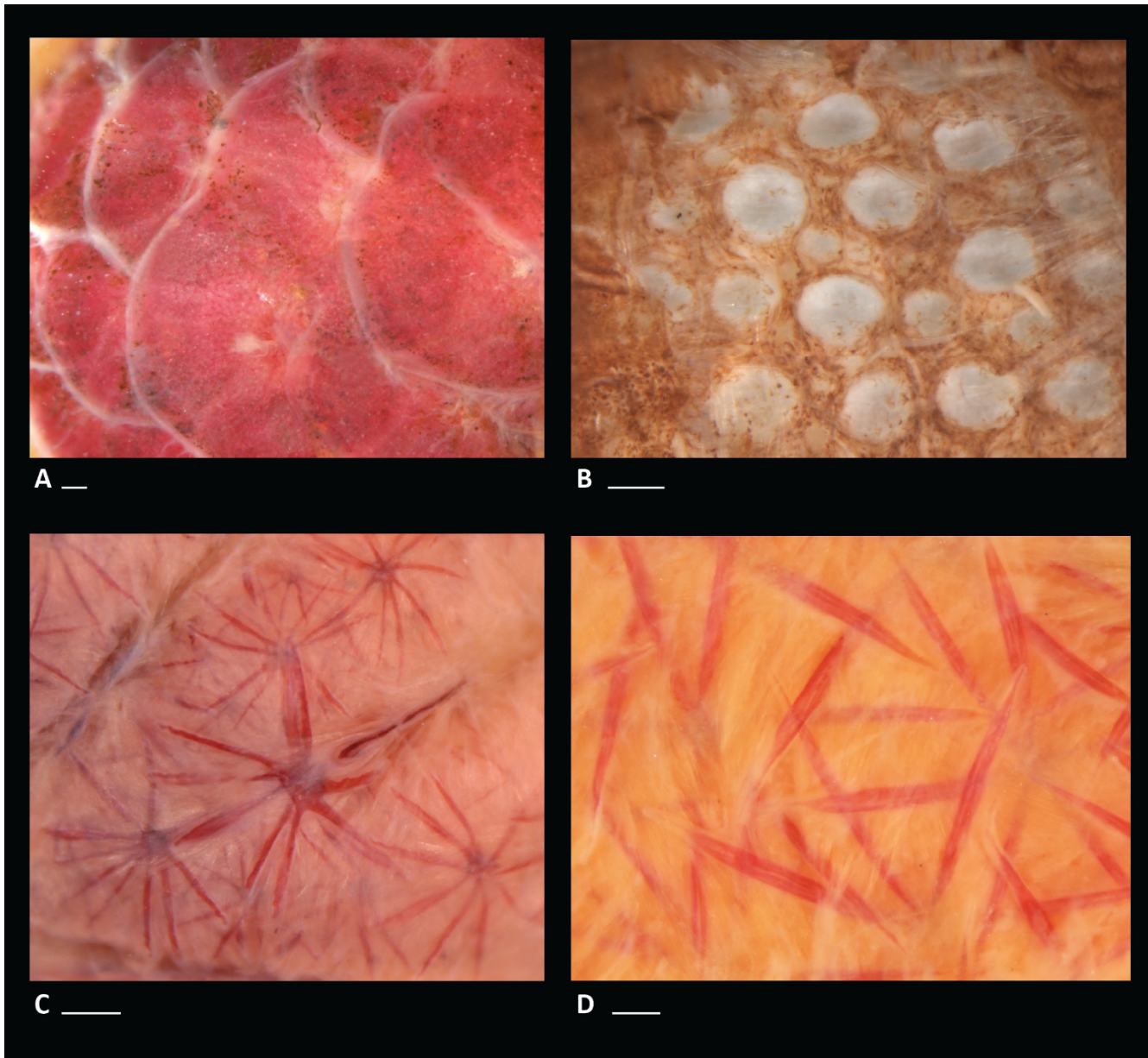


**FIGURE 56.** Inset of the muscular attachment of the pharyngeal-sac raker in Stromateiformes. Raker bases are visible after removal of the external most layer of the *sphincter oesophagi*. In A, Ariommatidae (*Ariomma melanum*: MZUSP 123246) the raker bases are large, round, and partially overlap each other. In B, Tetragonuridae (*Tetragonurus cuvieri*: MZUSP 123241) the round raker bases are small, do not overlap each other, and are poorly ossified. Both in C, Nomeidae (*Nomeus gronovii*: MZUSP 67590) and D, Stromateidae (*Stromateus brasiliensis*: MZUSP 51279) the raker bases exhibit large, well ossified, and exhibiting a stellate morphology. Scale bar: 0.5 mm.

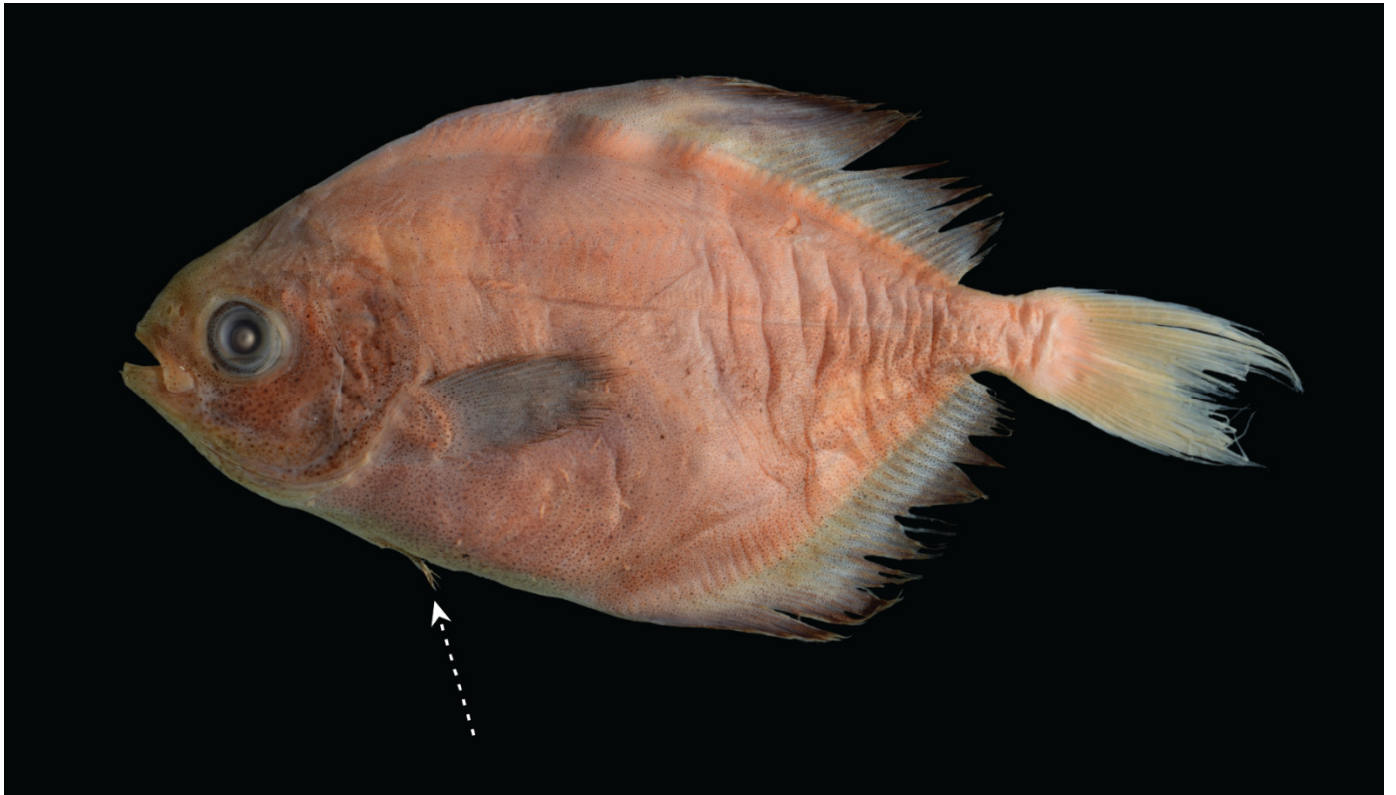


**FIGURE 57.** Left lateral view of an alcohol preserved juvenile specimen of *Stromateus fiatola* (Stromateidae: USNM UNCAT; 68.7 mm SL). Arrow indicates the pelvic fin.

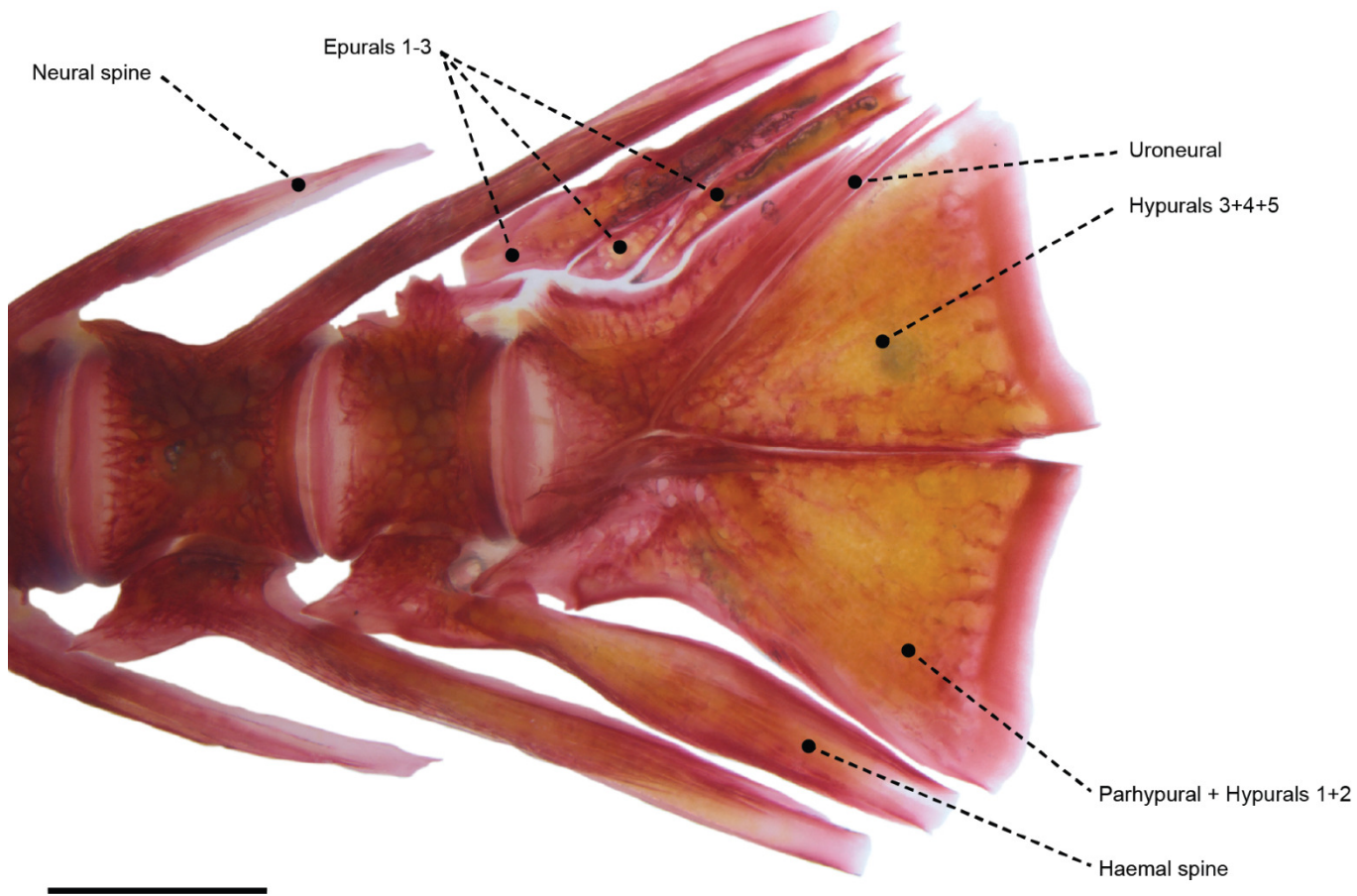


**FIGURE 58:** Caudal skeleton of a cleared and stained specimen of *Ariomma bondi* (Ariommatidae: MZUSP 86717) in left lateral view. Scale bar: 2 mm.

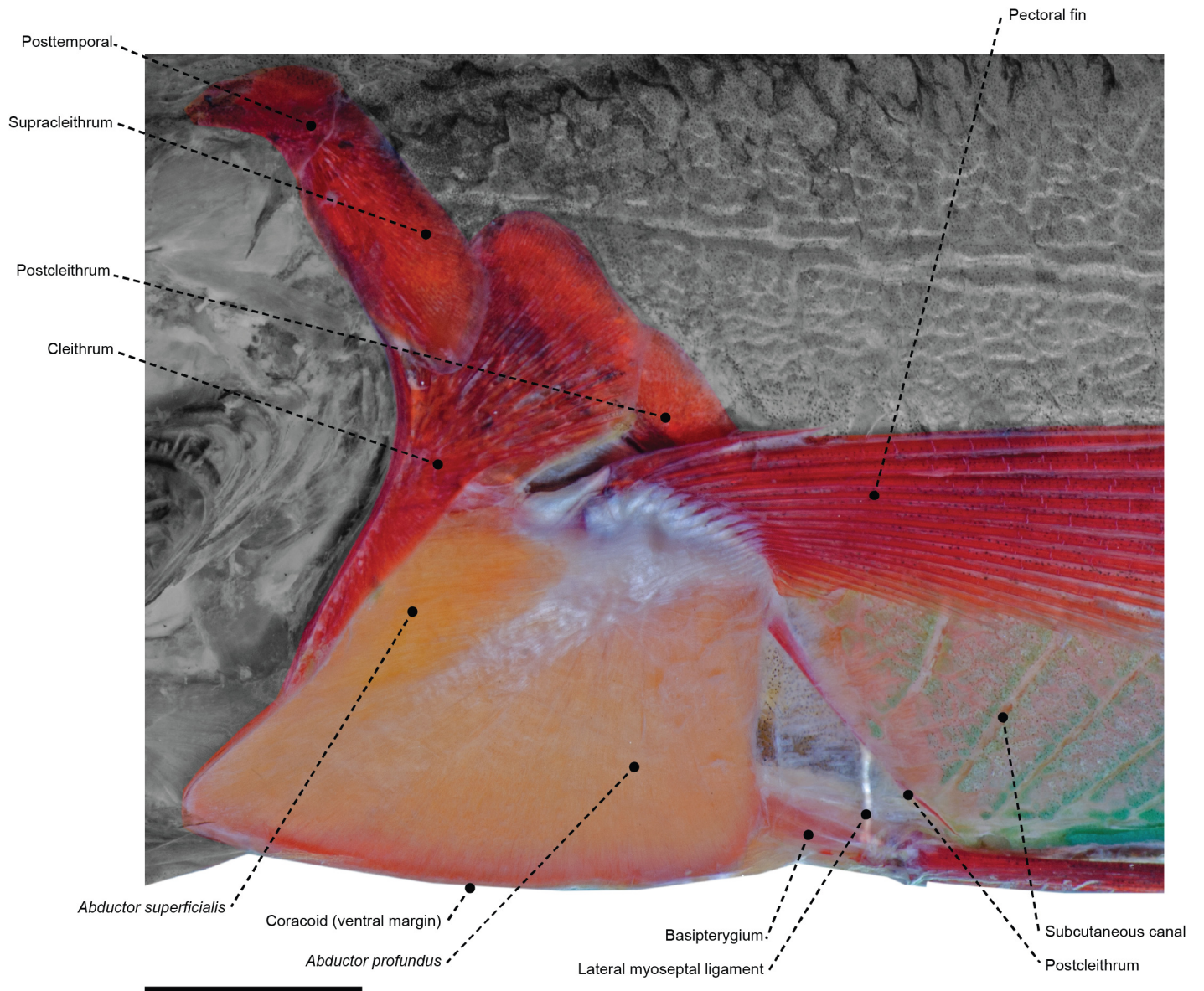


**FIGURE 59.** Pectoral and pelvic girdles and fins of *Cubiceps pauciradiatus* (Nomeidae: MZUSP 80701) in left lateral view. Note the lateral myoseptal ligament connecting the basipterygium to the postcleithrum. Scale bar: 5 mm.



**FIGURE 60:** Dorsal (A) and left lateral (B) views of the basipterygium of *Peprilus triacanthus* (Stromateidae: USNM 302441). In A, arrow indicates point of fusion between basipterygia; in B, arrow points to posteriorly oriented pelvic spine. Scale bar: 3 mm.

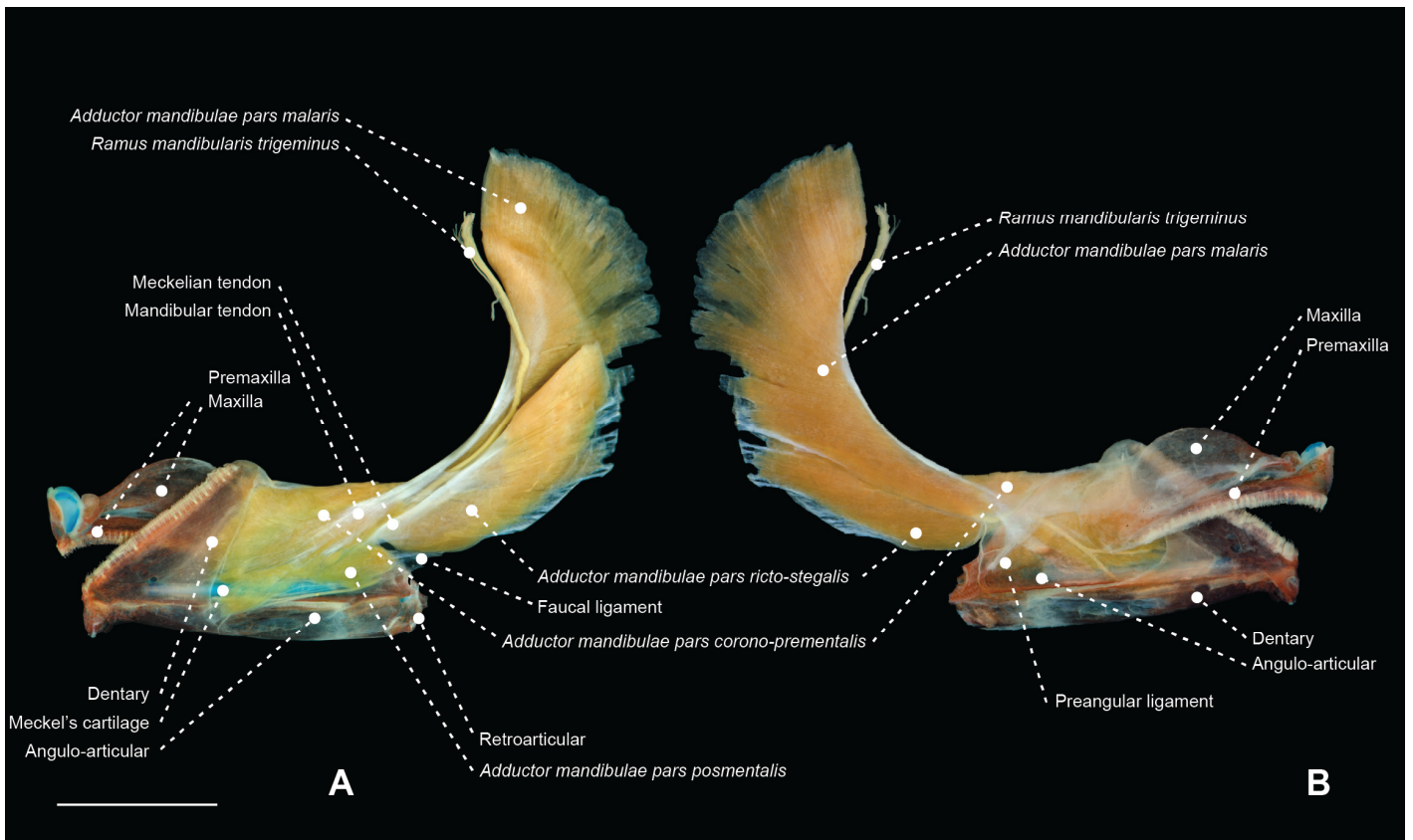


**FIGURE 61:** Left *adductor mandibulae* and associated structures of *Ariomma melanum* (Ariommatidae: MZUSP 123246) in (A) medial and (B) lateral views. Scale bar: 7 mm.

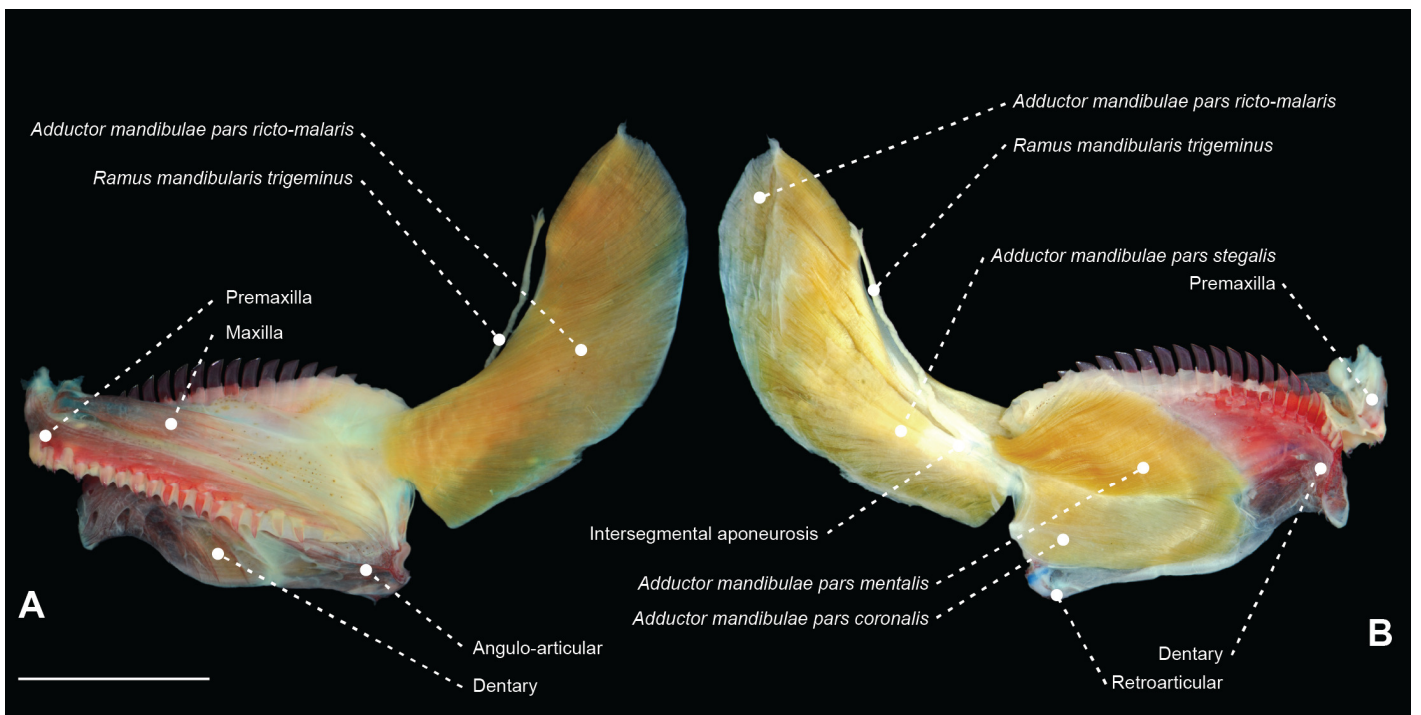


**FIGURE 62:** Left *adductor mandibulae* and associated structures of *Tetragonurus cuvieri* (Tetragonuridae: MZUSP 123241) in (A) lateral and (B) medial views. Scale bar: 5 mm.

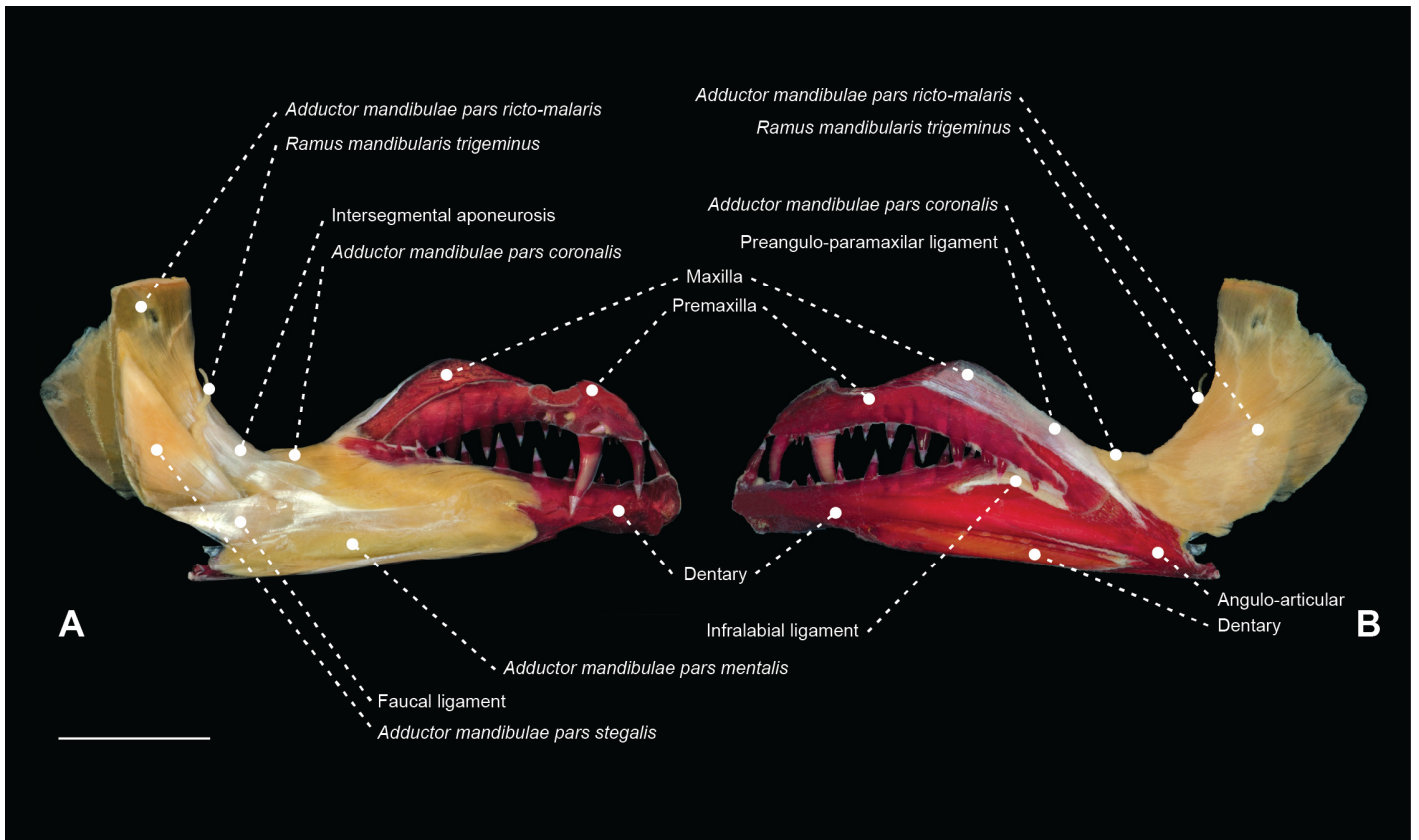


**FIGURE 63:** Left *adductor mandibulae* and associated structures of *Trichiurus lepturus* (Trichiuridae: MZUSP 8855) in (A) medial and (B) lateral views. Scale bar: 10 mm.

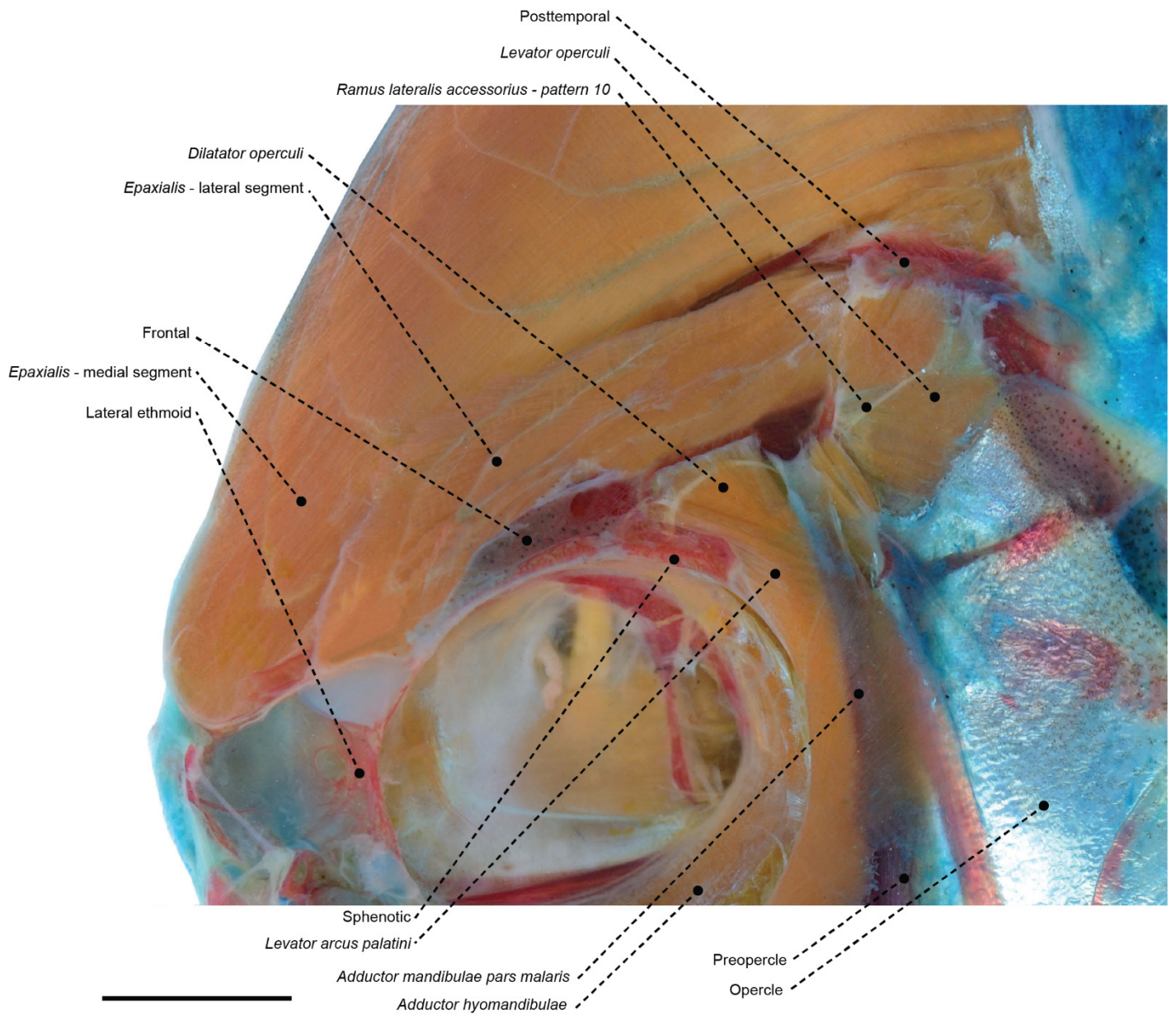


**FIGURE 64.** Inset of the temporal region of *Peprilus paru* (Stromateidae: MZUSP 67608) in left lateral view exhibiting associated muscles and bones. Eye and infraorbital series removed. Note the *ramus lateralis accessorius* pattern 10, emerging from the sphenotic and following caudally superficial to the levator arcus palatini, dilatator operculi, and levator operculi. Scale bar: 4 mm.

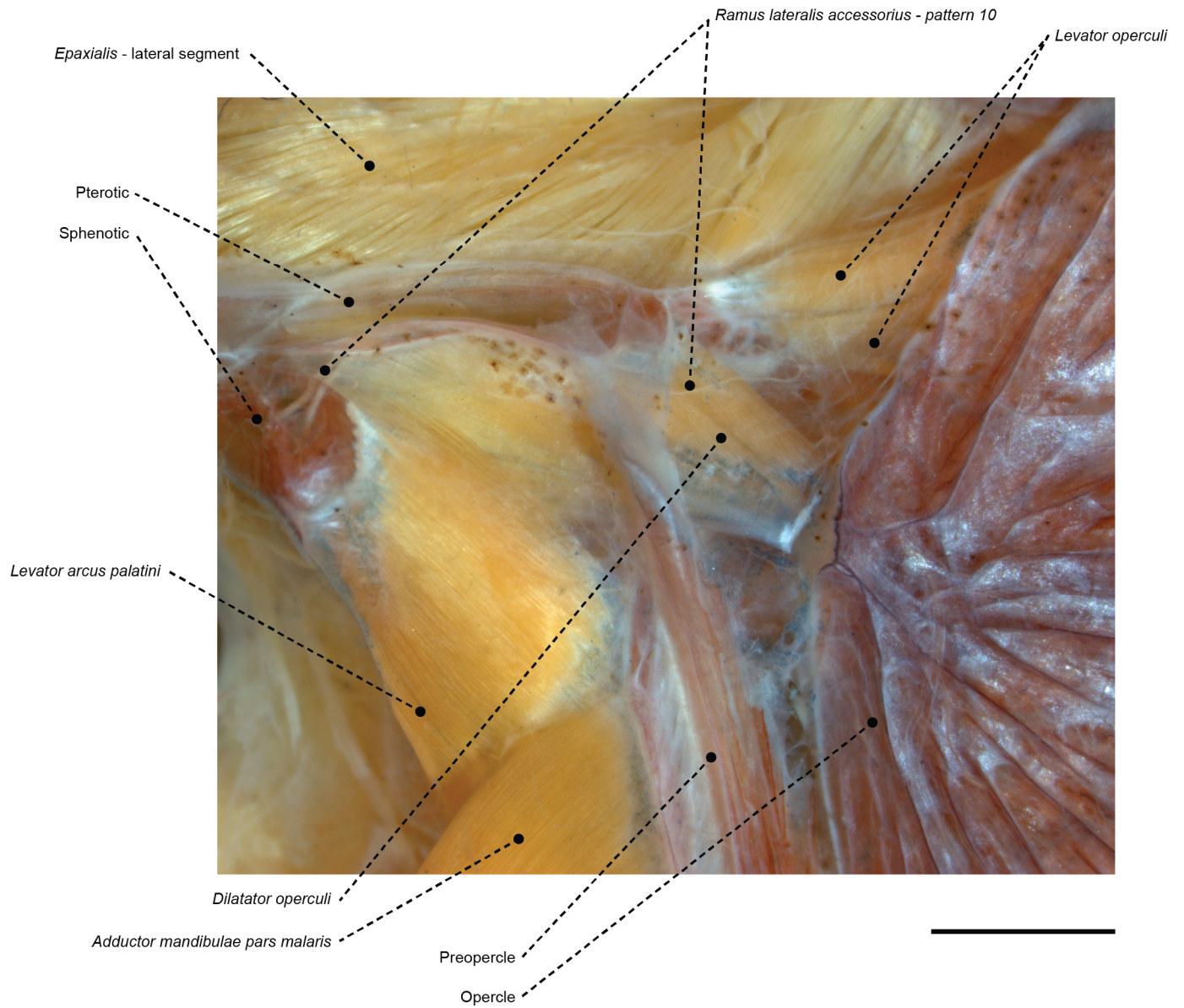


**FIGURE 65.** Inset of the temporal region of *Icichthys lockingtoni* (Centrolophidae: OS 16732) in left lateral view exhibiting associated muscles and bones. Note the *ramus lateralis accessorius* in a pattern 10 emerging from the sphenotic. Scale bar: 2 mm.

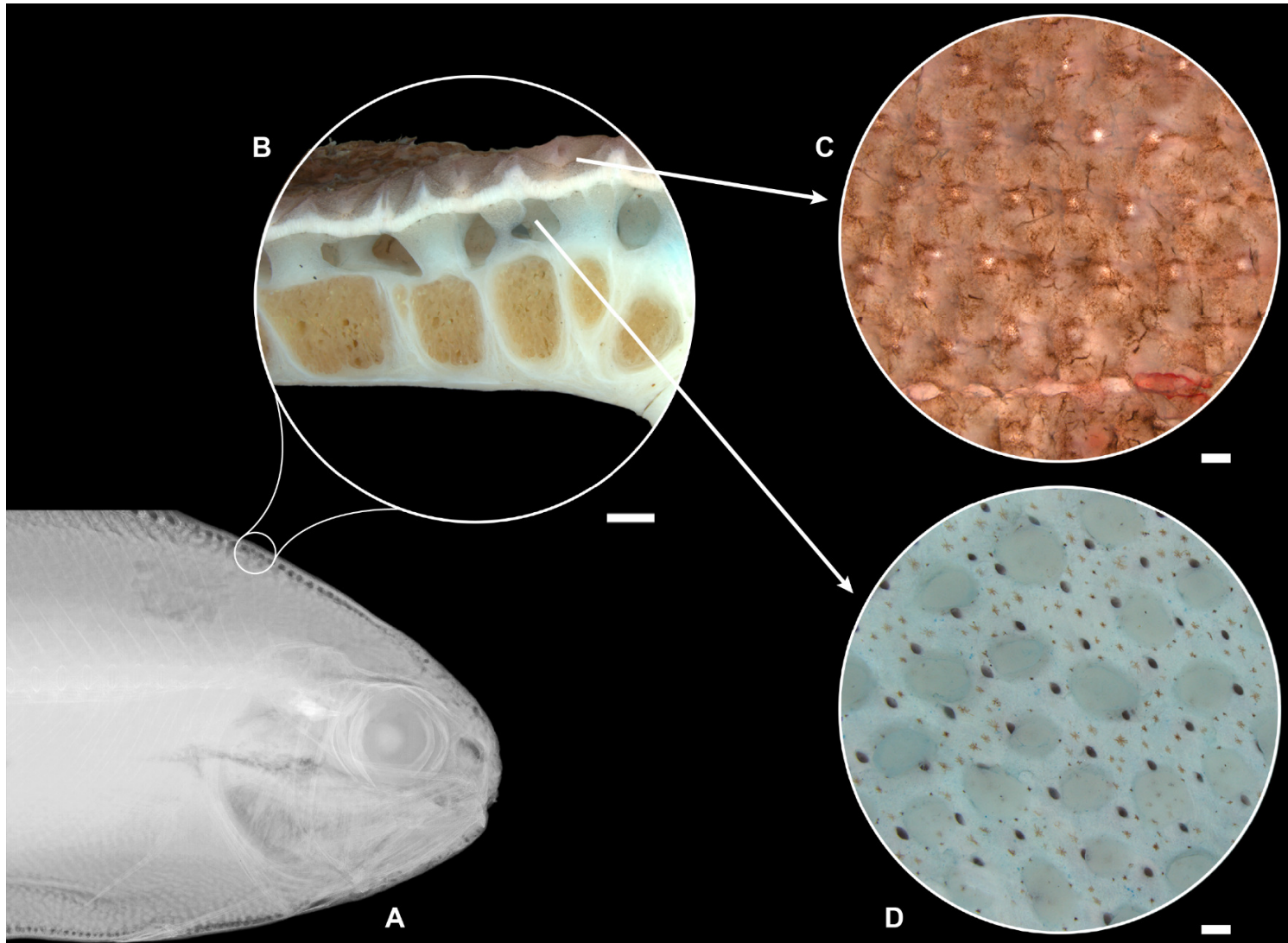


**FIGURE 66.** Subdermal canal plexus of *Tubbia tasmanica* (Centrolophidae: CSIRO H 6979-03). In A, the subdermal canals are visible in a radiographed specimen (325.2 mm SL). A transverse section of the superficial layers of skin and axial musculature is shown in B. A magnification of the external appearance of the skin surface is offered in C, and a photograph of opposite surface of the same piece is shown in D. Note pores connecting the external surface to the interdermal space in pictures C and D. Scale bar: 1 mm.

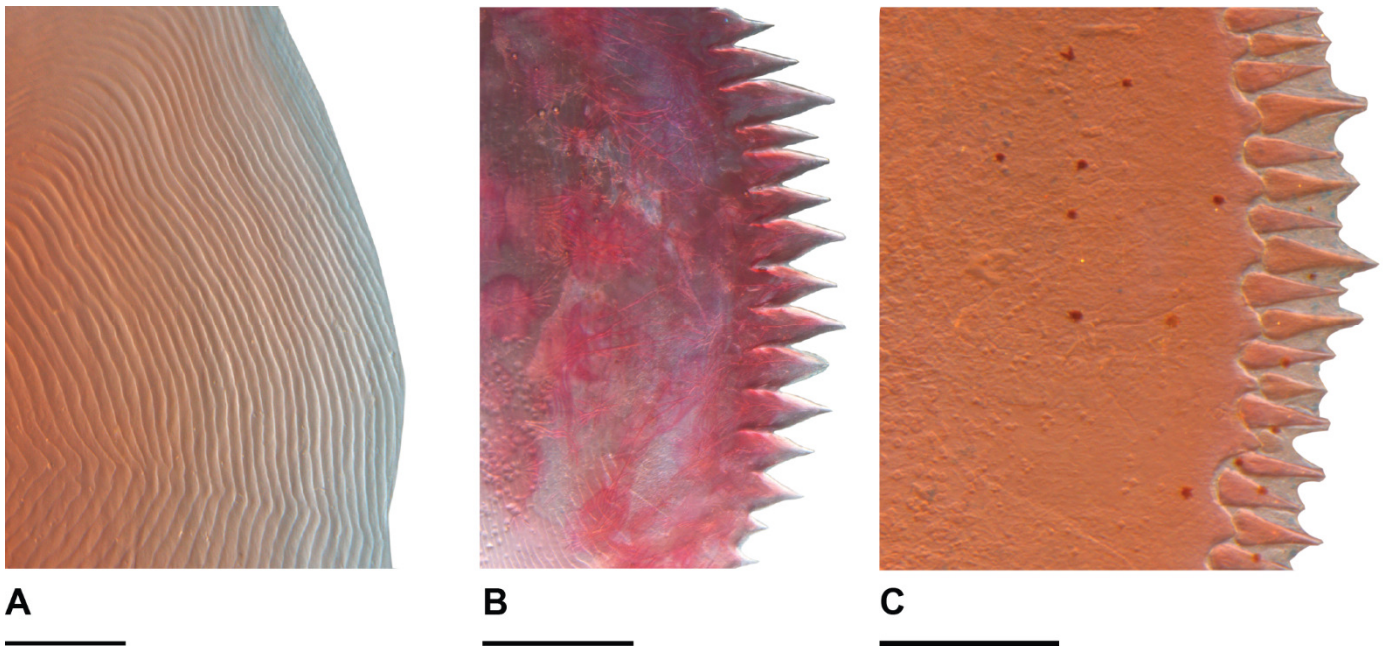


**FIGURE 67.** Photographs of alizarin-red stained percomorphacean scales. The posterior margin of a cycloid scale of *Cubiceps whiteleggii* (Nomeidae: MZUSP 67590) is shown in A. The same region of a spinoid scale of *Beryx splendens* (Berycidae: MZUSP 121649) is shown in B; and of a transforming ctenoid scale of *Apogon maculatus* (MZUSP 43155) is shown in C. Scale sampling was standardized to the region behind the left pectoral fin. Scale bar: 0.5 mm.

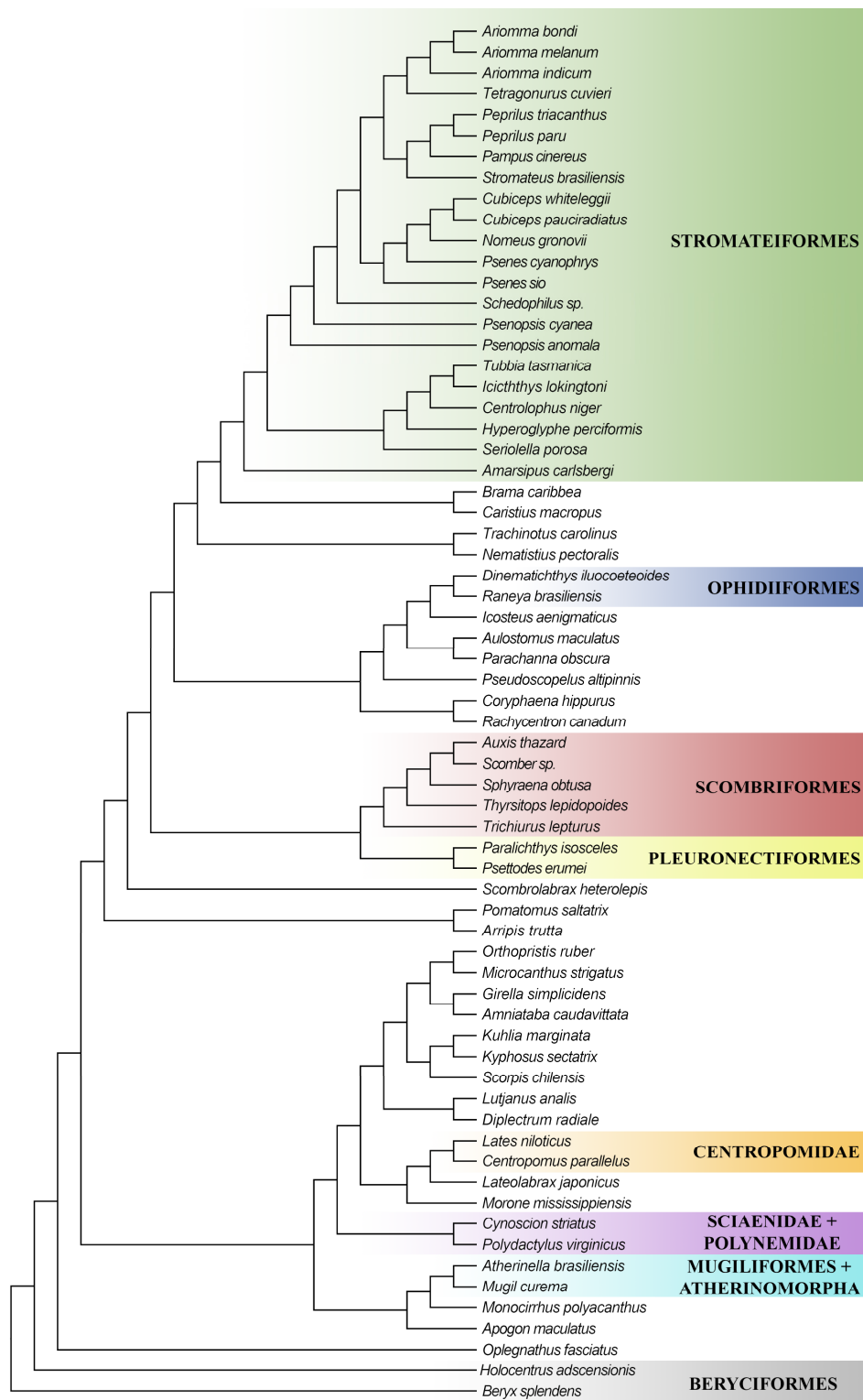


**FIGURE 68.** Most parsimonious tree resultant from an analysis employing Implicit Weighting against homoplasies under  $K = 6.808$ . Highlighted clades represent: Stromateiformes (dark green), Ophidiiformes (blue), Scombriformes (red), Pleuronectiformes (yellow) Centropomidae (orange), Sciaenidae + Polynemidae (purple), and Mugiliformes + Atherinomorpha (light blue). The monophyly of Beryciformes (highlighted in grey) was not tested herein, as the analysis was rooted in *Beryx splendens*.



FIGURE 69. Most parsimonious tree resultant from an analysis employing Implicit Weighting against homoplasies under K = 6.808 exported with TNT native node numbers.

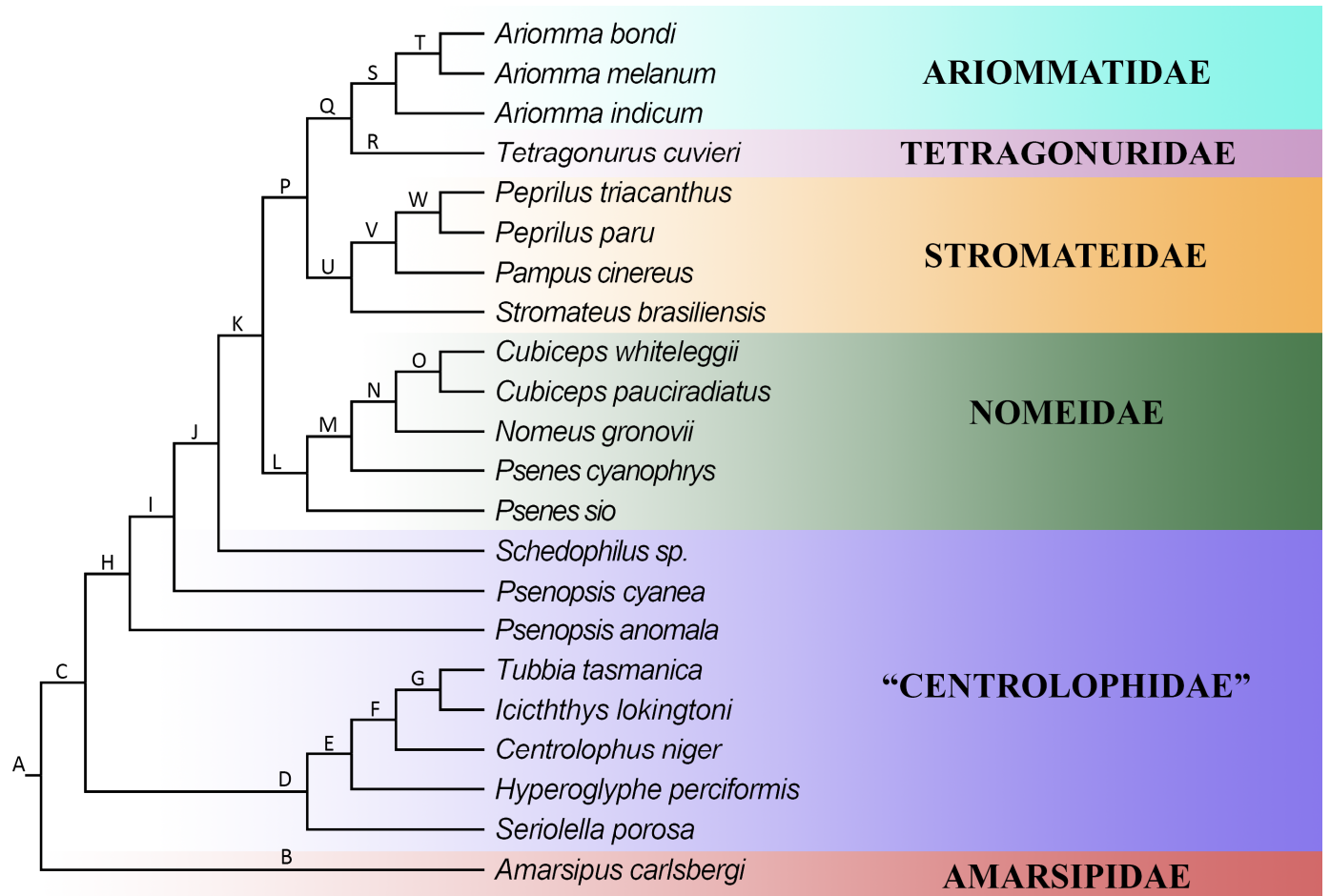


**FIGURE 70:** Interrelationships of the Stromateiformes resultant from an analysis employing Implicit Weighting against homoplasies, under  $K = 6.808$ . Highlighted taxa represent: Amarsipidae (red), Centrolophidae (blue), Nomeidae (green), Stromateidae (orange), Tetragnuridae (pink), and Ariommatidae (light blue). Letters A to W represent clades within Stromateiformes.



**FIGURE 71:** Left lateral view of an alcohol preserved specimen of (A) *Amarsipus carlsbergi* (Amarsipidae: SIO 75-122; 50.4 mm SL), and (B) *Tetragonurus cuvieri* (Tetragonuridae: MZUSP 123241; 94.7 mm SL).

## APPENDIX

### DATA MATRIX: QUANTITATIVE CHARACTERS

*Beryx splendens*: 0.04 0.17 0.05 0.38 0.50 0.38 1.00 0.12 0.25 0.11 0.89 0.25 0.01 0.21 0.21 0.00 0.75 0.00 0.73 0.66 0.64 0.50

*Holocentrus adscensionis*: 0.12 0.56 0.07 0.38 0.50 0.38 0.70 0.05 0.25 0.04 0.89 0.13 0.03 0.36 0.29 0.00 0.55 0.55 0.49 0.55 0.85 0.12

*Dinematichthys ilucoeteoides*: 0.50 0.00 0.53 0.75 0.00 0.81 0.00 0.34 0.00 0.35 0.56 0.00 0.14 0.00 0.00 0.25 0.45 0.72 0.23 0.28 0.36 0.76

*Raneya brasiliensis*: 0.86 0.00 0.89 0.63 0.00 0.75 0.00 0.60 0.00 0.61 0.00 0.00 0.28 0.00 0.00 0.25 0.33 0.82 0.11 0.00 0.15 0.83

*Apogon maculatus*: 0.03 0.33 0.02 0.13 0.50 0.13 0.50 0.01 0.08 0.02 0.67 0.13 0.01 0.64 0.50 0.25 0.65 0.17 0.52 0.55 0.60 0.07

*Aulostomus maculatus*: 0.22 0.67 0.15 0.38 0.00 0.00 0.50 0.14 0.08 0.14 0.00 0.00 0.24 0.21 0.21 1.00 0.80 0.30 0.00 1.00 1.00 0.08

*Icosteus aenigmaticus*: 0.34 0.00 0.38 0.56 0.00 0.63 0.40 0.20 0.00 0.22 1.00 0.00 0.30 0.43 0.29 0.50 0.32 0.71 0.32 0.41 0.29 0.50

*Brama caribbea*: 0.20 0.22 0.19 0.50 0.50 0.50 0.50 0.14 0.08 0.14 0.56 0.25 0.10 0.43 0.36 0.25 0.66 0.54 0.78 0.68 0.53 0.63

*Caristius macropus*: 0.20 0.00 0.23 0.50 0.50 0.50 0.50 0.10 0.00 0.11 0.67 0.00 0.10 0.43 0.57 0.25 0.24 0.85 0.50 0.47 0.38 0.55

*Pseudoscopelus altipinnis*: 0.15 0.50 0.10 0.19 0.50 0.19 0.50 0.06 0.17 0.05 0.67 0.00 0.10 0.64 0.64 0.25 0.49 0.53 0.39 0.48 0.46 0.49

*Pomatomus saltatrix*: 0.14 0.39 0.11 0.50 0.50 0.50 0.50 0.15 0.08 0.16 0.67 0.25 0.02 0.57 0.57 0.25 0.60 0.44 0.35 0.53 0.61 0.33

*Arripis georgianus*: 0.08 0.44 0.05 0.31 0.50 0.31 0.50 0.03 0.17 0.03 0.67 0.25 0.01 0.50 0.50 0.25 0.53 0.43 0.37 0.55 0.86 0.11

*Scombrolabrax heterolepis*: 0.14 0.67 0.07 0.38 0.50 0.38 0.50 0.08 0.08 0.09 0.67 0.00 0.05 0.64 0.64 0.25 0.54 0.46 0.68 0.64 0.86 0.21

*Sphyræna tome*: 0.02 0.28 0.02 0.19 0.50 0.19 0.50 0.02 0.00 0.03 0.67 0.00 0.01 0.57 0.57 0.25 0.69 0.18 0.16 0.69 0.80 0.00

*Thyrsitops lepidopoides*: 0.20 0.94 0.10 0.31 0.50 0.31 0.50 0.09 0.17 0.09 0.67 0.00 0.07 0.50 0.50 0.25 0.39 0.64 0.26 0.53 0.82 0.25

*Auxis thazard*: 0.05 0.44 0.02 0.81 0.50 0.81 0.50 0.03 0.00 0.05 0.67 0.00 0.11 0.86 1.00 0.25 0.47 0.66 0.25 0.43 0.84 0.32

*Scomber sp.*: 0.11 0.44 0.08 0.75 0.50 0.75 0.50 0.07 0.08 0.07 0.67 0.00 0.06 0.71 0.64 0.25 0.56 0.55 0.23 0.51 0.72 0.32

*Trichiurus lepturus*: 1.00 0.11 1.00 0.00 0.00 0.00 0.00 1.00 0.00 1.00 0.00 0.00 1.00 0.00 0.00 0.25 0.07 0.90 0.00 ? 0.11 0.82

*Amarsipus carlsbergi*: 0.18 0.56 0.13 0.50 0.50 0.50 0.50 0.13 0.17 0.13 0.67 0.25 0.17 0.86 0.86 0.50 0.45 0.41 0.45 0.26 0.28 0.40

*Ariomma indicum*: 0.10 0.50 0.06 0.88 0.50 0.88 0.50 0.07 0.17 0.07 0.67 0.25 0.06 0.57 0.50 0.50 0.54 0.60 0.74 0.61  
0.57 0.53

*Ariomma bondi*: 0.12 0.67 0.06 0.75 0.50 0.75 0.50 0.10 0.17 0.09 0.67 0.13 0.06 0.64 0.57 0.50 0.50 0.60 0.59 0.56 0.67  
0.38

*Psenopsis anomala*: 0.18 0.28 0.17 0.63 0.50 0.63 0.50 0.15 0.17 0.15 0.67 0.25 0.01 0.57 0.50 0.25 0.58 0.50 0.64 0.63  
0.46 0.59

*Psenopsis cyanea*: 0.15 0.33 0.13 0.63 0.50 0.63 0.50 0.13 0.17 0.13 0.67 0.25 0.01 0.64 0.57 0.25 0.52 0.54 0.50 0.46  
0.47 0.45

*Centrolophus niger*: 0.26 0.22 0.26 0.69 0.50 0.69 0.50 0.13 0.17 0.13 0.67 0.25 0.01 0.86 0.79 0.25 0.45 0.59 0.11 0.37  
0.45 0.33

*Schedophilus sp.*: 0.28 0.33 0.26 0.56 0.50 0.56 0.50 0.17 0.17 0.17 0.67 0.25 0.07 0.57 0.57 0.50 0.42 0.60 0.53 0.64 0.49  
0.49

*Seriocella violacea*: 0.26 0.39 0.23 0.56 0.50 0.56 0.50 0.11 0.17 0.11 0.67 0.25 0.01 0.71 0.57 0.25 0.49 0.56 0.52 0.49  
0.59 0.33

*Tubbia tasmanica*: 0.30 0.22 0.29 0.69 0.50 0.69 0.50 0.18 0.17 0.18 0.67 0.25 0.13 0.79 0.71 0.25 0.54 0.54 0.20 0.37  
0.31 0.56

*Icichthys lockingtoni*: 0.23 0.22 0.23 0.63 0.50 0.63 0.50 0.17 0.17 0.16 0.67 1.00 0.26 1.00 1.00 0.25 0.64 0.50 0.25 0.36  
0.45 0.41

*Hyperoglyphe perciformis*: 0.14 0.39 0.11 0.81 0.50 0.81 0.50 0.08 0.17 0.08 0.67 0.25 0.01 0.64 0.64 0.25 0.58 0.52 0.54  
0.55 0.66 0.29

*Psenes cyanophrys*: 0.18 0.56 0.13 0.50 0.50 0.50 0.50 0.17 0.17 0.16 0.56 0.25 0.06 0.43 0.43 0.50 0.51 0.66 0.81 0.60  
0.38 0.64

*Psenes sio*: 0.19 0.61 0.13 0.50 0.50 0.50 0.50 0.12 0.08 0.12 0.56 0.25 0.09 0.57 0.50 0.50 0.50 0.60 0.37 0.46 0.39 0.52

*Ariomma melanum*: 0.12 0.61 0.06 0.75 0.50 0.75 0.50 0.06 0.17 0.06 0.67 0.25 0.06 0.57 0.50 0.50 0.53 0.58 0.50 0.56  
0.65 0.40

*Cubiceps whiteleggii*: 0.15 0.67 0.08 0.63 0.50 0.63 0.50 0.08 0.17 0.08 0.67 0.25 0.06 0.57 0.57 0.50 0.56 0.55 0.69 0.64  
0.52 0.40

*Cubiceps pauciradiatus*: 0.11 0.50 0.06 0.50 0.50 0.50 0.50 0.06 0.08 0.07 0.67 0.25 0.06 0.50 0.43 0.50 0.52 0.45 0.75  
0.60 0.64 0.24

*Nomeus gronovii*: 0.20 0.56 0.15 0.75 0.50 0.75 0.50 0.14 0.17 0.14 0.67 0.25 0.12 0.64 0.57 0.50 0.48 0.49 0.68 0.53 0.55  
0.39

*Peprilus triacanthus*: 0.29 0.17 0.29 0.50 0.50 0.50 0.00 0.24 0.17 0.24 0.67 0.25 0.06 0.43 0.43 0.50 0.52 0.63 0.82 ? 0.26  
0.81

*Peprilus paru*: 0.30 0.33 0.27 0.50 0.50 0.50 0.00 0.24 0.25 0.23 0.67 0.25 0.04 0.36 0.29 0.50 0.70 0.72 1.00 ? 0.34 0.96

*Pampus cinereus*: 0.30 0.44 0.27 1.00 0.50 1.00 0.00 0.22 0.42 0.20 0.67 0.25 0.09 0.36 0.29 0.50 0.64 0.62 0.93 ? 0.50  
0.86

*Stromateus brasiliensis*: 0.27 0.56 0.22 0.69 0.50 0.69 0.00 0.25 0.17 0.24 0.67 0.25 0.17 0.64 0.57 0.50 0.50 0.64 0.56 ?  
0.26 0.72

*Tetragonurus cuvieri*: 0.15 1.00 0.03 0.38 0.50 0.38 0.50 0.03 0.00 0.04 0.67 0.00 0.21 0.71 0.57 0.50 0.62 0.23 0.25 0.43  
0.61 0.06

*Orthopristis ruber*: 0.13 0.61 0.07 0.50 0.50 0.50 0.50 0.04 0.17 0.04 0.67 0.25 0.02 0.79 0.71 0.50 0.61 0.53 0.64 0.58  
0.75 0.17

*Kuhlia marginata*: 0.07 0.50 0.03 0.19 0.50 0.19 0.50 0.04 0.17 0.04 0.67 0.25 0.01 0.79 0.64 0.50 0.59 0.38 0.43 0.59  
0.59 0.33

*Girella simplicidens*: 0.14 0.72 0.06 0.56 0.00 0.63 0.50 0.04 0.17 0.04 0.67 0.25 0.03 0.64 0.57 0.50 0.59 0.56 0.58 0.55  
0.69 0.22

*Kyphosus sectatrix*: 0.09 0.56 0.04 0.50 0.50 0.50 0.50 0.04 0.17 0.04 0.67 0.25 0.02 0.50 0.43 0.25 0.75 0.37 0.41 0.60  
0.62 0.26

*Microcanthus strigatus*: 0.12 0.56 0.07 0.38 0.50 0.38 0.50 0.06 0.17 0.05 0.67 0.25 0.01 0.57 0.50 0.50 0.74 0.62 0.63  
0.70 0.82 0.33

*Scorpius chilensis*: 0.20 0.50 0.15 0.50 0.50 0.50 0.50 0.15 0.17 0.15 0.67 0.25 0.01 0.79 0.71 0.25 0.59 0.52 0.51 0.61 0.54  
0.54

*Lutjanus analis*: 0.10 0.50 0.06 0.38 0.50 0.38 0.50 0.03 0.17 0.03 0.67 0.25 0.01 0.64 0.57 0.25 0.69 0.44 0.62 0.63 0.74  
0.16

*Cynoscion striatus*: 0.16 0.56 0.10 0.44 0.50 0.44 0.50 0.01 0.08 0.02 0.67 0.25 0.01 0.57 0.50 0.25 0.51 0.43 0.44 0.56  
0.90 0.02

*Amniataba caudavittata*: 0.07 0.61 0.02 0.31 0.50 0.31 0.50 0.02 0.17 0.02 0.67 0.25 0.01 0.57 0.57 0.50 0.66 0.51 0.41  
0.63 0.81 0.18

*Diplectrum radiale*: 0.08 0.50 0.04 0.44 0.50 0.44 0.50 0.01 0.17 0.01 0.67 0.25 0.01 0.71 0.64 0.25 0.52 0.48 0.52 0.45  
0.59 0.15

*Atherinella brasiliensis*: 0.00 0.22 0.00 0.25 0.00 0.31 0.50 0.08 0.00 0.09 0.67 0.00 0.11 0.57 0.71 0.50 1.00 0.04 0.50  
0.65 0.59 0.24

*Mugil curema*: 0.01 0.17 0.02 0.44 0.50 0.44 0.50 0.03 0.17 0.03 0.33 0.25 0.01 0.36 0.43 0.50 0.85 0.23 0.48 0.69 0.87  
0.09

*Monocirrhus polyacanthus*: 0.16 0.89 0.06 0.63 0.00 0.00 0.50 0.13 1.00 0.06 0.67 0.25 0.00 0.07 0.00 0.50 0.79 0.55 0.18  
0.67 0.57 0.61

*Trachinotus carolinus*: 0.17 0.33 0.15 0.50 0.50 0.50 0.50 0.12 0.17 0.11 0.67 0.25 0.01 0.50 0.43 0.25 0.58 0.59 0.48 0.55  
0.48 0.51

*Coryphaena hippurus*: 0.43 0.72 0.35 0.63 0.50 0.63 0.50 0.14 0.17 0.14 0.67 0.00 0.06 0.86 0.86 0.00 0.14 0.87 0.29 0.36  
0.48 0.49

*Rachycentron canadum*: 0.22 0.44 0.19 0.69 0.50 0.69 0.50 0.10 0.00 0.11 0.67 0.00 0.01 0.86 0.79 0.25 0.38 0.56 0.48  
0.41 0.46 0.44

*Nematistius pectoralis*: 0.18 0.44 0.15 0.44 0.50 0.44 0.50 0.09 0.17 0.09 0.67 0.25 0.01 0.64 0.57 0.25 0.45 0.63 0.30 0.54  
0.75 0.23

*Morone mississippiensis*: 0.07 0.50 0.03 0.38 0.50 0.38 0.50 0.03 0.17 0.03 0.67 0.25 0.01 0.71 0.64 0.25 0.65 0.32 0.50  
0.56 0.81 0.09

*Lateolabrax japonicus*: 0.10 0.61 0.04 0.44 0.50 0.44 0.50 0.02 0.17 0.02 0.67 0.25 0.08 0.86 0.71 0.25 0.55 0.41 0.33 0.56  
0.83 0.04

*Lates niloticus*: 0.06 0.33 0.04 0.38 0.50 0.38 0.50 0.03 0.17 0.03 0.67 0.25 0.01 0.50 0.43 0.25 0.73 0.38 0.42 0.59 0.89  
0.09

*Centropomus paralellus* 0.06 0.44 0.02 0.38 0.50 0.38 0.50 0.00 0.17 0.00 0.67 0.25 0.01 0.71 0.71 0.25 0.41 0.13 0.28  
0.41 0.40 0.02

*Oplegnathus fasciatus* 0.13 0.61 0.07 0.44 0.00 0.50 0.50 0.05 0.17 0.05 0.67 0.25 0.01 0.71 0.64 0.25 0.59 0.56 0.50 0.75  
0.77 0.29

*Polydactylus virginicus* 0.07 0.44 0.04 0.94 0.00 0.00 0.50 0.08 0.17 0.07 0.67 0.25 0.01 0.86 0.79 0.25 0.55 0.35 0.56 0.53  
0.52 0.23

*Paralichthys isosceles*: 0.55 0.00 0.58 0.06 1.00 0.00 0.50 0.41 0.00 0.42 0.44 0.00 0.11 0.07 0.00 0.25 0.00 1.00 0.35 0.38  
0.00 1.00

*Psettodes erumei*: 0.30 0.56 0.24 0.25 0.50 0.25 0.50 0.21 0.00 0.22 0.67 0.00 0.01 0.29 0.29 0.25 0.19 0.76 0.26 0.47  
0.22 0.76

*Parachanna obscura* 0.24 0.00 0.27 0.44 0.50 0.44 0.50 0.14 0.00 0.16 0.33 0.00 0.14 0.14 0.21 0.75 0.47 0.62 0.33 0.53  
0.37 0.58

DATA MATRIX: QUALITATIVE CHARACTERS

*Beryx splendens*: 1010001001010100111-10000000100100000-----0102010010100000  
0000101011001000001000120000-10-0211000000000000100000000-----0001000  
0000000000--01100110100--00000100000000-000-0000001000012110--010000

*Holocentrus adscensionis* 1010000111010100011-100000000-1-10000-----000001000010  
0000000010100--000000010001-0000-10-1211001000000000100100000-----0001  
0000000000000--01100100000--01000100000000-00000000101010012100--0100  
00

*Dinematichthys ilucoeteoides* 1100101000000100111-00000001110000000-----1-0-1-001  
011-201101000000--0100000111---0010-111001000000000000101000010-----0  
0010001010000000--011001000010100001001000000---0101-0001110111--0--1  
00000

*Raneya brasiliensis*: 1101100000100100111-00000111110000100-----1-0-1-001011-20  
110-000000--01000001-1---0010-1110010000000000000101001010-----0001000  
1010000000--111011000010100001101000000---0101-00010000010-0--100000

*Apogon maculatus*: 0000100001000100111-10000000110010100-----00110100010000  
0000000000--000000011001-0000-10-001010000002100100000000-----000000  
0001000000--11000100000--10100101000000-00000000101000010100--110000

*Aulostomus maculatus*: 000101-000000-01011-1100011-0-020-100-----011-0100100012  
0110-000000--01001----0----000--0-0111-----00000102000010-----000?00--10-  
000000--21101000000--00001101000000---1111-011100001010110100000

*Icosteus aenigmaticus*: 001110-000000111111-110000000-0110100-----0-01001001-2  
00001000000--01001----1---0000-00-002001101-02100100000010-----000000--  
01000100100011001001010001001000000000---1111-1-----100--101001

*Brama caribbea*: 100111-001001100111-10000010100000100-----0102--00100010000  
001000011100000000100120000-10-02110001000210000000000000-----01000010  
0100010010011100110110--0000101-000100---0001-0000011012100--0111-1

*Caristius macropus*: 000111-000000100111-110000100-0110100-----010-01001010120  
0001000000--0000000011---0000-10-02220000000000000100000010-----0000000  
0010000000--01101110110--001011000001010--000020000000011100--11100?

*Pseudoscopelus altipinnis*: 000111-0000001101101001000100-0010000-----011-0100110  
01000000000000--0100100011---0010-111010000001-00000100100010-----001  
00000011001000--211001000010000001000000000---011000111000001100--001  
000

*Pomatomus saltatrix*: 1010001001001100111-00000010100100100-----0101010010001  
000000110000--00000001100120001110-021100001-000111000010010-----0000  
00000000000000--11100100100--01100100000100-00000000101100112100--0100  
10

*Arripis georgianus*: 1010001001001100111-00000110100000100-----000100000100000  
1100110000--00000001100120001110-0020100100000011000000001-----000000  
0001-000010--11100100100--01100100100100-00000000101101110100--01000?

*Scombrolabrax heterolepis*: 0000000101000100111-100001100-1-00100-----0001010001  
000000000110000--0000000111---0001110-001010000000000100000000-----00  
00000001000?000--01100100100--01000101000000-000000001010000?10-0--01  
000?

*Sphyraena tome*: 100101-0000111101100101001100-0200100-----011-010010001001  
100110000--0000100111---001111110111101000100100010010010-----0000000  
0000011000--11101100100--01001101100100---0011-0101000011100--010000

*Thyrsitops lepidopoides*: 100001-000001100111-11100010100200100-----011001001100  
1001100001000--00000000100--0011100-021100101-001101000001000-----0000  
0000000010000--11100100100--01001101100100-000001-0101000011100--0100  
00

*Auxis thazard*: 100101-0000011111100111001100-0200100-----01110100110010111  
0-001000--0000000011---000111100020000000101101000000000-----001000000  
00011000--11100100100--01001101100000---0001-0001000001100--01???

*Scomber sp.*: 100001-0000010001101111001100-1-00100-----011101001100101110-  
001000--0000000011---000111100020001100101101000000000-----0010000000  
0011000--11101100100--00001101100000-000001-0101000011100--011000

*Trichiurus lepturus*: 110011-000000110111-111001100-0200100-----010-0101---01-0--  
---0000--1---00011---0011100-020010101-00110000101101-----0000000010-0  
01010--11100100100--01--111-000100-001---1-----101-10000

*Amarsipus carlsbergi*: 0000101000000001111-110000001-0010100-----011-0100110010  
00000110000--000000001012300010110002000001-000001000000000-----00000  
000010001000--111001001011000001101000110---0001-0101000001100--01100  
1

*Ariomma indicum*: 000001-000001011111-111100101000101011011100111000011001  
001110100000--00000001100120001000-01110111010000110000000001011100  
0-11000100010011111101110110--010010000001110110001-0001011001100--0  
11011

*Ariomma bondi*: 100001-000001011111-111100100-0000101101110011100001100100  
1110000000--0000000110-120001100-012101111-00001100000000010111000-1  
1000010010011011101110110--010010000001110110001-0001000011100--0110  
11

*Psenopsis anomala*: 000001-001000011111-1110001010001010100000-0101000011001  
000000110000--00000001100120001010-021100001-00001100000010-0-000000  
-10000010000010011100110110--01001100000111011000000101110111100--01  
1011

**Psenopsis cyanea:** 0000001001000011111-111000100-001010100000-01010000110010  
00000100000--000000011001200011110012100001-00001100000010-0-000000-  
100000100100100111001101111001001100000111011000000101100111100--01  
1011

**Centrolophus niger:** 000101-0010010111111-101000100-001010100000-0102000010000  
000000110000--00000001100120000-110020000001-0000110000001000-000000  
-1000001001001001110011010110010011000001111--0001-0101111111100--01  
1001

**Schedophilus sp.:** 000111-0000000111111-1?1000000-001010100000-010100001100100  
1100100000--00000001100120001010-002001111-00001100000010-0-000000-10  
000010010010010-00110110--010011000001110--0001-0101100111100--011011

**Seriolaella violacea:** 1000001001001011111-1010001010001010100000-0101000011001  
001100110000--00000001100120001110-011100001-0000110000001000-000000  
-10000010010010011100110110--011011000001111110001-0101100111100--01  
1001

**Tubbia tasmanica:** 0000001101000011111-101000100-000010100000-01020100100010  
00000110000--00000001100120000-110120010001-00000100000010-0-000000-1  
0000010010010010-0011010100011011000001111110001-0000111111100--0110  
11

**Icichthys lockingtoni:** 1001101101000011111-101000000-001011100000-010-010010001  
000001000000--000000011001200010110021100001-02101100000010-0-000000  
-000000100100100111001101010001001100000110---0001-0101111111100--011  
001

**Hyperoglyphe perciformis:** 1000101001001011111-1010001010001010100000-000100001  
1001000000110000--000000011001200010110002000000000000110000001000-0  
00000-10000010000010010-001101011001101100000110-110000001011111111  
00--010011

**Psenes cyanophrys:** 100101-0000010001101101000101000001010001110111000011001  
0011001100011000000001100120001000-00200011010000010000001000-00000  
0-10000010010010010-00110110--010011000001110--000020001111111100--01  
1011

**Psenes sio:** 000001-1010000111111-111000100-0010101000111011100001100100110  
01100011000000001100120001000-002011110100000100000010-0-000000-1000  
0010010010010-00110110--010010000001110--000000001111111100--011011

**Ariomma melanum:** 100001-0000010111111-111100101000001011011100111000011001  
001110000000--00000001100120001000-002001111-00001100000000010111000  
-11000010010011011101110110--010010000001110110001-0001011011100--01  
1001

**Cubiceps whiteleggii:** 000101-0000000001101111000100-0010101000111011100001100  
10011001000011100001001100120001000-002000101-00001100000000-0-00000  
0-10000010010010011100110110--010011000001110--000000001111111100--01  
1001

**Cubiceps pauciradiatus:** 000101-00000000011101111000100-1-1010100011101110000110  
010011001000011100001001100120001000-002000111-00001100000000-0-0000  
00-10000011010010011100110110--000011000001110--000000001111111100--0  
11001

**Nomeus gronovii:** 000101-0000000001101101000100-1-1010100011101110100110010  
011001000010000001001100120001000-002000111-00001100000000-0-000000-  
10000011010010010-00110110--010011000001110--0001-0001111111100--0110  
01

**Peprilus triacanthus:** 000101-000001011111-111110100-001011111011100010111--00  
001101100010--00110001100120001000-02110111010000110000001011110000  
0-00000010010010011-01111110--010010000001111--0-01-010110-111100--011  
011

**Peprilus paru:** 000101-000001011111-111110100-001011111011100010011--000011  
01100010--00110001100120001000-021101111-0[01]101100000010111100000-0  
0000010010010011-00111110--010010000001111--0-01-010110-111100--01101  
1

**Pampus cinereus:** 000101-000000011111-111110000-001011111011100010111--0000  
1101100000--01000000100120001000-021101111-02101100000010-11100000-1  
00000000100100111011101111001001-000001111--0101-010110-111100--01101  
1

**Stromateus brasiliensis:** 000101-000001011111-111110100-011011111011101010101--0  
1001101100000--01000001100120001000-121101111-0210110000001001110000  
0-000000100100100111011111110010010000001111--0101-010110-111100--01  
1011

**Tetragonurus cuvieri:** 000111-1010000001101111000000-0010001110110011-00001100  
1001101000000--00000001-1---0001100-020010001-00000000000010-10100000  
-10000001000111100-011001011001001101000100---0001-0101100112100--011  
011

**Orthopristis ruber:** 000101-001001111111-11000110111-00100-----00010000000000  
0000110000--0000000110011000102101010110100000001000000100-----000010  
00010001000--11-101001010001110000000100---0001-0000011110100--010000

**Kuhlia marginata:** 0011000001011100001-11000010100000100-----00010000010000  
0000110000--0000001110012000--0110101100000000011000000000-----000000  
0001000?000--20-00100000--01110100000000---0001-0101000010100--010000

**Girella simplicidens:** 000000000000111111-11000000102-00100-----00010000010000  
00000000000--00000001100110000-110000000101-0010101-1000100-----00000  
00001000?000--20-00100100--01110001000100-00000000001100110100--01000  
1

**Kyphosus sectatrix:** 0011000000011100100011000010100000100-----00010000010000  
00000110000--000000111001201010010001000101-000011000000100-----00000  
00000000?000--10-00100100--01110000000100---000000000111110100--01000  
0

**Microcanthus strigatus:** 000001-001011111111-11000110100000100-----000100000100  
0000000110000--00000011100110000-210001000001-021011000000100-----000  
0001001000?010---0-00100000--01110000000100-00000000001111110100--010  
000

**Scorpius chilensis:** 001001-001011100101-11000110100000100-----000100000100000  
000110000--0000000110012000101100111101100000001000000001-----0000000  
001000?000--11000100000--01110000000100-010001-0000111110100--010000

*Lutjanus analis*: 000001-001001100111-00000110110000100-----00010000010000000  
00000000--0000000110012000101100121000100000001001000100-----00000000  
01000000--11010100100--01110101000100-11000000101100110100--010000

*Cynoscion striatus*: 0000001001110111111-01000111112-01100-----001100001000010  
0000100000--00000001100120000-1110020000000000000001-100010-----000000  
00010001010---1010100000--11000100000000-10000000000101110110--0101-0

*Amniataba caudavittata*: 0010000001001111111-11000110101-00100-----00000000000  
00000000110010--00000001100010000-11001111010000000101-1000101-----00  
000000010001010--110001000010001110001000000-010001-0101110110100--0  
10000

*Diplectrum radiale*: 0000000001011100111-00000110111-00100-----000100000000000  
0000000000--00000001100120000-110001000000000000001001000100-----000000  
00010000000--110001000010010110101000100-110001-0101010010100--01000  
0

*Atherinella brasiliensis*: 000101-0000011111111-110001110-2-01100-----011-010011001  
001001000000--0100110111---1101100-010110011-100001000000000-----10001  
000010001100--20-10100000--00000101000000---0110100010000111010110000  
0

*Mugil curema*: 001101-000000011111-110001110-0-01100-----001-01000100000110  
1000000--0000110110---2000-00-000100011-00000000000010-----10001010--1  
0-1100---0-00100000--00000101100000---00100000011111010101100000

*Monocirrhus polyacanthus*: 0001101000010111111-110000100-1-00100-----0001000001  
00020000-000000--00000---00121000-20-0121000000000000100000010-----010  
00000000100000--10-00100100--00000101001000---0001-00010000100-101100  
000

*Trachinotus carolinus*: 010001-000001110111-11000010100000100-----0001010001000  
001101000000--00000001100120000-10-011000001-000000010000100-----0000  
0000010001000--20-00110110--01101000101000-00000000101000011100--0100  
01

*Coryphaena hippurus*: 110101-000000100110011000110110000100-----010-000011001  
00110-000000--0000000111---0001010-011110101-0210011-010000-----000000  
00010001000--11101110110--010011000010010--0001-0101000011100--01100?

*Rachycentron canadum*: 110111-0000001001000000001101100?0100-----000001001100  
1000000000000--0000000111---0001000-001000101-0000001-010000-----0000  
0000010000000--11-00100000--01001100000000---0001-0101000011100--00100  
0

*Nematistius pectoralis*: 110011-001001100111-00000110100100100-----010?000011001  
001100000000--00000001100000001010-001000001-000001001000000-----0000  
0000010000000--11100110110--01001100000000-000000001010001?1100--0100  
00

*Morone mississippiensis*: 0000000001011100110000000010110000100-----00010000010  
00000000110100--00000001100120000-110111100111-0000011-1000000-----00  
000000010001000--210011000011001100100000000-11000000001100110100--0  
10000

*Lateolabrax japonicus*: 1000000011010100111-00000110110000100-----001101000100  
0000000110100--00000001100120000-110011110100000000100100000-----000

000000100010[01]0--110011000010001100100000000-11000000001110010100--  
010000

**Lates niloticus:** 1010000011010100011-00000110100000100-----00110000010002000  
01110100--00000001100120000-110012110100000000000100000-----00000000  
010001010--110001000010011100100000000-11000000101101110110--010000

**Centropomus paralellus:** 101001-011010100011-00000110100000100-----000100000000  
0000000110000--00000001100120000-110011110111-0000011-000000-----0000  
0010010011000--110111000010001100100000100-10000000101001110110--010  
000

**Oplegnathus fasciatus:** 0000101001011101111-11000010100000100-----000100000100  
0200000110100--00000011100110000-110021000001-000011000000100-----000  
0000001000?000--11100100000--01100001000100-000001-0101000010100--010  
000

**Polydactylus virginicus:** 000011-011111100011-00000111112-01100-----0011000000000  
00000011000--0000100110012001111110020000000000001000010100-----0000  
0000010001010--11000100101000?000100100100-00000000000111110110--010  
010

**Paralichthys isosceles:** 000101-000000111111-10000110101-00000-----1-0-01001001-0  
0--0-000000--0000000011---0010-10-001010001-01100100000000-----0100000  
-10-000000--11100100100--01001000010000--0001-0001101110110--011000

**Psettodes erumei:** 100101-000000100100011000110101-00100-----010-000011001100  
00-000000--0000000111---0010-10-011110000001100100100010-----0100000-1  
0-00?010--111001001010001001100010000---0001-0001000010110--011000

**Parachanna obscura** 000011-000000100111-110001100-0100000-----1-000100100012  
00000000000--00001001101--0000-10-001000001-00000100001011-----000010  
00010101000--21-00000000--00000001001000-000011-0000000011100--100000

LIST OF SYNAPOMORPHIES FOR THE REFERENCE TREE (K= 6.808).

**Beryx splendens:** No autapomorphies.

**Holocentrus adscensionis:** Char. #9: 0.050-->0.040; Char. #11: 0.250-->0.130; Char. #12: 0.010-->0.030; Char. #16: 0.590-->0.550; Char. #18: 0.500-->0.490; Char. #19: 0.560-0.660-->0.550; Char. #20: 0.740-0.770-->0.850; Char. #21: 0.210-0.290-->0.120; Char. #28: 1-->0; Char. #29: 0-->1; Char. #30: 0-->1; Char. #38: 1-->0; Char. #50: 1-->0; Char. #52: 0-->1; Char. #54: 0-->1; Char. #68: 1-->0; Char. #113: 0-->1; Char. #119: 0-->1; Char. #131: 0-->1; Char. #202: 0-->1.

**Dinematichthys ilucoeteoides:** Char. #3: 0.630-->0.750; Char. #5: 0.750-->0.810; Char. #25: 1-->0; Char. #56: 1-->0; Char. #201: 0-->1; Char. #202: 0-->1; Char. #204: 0-->1.

**Raneya brasiliensis:** Char. #0: 0.500-->0.860; Char. #2: 0.530-->0.890; Char. #7: 0.340-->0.600; Char. #9: 0.350-->0.610; Char. #10: 0.560-->0.000; Char. #17: 0.720-->0.820; Char. #18: 0.230-->0.110; Char. #19: 0.280-->0.000; Char. #20: 0.290-0.360-->0.150; Char. #21: 0.760-->0.830; Char. #28: 1-->0; Char. #32: 0-->1; Char. #133: 0-->1; Char. #162: 0-->1; Char. #166: 0-->1; Char. #180: 0-->1; Char. #205: 1-->0.

**Apogon maculatus:** Char. #3: 0.380-0.440-->0.130; Char. #7: 0.030-0.050-->0.010; Char. #8: 0.170-->0.080; Char. #9: 0.030-0.050-->0.020; Char. #11: 0.250-->0.130; Char. #17: 0.230-0.430-->0.170; Char. #18: 0.500-->0.520; Char. #19: 0.560-->0.550; Char. #21: 0.160-0.240-->0.070; Char. #28: 1-->0; Char. #48: 1-->0; Char. #54: 0-->1; Char. #114: 1-->0; Char. #117: 0-->1; Char. #124: 0-->2; Char. #125: 0-->1; Char. #175: 0-->1.

**Aulostomus maculatus:** Char. #1: 0.000-0.440-->0.670; Char. #2: 0.170-0.270-->0.150; Char. #3: 0.440-->0.380; Char. #5: 0.440-->0.000; Char. #10: 0.330-->0.000; Char. #15: 0.750-->1.000; Char. #16: 0.470-->0.800; Char. #17: 0.560-0.620-->0.300; Char. #18: 0.320-0.330-->0.000; Char. #19: 0.530-->1.000; Char. #20: 0.370-0.460-->1.000; Char. #21: 0.490-0.500-->0.080; Char. #26: 1-->0; Char. #37: 0-->1; Char. #38: 1-->0; Char. #53: 1-->2; Char. #67: 0-->1; Char. #80: 0-->1; Char. #81: 0-->1; Char. #116: 0-->1; Char. #130: 0-->2; Char. #151: 0-->1; Char. #152: 1-->0; Char. #156: 1-->0; Char. #166: 0-->1; Char. #180: 0-->1; Char. #192: 0-->1; Char. #199: 0-->1; Char. #206: 1-->0; Char. #209: 0-->1.

**Icosteus aenigmaticus:** Char. #10: 0.560-0.670-->1.000; Char. #12: 0.140-0.280-->0.300; Char. #16: 0.330-0.450-->0.320; Char. #24: 0-->1; Char. #36: 0-->1; Char. #37: 0-->1; Char. #54: 0-->1; Char. #110: 1-->0; Char. #115: 1-->2; Char. #118: 0-->1; Char. #119: 0-->1; Char. #124: 0-->2; Char. #125: 0-->1; Char. #159: 0-->1; Char. #170: 0-->1; Char. #176: 0-->1; Char. #192: 0-->1; Char. #197: 0-->1; Char. #217: 0-->1.

**Brama caribbea:** Char. #7: 0.120-0.130-->0.140; Char. #9: 0.110-0.130-->0.140; Char. #10: 0.670-->0.560; Char. #14: 0.570-->0.360; Char. #16: 0.450-0.470-->0.660; Char. #18: 0.500-->0.780; Char. #19: 0.490-0.530-->0.680; Char. #20: 0.460-0.470-->0.530; Char. #21: 0.550-->0.630; Char. #22: 0-->1; Char. #31: 0-->1; Char. #34: 0-->1; Char. #43: 1-->0; Char. #89: 0-->1; Char. #120: 0-->1; Char. #124: 0-->2; Char. #125: 0-->1; Char. #128: 1-->0; Char. #144: 0-->1; Char. #149: 0-->1; Char. #159: 0-->1; Char. #180: 1-->0; Char. #181: 0-->1; Char. #202: 0-->1; Char. #203: 0-->1; Char. #206: 1-->2; Char. #215: 0-->1.

**Caristius macropus:** Char. #1: 0.220-->0.000; Char. #2: 0.190-->0.230; Char. #7: 0.120-0.130-->0.100; Char. #8: 0.080-->0.000; Char. #11: 0.250-->0.000; Char. #16: 0.450-0.470-->0.240; Char. #17: 0.540-0.590-->0.850; Char. #19: 0.490-0.530-->0.470; Char. #20: 0.460-0.470-->0.380; Char. #50: 1-->0; Char. #53: 0-->1; Char. #75: 0-->1; Char. #78: 0-->2; Char. #83: 0-->1; Char. #101: 0-->1; Char. #115: 1-->2; Char. #116: 1-->2; Char. #135: 0-->1; Char. #156: 1-->0; Char. #162: 1-->0; Char. #166: 0-->1; Char. #177: 0-->1; Char. #188: 0-->1; Char. #195: 1-->0; Char. #212: 0-->1.

**Pseudoscopelus altipinnis:** Char. #0: 0.180-0.220-->0.150; Char. #1: 0.440-->0.500; Char. #2: 0.170-0.190-->0.100; Char. #3: 0.440-0.500-->0.190; Char. #5: 0.440-0.500-->0.190; Char. #7: 0.120-0.130-->0.060; Char. #9: 0.110-0.130-->0.050; Char. #16: 0.450-0.470-->0.490; Char. #17: 0.560-0.590-->0.530; Char. #36: 0-->1; Char. #42: 1-->0; Char. #43: 1-->0; Char. #44: 0-->1; Char. #54: 0-->1; Char. #56: 1-->0; Char. #67: 0-->1; Char. #99: 1-->0; Char. #107: 0-->1; Char. #111: 0-->1; Char. #115: 1-->0; Char. #131: 0-->1; Char. #145: 0-->1; Char. #153: 0-->1; Char. #195: 1-->0; Char. #199: 0-->1; Char. #205: 1-->0.

**Pomatomus saltatrix:** Char. #1: 0.440-->0.390; Char. #2: 0.070-->0.110; Char. #3: 0.380-0.440-->0.500; Char. #5: 0.380-->0.500; Char. #7: 0.050-0.080-->0.150; Char. #9: 0.050-0.090-->0.160; Char. #16: 0.540-0.590-->0.600; Char. #18: 0.370-->0.350; Char. #19: 0.550-->0.530; Char. #20: 0.740-0.770-->0.610; Char. #21: 0.210-0.290-->0.330; Char. #53: 0-->1; Char. #66: 0-->1; Char. #73: 0-->1; Char. #74: 1-->0; Char. #77: 0-->1; Char. #114: 1-->2; Char. #116: 0-->1; Char. #121: 0-->1; Char. #126: 0-->1; Char. #133: 0-->1; Char. #136: 0-->1; Char. #152: 1-->0; Char. #206: 0-->2; Char. #216: 0-->1.

**Arripis georgianus:** Char. #0: 0.120-0.140-->0.080; Char. #2: 0.070-->0.050; Char. #3: 0.380-0.440-->0.310; Char. #5: 0.380-->0.310; Char. #7: 0.050-0.080-->0.030; Char. #9: 0.050-0.090-->0.030; Char. #13: 0.570-->0.500; Char. #14: 0.570-->0.500; Char. #16: 0.540-0.590-->0.530; Char. #17: 0.440-->0.430; Char. #20: 0.740-0.770-->0.860; Char. #21: 0.210-0.290-->0.110; Char. #70: 1-->0; Char. #80: 0-->1; Char. #81: 0-->1; Char. #114: 1-->0; Char. #115: 1-->2; Char. #120: 0-->1; Char. #137: 0-->1; Char. #158: 0-->1; Char. #183: 0-->1; Char. #203: 0-->1.

**Scombrolabrax heterolepis:** Char. #1: 0.440-0.500-->0.670; Char. #14: 0.570-->0.640; Char. #18: 0.390-0.500-->0.680; Char. #19: 0.550-0.560-->0.640; Char. #20: 0.740-0.770-->0.860; Char. #28: 1-->0; Char. #29: 0-->1; Char. #50: 1-->0; Char. #52: 0-->1; Char. #114: 1-->0; Char. #162: 1-->0; Char. #182: 0-->1; Char. #207: 1-->0.

**Sphyræna tome:** Char. #0: 0.050-0.110-->0.020; Char. #1: 0.440-->0.280; Char. #3: 0.250-0.310-->0.190; Char. #5: 0.250-0.310-->0.190; Char. #7: 0.030-0.070-->0.020; Char. #9: 0.050-0.070-->0.030; Char. #12: 0.060-0.070-->0.010; Char. #16: 0.470-0.560-->0.690; Char. #17: 0.550-0.640-->0.180; Char. #18: 0.230-0.250-->0.160; Char. #19: 0.510-0.530-->0.690; Char. #21: 0.250-0.320-->0.000; Char. #33: 0-->1; Char. #43: 1-->0; Char. #74: 1-->0; Char. #84: 0-->1; Char. #85: 0-->1; Char. #96: 0-->1; Char. #99: 0-->1; Char. #112: 0-->1; Char. #125: 1-->0; Char. #128: 1-->0; Char. #130: 0-->1; Char. #133: 0-->1; Char. #136: 0-->1; Char. #194: 0-->1.

**Thyrsitops lepidopoides:** Char. #1: 0.440-->0.940; Char. #8: 0.000-->0.170; Char. #20: 0.800-->0.820; Char. #47: 1-->0; Char. #68: 1-->0; Char. #101: 1-->0.

**Auxhis thazard:** Char. #3: 0.750-->0.810; Char. #5: 0.750-->0.810; Char. #12: 0.060-0.070-->0.110; Char. #13: 0.710-->0.860; Char. #14: 0.640-->1.000; Char. #17: 0.550-0.640-->0.660; Char. #19: 0.510-->0.430; Char. #20: 0.800-->0.840; Char. #37: 0-->1; Char. #119: 1-->0; Char. #198: 1-->0; Char. #205: 1-->0.

**Scomber sp.:** Char. #8: 0.000-->0.080; Char. #20: 0.800-->0.720; Char. #35: 1-->0; Char. #41: 0-->1; Char. #52: 0-->1; Char. #120: 0-->1; Char. #176: 1-->0.

**Trichiurus lepturus:** Char. #0: 0.200-0.300-->1.000; Char. #1: 0.440-->0.110; Char. #2: 0.170-0.240-->1.000; Char. #3: 0.250-0.310-->0.000; Char. #4: 0.500-->0.000; Char. #5: 0.250-0.310-->0.000; Char. #6: 0.500-->0.000; Char. #7: 0.120-0.210-->1.000; Char. #9: 0.110-0.220-->1.000; Char. #10: 0.670-->0.000; Char. #12: 0.060-0.070-->1.000; Char. #13: 0.290-0.500-->0.000; Char. #14: 0.290-0.500-->0.000; Char. #16: 0.190-0.390-->0.070; Char. #17: 0.640-0.760-->0.900; Char. #18: 0.230-0.260-->0.000; Char. #20: 0.220-0.470-->0.110; Char. #21: 0.490-0.760-->0.820; Char. #23: 0-->1; Char. #26: 0-->1; Char. #72: 0-->1; Char. #92: 0-->1; Char. #115: 1-->0; Char. #128: 1-->0; Char. #131: 0-->1; Char. #133: 0-->1; Char. #136: 0-->1; Char. #158: 0-->1; Char. #181: 0-->1; Char. #192: 0-->1; Char. #197: 0-->1; Char. #209: 0-->1.

**Amarsipus carlsbergi:** Char. #1: 0.390-0.440-->0.560; Char. #2: 0.170-0.190-->0.130; Char. #12: 0.060-0.100-->0.170; Char. #13: 0.640-0.710-->0.860; Char. #14: 0.570-->0.860; Char. #15: 0.250-->0.500; Char. #17: 0.540-->0.410; Char. #19: 0.490-0.530-->0.260; Char. #20: 0.460-0.470-->0.280; Char. #48: 1-->0; Char. #67: 0-->1; Char. #102: 0-->1; Char. #103: 1-->2; Char. #104: 2-->3; Char. #111: 0-->1; Char. #114: 1-->0; Char. #115: 1-->2; Char. #168: 1-->0; Char. #171: 1-->0; Char. #172: 0-->1; Char. #182: 0-->1; Char. #205: 1-->0.

**Ariomma indicum:** Char. #0: 0.120-->0.100; Char. #1: 0.560-0.610-->0.500; Char. #3: 0.750-->0.880; Char. #5: 0.750-->0.880; Char. #18: 0.530-0.590-->0.740; Char. #19: 0.560-->0.610; Char. #21: 0.400-0.520-->0.530; Char. #121: 1-->0; Char. #152: 0-->1; Char. #205: 1-->0.

**Ariomma bondi:** Char. #1: 0.610-->0.670; Char. #7: 0.070-->0.100; Char. #9: 0.070-->0.090; Char. #11: 0.250-->0.130; Char. #13: 0.570-->0.640; Char. #16: 0.530-->0.500; Char. #20: 0.650-->0.670; Char. #21: 0.400-->0.380; Char. #109: 0-->1.

**Psenopsis anomala:** Char. #1: 0.330-->0.280; Char. #7: 0.130-0.140-->0.150; Char. #9: 0.130-0.140-->0.150; Char. #14: 0.570-->0.500; Char. #16: 0.510-0.520-->0.580; Char. #17: 0.540-->0.500; Char. #18: 0.520-0.530-->0.640; Char. #19: 0.490-0.560-->0.630; Char. #21: 0.450-0.490-->0.590; Char. #114: 1-->2; Char. #156: 1-->0; Char. #202: 0-->1.

**Psenopsis cyanea:** Char. #0: 0.180-0.190-->0.150; Char. #18: 0.520-0.530-->0.500; Char. #19: 0.490-0.560-->0.460; Char. #109: 0-->1; Char. #111: 0-->1; Char. #172: 0-->1.

**Centrolophus niger:** Char. #16: 0.490-0.540-->0.450; Char. #17: 0.540-->0.590; Char. #18: 0.200-0.250-->0.110; Char. #27: 0-->1; Char. #77: 1-->0.

**Schedophilus sp.:** Char. #0: 0.180-0.190-->0.280; Char. #2: 0.130-0.170-->0.260; Char. #7: 0.130-0.140-->0.170; Char. #9: 0.130-0.140-->0.170; Char. #16: 0.510-0.520-->0.420; Char. #19: 0.490-0.560-->0.640; Char. #20: 0.460-0.470-->0.490; Char. #26: 0-->1; Char. #48: 1-->0.

**Seriollella violacea:** Char. #17: 0.540-->0.560; Char. #80: 0-->1; Char. #81: 0-->1; Char. #109: 0-->1.

**Tubbia:** Char. #0: 0.230-0.260-->0.300; Char. #2: 0.230-0.260-->0.290; Char. #7: 0.170-->0.180; Char. #9: 0.160-->0.180; Char. #20: 0.450-->0.310; Char. #21: 0.410-->0.560; Char. #54: 1-->0; Char. #113: 0-->1; Char. #117: 0-->1; Char. #127: 1-->0; Char. #163: 1-->0; Char. #198: 1-->0; Char. #200: 1-->0; Char. #216: 0-->1.

**Icichthys lockingtoni:** Char. #3: 0.690-->0.630; Char. #5: 0.690-->0.630; Char. #11: 0.250-->1.000; Char. #12: 0.130-->0.260; Char. #13: 0.790-0.860-->1.000; Char. #14: 0.710-0.790-->1.000; Char. #16: 0.540-->0.640; Char. #17: 0.540-->0.500; Char. #19: 0.370-->0.360; Char. #26: 0-->1; Char. #48: 1-->0; Char. #57: 0-->1; Char. #83: 0-->1; Char. #84: 1-->0; Char. #85: 1-->0; Char. #116: 0-->1; Char. #124: 0-->2; Char. #125: 0-->1; Char. #147: 1-->0; Char. #188: 1-->0.

**Hyperoglyphe perciformis:** Char. #0: 0.180-0.260-->0.140; Char. #2: 0.170-0.230-->0.110; Char. #3: 0.690-->0.810; Char. #5: 0.690-->0.810; Char. #7: 0.110-0.130-->0.080; Char. #9: 0.110-0.130-->0.080; Char. #16: 0.490-0.540-->0.580; Char. #17: 0.540-->0.520; Char. #18: 0.520-->0.540; Char. #19: 0.490-0.530-->0.550; Char. #20: 0.460-0.590-->0.660; Char. #21: 0.330-->0.290; Char. #26: 0-->1; Char. #66: 1-->0; Char. #114: 1-->0; Char. #115: 1-->2; Char. #121: 1-->0; Char. #156: 1-->0; Char. #163: 1-->0; Char. #188: 1-->0; Char. #195: 1-->0; Char. #214: 1-->0; Char. #216: 0-->1.

***Psenes cyanophrys***: Char. #7: 0.130-0.140-->0.170; Char. #9: 0.130-0.140-->0.160; Char. #13: 0.570-->0.430; Char. #14: 0.500-0.570-->0.430; Char. #17: 0.600-->0.660; Char. #18: 0.680-0.690-->0.810; Char. #20: 0.390-0.470-->0.380; Char. #21: 0.490-0.520-->0.640; Char. #22: 0-->1; Char. #34: 0-->1; Char. #50: 0-->1; Char. #54: 1-->0; Char. #196: 0-->2.

***Psenes sio***: Char. #1: 0.560-->0.610; Char. #7: 0.130-0.140-->0.120; Char. #8: 0.170-->0.080; Char. #9: 0.130-0.140-->0.120; Char. #16: 0.510-->0.500; Char. #18: 0.530-0.560-->0.370; Char. #19: 0.490-0.560-->0.460; Char. #25: 1-->0; Char. #29: 0-->1; Char. #31: 0-->1; Char. #117: 0-->1.

***Cubiceps baxteri***: Char. #7: 0.070-->0.060; Char. #9: 0.070-->0.060; Char. #17: 0.600-->0.580; Char. #18: 0.530-0.590-->0.500; Char. #114: 1-->0; Char. #216: 1-->0.

***Cubiceps whiteleggii***: Char. #1: 0.560-->0.670; Char. #16: 0.520-->0.560; Char. #19: 0.600-->0.640; Char. #120: 1-->0.

***Cubiceps pauciradiatus***: Char. #0: 0.150-->0.110; Char. #1: 0.560-->0.500; Char. #2: 0.080-->0.060; Char. #7: 0.080-->0.060; Char. #8: 0.170-->0.080; Char. #9: 0.080-->0.070; Char. #13: 0.570-->0.500; Char. #14: 0.500-0.570-->0.430; Char. #17: 0.490-0.550-->0.450; Char. #18: 0.690-->0.750; Char. #20: 0.520-0.550-->0.640; Char. #21: 0.390-0.400-->0.240; Char. #37: 0-->1; Char. #176: 1-->0.

***Nomeus gronovii***: Char. #0: 0.180-0.190-->0.200; Char. #2: 0.130-->0.150; Char. #3: 0.500-0.630-->0.750; Char. #5: 0.500-0.630-->0.750; Char. #12: 0.060-0.090-->0.120; Char. #13: 0.570-->0.640; Char. #16: 0.510-->0.480; Char. #70: 0-->1; Char. #90: 1-->0; Char. #195: 0-->1.

***Peprilus triacanthus***: Char. #1: 0.330-->0.170; Char. #2: 0.270-->0.290; Char. #9: 0.230-->0.240; Char. #20: 0.340-->0.260; Char. #121: 1-->0; Char. #125: 1-->0.

***Peprilus paru***: Char. #12: 0.060-->0.040; Char. #16: 0.520-0.640-->0.700; Char. #17: 0.630-->0.720; Char. #18: 0.820-0.930-->1.000; Char. #21: 0.810-0.860-->0.960; Char. #70: 1-->0; Char. #166: 1-->0.

***Pampus cinereus***: Char. #3: 0.560-0.690-->1.000; Char. #5: 0.560-0.690-->1.000; Char. #8: 0.170-0.250-->0.420; Char. #20: 0.340-0.470-->0.500; Char. #48: 1-->0; Char. #99: 1-->0; Char. #153: 1-->0.

***Stromateus brasiliensis***: Char. #7: 0.220-0.240-->0.250; Char. #9: 0.200-0.230-->0.240; Char. #12: 0.070-0.090-->0.170; Char. #13: 0.570-->0.640; Char. #16: 0.510-0.540-->0.500; Char. #17: 0.620-0.630-->0.640; Char. #20: 0.340-0.470-->0.260; Char. #53: 0-->1; Char. #113: 0-->1.

***Tetragonurus cuvieri***: Char. #1: 0.560-0.610-->1.000; Char. #2: 0.060-->0.030; Char. #3: 0.560-0.690-->0.380; Char. #5: 0.560-0.690-->0.380; Char. #7: 0.070-->0.030; Char. #8: 0.170-->0.000; Char. #9: 0.070-->0.040; Char. #11: 0.250-->0.000; Char. #12: 0.070-0.090-->0.210; Char. #13: 0.570-->0.710; Char. #16: 0.530-0.540-->0.620; Char. #17: 0.600-->0.230; Char. #18: 0.530-0.560-->0.250; Char. #19: 0.490-0.560-->0.430; Char. #21: 0.400-0.520-->0.060; Char. #26: 0-->1; Char. #29: 0-->1; Char. #31: 0-->1; Char. #36: 1-->0; Char. #37: 1-->0; Char. #40: 1-->0; Char. #48: 1-->0; Char. #56: 1-->0; Char. #101: 0-->1; Char. #109: 0-->1; Char. #115: 1-->0; Char. #117: 0-->1; Char. #118: 1-->0; Char. #119: 1-->0; Char. #120: 1-->0; Char. #127: 1-->0; Char. #128: 1-->0; Char. #154: 0-->1; Char. #156: 1-->0; Char. #158: 0-->1; Char. #162: 1-->0; Char. #168: 1-->0; Char. #171: 1-->0; Char. #182: 0-->1; Char. #187: 1-->0; Char. #188: 1-->0; Char. #206: 1-->2.

***Orthopristis ruber***: Char. #0: 0.120-->0.130; Char. #12: 0.010-->0.020; Char. #13: 0.640-0.710-->0.790; Char. #14: 0.570-0.640-->0.710; Char. #18: 0.630-->0.640; Char. #21: 0.180-0.220-->0.170; Char. #25: 0-->1; Char. #51: 0-->1; Char. #74: 1-->0; Char. #108: 0-->1; Char. #113: 0-->1; Char. #118: 0-->1; Char. #120: 0-->1; Char. #147: 0-->1; Char. #165: 0-->1; Char. #170: 0-->1; Char. #172: 0-->1; Char. #200: 1-->0; Char. #201: 1-->0.

***Kuhlia marginata***: Char. #0: 0.090-->0.070; Char. #2: 0.040-->0.030; Char. #3: 0.380-0.500-->0.190; Char. #5: 0.380-0.500-->0.190; Char. #15: 0.250-->0.500; Char. #38: 1-->0; Char. #112: 0-->1; Char. #115: 1-->0; Char. #162: 1-->2; Char. #180: 0-->1; Char. #186: 1-->0; Char. #198: 0-->1; Char. #201: 1-->0; Char. #202: 1-->0; Char. #204: 1-->0.

***Girella simplicidens***: Char. #0: 0.090-0.120-->0.140; Char. #1: 0.610-->0.720; Char. #3: 0.380-0.500-->0.560; Char. #4: 0.500-->0.000; Char. #5: 0.380-0.500-->0.630; Char. #12: 0.010-->0.030; Char. #17: 0.510-0.530-->0.560; Char. #19: 0.580-0.600-->0.550; Char. #20: 0.740-0.750-->0.690; Char. #31: 1-->0; Char. #47: 1-->0; Char. #48: 1-->0; Char. #84: 1-->0; Char. #85: 1-->0; Char. #115: 1-->0; Char. #121: 0-->1; Char. #125: 0-->1; Char. #162: 1-->2; Char. #163: 1-->0; Char. #170: 0-->1; Char. #202: 1-->0; Char. #217: 0-->1.

**Kyphosus sectatrix:** Char. #1: 0.500-->0.560; Char. #12: 0.010-->0.020; Char. #13: 0.640-0.790-->0.500; Char. #14: 0.570-0.640-->0.430; Char. #16: 0.590-->0.750; Char. #17: 0.380-->0.370; Char. #18: 0.430-->0.410; Char. #31: 1-->0; Char. #40: 1-->0; Char. #106: 0-->1; Char. #114: 1-->0; Char. #121: 0-->1; Char. #152: 1-->0; Char. #170: 0-->1.

**Microcanthus strigatus:** Char. #7: 0.040-->0.060; Char. #9: 0.040-->0.050; Char. #13: 0.640-0.710-->0.570; Char. #14: 0.570-0.640-->0.500; Char. #16: 0.610-->0.740; Char. #17: 0.530-->0.620; Char. #19: 0.580-0.600-->0.700; Char. #20: 0.750-->0.820; Char. #21: 0.180-0.220-->0.330; Char. #98: 0-->1; Char. #121: 0-->1; Char. #124: 0-->2; Char. #125: 0-->1; Char. #149: 0-->1; Char. #158: 0-->1; Char. #163: 1-->0.

**Scorpius chilensis:** Char. #0: 0.090-0.120-->0.200; Char. #2: 0.040-0.060-->0.150; Char. #7: 0.040-->0.150; Char. #9: 0.040-->0.150; Char. #14: 0.570-0.640-->0.710; Char. #19: 0.590-0.600-->0.610; Char. #20: 0.590-0.620-->0.540; Char. #21: 0.260-0.330-->0.540; Char. #27: 0-->1; Char. #120: 0-->1; Char. #137: 0-->1.

**Lutjanus analis:** Char. #16: 0.590-->0.690; Char. #18: 0.520-->0.620; Char. #19: 0.560-0.600-->0.630; Char. #27: 0-->1; Char. #33: 1-->0; Char. #108: 0-->1; Char. #115: 1-->2; Char. #120: 0-->1; Char. #165: 0-->1; Char. #170: 0-->1.

**Cynoscion striatus:** Char. #0: 0.070-0.100-->0.160; Char. #1: 0.440-0.500-->0.560; Char. #2: 0.040-0.060-->0.100; Char. #5: 0.380-->0.440; Char. #7: 0.030-0.050-->0.010; Char. #8: 0.170-->0.080; Char. #9: 0.030-0.050-->0.020; Char. #13: 0.640-0.710-->0.570; Char. #14: 0.570-0.640-->0.500; Char. #16: 0.550-->0.510; Char. #18: 0.500-->0.440; Char. #20: 0.740-0.770-->0.900; Char. #21: 0.160-0.230-->0.020; Char. #36: 0-->1; Char. #37: 0-->1; Char. #43: 0-->1; Char. #73: 0-->1; Char. #78: 0-->1; Char. #85: 1-->0; Char. #128: 1-->0; Char. #129: 0-->1; Char. #165: 0-->1; Char. #175: 0-->1; Char. #215: 0-->1.

**Ambiatoba caudavittata:** Char. #0: 0.090-0.120-->0.070; Char. #2: 0.040-0.060-->0.020; Char. #3: 0.380-0.500-->0.310; Char. #5: 0.380-0.500-->0.310; Char. #7: 0.040-->0.020; Char. #9: 0.040-->0.020; Char. #13: 0.640-->0.570; Char. #16: 0.590-0.610-->0.660; Char. #18: 0.510-0.580-->0.410; Char. #19: 0.580-0.600-->0.630; Char. #20: 0.740-0.750-->0.810; Char. #24: 0-->1; Char. #68: 1-->0; Char. #74: 1-->0; Char. #88: 0-->1; Char. #103: 1-->0; Char. #137: 0-->1; Char. #158: 0-->1; Char. #172: 0-->1; Char. #186: 1-->0; Char. #198: 0-->1.

**Diplectrum radiale:** Char. #7: 0.030-->0.010; Char. #9: 0.030-->0.010; Char. #16: 0.590-->0.520; Char. #19: 0.560-0.600-->0.450; Char. #20: 0.740-->0.590; Char. #21: 0.160-->0.150; Char. #52: 0-->1; Char. #74: 1-->0; Char. #114: 1-->0; Char. #172: 0-->1; Char. #175: 0-->1; Char. #176: 1-->0; Char. #201: 1-->0; Char. #204: 1-->0.

**Atherinella brasiliensis:** Char. #0: 0.010-->0.000; Char. #2: 0.020-->0.000; Char. #3: 0.380-0.440-->0.250; Char. #8: 0.170-->0.000; Char. #9: 0.030-0.060-->0.090; Char. #11: 0.250-->0.000; Char. #12: 0.010-->0.110; Char. #14: 0.430-0.500-->0.710; Char. #16: 0.850-->1.000; Char. #17: 0.230-->0.040; Char. #34: 0-->1; Char. #52: 0-->2; Char. #66: 0-->1; Char. #73: 0-->1; Char. #77: 0-->1; Char. #93: 0-->1; Char. #101: 0-->1; Char. #106: 0-->1; Char. #108: 0-->1; Char. #117: 0-->1; Char. #123: 0-->1; Char. #165: 0-->1; Char. #193: 0-->1; Char. #196: 0-->1; Char. #206: 0-->1.

**Mugil curema:** Char. #1: 0.220-->0.170; Char. #5: 0.310-->0.440; Char. #10: 0.670-->0.330; Char. #19: 0.650-0.670-->0.690; Char. #20: 0.590-0.600-->0.870; Char. #21: 0.160-0.240-->0.090; Char. #24: 0-->1; Char. #35: 1-->0; Char. #81: 0-->1; Char. #105: 1-->2; Char. #114: 1-->0; Char. #128: 1-->0; Char. #149: 0-->1; Char. #153: 0-->1; Char. #183: 0-->1; Char. #200: 1-->0; Char. #201: 0-->1; Char. #202: 0-->1; Char. #203: 0-->1; Char. #204: 0-->1.

**Monocirrhus polyacanthus:** Char. #0: 0.030-0.100-->0.160; Char. #1: 0.330-0.500-->0.890; Char. #3: 0.380-0.440-->0.630; Char. #5: 0.130-0.310-->0.000; Char. #7: 0.030-0.080-->0.130; Char. #8: 0.170-->1.000; Char. #12: 0.010-->0.000; Char. #13: 0.360-0.570-->0.070; Char. #14: 0.430-0.500-->0.000; Char. #17: 0.230-0.430-->0.550; Char. #18: 0.480-0.500-->0.180; Char. #20: 0.590-0.600-->0.570; Char. #21: 0.160-0.240-->0.610; Char. #52: 0-->1; Char. #70: 1-->0; Char. #78: 0-->2; Char. #110: 1-->2; Char. #115: 1-->2; Char. #144: 0-->1; Char. #152: 1-->0; Char. #154: 0-->1; Char. #170: 0-->1; Char. #185: 0-->1; Char. #195: 0-->1; Char. #207: 1-->0.

**Trachinotus carolinus:** Char. #0: 0.180-->0.170; Char. #1: 0.390-0.440-->0.330; Char. #13: 0.640-->0.500; Char. #14: 0.570-->0.430; Char. #16: 0.450-0.470-->0.580; Char. #19: 0.540-->0.550; Char. #21: 0.490-->0.510; Char. #26: 1-->0; Char. #36: 0-->1; Char. #66: 1-->0; Char. #73: 1-->0; Char. #77: 1-->0; Char. #83: 0-->1; Char. #108: 1-->0; Char. #128: 1-->0; Char. #130: 0-->1; Char. #135: 0-->1; Char. #162: 1-->2; Char. #163: 1-->0; Char. #177: 0-->1; Char. #180: 1-->0; Char. #183: 0-->1; Char. #185: 0-->1.

**Coryphaena hippurus:** Char. #0: 0.220-->0.430; Char. #1: 0.440-->0.720; Char. #2: 0.190-->0.350; Char. #7: 0.120-0.130-->0.140; Char. #9: 0.110-0.130-->0.140; Char. #14: 0.790-->0.860; Char. #15: 0.250-->0.000; Char. #16: 0.380-->0.140;

Char. #17: 0.560-0.590-->0.870; Char. #18: 0.390-0.480-->0.290; Char. #19: 0.410-->0.360; Char. #20: 0.460-0.470-->0.480; Char. #26: 1-->0; Char. #70: 1-->0; Char. #80: 0-->1; Char. #81: 0-->1; Char. #116: 0-->1; Char. #117: 0-->1; Char. #124: 0-->2; Char. #125: 0-->1; Char. #166: 0-->1; Char. #168: 0-->1; Char. #171: 0-->1; Char. #185: 0-->1; Char. #188: 0-->1.

***Rachycentron canadum***: Char. #3: 0.630-->0.690; Char. #5: 0.630-->0.690; Char. #7: 0.120-0.130-->0.100; Char. #8: 0.080-0.170-->0.000; Char. #12: 0.060-->0.010; Char. #21: 0.490-->0.440; Char. #39: 1-->0; Char. #42: 1-->0; Char. #43: 1-->0; Char. #66: 1-->0; Char. #110: 1-->0; Char. #114: 1-->0; Char. #128: 1-->0; Char. #156: 1-->0.

***Nematistius pectoralis***: Char. #7: 0.120-->0.090; Char. #9: 0.110-->0.090; Char. #17: 0.590-->0.630; Char. #18: 0.390-0.480-->0.300; Char. #20: 0.480-->0.750; Char. #21: 0.490-->0.230; Char. #22: 0-->1; Char. #31: 0-->1; Char. #42: 1-->0; Char. #43: 1-->0; Char. #53: 0-->1; Char. #70: 1-->0; Char. #103: 1-->0; Char. #104: 2-->0; Char. #114: 1-->0; Char. #131: 0-->1; Char. #156: 1-->0; Char. #204: 0-->1.

***Morone mississippiensis***: Char. #2: 0.040-->0.030; Char. #16: 0.590-->0.650; Char. #17: 0.380-0.410-->0.320; Char. #40: 1-->0; Char. #47: 1-->0; Char. #113: 0-->1; Char. #120: 0-->1; Char. #121: 0-->1; Char. #129: 0-->1; Char. #162: 1-->2; Char. #173: 0-->1.

***Lateolabrax japonicus***: Char. #1: 0.500-->0.610; Char. #5: 0.380-->0.440; Char. #12: 0.010-->0.080; Char. #13: 0.710-->0.860; Char. #70: 0-->1; Char. #202: 0-->1; Char. #204: 1-->0.

**Lates**: Char. #1: 0.440-->0.330; Char. #13: 0.710-->0.500; Char. #14: 0.640-0.710-->0.430; Char. #16: 0.550-0.590-->0.730; Char. #19: 0.560-->0.590; Char. #20: 0.810-0.830-->0.890; Char. #78: 0-->2; Char. #83: 0-->1; Char. #115: 1-->2; Char. #128: 1-->0; Char. #158: 0-->1; Char. #166: 1-->0; Char. #175: 0-->1.

***Centropomus parallelus***: Char. #2: 0.040-->0.020; Char. #7: 0.020-0.030-->0.000; Char. #9: 0.020-0.030-->0.000; Char. #16: 0.550-0.590-->0.410; Char. #17: 0.380-->0.130; Char. #18: 0.330-0.420-->0.280; Char. #19: 0.560-->0.410; Char. #20: 0.810-0.830-->0.400; Char. #21: 0.040-0.090-->0.020; Char. #27: 0-->1; Char. #74: 1-->0; Char. #87: 1-->0; Char. #120: 0-->1; Char. #121: 0-->1; Char. #129: 0-->1; Char. #131: 1-->0; Char. #149: 0-->1; Char. #155: 0-->1; Char. #165: 0-->1; Char. #186: 0-->1; Char. #191: 1-->0; Char. #201: 1-->0.

***Oplegnathus fasciatus***: Char. #1: 0.440-0.560-->0.610; Char. #4: 0.500-->0.000; Char. #5: 0.380-->0.500; Char. #13: 0.640-->0.710; Char. #14: 0.570-->0.640; Char. #17: 0.440-0.550-->0.560; Char. #19: 0.560-0.660-->0.750; Char. #26: 0-->1; Char. #37: 0-->1; Char. #43: 0-->1; Char. #70: 1-->0; Char. #78: 0-->2; Char. #98: 0-->1; Char. #104: 2-->1; Char. #111: 0-->1; Char. #121: 0-->1; Char. #127: 0-->1; Char. #180: 1-->0; Char. #182: 0-->1; Char. #186: 0-->1; Char. #195: 0-->1.

***Polydactylus virginicus***: Char. #3: 0.440-->0.940; Char. #4: 0.500-->0.000; Char. #5: 0.380-->0.000; Char. #7: 0.030-0.050-->0.080; Char. #9: 0.030-0.050-->0.070; Char. #13: 0.640-0.710-->0.860; Char. #14: 0.570-0.640-->0.790; Char. #17: 0.380-0.430-->0.350; Char. #18: 0.500-->0.560; Char. #19: 0.560-->0.530; Char. #20: 0.740-0.770-->0.520; Char. #26: 0-->1; Char. #27: 0-->1; Char. #30: 0-->1; Char. #38: 1-->0; Char. #96: 0-->1; Char. #107: 0-->1; Char. #108: 0-->1; Char. #133: 0-->1; Char. #170: 0-->1; Char. #172: 0-->1; Char. #183: 0-->1; Char. #186: 0-->1; Char. #202: 0-->1.

***Paralichthys isosceles***: Char. #0: 0.300-->0.550; Char. #1: 0.440-->0.000; Char. #2: 0.240-->0.580; Char. #3: 0.250-->0.060; Char. #4: 0.500-->1.000; Char. #5: 0.250-->0.000; Char. #7: 0.210-->0.410; Char. #9: 0.220-->0.420; Char. #10: 0.670-->0.440; Char. #12: 0.060-0.070-->0.110; Char. #13: 0.290-->0.070; Char. #14: 0.290-->0.000; Char. #16: 0.190-->0.000; Char. #17: 0.760-->1.000; Char. #19: 0.470-->0.380; Char. #20: 0.220-->0.000; Char. #21: 0.760-->1.000; Char. #37: 0-->1; Char. #43: 1-->0; Char. #56: 1-->0; Char. #65: 0-->1; Char. #74: 1-->0; Char. #76: 0-->1; Char. #114: 1-->0; Char. #180: 1-->0; Char. #201: 0-->1; Char. #203: 0-->1; Char. #204: 0-->1.

***Psettodes erumei***: Char. #1: 0.440-->0.560; Char. #12: 0.060-0.070-->0.010; Char. #39: 1-->0; Char. #40: 1-->0; Char. #70: 1-->0; Char. #78: 0-->1; Char. #116: 0-->1; Char. #121: 1-->0; Char. #131: 0-->1; Char. #135: 0-->1; Char. #158: 0-->1; Char. #172: 0-->1.

***Parachanna obscura***: Char. #13: 0.210-->0.140; Char. #21: 0.490-0.500-->0.580; Char. #25: 1-->0; Char. #56: 1-->0; Char. #93: 1-->0; Char. #133: 0-->1; Char. #136: 0-->1; Char. #147: 0-->1; Char. #154: 0-->1; Char. #179: 1-->0; Char. #185: 0-->1; Char. #193: 1-->0; Char. #200: 1-->0.

**Node 68**: No synapomorphies

**Node 69:** Char. #0: 0.340-->0.500; Char. #2: 0.380-->0.530; Char. #3: 0.560-->0.630; Char. #5: 0.630-->0.750; Char. #6: 0.400-->0.000; Char. #7: 0.200-->0.340; Char. #9: 0.220-->0.350; Char. #13: 0.210-0.430-->0.000; Char. #14: 0.210-0.290-->0.000; Char. #17: 0.710-->0.720; Char. #18: 0.320-->0.230; Char. #19: 0.410-->0.280; Char. #21: 0.500-->0.760; Char. #22: 0-->1; Char. #23: 0-->1; Char. #42: 1-->0; Char. #43: 1-->0; Char. #49: 0-->1; Char. #50: 0-->1; Char. #69: 0-->1; Char. #75: 0-->1; Char. #80: 0-->1; Char. #81: 0-->1; Char. #96: 1-->0; Char. #107: 0-->1; Char. #111: 0-->1; Char. #121: 1-->0; Char. #130: 0-->1; Char. #146: 0-->1; Char. #156: 1-->0; Char. #174: 0-->1; Char. #194: 1-->0.

**Node 70:** Char. #0: 0.220-0.240-->0.340; Char. #2: 0.170-0.270-->0.380; Char. #3: 0.440-0.500-->0.560; Char. #5: 0.440-0.500-->0.630; Char. #6: 0.500-->0.400; Char. #7: 0.140-->0.200; Char. #9: 0.140-0.160-->0.220; Char. #17: 0.560-0.620-->0.710; Char. #19: 0.480-->0.410; Char. #20: 0.370-0.460-->0.290-0.360; Char. #27: 1-->0; Char. #76: 0-->1; Char. #83: 0-->1; Char. #162: 2-->0.

**Node 71:** Char. #7: 0.120-0.130-->0.140; Char. #9: 0.110-0.130-->0.140-0.160; Char. #12: 0.100-->0.140-0.240; Char. #13: 0.640-->0.210-0.430; Char. #14: 0.570-0.640-->0.210-0.290; Char. #18: 0.390-->0.320-0.330; Char. #74: 1-->0; Char. #78: 0-->2; Char. #212: 0-->1.

**Node 72:** Char. #12: 0.060-0.070-->0.100; Char. #50: 1-->0; Char. #93: 0-->1; Char. #96: 0-->1; Char. #108: 1-->0; Char. #135: 0-->1; Char. #162: 1-->2; Char. #176: 1-->0; Char. #180: 1-->0; Char. #193: 0-->1; Char. #194: 0-->1.

**Node 73:** Char. #19: 0.490-0.530-->0.480; Char. #25: 0-->1; Char. #51: 0-->1; Char. #68: 1-->0.

**Node 74:** Char. #5: 0.380-->0.440-0.500; Char. #26: 0-->1; Char. #109: 1-->0.

**Node 75:** Char. #0: 0.140-->0.180-0.220; Char. #2: 0.070-->0.170-0.190; Char. #7: 0.080-->0.120-0.130; Char. #9: 0.090-->0.110-0.130; Char. #12: 0.050-->0.060-0.070; Char. #16: 0.540-->0.450-0.470; Char. #17: 0.460-->0.560-0.590; Char. #19: 0.550-0.560-->0.490-0.530; Char. #20: 0.740-0.770-->0.460-0.470; Char. #21: 0.210-0.290-->0.490; Char. #27: 0-->1; Char. #31: 1-->0; Char. #43: 0-->1; Char. #66: 0-->1; Char. #73: 0-->1; Char. #77: 0-->1; Char. #84: 1-->0; Char. #85: 1-->0; Char. #121: 0-->1; Char. #179: 0-->1; Char. #195: 0-->1.

**Node 76:** Char. #11: 0.250-->0.000; Char. #12: 0.010-0.020-->0.050; Char. #101: 0-->1; Char. #206: 0-->1.

**Node 77:** Char. #108: 0-->1; Char. #170: 0-->1.

**Node 78:** Char. #87: 1-->0; Char. #114: 2-->1.

**Node 79:** Char. #6: 0.700-->0.500; Char. #8: 0.250-->0.170; Char. #10: 0.890-->0.670; Char. #13: 0.360-->0.640; Char. #14: 0.290-->0.570; Char. #15: 0.000-->0.250; Char. #22: 1-->0; Char. #24: 1-->0; Char. #48: 0-->1; Char. #56: 0-->1; Char. #74: 0-->1; Char. #75: 1-->0; Char. #84: 0-->1; Char. #100: 0-->1; Char. #116: 1-->0; Char. #146: 1-->0; Char. #152: 0-->1; Char. #162: 0-->1; Char. #206: 2-->0.

**Node 80:** Char. #5: 0.380-->0.130-0.310; Char. #14: 0.570-->0.500; Char. #16: 0.590-->0.650; Char. #20: 0.740-0.770-->0.600; Char. #84: 1-->0; Char. #85: 1-->0; Char. #176: 1-->0; Char. #182: 0-->1; Char. #212: 0-->1.

**Node 81:** Char. #0: 0.120-0.130-->0.070-0.100; Char. #2: 0.070-->0.040-0.060; Char. #17: 0.440-0.460-->0.380-0.430; Char. #51: 0-->1; Char. #164: 1-->0.

**Node 82:** Char. #10: 0.560-0.670-->0.330; Char. #15: 0.250-0.500-->0.750; Char. #19: 0.480-->0.530; Char. #101: 1-->0; Char. #167: 1-->0.

**Node 83:** Char. #1: 0.390-0.440-->0.220; Char. #13: 0.640-->0.430; Char. #21: 0.490-->0.550; Char. #25: 0-->1; Char. #74: 1-->0; Char. #108: 1-->0; Char. #114: 1-->2; Char. #121: 1-->0; Char. #198: 1-->0; Char. #200: 1-->0.

**Node 84:** Char. #186: 0-->1.

**Node 85:** Char. #11: 0.000-->0.250; Char. #101: 1-->0; Char. #168: 0-->1; Char. #171: 0-->1.

**Node 86:** Char. #13: 0.640-->0.570; Char. #18: 0.390-0.500-->0.370; Char. #22: 0-->1; Char. #24: 0-->1; Char. #42: 1-->0; Char. #127: 0-->1; Char. #186: 0-->1; Char. #201: 0-->1; Char. #204: 0-->1.

**Node 87:** Char. #0: 0.200-->0.050-0.110; Char. #2: 0.100-->0.020-0.080; Char. #7: 0.090-->0.030-0.070; Char. #9: 0.090-->0.050-0.070; Char. #13: 0.500-->0.570; Char. #14: 0.500-->0.570; Char. #16: 0.390-->0.470-0.560; Char. #40: 1-->0; Char. #111: 0-->1; Char. #121: 1-->0; Char. #123: 0-->1.

**Node 88:** Char. #2: 0.170-0.240-->0.100; Char. #7: 0.120-0.210-->0.090; Char. #9: 0.110-0.220-->0.090; Char. #20: 0.220-0.470-->0.800; Char. #21: 0.490-0.760-->0.250-0.320; Char. #34: 0-->1; Char. #67: 0-->1; Char. #155: 0-->1; Char. #183: 0-->1.

**Node 89:** Char. #44: 0-->1; Char. #119: 0-->1; Char. #126: 0-->1; Char. #186: 0-->1.

**Node 90:** Char. #3: 0.380-0.440-->0.250-0.310; Char. #5: 0.380-->0.250-0.310; Char. #8: 0.080-0.170-->0.000; Char. #13: 0.640-->0.290-0.500; Char. #14: 0.570-->0.290-0.500; Char. #16: 0.450-0.470-->0.190-0.390; Char. #17: 0.560-0.590-->0.640-0.760; Char. #18: 0.390-0.480-->0.260-0.350; Char. #107: 0-->1; Char. #125: 0-->1; Char. #152: 1-->0.

**Node 91:** Char. #3: 0.250-0.310-->0.750; Char. #5: 0.250-0.310-->0.750; Char. #13: 0.570-->0.710; Char. #14: 0.570-->0.640; Char. #79: 0-->1; Char. #107: 1-->0; Char. #114: 1-->0; Char. #115: 1-->2; Char. #145: 0-->1; Char. #186: 1-->0.

**Node 92:** Char. #35: 1-->0; Char. #37: 0-->1; Char. #85: 0-->1; Char. #187: 0-->1.

**Node 93:** Char. #0: 0.150-->0.120; Char. #3: 0.560-0.690-->0.750; Char. #5: 0.560-0.690-->0.750; Char. #12: 0.070-0.090-->0.060; Char. #25: 1-->0; Char. #61: 0-->1; Char. #82: 0-->1; Char. #135: 1-->0; Char. #141: 0-->1; Char. #142: 0-->1; Char. #148: 0-->1; Char. #198: 1-->0; Char. #201: 1-->0; Char. #204: 1-->0.

**Node 94:** Char. #0: 0.180-0.190-->0.150; Char. #2: 0.130-0.170-->0.060; Char. #7: 0.130-0.140-->0.070; Char. #9: 0.130-0.140-->0.070; Char. #20: 0.390-0.470-->0.570-0.610; Char. #64: 1-->0; Char. #160: 0-->1.

**Node 95:** Char. #59: 0-->1; Char. #115: 2-->1; Char. #138: 0-->1; Char. #140: 0-->1; Char. #166: 0-->1.

**Node 96:** Char. #1: 0.330-->0.560; Char. #62: 0-->1; Char. #63: 0-->1; Char. #110: 1-->0.

**Node 97:** Char. #12: 0.010-->0.070; Char. #15: 0.250-->0.500; Char. #17: 0.540-->0.600; Char. #25: 0-->1; Char. #31: 1-->0; Char. #80: 0-->1; Char. #81: 0-->1; Char. #118: 0-->1; Char. #119: 0-->1; Char. #120: 0-->1.

**Node 98:** Char. #50: 1-->0; Char. #85: 1-->0; Char. #115: 1-->2.

**Node 99:** Char. #1: 0.390-->0.330; Char. #216: 0-->1.

**Node 100:** Char. #3: 0.500-->0.560-0.630; Char. #5: 0.500-->0.560-0.630; Char. #12: 0.060-0.100-->0.010; Char. #16: 0.450-0.470-->0.490-0.520; Char. #18: 0.450-0.500-->0.520; Char. #26: 1-->0; Char. #31: 0-->1; Char. #36: 0-->1; Char. #44: 0-->1; Char. #58: 0-->1; Char. #70: 1-->0; Char. #127: 0-->1; Char. #135: 0-->1; Char. #147: 0-->1; Char. #152: 1-->0; Char. #153: 0-->1; Char. #159: 0-->1; Char. #188: 0-->1; Char. #201: 0-->1; Char. #204: 0-->1.

**Node 101:** Char. #20: 0.570-0.610-->0.650; Char. #22: 0-->1; Char. #54: 1-->0; Char. #115: 1-->2.

**Node 102:** Char. #1: 0.390-->0.220; Char. #13: 0.640-0.710-->0.790-0.860; Char. #14: 0.640-->0.710-0.790; Char. #18: 0.520-->0.200-0.250; Char. #19: 0.490-0.530-->0.370; Char. #20: 0.460-0.590-->0.450; Char. #50: 1-->0; Char. #68: 1-->2; Char. #74: 1-->0; Char. #114: 1-->2.

**Node 103:** Char. #3: 0.560-0.630-->0.690; Char. #5: 0.560-0.630-->0.690; Char. #14: 0.570-->0.640; Char. #111: 0-->1; Char. #171: 1-->0; Char. #172: 0-->1; Char. #202: 0-->1; Char. #203: 0-->1.

**Node 104:** Char. #21: 0.400-0.490-->0.330; Char. #34: 0-->1; Char. #43: 1-->0; Char. #189: 0-->1 ;

**Node 105:** Char. #7: 0.130-->0.170; Char. #9: 0.130-->0.160; Char. #12: 0.010-->0.130; Char. #21: 0.330-->0.410; Char. #29: 0-->1; Char. #34: 1-->0; Char. #70: 0-->1; Char. #173: 1-->0.

**Node 106:** Char. #18: 0.530-0.560-->0.680-0.690; Char. #36: 1-->0; Char. #37: 1-->0; Char. #40: 1-->0; Char. #118: 1-->0.

**Node 107:** Char. #89: 0-->1; Char. #198: 1-->0; Char. #202: 0-->1.

**Node 108:** Char. #0: 0.180-0.190-->0.150; Char. #2: 0.130-->0.080; Char. #7: 0.130-0.140-->0.080; Char. #9: 0.130-0.140->0.080; Char. #16: 0.510-->0.520; Char. #91: 0-->1; Char. #163: 0-->1.

**Node 109:** Char. #17: 0.600-->0.490-0.550; Char. #20: 0.390-0.470-->0.520-0.550; Char. #21: 0.490-0.520-->0.390-0.400; Char. #96: 0-->1; Char. #135: 1-->0; Char. #216: 1-->0.

**Node 110:** Char. #1: 0.440-->0.330; Char. #3: 0.560-0.690-->0.500; Char. #5: 0.560-0.690-->0.500; Char. #12: 0.070-0.090->0.060; Char. #88: 0-->1; Char. #94: 0-->1; Char. #95: 0-->1.

**Node 111:** Char. #0: 0.270-->0.290-0.300; Char. #1: 0.560-->0.440; Char. #2: 0.220-->0.270; Char. #13: 0.570-->0.360-0.430; Char. #14: 0.500-0.570-->0.290-0.430; Char. #18: 0.560-->0.820-0.930; Char. #21: 0.720-->0.810-0.860; Char. #66: 1-->0; Char. #71: 0-->1; Char. #77: 1-->0.

**Node 112:** Char. #0: 0.180-0.190-->0.270; Char. #2: 0.130-0.170-->0.220; Char. #6: 0.500-->0.000; Char. #7: 0.130-0.140->0.220-0.240; Char. #9: 0.130-0.140-->0.200-0.230; Char. #17: 0.600-->0.620-0.630; Char. #21: 0.490-0.520-->0.720; Char. #46: 0-->1; Char. #57: 0-->1; Char. #70: 0-->1; Char. #72: 0-->1; Char. #125: 0-->1; Char. #189: 0-->1; Char. #193: 0->1.

**Node 113:** Char. #2: 0.040-0.060-->0.070; Char. #18: 0.510-0.580-->0.630; Char. #27: 0-->1; Char. #110: 1-->2.

**Node 114:** Char. #1: 0.500-->0.560-0.610; Char. #15: 0.250-->0.500; Char. #36: 0-->1; Char. #37: 0-->1; Char. #104: 2-->1.

**Node 115:** Char. #42: 0-->1; Char. #43: 0-->1; Char. #51: 1-->0; Char. #180: 1-->0.

**Node 116:** Char. #17: 0.380-0.430-->0.440-0.480; Char. #18: 0.500-->0.510-0.520; Char. #178: 0-->1; Char. #186: 0-->1.

**Node 117:** Char. #28: 1-->0; Char. #191: 0-->1.

**Node 118:** Char. #42: 1-->0; Char. #70: 1-->0; Char. #111: 0-->1; Char. #156: 0-->1; Char. #201: 0-->1; Char. #204: 0-->1.

**Node 119:** Char. #17: 0.440-0.520-->0.380; Char. #18: 0.510-->0.430; Char. #25: 0-->1; Char. #47: 1-->0; Char. #98: 0-->1; Char. #110: 1-->0; Char. #163: 1-->0.

**Node 120:** Char. #20: 0.740-0.750-->0.590-0.620; Char. #21: 0.180-0.220-->0.260-0.330; Char. #24: 0-->1; Char. #39: 1-->0; Char. #108: 0-->1.

**Node 121:** Char. #128: 1-->0; Char. #129: 0-->1; Char. #182: 0-->1.

**Node 122:** Char. #84: 1-->0; Char. #85: 1-->0; Char. #156: 1-->0; Char. #182: 0-->1; Char. #198: 0-->1.

**Node 123:** Char. #16: 0.590-->0.550; Char. #32: 0-->1; Char. #49: 0-->1; Char. #52: 0-->2; Char. #55: 0-->1; Char. #74: 1-->0; Char. #112: 0-->1; Char. #114: 1-->0; Char. #115: 1-->2; Char. #158: 0-->1; Char. #200: 1-->0; Char. #203: 0-->1; Char. #208: 0-->1.

**Node 124:** Char. #0: 0.030-0.100-->0.010; Char. #1: 0.330-0.500-->0.220; Char. #16: 0.790-->0.850; Char. #27: 0-->1; Char. #49: 0-->1; Char. #55: 0-->1; Char. #80: 0-->1; Char. #96: 0-->1; Char. #110: 1-->0; Char. #115: 1-->0; Char. #120: 0-->1; Char. #121: 0-->1; Char. #143: 0-->1; Char. #147: 0-->1; Char. #156: 0-->1; Char. #157: 0-->1; Char. #194: 0-->1.

**Node 125:** Char. #13: 0.640-->0.360-0.570; Char. #15: 0.250-->0.500; Char. #16: 0.650-->0.790; Char. #19: 0.560-->0.650-0.670; Char. #25: 0-->1; Char. #31: 1-->0; Char. #36: 0-->1; Char. #37: 0-->1; Char. #43: 0-->1; Char. #50: 1-->0; Char. #105: 0-->1; Char. #116: 0-->1; Char. #163: 1-->0; Char. #209: 0-->1; Char. #213: 1-->0.

**Node 126:** Char. #2: 0.170-0.190-->0.150; Char. #12: 0.060-0.070-->0.010; Char. #19: 0.490-0.530-->0.540; Char. #20: 0.460-0.470-->0.480; Char. #23: 0-->1; Char. #34: 0-->1; Char. #80: 0-->1; Char. #81: 0-->1; Char. #195: 1-->0.

**Node 127:** Char. #3: 0.440-0.500-->0.630; Char. #5: 0.440-0.500-->0.630; Char. #13: 0.640-->0.860; Char. #14: 0.570-0.640-->0.790; Char. #16: 0.450-0.470-->0.380; Char. #19: 0.480-->0.410; Char. #22: 0-->1; Char. #23: 0-->1; Char. #119: 0-->1; Char. #129: 0-->1; Char. #132: 0-->1.

**Node 128:** Char. #20: 0.740-0.770-->0.810; Char. #21: 0.160-0.220-->0.090; Char. #87: 0-->1; Char. #166: 0-->1; Char. #172: 0-->1.

**Node 129:** Char. #18: 0.500-->0.330-0.420; Char. #22: 0-->1; Char. #30: 0-->1; Char. #117: 0-->1.

**Node 130:** Char. #0: 0.070-0.100-->0.060; Char. #1: 0.500-->0.440; Char. #24: 0-->1; Char. #38: 1-->0; Char. #51: 1-->0; Char. #198: 0-->1; Char. #203: 0-->1; Char. #208: 0-->1.

**Node 131:** Char. #19: 0.490-0.530-->0.470; Char. #25: 0-->1; Char. #52: 0-->1; Char. #108: 1-->0; Char. #124: 0-->1; Char. #144: 0-->1; Char. #184: 0-->1; Char. #198: 1-->0; Char. #206: 1-->0; Char. #208: 0-->1.

**BREMER SUPPORT (RELATIVE AND ABSOLUTE) FOR THE REFERENCE TREE (K= 6.808).**

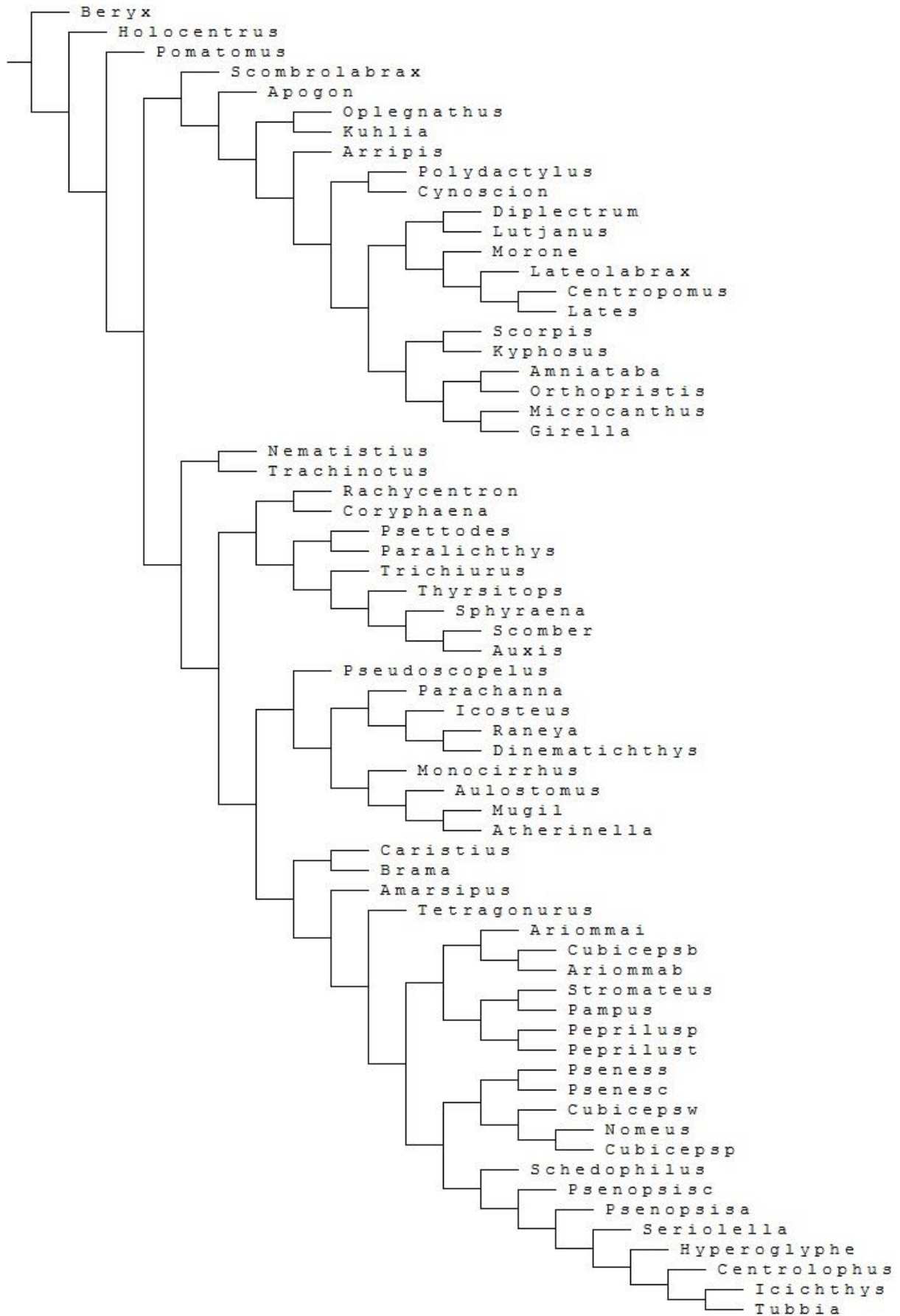
Relative bremer supports (from 14999 trees, cut 0)



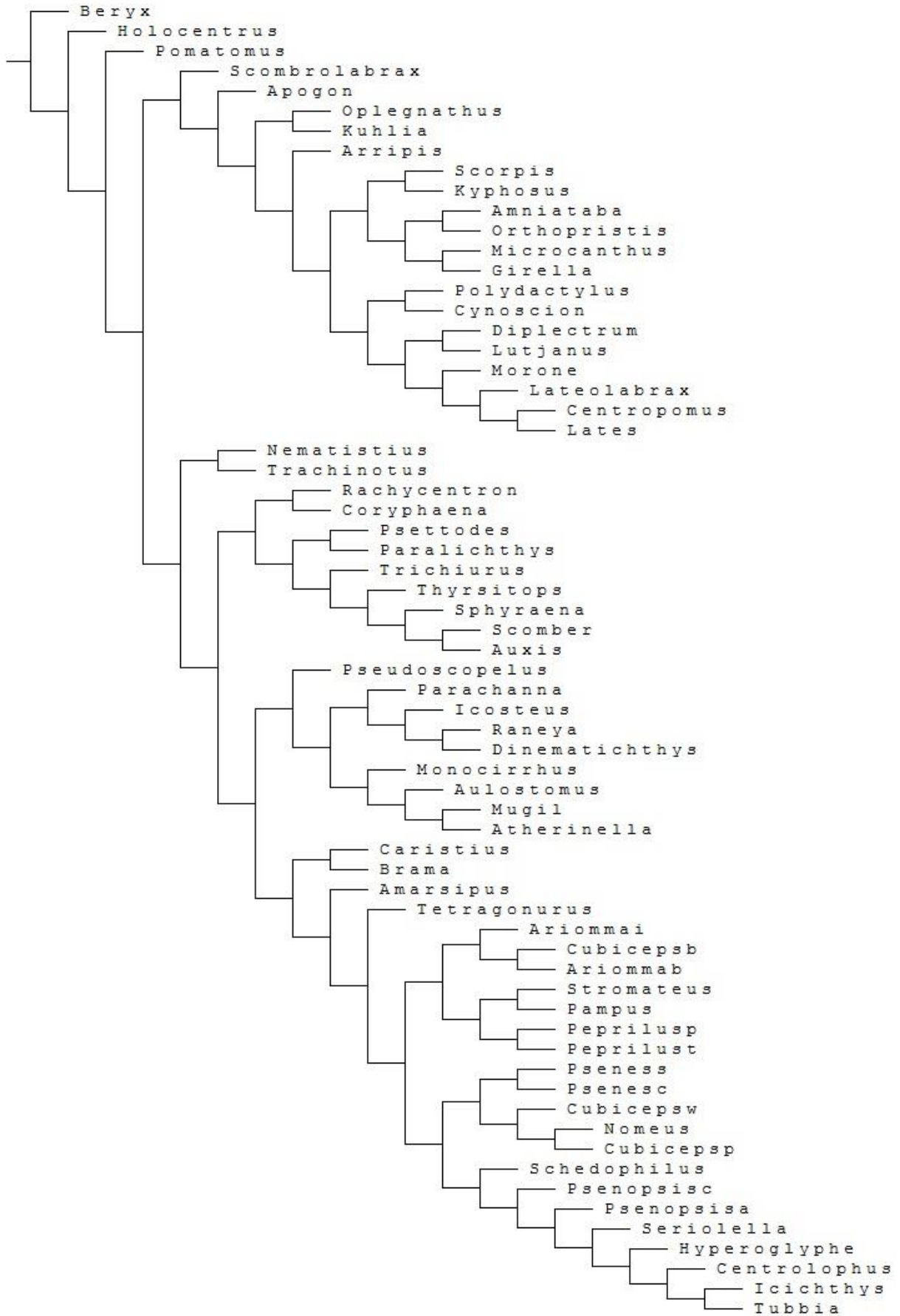


THE TWO MOST PARSIMONIOUS TREES RESULTANT FROM AN EQUAL WEIGHT SEARCH:

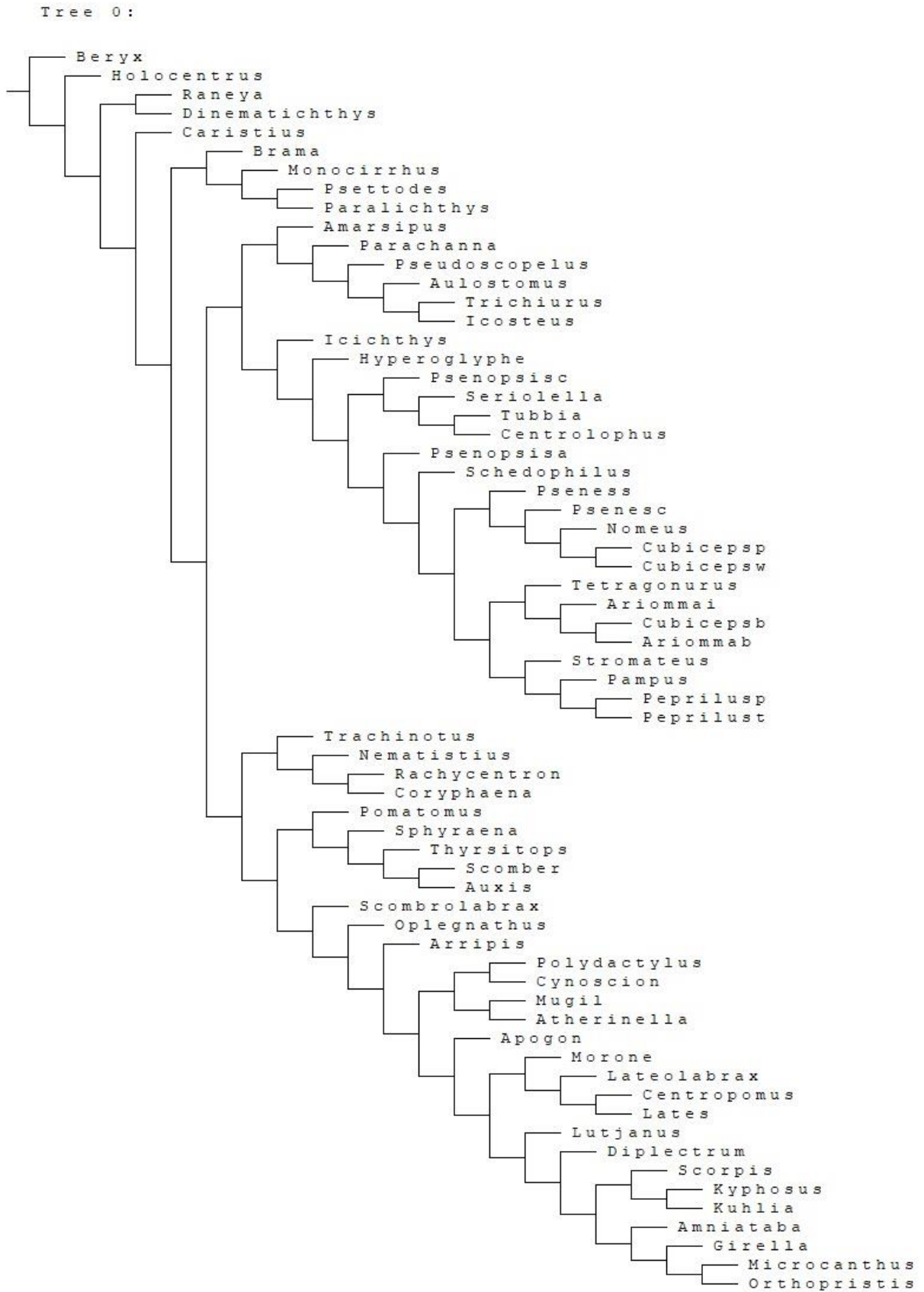
Tree 0:



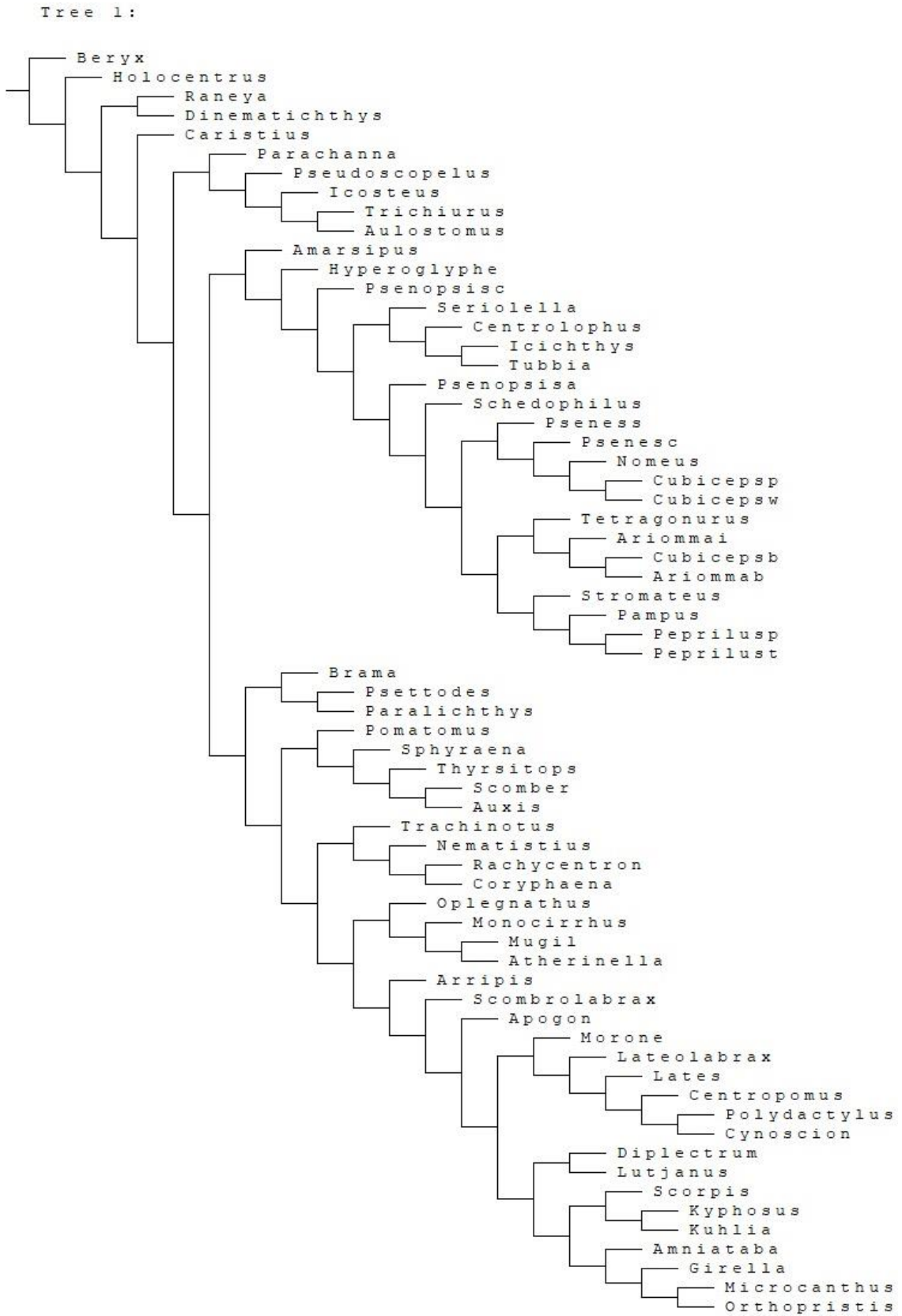
Tree 1:



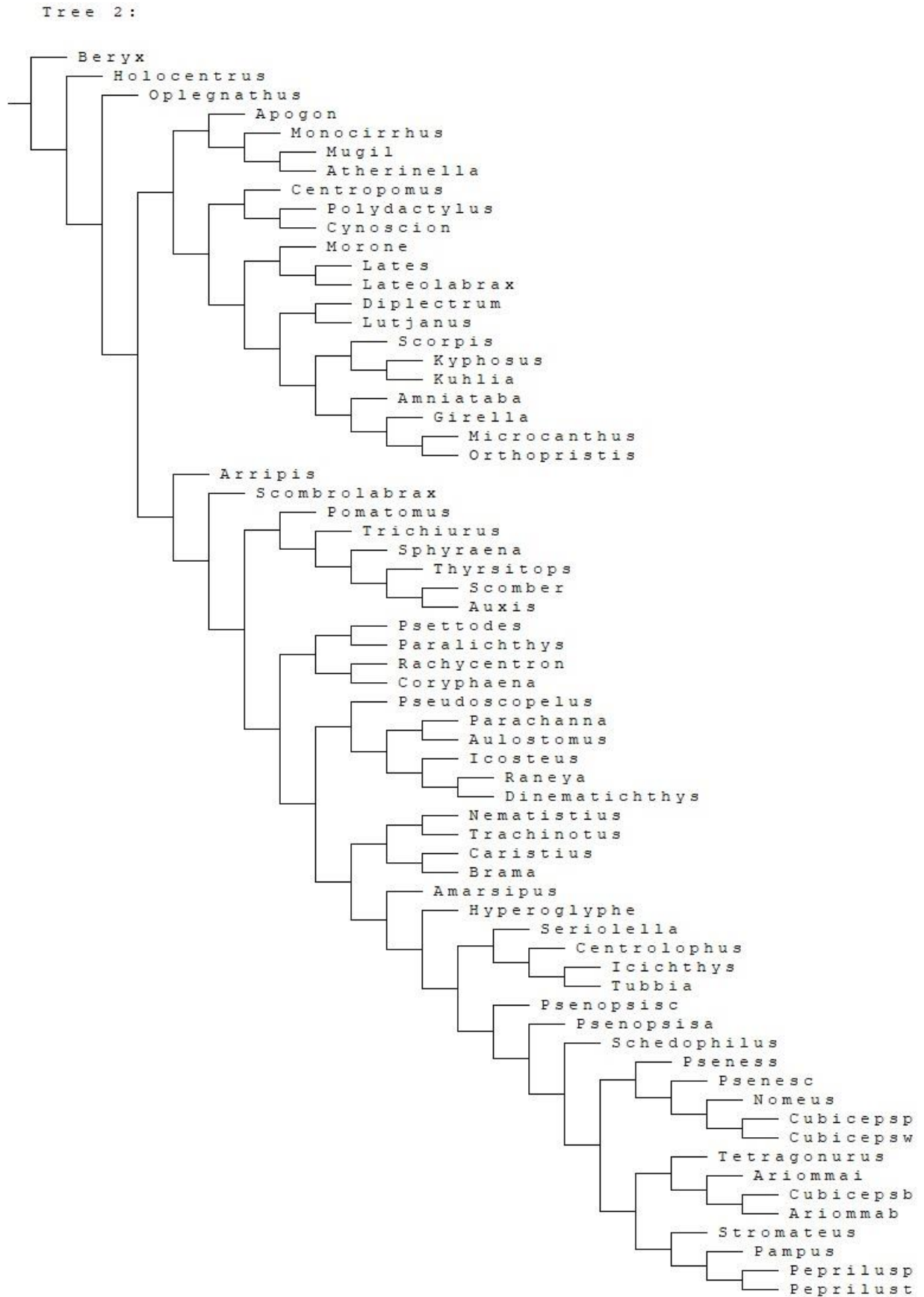
MOST PARSIMONIOUS TREES RESULTANT FROM AN IMPLICIT WEIGHT SEARCH (K = 1):



MOST PARSIMONIOUS TREES RESULTANT FROM AN IMPLICIT WEIGHT SEARCH (K = 1.885):



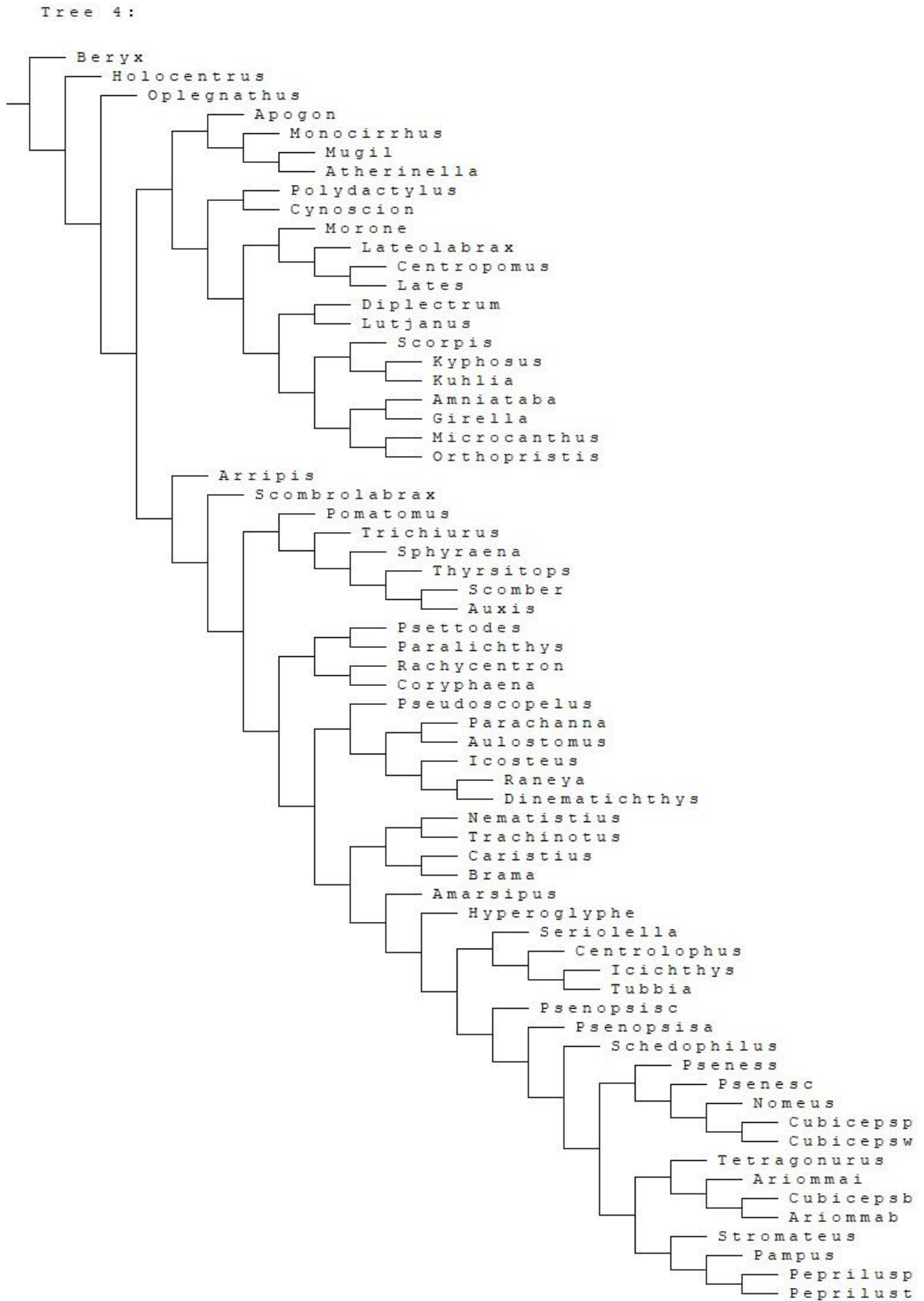
MOST PARSIMONIOUS TREES RESULTANT FROM AN IMPLICIT WEIGHT SEARCH (K = 2.849):



MOST PARSIMONIOUS TREES RESULTANT FROM AN IMPLICIT WEIGHT SEARCH (K = 3.957):

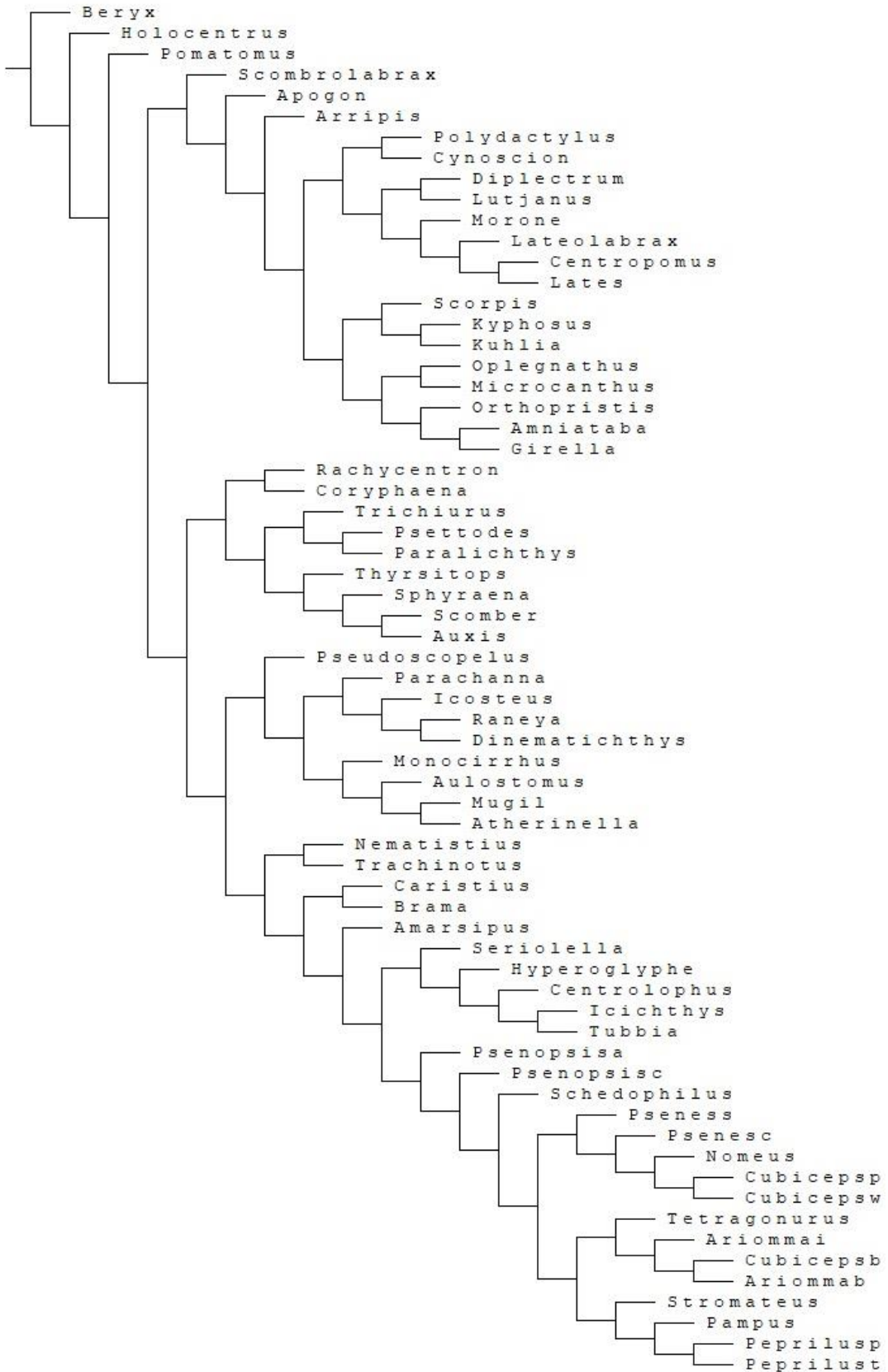


MOST PARSIMONIOUS TREES RESULTANT FROM AN IMPLICIT WEIGHT SEARCH (K = 5.267):

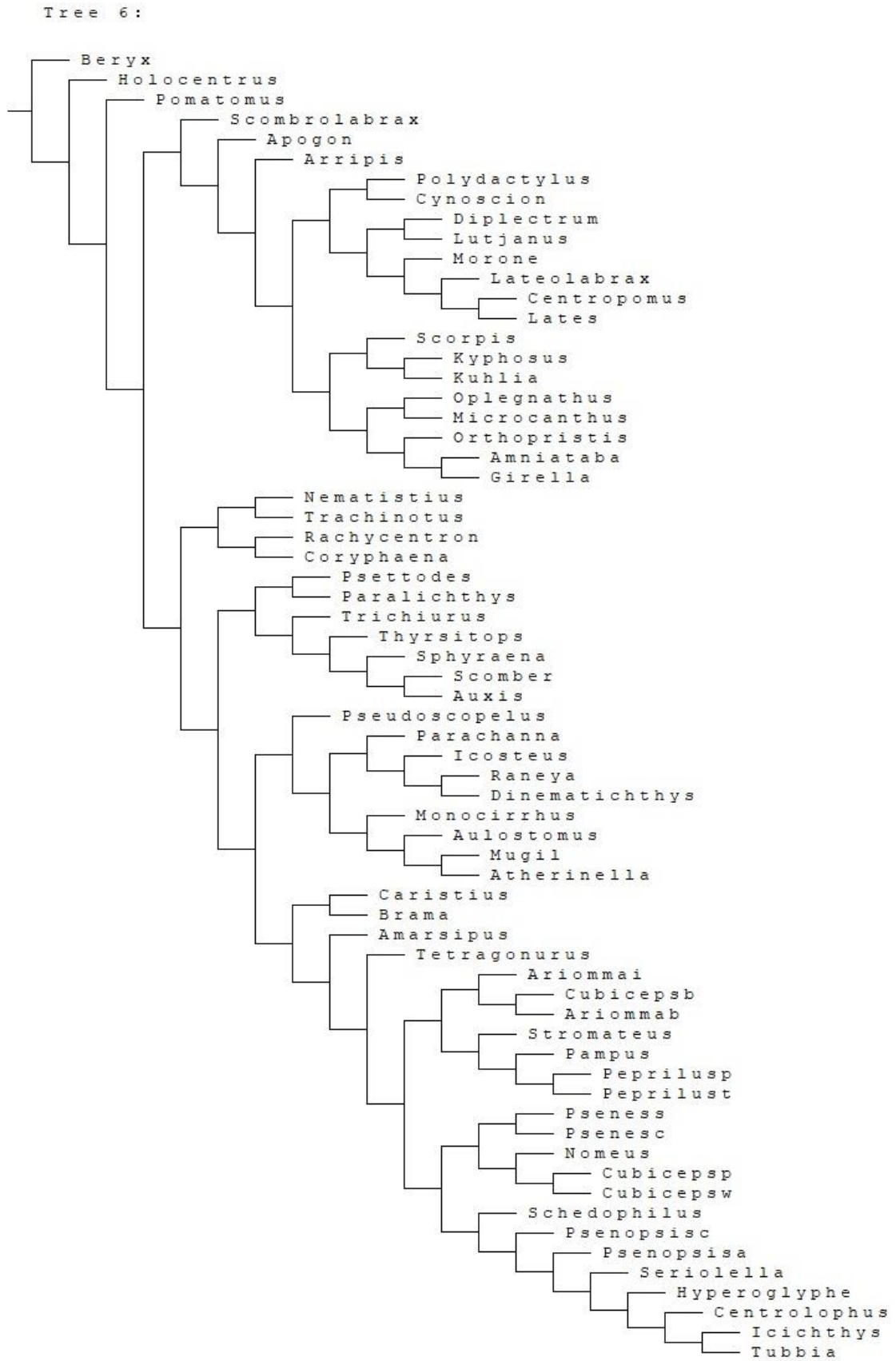


MOST PARSIMONIOUS TREES RESULTANT FROM AN IMPLICIT WEIGHT SEARCH (K = 8.654):

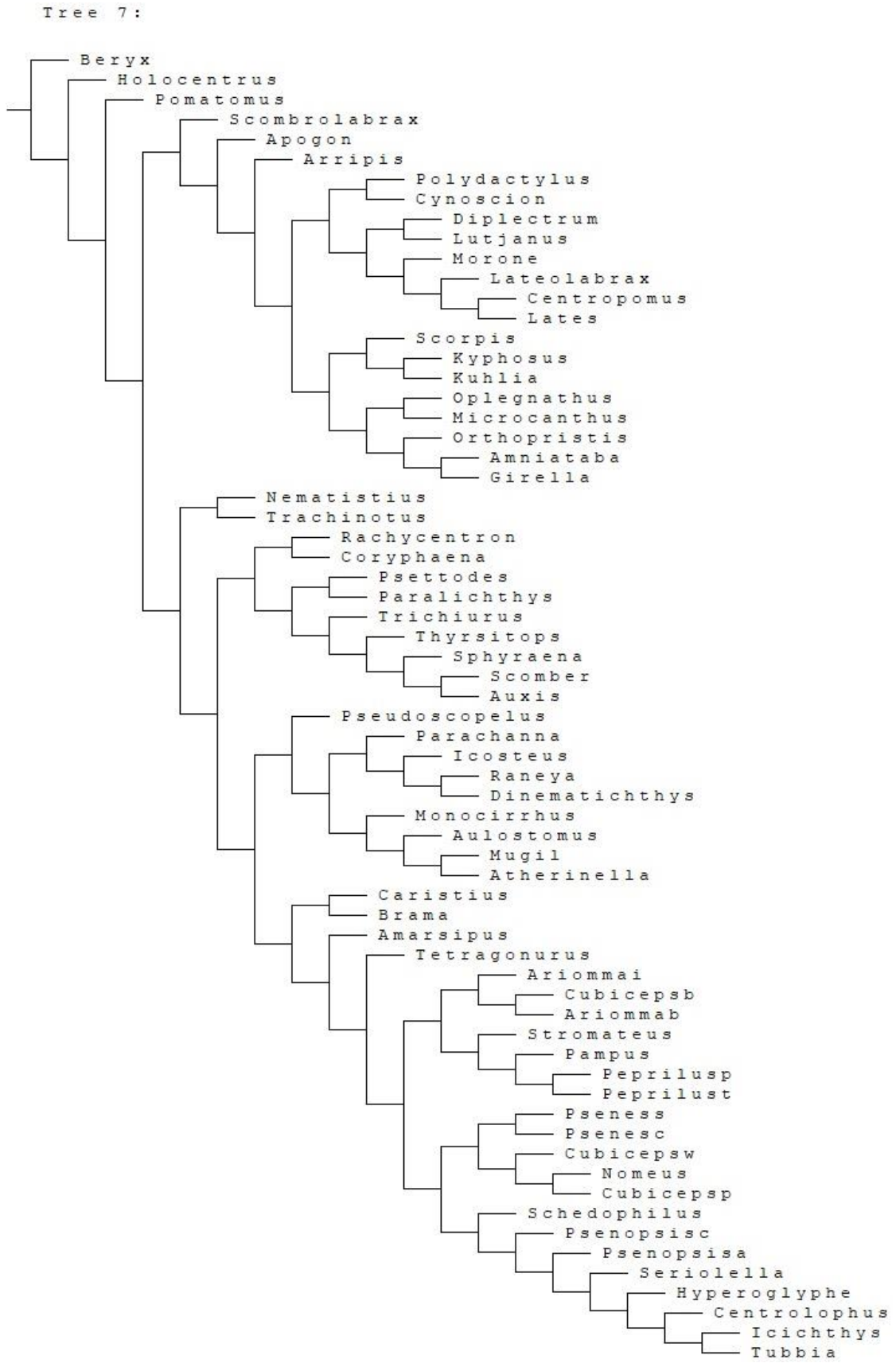
Tree 5:



MOST PARSIMONIOUS TREES RESULTANT FROM AN IMPLICIT WEIGHT SEARCH (K = 10.628):

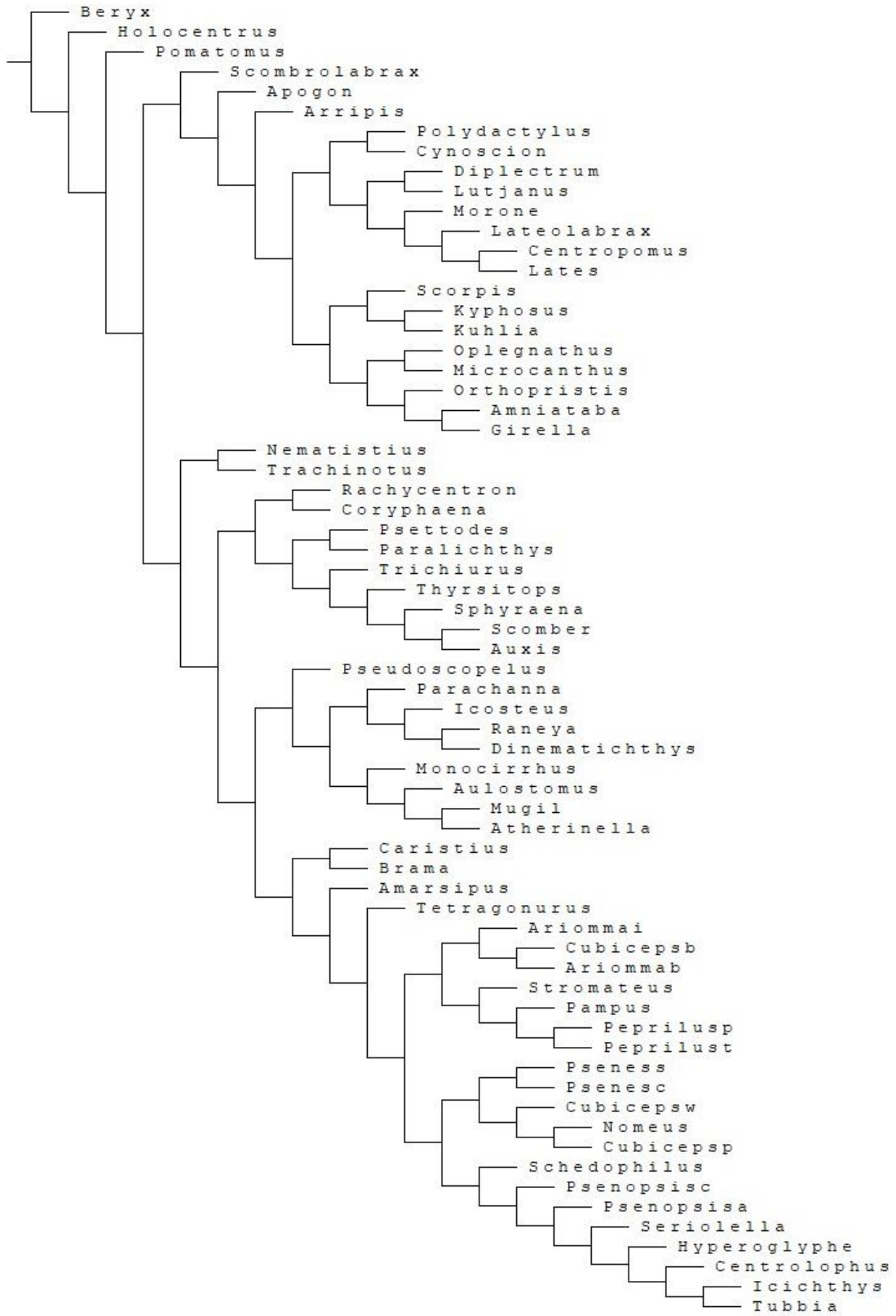


MOST PARSIMONIOUS TREES RESULTANT FROM AN IMPLICIT WEIGHT SEARCH (K = 13.703):



MOST PARSIMONIOUS TREES RESULTANT FROM AN IMPLICIT WEIGHT SEARCH (K = 17.274):

Tree 8:



MOST PARSIMONIOUS TREES RESULTANT FROM AN IMPLICIT WEIGHT SEARCH (K = 22):

